UNIVERSITÀ DEGLI STUDI DELL'AQUILA
DIPARTIMENTO DI INGEGNERIA INDUSTRIALE E DELL'INFORMAZIONE E DI ECONOMIA

Dottorato di Ricerca in Ingegneria Industriale e dell'Informazione e di Economia

Curriculum Ingegneria chimica

XXXII ciclo

Titolo della tesi

Reduction of CO_2 emissions: strategic utilization and storage options

SSD ING-IND/24

Dottorando

Grazia Leonzio

Coordinatore del corso

Prof. Giuseppe Ferri

Tutor

Prof. Pier Ugo Foscolo

Co-Tutor

Prof. David Bogle

Prof. Edwin Zondervan

A.A. 2018/2019

Abstract

The major contribution to global warming and climate change is due to increasing emissions of greenhouse gases by fossil fuels utilization. To be more precise, globally, 32.5 Gt of emissions were registered in 2017, while carbon dioxide concentration in the atmosphere achieved a value of 404 ppm. Urgent actions are needed to face this environmental problem. In this context, carbon capture utilization and storage supply chains have been recognized as a critical measure to reduce emissions and mitigate the anthropogenic impact on the Earth. In Europe, Germany, Italy and the UK are the Countries with higher carbon dioxide emissions. Then, carbon capture utilization and storage supply chains are here designed and discussed for these European Countries. Moreover, it is interesting to analyze and study in depth the most important utilization route of carbon dioxide that can be considered inside a carbon supply chain, as reported in the literature: the hydrogenation of carbon dioxide to methanol production. These topics are investigated in this Thesis at the level of mathematical and numerical modeling, using different computational tools as AIMMS, MATLAB® and Aspen Plus®. The development of a mixed integer linear programming model (deterministic and stochastic) is thus achieved to design carbon supply chains, including its life cycle assessment analysis, and the development of a 1-D and 2-D model for a methanol reactor with the separation of methanol and water by condensation after the recycle of unconverted gases, following its equilibrium study.

After a brief introduction, Chapter II is focused on the study regarding the hydrogenation of carbon dioxide to methanol. An equilibrium analysis of three different reactor configurations (once-through reactor, reactor with the recycle of unconverted gases after the separation of methanol and water by condensation; reactor equipped with membrane permeable to water) is developed in Aspen Plus®. It is found that despite the thermodynamic and kinetic limitations, the reaction is technically feasible. Also, the best efficiency in terms of yield and conversion is obtained with the second configuration mentioned above. Then, for this system a 1-D and 2-D model are developed in MATLAB®: a sensitivity analysis shows the effect of some parameters on the system behavior, while a comparison between a structured and non-structured reactor is considered through the 2-D model, demonstrating the better efficiency of the first case.

The following Chapters are about the analysis of carbon capture utilization and storage supply chains.

In Chapter III, the mixed integer linear programming model for the carbon supply chain is described and applied to Germany. Here, carbon dioxide is stored and used to produce methanol via methane dry reforming. Three different cases are considered, according to the hydrogen production route required to correct feed composition: hydrogen by external reforming, hydrogen by external water electrolysis utilizing renewable power sources, hydrogen by internal steam reforming. By the minimization of total costs, results show that the second case is the best option, because a higher amount of carbon dioxide is consumed to produce the same amount of methanol (then the lowest value of global potential is obtained). Also, the supply chain has the lowest global cost, even though higher economic incentives are required to get the defined methane production cost. However, the suggested framework produces 203 Mton/year of methanol,

then Germany would have a predominant role inside the world methanol market, in coming years. Carbon tax and economic incentives are required to have a profitable system according to an economic point of view ensuring a methanol production cost of 340 €/ton.

In order to overcome the problem of methanol overproduction found in the previous Chapter, in Chapter IV, the same mathematical model is proposed for Germany, however in the utilization section different products are assumed: beside methanol, concrete by curing, wheat, lignin for polyethylene, calcium carbonate, urea, polyurethane and concrete by red mud. The framework is designed and optimized minimizing total costs that are equal to 97.9 billion €/year; the net present value is 675 billion€, while the payback period is 2.71 years: the economic profitability is ensured only by imposing a carbon tax. A Monte Carlo simulation is carried out to evaluate the uncertainty regarding the selling price of carbon-dioxide-based products and their national demand.

In Chapter V, the mathematical model of carbon capture utilization and storage supply chain is applied to Italian regions: carbon dioxide is stored and used to produce methane through a power to gas system. Here, different frameworks with different storage sites for the carbon capture utilization supply chain are compared and designed through the minimization of total costs. It is found that carbon tax and economic incentives are required to have profitable solutions. Among them, the system with offshore Adriatic sea as storage site is the best option, due to the lowest supply chain cost ($7.34 \cdot 10^4$ million €/year) and the lowest level of economic incentives (80 €/tonCO_2 for carbon tax and 260 €/MWh for methane production). Then, it is also found that a carbon capture and utilization supply chain (i.e. without storage) is economically less favorable and a storage site is important in the management of carbon dioxide.

In Chapter VI, the mathematical model for carbon capture utilization and storage supply chain is applied to the UK. Three different frameworks are considered with different storage sites, as Bunter Sandstone, Scottish off-shore and Ormskirk Sandstone. Carbon dioxide can be used to produce calcium carbonate, concrete, tomatoes, polyurethane, methanol and methane. Total costs are minimized to design and optimize these carbon supply chains, while reducing significantly carbon dioxide emissions. Results show that the system with Bunter Sandstone as storage site is the most economically profitable solution, due to the highest value of net present value (0.554 trillion€) and lowest value of payback period (2.85 years). Only carbon tax is needed to have a profitable solution from an economic point of view. Total costs are 1.04 billion€/year.

The previous supply chains are designed through the minimization of the objective function expressing total costs. However, in order to have a description of a more realistic system, carbon tax remission, revenues and economic incentives are subtracted in the objective function to be minimized, as considered in Chapter VII. These new terms are taken into account at three different levels, according to their values on the market, then a scenario analysis is developed for the carbon capture utilization and storage supply chains of Germany, Italy and the UK. Results show that carbon tax influences only the total value of the objective function, while economic incentives and revenues have a significant effect also on the topology of the supply chain.

The supply chains developed on large scale require a lot of energy for their operation, then additional emissions are produced. It is necessary to develop a life cycle assessment analysis to verify that the proposed frameworks achieve the target set by the environmental policy for reduction of carbon dioxide emissions. In Chapter VIII, a life cycle assessment analysis is carried out for the best supply chains of Italy, Germany and the UK. Results show that these Countries will be able to achieve the carbon dioxide reduction target fixed by the environmental policy, by putting into operation the carbon supply chain designed for each Country. A sensitivity analysis is also carried out increasing the amount of carbon dioxide sent to the utilization section and reducing that sent to the storage section, keeping constant the overall amount of captured carbon dioxide. For the supply chains of Germany and the UK, a higher environmental impact is produced at a higher utilization rate of carbon dioxide. An opposite effect is produced for the supply chain of Italy, using a power to gas system. This last is the most attractive and mature process that contributes to reduce the environmental impact, although the high costs especially in the hydrogen production section.

In addition to economic aspects, also the environmental aspect is important to design a carbon supply chain. For this reason, in Chapter IX, the best framework of Italy, Germany and the UK are reformulated as a multi-objective problem, minimizing total costs and maximizing the amount of captured carbon dioxide, simultaneously. The augmented ε-constraint method and the traditional ε-constraint method are both used to solve these problems, and the first one shows a better efficiency. Pareto fronts with trade-off conditions are obtained and two guidelines, based on the shortest distance from the Utopia point and on the minimum net total costs, respectively, are suggested to choose the operating point for a decision maker. It is found that the scenario suggested for the CCUS supply chain of Germany is closer to Utopia conditions than those suggested for the other two supply chains: a better trade-off between the two objective functions is then achieved, even if the system has the highest costs.

These supply chains are dynamic systems, then they can be described through a stochastic model. For this reason, in Chapter X the best framework for Germany, Italy and the UK are modelled through a two stage stochastic model, minimizing the expected total costs, under the uncertainties of the production costs of carbon-dioxide-based compounds, achieving the minimum target for carbon dioxide emissions reduction. It is found that the expected total costs for the carbon capture utilization and storage supply chain of Italy, Germany and the UK are respectively 77.265 billion€/year, 35.17 million€/year, 19094 €/year. A comparison with the respective deterministic model is considered through the evaluation of the expected value of perfect information and the value of stochastic solution. Results show that the uncertain production cost in the stochastic model does not have a significant effect on the results, then there are few advantages on solving the stochastic model instead of the deterministic one.

In the previous analyses about carbon supply chains, two different pipelines are considered to connect different sites, for the storage and for the utilization section, respectively. It is supposed that almost pure carbon dioxide is transported from the capture to the storage site, while the purity of carbon dioxide needed by the production processes is achieved in the specific utilization site. In order to have an unique pipeline for carbon dioxide transport, at 150 bar and purity higher than 90% molar, for both utilization and storage

sites, the mixed integer linear programming model is reformulated to this aim and applied to the German case of study, producing more products. The system is designed and optimized through the minimization of total costs. Results show that the new supply chain costs 0.104 trillion€/year, achieving the minimum target for emissions reduction at a slightly higher relative cost compared to the previous scheme.

From the previous studies considering an innovative model to design carbon capture utilization and storage supply chains and their life cycle assessment analysis, it is evident that these frameworks are valid solutions to solve the problem related to carbon dioxide undue emissions. It is important to underline that carbon dioxide can be used to produce different, useful compounds in these systems, selling of which on the market may produce an income. Also it results that in this management it is important to have a storage site as a complementary aspect of carbon dioxide utilization. Moreover, deterministic (with a single or a multiple optimization) models are able to provide a valid description of these systems.

In future works, it is recommended to analyze more complex supply chains with more storage and utilization sites, keeping the ratio between utilization and storage above a given threshold limit dictated by the need to establish a circular carbon economy. It is also interesting to develop a unique structure for Europe, where all Countries are bound to reduce their emissions in next years.

Visiting research periods

During the PhD, different visiting research periods were spent, in particular, at the Bremen University (Germany), for 1 year, and at the University College of London (UK), for six months. The research activities at the Bremen University were carried out under the supervision of Prof. Edwin Zondervan, aimed to develop mathematical models of different carbon capture, utilization and storage (CCUS) supply chains. The research activities at the University College of London, under the supervision of Prof. David Bogle, aimed to develop life cycle assessment (LCA) analyses of CCUS supply chains.

Publications

The following articles related to the PhD programme are published:

G. Leonzio, State of art and perspectives about the production of methanol, dimethyl ether and syngas by carbon dioxide hydrogenation, 2018. Journal of CO_2 utilization, 27, 326-354.

G. Leonzio, E. Zondervan, P.U. Foscolo, Methanol production by CO_2 hydrogenation: Analysis and simulation of reactor performance, 2019. International Journal of Hydrogen Energy, 44 7915-7933.

G. Leonzio, P.U. Foscolo, E. Zondervan, An outlook towards 2030: optimization and design of a CCUS supply chain in Germany, 2019. Computer and chemical engineering journal, 125 499–513.

G. Leonzio, P.U. Foscolo, E. Zondervan, Sustainable utilization and storage of carbon dioxide: analysis and design of an innovative supply chain, 2019. Computer and chemical engineering journal. 131 106569

G. Leonzio, P.U. Foscolo, D. Bogle, E. Zondervan, Scenario analysis of carbon capture, utilization (particularly producing methane and methanol) and storage (CCUS) systems, Industrial & Engineering Chemistry Research. 2020. In press

G. Leonzio, D. Bogle, P.U. Foscolo, E. Zondervan. Optimization of CCUS supply chains in the UK: a strategic role for emissions reduction, 2020. Chemical Engineering Research and Design. 155 211-228

G. Leonzio, P.U. Foscolo, Analysis of a 2-D model of a packed bed reactor for methanol production by means of CO_2 hydrogenation, 2020 International Journal of Hydrogen Energy. 45 (18) 10648-10663

Other articles are under review:

G. Leonzio, E. Zondervan, Analysis and optimization of carbon supply chain integrated by power to gas process in Italy, Journal of Cleaner Production.

Life cycle assessment analysis of a carbon capture utilization and storage supply chain in Italy and Germany: comparison between carbon dioxide storage and utilization system, Journal of Cleaner Production.

Other articles are to be submitted:

Design and analysis of CCUS supply chains for European countries under the uncertainty.

Multi-objective optimization of CCUS supply chains for the European countries with higher carbon dioxide emissions.

Contents

Chapter I

Introduction

In this chapter, a brief overview of carbon dioxide, as an important gas inside the natural carbon cycle, carbon dioxide emissions, for the world and particularly for the three higher-emitter countries in Europe, and carbon dioxide supply chains is provided, underlining the central and important environmental problem that researchers have faced, in the last decades. Climate change and global warming require urgent actions for a better living in the coming future, as underlined by many international agreements. Moreover, a literature analysis about the main topics of this work (carbon dioxide utilization, carbon supply chain modelling, life cycle assessment analysis of carbon supply chains and modelling of a methanol reactor) is presented. Then, the scope and the outline of this thesis are provided.

I.1 Carbon dioxide

Carbon dioxide (CO_2) is a colorless and odorless gas. It consists of a carbon atom bonded with a double covalent bond to two oxygen atoms. Although much less abundant than nitrogen and oxygen, CO_2 is an important gas in the Earth's atmosphere, because it is used by plants to produce water (H_2O) and light-energy carbohydrates, through photosynthesis, an important step in the natural carbon cycle, shown in figure I.1. In this natural cycle, carbon moves from the atmosphere, in the form of CO_2, to plants, from plants to animals, from plants and animals to soils, from living things like plants and animals to the atmosphere, from fossil fuels to the atmosphere (when fuels are burned), and from the atmosphere to the ocean. Then the element carbon is part of seawater, atmosphere, rocks, soils and all living things: it moves from one of these to another as a part of the carbon cycle. Recently, however, this bio-geochemical cycle has been altered due to human activities that discharge more CO_2 into the atmosphere, influencing natural sinks such as forests. This has created the so-called climate change and warming impact phenomena. In fact, in addition to water vapor (H_2O), methane (CH_4), nitrous oxide (N_2O), ozone (O_3), chlorofluorocarbons (CFCs) and hydrofluorocarbons (HCFCs), CO_2 is an important greenhouse gas (GHG): its contribution is 82% (EPA, 2019). As a GHG gas, CO_2 is able to absorb and emit infrared radiations (long waves) in the wavelength range emitted by Earth. These GHGs then trap heat near the Earth's surface, keeping it much warmer than it would otherwise be. In fact, most of solar radiation is absorbed by the Earth's surface and warms it. Some solar radiation is reflected by the Earth and the atmosphere. This is because the greenhouse gases let the sun's short wave reach the Earth. On the other hand, the Earth also emits some of the absorbed energy as infrared radiations. Some of these pass through the atmosphere. Some is absorbed and re-emitted in all directions by greenhouse molecules. The effect of this is to warm the Earth's surface and the lower atmosphere. Climate change can be defined as a significant long term (decades or longer) change of the climate, then of the weather, in the Earth, due to the higher concentration of CO_2. This can be verified by temperature, rainfall or wind in a specific area.

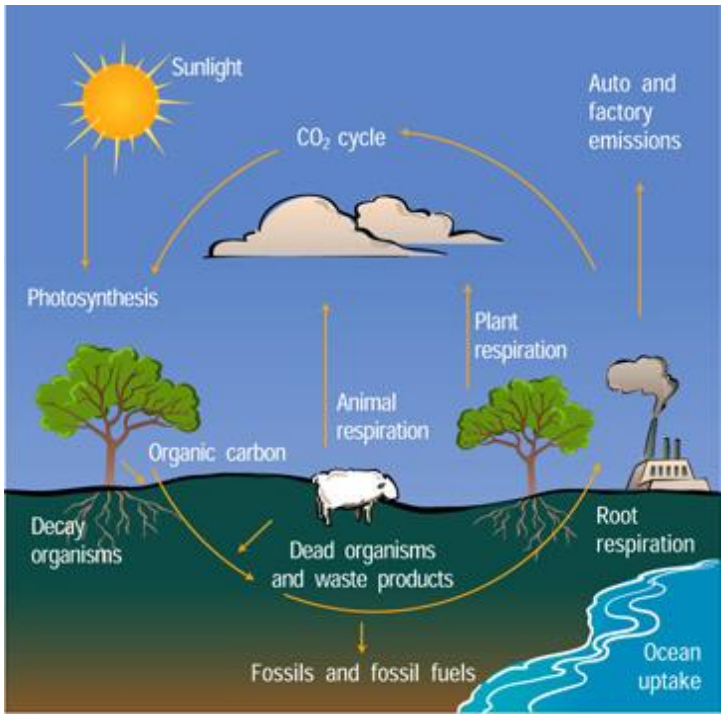

Figure I.1 Simple diagram of natural carbon cycle underling the terrestrial parts of the cycle (UCAR, 2019)

The physical and chemical properties of CO_2 are reported in table I.1 (Song, 2006).

Table I.1 Physical and chemical properties of CO_2 (Song, 2006)

Property	**Value**	
Molecular weight	44.01	g/mol
Heat of formation at 25°C	-393.5	kJ/mol
Entropy of formation at 25 °C	213.6	J/molK
Gibbs free energy of formation at 25 °C	-394.3	kJ/mol
Latent heat of vaporization at 0 °C	231.3	J/g
Sublimation point at 1 atm	-78.5	°C
Triple point at 5.1 atm	-56.5	°C
Triple point pressure	5.12	atm
Critical temperature	31.04	°C
Critical pressure	72.93	atm
Critical density	468	kg/m^3

In figure I.2, the phase diagram of CO_2 is reported, suggesting the phase of this gas for a specific temperature and pressure. Liquid CO_2 cannot exist at pressure lower than that of triple point of 5.1 atm. On the other hand, at 1 atm, solid CO_2 sublimes directly to the gas phase with a temperature of −78.5°C

(sublimation temperature). For conditions above the critical point (72.93 bar and 31.04 °C), supercritical CO_2 is present.

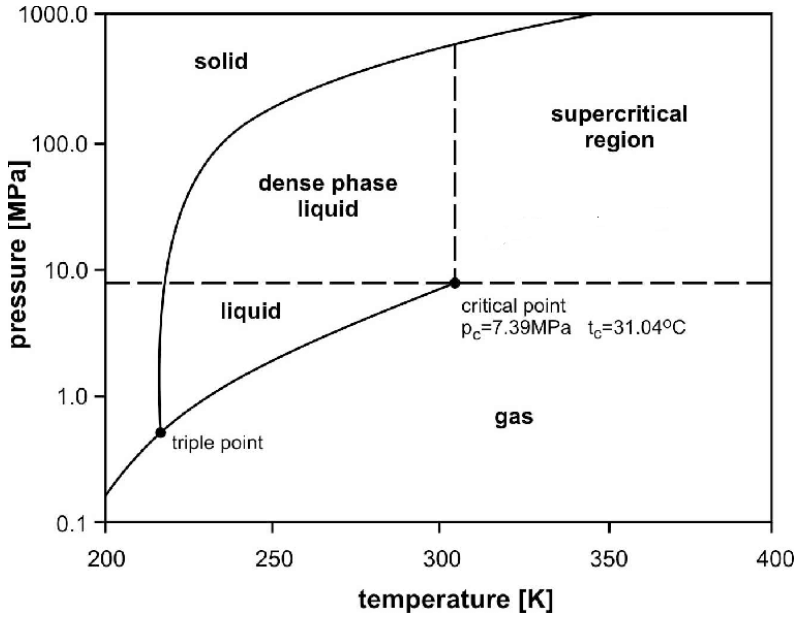

Figure I.2 Phase diagram of CO_2 (Witkowski et al., 2014)

I.2 Carbon dioxide emissions

In the last decades, the world was characterized by a rapid industrialization and urbanization. The World Bank (2017) reported that the gross domestic product (GDP) has increased from $37224 billion US in 1990 to $72247 billion US in 2014, with an average annual growth rate of 2.7%. On the other hand, the global population size has increased from 5.3 billion in 1990 to 7.3 billion in 2014, with an average annual growth rate of 1.3% (World Bank, 2017). These growths have led to a rapid increase of global energy consumption: from 8133 million tonnes of oil equivalent (Mtoe) in 1990 to 12928 Mtoe in 2014 (BP, 2017). As a consequence, carbon dioxide emissions have increased over last few years, generating the so called global warming and climate change phenomena, due to its heat–trapping property. Since the industrial revolution, the average global temperature has increased by about 1 °C and is currently rising by about 0.2 °C per decade (Allen et al., 2018). In the extreme scenario, it can increase up to 4.8 °C (Stocker et al., 2013).

In 2018, CO_2 concentration was about 400 parts per million (ppm) (it increased 2-3 ppm/yr), the highest level over the last years (NOAA, 2019), while CO_2 emissions in 2017 were about 36.2 billion tonnes (Le Quéré et al., 2018).China is the world's largest CO_2 emitter, accounting for more than one-quarter of emissions. This is followed by the USA (15%), EU-28 (10%), India (7%) and Russia (5%), as shown in figure I.3.

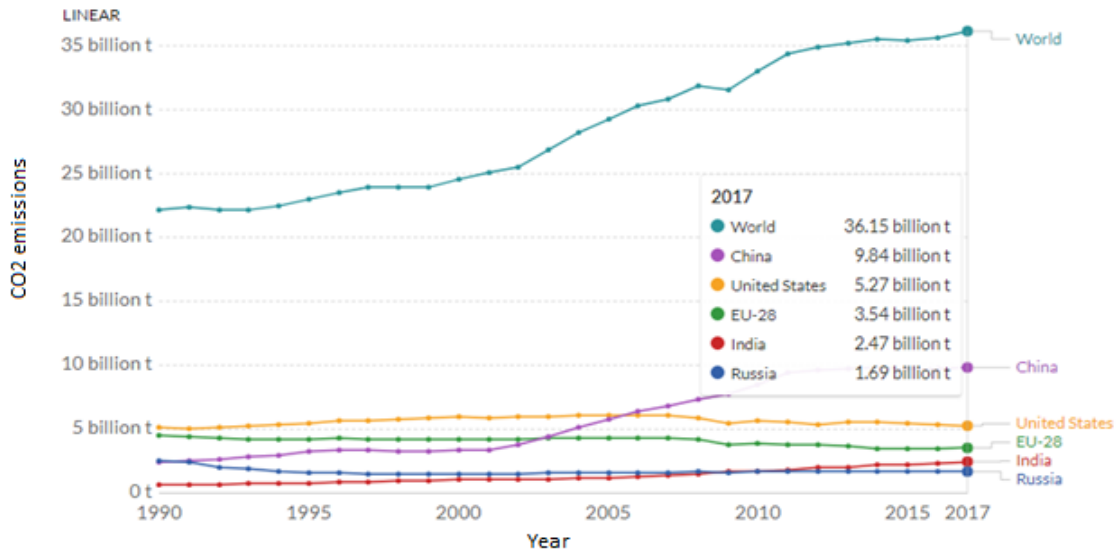

Figure I.3 Trend of carbon dioxide emissions for the world and the most emitter countries (Le Quéré et al., 2018)

As illustrated in figure I.4, globally about half of CO_2 emissions are related to energy production (electricity and heat production), while transport and manufacturing industries both contributed to about 20%, residential, commercial and public services contributed to about 9%, with other sectors contributing to about 1-2% (IEA, 2014).

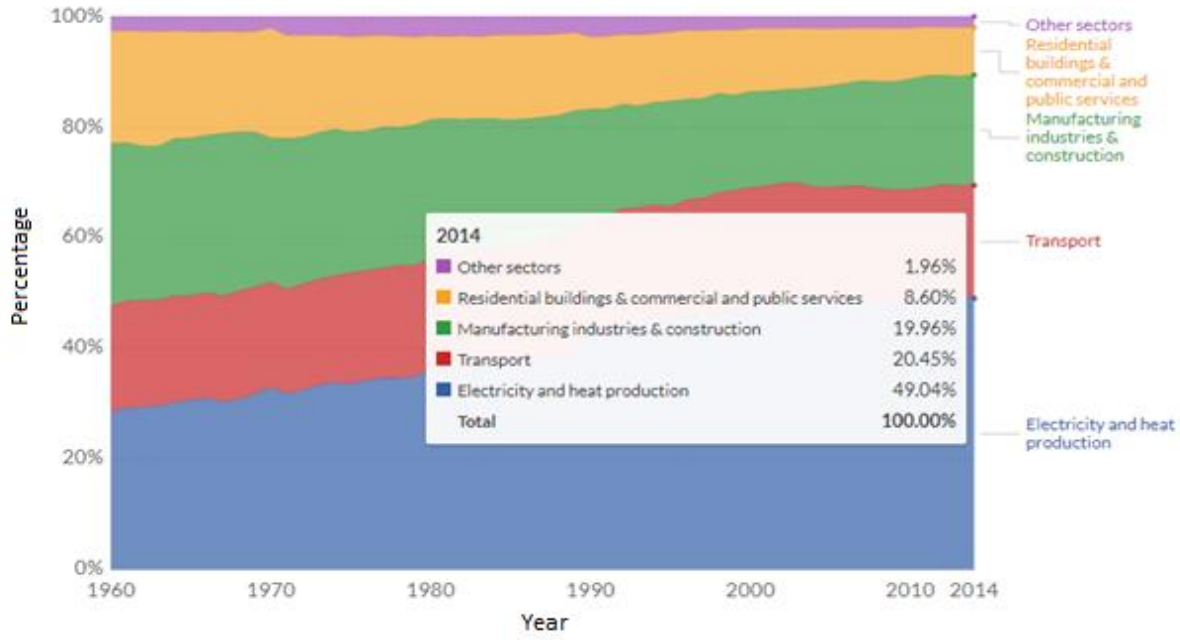

Figure I.4 Global CO_2 emissions by sector (IEA, 2014)

To solve this environmental problem, different international agreements were reached. The recent and the most important one is the 21st Conference of the Parties (COP21) of the United Nations Framework Convention on Climate Change (UNFCCC), held in Paris on the 12th of December 2015 (and therefore referred to as the Paris Agreement) and entered into force on the 4th November 2016. The most important established goals are the following (United Nation, 2015):

(a) "*Holding the increase in the global average temperature to well below 2 °C (…) and to pursue efforts to limit the temperature increase to 1.5 °C above pre-industrial levels*";

(b) "*Increasing the ability to adapt (…) and foster climate resilience and low greenhouse gas emissions development*";

(c) "*Making finance flows consistent with a pathway towards low GHG emissions and climate resilient development*".

In respect of this, each signed country defined their own national determined contribution (NDC). This agreement was also signed by the European Union (EU), where Germany, the United Kingdom and Italy had higher CO_2 emissions, respectively of 720 Mton, 420 Mton 320 Mton in 2014, as shown in figure I.5 (World Bank, 2019).

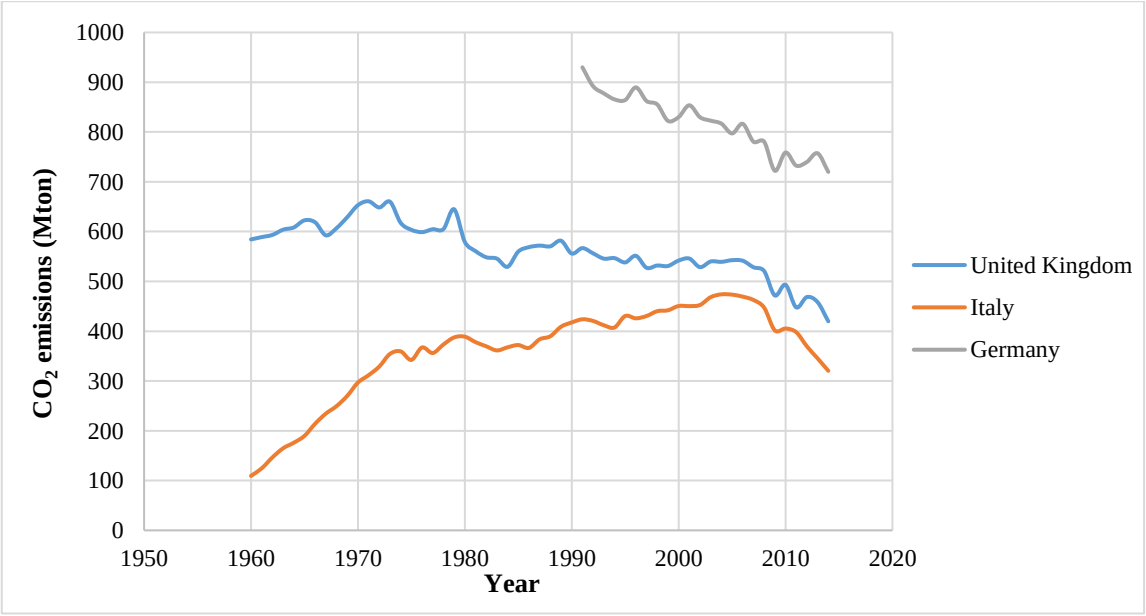

Figure I.5 Trend of CO_2 emissions for Germany, the United Kingdom and Italy (World Bank, 2019)

The EU's national determined contribution (NDC) under the Paris Agreement is to reduce GHG emissions by at least 40%, increase the use of renewable energy by 32%, and improve the energy efficiency by 32.5% by 2030, compared to the level of 1990 (European Commission, 2019). Overall, this strategy aims at creating a low-carbon economy and a more efficient and sustainable energy system.

The previous environmental European strategy was the Europe 2020, valid for the decade 2010-2020, and includes the so called 20/20/20 targets: 20% reduction of greenhouse gas emissions by 2020, 20% increase of renewable share in primary energy sources, 20% increase of efficiency in energy utilization, compared to 1990 levels (European Commission, 2011).

I.3 Carbon dioxide storage, utilization and carbon supply chain

In order to reduce CO_2 emissions and solve this environmental problem, CO_2 can either be stored or used. There are different options of using it, as shown in figure I.6. CO_2 can be used as a feedstock and then valorized for direct utilization (e.g. in food industry, power generation, oil and gas recovery, wastewater treatment, solvents for pharma, fire extinguishers, etc.), biological conversion (e.g. for biological methanation or in horticulture), chemical conversion (e.g. to produce polymers, valuable chemicals, fuels and commodities) and mineralization (e.g. to produce concrete and carbonates). Actually, CO_2 is mainly used for urea, carbonate and methanol production (Aresta et al., 2013). In 2016, global CO_2 utilization was about 300 Mton, while it is expected to be of 1.5-2 Gton/year in the long term (actually, two orders of magnitude and in the long term one order of magnitude lower than the current global emissions) (von der Assen et al., 2016). It is important to increase the social acceptance of CO_2 utilization, which is actually very low (Jones et al., 2017).

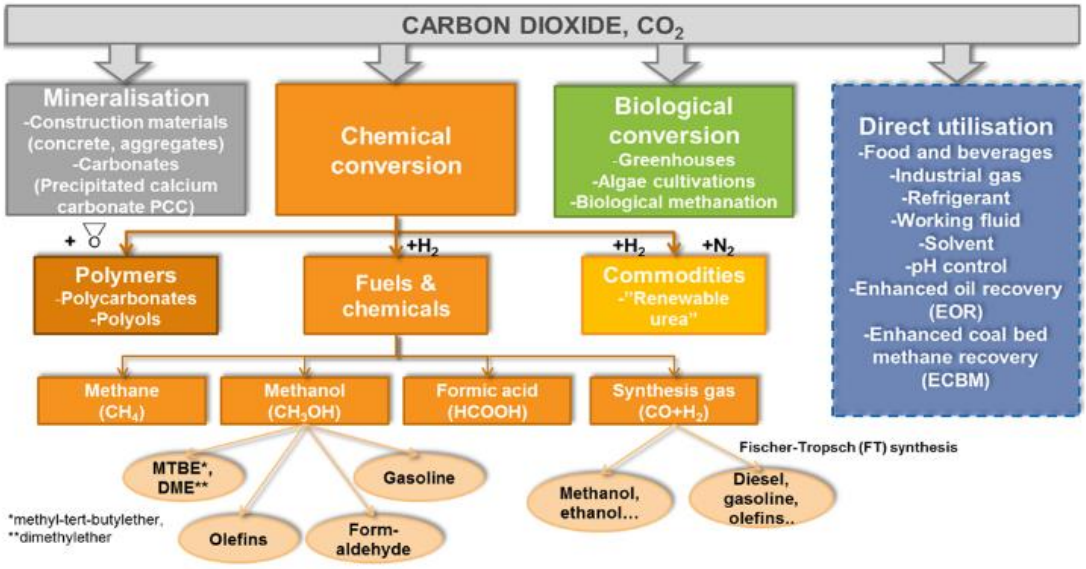

Figure I.6 Utilization routes of CO_2 (BioCO2, 2019)

CO_2 can be stored in geological formations or in the oceans' water (Ajayi et al., 2019). Geological sequestration is the most commonly used technology, where CO_2 is injected into depleted oil and gas reservoirs, deep saline aquifers or unexploitable coal beds. Saline aquifers as porous and permeable reservoir rocks that contain saline fluid in the pore spaces between the rock grains and are characterized by a huge storage capacity (Grobe et al., 2009). Oil and gas reservoirs are fields that produced oil and gas in the past, but now are considered uneconomical for further production of hydrocarbons. In the unminable coal beds, CO_2 is used for the recovery of methane from the coal bed during the enhanced coal bed methane recovery process: the injected CO_2 is trapped being adsorbed on the surface of the coal, while CH_4 is released and produced.

To have a good sequestration, CO_2 should be injected in a supercritical phase (it has the properties of a liquid but flows as a gas): it has a higher density than the gaseous phase, reducing then the buoyancy differential between CO_2 and in situ fluids and requiring a storage volume much lower than that required by the same gas at atmospheric conditions. There are four mechanisms to trap CO_2 in the subsurface: physical trapping (structural trapping, residual or capillary trapping, sorption trapping), maintaining its physical nature, and geochemical trapping (solubility trapping and mineral trapping), changing its physical and chemical nature (Ajayi et al., 2019). CO_2 is trapped via physical trapping for a period lower than 100 years, while a long term storage is ensured with geochemical trapping (Juanes et al., 2006). In structural trapping, the injected supercritical CO_2 migrates upward through the porous and permeable rock as a result of the buoyancy effect created by its density difference compared to other reservoir fluids and laterally via preferential pathways until a cap rock, fault or other sealed discontinuity is reached. In residual trapping, CO_2 flows among the rock grains, displacing the existing fluid. However, a small portion of this gas can be left behind as disconnected, residual or droplets in the pore spaces. In solubility trapping, CO2 dissolves in the brine that is present in the pore spaces within the rock. Weak carbonic acid is produced that is decomposed into H^+ and HCO_3^- ions. In mineral trapping, CO_2 reacts with solid minerals in the rocks to produce calcite.

Ocean sequestration has the highest potential for CO_2 capture, estimated at 40000 Gton of CO_2 (Lal, 2008). In this case, CO_2 is injected and deposited into the sea water at a depth below 1 km by using moving ships, fixed pipelines or offshore platforms. At this depth, water has a lower density than the injected CO_2 then the last dissolves and disperses into the water body (Metz et al. 2005). However, there are problems of acidity for the marine life near the injection point. This technology is still at the research stage, without any pilot tests (Ajayi et al., 2019).

CO_2 utilization and storage are two important elements of a carbon supply chain system. It is possible to have a carbon capture and storage (CCS) supply chain, a carbon capture and utilization (CCU) supply chain and a carbon capture, utilization and storage (CCUS) supply chain. In a CCS supply chain, carbon dioxide is captured, transported and sent to the storage site. In a CCU supply chain, carbon dioxide is captured, transported and sent to the utilization section, while in a CCUS supply chain carbon dioxide is captured,

transported and sent to the storage and utilization sections. The conceptual schemes of these different supply chains are shown in figure I.7.

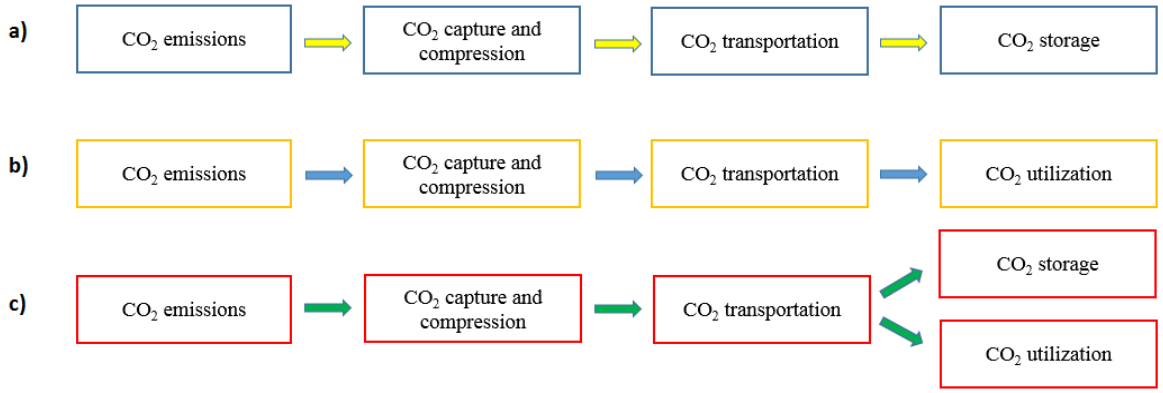

Figure I.7 Conceptual scheme of a) CCS supply chain, b) CCU supply chain, c) CCUS supply chain (Leonzio et al., 2020).

CO_2 is generally transported via pipeline, as the most mature technology to transport a huge amount of CO_2 at low costs (Kalyanarengan Ravi et al., 2017). However, CO_2 can be transported also by truck and rail (for small quantities) or by ship (Global CCS Institute, 2019). Generally, pipelines are made of carbon steel (Leung et al., 2014).

Regarding the CO_2 capture process, different technologies may be used: absorption, adsorption, membrane, chemical looping combustion, cryogenic technology, and hybrid technology (Song et al., 2018).

The absorption can be chemical or physical. Solvents like Rectisol, Selexol and Purisol are used for physical absorption, however chemical absorption is preferred due to its higher absorption capacity at low CO_2 partial pressure (Leonzio, 2018). Chemical solutions for absorption such as Monoethanolamine (MEA), Diethanol amine (DEA), Nmethyldiethanolamine (MDEA) and Di-2-propanolamine (DIPA) are generally used (Mamun et al., 2007). Diglycolamine (DGA), 2-(2-aminoethylamino) Ethanol (AEE), 2-amino 2-methyl 1-propanol (AMP), N-2-aminoethyl 1,3-propanediamine (AEPDNH2), Triethanol amine (TEA), Triethylene tetra amine (TETA), Piperazine (PZ), Glucosamine (GA), NaOH, NH_3, K_2CO_3, KOH, Na_2CO_3, etc. are absorbent solutions that can be used, however with some limitations for application in industrial plants at large scale, for degradation, corrosion, high energy for regeneration, environmental impact. In recent years, ionic liquids (ILs) (salts that are liquid at a low temperature) have received the attention by the research community due to their better properties, compared to traditional solvents: low volatility, environmentally friendly, non-corrosive, high thermal and electrochemical stability, excellent chemical tunabilities. These ensure a lower energy for regeneration, lower losses of solvent, even if the high costs

and the recovery is not easy (Leonzio, 2018; Wappel et al., 2010). Actually, absorption is the most mature process to capture CO_2 (Leung et al., 2014).

In the adsorption system, two or three adsorption chambers are present: the first receives the feed for CO_2 adsorption, the second for its desorption, while the last is in stand-by for the first one (Thiruvenkatachari et al., 2009). The system operates continuously, changing pressure in PSA (pressure swing adsorption) and VPSA (vacuum pressure swing adsorption) systems, temperature in TSA (temperature swing adsorption) systems or voltage electric current in electrical swing adsorption (ESA) systems. It is possible to combine pressure swing adsorption and temperature swing adsorption in PTSA systems (pressure and temperature swing adsorption) that could reduce power consumption by 11% with respect to a pressure swing adsorption system (Gupta, 2003). In addition to liquid sorbents, characterized by corrosion, solid sorbents have been studied to recover CO_2 and are divided at low temperatures (< 200 °C), intermediate temperatures (200-400 °C) and high temperatures (> 400 °C) (Wang et al., 2014; Li et al., 2010) Solid amine-based adsorbents, carbon–based sorbents, graphite/graphene-based adsorbents, zeolite-based adsorbents, metal–organic-based sorbents, silica-based adsorbents, polymer-based adsorbents, clay-based adsorbents, alkali metal carbonate-based adsorbents, immobilized ionic liquid-based adsorbents are used at low temperatures.

LDH-based sorbents and MgO-based sorbents are used at intermediate temperatures. CaO-based sorbents, alkali zirconate-based sorbents and alkali silicate-based sorbents are used at high temperatures.

In an adsorption process, no wastewaters are produced and low energy is required, even if there are some disadvantages due to the low selectivity for CO_2 and regeneration and reusability of adsorbents (Mondal et al., 2012).

With regard to the adsorption process it is interesting to consider processes where CO_2 is captured in the reaction environment. One of these is the sorption enhanced steam methane reforming (SESMR) which is able to produce H_2 by a more environmental friendly exploitation of natural gas and at a lower temperature and pressure than the conventional steam methane reforming method (Aloisi et al., 2017; Di Giuliano and Gallucci, 2018). In this case, bi-functional catalyst-sorbent materials are taken into account, containing both CaO sorbent grains to capture CO_2 and nickel catalytic sites to promote the reaction (Di Giuliano et al., 2018a; Di Giuliano, 2019). CaO is usually the first choice because of its high sorption capacity and rate of carbonation reaction with CO_2 (Di Giuliano et al., 2018b).

Membranes could be classified into three types based on the method employed: non-dispersive contact via micro-porous membranes, gas permeation through dense membranes, and through supported liquid membranes (Sreedhar et al., 2017). The first type has a better mass transfer compared to the other types, while dense membranes can be divided in ceramic and polymeric. Ceramic membranes have higher thermal, mechanical and chemical stability than the polymeric types. The mechanical stability of polymeric membranes is increased by using an appropriate support, while inserted inorganic materials increase the thermal stability of the system. In supported liquid membranes (SLM), also called immobilized liquid membranes, liquid is supported on the surface of a solid or could be filled inside the pores. The transport

mechanism is solution-diffusion type. Although SLMs are not commercialized at an industrial scale, promising results have been reported in the lab scale (Cheng et al., 2014). Some commonly used solvents in SLMs include primary amines such as monoethanolamine (MEA), 2-amino-2-methyl-1-proponol (AMP), secondary amines such as diethanolamine (DEA) and tertiary amines such as methyl diethanolamine (MDEA), aqueous ammonia (Yeh et al. 2005), Selexol, Rectisol (White et al., 2003) and fluorinated solvents (Kenarsari et al., 2013). Generally, in membrane technology, where no regeneration energy is required, simple modular systems are used and waste streams are not produced, and even if can be plugged by impurities in the gas stream. Actually, the process is still under development and it is not applicable on a large scale.

In chemical looping combustion for carbon capture system, combustion is divided in two steps: oxidation and reduction reaction by using oxygen (in the form of solid metal oxides such as Fe_2O_3, NiO, CuO, Mn_2O_3 called solid oxygen carrier), moving between the two separated phases, with two fluidized bed reactors, one for air and one for fuel (Song et al., 2019). In the first reactor, metal oxides are oxidized by the oxygen of air. In the second reactor, metal oxides are reduced by fuel, which is oxidized to CO_2 and H_2O. CO_2 is then separated from H_2O and then captured by condensation. NO_x formations are minimized, because combustion is carried out in the absence of N_2 with an oxygen carrier that is re-oxidized in the air reactor at lower temperature. Energy penalties are reduced, then lower operating costs are involved. However, there are only a few large-scale plants using this process (most of them are at lab scale), also with some problems, such as the low stability of oxygen carrier, the slow reaction rate of redox reaction and the removal of sulfur by fuel to avoid poisoning problems (Solunke and Veser, 2011).

The cryogenic separation is based on the phase change of CO_2 to separate it from exhaust or process gases. In particular, CO_2 is cooled to about -140 °C, so that it is de-sublimated, passing from a gas to a solid phase. The CO_2 solid is separated from the remaining gas, pressurized and melted, while the other gases are released into the atmosphere. However, the cryogenic separation is an energy intensive process compared to other technologies, due to the high amount of energy required for gas cooling and compression (Shafiee et al., 2017). Also, the phase behavior of CO_2 is complex and it easily leads to the formation of solids which plug equipment and severely reduce heat transfer rates resulting in the reduction of process efficiency (Mondal et al., 2012). On the other hand, chemical solvents are not required. Researches have been limited only to specific situations, including high pressure feed streams such as natural gas treatment (Hart, 2009), CO_2/O_2 combustion cycles (Meratla, 1997) and concentrated CO_2 mixtures (Zanganeh et al., 2009). According to the used cold energy source, this technology is classified in packed bed, AnSU, CryoCell, distillation, stirling cooler if liquid nitrogen gas, liquefied natural gas, chiller, compressor and cooler, stirling cooler are respectively used to cool a CO_2 stream (Song et al., 2019).

Hybrid capture technologies are developed by the combination of two or more technologies, in order to overcome their limitations and disadvantages, ensuring then higher efficiencies. These hybrid technologies are classified in absorption-based, adsorption-based, membrane-based and cryogenic-based hybrid

processes and can be combined in series, parallel or simply integrated (Song et al., 2018). This strategy mostly combines a first step of CO_2 pre-concentration using membrane unit separation with a second step of CO_2 concentration and compression, as in Figure I.8.

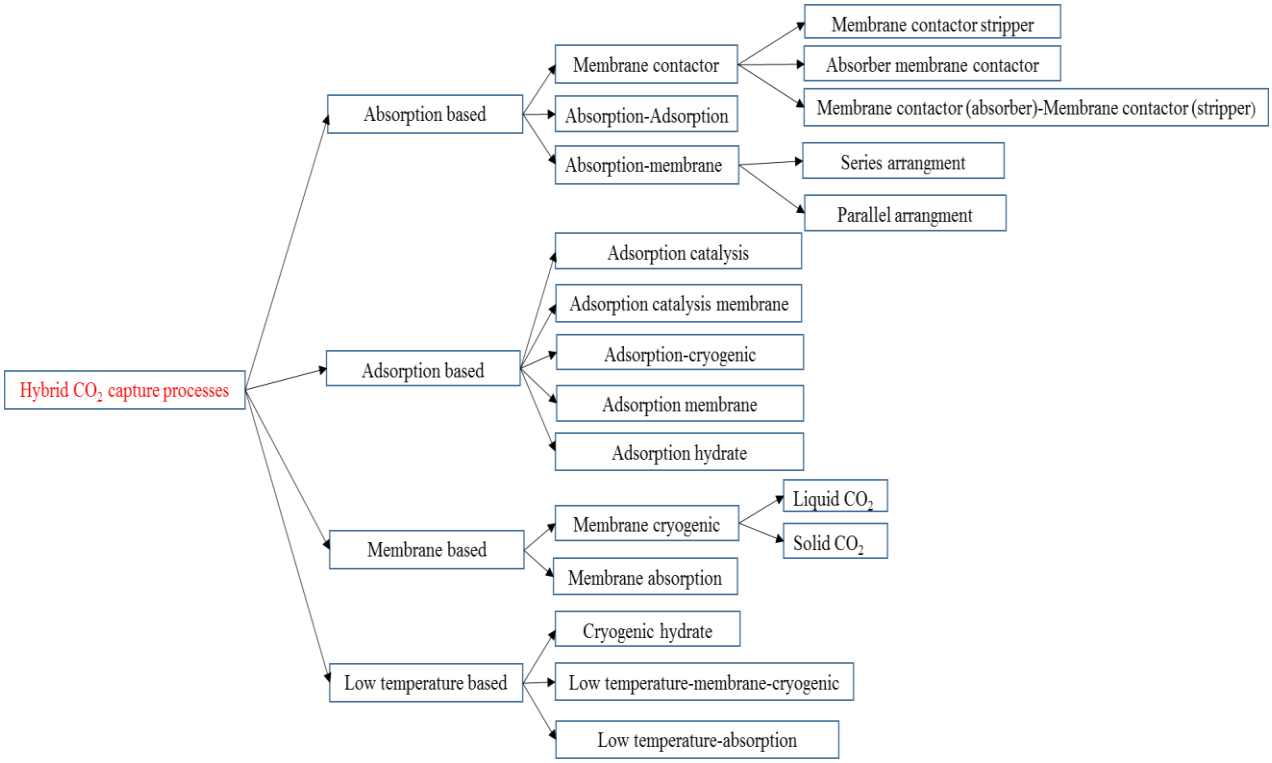

Figure I.8 Existing hybrid CO_2 capture processes: absorption based, adsorption based, membrane based and low temperature based (Song et al., 2018)

Another innovative technology to separate CO_2 is the molten carbon fuel cells (MCFC), an attractive technology for CO_2 separation and electricity production, as shown in Figure I.9 (Leonzio, 2018). It is a high-temperature cell, operating at around 650 °C and its electrolyte is a mixture of alkali metal carbonates that are solid at room temperature but liquid at the cell operating temperature. This cell can reach efficiencies of around 60%. At the anode, hydrogen is oxidized by carbonate ions and CO_2 and water are produced with two electrons (see Eq. I.1), while at the cathode, oxygen is reduced with CO_2 to produce carbonate ions (see Eq. I.2). In this way, CO_2 is separated by the cathode and concentrated in the anode through the cell reaction. Overall, natural gas can be used to fuel this cell.

$$H_2 + {CO_3}^{2-} \rightarrow H_2O + CO_2 + 2e^- \qquad (I.1)$$

$$\frac{1}{2}O_2 + CO_2 + 2e^- \rightarrow {CO_3}^{2-} \qquad (I.2)$$

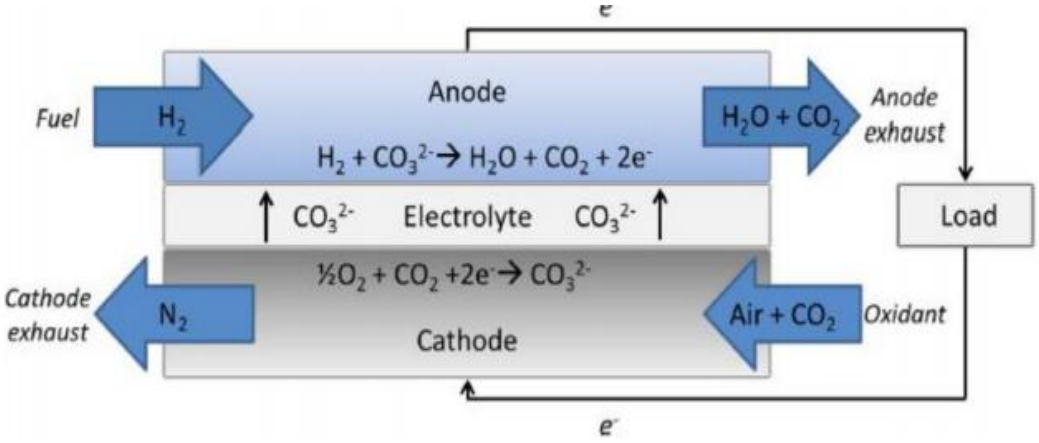

Figure I.9 The working principle of the MCFC (Leonzio, 2018)

In addition to MCFC, solid oxide fuel cell (SOFC) can be used to capture CO_2, because a stream with a high CO_2 content is formed at the anode (Haines et al., 2002). These systems work at very high temperatures, the highest among all types of fuel cells, from 800 ºC to 1000 °C, and can have efficiencies of over 60% when converting fuel (H_2, CH_4 or syngas) to electricity. The reactions that are involved at the anode, cathode and anode/interface respectively are the following (see Eqs. I.3 and I.5) (Garrison, 2019):

$$CO + H_2O \rightarrow CO_2 + H_2 \quad (I.3)$$

$$O_2 + 4e^- \rightarrow 2O^{2-} \quad (I.4)$$

$$O^{2-} + H_2 \rightarrow H_2O + 2e^- \quad (I.5)$$

CO_2 is produced, then can be captured. Air flows from the cathode (also called the "air electrode"). When an oxygen molecule contacts the cathode/electrolyte interface, it catalytically acquires four electrons from the cathode and splits into two oxygen ions (see Eq. I.4). The oxygen ions diffuse into the electrolyte material and migrate to the other side of the cell where they encounter the anode (also called the "fuel electrode"). The oxygen ions encounter the fuel at the anode/electrolyte interface and react catalytically, producing H_2O, CO_2, heat, and most importantly for the electric cycle, two electrons (see Eqs. I.3 and I.5). The electron transport takes place through the anode to the external circuit and back to the cathode, providing a source of useful electrical energy in an external circuit. A schematic representation of SOFC is illustrated in Figure I.10 (Garrison, 2019).

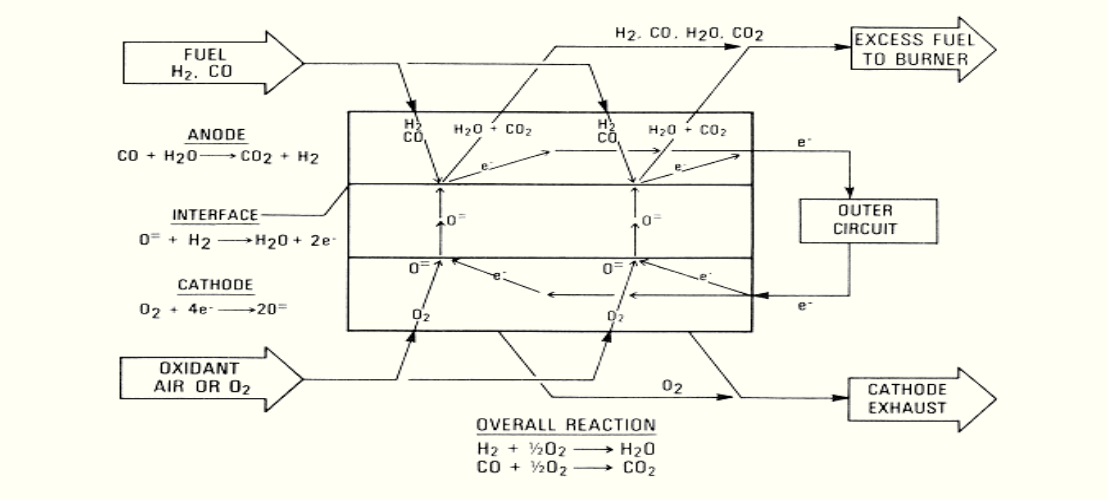

Figure I.10 The working principle of the SOFC (Garrison, 2019)

A comparison between the main capture technologies (absorption, adsorption, membrane and cryogenic) is shown in table I.2.

Table I.2 Comparative analysis of different technologies (Mondal et al., 2012)

Parameter	Absorption	Adsorption	Membrane	Cryogenic
Operating flexibility	Moderate	Moderate	High (CO_2>20%) Low (CO_2<20%)	Low
Response to variation	Rapid (5-15 min)	-	Istantaneous	Slow
Start-up after the variation	1 h	-	Extremely short (10 min)	8-24 h
Turndown	Down to 30%		Down to 10%	Down to 50%
Reliability	Moderate	Moderate	100%	Limited
Control requirements	High	High	Low	High
Ease of expansion	Moderate	Moderate	Very high	Very low
Energy requirements	4-6MJ/kgCO_2	2-3 MJ/kgCO_2	0.5-6 MJ/kgCO_2	6-10 MJ/kgCO_2
CO_2 recovery	90-98%	80-95%	80-90%	>95%

I.4 Literature analysis

I.4.1 Carbon dioxide utilization pathways

CO_2, being a waste emission, can be valorized as a feedstock and used in different pathways, according to the principles of circular economy. Another important aspect, is the fact that CO_2, through its utilization is an important molecule that can help the introduction of renewable energy resources into the chemical and

energy chains (Ampelli et al., 2015). Then, CO_2 utilization has an important role for suitable chemical, energy and process industries, for resource and energy efficient development. In the literature, there are different pathways for CO_2 utilization, that have been investigated and discussed (Hepburn et al., 2019):

- *Chemicals*
- *Fuels*
- *Concrete building materials*
- *Mineral carbonation*
- *Oil and methane recovery*
- *Horticulture and algae production*
- *Direct use*

Each pathway is characterized by a defined potential development, economic perspective, use of energy and amount of CO_2, time of sequestration, and environmental impact (Ampelli et al., 2015). These aspects are also enclosed in the definition of technology readiness level (TRL), shown for the most important CO_2-based compounds in figure I.11, for which the timeframe of deployment has been assigned with a detailed literature analysis (Chauvy et al., 2019). The meaning of different TRL values is shown in table I.3.

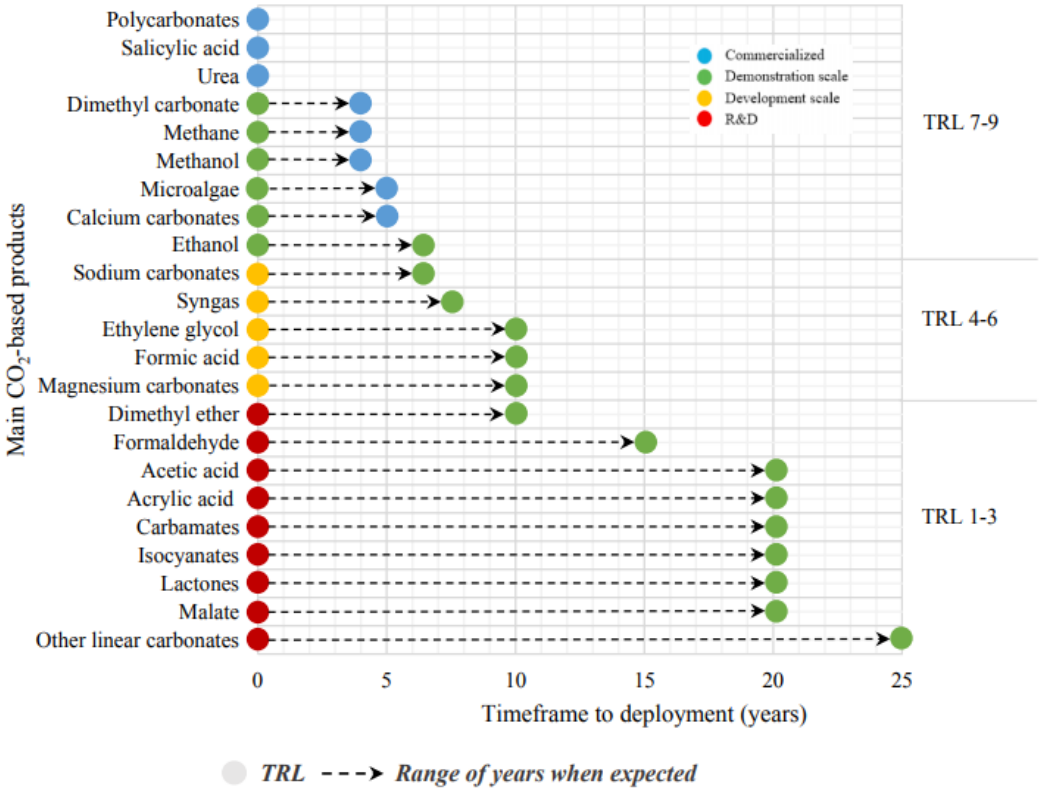

Figure I.11 TRL for main CO_2-based products (Chauvy et al., 2019)

Table I.3 TRL scale for CCU evaluation (Chauvy et al., 2019)

TRL	Description	
1	Research and development	Published research that identifies the principles that underlie the technology
2	Basic technology research	Publications or other references that outline the application being considered, and that provide analysis to support the concept
3	Research to prove feasibility	Active research and development has been initiated
4	Development scale	Determination if individual components work together as a system
5	Technology development	The basic technological components are integrated so that the system configuration is similar to the final application in almost all respects
6	Technology demonstration	True engineering development of the technology as an operational system
7	Demonstration scale	Actual system prototype
8	System commissioning	The technology has been proven to work in its final form and under expected conditions
9	System operations	The technology is in its final form and operates under the full range of operating mission conditions

I.4.1.1 Chemicals

It consists on the catalytic chemical conversion of CO_2 into chemical products, such as urea (Perez- Fortes et al., 2014) and polycarbonate polyols (Langanke et al., 2014) for polymer production (polyurethane). Urea is produced from ammonia (NH_3), obtained by Haber-Bosch process, and CO_2, according to the following reaction (see Eqs. I.6-I.7):

$$2 \cdot NH_3 + CO_2 \leftrightarrow NH_2CO_2NH_4 \qquad \Delta H = 157.5\ kJ/mol \qquad (I.6)$$

$$NH_2CO_2NH_4 \leftrightarrow NH_2CONH_2 + H_2O \qquad \Delta H = -26.44\ kJ/mol \qquad (I.7)$$

with ammonium carbamate as intermediate step. It is non-toxic and can be used as fertilizer or for polymer synthesis (melamine and ureaformaldehyde resins) (Mikulčić et al., 2019). Actually, urea production is the largest-scale process for CO_2 utilization: 140 $MtCO_2$/year are used to produce 200 Mt/year of urea (Jarvis and Samsatli, 2018). For this route, the value of TRL is of 9 (Chauvy et al., 2019).

Polyols (usually polyether and polyester) are a petroleum derived product and it catalytically reacts with isocyanate to produce polyurethane (Garcia Ramos et al., 2016). However, polyether carbonate polyols can be produced in a more environmental way with the reaction of CO_2 and epoxides (alkylene oxide) (Artzet al., 2018; Mullet et al., 2016). Actually, the company Bayer (Covestro) is focusing on the production of polyols for polyurethane and the value of TRL is 8-9 (Fernández-Dacosta et al., 2017; Chauvy et al., 2019). The mechanical properties of polyurethane are comparable with one obtained through a traditional way. Other commercialized products from CO_2 are polycarbonate and Salicylic acid. At research stage there are other chemicals, such as carboxylic acids (acetic acid), carbamates (linear and cyclic), formaldehyde,

isocyanates, etc. In this pathway, the expected storage time of CO_2 depends on the produced chemical (days/decades), while the likelihood of release during storage is high (Hepburn et al., 2019).

I.4.1.2 Fuels

In this case, a catalytic hydrogenation reaction is applied to convert CO_2 into fuels (methane, methanol, ethanol, dimethyl ether, syngas, hydrocarbons, etc.). Methanol, methane and syngas are the most important products. In fact, methanol, among fuel liquids, while methane, among gas fuels, have the highest value of EXc, as the carbon fuel exergy content per mole of carbon. The exergy of a fuel refers to the maximum reversible work that can be generated from it. Thus, choosing fuels with higher value of EX_C reduces the carbon demand for storing a unit of exergy. Al-musleh et al. (2014) suggest that the value of EXc for methanol and methane is respectively of 693 MJ/kmol C and 806 MJ/kmol C.

Syngas is suggested because can be used to produce different fuels (hydrocarbons, methanol, dimethyl ether). However, methanol is preferred over methane for different reasons: the higher maturity of the technology, the liquid phase that is easy to store and transport, versatility to transform in other chemicals (a gas in comparison with a liquid has many constraints in terms of storage, distribution and use), the production process made of a reduced number of steps and a simpler separation (Ampelli et al., 2015). In addition, methanol synthesis is more efficient, because takes place at milder conditions and requires less hydrogen (H_2).

Methanol is an important primary raw material for the energy and chemical industries, due to its wide applications ranging from energy uses (e.g., as a fuel by itself, or to be blended with gasoline) to chemical uses (e.g., as a solvent, or to be converted to formaldehyde, acetic acid, methyl methacrylate, dimethyl terephthalate, methylamines, chloromethane, dimethyl carbonate and methyl tertiary butyl ether, dimethyl ether, etc.) (Bertau et al., 2014). It can also be transformed to ethylene and propylene via methanol-to-olefin (MTO) processes (Speybroeck et al., 2014). The conventional raw material for methanol production is syngas, obtained by steam reforming or partial oxidation of natural gas or by biomass gasification, according to the following reactions (Graaf et al., 1988a) (see Eqs. I.8-I.10):

$$CO + 2 \cdot H_2 \leftrightarrow CH_3OH \qquad \Delta H = -90.8\ kJ/mol \qquad (I.8)$$

$$CO_2 + H_2 \leftrightarrow CO + H_2O \qquad \Delta H = 41.6\ kJ/mol \qquad (I.9)$$

$$CO_2 + 3 \cdot H_2 \leftrightarrow CH_3OH + H_2O \qquad \Delta H = -49.2\ kJ/mol \qquad (I.10)$$

However, when methanol is produced via CO_2 hydrogenation (with a stoichiometric H_2/CO_2 ratio of 3), only the independent reactions I.10 and I.9 are considered (see Eq. I.5-I.6) (Leonzio, 2018).

H_2 can be produced from renewable energy via water electrolysis, can be obtained by coke oven gas, chlorine alkali plant or from the conventional way like syngas, methane steam reforming and petrochemical plants. In addition to the hydrogenation reaction, the co-electrolysis of CO_2 and H_2O and the electro-catalytic reduction of CO_2 are investigated to produce methanol, as reported in table I.4.

Table I.4 Analysis of the open literature for methanol production

Hydrogenation of syngas	**Type of reactor**	**Pressure (bar)**	**Temperature (K)**	**Catalyst**	**Methanol production**	
Luu et al. (2016)	Packed bed	50-100	503-538	$Cu/ZnO/Al_2O_3$	776 ton/h	
Zhang et al. (2017)	Packed bed	80	523	Cu		
Zhang et al. (2017)	Packed bed	80	523	Cu	83.54 kmol/h	
Storch et al. (2016)		100	525-538			
Gai et al. (2016)		40	483		5.6 kmol/day	
Martin and Grossmann (2016)		50-100	473-573		207 Mgal/year	
Iaquaniello et al. (2017)			493		105000 t/year	
Specht et al. (1999)					2.2 t/h	
Co-electrolysis of CO_2 and H_2O	**Type of reactor**	**Pressure (bar)**	**Temperature (K)**	**Catalyst**	**Methanol production**	**Type of electrolysis**
Al-Kalbani et al. (2016)	Packed bed		538-131		1500 ton/day	SOEC
Rivera-Tinoco et al. (2016)	Packed bed	80	533	$Cu/ZnO/Al_2O_3$		PEM/SOEC
Hydrogenation of CO_2	**Type of reactor**	**Pressure (bar)**	**Temperature (K)**	**Catalyst**	**Methanol production**	**Hydrogen source**
Kiss et al. (2016)	Packed bed	50-100	473-573	Cu/Zn/Al/Zr	100 kt/year	Chlor-alkali
Atsonios et al. (2016)	Membrane reactor	65	523	Cu-Zn-Al	94.38 ton/year	KOH water electrolysis
Peres Fortes et al. (2016)	Packed bed	76	483	$Cu/ZnO/Al_2O_3$		PEM
Bellotti et al. (2016)		50-100	523-573	$Cu/ZnO/Al_2O_3$	97 kg/h	PEM
Harp et al. (2015)		50-100	523	Zn	452 t/day	Steelwork
Electrocatalytic reactor	**Type reactor**	**Pressure (bar)**	**Temperature (K)**	**Catalyst**	**Methanol production**	
Gai et al. (2016)		80	403		5.6 kmol/day	

The TRL value for hydrogenation reaction is of 8-9 (the "George Olah" plant in Iceland is close to a commercial plant), while other routes are at research and development scale (TRL of 1-3) (Chauvy et al., 2019). Chauvy et al. (2019) suggest an interesting SWOT analysis about strengths, weaknesses, opportunities and threats for the hydrogenation reaction of CO_2 to methanol. Strengths for methanol production via CO_2 hydrogenation are the following: a big market, it is a raw material for synthetic hydrocarbons and it is a liquid under ambient conditions, so that it is easy to handle. Weaknesses for this route are, instead, the following: the use of hydrogen that should be produced by renewable energies increasing the cost, the lack of a suitable catalyst, it is toxic and flammable so that, it must be handled properly. On the other hand, opportunities are: a methanol based economy replacing fossil fuels as a storage of energy, fuel and raw materials for synthetic hydrocarbons, the increase of consumption due to the emerging application technologies. Threats are the following: the evolution of CO_2 and H_2 price, the possibility to have "catastrophic" events in all phases of the methanol value chain and the bio-methanol produced from other feedstocks. Different reactors can be used for the production of methanol. For a gas phase technology, an isothermal or adiabatic reactor can be used. In addition, liquid phase reactors and membrane reactors can be used for this synthesis (Leonzio, 2018). Adiabatic reactors are proposed by the Imperial Chemical Industries, Casale (Wang et al., 2013), Toyo Engineering Corporation (Toyo Engineering, 2015), Haldor Topsoe, Kellogg (Leonzio, 2018) and Rahimpour (2008). Overall, these type of reactors consists of adiabatic fixed beds with intermediate refrigeration to control temperature. Isothermal reactors are proposed by Linde (Linde Engineering, 2015), Lurgi (Haid and Koss, 2001), Mitsubishi Gas Chemical (MGC) and Mitsubishi Heavy Industry (MHI) (Leonzio, 2018), Casale (Bozzano and Manenti, 2016). These are shell and tube reactors with catalyst inside (Lurgi, MGC, MHI) or outside tubes (radial steam-raising converter and tube cooled converter). Liquid reactors, compared to other technologies, allow a good control of temperature due to a large heat capacity of a liquid to absorb the generated heat (Xu et al., 2009). Air Products proposes a slurry liquid phase technology (LPMEOH™) (Leonzio, 2018): the catalyst is suspended in an inert mineral oil, allowing very efficient heat and mass transfer. Compared to tubular fixed bed reactors, operating and capital costs are lower. The system assures a high conversion with a low recycle. Membrane reactors allow the removal of a product (methanol or water or both) improving the efficiency. Gallucci et al. (2004) using a zeolite membrane reactor, find that CO_2 conversion (X_{CO2}=11.6%), methanol selectivity (S_{MeOH}=75%) and yield (Y_{MeOH}=8.7%) are higher than those obtained in a conventional reactor (X_{CO2}=5%, S_{MeOH}=48% and Y_{MeOH}=2.4%) at 483 K, 20 bar, H_2/CO_2 ratio of 3 and space velocity of 6000 1/h. Other membrane reactors for methanol synthesis are analyzed by Parvasi et al. (2009), Rahimpour and Ghader (2003), Farsi and Jahanmiri (2011), Barbieri et al. (2002). In addition to these types of reactors, a gas phase fluidized bed reactor is developed by the New Energy and Industrial Technology Development Organization (NEDO) and Petroleum Endowment Center (PEC) in Japan: the catalyst particles are fluidized by the fresh gas fed at the bottom. The temperature is controlled by cooling pipes that recover the heat of reaction at high pressure. These reactors ensure a good conversion,

less pressure drop, elimination of diffusion limitations, good heat transfer capability and a more compact design (Abashar et al., 2004).

Methane is produced by CO_2 and H_2, according to the Sabatier reaction (see Eq. I.11) (Catarina Faria et al., 2018):

$$CO_2 + 4 \cdot H_2 \leftrightarrow CH_4 + 2 \cdot H_2O \qquad \Delta H = -165\ kJ/mol \qquad (I.11)$$

To be more precise, the methanation reaction is the combination of the carbon monoxide (CO) methanation and reverse water gas shift (RWGS) reaction (Bassano et al., 2019) (see Eqs. I.12-I.13):

$$CO + 3 \cdot H_2 \leftrightarrow CH_4 + H_2O \qquad \Delta H = -206\ kJ/mol \qquad (I.12)$$

$$CO_2 + H_2 \leftrightarrow CO + 2 \cdot H_2O \qquad \Delta H = 41\ kJ/mol \qquad (I.13)$$

The H_2/CO_2 ratio for methane production should be 4 (Leonzio, 2018). The obtained methane is called substitute natural gas (SNG), with physical and chemical properties very close to that of commercial natural gas (Riccia et al, 2019). When H_2 is produced by renewable energies, such as solar or wind energy, via H_2O electrolysis the process is known as Power-to-Gas: renewable electric energy can be transformed into storable methane via electrolysis and subsequent methanation. Power-to-Gas system is a promising way to manage and store fluctuating electricity produced by renewable energy sources, then a highly effective integration of renewables. It can be used not only as an energy storage technology, but also as a tool for balancing electric and gas grids (Lewandowska-Bernat and Desideri, 2017). For power to methane technology, it is estimated that the energy efficiency from renewable energies to gas is about 30-40%, a value similar to that obtained by conventional power plants (this should be about 40-50% by 2030) (Sauer et al., 2012). The TRL value for this hydrogenation reaction is of 7, tests are limited to demonstration plant. A lower value of TRL is considered for the other routes of methane production: 4 for the electrochemical reduction of CO_2, 3-4 for the microbial conversion of CO_2 and 3 for the photo-electrochemical reduction of CO_2 (Chauvy et al. 2019). Existing projects, on catalytic hydrogenation of CO_2 in a Power-to-Gas process, are present in Germany, Switzerland, United State, Austria, Japan, The Netherlands, Poland, France, Canada and Thailand (Bailera et al., 2017; Chwoła et al., 2020). Plants with higher installed power are located in Germany (30.7 MW_{el}) followed by Denmark (2.53 MW_{el}), Canada and the United States of America (both about 0.45 MW_{el}) (Therma et al., 2019).

Water electrolysis systems are classified on alkaline electrolysis (AEL), polymer electrolyte membrane electrolysis (PEM) and solid oxide electrolysis cell (SOEC). AEL is the most mature technology, while SOEC is still at pre-commercial scale. Specific electrical energy consumption of AEL, PEM and SOEC is respectively of 4.2-4.8 kWh/Nm^3, 4.4-5 kWh/Nm^3 and 3 kWh/Nm^3, while capital costs are of 1000 €/kWel–1200 €/kWe, 1800–2300 €/kWe and above 2000 €/kWe (Schmidt et al., 2017; Buttler and Spliethoff, 2018). Cascades of fixed bed reactors with intercooling, cooled fixed-bed reactors, fluidized-bed reactors, structured reactors and three-phase reactors may be used for methanation reaction (Rönsch et al., 2016).

Most of studies present in the literature are about process and system analysis of Power-to-Gas process, in addition to a simple analysis of methanation reaction (Bassano et al., 2019). Blanco et al. (2018), analyze the potential application of this system in Europe with two different scenarios: a reduction of 85% and 90% of emission by 2050 compared to 1990 level. They find that Power-to-Gas will come to place only with lower costs. Countries with a high availability of renewable energy will tend to use hydro, geothermal, biomass or nuclear energy to compensate the fluctuations of solar and wind energy. Brunner and Thomas (2014) consider an analysis of a Power-to-Gas process for the federal state of Baden-Wurttemberg in Germany. An analysis of a Power-to-Gas system integrated by a large scale electricity generation, based on renewable energies, is considered in Vanderwalle et al. (2015). Dickinson et al. (2010) study a Power-to-Gas process by combining hydrogen from geothermal energy via electrolysis and carbon dioxide from natural gas power plants in Australia. Kötter et al. (2015) consider to use 100% of renewable energy for a Power-to-Gas system in Germany. They find that in this case, the levelled cost of electricity (LCOE) of 11 ct/kWhel is lower than that estimated by using batteries to store energies. An economic analysis is developed by Gassner and Maréchal (2012), Buchholz et al. (2014), Tsuparia et al. (2016), Petersa et al. (2019) finding a methane cost in the range of € 3.51-3.88 per kg. An economic analysis for Germany is carried out by Leonzio (2017), suggesting the need of economic incentives to have a profitable system. Balan et al. (2016) perform a technical and economic analysis for a Power-to-Gas in Romania. A new methodology for sizing is proposed, based on analyzing different threshold values for the price of energy. The economic evaluation consists in a discounted cash flow analysis: the results suggest that the system is not financially viable without taking into consideration economic incentives. Economic incentives are also required by Blanco and Faaij (2018) for this synthesis. In this context, an economic optimization is considered by Gorre et al. (2020): a potential cost reduction of up to 17% in synthetic natural gas production is achieved in optimal conditions.

From this analysis it results, that there is a great interest on increase the integration of renewable energies and that this technology is characterized by high costs, then economic incentives are required. A SWOT analysis for methanation reaction is also suggested by Chauvy et al. (2019). A strength is the fact that methane has a big market. Opportunities are the following: a reaction highly exothermic with the possibility to reuse the heat from the conversion, the produced methane can be transported using the current gas grid and infrastructure, the possibility to fit renewable methane and renewable hydrogen economies. Weaknesses are: the use of H_2 that should be produced by renewable energies at high costs, the reaction is highly exothermic and should be controlled, it is flammable and it is in competition with natural gas. Threats are the following: the evolution of CO_2 and H_2 price, the competition with biogas from fermentation.

Generally, syngas can be produced from coal, petroleum coke, natural gas, biomass and even from organic wastes (Tao et al., 2011). However, syngas may be produced from CO_2 in different ways, as reported in table I.5. Overall, it is possible to have, according to the temperature, thermal and non-thermal (dielectric barrier discharge, glow discharge, corona discharge, plasma jets) plasma, producing effective electrons able

to fragment CH_4 molecule to form CH_i radicals that react with additive gases such as CO_2 to form products. Reactions of CO_2 reforming of CH_4 to syngas are involved, however these techniques have not been practically commercialized so far (Tao et al., 2011).

Table I.5 Investigated technologies to produce syngas by CO_2

Glow discarges
Li et al. (2009)
Dielectric barrier discharges
Wang et al. (2011)
Pham et al. (2011)
Ozkan et al. (2015)
Song et al. (2004)
Nguyen et al. (2019)
Plasma jets
Ni et al. (2011)
Rutberg et al. (2015)
Thermal plasma
Yanpeng et al. (2014)
Methane dry reforming
Gokon et al. (2011)
Dou et al. (2019)
Wang et al. (2019)
Microwave-assisted dry reforming
Fidalgo et al. (2008)
Co-electrolysis of H_2O and CO_2
Pardala et al. (2017)
Liu et al. (2016)
Stoots et al. (2009)
Delacourt et al. (2008)
Kleiminger et al. (2015)
How and Xie (2019)
Zhou et al. (2019)
Acid Gas To Syngas (AG2STM)
Bassani et al. (2016)

Li et al. (2009) analyze operating parameters of a glow discharge plasma reactor. They find that under the experimental conditions of CH_4/CO_2 rate at 4/6, input power at 69.85 W and feed flow rate at 2200 mL/min, the conversion of CH_4 and CO_2 are of 60.97% and 49.91%, the selectivity of H_2 and CO are 89.30% and 72.58%, H_2/CO rate is 1.5, respectively. Ozkan et al. (2015) study the dielectric barrier discharge (DBD) to generate syngas by CO_2 and CH_4. Some parameters are evaluated: CO_2 and CH_4 flow rates, the power supplied to the DBD and the nature of the carrier gas (Ar or He). In particular, power has a positive effect

on carbon dioxide and methane conversion and in syngas production, with a linear increase. A plasma jet is analyzed by Ni et al. (2011): under optimum experimental conditions, the energy conversion efficiency reaches up to maximum value of 1.87 mol/kJ and the highest energy efficiency of 74.63% is achieved, which is higher than that of other plasma processes. The good performances of a thermal plasma reactor are verified by Yanpeng et al. (2014): thermodynamic and experimental studies show that the CO_2/CH_4 volume ratio and the total feed flow rate are important parameters in the reforming process. Then, for thermal and non-thermal plasma reactors, operating parameters are analyzed in the existing literature.

Another technique for syngas production using CO_2 and that has not reached the commercialized level is the methane dry reforming. The value of TRL is, in fact, of 6 (Chauvy et al., 2019). It is an endothermic reaction that requires a lot of energy (Farniaei et al., 2014; Leonzio, 2018) (see Eq. I.14):

$$CO_2 + CH_4 \leftrightarrow 2CO + 2{\cdot}H_2 \qquad \Delta H = 247.3\ kJ/mol \qquad (I.14)$$

Most of the literature analysis is about the searching and analysis of an appropriate catalyst (Gokon et al., 2011; Wang et al., 2019; Dou et al., 2019).

Methane dry reforming can be developed also using microwaves, under the micro-wave assisted dry reforming of methane: it is a combination of catalytic CH_4 decomposition and CO_2 gasification producing syngas (Leonzio, 2018). A comparison with the traditional dry reforming reaction is considered in the work of Fidalgo et al. (2008), showing higher CH_4 and CO_2 conversion for the microwave heating. Under microwave heating, various operating variables are studied in order to determine the best conditions for performing dry reforming with high conversions and the most suitable H_2/CO ratio.

Another technology to produce syngas is the co-electrolysis of CO_2 and H_2O. According to this principle, the reactions in the cathode are the following (see Eqs. I.15-I.16) (Li et al., 2013):

$$CO_2 + 2e^- \rightarrow CO + O^{2-} \qquad (I.15)$$

$$H_2O + 2e^- \rightarrow H_2 + O^{2-} \qquad (I.16)$$

At the anode occurs the following reaction (see Eq. I.17) (Li et al., 2013):

$$2{\cdot}O^{2-} \rightarrow O_2 + 4{\cdot}e^- \qquad (I.17)$$

Literature works demonstrate the feasibility of this technique at large scale and analyze different configurations. Liu et al. (2016) analyze the separate electrolysis of CO_2 and H_2O and the co-electrolysis of these molecules. Results show that the simultaneous electrolysis in a single electrolyzer is possible as well as the industrial production. Stoots et al. (2009) study experimentally the simultaneous high-temperature electrolysis of H_2O and CO_2 using solid-oxide electrolysis cells. Results show that this technology significantly increases the yield of syngas over the reverse water gas shift reaction equilibrium composition: the process appears to be a promising technique for large-scale syngas production. An electrolyzer system using also ionic liquid (1-butyl-3-methylimidazolium triflate) is suggested by Pardal et

al. (2017) in order to have high selectivities, tunable H_2/CO ratio and low energetic requirements. Delacourt et al. (2008) modify a proton exchange membrane with the insertion of a pH-buffer layer (aqueous $KHCO_3$) between the silver-based cathode catalyst layer and the Nafion membrane improving the cathode selectivity for CO_2 reduction to CO. Kleiminger et al. (2015) use a micro-tubular solid oxide electrolyzer with yttria-stabilized zirconia (YSZ) electrolyte, Ni-YSZ cermet cathode and strontium(II)-doped lanthanum manganite (LSM) oxygen-evolving anode, for the co-electrolysis of H_2O and CO_2 to produce syngas. The value of TRL for this technology is of 4-5 (Chauvy et al., 2019).

In a similar field, Bassani et al. (2016) propose a novel Acid Gas To Syngas (AG2STM) technology to the gasification of solid fuels (coal or biomass), where H_2S and CO_2 are converted into syngas, by means of a regenerative thermal reactor. The process allows to reduce the environmental impact of coal uses and, at the same time, to improve the yield of coal gasification processes thanks to the innovative idea of coupling the reducing potential of H_2S with CO_2.

New researches regard the production of syngas using solar cells that efficiently convert carbon dioxide from air directly into synthesis gas, using only sunlight for energy source (Leonzio, 2018).

In this pathway for fuel production, the expected storage time of CO_2 depends on the produced fuel (weeks/months), while the likelihood of release during storage is high (Hepburn et al., 2019).

Figure I.12 shows the main fuels that may be obtained from CO_2, through different reactions.

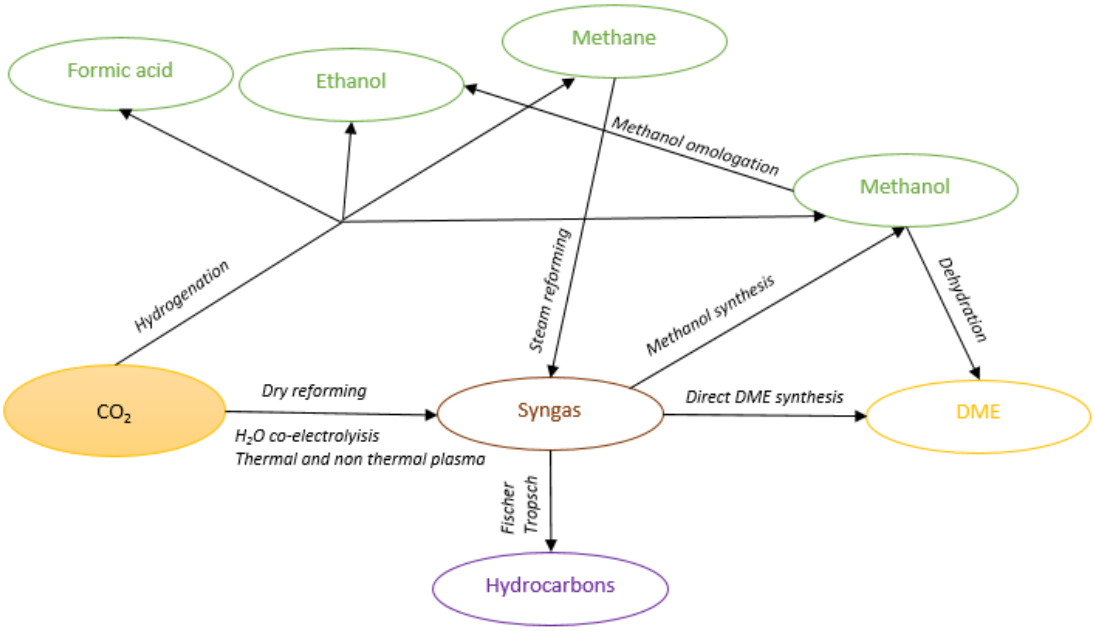

Figure I.12 Principal fuels obtained from CO_2 (Leonzio, 2019)

I.4.1.3 Concrete building materials

Concrete is a mixture of cement, fine aggregate like sand and coarse aggregate like gravel or crushed stone. Natural and accelerated curing carbonation can occur and they have been studied (Galan et al., 2010; Monkman and Shao, 2006). Natural curing carbonation occurs in air: cement hydration products, mainly calcium hydroxide and calcium-silicate-hydrates, react with atmospheric CO_2 to produce calcium carbonate ($CaCO_3$), improving the mechanical properties and reducing the subsequent drying shrinkage of concrete product (Baojian et al., 2013). However, it is a slow process and it is a problem for steel reinforced concrete structure because the carbonation decreases the concrete pH, improving the corrosion of reinforcing steel. In the accelerated curing carbonation, on the other hand, CO_2 is injected into the curing vessel at room temperature, then CO_2, diffusing into the fresh concrete under low pressure, reacts with cement components or hydration products like $3CaO{\cdot}SiO_2$, $2CaO{\cdot}SiO_2$ to produce $CaCO_3$ and strength-contributing phases, such as calcium silicate hydrates, according to the following reactions (see Eqs. I.18-I.19) (Xuan et al., 2018; Khan et al., 2018):

$$2(3CaO{\cdot}SiO_2) + 3CO_2 + 3H_2O \rightarrow 3CaO{\cdot}2SiO_2{\cdot}3H_2O + 3CaCO_3 \quad \text{(I. 18)}$$

$$2(2CaO{\cdot}SiO_2) + CO_2 + 3H_2O \rightarrow 3CaO{\cdot}2SiO_2{\cdot}3H_2O + CaCO_3 \quad \text{(I. 19)}$$

If initial hydration as pre-condition is introduced before carbonation, hydration products such as calcium hydroxide (CH) and calcium-silicate-hydrate (C-S-H) can also be carbonated, according to the following reactions (see Eqs. I.20-I.21) (He et al., 2019):

$$Ca(OH)_2 + CO_2 \rightarrow CaCO_3 + H_2O \quad \text{(I. 20)}$$

$$3CaO{\cdot}2SiO_2{\cdot}3H_2O + 3CO_2 \rightarrow 3CaCO_3 + 2SiO_2 + 3H_2O \quad \text{(I. 21)}$$

Overall, gaseous CO_2, after its dissolution into H_2O, is converted into a solid calcium carbonate during an accelerated curing process. For applications without reinforcing steel, the carbonated concrete products have better performances in terms of compressive strength, abrasion resistance, durability, stable dimensions, due to the near-complete depletion of calcium hydroxide (Baojian et al., 2013; Shi-Cong et al., 2014). Costs are also reduced due to the lower cement content. However, it is most suitable for concrete products, such as blocks and cement boards.

Also, these properties can be acquired in few hours against the natural carbonation of concrete in air (El-Hassan, 2014; Zhan et al., 2016) and in any case this process depends on CO_2 concentration, pressure, time of exposure, relative humidity etc. (Shi et al., 2013). Khan et al. (2018) find that in the accelerated curing carbonation, concrete achieves in only 4 hours the strength that should be achieved in 28 days, with natural curing carbonation. Xuan et al. (2018) find that important parameters to improve the maturity and strength of concrete are: a high CO_2 concentration, a fast gas flow rate and a moderate relative humidity. On the other hand, Monkman et al. (2016) report that with accelerated concrete curing the durability of the concrete

is not compromised, but better performances (compressive strength, linear shrinkage, etc.) are obtained. The value of TRL for concrete curing is of 7-8 (Alberici et al., 2017).

In addition, concrete can be produced from CO_2, through the red mud or "bauxite residue", obtained by bauxite treatment during alumina production (two tons of red mud are produced by one ton of bauxite, according to the bauxite characteristics and processing parameters) (Klauber and Gräfe, 2009). Red mud is mainly composed by Al_2O_3, Fe_2O_3, SiO_2, TiO_2, CaO, Na_2O, then it has an alkaline character with an high pH (10.5-12.5) (Patricio et al., 2017a; Ribeiro and Morelli, 2011). However, if the red mud is carbonated with CO_2, the pH decreases and it can be valorized and used as additive for building materials: it can be used to produce concrete reducing the cement content (Sutar et al., 2014). Several studies are related to the use of red mud in concrete production. Ribeiro et al. (2012) suggest that the utilization of red mud in concrete production can improve the corrosion resistance, with an optimal composition value between 20% wt and 30% wt. Better mechanical properties than the conventional concrete are obtained by Nikbin et al. (2018). Liu and Poon (2016) replace fly ash with red mud in concrete improving the compressive strength, splitting tensile strength and elasticity modulus; on the other hand, drying shrinkage is decreased. Rathod et al. (2014) find that the optimal value of red mud composition in concrete is of 25% wt. Similar analyses are carried out by Sai (2017), Colella et al. (2007), Feng and Peng (2005), Hauri (2006), Dindi et al. (2019). Overall, the literature works analyze the production process finding better operating conditions for this pathway. This pathway has a value of TRL of 9 (Patricio et al., 2017a).

In concrete production, the expected storage time of CO_2 may be of centuries, while the likelihood of release during storage is low (Hepburn et al., 2019).

I.4.1.4 Mineral carbonation

Mineral carbonation reaction can be in-situ or ex-situ (Chang et al., 2017a). The first case occurs into geological storages, when CO_2 reacts with alkaline minerals present in the geological formation and it is transformed into a mineral carbonate. The ex-situ reaction, on the other hand, occurs chemically in an industrial plant, through a reaction between CO_2 and alkaline earth metals mostly calcium (Ca) or magnesium (Mg), obtained from the nature via silicate minerals (wollastonite, olivine, serpentine, etc.) or from industrial by-products or waste materials (coal fly ash, steel and stainless-steel slags, and cement and lime kiln dusts, basic oxygen furnace slag) (Gerdemann et al., 2007; Pan et al., 2012). In this case a precipitated mineral carbonate is produced. In particular, for the in-situ and ex-situ carbonation, the reaction is between the metal oxide bearing the mineral and CO_2, as fellows (see Eq. I.22):

$$Metal\ oxide + CO_2 \rightarrow Mineral\ carbonate + Heat \qquad (I.22)$$

In addition to $CaCO_3$ and magnesium carbonate ($MgCO_3$), sodium carbonate ($NaCO_3$) and sodium bicarbonate ($NaHCO_3$) may be produced. The TRL value for the process producing $CaCO_3$, $MgCO_3$, $NaCO_3$ and $NaHCO_3$ is respectively of 7, 3-4, 6 and 8-9 (Chauvy et al., 2019).

Compared to the in-situ reaction, the ex-situ reaction allows to valorize also industrial hazardous wastes, containing the considered metals and to use the obtained mineral carbonate products for different aims. In fact, for example, $CaCO_3$ may be used as adhesive, sealants, in food and pharmaceutical sector, in paint, rubber and paper industry, for construction materials (Eloneva et al., 2008). In addition, while in the in-situ reaction CO_2 is just injected into geological formations containing alkaline metals, the ex-situ mineral carbonation involves different processes as mining, grinding, and/or pre-treatment processes to ensure Ca- or Mg-bearing mineral feedstock. The different applications of mineral carbonates are related to their physicochemical characteristics such as particle size, shape, density, color, brightness, that can be governed through operating parameters as pH, temperature, concentration, additives, stirring, reaction time, etc. (Zhang et al., 2013; Chang et al., 2017b).

Literature works are mainly considering steel slag as raw material to produce precipitated calcium carbonate. In the work of Zappa (2014) calcium is extracted from steel slag by using a solution of ammonium chloride (NH_4Cl). The author reports that temperature, calcium concentration, NH_4Cl solvent concentration, CO_2 flow rate and agitation speed have important effects on the mineralization and quality of the precipitated calcium carbonate. In particular, a lower dimension can be obtained reducing temperature, calcium and NH_4Cl concentration, CO_2 flow rate and increasing the agitation speed. An economic analysis of the process is also developed: the production cost for the precipitated calcium carbonate is of 65 €/ton. A techno-economic analysis of a process, called KIST, to produce calcium carbonate from steel slag is carried out by Lee et al. (2020): results suggest the cost of 483 USD/ton $CaCO_3$, then the process is feasible. Said et al. (2013) consider a parametric analysis of this process. They find that grinding the materials of steel slag to a smaller size can improve the efficiency and chemical conversion rates (reactor size and resident time are decreased improving the extraction efficiency), while the smallest solid to liquid ratio ensures the maximum calcium extraction efficiency. A feasibility study for $CaCO_3$ production from basic oxygen furnace slag is proposed by Kim et al. (2020). It is evident that, the most of literature works are regarding the analysis of the mineralization process, finding the costs and the influence of some operating parameters.

As in concrete production, the expected storage time of CO_2 in mineral carbonates may be of centuries in a stable, inert and solid form, while the likelihood of release during storage is low due to the stability of mineral carbonates (Hepburn et al., 2019; Zevenhoven et al., 2006).

I.4.1.5 Oil and methane recovery

CO_2 can be used for oil and gas (methane) recovery, respectively in CO_2 enhanced oil recovery (CO_2-EOR) and CO_2-enhanced coalbed methane (CO_2-ECBM) technologies. It is a way to store CO_2, but at the same time, CO_2 is used as injection fluid to recover oil and methane from the respective reservoirs. In CO_2-enhanced coalbed methane, CO_2 is used to extracts CH_4 from the coalbed: the injected gas allows CH_4 to desorb from the coalbed, changing the adsorption rate between gases and micro-pores in the seam, while

CO_2 is adsorbed and then stored (Cho et al., 2019). In fact, coalbed methane reservoirs are naturally fractured rocks, consisting of cleats and matrix, which micro-pores contain a considerable amount of methane adsorbed on the walls (Verma and Sirvaiya, 2016). This phenome can be explained by geometrical and physical/chemical properties of gas molecules (Sayyafzadeh et al., 2015). In fact, CO_2 molecules are smaller than CH_4 molecules and also have a linear shape, facilitating CO_2 entrance to more restricted pore spaces and dislocating the pre-adsorbed CH_4 molecules out of micro-pore surfaces. Moreover, CO_2 has a more favorable interaction enthalpy than hydrocarbons, increasing CO_2 solubility in coals compared to CH_4. An overview about this technology and the investigations that should be done is suggested by Li and Fang (2014) and Lau et al. (2017). Other studies present in the literature are about the analysis of geological and physical characteristics of a coalbed methane, underlining the process performances, as CO_2 injection and CH_4 separation. Mazzotti et al. (2009) show the best performances and efficiencies obtained by using CO_2 and not another gas (e.g. nitrogen or a mixture of nitrogen and carbon dioxide), due to the grater affinity of coal towards CO_2. Guan et al. (2018) analyze the adsorption capacity of CH_4 and CO_2 for an Illinois coal at different temperatures and find that these are correlated. In particular, the adsorption capacity of these gases decreases at higher temperatures, until a critical temperature value, where this dependence is vanished. Liu et al. (2013) propose a mathematical model to evaluate the wellhead and bottom-hole pressure, considered as important parameters. In the work of Sinayuc et al. (2011), the effect of some parameters, such as the layout and number of wells, composition of injected gas and permeability on CH_4 production are evaluated. In a more accurate analysis, Dai et al. (2017) find that the reservoir thickness, permeability, and porosity are key parameters controlling the CO_2 injection and CH_4 production rates. In particular, reservoir thickness, permeability, porosity have a positive effect on CO_2 injection rate and CH_4 production rate. The effect of injection pressure and initial reservoirs temperature on the process is analyzed by Fan et al. (2018) through a simulation in COMSOL Multiphysics. The authors find that the amount of stored CO_2 and extracted CH_4 decrease at higher reservoir temperature, and increase at higher pressure. The positive effect of pressure is also documented in the work of Yin et al. (2017). The optimal CO_2 composition for gas recovery is find by Sayyafzadeh and Keshavarz (2016), based on the economic calculation of net present value. Studies for micro-pilot tests are carried out by Wong (2007) and Ye (2007). In recent years, also liquid CO_2 is used for this technology: a higher pressure and volume is able to crack the coal seams and to improve the gas extraction (Chen et al., 2017; Hu et al., 2018; Wen et al., 2020).

The TRL value for this utilization option is of 7 (demonstration scale) (Bui et al., 2018).

In CO_2-EOR, as already mentioned, CO_2 is used to extract oil from reservoirs. This technology is based on chemical and physical mechanisms, involved during the interaction of CO_2 with rocks and fluids that are present in the reservoir. In particular, CO_2 has excellent dissolution properties and above the minimum miscibility pressure, becomes miscible with the in-situ oil, dragging the oil out of pores through different mechanisms, as interfacial-tension and viscosity reduction, and oil swelling (Farajzadeh et al., 2020). Besides the United States, China and countries in the Middle East have expressed strong interest in using

CO_2-EOR (Azzolina et al., 2016). In 2014, 136 active CO_2-EOR projects were identified in the United States (Koottungal, 2014).

Studies present in the literature are mainly about the optimization of the process, techno-economic and environmental analysis. Generally, the co-optimization of CO_2 storage and oil recovery is considered by Kamali and Cinar (2014), Ampomah et al. (2017), Wang et al. (2018), Chen and Pawar (2019). In the work of AlMazrouei et al. (2017) two different optimizations are suggested for a CO_2-EOR in California: one is minimizing the costs, the other one is maximizing the revenues. The second one is preferable according to the market dynamics. Wei et al. (2015) perform a techno-economic analysis for an oil field in China. A sensitivity analysis shows that oil production and CO_2 storage are very sensitive to crude oil price, CO_2 cost, project lifetime, discount rate and tax policy. Also, high oil price, short project lifetime, low discount rate, low CO_2 cost, and low tax policy can greatly increase the net income. Key parameters for a techno-economic analysis are also investigated in the work of Jiang et al. (2019). These parameters are: the porosity, net pay, CO_2 injection, depth, oil formation factor, and oil saturation. The net present value of the process is maximized by Kwak and Kim (2017), while Kemp and Kasim (2013) find that high CO_2 costs can provide negative values of net present value. Many other literature works regard a techno-economic analysis, suggesting the potential of this technology and its capacity to reduce CO_2 emissions (Davidson et al., 2011; Rubin et al., 2013; King et al., 2011; Mendelevitch, 2014). In addition to these feasibility studies, environmental analyses are also developed, in order to evaluate the emissions of this technology. Jaramillo et al. (2009) propone a model to calculate the cumulative CO_2 emissions over the life cycle of the considered process, including CO_2 capture from a power plant, CO_2 transportation, oil exploration and transportation, crude oil refining and its combustion. A detailed gate-to-gate, cradle to gate and cradle to grave life cycle assessment (LCA) analysis for a CO_2-EOR system is developed by Cooney et al. (2015): they find that it is more environmentally beneficial to use anthropogenic CO_2 sources than natural CO_2. Azzolina et al. (2016) in their study find that CO_2-EOR process produces oil with an emission factor of about 300 $kgCO_{2\text{-}eq}$/bbl, lower than the conventional process (500 $kgCO_{2\text{-}eq}$/bbl). In this study, CO_2 is captured from a coal-fired power plant. Greenhouse gas emissions reduction per unit of produced oil are obtained through this kind of system in an offshore EOR in the North Sea, in the work of Stewart and Haszeldine (2015). Overall, environmental benefits of this technology are reported in the literature. For this pathway the value of TRL is of 9, then it is at commercial scale (Bui et al., 2018). In both discussed pathway, CO_2 is stored as a geological sequestration, then for millennia and the likelihood of release during storage is low (Hepburn et al., 2018).

I.4.1.6 Horticulture and algae production

CO_2 may be used for horticulture and algae production by using greenhouses with CO_2 enrichment. CO_2 enrichment is a technique used to enhance the photosynthesis, resulting in improved yields and income (Chalabi et al., 2002). It is important to underline that these benefits are present only for plants with C3

photosynthesis pathway and not for plants with C4 pathway (Dion et al., 2011). C3 pathway includes cereals (wheat, rice, barley, oats, rye, triticale, etc.), all legumes (dry bean, soybean, peanut, mung bean, faba bean, cowpea, common pea, chickpea, pigeon pea, lentil, etc.), nearly all fruits (including banana, coconut, etc.), roots and tubers (potato, taro, yams, sweet potato, cassava, etc.). C3 is also the pathway for sugar beet, fibre crops (cotton, jute, sisal, etc.) and oil crops (sesame, sunflower, rapeseed, safflower etc.), algae and for trees. On the other hand, C4 pathway includes corn (maize), sorghum, millet and sugarcane. Then, C3 plants are the most common greenhouse crops, even if they are less efficient to fix CO_2 at ambient concentrations (about 388 ppm) (Dion et al., 2011). However, for these crops, a higher CO_2 concentration determines a higher photosynthetic rate, creating more carbohydrates that translates into an increased biomass (Sanchez-Guerrero et al., 2009). Generally, this positive effect for greenhouse crops is obtained for CO_2 concentrations between 700 and 1000 ppm, which produces a yield increases from 21% to 61% in dry mass (Jaffrin et al. 2003). On the other hand, the photosynthesis can improve also up to 50% (Patricio et al., 2017a). The positive effect of CO_2 on the yield of important crops has been reviewed with respect to rice, wheat, soybeans and grain (Dong et al., 2020; Senghor et al., 2017).

Also, this positive effects strongly depend on different greenhouse environmental parameters, such as temperature, relative humidity, nutrients and irrigation schedule. Several researches have been developed to optimize the level of CO_2 injection into greenhouses according to these factors (Klaring et al. 2007; Edwards, 2008; Rachmilevitch et al., 2004). The economic benefits of CO_2 enrichment technology are reported by Marchi et al. (2018), considering the saving related to the use of carbon emissions from the industrial process and the additional revenues due to the increase of the yield of products (tomatoes, cucumbers and strawberries). It is evident that for the horticulture production, most of literature works want to underline the better efficiencies obtained at a higher CO_2 concentration. Few works are about an economic analysis of this pathway.

Interesting considerations are reported in the literature for algae cultivation, that can be used as feedstocks for biofuels, such as biodiesel (Hallenbeck et al., 2014; Choia et al., 2014), pyro-oil (Pisal and Lele, 2005) and other bio-chemicals (Pradhan et al., 2015). Compared to other C3 plants algae can tolerate higher ranges of temperature, pH value and CO_2 composition (Olaizola et al., 2003); moreover these are able to fix CO_2 at a rate several times higher than plants showing their high photosynthetic efficiencies (Bhola et al., 2014). From the literature review, it is clear that algae may be cultivated either in open raceway ponds or in photo-bioreactors used to enhance the photosynthetic process (Pradhan et al., 2015). Several works suggest the way to improve the efficiency of these reactors (Zittelli et al., 2013; Ugwu et al., 2008).

The TRL value for horticulture and algae production is 9 and 8-9, respectively (Patricio et al., 2017a; Tcvetkov et al., 2019). The expected storage time of CO_2 depends on the product and can be of weeks or months, while the likelihood of release during storage is high (Hepburn et al., 2018).

I.4.1.7 Direct use

CO_2 can be used in various processes of food industry, as an inert to prevent the food spoilage and in packaging applications, when it is used both in modified and controlled atmosphere packaging. CO_2 is also used in beverage carbonation (Linde, 2019), in coffee decaffeination as an extraction solvent at supercritical conditions (AHDB, 2019), and wine making, as a seal gas to prevent oxidation of the wine during maturation (Global CCS Institute, 2011). CO_2 is used also in metal industry, as a shrouding gas to prevent oxidation in a welding process, or in basic oxygen furnaces for dust suppression (Leeson et al., 2017).

Other industrial direct uses of CO_2, include pulp and paper processing, to reduce the pH value during pulp washing operations (Linde, 2012), water treatment (it is used for the re-mineralization of water following reverse osmosis and for pH control) (Girdon et al., 2006), printed circuit board manufacture (as a cleaning fluid) (Pieri et al., 2018), and power generation (in the supercritical form as a power cycle working fluid) (Global CCS Institute, 2011). CO_2 can be also used in pneumatic applications, in fire extinguishers and in industrial fire protection systems (Pieri et al., 2018), in refrigeration units (larger industrial air conditioning and refrigeration systems) as the working fluid, replacing other more toxic refrigerant gases (Leeson et al., 2017).

I.4.2 Carbon supply chains modelling

I.4.2.1 CCS supply chains modelling

From the literature analysis of CCS supply chains, it is evident the necessity to investigate the design, costs and integration of these frameworks for different geographic contexts. To this purpose, optimization techniques, especially mixed integer linear programming (MILP) models, are developed to have some preliminary information for an early planning of large scale network.

Tan et al. (2012) suggest a MILP model to match CO_2 sources and sinks in CCS systems, taken into account the storage limitations of the sinks. In the subsequent work, Tan et al. (2013) design the system under the constraints of temporal, injection rate and storage capacity.

A revision of different mathematical models published in the last decade for Europe and the United States is presented by Tapia et al. (2018). Kalyanarengan Ravi et al. (2017) design and optimize the minimization of the total costs for a CCS supply chain in The Netherlands. As an important point of this work, the fraction of captured CO_2 is chosen through the optimization and it is not considered a constant, as in the previous works. Other countries are also considered. In fact, other CCS supply chain models are developed for Norway by Bakken and von Streng Velken (2008) and Klokk et al. (2010), The North Sea regions by Strachan et al. (2011), Texas by Middleton et al. (2012), Europe by Odenberger and Johnsson (2010) and d'Amore and Bezzo (2017), the UK by Akgul et al. (2014), western Nebraska by Wildgust et al. (2019),

China by Fan et al. (2018), Japan by Tanaka et al. (2017), India by Garg et al. (2017), Quatar by Zhang et al. (2017).

These works consider mainly a deterministic economic optimization (trough the minimization of the total costs or the maximization of the profit) and the total costs of the framework are calculated. It is evident that, the major obstacle towards large scale deployment of this system are its high costs (Zhang et al., 2017; Budinis et al., 2018). For this reason, economic subsidies are needed as suggested by Zhu et al. (2015) considering a long term perspective (2050).

In addition to the economic analysis, social risks and acceptances are discussed. In fact, CO_2 is a non-toxic and non-flammable gas, but has a higher density than air, and therefore in presence of a leakage it could locally accumulate up to a dangerous concentration. Then, in the work of d'Amore et al. (2018) social risks are considered in the economic analysis: social risk has not a significant effect on the costs, but limits only the sequestration potential. Social acceptances are taken into account in the work of d'Amore et al. (2020): the developed mathematical model minimizes the total costs and maximizes the community acceptance. Yang et al. (2016) report that public cognition, economic benefits, and environmentalism have a positive effect on the public acceptance of CCS systems, while potential risks have a strong negative effect.

However, in the modelling of supply chains, uncertainties can be also taken into account and these can be related to policy, technology, engineering performance, economics, market forces, CO_2 injection and storage (Middleton and Yaw, 2018). Zhu and Fan (2011) evaluate the investment needed for a CCS under the uncertainties of fuel price, investment costs, capture costs and carbon price. Santibanez-Gonzalez (2017) develop a novel stochastic mixed integer linear optimization model for a CCS supply chain in Brazil, considering also carbon tax. A two stage stochastic model is developed by Han and Lee (2012) for the eastern coast of Korea: uncertainties in product prices, operating costs, and CO_2 emissions are considered, while the total profit is maximized. Also, Nie et al. (2017) propose a CCS optimization for the UK under market prices uncertainty while, d'Amore et al. (2019) maximize the resiliency of a European CCS supply chain under the uncertainty of geological storage capacities. Similarly, Jeong et al. (2018) find the minimum costs of a CCS supply chain under geological uncertainties (brine formation and leakage in storage). Sink physical and investment limit uncertainties are present in the two stage stochastic MILP model developed by Zhang et al. (2018). Another non-deterministic study is suggested by Jin et al. (2017), minimizing the total costs under multiple uncertainties (fuel costs, CCS investment, mitigation level, etc.).

In some cases, multi objective optimization analyses are considered. Lee et al. (2017) propose a MILP stochastic programming for the optimization of a CCS infrastructure in South Korea, while simultaneously including cost, environmental impact and financial risk measures within the multi-objective mathematical framework.

The majority of the published studies focuses only on the economic assessment of the carbon scheme, in a stochastic or deterministic model.

I.4.2.2 CCU supply chains modelling

Few works are present in the literature about CCU supply chains. A techno-economic analysis for two CCU systems producing methanol and calcium carbonate via carbonation of flay ash is reported in Perez-Fortes et al. (2014). Methanol is also produced in the work of Kourkoumpas et al. (2016), capturing CO_2 from a lignite fired power plant. A techno-economic analysis is performed and it is found a methanol production cost of 421 €/ton. In Duraccio et al. (2015), the CCU framework considers the capture of CO_2 from a power plant and its utilization for sugar production: for the sugar factory a reduction of 42% of costs is ensured. Patricio et al. (2017b) consider a CCU supply chain for Sweden, where CO_2 is used for mineral carbonation, tomatoes and algae production, methanol and methane synthesis, pH control, lignin production, polymer synthesis and concrete curing. In this case, CO_2 emissions could be reduced of 250,000 tCO_2 per year. Dimethyl ether is produced in the CCU framework developed by Michailos et al. (2019): the minimum deterministic selling price of this CO_2-based product is of 2193 €/ton while, with the uncertainty of renewable energy price this cost is in the range of 1828–2322€.

Optimization models are also developed. Lainez-Aguirre et al. (2017) develop a MILP model for a CCU framework where CO_2 captured from the co-combustion of biomass and coal is used to produce methanol. In the model, the net present value is maximized satisfying the electricity demand, methanol demand and CO_2 emissions reduction. The potential production of synthetic hydrocarbons capturing CO_2 from cement plants in a CCU system is discussed by Farfan et al. (2019), while in the work of Valderrama et al. (2019) CO_2 is mainly captured and used to produce polymers. A model for a CCU supply chain, integrated in a steelmaking plant and producing methanol, is suggested by Ghambari et al. (2015): the system is designed by the maximization of the net present value.

The most of CCU supply chain studies reported in the literature are then regarding a feasibility and economic analysis.

I.4.2.3 CCUS supply chains modelling

Generally, mathematical models of CCUS supply chains that are present in the literature can be classified in deterministic, stochastic and multi objective optimization models. Deterministic models, particularly MILP models, are mostly about CO_2-EOR systems optimized for an economic point of view. Only Yao et al. (2018) present a business model of these systems. In fact, with the decline in oil discoveries during the last decades it is believed that EOR technologies will play a key role to meet the energy demand in years to come.

Regarding the optimization, Hasan et al. (2014) design a CCUS supply chain with CO_2-EOR for the United States and find that it is possible to reduce 50%-80% of CO_2 emissions with an annual cost of $58.1-106.6 billion, generating $3.4-3.6 billion of revenues per year. In the followed work, Hasan et al. (2015), find that for a CO_2-EOR framework it is possible to reduce 50% of CO_2 emissions at a cost of $35.63/ton captured CO_2. A simultaneous design methodology is also presented. In both studies the total costs are minimized.

The total costs are also minimized in the work of Zhang et al. (2018), where this kind of framework is developed for the north eastern China. The system is able to reduce 50% of stationary emissions with an annual cost of $2.3 billion and $0.77 billion of revenues. A similar case study for China is also developed by Sun et al. (2018). The important role of CCUS supply chains for China is recognized by Yu et al. (2019): these allow the energy transaction and a low carbon development at lower costs. However, Fan et al. (2019) report that economic incentives are required for China to avoid that these systems remain in the 'technology valley of death'. The need of subsidies for the development of CCUS project with oil recovery in China is also suggested by Yang et al. (2019).

In addition to the minimization of the total costs, different optimization methods are used by Rahmawati et al. (2015) to maximize the net present value of a CCUS supply chain with CO_2-EOR, comparing the obtained results with other injection strategies. The net present value is also optimized for these systems by Jahangiri and Zhang (2012). In Middleton et al. (2015) a CCUS supply chain is developed for the U.S. Gulf Coast region and in nearby regions (Texas, Louisiana, Mississipi, New Mexico, Oklahoma and Kansas) reducing 50 Mton of emissions and producing 200 million bbl/yr of oil, while in Klokk et al. (2010) a CO_2-EOR supply chain is optimized for the Norwegian regions, maximizing the net present value. The optimal value of the net present value is find by Agralı et al. (2018) in the modelling of a CO_2-EOR system in Turkey. For the authors, economic incentives are important for the commercialization of these carbon schemes. A similar economic analysis is also carried out by Guo et al. (2020).

Other considerations are presented in the work of Tapia et al. (2016a). The authors consider a MILP model for these supply chains with three important issues: the scheduling of CCUS operations, the allocation of CO_2 supply for CO_2-EOR operations and the matching between CO_2 sources and geological storages. In the followed work, Tapia et al. (2016b) consider the uncertainties of oil price, reservoir oil capacity and oil yield through a Monte Carlo simulation. An economic evaluation of CCUS supply chains with CO_2-EOR in Poland is carried out by Mathisen and Skagestad (2017) considering a sensitivity analysis for the price of oil and of CO_2.

In the deterministic models, CO_2 can be used also to produce other different products. Ochoa Bique et al. (2018) integrate a CO_2 and a H_2 supply chain in Germany in order to produce methanol in a sustainable way via hydrogenation. Results show that this solution is feasible only when the electricity for the electrolyzer is delivered for free.

Generally, the above models consider only one single objective function. However, more objective functions can be taken into account simultaneously for the optimization and design of the best supply chain. A tread-off between the different objective functions is in this case obtained. Leach et al. (2011) suggest a co-optimization of oil production and CO_2 storage for a CO_2-EOR supply chain: only at very high taxes does a trade-off between revenues from oil output and sequestration arise. Yue and You (2015) present a non-convex mixed integer nonlinear programming (MINLP) model for Texas to optimize the CCUS system according to both economic and environmental criteria using a multi-objective optimization approach. CO_2

is used to cultivate algae for biofuel production. 80% of carbon dioxide emissions are reduced at a price that is lower compared to other mitigation technologies.

Stochastic models are also present in the literature to consider the uncertainty of different parameters.

Huang et al. (2014) analyze a CCUS supply chain with CO_2-ECBM utilization option through a MINLP model. The profit is maximized considering uncertainties in natural gas price and carbon credit. A stochastic simulation for a CO_2-EOR system in the Danish North Sea is presented in the work of Suicmez et al. (2019). The price of the oil and the CO_2, discount and hydrocarbon tax rates are the stochastic parameters. Results show that the NPV distribution is between −491 and 1,203 million USD with the most likely value of 124 million USD. Uncertainties on coal price and carbon trading price are considered for a CCUS supply chain with CO_2-EOR in China in Fan et al. (2019). Lee et al. (2019) develop a two stage stochastic model for a CCUS supply chain producing polymer and bio-butanol in Korea. The annual profit is maximized, while the environmental impact and risk due to the uncertainties are minimized simultaneously. Operating costs, carbon dioxide sources, energy consumption are the stochastic parameters.

Also for this kind of supply chain, the literature works are mainly about economic considerations and in few cases the environmental aspect is considered in the objective function through a minimization or a maximization. This underlines that the costs are an important aspect for the development of these technologies. Moreover, few CO_2-based products are considered in the CCUS supply chain, mainly focused on CO_2-EOR technology. There is, also, a lack of studies considering the uncertainties in the model.

I.4.3 Life cycle assessment analysis of carbon supply chains

Life cycle assessment (LCA) analyses of carbon supply chains are reported in the literature in order to evaluate their net environmental impact and verify that these systems can effectively reduce emissions.

Different LCA studies are related to CCS supply chains. These studies differ in terms of the capture technology, details in modelled process, completeness of the life cycle inventory analysis and the emissions included in the assessment. A review of this analysis for CCS systems is reported by Cuellar-Franca and Azapagic (2015), underling that with CO_2 capture and storage, the global warming potential (GWP) of a power plant can be reduced of 63-82%, depending on the capture option. However, there are an increase of acidification and human toxicity. The same result is found by Zapp et al. (2012) and Oreggioni et al. (2017): the GWP decreases, while acidification, toxicity, resource depletion increase for a CCS with different capture technologies. Human toxicity, acidification and eutrophication increase with a decrement of the GWP in the work of Tang et al. (2014), analyzing a coal fired power plant with a CCS system in Japan.

In the work of Singh et al. (2011a), the application of a CCS system to a natural gas combined cycle (NGCC) for electricity generation can reduce the GWP by 64%, but with an increase of 43% in acidification, 35% in eutrophication, and 120–170% in various toxicity impacts.

A net reduction of the GWP for different power plants with a CCS system is in the order of 65–84% for a pulverized coal-fired power plant, 68–87% for an integrated gasification combined cycle, 47–80% for a natural gas combined cycle, and 76–97% for an oxyfuel plant (Corsten et al., 2013).

A reduction of the GWP, through the use of a CCS, is also reported by Volkart et al. (2013): it is of 68-92% for fossil power plants and 39-78% for cement plants.

The advantages of CCS systems are also documented in the work of Viebahn et al. (2007), Pehnt and Henkel (2009), Nie et al. (2011) and Singh et al. (2011a).

Pehnt and Henkel (2009) develop a LCA analysis of a CCS supply chain located in Germany (Lausitz region), storing CO_2 in a depleted gas field. CO_2 is captured from a lignite power plant with post-combustion, pre-combustion and oxy-fuel technologies. Results show that a reduction of all impact categories is present in pre-combustion capture technology. Nie et al. (2011) find that a post-combustion and oxy-fuel combustion CCS case can reduce the GWP by 78.8% and 80.0% respectively, compared to a conventional power plant without a CCS. Analogous results, for GWP reductions, are reported by Corsten et al. (2013), considering a NGCC, oxy-fuel and pulverized coal plant with a carbon storage system. Reductions of CO_2 emissions by 72-90% for a power plant with a CCS system are also obtained by Viebahn et al. (2007). Similarly, in Korre et al (2010) it is reported that a power plant with CCS can reduce the GWP of 80%, compared to a plant without the capture and storage of CO_2, while in Koornneef et al. (2008) the use of CCS in a pulverized coal power plant reduces greenhouse emissions to 243 g/kWh.

Better results are found in Yang et al. (2019): a pulverized biomass/coal co-firing power plant with CCS can have near zero emissions at a co-firing ratio of 25%. A similar analysis is carried out by Yi et al. (2018), evaluating the environmental analysis of a biomass co-firing plant with and without CCS in the UK and finding that in specific conditions negative emissions can be achieved.

It is important to underline that, the reduction of emissions depends on the capture technology (Singh et al. 2011b; Modahl et al., 2011). Moreover, in the work of Khoo and Tan (2006) different capture technologies and storage options are compared: lower environmental impact is ensured by using the chemical absorption and enhanced oil recovery.

A first more detailed cradle-to-grave LCA analysis for a CCS supply chain is studied by Petrescu et al. (2017). CO_2 is captured from a supercritical pulverized-coal process by using MDEA, an aqueous ammonia and calcium looping. Results show that the considered capture technologies do not allow a complete reduction of all impact categories.

Generally, for CCS supply chains, the impact of CO_2 transportation and storage is slightly significant in the whole life cycle of the system (Pehnt and Henkel, 2009; Singh et al., 2011a; Nie et al., 2011).

Regarding CCU supply chains, Cuellar-Franca and Azapagic (2015) suggest that GWP values are lower for CCS systems and not for CCU frameworks, even if the first can have higher values for other impact categories. The same conclusion is achieved by Aldaco et al. (2019) analyzing a CCU supply chain producing formic acid: a CCS technology can ensure higher reduction of CO_2 emissions, but a CCU system

has better economic potentials and lower fossil consumptions, especially when renewable energies are integrated into the process.

Other LCA analyses are carried out for CCU supply chains, where CO_2 may be used for mineral carbonation (Khoo et al., 2011a,b; Nduagu et al., 2012; Pan et al., 2017). In Khoo et al. (2011a), CO_2 is captured from a natural gas combined cycle power plant and used to produce $MgCO_3$: 106.9-175.9 kg of CO_2 can be avoided per 1 MWh. A higher value of avoided CO_2 can be achieved through the direct mineralization, as found in Khoo et al. (2011b): 215-154 kg of CO_2 can be avoided per 1 MWh. Environmental advantages for this process are also reported by Nduagu et al. (2012): 483 kg of CO_2 can be avoided per 1 ton of mineralized CO_2, while in Pan et al. (2017) 1 ton of $CO_{2\text{-eq}}$ can be avoided per 1 ton of steel slag. Han and Lee (2013) develop a mathematical model to evaluate the environmental impact of a CCU supply chain, where CO_2 is used to produce polymers and bio-butanol, in Korea. Results show that in order to reduce the environmental impact, it is important to reduce gas-MEA capture systems.

Von der Assen and Bardow (2014) analyze a LCA analysis for a CCU supply chain, where CO_2, captured from lignite power plant, is used for polyol production in the polyurethane industry. Results show that the production of polyol at 20 %wt of CO_2 can reduce the GHG emissions by 11-19% and save the fossil resources by 13-16%.

LCA analyses are present in the literature also for CCUS supply chains, especially for CO_2-EOR systems. This has higher CO_2 emissions compared to a CCS supply chain (Yujia et al., 2014).

Hertwich et al. (2008) carry out a LCA analysis for a supply chain with CO_2-EOR in the utilization section, set in Halten (Norwegian Sea). In the system, CO_2 from a combined cycle power plant is captured by post-combustion ammine absorption. A reduction of GHG emissions of 80% is obtained.

Other studies about LCA analyses for CO_2-EOR technology are developed showing the environmental advantages of this system. Cooney et al. (2015) study a LCA analysis for CO_2-EOR in a carbon supply chain, considering different system boundaries: gate-to-gate, cradle-to-gate and cradle-to-grave. Results show that only the anthropogenic CO_2-EOR case provides emissions lower than the conventionally produced crude. Environmental benefits are also suggested by Lacy et al. (2015): in a CO_2-EOR supply chain, 251 kg $CO_{2\text{-eq}}$ per oil barrel are calculated.

Hussain et al. (2013) find that a coal and biomass IGCC with CO_2-EOR, as well as a natural gas and biogas NGCC with CO_2-EOR, can be attractive alternatives for reducing GHG emissions.

Negative carbon emissions are obtained by Hornafius and Hornafius (2015) in a CCUS supply chain where CO_2 is used for the recovery of oil. Azzolina et al. (2017) analyzing a CCUS system with CO_2-EOR find that the produced oil is a lower carbon fuel with an emission factor lower than the traditional oil production.

An environmental analysis is also considered by Jiang et al. (2017): using a CO_2-EOR system it is found that total CO_2 emissions are of 114.69-121.50 Mt $CO_{2\text{-eq}}$, 222.95-236.19 Mt $CO_{2\text{-eq}}$, and 49.09-51.96 Mt $CO_{2\text{-eq}}$ for a IGCC, PC, and oxy-fuel plant, respectively.

A more detailed study can characterize the analyzed system with specific geographic information. On this point of view, Abotalib et al. (2016) develop a LCA analysis for a carbon supply chain with CO_2-EOR as utilization site in the USA. Results show that the supply chain using CO_2 from ethanol plant is the best alternative and the environmental analysis depended on the specific crude recovery rate.

Other products can be considered in a CCUS supply chain.

In the work of Yue and You (2015) CO_2 is stored and used to cultivate algae for biofuel production, in Texas. Environmental and economic analyses are developed by using a mixed integer non-linear programming model. Results show that a reduction of 80% on CO_2 emission can produce 187 Mgal of renewable diesel, while CO_2 can be stored and used at an average cost of 45.5 \$/tonCO_2. A LCA analysis for a CCUS supply chain in refineries producing dimethyl ether and polyol is developed by Fernandez-Dacosta et al. (2018). They find that the combination of CO_2 utilization and storage is the best alternative to reduce the climate change potential, being at the same time economically feasible.

From the above literature analysis, it results that only a few CO_2-based products are taken into consideration for a LCA analysis of a carbon supply chain. Also, the previous studies are not considering the application of a LCA analysis on a carbon supply chain at large scale and a simple analysis is considered in order to evaluate and quantify the befits of these technologies.

I.4.4 Modelling of a methanol reactor

Due to the environmental problems that have arisen in recent years, as mentioned above methanol has received the attention of many researchers, being a key product of large-scale chemistry for the development of a circular economy. Different works are present in the literature about modelling of a methanol reactor, in dynamic and steady state conditions, mainly fed by the syngas.

Each of them is based on specific assumptions, with the aim to simplify complex phenomena and to reduce computational time (Bozzano and Manenti, 2016). Manenti et al. (2011) suggest three different classes to group together mathematical models for a methanol reactor: pseudo-homogeneous models, described by means of molar balances (composition and temperature gradients between gas and solid phases and the progressive decrease in the molar flow rate are neglected), pseudo-homogeneous models based on mass balance (only gradients between solid and gas phase are neglected, while mole numbers are decreasing along the reactor) and heterogeneous models (gradients between gas and solid phase and the decrease in the number of total moles are considered).

Models can be also classified as one- (1-D) and two-dimensional (2-D) models, where radial phenomena are considered in the latter approach.

Kordabadi and Jahanmiri (2005) develop a mathematical heterogeneous model in order to find the temperature profile along the reactor, maximizing the methanol production rate at steady state and dynamic conditions. They find that, in the optimal conditions, the yield is improved by 2.9% with reference to that

in the base case. More complex reactor systems are also considered. Rahimpour (2008) models two stages methanol reactors: syngas is heated by heat released in the second reactor and then is fed to the first reactor. In this way, a better temperature profile ensures lower catalyst deactivation and higher methanol production. In a different work, Rahimpour et al. (2009) develop a one-dimensional pseudo-homogeneous model for a spherical reactor in order to maximize the methanol production. A spherical reactor is also considered by Sadeghi et al. (2014): reactor size, overall feed flow rate and composition, inlet temperature have significant effect on catalyst activity and methanol production. A similar work is developed by Parvasi et al. (2008). Modelling an industrial methanol reactor is carried out by Yusup et al. (2010) in order to evaluate the effect of inlet temperature, coolant inlet temperature and flow rate on the reactor performance.

Modelling membrane reactors, permeable to H_2O, for methanol production is also investigated (Rahimpour and Elekaei, 2009; Gallucci and Basile, 2007; Farsi and Jahanmiri, 2012; Samimi et al., 2018), as well as methanol reactor with the adsorption of CO and H_2O (Leonzio, 2020) or with the adsorption of only H_2O (Bayat et al., 2014; Abashar and Al-Rabiah, 2018).

Regarding dynamic models, Abrol and Hilton (2012) develop a dynamic model for a reactor-separator system, with the aim to evaluate the performances of the process at different flow rate of syngas. In addition, Manenti et al. (2013) analyze a dynamic model for a methanol reactor and study the transformation of the hyperbolic PDE system into a parabolic PDE system that allows to estimate accurately the location of the hot spot, in a short computing time.

Regarding the optimization purpose, Bozzano et al. (2017) carry out a numerical optimization to find the optimal composition of syngas, with the aim to maximize methanol production. An additional optimization work is developed by Vita et al. (2018).

Few works consider radial phenomena inside a methanol reactor. In addition to Hartig and Keil (1993), Montebelli et al. (2013) develop a two dimensional heterogeneous model comparing a structured multi-tubular reactor, loaded with copper honeycomb monoliths or alternatively with open cell foams, with a packed bed of catalyst pellets. Results show that the structured reactor is predicted to operate with a lower recycle ratio and hot spot temperature. A two dimensional pseudo-homogeneous model is also proposed by Meyer et al. (2016) comparing two different kinetic approaches (Graaf et al. (1988b) and Vanden Bussche and Froment (1996)) and assuming only CO_2 and H_2 in the feed. Axial profiles show that the latter kinetic model predicts higher reverse water gas shift and methanol formation reaction rates than those calculated by the former kinetic model, especially in the first section of the reactor.

Some mathematical models take into account also catalyst deactivation, as in Løvik et al. (1999), Rezaie et al. (2005). Zahedi et al. (2005) and in Farsi and Jahanmiri (2014) considering a dynamic heterogeneous one-dimensional model for a membrane reactor permeable to H_2O.

When the modelling of a methanol reactor is developed, different kinetic models can be considered.

Vanden Bussche and Froment (1996) as well as Kubota et al. (2001) and Askgaard et al. (1995) suggest to use two independent reactions (CO_2 hydrogenation and reverse water gas shift reaction). On the other hand,

three reactions (hydrogenation of CO_2 and CO with reverse water gas shift) are considered by Graaf et al. (1988), Seidel et al. (2018) and Takagawa et al. (1987). Another mechanism supposes the hydrogenation of CO_2 and CO without considering the water gas shift reaction. Klier et al. (1982), Ma et al. (2009) and McNeil et al. (1989) develop a kinetic based on this assumption. The last mechanism is assumed by Villa et al. (1985): they consider CO as the main carbon source for methanol.

A comparison between Graaf et al. (1988), Vanden Bussche and Froment (1996), Seidel et al. (2018), Ma et al. (2009) and Villa et al. (1985) is suggested by Slotboom et al. (2020), considering a large database of experimental data. Results show that the model of Seidel et al. (2018) better predict the data in terms of a mean squared error analysis, but is complex and has highly correlated parameters. For this reason, in the work of Slotboom et al. (2020) a new kinetic model with six parameters and based on that of Vanden Bussche and Froment (1996) is proposed and regressed with experimental data. Results show that the suggested new model describes the trend of experimental data very well and it is statistically valid.

From the above literature analysis it is evident that a thorough investigation is still lacking about the packed bed methanol reactor described with a two dimensional model, fed by CO_2 and H_2. In fact, most of published works are about the one dimensional model for an optimization aim, or to evaluate specific aspects like catalyst deactivation or reaction rate equations. Moreover, a comparison between different reactor schemes (that want to overcome thermodynamic and kinetic limitations) based on the efficiency is missing in the literature.

I.5 Scope of the thesis

As already mentioned in this introduction, in Europe, Germany, the UK and Italy are the countries with higher CO_2 emissions.

The principal aim of this research is to develop a mathematical model to design and optimize a large scale CCUS supply chain for these European countries that can be suggested as a solution to meet the various targets for GHG emissions reduction.

For a more realistic analysis, the developed models are considered under a deterministic and stochastic point of view, also considering a simultaneous optimization of economic and environmental aspects.

In addition, to be sure that the suggested carbon supply chains can achieve the set targets, a LCA analysis is developed.

In a circular economy, CO_2 utilization is the main objective and not its storage, because this last option leads to an accumulation of this gas. Then, it is not possible to solve the problem of CO_2 emissions only with the storage, but the utilization option should have an important role. With this consideration, the most important utilization pathway, as reported in the literature, as the methanol production via hydrogenation reaction, is analyzed more deeply, developing 1-D and 2-D models for a Lurgy reactor, i.e. with heat transfer at the catalytic tube surface. Also, an equilibrium analysis of different reactor configurations

designed to overcome the thermodynamic limitation is carried out. This is, then, another aim of this research.

I.6 Thesis outline

Chapter 2 focuses on an equilibrium analysis of different reactor configurations, fed by CO_2 and H_2, aimed at methanol production. A 1-D and 2-D mathematical model for the most efficient methanol reactor are also presented, under kinetic regime.

Chapter 3 describes the mathematical model utilized to design carbon dioxide supply chains and suggests a CCUS supply chain of Germany, where CO_2 is used to produce methanol via methane dry reforming. An excessive methanol production is predicted in order to meet the environmental constraints imposed on Germany, at the minimum cost.

Chapter 4 is addressed to overcome the problem underlined in the previous chapter, then for the CCUS supply chain of Germany more utilization options are considered in the utilization section.

Chapter 5 presents a mathematical model for the design and optimization of different CCUS supply chains of Italy. These have different storage sites and a comparison with a CCU system is also considered.

Chapter 6 describes the mathematical model for a CCUS supply chain of the UK: three different storage sites are taken into account.

In Chapter 7, for the carbon supply chains studied previously, an innovative objective function is taken into account considering carbon tax, economic incentives and revenues. A sensitivity analysis is performed to verify which terms are more significant.

Chapter 8 presents a LCA analysis for the carbon supply chains developed before, and a sensitivity analysis is carried out to evaluate the influence of CO_2 storage and utilization on the environmental impact.

Chapter 9 considers a multiple objective optimization of the CCUS framework of Italy, Germany and the UK: total costs and CO_2 captured are simultaneously optimized.

In Chapter 10, the deterministic models of supply chains are converted into stochastic models, to take into account the uncertainty of the production cost of different CO_2-based products.

Chapter 11 presents the improvements done in the mathematical model describing the supply chains.

Finally, overall conclusions and outlooks are presented in Chapter 12.

References

Abashar, M.E.E. 2004. Coupling of steam and dry reforming of methane in catalytic fluidized bed membrane reactors, Int. J. Hydrogen Energy 29 (8) 799–808.

Abashar, M.E.E.E., Al-Rabiah, A.A. 2018. Investigation of the efficiency of sorption-enhanced methanol synthesis process in circulating fast fluidized bed reactors. Fuel Processing Technology 179 387–398

Abrol, S., Hilton, C.M. 2012. Modeling, simulation and advanced control of methanol production from variable synthesis gas feed. Comput. Chem. Eng. 40, 117-131.

Abotalib, M., Zhao, F., Clarens, A., 2016. Deployment of a Geographical Information System Life Cycle Assessment Integrated Framework for Exploring the Opportunities and Challenges of Enhanced Oil Recovery Using Industrial CO2 Supply in the United States, ACS Sustainable Chem. Eng. 4, 4743−4751.

Agralıa, S., Üçtug, F.G., Türkmen, B.A. 2018. An optimization model for carbon capture & storage/utilization vs. carbon trading: A case study of fossil-fired power plants in Turkey. Journal of Environmental Management 215 305-315

AHDB Horticulture. 2019. Available at: https://horticulture.ahdb.org.uk/sources-co2

Ajayi, T., Gomes, J.S., Bera, A., 2019. A review of CO_2 storage in geological formations emphasizing modeling, monitoring and capacity estimation approaches, Petroleum Science, 16, 1028–1063.

Akgul, O., Mac Dowell, N., Papageorgiou, L.G., Shah, N., 2014. A mixed integer nonlinear programming (MINLP) supply chain optimisation framework for carbon negative electricity generation using biomass to energy with CCS (BECCS) in the UK. Int. J. Greenhouse Gas Control 28, 189–202.

Alberici, S., 2017 et al. Assessing the potential of CO2 utilization in the UK. Report Available at: https://assets.publishing.service.gov.uk/government/uploads/system/uploads/attachment_data/file/799293/SISUK17099AssessingCO2_utilisationUK_ReportFinal_260517v2__1_.pdf

Aldaco, R., Butnar, I., Margallo, M., Laso, J., Rumayor, M., Dominguez-Ramos, A., Irabien, A., Dodds, P.E., 2019. Bringing value to the chemical industry from capture, storage and use of CO2: A dynamic LCA of formic acid production, Science of the Total Environment 663, 738–753

Al-Kalbani, H., Xuan, J., García, S., Wang, H. 2016. Comparative energetic assessment of methanol production from CO2: chemical versus electrochemical process, Appl. Energy 165, 1–13.

Al-musleh, E.I., Mallapragada, D.S., Agrawal, R. 2014. Continuous power supply from a baseload renewable power plant, Appl. Energy 122, 83–93.

Ampelli, C., Perathoner, S., Centi, G. 2015 CO_2 utilization: an enabling element to move to a resource- and energy-efficient chemical and fuel production. Phil. Trans. R. Soc. A 373: 20140177.

Ampomah, W., Balch, R.S., Grigg, R.B., McPherson, B., Will, R.A., Lee, S.Y., Dai, Z., Pan, F. 2016. Co-optimization of CO_2-EOR and storage processes in mature oil reservoirs, Greenh. Gases Sci. Technol. 7, 128–142.

Allen, M., Dube, O.P., Solecki, W., Aragón-Durand, F., et al. 2018. Chapter 1: Framing and Context. IPCC SR15 2018. 47–91.

Aloisi, I., Di Giuliano, A., Di Carlo, A., Foscolo, P.U., Courson, C., Gallucci, K. 2017. Sorption enhanced catalytic Steam Methane Reforming: Experimental data and simulations describing the behaviour of bi-functional particles. Chemical Engineering Journal 314 570–582.

Aresta, M., Dibenedetto, A., Angelini, A., 2013. The changing paradigm in CO_2 utilization. Journal of CO_2 Utilization 3–4, 65–73.

Artz, J., Muller, T.E., Thenert, K., Kleinekorte, J., Meys, R., Sternberg, A., Bardow, A. 2018. Sustainable Conversion of Carbon Dioxide: An Integrated Review of Catalysis and Life Cycle Assessment. Chem. Rev. 118, 434−504

Askgaard, T.S., Norskov, J.K., Ovesen, C.V., Stoltze, P. 1995. A Kinetic Model of Methanol Synthesis, Journal of Catalysis 156 (2) 229–242

Atsonios, K., Panopoulos, K.D., Kakaras, E. 2016. Thermocatalytic CO2 hydrogenation for methanol and ethanol production: process improvements, Int. J. Hydrogen Energy 41, 792–806.

Atsonios, K., Panopoulos, K.D., Kakaras, E. 2016. Investigation of technical and economic aspects for methanol production through CO2 hydrogenation, Int. J. Hydrogen Energy 41, 2202–2214.

Azzolina, N.A., Peck, W.D., Hamling, J.A., Gorecki, C.D., Ayash, S.C., Doll, T.E., et al. 2016. How green is my oil? A detailed look at greenhouse gas accounting for CO2-enhanced oil recovery (CO2-EOR) sites. Int J Greenhouse Gas Control 51 369–79.

Azzolina, N.A., Hamling, J.A., Peck, W.D., Gorecki, C.D., Nakles, D.V., and Melzer, L.S., 2017. A life cycle analysis of incremental oil produced via CO2 EOR, Energy Procedia 114, 6588 – 6596.

Baileraa, M., Lisbona, P., Romeo, L.M., Espatolero, S. 2017. Power-to-Gas projects review: Lab, pilot and demo plants for storing renewable energy and CO2. Renewable and Sustainable Energy Reviews 69, 292–312.

Bakken, B.H., von Streng Velken, I., 2008. Linear models for optimization of infrastructure for CO2 capture and storage. IEEE T. Energy Conver. 23, 824–833.

Balan, O.M., Buga, M.R., Bildea, C.S. 2016. Conceptual design, performance and economic evaluation of carbon dioxide methanation plant. Rev. Chim. 67 (11) 2237-2242.

Baojian, Z., Chisun, P., Caijun, S., 2013. CO2 curing for improving the properties of concrete blocks containing recycled aggregates, Cement & Concrete Composites 42, 1–8.

Barbieri, G., Marigliano, G., Golemme, G., Drioli, E. 2002. Simulation of CO2 hydrogenation with CH3OH removal in a zeolite membrane reactor, Chem. Eng. J. 85 53–59.

Bassani, A., Pirola, C., Maggio, E., Pettinau, A., Frau, C., Bozzano, G., Pierucci, S., Ranzi, E., Manenti, F. 2016. Acid Gas to Syngas (AG2STM) technology applied to solid fuel gasification: Cutting H2S and CO2 emissions by improving syngas production, Appl. Energy 184, 1284–1291

Bassano, C., Deiana, P., Lietti, L., Visconti, C.G., 2019. P2G movable modular plant operation on synthetic methane production from CO2 and hydrogen from renewables sources. Fuel 253, 1071-1079.

Bayat, M., Dehghani, Z., Rahimpour, M.R., 2014. Sorption-enhanced methanol synthesis in a dual-bed reactor: Dynamic modeling and simulation. Journal of the Taiwan Institute of Chemical Engineers 45 2307–2318

Bellotti, D., Rivarolo, M., Magistri, L., Massardo, A.F. 2017. Feasibility study of methanol production plant from hydrogen and captured carbon dioxide, J. CO_2 Util. 21, 132–138

Bertau, M. Offermanns, H., Plass, L., Schmidt, F., Wernicke, H.J. 2014. Methanol: The Basic Chemical and Energy Feedstock of the Future, Springer-Verlag, Berlin Heidelberg.

Bhola, V., Swalaha, F., Kumar, R.R., Singh, M., Bux, F. 2014. Overview of the potential of microalgae for CO2 sequestration. Int. J. Environ. Sci. Technol. 11:2103–2118

BioCO_2, 2019. Available at: https://www.vtt.fi/sites/BioCO_2/en

Blanco, H., Nijs, W., Ruf, J., Faaij, A. 2018. Potential of power-to-methane in the EU energy transition to a low carbon system using cost optimization, Appl. Energy 232, 323–340.

Blanco, H., Faaij, A. 2018. A review at the role of storage in energy systems with a focus on Power-to-Gas and long-term storage. Renew Sustain Energy Rev 81, 1049–86.

BP, 2017. BP statistical review of world energy 2017. Available at: http://www.bp.com/en/global/corporate/energy-economics/statistical-review-of-world-energy/downloads.html

Bozzano, G., Manenti, F. 2016. Efficient methanol synthesis: perspectives, technologies and optimization strategies, Prog. Energy Combust. Sci. 56, 71–105.

Bozzano, G., Pirola, C., Italiano, C., Pelosato, R., Vita, A., Manenti, F. 2017. Biogas: a possible new pathway to methanol?. In: Espu~na, A., Graells, M., Puigjaner, L. (Eds.), 27th European Symposium on Computer Aided Process Engineering, 40 (2017) 523-528.

Brunner, C., Thomas, A. 2014. Arbeitspaket 6: Gasnetzanalysen und Wirtschaftlichkeitsbetrachtung, Wasser-Praxis 65, 59–65.

Buchholz, O.S., van der Ham, A.G.J., Veneman, R., Brilman, D.W.F., Kersten, S.R.A. 2014. Power-to-gas: storing surplus electrical energy. A design study, Energy Procedia 63, 7993–8009.

Budinis, S., Krevor, S., Dowell, N.M., Brandon, N., Hawkes, A. 2018. An assessment of CCS costs, barriers and potential. Energy Strategy Reviews 22 61–81

Bui, M., et al. 2018. Carbon capture and storage (CCS): the way forward. Energy Environ. Sci.,11, 1062-1176

Buttler, A., Spliethoff, H. 2018. Current status of water electrolysis for energy storage, grid balancing and sector coupling via power-to-gas and power-to-liquids: a review. Renew Sustain Energy Rev 82 2440–54.

Catarina Faria, A., Miguel, C.V., Madeira, L.M., 2018. Thermodynamic analysis of the CO_2 methanation reaction with in situ water removal for biogas upgrading, Journal of CO_2 Utilization 26, 271–280.

Chalabi, Z.S., Biro, A., Bailey, B.J., Aikman, D.P., Cockshull, K.E. 2002. Optimal control strategies for carbon dioxide enrichment in greenhouse tomato cropsdpart 1: using pure carbon dioxide. Biosyst Eng 81 421.

Chang, R., Choi, D., Kim, M. H., and Park, Y. 2017b. Tuning crystal polymorphisms and structural investigation of precipitated calcium carbonates for CO2 mineralization. *ACS Sustain. Chem. Eng.* 5, 1659–1667

Chang, R., Kim, S., Lee, S., Choi, S., Kim, M., and Park, Y. 2017a Calcium Carbonate Precipitation for CO2 Storage and Utilization: A Review of the Carbonate Crystallization and Polymorphism. Front. Energy Res. 5 (17) 1-12.

Chauvy, R., Meunier, N., Thomas, D., De Weireld, G. 2019. Selecting emerging CO_2 utilization products for short- to mid-term deployment. Applied energy 236 662-680.

Chen, H., Wang, Z., Chen, X., Chen, X., Wang, L., 2017. Increasing permeability of coal seams using the phase energy of liquid carbon dioxide. Journal of CO2 Utilization, 19, 112–119.

Chen, B., Pawar, R.J. 2019. Capacity assessment and co-optimization of CO2 storage and enhanced oil recovery in residual oil zones. Journal of Petroleum Science and Engineering 182, 106342

Cheng, L.H., Rahaman, M.S.A., Yao, R., Zhang, L., Xu, X.H., Chen, H.L. 2014. Study on microporous supported ionic liquid membranes for carbon dioxide capture, Int. J. Greenh. Gas Control 21 82–90.

Chwoła, T., Spietz, T., Więcław-Solny, L., Tatarczuk, A., Krótki, A., Dobra, S., Wilk, A., Tchórz, J., Stec, M., Zde, J. 2020. Pilot plant initial results for the methanation process using CO2 from amine scrubbing at the Łaziska power plant in Poland. Fuel. 263 116804.

Cho, S., Kim, S., Kim, J. 2019. Life-cycle energy, cost, and CO2 emission of CO2-enhanced coalbed methane (ECBM) recovery framework. Journal of Natural Gas Science and Engineering 70, 102953.

Choia, J.H., Woob, H.C., Suha, D.J., 2014. Pyrolysis of seaweeds for bio-oil and bio-char production, Chem. Eng. Trans. 37, 121–126.

Colella, C., Cejka, J., Van Bekkum, H., Corma, A., Schueth, F., 2007. Introduction to Zeolite Science and Practice. Elsevier, Amsterdam, 999-1035.

Cooney, G., Littlefield, J., Marriott, J., Skone, T.J. 2015. Evaluating the climate benefits of CO2-enhanced oil recovery using life cycle analysis. Environ Sci Technol 49 (12) 7491–500.

Corsten M., Ramirez A., Shen L., Koornneef J., Faaij A. 2013. Environmental impact assessment of CCS chains e lessons learned and limitations from LCA literature. Int J Greenh Gas Control 13, 59-71.

Cuellar-Franca, R.M., Azapagic, A., 2015b. Carbon capture, storage and utilisation technologies: a critical analysis and comparison of their life cycle environmental impacts. J. CO2 Util. 9, 82–102.

d'Amore, F., Sunny, N., Iruretagoyena, D., Bezzo, F., Shah, N., 2019. European supply chains for carbon capture, transport and sequestration, with uncertainties in geological storage capacity: insights from economic optimisation. Comput. Chem. Eng. 129, 106521

d'Amore, F., Bezzo, F., 2017. Economic optimisation of European supply chains for CO2 capture, transport and sequestration. Int. J. Greenh. Gas Control 65.

d'Amore, F., Mocellin, P., Vianello, C., Maschio, G., Bezzo, F., 2018. Economic optimisation of European supply chains for CO2 capture, transport and sequestration, including societal risk analysis and risk mitigation measures. Appl. Energy 223, 401-415.

Daia, Z., Viswanathan, H., Xiao, T., Middleton, R., Pan, F., Ampomah, W., Yang, C., Zhoud, Y., Jia, W., Lee, S.Y., Cather, M., Balch, R., McPherson, B. 2017. CO2 Sequestration and Enhanced Oil Recovery at Depleted Oil/Gas Reservoirs. Energy Procedia 114, 6957–6967.

Davidson, C.L., Dahowski, R.T., Dooley, J.J., 2011. A quantitative comparison of the cost of employing EOR-coupled CCS supplemented with secondary DSF storage for two large CO2 point sources. Energy Procedia 4, 2361–2368.

Delacourt, C., Ridgway, P.L., Kerr, J.B., Newman, J. 2008. Design of an electrochemical cell making syngas (CO + H2) from CO2 and H2O reduction at room temperature, J. Electrochem. Soc. 155 (1) B42–B49.

Di Giuliano, A., Gallucci, K. 2018. Sorption enhanced steam methane reforming based on nickel and calcium looping: a review. Chemical Engineering & Processing: Process Intensification 130 240–252

Di Giuliano, A., Giancaterino, F., Courson, C., Foscolo, P.U., Gallucci, K. 2018a. Development of a Ni-CaO-mayenite combined sorbent-catalyst material for multicycle sorption enhanced steam methane reforming. Fuel 234 687–699

Di Giuliano, A., Giancaterino, F., Gallucci, K., Foscolo, P.U., Courson, C. 2018b. Catalytic and sorbent materials based on mayenite for sorption enhanced steam methane reforming with different packed-bed configurations. International Journal of Hydrogen Energy. 43 21279-21289.

Di Giuliano, A., Gallucci, K., Giancaterino, F., Courson, C., Foscolo, P.U. 2019. Multicycle sorption enhanced steam methane reforming with different sorbent regeneration conditions: Experimental and modelling study. Chemical Engineering Journal 377 119874.

Dickinson, R.R., Battye, D.L., Linton, V.M., Ashman, P.J., Nathan, G.J. 2010. Alternative carriers for remote renewable energy sources using existing CNG infrastructure, Int. J. Hydrogen Energy 35 (3) 1321–1329.

Dindi, A., Quang, D.V., Vega, L.F., Nashef, E., Abu-Zahr, M.R.M. 2019. Applications of fly ash for CO2 capture, utilization, and storage. Journal of CO_2 Utilization 29, 82–102.

Dion, L.M., Lefsrud, M., Orsat, V. 2011. Review of CO2 recovery methods from the exhaust gas of biomass heating systems for safe enrichment in greenhouses. Biomass and bioenergy 35 3422-3432.

Dong, J., Gruda, N., Li, X., Tang, Y., Zhang, P., Duan, Z. 2020. Sustainable vegetable production under changing climate: The impact of elevated CO2 on yield of vegetables and the interactions with environments-A review, Journal of Cleaner Production 253, 119920.

Dou, J., Zhang, R., Hao, X., Bao, Z., Wu, T., Wang, B., Yu, F. 2019. Sandwiched SiO2@Ni@ZrO2 as a coke resistant nanocatalyst for dry reforming of methane. Applied Catalysis B: Environmental 254 (2019) 612–623.

Duraccio, V., Gnoni, M.G., Elia, V. 2015. Carbon capture and reuse in an industrial district: A technical and economic feasibility study. Journal of CO2 Utilization 10 23–29.

Edwards, D.R. 2008. Towards a plant-based method of guiding CO2 enrichment in greenhouse tomato. Plant Science Department. Vancouver: University of British Columbia.

El-Hassan, H., Shao, Y.X., 2014. Carbon storage through concrete block carbonation curing, J. Clean Energy Technol. 2 (3), 287-291.

Eloneva, S., Teir, S., Salminen, J., Fogelholm, C.-J., and Zevenhoven, R. 2008a. Fixation of CO2 by carbonating calcium derived from blast furnace slag. Energy 33, 1461–1467.

EPA, 2019. United States Environmental Protection Agency. Available at: https://www.epa.gov/ghgemissions/overview-greenhouse-gases

European Commission, 2011, A Resource-efficient Europee-flagship Initiative under the Europe 2020 Strategy, COM, 2011, p. 21

European Commission, 2019, 2030 climate & energy framework, Available at: https://ec.europa.eu/clima/policies/strategies/2030_en

Fan, J.L., Xu, M., Lid, F., Yang, L., Zhang, X. 2018. Carbon capture and storage (CCS) retrofit potential of coal-fired power plants in China: The technology lock-in and cost optimization perspective. Applied Energy 229 326–334.

Fan, J.L., Xu, M., Yang, L., Zhang, X., Lie, F., 2019. How can carbon capture utilization and storage be incentivized in China? A perspective based on the 45Q tax credit provisions, Energy Policy 132, 1229–1240.

Fana, Y., Deng, C., Zhanga, X., Lid, F., Wanga, X., Qiao, L. 2018. Numerical study of CO2-enhanced coalbed methane recovery. International Journal of Greenhouse Gas Control 76, 12–23.

Farajzadeha, R., Eftekhari, A.A., Dafnomilisa, G., Lake, W., Bruining, J. 2020. On the sustainability of CO2 storage through CO2 – Enhanced oil recovery. Applied Energy 261, 114467.

Farfan, J., Fasihi, M., Breyer, C. 2019. Trends in the global cement industry and opportunities for long-term sustainable CCU potential for Power-to-X. Journal of Cleaner Production 217 821-835.

Farniaei, M., Abbasi, M., Rahnama, H., Rahimpour, M.R., Shariati, A. 2014. Syngas production in a novel methane dry reformer by utilizing of tri-reforming process for energy supplying: modeling and simulation, J. Nat. Gas Eng. 20, 132–146.

Farsi, M., Jahanmiri, A. 2011. Application of water vapor and hydrogen perm-selective membranes in an industrial fixed-bed reactor for large scale methanol production, Chem. Eng. Res. Des. 89 (12) 2728–2735.

Farsi, M., Jahanmiri, A. 2012. Dynamic modeling of a H2O-permselective membrane reactor to enhance methanol synthesis from syngas considering catalyst deactivation. Journal of Natural Gas Chemistry 21 407–414.

Farsi, M., Jahanmiri, A. 2014. Dynamic modeling and operability analysis of a dual-membrane fixed bed reactor to produce methanol considering catalyst deactivation. Journal of Industrial and Engineering Chemistry 20 2927–2933

Feng, N., Peng, G., 2005. Applications of natural zeolite to construction and building materials in China. Constr. Build. Mater. 19 (8), 579-584.

Fernández-Dacosta, C., Van Der Spek, M., Hung, C.R., Oregionni, G.D., Skagestad, R., Parihar, P., et al. 2017. Prospective techno-economic and environmental assessment of carbon capture at a refinery and CO2 utilisation in polyol synthesis. J CO2 Util 21 405–22.

Fidalgo, F., Domínguez, A., Pis, J.J., Menéndez, J.A. 2008. Microwave-assisted dry reforming of methane. International Journal of Hydrogen Energy. 33 (16) 4337-4344.

Gai, S., Yub, J., Yuc, H., Eagle, J., Zhao, H., Lucas, J., Doroodchi, E., Moghtaderi, B. 2016. Process simulation of a near-zero-carbon-emission power plant using CO2 as the renewable energy storage medium, Int. J. Greenh. Gas Control 47, 240–249.

Galan, I., Andrade, C., Mora, P., Sanjuan, M.A. 2010. Sequestration of CO2 by concrete carbonation, Environ. Sci. Technol. 44 (8) (2010) 3181-3186

Gallucci, F., Paturzo, L., Basile, A. 2004. An experimental study of CO_2 hydrogenation into methanol involving a zeolite membrane reactor, Chem. Eng. Process 43, 1029–1036.

Gallucci, F., Basile, A. 2007. A theoretical analysis of methanol synthesis from CO2 and H2 in a ceramic membrane reactor, International Journal of Hydrogen Energy 32 5050–5058.

Garga, A., Shuklaa, P.R., Parihara, S., Singh, U., Kankal, 2017. Cost-effective architecture of carbon capture and storage (CCS) grid in India. International Journal of Greenhouse Gas Control 66 129–146.

Garcia Ramos et al. (2016) A thermoplastic polyurethane based on polyether carbonate polyol. Patent WO 2016/120399 Al

Garrison, E., 2019. Available at: https://mypages.iit.edu/~smart/garrear/fuelcells.htm

Gassner, M., Maréchal, M. 2012. Thermo-economic optimisation of the polygeneration of synthetic natural gas (SNG), power and heat from lignocellulosic biomass by gasification and methanation, Energy Environ. Sci. 5 (2) 5768.

Gerdemann, S. J., O'Connor, W. K., Dahlin, D. C., Penner, L. R., and Rush, H. 2007. Ex situ aqueous mineral carbonation. Environ. Sci. Technol. 41, 2587–2593.

Ghanbari, H., Helle, M., Saxén, H. 2015. Optimization of an Integrated Steel Plant with Carbon Capturing and Utilization Processes. IFAC-PapersOnLine 48-17 012–017

Girdon, P., Gloger, C., Gonzalez, D., Henneqiun, J., Krinninger, K., de Lorenzi, L., Wilyman, P. 2006 Minimum Specifications for Food Gas Applications; European Industrial Gases Association AISBL: Brussels, Belgium.

Global CCS Institute, 2019. Available at: https://www.globalccsinstitute.com/wp-content/uploads/2018/12/Global-CCS-Institute-Fact-Sheet_Transporting-CO2-1.pdf

Global CCS Institute. 2011. Accelerating the Uptake of CCS: Industrial Use of Captured Carbon Dioxide; Parsons Brickerhoff: New York, NY, USA.

Gorrea, J., Ruossa, F., Karjunenb, H., Schaffertc, J., Tynjälä, T. 2020. Cost benefits of optimizing hydrogen storage and methanation capacities for Power-to-Gas plants in dynamic operation. Applied Energy, 257 113967.

Gokon, N. et al., 2011. Kinetics of methane reforming over Ru/γ-Al2O3-catalyzed metallic foam at 650–900 °C for solar receiver-absorbers, Int. J. Hydrogen Energy 36 (1) 203–215.

Graaf, G.H., Winkelman, J.G.M., Stamhuis, E.J., Beenackers, A.A.C.M. 1988a. Kinetics of the three phase methanol synthesis, Chem. Eng. Sci. 43, 2161–2168.

Graaf, G.H., Stamhuis, E.J., Beenackers, A. 1988b. Kinetics of low-pressure methanol synthesis, Chem. Eng. Sci. 43 (12), 3185-3195.

Grobe, M., Pashin, J.C., Dodge, R.L. 2009. Carbon dioxide sequestration in geological media: state of the science. In: AAPG studies in geology. American Association of Petroleum Geologists, Tulsa, OK; p xi, 715.

Guan, C., Liu, S., Li, C., Wang, Y., Zhao, Y. 2018. The temperature effect on the methane and CO_2 adsorption capacities of Illinois coal. Fuel, 211 241-250.

Guo, J.X., Huang, C., Wang, J.L., Meng, X.Y. 2020. Integrated operation for the planning of CO2 capture path in CCS–EOR project. Journal of Petroleum Science and Engineering. In press.

Gupta, M., Coyle, I., Thambimuthu, K. 2003. Strawman document for CO_2 capture and storage technology roadmap. Canada: Canmet Energy Technology Centre, Natural Resources.

Haid, J., Koss, U. 2001. Lurgi's Mega-Methanol technology opens the door for a new era in down-stream applications, Stud. Surf. Sci. Catal. 136, 399–404.

Haines, M.R., Heidug, W.K., Li., K.J., Moore, J.B. 2002. Progress with the development of a capturing CO2 solid oxide fuel cell. Journal of Power source. 106 377-380.

Hallenbeck, P.C., Leite, G.B., Abdelaziz, A.E.M. 2014. Exploring the diversity of microalgal physiology for applications in waste water treatment and biofuel production, Algal Res. 6, 111–118.

Han, J.H., Lee, I.B., 2012. Multiperiod stochastic optimization model for carbon capture and storage infrastructure under uncertainty in CO2 emissions, product prices, and operating costs. Ind. Eng. Chem. Res. 51, 11445-11457.

Han, J.H., Lee, I.B., 2013. A Comprehensive Infrastructure Assessment Model for Carbon Capture and Storage Responding to Climate Change under Uncertainty, Ind. Eng. Chem. Res. 52, 3805−3815.

Harp, G., Harp, K.C., Bergins, T.G., Buddenberg, T., Drach, I., Koytsoumpa, E.I., Sigurbjornsson, O. 2015. Application of Power to Methanol Technology to Integrated Steelworks for Profitability, Conversion Efficiency, and CO2 Reduction, Available at: http://www.mefco2.eu/pdf/2.%20Application%20of%20Power%20to%20Methanol%20Technology%20to%20Integrated%20Steelworks%20for%20Profitability,%20Conversion%20Efficiency,%20and%20CO2.pdf

Hart, A., Gnanendran, N., 2009. Cryogenic CO_2 capture in natural gas, Energy Procedia 1 697–706.

Hartig, F., Keil, F.J., 1993. Large-scale spherical fixed bed reactors: modeling and optimization, Ind. Eng. Chem. Res. 32 (3), 424-437.

Hasan, M.M.F., Boukouvala, F., First, E.L., Floudas, C.A., 2014. Nationwide, Regional, and Statewide CO2 Capture, Utilization, and Sequestration Supply Chain Network Optimization, Ind. Eng. Chem. Res. 53, 7489−7506.

Hasan, M.M.F., First, E.L., Boukouvala, F., Floudas, C.A., 2015. A multi-scale framework for CO2 capture, utilization, and sequestration: CCUS and CCU, Computers and Chemical Engineering 81, 2–21.

Hauri, F., 2006. Natural zeolite from southern Germany: applications in concrete. In: Bowman, R.S., Delap, S.E. (Eds.), Proceedings of 7th International Conference on the Occurrence, Properties, and Utilization of Natural Zeolites. Socorro, 130-131.

He, Z., Jia, Z., Wang, S., Mahoutian, M., Shao, Y. 2019. Maximizing CO2 sequestration in cement-bonded fiberboards through carbonation curing. Construction and Building Materials 213, 51–60

Hepburn, C., Adlen, E., Beddington, J., Carter, E.A., Fuss, S., Dowell, N.M., Minx, J.C., Smith, P., Williams, C.K., 2019. The technological and economic prospects for CO_2 utilization and removal. Nature 575, 87-97.

Hertwich, E.G., Aaberg, M., Singh, B., Strømman, A.H., 2008. Life-cycle assessment of carbon dioxide capture for enhanced oil recovery. Chin. J. Chem. Eng. 16 (3) 343–353.

Hornafius, K.Y., Hornafius, J.S. 2015. Carbon negative oil: A pathway for CO2 emission reduction goals. Int. J. Greenhouse Gas Control 37, 492−503.

Hou, S., Xie, K. 2019. Enhancing the performance of high-temperature H2O/CO2 co-electrolysis process on the solid oxide Sr2Fe1.6Mo0.5O6-d-SDC/ LSGM/Sr2Fe1.5Mo0.5O6-d-SDC cell. Electrochimica Acta 301, 63-68.

Hu, G.Z., He, W.R., Sun, M., 2018. Enhancing coal seam gas using liquid CO2 phase-transition blasting with crossmeasure borehole. Journal of Natural Gas Science and Engineering, 60, 164–173.

Huang, Y., Zheng, Q.P., Fan, N., Aminian, K., 2014. Optimal scheduling for enhanced coal bed methane production through CO2injection. Appl. Energy 113, 1475–1483.

Hussain, D., Dzombak, D.A., Jaramillo, P., Lowry, G.V. 2013. Comparative lifecycle inventory (LCI) of greenhouse gas (GHG) emissions of enhanced oil recovery (EOR) methods using different CO2 sources. Int. J. Greenhouse Gas Control. 16, 129−144.

Iaquaniello, G., Centi, G., Salladini, A., Palo, E., Perathoner, S., Spadaccini, L. 2017. Wasteto-methanol: process and economics assessment, Bioresour. Technol. 243, 611–619.

IEA, 2014. IEA Statistics OECD/IEA Available at: http://www.iea.org/stats/index.asp

Jaffrin, A., Bentounes, N., Joan, A.M., Makhlouf, S. 2003. Landfill biogas for heating greenhouses and providing carbon dioxide supplement for plant growth. Biosyst Eng 86 113.

Jahangiri, H.R., Zhang, D. 2012. Ensemble based co-optimization of carbon dioxide sequestration and enhanced oil recovery. International Journal of Greenhouse Gas Control 8 22–33.

Jaramillo, P., Griffin. W.M., McCoy, S.T. 2009. Life Cycle Inventory of CO2 in an Enhanced Oil Recovery System;

Jarvis, S.M., Samsatli, S. 2018. Technologies and infrastructures underpinning future CO2 value chains: A comprehensive review and comparative analysis. Renew. Sustain. Energy Rev. 85, 46–68.

Jeong, H., Sun, A.Y., Zhang, X., 2018. Cost-optimal design of pressure-based monitoring networks for carbon sequestration projects, with consideration of geological uncertainty. Int. J. Greenh. Gas Control 71, 278–292. doi:10.1016/j.ijggc.2018.02. 014.

Jiang, Y., Lei, Y., Yang, Y., Wang, F., 2018. Life Cycle CO2 Emission Estimation of CCS-EOR System Using Different CO2 Sources, Pol. J. Environ. Stud. 27, 6, 2573-2583

Jiang, J., Rui, Z., Hazlett, R., Lu, J., 2019. An integrated technical-economic model for evaluating CO2 enhanced oil recovery development. Applied Energy 247, 190–211.

Jin, S.W., Li, Y.P., Nie, S., Sun, J., 2017. The potential role of carbon capture and storage technology in sustainable electric-power systems under multiple uncertainties. Renew. Sustain. Energy Rev. 80, 467–480

Jones, C.R., Olfe-Kräutlein, B., Naims, H., Armstrong, K. 2017. The social acceptance of carbon dioxide utilisation: a review and research agenda, Front. Energy Res. 5, 1–14.

Juanes, R., Spiteri, E.J., Orr, F.M., Blunt, M.J. 2006. Impact of relative permeability hysteresis on geological CO_2 storage. Water Resour Res.

Kalyanarengan Ravi, N., Van Sint Annaland, M., Fransoo, J.C., Grievink, J., Zondervan, E., 2017. Development and implementation of supply chain optimization framework for CO2 capture and storage in the Netherlands. Comp. Chem. Eng. 102 40–51.

Kamali, F., and Cinar, Y., 2014. Co-Optimizing Enhanced Oil Recovery and CO_2 Storage by Simultaneous Water and CO_2 Injection, Energy exploration and exploitation, 32 (2) 281-300.

Kemp, A.G., Kasim, S., 2013. The economics of CO2-EOR cluster developments in the UK Central North Sea. Energy Policy 62, 1344–1355

Kenarsari, S.D., Yang, D., Jiang, G., Zhang, S., Wang, J., Russell, A.G., Wei, Q., Fan, M. 2013. Review of recent advances in carbon dioxide separation and capture, RSC Adv. 3 (45) 22739–22773.

Khan, M.T., Saud, K.R., M.Irfan, K.A., Ibrahim, 2018. Curing of Concrete by Carbon Dioxide. International Research Journal of Engineering and Technology. 5 (4) 4410-4414.

Khoo, H.H., Tan, RBH, 2006, Life cycle investigation of CO2 recovery and sequestration", Environmental science & technology, 40, 12, 4016-4024.

Kim, S.H., Jeong, S., Chung, H., Nam, K. 2020. Mechanism for alkaline leachate reduction through calcium carbonate precipitation on basic oxygen furnace slag by different carbonate sources: Application of NaHCO3 and CO2 gas. Waste Management 103 122–127.

King, C., Coleman, S., Cohen, S., Gülen, G., 2011. The economics of an integrated CO2 capture and sequestration system: Texas Gulf Coast case study. Energy Procedia 4, 2588–2595.

Klaring, H.P., Hauschild, C., Heißner, A., Bar-Yosef, B. 2007. Modelbased control of CO2 concentration in greenhouses at ambient levels increases cucumber yield. Agr Forest Meteor 143 208.

Klauber, C., Gräfe, M., 2009. Power, G. Review of Bauxite Residue "Re-use" Options. CSIRO Document DMR-3609, 2009. Available online: http://www.asiapacificpartnership.org/pdf/Aluminium/6th_aluminium_tf_meeting/Review_of_Bauxite_Residue_Re-use_Options_Aug09_sec.pdf

Kleiminger, L., Li, T., Li, K., Kelsall, G.H. 2015. Syngas (CO-H2) production using high temperature micro-tubular solid oxide electrolysers, Electrochim. Acta 179, 565–577.

Klier, K., Chatikavanij, V., Herman, R.G., Simmons, G.W. 1982. Catalytic synthesis of methanol from CO/H2: IV. The effects of carbon dioxide, Journal of Catalysis 74 (2) 343–360.

Klokk, Schreiner, P.F., Pagès-Bernaus, A., Tomasgard, A., 2010. Optimizing a CO2 value chain for the norwegian continental shelf. Energy Policy 38, 6604–6614.

Khoo, H.H., Bu, J., Wong, R.L., Kuan, S.Y., Sharratt, P.N., 2011a. Carbon capture and utilization: Preliminary life cycle CO2, energy, and cost results of potential mineral Carbonation, Energy Proc. 4, 2494–2501.

Khoo, H.H., Sharratt, P.N., Bu, J., Yeo, T.Y., Borgna, A., Highfield, J.G., Bjorklof, T.G., Zevenhoven, R. 2011b. Carbon capture and mineralization in Singapore: Preliminary environmental impacts and costs via LCA. Ind. Eng. Chem. Res. 50 (19) 11350–11357.

Kiss, A.A., Pragt, J.J., Vos, H.J., Bargeman, G., de Groot, M.T. 2016. Novel efficient process for methanol synthesis by CO2 hydrogenation, Chem. Eng. J. 284, 260–269.

Koornneef J., van Keulen T., Faaij A., Turkenburg W. 2008. Life cycle assessment of a pulverized coal power plant with post-combustion capture, transport and storage of CO2. International Journal of Greenhouse Gas Control 2, 448-467.

Koottungal, L., 2014. 2014 worldwide EOR survey. Oil Gas J. (April).

Kordabadi, H., Jahanmiri, A. 2005. Optimization of methanol synthesis reactor using genetic algorithms, Chemical Engineering Journal 108 249–255

Korre, A., Nie, Z., Durucan, S., 2010. Life cycle modelling of fossil fuel power generation with post-combustion CO2 capture. Int. J. Greenhouse Gas Control. 4, 289–300.

Kötter, E., Schneider, L., Sehnke, F., Ohnmeiss, K., Schröer, R. 2015. Sensitivities of powerto-gas within an optimised energy system, Energy Procedia 73, 190–199.

Kourkoumpas, D.S., Papadimou, E., Atsonios, K., Karellas, S., Grammelis, P., Kakaras, E. 2016. Implementation of the Power to Methanol concept by using CO2 from lignite power plants: Techno-economic investigation. International Journal of Hydrogen Energy. 41 16674-16668.

Kubota, T., Hayakawa, I., Mabuse, H., Mori, K., Ushikoshi, K., Watanabe, T., Saito, M. 2001. Kinetic study of methanol synthesis from carbon dioxide and hydrogen, Appl. Organometal. Chem. 15 121–126.

Kwak, D.H., Kim, J.K. 2017. Techno-economic evaluation of CO2 enhanced oil recovery (EOR) with the optimization of CO2 supply. Int J Greenhouse Gas Control 58, 169–84.

Lacy, R., Molina, M., Vaca, M., Serrald, C., Hernandez, G., Rios, G., Guzman, E., Hernandez, R., Perez, R. 2015. Life-cycle GHG assessment of carbon capture, use and geological storage (CCUS) for linked primary energy and electricity production. International Journal of Greenhouse Gas Control 42 165–174.

Lainez-Aguirrea, J.M., Pérez-Fortes, M., Puigjanerb, P., 2017. Economic evaluation of bio-based supply chains with CO2 capture andutilisation, Computers and Chemical Engineering 102, 213–225.

Lal, R. 2008. Carbon sequestration. Philos Trans R Soc Lond B Biol Sci. 363 (1492) 815–30.

Langanke, J. et al. 2014. Carbon dioxide (CO_2) as sustainable feedstock for polyurethane production. Green Chem. 16, 1865–1870.

Lau, H.C., Li, H., Huang, S., 2017. Challenges and Opportunities of Coalbed Methane Development in China, Energy Fuels, 31, 5, 4588-4602.

Leach, A., Mason, C.F., van 't Veld, K. 2011. Co-optimization of enhanced oil recovery and carbon sequestration. Resource and Energy Economics 33 893–912.

Le Quéré et al. 2018. Global Carbon Project; Carbon Dioxide Information Analysis Centre (CDIAC).

Lee, S.Y., Lee, J.U., Lee, I.B., Han, J. 2017. Design under uncertainty of carbon capture and storage infrastructure considering cost, environmental impact, and preference on risk. Appl Energy 189 725–38

Lee, J., Ryu, K.H., Ha, H.Y., Jung, K-D., Lee, J.H. 2020. Techno-economic and environmental evaluation of nano calcium carbonate production utilizing the steel slag. Journal of CO_2 Utilization 37, 113–121.

Leeson, D., Mac Dowell, N., Shah, N., Petit, C., Fennell, P.S. 2017. A Techno-economic analysis and systematic review of carbon capture and storage (CCS) applied to the iron and steel, cement, oil refining and pulp and paper industries, as well as other high purity source. Int. J. Greenh. Gas Control 61, 71–84.

Leonzio, G., 2018. State of art and perspectives about the production of methanol, dimethyl ether and syngas by carbon dioxide hydrogenation, Journal of CO_2 utilization, 27, 326-354.

Leonzio, G. 2019. Carbon Capture Utilization and Storage Supply Chain: Analysis, Modeling and Optimization. Sustainable Agriculture Reviews 37, 37-72

Leonzio, G., D. Bogle, P.U. Foscolo, 2020. Life cycle assessment of a carbon capture utilization and storage supply chain in Italy and Germany: comparison between carbon dioxide storage and utilization systems. To be submitted.

Leonzio, G. 2020. Analysis and optimization of a methanol reactor with the adsorption of carbon monoxide and water, Renewable Energy 146 2744-2757.Leung, D.Y.C., Caramanna, G., Maroto-Valer, M.M. 2014. An overview of current status of carbon dioxide capture and storage technologies, Renewable and Sustainable Energy Reviews. 39 42-433.

Lewandowska-Bernat, A., Desideri, U., 2017. Opportunities of Power-to-Gas technology. Energy Procedia 105, 4569 – 4574.

Li, X., Fang, Z., 2014. Current status and technical challenges of CO_2 storage in coal seams and enhanced coalbed methane recovery: an overview. International Journal of Coal Science & Technology. 1 (1) 93-102.

Li, L., Wen, X., Fu, X., Wang, F., Zhao, N., Xiao, F.K. et al., 2010. MgO/Al_2O_3 sorbent for CO_2 capture, Energy Fuels 24, 5773–5780.

Li, D., Li, X., Bai, M., Tao, X., Shang, S., Dai, X., Yin, Y., 2009. CO2 reforming of CH4 by atmospheric pressure glow discharge plasma: A high conversion ability, International Journal of Hydrogen Energy, 34 (1) 308-313.

Li, W., Wang, H., Shi, Y., Cai, N. 2013. Performance and methane production characteristics of H_2O-CO_2 co-electrolysis in solid-oxide electrolysis cells, Int. J. Hydrogen Energy 38, 11104–11109.

Linde, 2019. Available at: http://www.linde-gas.com/en/processes/freezing_and_cooling/metal_cooling/index.html

Linde. 2012. Gas Applications for the Pulp and Paper Industry; Linde North America Inc.: New York, NY, USA.

Linde Engineering. 2015. Available at: https://www.linde-engineering.com/en/process_plants/hydrogen_and_synthesis_gas_plants/gas_generation/isothermal_reactor/index.html.

Liu, Z., Masel, R.I., Chen, Q., Kutz, R., Yang, H., Lewinski, K., Kaplun, M., Luopa, S., Lutz,m D.R. 2016. Electrochemical generation of syngas from water and carbon dioxide at industrially important rates, J. CO2 Util. 15, 50–56.

Liu, R.X., Poon, C.S. 2016. Utilization of red mud derived from bauxite in self-compacting concrete, Journal of Cleaner Production 112, 384-391.

Liu, M., Bai, B., Li, X. 2013. A Unified Formula for Determination of Wellhead Pressure and Bottom-hole Pressure. Energy Procedia, 37, 3291-3298.

Løvik, I., Hillestad, M., Hertzberg, T., 1999. Modeling and optimization of a reactor system with deactivating catalyst. Comput. Chem. Eng. 23, S839-S842.

Luu, M.T., Milani, D., Abbas, A. 2016. Analysis of CO2 utilization for methanol synthesis integrated with enhanced gas recovery, J. Clean. Prod. 112, 3540–3554.

Ma, H., Ying, W., Fang, D. 2009. Study on methanol synthesis from coal-based syngas, J. Coal Sci. Eng. (China) 15 (1) 98–103.

Mamun, S., Dindore, V.Y., Svendsen, H.F. 2007. Kinetics of the reaction of carbon dioxide with aqueous solutions of 2-((2-aminoethyl) amino) ethanol. Industrial & Engineering Chemistry Research. 46, 385-94.

Manenti, F., Cieri, S., Restelli, M. 2011. Considerations on the steady-state modeling of methanol reactor synthesis fixed bed reactor. Chemical Engineering Science. 66 152-162.

Manenti, F., Cieri, S., Restelli, M., Bozzano, G., 2013. Dynamic modeling of the methanol synthesis fixed-bed reactor, Computers and Chemical Engineering 48 325–334.

Marchia, B., Zanonia, S., Pasetti, M. 2018. Industrial symbiosis for greener horticulture practices: the CO2 enrichment from energy intensive industrial processes. Procedia CIRP 69, 562 – 567.

Martína, M., Grossmann, I.E. 2017. Towards zero CO2 emissions in the production of methanol from switchgrass. CO2 to methanol, Comput. Chem. Eng. 105, 308–3016.

Mathisena, A., Skagestad, R., 2017. Utilization of CO2 from emitters in Poland for CO2-EOR, Energy Procedia 114, 6721 – 6729.

Mazzotti, M., Pini, R., Storti, G. 2009. Enhanced coalbed methane recovery. The Journal of Supercritical Fluids, 47 (3) 619-627.

McNeil, M.A., Schack, C.J., Rinker, R.G. 1989. Methanol synthesis from hydrogen, carbon monoxide and carbon dioxide over a CuO/ZnO/Al2O3 catalyst: II. Development of a phenomenological rate expression, Applied Catalysis 50 (1) 265–285.

Mendelevitch, R. 2014. The role of CO2-EOR for the development of a CCTS infrastructure in the North Sea Region A techno-economic model and applications. International Journal of Greenhouse Gas Control 20, 132–159.

Meratla, Z., 1997. Combining cryogenic flue gas emission remediation with a CO2O2 combustion cycle, Energy Convers. Manag. 38 S147–S152.

Metz, B, Davidson, O, de Coninck, H, Loos, M, Meyer, L. Carbon dioxide capture and storage, intergovernmental panel on climate change, Geneva (Switzerland). Working group III; 2005.

Meyer, J.J., Tan, P., Apfelbacher, A., Daschner, R., Hornung, A. 2016. Modeling of a Methanol Synthesis Reactor for Storage of Renewable Energy and Conversion of CO2 – Comparison of Two Kinetic Models, Chem. Eng. Technol. 39 (2) 233–245

Michailos, S., McCord, S., Sick, V., Stokes, G., Styring, P. 2019. Dimethyl ether synthesis via captured CO2 hydrogenation within the power to liquids concept: A techno-economic assessment. Energy Conversion and Management 184 262–276.

Middleton, R.S., Yaw, S. 2018. The cost of getting CCS wrong: Uncertainty, infrastructure design, and stranded CO2. International Journal of Greenhouse Gas Control 70, 1–11.

Middleton, R.S., Levine, J., Bielicki, J., Carey, J.W., Viswanathan, H.S., Stauffer, P.H., 2015. Jumpstarting commercial-scale CO2 capture and storage with ethylene production and enhanced oil recovery in the U.S. Gulf, Greenhouse Gases: Science and Technology, 5, 3, 241–253.

Middleton, R.S., Kuby, M.J., Wei, R., Keating, G.N., Pawar, R.J., 2012. A dynamic model for optimally phasing in CO2 capture and storage infrastructure. Environ. Modell. Softw. 37, 193–205.

Mikulčića, H., Skovc, I.R., Dominkovićd, D.F., Alwie, S.R.W., Manane, Z.A., Tanf, R., Duićb, N., Mohamade, S.N.H., Wang, X., 2019. Flexible Carbon Capture and Utilization technologies in future energysystems and the utilization pathways of captured CO_2, Renewable and Sustainable Energy Reviews, 114 109338.

Modahl, I.S., Nyland, C.A., Raadal, H.L., Kårstad, O., Torp, T.A., Hagemann, R. 2011. Life cycle assessment of gas power with CCS - a study showing the environmental benefits of system integration. Energy Procedia 4 2470–2477.

Mondal, M.K., Balsora, H.K., Varshney, P. 2012. Progress and trends in CO_2 capture/separation technologies: A review. Energy 46 431-444.

Monkman, S., Shao, Y.X. 2006. Assessing the carbonation behavior of cementitious materials, J. Mater Civ. Eng. 18 (6) 768-776.

Montebelli, A., Visconti, C.G., Groppi, G., Tronconi, E., Ferreira, C., Kohler, S. 2013. Enabling small scale methanol synthesis reactors through the adoption of highly structured catalyst. Catal. Today 215 176-185.

Muller et al. (2016). Polyether carbonate polyol production method. Patent US 9.273,183 B2

Nduagu, E., Bergerson, J., Zevenhoven, R. 2012. Life cycle assessment of CO2 sequestration in magnesium silicate rock–A comparative study, Energy Convers. Manage. 55, 116–126.

Nguyen, D.B., Trinh, Q.H., Hossain, M.M., Lee, W.G., Mok, Y.S. 2019. Enhancement of plasma-assisted catalytic CO2 reforming of CH4 to syngas by avoiding outside air discharges from ground electrode. International Journal of Hydrogen Energy, In press.

Ni, G., Lan, Y., Cheng, C., Meng, Y., Wang, X. 2011. Reforming of methane and carbon dioxide by DC water plasma at atmospheric pressure. International Journal of Hydrogen Energy, 36 (20) 12869-12876.

Nie, Z., Korre, A., Elahi, N., Durucan, S., 2017. Real options analysis of CO2 transport and storage in the UK continental shelf under geological and market uncertainties and the viability of subsidies for market development. Energy Procedia 114, 6612-6622

Nie, Z., Korre, A., Durucan, S., 2011. Life cycle modelling and comparative assessment of the environmental impacts of oxy-fuel and post-combustion CO_2 capture, transport and injection processes**.** Energy Proc. 4, 2510–2517

Nikbin, I.M., Aliaghazadeh, M., Charkhtab, Sb., Fathollahpour, A. 2018. Environmental impacts and mechanical properties of lightweight concrete containing bauxite residue (red mud). Journal of Cleaner Production 172, 2683-2694.

NOOA, 2019. Available at.: https://www.esrl.noaa.gov/gmd/ccgg/trends/ff.html

Ochoa Bique, A., Nguyen, T.B.H., Leonzio, G., Galanopoulos, C., Zondervan, E. 2018. Integration of carbon dioxide and hydrogen supply chains, Computer Aided Chemical Engineering, 43, 1413-1418.

Odenberger, M., Johnsson, F., 2010. Pathways for the European electricity supply system to 2050-The role of CCS to meet stringent CO2 reduction targets. Int. J. Greenhouse Gas Control 4, 327–340.

Olaizola, O., 2003. Microalgal removal of CO2 from flue gases: changes in medium pH and flue gas composition do not appear to affect the photochemical yield of microalgal cultures, Biotechnol. Bioprocess Eng. 8 360–367.

Oreggioni, O.G., Singh, B., Hung, C., van der Spek, M.W., Skagestad, R., Eldrup, N.H., Ramirez, A., Strømman, A.H., 2017. Comparative environmental life cycle assessment of oxyfuel and postcombustion capture with MEA and AMP/PZ - Case studies from the EDDiCCUT project. Energy Procedia 114 6604 – 6611.

Pan, S.Y., Chang, E.E., and Chiang, P.C. 2012. CO2 capture by accelerated carbonation of alkaline wastes: a review on its principles and applications. Aerosol Air Qual. Res. 12, 770–791

Pan, S.Y., Shah, K.J., Chen, Y.H.., Wang, M.H., Chiang, P.C., 2017. Deployment of Accelerated Carbonation Using Alkaline Solid Wastes for Carbon Mineralization and Utilization Toward a Circular Economy, ACS Sustainable Chem. Eng. 5, 6429−6437.

Pardal, T., Messias, S., Sousa, M., Reis Machado, A.S., Rangel, C.M., Nunesc, D., Pinto, J.V., Martins, R., Nunes da Ponte, M. 2017. Syngas production by electrochemical CO2 reduction in an ionic liquid based-electrolyte, J. CO2 Util. 18 62–72.

Parvasi, P., Khosravanipour Mostafazadeh, A., Rahimpour, M.R. 2009. Dynamic modeling and optimization of a novel methanol synthesis loop with hydrogen permselective membrane reactor, Int. J. Hydrogen Energy 34 (9) 3717–3733.

Parvasi, P., Rahimpour, M.R., Jahanmiri, A. 2008. Incorporation of dynamic flexibility in the design of a methanol synthesis loop in the presence of catalyst deactivation. Chem. Eng. Technol. 31 (1) 116-132.

Patricio, J., Angelis-Dimakis, A., Castillo-Castillo, A., Kalmykova, Y., Rosado, L. 2017a. Region prioritization for the development of carbon capture and utilization technologies. Journal of CO2 Utilization 17, 50–59.

Patricio, J., Angelis-Dimakis, A., Castillo-Castillo, A., Kalmykova, Y., Rosado, L. 2017b. Method to identify opportunities for CCU at regional level — Matching sources and receivers. Journal of CO_2 Utilization 22 (2017) 330–345.

Pehnt A., Henkel J. 2009. Life cycle assessment of carbon dioxide capture and storage from lignite power plants. Int J Greenh Gas Control 3, 49-66.

Pérez-Fortes, M., Bocin-Dumitriu, A. & Tzimas, E. 2014. CO2 utilization pathways: Techno-economic assessment and market opportunities. Energy Procedia 63, 7968–7975.

Pérez-Fortes, M., Bocin-Dumitriu, A., Tzimas, E. 2014. Techno-Economic Assessment of Carbon Utilisation Potential in Europe. Chemical Engineering Transactions, 39, 1453-1458

Pérez-Fortes, M., Schöneberger, J.C., Boulamanti, A., Tzimas, E. 2016. Methanol synthesis using captured CO2 as raw material: techno-economic and environmental assessment, Appl. Energy 161, 718–732.

Petersa, R., Baltruweita, M., Grubea, T., Can Samsuna, R., Stolten, D. 2019. A techno economic analysis of the Power-to-Gas route, Journal of CO_2 Utilization 34, 616–634.

Petrescu, L., Bonalumi, D., Valenti, G., Cormos, A.M., Cormos, C.C., 2017. Life Cycle Assessment for supercritical pulverized coal power plants with post-combustion carbon capture and storage, Journal of Cleaner Production 157, 10-21.

Pham, M., Goujard, V., Tatibouet, J.M., Batiot-Dupeyrat, C. 2011. Activation of methane and carbon dioxide in a dielectric-barrier discharge-plasma reactor to produce hydrocarbons—Influence of La_2O_3/γ-Al_2O_3 catalyst. Catal. Today 171 (2011) 67–71.

Pieri, T., Nikitas, A., Castillo-Castillo, A., Angelis-Dimakis, A. 2018. Holistic Assessment of Carbon Capture and Utilization Value Chains. Environments 5, 108, 1-17.

Pisal, D.S., Lele, S.S. 2005. Carotenoid production from microalgae, Dunalliella salina, Indian J. Biotechnol. 4, 476–483.

Pradhan, L., Bhattacharjee, V., Mitra, R., Bhattacharya, I., Chowdhury, R., 2015. Biosequestration of CO2 using power plant algae (Rhizoclonium hieroglyphicum JUCHE2) in a Flat Plate Photobio-Bubble-Reactor – Experimental and modeling. Chemical Engineering Journal 275 381–390.

Quadrelli, E.A., Centi, G., Duplan, J.L., Perathoner, S. 2011. Carbon dioxide recycling: emerging large-scale technologies with industrial potential. Chem Sus Chem 4 1194–215.

Rachmilevitch, S., Cousins, A.B., Bloom, A.J. 2004. Nitrate assimilation in plant shoots depends on photorespiration. In: Proceedings of the National Academy of Sciences of the United States of America 101 11506.

Rahmawati, S.D., Hoda, M.F., Kuntadi, A., 2015. CO2 injection project analysis using application of integrated model and optimization. In: SPE Middle East Oil and Gas Show and Conference, MEOS, Proceedings, 1916–1926

Rahimpour, M.R., 2008. A two-stage catalyst bed concept for conversion of carbon dioxide into methanol, Fuel Process Technol. 89, 556–566.

Rahimpour, M.R., Ghader, S. 2003. Theoretical investigation of a Pd-membrane reactor for methanol synthesis, Chem. Eng. Technol. 26 (8) 902–907.

Rahimpour, M.R., Elekaei, H. 2009. Enhancement of methanol production in a novel fluidized-bed hydrogen-permselective membrane reactor in the presence of catalyst deactivation, International Journal of Hydrogen Energy, 34 (2009) 2208-2223.

Rahimpour, M.R., Parvasi, P., Setoodeh, P. 2009. Dynamic optimization of a novel radial-flow, spherical-bed methanol synthesis reactor in the presence of catalyst deactivation using Differential Evolution (DE) algorithm. Int. J. Hydrogen Energy 34 (15) 6221-6230.

Rathod, R.R., Suryawanshi, N.T., Memade, P.D. 2014. Evaluation of the properties of Red Mud Concrete, IOSR Journal of Mechanical and Civil Engineering (IOSR-JMCE) ISSN: 2278-1684, 31-34

Rezaie, N., Jahanmiri, A., Moghtaderi, B., Rahimpour, M.R. 2005. A comparison of homogeneous and heterogeneous dynamic models for industrial methanol reactors in the presence of catalyst deactivation. Chem. Eng. Process. 44 (8) 911-921.

Ribeiro, D.V., Labrincha, J.A., Morelli, M.R., 2012. Effect of the addition of red mud on the corrosion parameters of reinforced concrete. Cem. Concr. Res. 42, 124-133.

Ribeiro, D.V., Morelli, M.R. 2011. Use of red mud as addition for Portland cement mortars. Available at.: https://inis.iaea.org/collection/NCLCollectionStore/_Public/47/081/47081549.pdf

Riccia, A., Truda, L., Palma, V. 2019. Study of the role of chemical support and structured carrier on the CO2 methanation reaction. Chemical Engineering Journal. 377, 120461.

Rivera-Tinoco, R., Farran, M., Bouallou, C., Aupretre, F., Valentin, S., Millet, P., Ngameni, J.R. 2016. Investigation of power-to-methanol processes coupling electrolytic hydrogen production and catalytic CO2 reduction, Int. J. Hydrogen Energy 41, 4546–4559.

Rönsch, S., Schneider, J., Matthischke, S., Schlüter, M., Götz, M., Lefebvre, J., et al. 2016. Review on methanation – from fundamentals to current projects. Fuel 166 276–96.

Rubin, E.S., Short, C., Booras, G., Davison, J., Ekstrom, C., Matuszewski, M., McCoy, S., 2013. A proposed methodology for CO2 capture and storage cost estimates. Int. J. Greenh. Gas Control 17, 488–503.

Rutberg, P.G., Kuznetsov, V.A., Popov, V.E., Popov, D.S., Surov, A.V., Subbotin, D.I., Bratsev, A.N. 2015. Conversion of methane by CO2+H2O+CH4 plasma. Applied Energy 148 159–168.

Samimi, F., Karimipourfard, D., Rahimpour, M.R., 2018. Green methanol synthesis process from carbon dioxide via reverse water gas shift reaction in a membrane reactor. Chemical Engineering Research and Design. 140 44-67.

Sai, P.S., 2017. Strength properties of concrete by using red mud as a replacement of cement with hydrated lime. International Journal of Civil Engineering and Technology (IJCIET) 8 (3) 38–49.

Sauer, D.U., Fuchs, G., Lunz, B., Leuthold, M., 2012. Technology Overview on Electricity Storage - Overview on the potential and on the deployment perspectives of electricity storage technologies.

Sanchez-Guerrero, M.C., Lorenzo, P., Medrano, E., Baille, A., Castilla, N. 2009. Effects of EC-based irrigation scheduling and CO2 enrichment on water use efficiency of a greenhouse cucumber crop. Agr Water Manag 96 429.

Sayyafzadeh, M., Keshavarz, A., 2016. Optimisation of gas mixture injection for enhanced coalbed methane recovery using a parallel genetic algorithm. Journal of Natural Gas Science and Engineering, 33, 942-953.

Sayyafzadeh, M., Keshavarz, A., Alias, A.R.M., Dong, K.A., Manser, M. 2015. Investigation of varying-composition gas injection for coalbed methane recovery enhancement: A simulation-based study. Journal of Natural Gas Science and Engineering 27, 1205-1212.

Schmidt, O., Gambhir, A., Staffell, I., Hawkes, A., Nelson, J., Few, S.2017. Future cost and performance of water electrolysis: an expert elicitation study. Int J Hydrogen Energy 42 (52) 30470–92.

Sadeghi, S., Vafajoo, L., Kazemeini, M., Fattahi, M. 2014. Modeling of the Methanol Synthesis Catalyst Deactivation in a Spherical Bed Reactor: An Environmental Challenge, APCBEE Procedia 10 84 – 90.

Seidel, C., Jorke, A., Vollbrecht, B., Seidel-Morgenstern, A., Kienle, A. 2018. Kinetic modeling of methanol synthesis from renewable resources, Chemical Engineering Science 175 130–138.

Senghora, A., Dioha, R.M.N., Müllerb, C., Youm, I., 2017. Cereal crops for biogas production: A review of possible impact of elevated CO2. Renewable and Sustainable Energy Reviews 71, 548–554

Shafiee, A., Nomvar, M., Liu, Z., Abbas, A. 2017. Automated process synthesis for optimal flowsheet design of a hybrid membrane cryogenic carbon capture process, J. Clean. Prod. 150 309–323.

Shi, C.S., Liu, M., He, P.P., Ou, Z.H. 2013. Factors affecting kinetics of CO2 curing of concrete, J. Sustain. Cement-Based Mater. 1 (1-2) 24-33

Shi-Cong, K., Bao-jian, Z., Chi-Sun, P., 2014. Use of a CO2 curing step to improve the properties of concrete prepared with recycled aggregates, Cement & Concrete Composites 45, 22–28.

Sinayuc, C., Shi, J.Q., Imrie, E.C., Syed, S.A., Korre, A., Durucan, S. 2011. Implementation of horizontal well CBM/ECBM technology and the assessment of effective CO2 storage capacity in a Scottish coalfield. Energy Procedia 4, 2150–2156.

Singh, B., Strømman, A.H., Hertwich, E. 2011a. Life cycle assessment of natural gas combined cycle power plant with post-combustion carbon capture, transport and storage, Int. J. Greenhouse Gas Control 5 (3) 457–466.

Singh B., Strømman A.H., Hertwich E.G. 2011b. Comparative life cycle environmental assessment of CCS technologies. Int J Greenhouse Gas Control 5 (4) 911–921.

Slotbooma, Y., Bosa, M.J., Piepera, J., Vrieswijka, V., Likozarb, B., Kerstena, S.R..A., Brilman, D.W.F. 2020. Critical assessment of steady-state kinetic models for the synthesis of methanol over an industrial Cu/ZnO/Al2O3 catalyst. Chemical Engineering Journal 389 124181.

Solunke, R.D., Veser, G. 2011. Integrating desulfurization with CO_2-capture in chemical looping combustion. Fuel, 90 608–17.

Song, C. 2006. Global challenges and strategies for control, conversion and utilization of CO_2 for sustainable development involving energy, catalysis, adsorption and chemical processing, Catalysis Today 115, 2–32.

Song ,C., Liu, Q., Ji, N., Deng, S., Zhao, J., Li, Y., Song, Y., Lid, H., 2018. Alternative pathways for efficient CO_2 capture by hybrid processes—A review, Renewable and Sustainable Energy Reviews 82 215–231.

Song, C., Liua, Q., Deng, S., Li, H., Kitamura, Y., 2019. Cryogenic-based CO2 capture technologies: State-of-the-art developments and current challenges, Renewable and Sustainable Energy Reviews, 101 265–278.

Song, H.K, Choi, J.W., Yue, S.H., Lee, H., Na, B.K. 2004. Synthesis gas production via dielectric barrier discharge over Ni/γ-Al2O3 catalyst. Catalysis Today. 89 (1-2) 27-33.

Speybroeck, V.V., De Wispelaere, K., Van der Mynsbrugge, J., Vandichel, M., Hemelsoet, K., Waroquier, M. 2014. First principle chemical kinetics in zeolites: the methanol-to-olefin process as a case study, Chem. Soc. Rev. 43, 7326–7357.

Specht, M., Bandi, A., Baumgart, F., Murray, C.N., Gretz, J., Eliasson, B., Riemer, P.W.F., Wokaun A. 1999. Synthesis of methanol from biomass/CO2 resources, greenhouse gas control technologies, 723, Pergamon, Amsterdam.

Sreedhar, I., Nahar, T., Venugopal, A., Srinivas, B., 2017. Carbon capture by absorption–path covered and ahead, Renew. Sustain. Energy Rev. 76, 1080–1107.

Stewart, R.J., Haszeldine, R.S., 2015. Can producing oil store carbon? Greenhouse Gas footprint of CO2-EOR, offshore North Sea. Environ. Sci. Technol. 49 (9), 5788–5795

Stocker, T.F., Qin, D., Plattner, G.K., Alexander, L.V., et al. 2013. Technical Summary. IPCC AR5 WG1 2013. 33–115.

Stoots, C.M., O'Brien, J.E., Herring, J.S., Hartvigsen, J.J. 2009. Syngas production via high-temperature co-electrolysis of steam and carbon dioxide, J. Fuel Cell Sci. Technol. 6 011014.

Storch, H.V., Roeb, M., Stadler, H., Sattler, C., Bardow, A., Hoffschmidt, B. 2016. On theassessment of renewable industrial processes: case study for solar co-production of methanol and power, Appl. Energy 183, 121–132.

Strachan, N., Hoefnagels, R., Ramírez, A., van den Broek, M., Fidje, A., Espegren, K., Grohnheit, P.E., et al., 2011. CCS in the North Sea region: a comparison on the cost effectiveness of storing CO2 in the Utsira formation at regional and national scales. Int. J. Greenhouse Gas Control 5, 1517–1532.

Sun, L., Dou, H., Li, Z., Hu, Y., Hao, X., 2018. Assessment of CO2 storage potential and carbon capture, utilization and storage prospect in China, Journal of the Energy Institute 91, 970-977.

Sutar, H., Mishra, S.C., Sahoo, S.K., Chakraverty, A.P., Maharana, H.S. 2014. Progress of Red Mud Utilization: An Overview, American Chemical Science Journal 4 (3) 255-279.

Suicmez V.S. 2019. Feasibility study for carbon capture utilization and storage (CCUS) in the Danish North Sea. Journal of Natural Gas Science and Engineering 68 102924.

Takagawa, M., Ohsugi, M. 1987. Study on reaction rates for methanol synthesis from carbon monoxide, carbon dioxide, and hydrogen, Journal of Catalysis 107 (1) 161–172

Tan, R.R., Aviso, K.B., Bandyopadhyay, S., Ng, D.K.S., 2012. Continuous-time optimization model for source–sink matching in carbon capture and storage systems. Ind. Eng. Chem. Res. 51, 10015–10020.

Tan, R.R., Aviso, K.B., Bandyopadhyay, S., Ng, D.K.S., 2013. Optimal source-sink matching in carbon capture and storage systems with time injection rate, and capacity constraints. Environ. Progress Sustain. Energy 32, 411–416.

Tanaka, Y., Sawada, Y., Tanase, D., Tanaka, J., Shiomi, S., Kasukawa, T. 2017. Tomakomai CCS Demonstration Project of Japan, CO2 Injection in Process. Energy Procedia 114 5836 – 5846.

Tang, Yokoyama, T., Kubota, H., Shimota, A. 2014. Life cycle assessment of a pulverized coal-fired power plant with CCS technology in Japan. Energy Procedia 63 743 –7443.

Tao, X., Bai, M., Li, X., Long, H., Shang, S., Yin, Y., Dai, X. 2011. CH4-CO2 reforming by plasma e challenges and opportunities. Progress in Energy and Combustion Science 37, 113-124.

Tapia, J.F.D., Lee, J.Y., Ooi, R.E.H., Foo, D.C.Y., Tan, R.R., 2016b. Optimal CO2 allocation and scheduling in enhanced oil recovery (EOR) operations. Appl. Energy 184, 337–345.

Tapia, J.F.D., Lee, J.Y., Ooi, R.E.H., Foo, D.C.Y., Tan, R.R., 2016a. Planning and scheduling of CO2 capture, utilization and storage (CCUS) operations as a strip packing problem. Process Saf. Environ. Prot. 104, 358–372.

Tapia, J.F.D., Lee, J.Y., Ooi, R.E.H., Foo, D.C.Y., Tan, R.R., 2018. A review of optimization and decision-making models for the planning of CO2 capture, utilization and storage (CCUS) systems. Sustain. Prod. Consum. 13, 1-15.

Tcvetkov, P., Cherepovitsyn, A., Fedoseev, S. 2019. The Changing Role of CO2 in the Transition to a Circular Economy: Review of Carbon Sequestration Projects. Sustainability 11, 5834

Thema, M., Bauer, F., Sterner, M., 2019. Power-to-Gas: Electrolysis and methanation status review. Renewable and Sustainable Energy Reviews 112, 775–787.

Thiruvenkatachari, R., Su, S., An, H., Yu, X.X. 2009. Post combustion CO_2 capture by carbon fibre monolithic adsorbents. Prog Energy Combust 35 438–55.

Toyo Engineering. 2015. Available at: http://www.toyo-eng.com/jp/en/products/petrochmical/ methanol.

Tsuparia, E., Kärki, J., Vakkilainen, E. 2016. Economic feasibility of power-to-gas integrated with biomass fired CHP plant. Journal of energy storage. 5, 62-69.

UCAR, 2019. Available at: https://scied.ucar.edu/carbon-cycle

Ugwu, C.U., Aoyagi, H., Uchiyama, H. 2008. Photobioreactors for mass cultivation of algae, Bioresour. Technol. 99 4021–4028.

United Nations, 2015. The Paris agreement. Available online at: https://unfccc.int/sites/default/files/english_paris_agreement.pdf.

Valderramaa, M.A.M., van Puttenb, R.G., Gruter, G.J.M., 2019. The potential of oxalic – and glycolic acid based polyesters (review). Towards CO2 as a feedstock (Carbon Capture and Utilization – CCU). European Polymer Journal 119 445–468.

Vanden Bussche, K.M., Froment, G.F. 1996. A Steady-State Kinetic Model for Methanol Synthesis and the Water Gas Shift Reaction on a Commercial Cu/ZnO/Al2O3 Catalyst, J. Catal. 161 (1) 1-10.

Vandewalle, J., Bruninx, K., D'haeseleer, W. 2015. Effects of large-scale Power-to-Gas conversion on the power, gas and carbon sectors and their interactions. Energy Conversion and Management 94, 28–39.

Verma, A.K., Sirvaiya, A. 2016. Comparative analysis of intelligent models for prediction of Langmuir constants for CO_2 adsorption of Gondwana coals in India, Geomechanics and Geophysics for Geo-Energy and Geo-Resources, 2 (2) 97-109.

Viebahn, P., Nitsch, J., Fischedick, M., Esken, A., Schuwer, D., Supersberger, N., Zuberbuhler, U., Edenhofer, O., 2007 Comparison of carbon capture and storage with renewable energy technologies regarding structural, economic, and ecological aspects in Germany. Int J Greenhouse Gas Control 1 121–133.

Villa, P., Forzatti, P., Buzzi-Ferraris, G., Garone, G., Pasquon, I. 1985. Synthesis of alcohols from carbon oxides and hydrogen. 1. Kinetics of the low-pressure methanol synthesis, Ind. Eng. Chem. Process Des. Develop. 24 (1) 12–19

Vita, A., Italiano, C., Previtali, D., Fabiano, C., Palella, A., Freni, F., Bozzano, G., Pino, L., Manenti, L., 2018. Methanol synthesis from biogas: a thermodynamic analysis. Renew. Energy 118, 673-684.

Volkart, K., Bauer, C., Boulet, C., 2013. Life cycle assessment of carbon capture and storage in power generation and industry in Europe, International Journal of Greenhouse Gas Control 16, 91–106.

von der Assen, N., Müller, L.J., Steingrube, A., Voll, P., Bardow, A., 2016. Selecting CO_2 Sources for CO_2 Utilization by Environmental-Merit Order-Curves, Environ. Sci. Technol. 50, 1093−1101.

von der Assen N., and Bardow, A., 2014. Life cycle assessment of polyols for polyurethane production using CO2 as feedstock: insights from an industrial case study, Green Chem., 16, 3272–3280.

Wang, J., Huang, L., Yang, R., Zhang, Z., Wu, J., Gao, Y., Wang, Q., O'Hare, D., Zhong, Z. 2014. Recent advances in solid sorbents for CO2 capture and new development trends. Energy Environ. Sci., 2014, 7, 3478

Wang, F., Wang, Y., Zhang, L., Zhu, J., Han, B., Fan, W., Xu, L., Yu, H., Cai, W., Li, Z., Deng, Z., Shi, W. 2019. Performance enhancement of methane dry reforming reaction for syngas production over Ir/Ce0.9La0.1O2-nanorods catalysts. Catalysis today, In proof.

Wang, X., Veld, K.v.t., Marcy, P., Huzurbazar, S., Alvarado, V., 2018. Economic co-optimization of oil recovery and CO2 sequestration. Appl. Energy 222, 132–147.

Wang, Q., Shi, H., Yan, B., Jin, Y., Cheng, Y. 2011. Steam enhanced carbon dioxide reforming of methane in DBD plasma reactor. Int. J. Hydrogen Energy 36 (14) 8301-8306

Wappel, D., Gronald, G., Kalb, R., Draxler, J. 2010. Ionic liquids for post-combustion CO_2 absorption, Int. J. Greenh. Gas Control 4 (3) 486–494.

Wei, N., Li, X., Dahowski, R.T., Davidson, C.L., Liu, S., Zha, Y. 2015. Economic evaluation on CO2-EOR of onshore oil fields in China. Int J Greenhouse Gas Control 37 170–81.

Wen, H., Cheng, X., Chen, J., Zhang, C., Yu, Z., Li, Z., Fan, S., Wei, G., Cheng, B. 2020. Micro-pilot test for optimized pre-extraction boreholes and enhanced coalbed methane recovery by injection of liquid carbon dioxide in the Sangshuping coal mine. Process Safety and Environmental Protection, In press.

Wildgust, N., Leroux, K.M., Botnen, B.W., Daly, D.J., Jensen, M.D., Kalenze, N.S., Burton-Kelly, M.E., Dalkhaa, C., Doll, T.E., Gorecki, C.D. 2019. Pre-feasibility study of CCS in western Nebraska. International Journal of Greenhouse Gas Control 84 1–12.

Witkowski, A., Majkut, M., Rulik, S., 2014. Analysis of pipeline transportation systems for carbon dioxide sequestration, Archives of Thermodynamics. 35 (1) 117-140.

White, C.M., Strazisar, B.R., Granite, E.J., Hoffman, J.S., Pennline, H.W., 2003. Separation and capture of CO_2 from large stationary sources and sequestration in geological formations-coalbeds and deep saline aquifers. J. Air Waste Manage. Assoc. 53 645–715.

Wong, S., Law, D., Deng, X., Robinson, J., Kadatz, B., Gunter, W.D., et al., 2007. Enhanced coalbed methane and CO2 storage in anthracitic coals—micro-pilot test at south Qinshui, Shanxi, China. International Journal of Greenhouse Gas Control 1(2), 215–222.

World Bank, 2017. World development indicators. Available at: http://databank.worldbank.org/data/reports.aspx?source=World%20Development%20Indicators.

World Bank, 2019. World development indicators. Available at: https://data.worldbank.org/indicator/EN.ATM.CO2E.KT

Xu, B., Yang, R., Meng, F., Reubroycharoen, P., Vitidsant, T., Zhang, Y., Yoneyama, Y., Tsubaki, N. 2009. A new method of low temperature methanol synthesis, Catal. Surv. Asia 13, 147–163.

Xuan, D., Zhan, B., Sun Poon, C., 2018. A maturity approach to estimate compressive strength development of CO2-cured concrete blocks. Cement and Concrete Composites 85, 153-160.

Yang, L., Zhang, X., Mcalinden, K.J. 2016. The effect of trust on people's acceptance of CCS (carbon capture and storage) technologies: evidence from a survey in the People's Republic of China. Energy 96 69–79.

Yang, L., Xu, M., Yang, Y., Fan, J., Zhang, X. 2019. Comparison of subsidy schemes for carbon capture utilization and storage (CCUS) investment based on real option approach: Evidence from China. Applied Energy 255 113828.

Yang, B., Wei, Y.M., Hou, Y., Li, H., Wang, P. 2019. Life cycle environmental impact assessment of fuel mix-based biomass cofiring plants with CO2 capture and storage. Applied Energy 252 113483.

Yao, X., Zhong, P., Zhang, X., Zhud, L. 2018. Business model design for the carbon capture utilization and storage (CCUS) project in China, Energy Policy 121, 519–533.

Ye, J.P., Feng, S.L., Fan, Z.Q., Wang, G.Q., Gunter, W.D., Sam, W., et al., 2007. Micro-pilot test for enhanced coalbed methane recovery by injecting carbon dioxide in south part of Qinshui Basin. Acta Petrolei Sinica 28(4), 77–80

Yeh, J.T., Resnik, K.P., Rygle, K., Pennline, H.W., 2005. Semi-batch absorption and regeneration studies for CO_2 capture by aqueous ammonia, Fuel Process Technol. 86, 1533–1546.

Yi, Q., Zhao, Y., Huang, Y., Wei, G., Hao, Y., Feng, J., et al. 2018. Life cycle energy-economic-CO2 emissions evaluation of biomass/coal, with and without CO2 capture and storage, in a pulverized fuel combustion power plant in the United Kingdom. Appl Energy 225 258–72.

Yin, G., Deng, B., Li, M., Zhang, D., Wang, W., Li, W., Shang, D. 2017. Impact of injection pressure on CO2–enhanced coalbed methane recovery considering mass transfer between coal fracture and matrix. Fuel 196, 288–297.

Yu, S., Horinga, J., Liu, Q., Dahowski, R., Davidson, C., Edmonds, J., Liu, B., Mcjeona, H., McLeod, J., Patel, P., Clarke, L. 2019. CCUS in China's mitigation strategy: insights from integrated assessment modeling, International Journal of Greenhouse Gas Control 84, 204–218.

Yue D., You F., 2015, Integration of geological sequestration and microalgae biofixation supply chains for better greenhouse gas emission abatement, Chemical Engineering Transactions, 45, 487-492.

Yujia, W., Zhaofeng, X., Zheng, L. 2014. Lifecycle Analysis of Coal-fired Power Plants with CCS in China. Energy Procedia 63 7444–7451.

Yusup, S., Anh, N.P., Zabiri, H. 2010. A Simulation study of an industrial methanol reactor based simplified steady state model, , IJRRAS 5 (3) 213-222.

Zahedi, G., Jahanmiri, A., Rahimpor, M., 2005. A neural network approach for prediction of the CuOeZnOeAl2O3 catalyst deactivation. Int. J. Chem. React. Eng. 3. Article A8.

Zanganeh, K.E., Shafeen, A., Salvador, C. 2009. CO_2 capture and development of an advanced pilot-scale cryogenic separation and compression unit, Energy Procedia 1 247–252.

Zapp, P., Schreiber, A., Marx, J., Haines, M., Hake, J.F., Gale, J. 2012. Overall environmental impacts of CCS technologies—A life cycle approach. International Journal of Greenhouse Gas Control 8 12–21.

Zappa, W., 2014. Pilot-Scale Experimental Work on the Production of Precipitated Calcium Carbonate (PCC) from Steel Slag for CO2 Fixation. Master Thesis, Aalto University. Department of Energy Technology.

Zevenhoven, R., Eloneva, S., Teir, S. 2006. Chemical fixation of CO2 in carbonates: routes to valuable products and long-term storage, Catal. Today 115 (1-4) 73‑79.

Zhan, B.J., Xuan, D.X., Poon, C.S., Shi, C.J. 2016. Effect of curing parameters on CO2 curing of concrete blocks containing recycled aggregates, Cem. Concr. Comp. 71, 122-130.

Zhang, S., Liu, L., Zhang, L., Meng, Q., Du, J., 2018. Optimal planning for regional carbon capture and storage systems under uncertainty. Chem. Eng. Trans. 70, 1207–1212

Zhang, D., Alhorr, Y., Elsarrag, E., Marafia, A.H., Lettieri, P., Papageorgiou, L. 2017. Fair design of CCS infrastructure for power plants in Qatar under carbon trading scheme. International Journal of Greenhouse Gas Control 56 43–54.

Zhang, C., Jun, K.W., Gao, R., Kwak, G., Park, H.G. 2017. Carbon dioxide utilization in a gas-to-methanol process combined with CO2/steam-mixed reforming: technoeconomic analysis, Fuel 190, 303–311.

Zhang, A., Liu, L., Zhang, L., Zhuang, Y., Du, J. 2018. An optimization model for carbon capture utilization and storage supply chain: A case study in Northeastern China, Applied Energy 231, 194–206.

Zhao, H., Park, Y., Lee, D. H., and Park, A.-H. A. 2013. Tuning the dissolution kinetics of wollastonite *via* chelating agents for CO2 sequestration with integrated synthesis of precipitated calcium carbonates. *Phys. Chem. Chem. Phys.* 15

Zhou, J., Ma, Z., Zhang, L., Liu, C., Pu, J., Chen, X., Zheng, Y., Chan, S.H. 2019. Study of CO2 and H2O direct co-electrolysis in an electrolyte-supported solid oxide electrolysis cell by aqueous tape casting technique. International Journal of Hydrogen Energy. 44 28939- 28946.

Zhu, L., Fan, Y., 2011. A real options-based CCS investment evaluation model: case study of China's power generation sector. Appl. Energy 88, 4320-4333.

Zhu, L., Duan, H.B., Fan, Y. 2015. CO2 mitigation potential of CCS in China e an evaluation based on an integrated assessment model. Journal of Cleaner Production 103 (2015) 934-947.

Zittelli, G.C., Biondi, N., Rodolfi, L., Tredici, M.R. 2013. Photobioreactors for mass production of microalgae, in: Amos Richmond, Hu Qiang (Eds.), Handbook of Microalgal Culture: Applied Phycology and Biotechnology, second ed., John Wiley & Sons Ltd., Oxford, UK, 225–266

Chapter II

Analysis of methanol reactors with CO_2 hydrogenation

This chapter is focused on the analysis of methanol reactors for carbon dioxide hydrogenation. The aim is to focus on pro and contras regarding the feasibility of carbon dioxide utilization, with specific reference to an important reaction path, carbon dioxide hydrogenation, and a major chemical commodity, methanol, available for a variety of chemical syntheses and as a transportation fuel.
At first, an equilibrium analysis of three different reactor configurations (once-through reactor, reactor with the recycle of unconverted gases after the separation of methanol and water by condensation; reactor equipped with membrane permeable to water) is developed in Aspen Plus®. Results demonstrate the feasibility of this reaction pathway and the best efficiencies are obtained in the configuration that separates methanol and water by condensation and recycles the unconverted gases. This process configuration is then assumed to analyze the behavior of a catalytic packed bed reactor. 1-D and 2-D models are developed in MATLAB® applying a literature kinetic approach: a sensitivity analysis shows the effect of some parameters on the system, while a comparison between a structured and non-structured reactor packing, characterized by quite different thermal conductivity, is considered through the 2-D model, demonstrating a better efficiency of the structured packing.

II.1 Introduction

This chapter is aimed at investigating a potential utilization route of carbon dioxide, i.e. its conversion to methanol by means of the hydrogenation reaction, amenable to important industrial applications (two industrial plants reported in the literature are reproduced and analyzed in the Appendix). As a matter of facts, the opportunity to convert carbon dioxide (CO_2) into useful products is the core subject of this Thesis and its following chapters, where strategies are described and evaluated by means of numerical models to combine capture and sequestration of carbon dioxide, so to reduce its impact on climate change, with its economic utilization, in order to develop the so called carbon capture, utilization and storage (CCUS) supply chains.

Methanol (CH_3OH) is among the most important products that can be obtained from CO_2 via hydrogenation reaction (Ampelli et al., 2015). As already mentioned in the first Chapter, methanol can be used as a fuel for combustion engines or in fuel cells for electricity production and on the other hand, it is a raw material for the synthesis of other important chemicals (Meyer et al., 2016).

Methanol production is generally carried out according to the indirect route, feeding syngas to a catalytic reactor and regulating the feed composition according to the stoichiometric number ($[H_2]-[CO_2]/[CO]+[CO_2]$) (Machado et al., 2014). However, a green process, responding to the principles of circular economy, can be developed according to the direct route, feeding CO_2 and hydrogen (H_2). In this case, CO_2 is captured from power plants, petrochemical and cement industries, paper mill and steel plants, etc., while H_2 is produced via water electrolysis exploiting renewable energies or can be obtained from coke

oven gases, steelwork and chlor-alkali plants, etc. (Leonzio, 2018). These routes are overall characterized by exothermic reactions, with a decrease of the total number of moles, favored at lower temperatures and higher pressures (Manenti et al., 2014). Generally, the direct route is carried out in a range of temperature and pressure of 473-553 K and 15-55 bar respectively, over a $Cu/ZnO/Al_2O_3$ catalyst (Vanden Bussche and Froment, 1996). However, higher pressures up to 100 bar can be considered (Meyer et al., 2016). The catalyst used commercially is active at temperatures higher than 473 K, while, for temperatures higher than 553 K, catalyst deactivation occurs, which means that the reaction conditions are limited by kinetic constraints (Manenti et al., 2014). In addition, thermodynamic limitations are present for this synthesis then, strategies should be suggested to overcome this problem. As a common chemical process, the recycle and the removal of products can be a valid solutions to overcome the thermodynamic limitation, shifting the chemical equilibrium to the product side. Moreover, the feasibility through an equilibrium analysis of the suggested strategies to solve the thermodynamic problem is missing in the literature for the direct route. In this chapter, then, a reacting system with the recycle of unconverted gases, after the separation of CH_3OH and water (H_2O) by condensation, and a membrane reactor permeable to H_2O are proposed to overcome the thermodynamic limit. An equilibrium analysis is considered to evaluate their feasibility and their efficiency (in terms of conversion, yield and selectivity) and to compare these configurations with a simple once-through reactor. These configurations are all studied in Aspen Plus® through an equilibrium reactor. A real, non-equilibrium catalytic packed bed reactor is then considered with reference to a successful industrial strategy, as the multi-tubular Lurgi reactor equipped with a shell cooling system and operated with the recycle of unconverted gases after the separation of CH_3OH and H_2O. 1-D and 2-D mathematical models are developed in MATLAB® to study the effect of some parameters on the system and to compare a structured catalytic packing with a non-structured one. Few analyses utilizing a 2-D model for a methanol reactor are present in the literature, particularly when the plant feedstock is made of carbon dioxide and hydrogen.

II.2 Materials and methods

II.2.1 Methanol reactor configurations examined in the equilibrium analysis

The following independent reactions are assumed to occur during CO_2 hydrogenation to CH_3OH (see Eqs. II.1-II.2):

$$CO_2 + 3H_2 \rightleftarrows CH_3OH + H_2O \qquad \Delta H^0_{298} = -49.5\ kJ/mol_{CO_2} \qquad (II.1)$$

$$CO_2 + H_2 \rightleftarrows CO + H_2O \qquad \Delta H^0_{298} = 41.2\ kJ/mol_{CO_2} \qquad (II.2)$$

The first reaction is exothermic with the reduction of mole number, while the second reaction (reverse water gas shift reaction) is endothermic without change in the mole number. Overall, as mentioned above, the synthesis is exothermic with a reduction of mole number.

The first stoichiometric expression (II.1) is a linear combination of equation II.2 and the following one, that characterizes the production of CH_3OH from syngas (see Eq. II.3):

$$CO + 2H_2 \leftrightarrow CH_3OH \qquad \Delta H_{298\,K} = -90{,}55\ kJ/mol \qquad (II.3)$$

The equilibrium constants for reaction II.1 and II.2 are reported in Vanden Bussche and Froment (1996), with the numerical values defined by Graaf et al. (1986) (see Eqs. II.4-II.5):

$$\log_{10} K_{eq,1} = \frac{3066}{T} - 10.592 \qquad (II.4)$$

$$\log_{10} K_{eq,2} = \frac{-2073}{T} + 2.029 \qquad (II.5)$$

where T indicates temperature expressed in Kelvin degrees. In order to overcome the thermodynamic limitation in methanol synthesis, two different reactor configurations are suggested, analyzed to verify the technical feasibility with CO_2 and H_2 in the feed, and compared with the simple once-through reactor, as in Figure II.1a. In particular, a reactor with the recycle of unconverted gases after the separation of CH_3OH and H_2O to shift the reaction equilibrium towards products, as in Figure II.1b, and a membrane reactor with simultaneous separation of H_2O, to shift the reaction also towards products, as in Figure II.1c, are considered. Regarding the first option, Khalilpourmeymandi et al. (2017) find that the recycle of CO, CO_2 and H_2 allows to have a higher methanol production, compared to the recycle of only CO and H_2. A methanol reactor with H_2O vapors separation through a membrane is also suggested by Gallucci and Basile (2007), underlining its advantages.

The investigated reactors are considered as equilibrium reactors, characterized by the chemical reactions described with the stoichiometric expressions reported in Eq. II.1 and II.2 and respective equilibrium constants as in Eq. II.4 and II.5.

To obtain conversion and selectivity for these reactor configurations and to find equilibrium values of methanol synthesis from pure CO_2 hydrogenation, their modeling is developed using Aspen Plus® software with Redlich-Kwong-Soave (RKS) as thermodynamic model.

The feeding stream is composed by CO_2 and H_2 in stoichiometric ratio. The membrane reactor is modelled using six stages of equilibrium reactors and H_2O separators in order to simulate the simultaneous reaction and H_2O separation process. In this case, a system operating under thermodynamic equilibrium conditions is simulated, so that the obtained final result is expected to be quite independent from the process path (simulation of reaction steps and simultaneous steam separation by means of a sequence of subsequent

operations chosen from among the software standard units). H_2O flowing through the membrane is considered to be a fraction, α, of its mass in the reaction ambient (permeation factor of membrane).

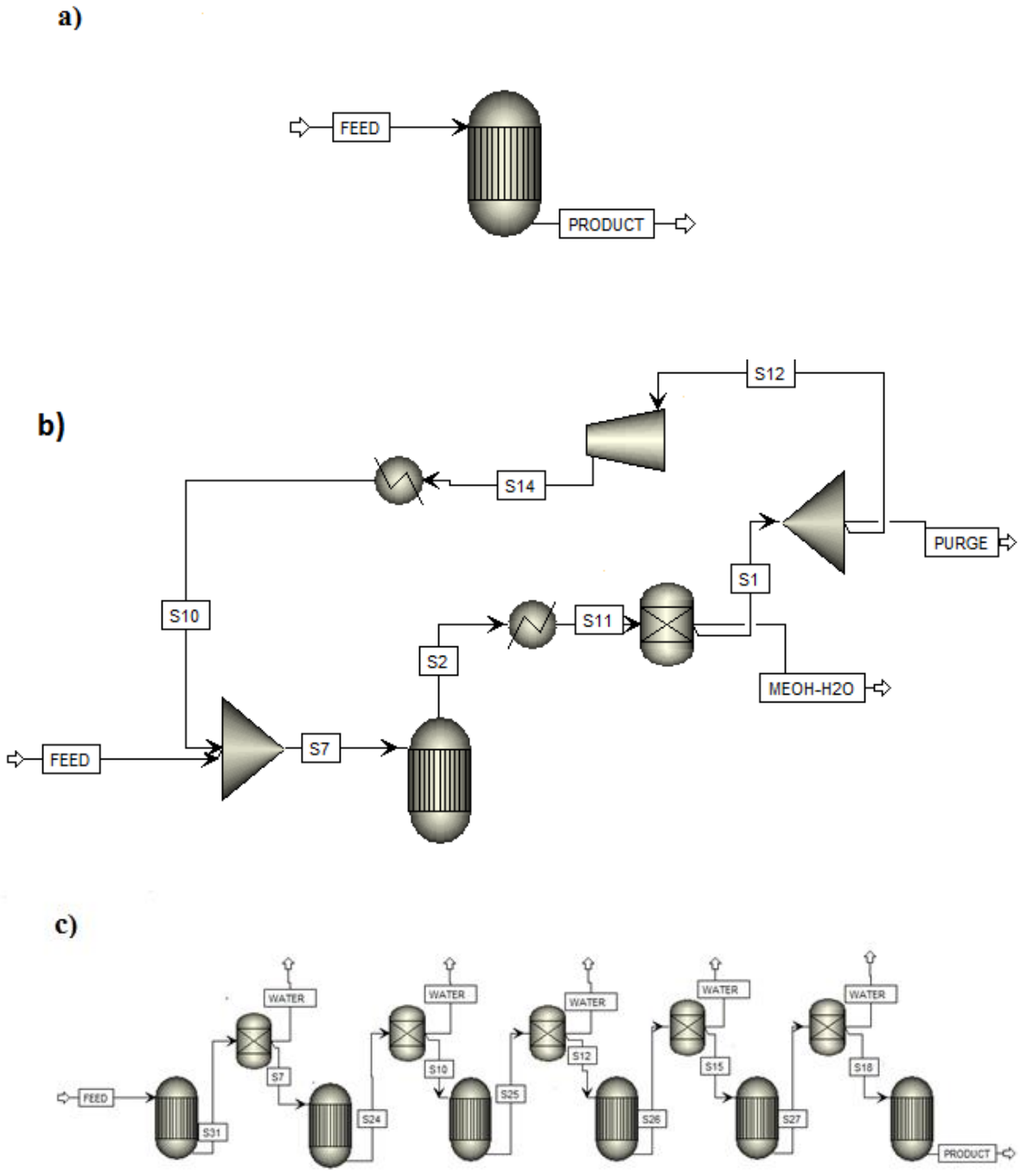

Figure II.1: Methanol reactor configurations studied in Aspen Plus® at equilibrium conditions: a) once-through equilibrium reactor; b) equilibrium reactor with the recycle of CO-CO_2-H_2 and separation of CH_3OH-H_2O by condensation; c) membrane reactor with H_2O separation (Leonzio et al., 2019)

In particular, for α=0 the reactor is without steam separation: steam is not transferred through the membrane and steam partial pressure on the reaction side is equal to that found without the membrane, at the same operating and equilibrium conditions. For α=1 the membrane is considered to be able to extract from the reaction ambient all H_2O produced there, then all steam passes through the membrane, that has an infinite surface area and the steam partial pressure inside the reactor (reaction side) is equal to that in the permeate side (1 bar). Positive driving force (the difference between steam partial pressure in the retentate and permeate side) is always verified.

It is interesting to analyze the analytical procedure for the calculation of these reactor configurations. This procedure is based on the application of the stoichiometric table and the equilibrium constants, expressed as functions of the extent of reactions II.1 and II.2. Setting a value of temperature and pressure, a solvable equations system is obtained.

At first, the once through reactor is taken into account. Table II.1 is the stoichiometric table, considered for reactions 1 and 2, where ξ_1 is the extent for reaction 1 and ξ_2 is the extent for reaction 2 at equilibrium conditions, In the calculation, it is assumed that the feed flow rate is composed of 1 mol/h of CO_2 and 3 mol/h of H_2 (stoichiometric conditions for reaction 1).

Table II.1 Stoichiometric table for reactions II.1 and II.2 for a feeding mixture of CO_2-H_2 (1:3) in a once-through reactor

	CO_2	H_2	CH_3OH	H_2O	CO
Feed	1	3	0	0	0
Consumed/Produced by reaction 1	$-\xi_1$	$-3\xi_1$	$+\xi_1$	$+\xi_1$	
Consumed/Produced by reaction 2	$-\xi_2$	$-\xi_2$		$+\xi_2$	$+\xi_2$
Equilibrium	$1-\xi_1-\xi_2$	$3-3\xi_1-\xi_2$	$+\xi_1$	$\xi_1+\xi_2$	$+\xi_2$

Assuming that partial pressures can reasonably approximate fugacities, the following equations are obtained to link the equilibrium constants to the reaction extents, ξ_1 and ξ_2, respectively (see Eqs. II.6-II.7):

$$K_{eq,1} = \frac{\left[\frac{\xi 1}{4-2\xi 1}\right]\cdot\left[\frac{\xi 1+\xi 2}{4-2\xi 1}\right]}{\left[\frac{1-\xi 1-\xi 2}{4-2\xi 1}\right]\cdot\left[\frac{3-3\xi 1-\xi 2}{4-2\xi 1}\right]^3}\cdot\frac{1}{P^2} \qquad (II.6)$$

$$K_{eq,2} = \frac{\left[\frac{\xi 1+\xi 2}{4-\xi 1}\right]\cdot\left[\frac{\xi 2}{4-\xi 1}\right]}{\left[\frac{1-\xi 1-\xi 2}{4-2\xi 1}\right]\cdot\left[\frac{3-3\xi 1-\xi 2}{4-2\xi 1}\right]} \qquad (II.7)$$

This is a system of two equations in two unknowns, when pressure and temperature are fixed: the extent of both reactions at thermodynamic equilibrium conditions is obtained.

It is interesting to analyze the once-through reactor also when it is fed by a mixture of CO_2, H_2 and CO. It is assumed that the feed is composed by 1 mol/h of CO_2, 5 mol/h of H_2 and 1 mol/h of CO: it is in stoichiometric condition for CH_3OH reaction: the required H_2 is equal to two moles for each mole of CO and three moles for each mole of CO_2. In this condition, the stoichiometric number S ($[H_2]-[CO_2]/[CO_2]+[CO]$) is equal to 2. Table II.2 shows the stoichiometric table for this reactor fed by a mixture with the composition defined above.

Table II.2 Stoichiometric table for reactions II.1 and II.2 with a feeding mixture of CO-CO_2-H_2 (1mol/h, 1 mol/h, 5 mol/h)

	CO_2	H_2	CH_3OH	H_2O	CO
Feed	1	5	0	0	1
Consumed/Produced by reaction 1	$-\xi_1$	$-3\xi_1$	$+\xi_1$	$+\xi_1$	
Consumed/Produced by reaction 2	$-\xi_2$	$-\xi_2$		$+\xi_2$	$+\xi_2$
Equilibrium	$1-\xi_1-\xi_2$	$5-3\xi_1-\xi_2$	$+\xi_1$	$\xi_1+\xi_2$	$1+\xi_2$

In these conditions, the relationships among the equilibrium constants and the extent of reactions are the following (see Eqs. II.8-II.9):

$$K_{eq,1} = \frac{\left[\frac{\xi1}{7-2\xi1}\right]\cdot\left[\frac{\xi1+\xi2}{7-2\xi1}\right]}{\left[\frac{1-\xi1-\xi2}{7-2\xi1}\right]\cdot\left[\frac{5-3\xi1-\xi2}{7-2\xi1}\right]^3}\cdot\frac{1}{P^2} \qquad (II.8)$$

$$K_{eq,2} = \frac{\left[\frac{\xi1+\xi2}{7-\xi1}\right]\cdot\left[\frac{1+\xi2}{7-\xi1}\right]}{\left[\frac{1-\xi1-\xi2}{7-2\xi1}\right]\cdot\left[\frac{5-3\xi1-\xi2}{7-2\xi1}\right]} \qquad (II.9)$$

Also in this case, setting the value for temperature and pressure, a solvable system in two equations with two unknowns, as ξ_1 and ξ_2 is present. With this feed composition, CO may be consumed when equilibrium conditions are established, so negative values for the reaction extent are also possible.

For the analysis of CH_3OH reactor with the recycle of unconverted gases after the condensation of CH_3OH and H_2O it is useful to consider the scheme reported in Figure II.2.

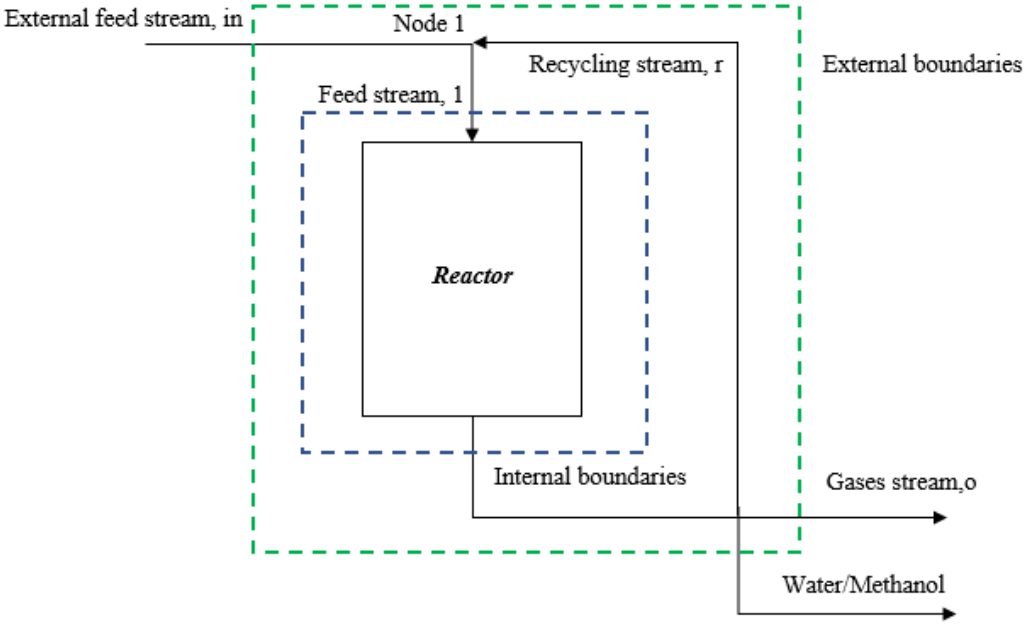

Figure II.2 Scheme of reactor with the recycle of CO-CO_2-H_2 and separation by condensation of H_2O and CH_3OH

Considering a material balance around node 1 where the external feed is linked to the recycling stream, the following relations are valid for CO_2, H_2 and CO (see Eqs. II.10-II.12):

$$CO_{2,1} = CO_{2,in} + CO_{2,r} = CO_{2,in} + R \cdot CO_{2,o} \quad (II.10)$$

$$H_{2,1} = H_{2,in} + H_{2,r} = H_{2,in} + R \cdot H_{2,o} \quad (II.11)$$

$$CO_1 = CO_{o,r} = R \cdot CO_o \quad (II.12)$$

where R is the recycling ratio (0%-100%), in is referred to the external feed stream at the inlet of the process, o is referred to the gases stream at the outlet of the process after the separation of H_2O and CH_3OH by condensation and r is referred to the recycling stream of H_2-CO_2-CO. A stoichiometric table as in Table II.3 is obtained, considering an external feed stream containing 1 mol/h of CO_2 and 3 mol/h of H_2. The feed is then in stoichiometric conditions as far as CH_3OH production is concerned (reaction II.1).

Table II.3 Stoichiometric table for reactions II.1 and II.2 with a feeding mixture of CO_2-H_2 (1:3), with recycle of CO-CO_2-H_2 and separation of CH_3OH-H_2O by condensation

	CO_2	H_2	CH_3OH	H_2O	CO
Feed	$1+RCO_{2,o}$	$3+RH_{2,o}$	0	0	RCO_o
Consumed/Produced by reaction 1	$-\xi_1$	$-3\xi_1$	$+\xi_1$	$+\xi_1$	
Consumed/Produced by reaction 2	$-\xi_2$	$-\xi_2$		$+\xi_2$	$+\xi_2$
Equilibrium	$1+RCO_{2,o}-\xi_1-\xi_2$	$3+RH_{2,o}-3\xi_1-\xi_2$	$+\xi_1$	$\xi_1+\xi_2$	$RCO_o+\xi_2$

In these conditions, the equilibrium reaction extents as functions of equilibrium constants and recycling ratio are given by (see Eqs. II.13-II.14):

$$K_{eq,1} = \frac{\left[\frac{\xi 1}{\frac{4-2\xi 1(1-\mathrm{R})-\mathrm{R}\xi 2}{1-R}}\right]\cdot\left[\frac{\xi 1+\xi 2}{\frac{4-2\xi 1(1-\mathrm{R})-\mathrm{R}\xi 2}{1-R}}\right]}{\left[\frac{1+\mathrm{R}CO_{2,o}-\xi 1-\xi 2}{\frac{4-2\xi 1(1-\mathrm{R})-\mathrm{R}\xi 2}{1-R}}\right]\cdot\left[\frac{3+\mathrm{R}H_{2,o}-3\xi 1-\xi 2}{\frac{4-2\xi 1(1-\mathrm{R})-\mathrm{R}\xi 2}{1-R}}\right]^3}\cdot\frac{1}{P^2} \qquad (II.13)$$

$$K_{eq,2} = \frac{\left[\frac{\mathrm{RCO}_o+\xi 2}{\frac{4-2\xi 1(1-\mathrm{R})-\mathrm{R}\xi 2}{1-R}}\right]\cdot\left[\frac{\xi 1+\xi 2}{\frac{4-2\xi 1(1-\mathrm{R})-\mathrm{R}\xi 2}{1-R}}\right]}{\left[\frac{1+\mathrm{R}CO_{2,o}-\xi 1-\xi 2}{\frac{4-2\xi 1(1-\mathrm{R})-\mathrm{R}\xi 2}{1-R}}\right]\cdot\left[\frac{3+\mathrm{R}H_{2,o}-3\xi 1-\xi 2}{\frac{4-2\xi 1(1-\mathrm{R})-\mathrm{R}\xi 2}{1-R}}\right]} \qquad (II.14)$$

Setting temperature, pressure and recycling ratio, the system of two equations in two unknowns, provides the equilibrium conditions for CH_3OH production. When R is equal to 0, the two equations are equal to the previous case, that without recycling. The study of this system can be divided in two sections: the first referred to internal boundaries, while the second referred to external boundaries. The results considered in this Thesis are those referred to the internal boundaries, so those relevant for the reactor behavior.

In a membrane reactor, H_2O is removed from reaction products and the equilibrium is shifted towards products. The flux of H_2O through a zeolite membrane is expressed by the following relation (see Eq. II.15):

$$J_{H2O} = Perm_{H2O}\cdot\left(P_{H2O,r}-P_{H2O,p}\right) \qquad (II.15)$$

where $Perm_{H2O}$ is the permeance of H_2O through the membrane (10^{-7}-10^{-6} $mols^{-1}m^{-2}Pa^{-1}$ at 523 K), $P_{H2O,r}$ is H_2O partial pressure on the retentate side and $P_{H2O,p}$ is H_2O partial pressure on the permeate side.

For this case, a stoichiometric table for the two reactions as in Table II.4 is developed, for a feed stream with 1 mol/h of CO_2 and 3 mol/h of H_2.

Table II.4 Stoichiometric table for reactions II.1 and II.2 with a feeding mixture of CO_2-H_2 (1:3) to the membrane reactor

	CO_2	H_2	CH_3OH	H_2O	CO
Feed	1	3	0	0	0
Consumed/Produced by reaction 1 and 2	$-\xi_1-\xi_2$	$-3\xi_1-\xi_2$	$+\xi_1$	$+\xi_1+\xi_2-J_{H2O}$ S	$+\xi_2$
Equilibrium	$1-\xi_1-\xi_2$	$3-3\xi_1-\xi_2$	$+\xi_1$	$\xi_1+\xi_2-J_{H2O}$ S	$+\xi_2$

To find the equilibrium conditions, three equations are available: the expressions for the two equilibrium ratios of partial pressures and the expression for the total moles of the system (H_2O partial pressure in the permeate side is set to 1 bar) (see Eqs. II.16-II.18):

$$K_{eq,1} = \frac{\left[\frac{\xi 1}{total\ moles}\right] \cdot \left[P_{H2O,o} - \Delta P_{H2O} \cdot \alpha\right]}{\left[\frac{1-\xi 1-\xi 2}{total\ moles}\right] \cdot \left[\frac{3-3\xi 1-\xi 2}{total\ moles}\right]^3} \cdot \frac{1}{P^2} \quad (II.16)$$

$$K_{eq,2} = \frac{\left[\frac{\xi 2}{total\ moles}\right] \cdot \left[P_{H2O,o} - \Delta P_{H2O} \cdot \alpha\right]}{\left[\frac{1-\xi 1-\xi 2}{total\ moles}\right] \cdot \left[\frac{3-3\xi 1-\xi 2}{total\ moles}\right]} \quad (II.17)$$

$$1 = \frac{1-\xi 1-\xi 2}{total\ moles} + \frac{3-3\xi 1-\xi 2}{total\ moles} + \frac{\xi 2}{total\ moles} + \frac{\xi 1}{total\ moles} + \left(P_{H2O,o} - \Delta P_{H2O} \cdot \alpha\right) \quad (II.18)$$

where (see Eqs. II.19-II.20):

$$P_{H2O,o} = \frac{\xi 1 + \xi 2}{4 - 2\xi 1} \cdot P \quad (II.19)$$

$$\Delta P_{H2O} = P_{H2O,o} - 1 \quad (II.20)$$

with α a factor varying in the range between 0 and 1.

Starting from a mixture with CO_2 and H_2, CO_2 conversion to CH_3OH can be defined as in the following relation (see Eq. II.21):

$$\chi_{co2} = \frac{CO_{2,in} - (CO_{2,out} + CO_{out})}{CO_{2,in}} = \xi_1 \quad (II.21)$$

Then, CO_2 conversion to CH_3OH corresponds to the extent of reaction 1. Equation II.8 also quantifies CH_3OH yield with respect to CO_2 in the feeding stream. In fact, CH_3OH yield is defined, for a feeding mixture of CO_2-H_2, by the following relation (see Eq. II.22):

$$MeOH\ yield = \frac{MeOH}{CO_{2,in}} = \chi_{co2} = \xi_1 \quad (II.22)$$

Global CO_2 conversion is defined as (see eq. II.23):

$$\chi_{co2,gloabal} = \frac{CO_{2,in} - CO_{2,out}}{CO_{2,in}} = \xi_1 + \xi_2 \quad (II.23)$$

Global CO_2 conversion is equal to the sum of the extent of reactions 1 and 2.

CH_3OH selectivity can be defined as (see Eq. II.24):

$$MeOH\ selectivity = \frac{MeOH}{CO_{2,in} - CO_{2,out}} = \frac{\xi_1}{\xi_1 + \xi_2} \quad (II.24)$$

When the feed contains CO-CO_2-H_2, carbon conversion to CH_3OH is defined by the following relation (see Eq. II.25):

$$\chi_c = \frac{(CO_{2,in} + CO_{in}) - (CO_{2,out} + CO_{out})}{(CO_{2,in} + CO_{in})} = \xi_1 \qquad (II.25)$$

Carbon conversion to CH_3OH is equal to the extent of reaction 1. On the other hand, CH_3OH yield is defined as (see Eq. II.26):

$$MeOH\ yield = \frac{MeOH}{CO_{2,in} + CO_{in}} = \chi_c = \xi_1 \qquad (II.26)$$

Related to the analysis of an equilibrium reactor it is the analysis an adiabatic plug flow reactor with the recycle of unconverted gases after the separation of CH_3OH and H_2O by condensation. This adiabatic reactor, considering two reactions (reaction II.1 and II.2), is described by the following energy and material balances in stationary conditions considering an infinitesimal volume (see Eqs. II.27-II.29):

$$\sum_i F_{i,1} \cdot c_{p,i1} \cdot dT + \Delta H_1 \cdot r_1 \cdot dV + \Delta H_2 \cdot r_2 \cdot dV = 0 \qquad (II.27)$$

$$F_{co2,1} \cdot d\varepsilon_1 = r_1 \cdot dV \qquad (II.28)$$

$$F_{co2,1} \cdot d\varepsilon_2 = r_2 \cdot dV \qquad (II.29)$$

where $F_{i,1}$ is the molar flow rate of i component at the inlet of reactor, T is temperature, $cp_{i,1}$ is the heat capacity at constant pressure for i component at the inlet of reactor, r_1 and r_2 are the reaction rate for Eq. II.1 and II.2 respectively, ΔH_1 and ΔH_2 are the heat of reaction for reaction II.1 and II.2 respectively, V is the volume of reactor, ε_1 and ε_2 are respectively the extent of reaction II.1 and II.2 for the adiabatic reactor, $F_{co2,1}$ is the molar flow rate of CO_2 at the inlet of reactor. Through appropriate mathematical steps and combining these above reactions, it is possible to obtain the following relation (see Eq. II.30):

$$\sum_i F_{i,1} \cdot c_{p,i1} \cdot (T - T_1) + \Delta H_1 \cdot \varepsilon_1 \cdot F_{co2,1} + \Delta H_2 \cdot \varepsilon_2 \cdot F_{co2,1} = 0 \qquad (II.30)$$

describing the trajectory of the process as a function of temperature. Overall, there are three equations with three main unknowns as T, ε_1 and ε_2. It is necessary, in order to solve the problem, to consider also molar balances with the energy balance. This means that a kinetic model is required. However, it is possible approximate the ξ_1/ξ_2 ratio of equilibrium condition (calculated before) to the $\varepsilon_1/\varepsilon_2$ ratio of adiabatic case at the same temperature, at the outlet of reactor. This simplifying hypothesis means that the selectivity of a CH_3OH equilibrium reactor is the same of that an adiabatic reactor, at the outlet of reactor. This assumption is justified by the fact that in this analysis, it is interesting the equilibrium approach, then the previous equality about selectivity is ensured. Setting a value of temperature it is possible to know the selectivity for the equilibrium and then for the adiabatic reactor; the selectivity is also expressed as a function of the

extents of each reaction and combined with the assumption about the ratio ξ_1/ξ_2, the value of ε_1 and ε_2 are evaluated. Doing the calculation for different values of temperature, it is possible to find the trajectory of the adiabatic reactor approaching the equilibrium condition.

II.2.2 Kinetic model for methanol synthesis

The kinetic mechanism of carbon dioxide hydrogenation is an active area of research as documented by different literature works studying the pathway leading to methanol formation from CO_2 on different catalysts and catalyst active sites (Hus et al., 2017a,b), also combining the density functional theory computations with the mesoscopic kinetic Monte Carlo (Kopac et al., 2017).

As discussed in Chapter I, different kinetic models based on different assumptions are reviewed by Slotboom et al. (2020), suggesting also a new model, the parameters of which are fitted by experimental data.

In this research, the Vanden Bussche and Froment (1996) kinetic model, based on the mechanism of CO_2 hydrogenation for CH_3OH production, is considered to model the methanol reactor.

The expressions for the reaction rates as functions of partial pressures are the following respectively for reaction II.1 and II.2 (see Eqs. II.31-II.32) (Vanden Bussche and Froment, 1996):

$$\boldsymbol{r_1} = \frac{k_1 \cdot p_{CO2} \cdot p_{H2} \cdot \left(1 - \frac{p_{CH_3OH} \cdot p_{H2O}}{K_{eq,1} \cdot p^3_{H2} \cdot p_{CO2}}\right)}{\left(1 + k_C \cdot \frac{p_{H2O}}{p_{H2}} + k_a \cdot \sqrt{p_{H2}} + k_b \cdot p_{H2O}\right)^3} \qquad (II.31)$$

$$\boldsymbol{r_2} = \frac{k_2 \cdot p_{CO2} \cdot \left(1 - \frac{p_{CO} \cdot p_{H2O}}{K_{eq,2} \cdot p_{H2} \cdot p_{CO2}}\right)}{\left(1 + k_C \cdot \frac{p_{H2O}}{p_{H2}} + k_a \cdot \sqrt{p_{H2}} + k_b \cdot p_{H2O}\right)} \qquad (II.32)$$

with k_1, k_2, k_c, k_a and k_b the reaction rate kinetic constants (see numerical values in the Appendix), p_{CH3OH} the partial pressure of CH_3OH, p_{CO} the partial pressure of carbon monoxide (CO), p_{CO2} the partial pressure of CO_2, p_{H2} the partial pressure of H_2, p_{H2O} the partial pressure of H_2O, K_{eq1} and K_{eq2} the equilibrium constant of reaction 1 and 2 respectively.

II.2.3 Mathematical model for a methanol reactor in kinetic regime

For the reactor configuration reported in Figure II.3 a mathematical model is developed in MATLAB® in 1-D and 2-D.

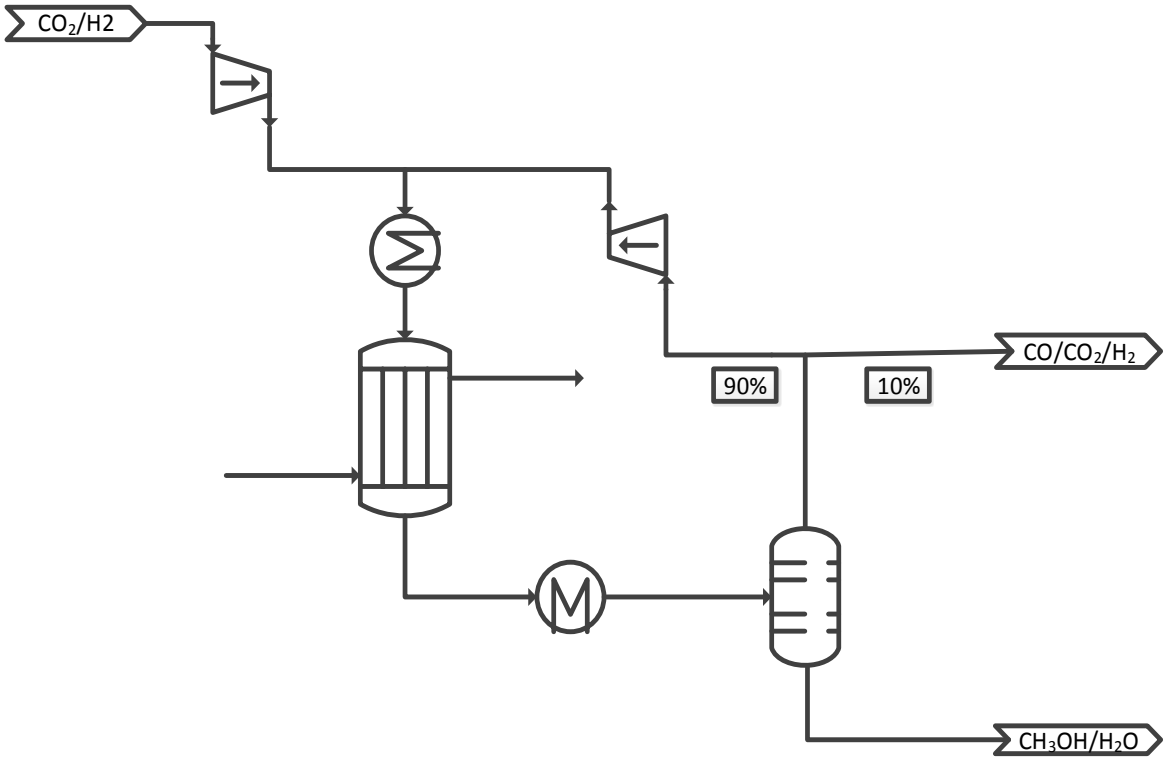

Figure II.3 Process scheme adopted in the mathematical kinetic model of a methanol reactor with 90% of recycle of unconverted gases after the separation of CH_3OH and H_2O by condensation (Leonzio et al., 2019)

A Lurgi type multi-tubular reactor is considered here: tubes are packed with a catalyst ($CuO/ZnO/Al_2O_3$) for the synthesis reactions, while on the shell side boiling water is flowing for the refrigeration. In the process scheme shown in Figure II.3, a recycle of unconverted gases, CO_2, CO and H_2, is present and the recycle ratio is set at 90%, after the separation of CH_3OH and H_2O by condensation. The external feed stream, fixed at 100 mol/s, is composed by CO_2 and H_2 with the stoichiometric molar ratio 1:3. Table II.1 summarizes the reactor operating conditions, considered for the two models, as suggested by Yusup et al. (2010).

Regarding the 2-D model, the same density value shown in Table II.5 is fixed for both the structured and non-structured packing, and the active catalyst load is also assumed to be the same: as a result, with a given geometric configuration and corresponding operating conditions, close values of the gas hourly space velocity are maintained in the reactor for structured and non-structured packing, respectively. The nominal diameter of catalyst pellets is defined as the diameter of a sphere with the same surface-to-volume ratio. To allow a straight comparison, cells or channels of the structured packing are characterized by the same nominal size.

Table II.5 Methanol reactor, Lurgy type, operating conditions (Leonzio and Foscolo, 2020)

Tube number	150	
Tube length	8	m
Tube ID diameter	0.0508	m
Density of catalyst packing	1100	kg/m^3
Nominal diameter of catalyst packing	0.0054	m
Thermal conductivity of catalyst pellets	0.38	W/(m K)
Thermal conductivity of structured catalyst	350	W/(m K)
Reactor fresh feeding flow rate	100	mol/s
Inlet pressure	55	bar
Inlet temperature	498	K
Refrigerant temperature	523	K

II.2.3.1 1-D mathematical model

For the above mentioned reactor configuration, a 1-D mathematical model in steady state conditions is developed in MATLAB®, solved with the ode45, with the following assumptions (Manenti et al., 2011):

- negligible axial dispersion;
- negligible radial diffusion (concentration, velocity and temperature profiles are assumed constant), due to the small ratio of reactor diameter to reactor length, leading to a 1-D model;
- uniform catalytic particles (constant temperature and pressure profiles within the catalytic pellet, due to the small size of the pellet and the relatively low chemical reaction intrinsic rate at the moderate temperature level of the reactor): the Weisz-Prater parameter, defined as follows (see Eq. II.33) (Fogler, 2004):

$$C_{wp} = \frac{r_{obs,i} \cdot \rho_c \cdot {R_p}^2}{D_e \cdot C_{s,i}} \qquad (II.33)$$

  is estimated to be << 1 (C_{wp}≈0.03), where $r_{obs,i}$ is the measured value of the reaction rate for component i, $C_{s,i}$ is the concentration of component i at the pellet surface, D_e is the effective diffusivity, R_p is the pellet radius, ρ_c is the density of catalyst particle;

- negligible catalyst deactivation: temperature is lower than levels where sintering phenomena may occur (the life cycle of the commercial catalyst is in the order of two years and no sulfur species are considered in this case);
- negligible side reactions except for the reverse water gas shift, due to the high catalyst selectivity;
- pseudo-homogeneous model: gradients between gas and solid phase are neglected due to the small size of particles;

The mathematical model is composed of the molar balances, the energy balance and the Ergun equation to estimate pressure drop along the reactor. The recycle of gases, with a recycle ratio of 90%, after the separation of CH_3OH and H_2O by condensation, is taken into account in the boundary conditions, which establish molar flows and concentrations entering the reactor by adding together the plant feeding stream and the recycle stream.

The material balances for each component in steady state conditions assume that the variation of the convective molar flow of each chemical compound matches the corresponding reaction rate (see Eqs. II.34-II.38):

$$\frac{dF_{CH3OH}}{dw} = r_{CH3OH} = r_1 \qquad (II.34)$$

$$\frac{dF_{H2O}}{dw} = r_{H2O} = r_1 + r_2 \qquad (II.35)$$

$$\frac{dF_{CO2}}{dw} = r_{CO2} = -r_1 - r_2 \qquad (II.36)$$

$$\frac{dF_{CO}}{dw} = r_{CO} = r_2 \qquad (II.37)$$

$$\frac{dF_{H2}}{dw} = r_{H2} = -3 \cdot r_1 - r_2 \qquad (II.38)$$

where *Fi* is the molar flow rate of i component (CH_3OH, H_2O, CO_2, CO, H_2) in mol/s, r_1 and r_2 are the reaction rates for CH_3OH and CO formation, respectively, referred to reactions (1) and (2) and expressed by Eqs. II.1 and II.2 in mol/(kg s), *w* the mass of catalyst in kg. The composition profile for each component is then obtained.

The energy balance and Ergun equations are used to calculate the temperature and pressure profiles, respectively from (see Eqs. II.39-II.42):

$$\frac{dT}{dw} = \frac{U \cdot a \cdot (T_j - T)}{F \cdot C_{pm}} - \frac{\Delta H_1^{rxn} \cdot r_1}{F \cdot C_{pm}} - \frac{\Delta H_2^{rxn} \cdot r_2}{F \cdot C_{pm}} \qquad (II.39)$$

$$\frac{dP}{dw} = -\frac{G}{\rho \cdot g_c \cdot d_p} \cdot \left(\frac{1-\varepsilon}{\varepsilon^3}\right) \cdot \left[\frac{150 \cdot (1-\varepsilon) \cdot \mu}{d_p} + 1.75 \cdot G\right] \cdot \frac{z}{w} \qquad (II.40)$$

$$\frac{z}{w} = \frac{1}{S \cdot (1-\varepsilon) \cdot \rho_c} \qquad (II.41)$$

$$a = \frac{4}{d_t \cdot (1-\varepsilon) \cdot \rho_c} \qquad (II.42)$$

where *F* is the total molar flow rate in mol/s, *w* is the mass of catalyst in kg, *T* is the temperature in K, *U* is the global coefficient of heat exchange in J/(m^2 s K), *a* is the specific surface area of heat exchange in

m^2/(kg cat), T_j is the temperature of the heat exchange fluid in K, C_{pm} is the average specific heat in J/(mol K), ΔH^{rxn} is the heat of reaction in J/mol, r is the reaction rate for reactions 1 and 2, respectively, in mol/(kg s), P is the pressure in Pa, G is the superficial mass velocity in kg/(s m^2), ρ is the gas density in kg/m^3, g_c is a conversion factor in kg/m/s^2N, d_p is the average equivalent diameter of catalyst pellets in the bed in m, ε is the bed porosity, μ is the fluid viscosity in Pa s, z is reactor length in m, d_t is the tube diameter in m, S the tube cross section surface area in m^2, ρ_c is the density of catalyst pellets in kg/m^3.

II.2.3.2 2-D mathematical model

A 2-D steady-state mathematical model is developed considering balance equations around the generic, toroidal volume element of the reactor with the following assumptions:

- negligible axial diffusion, due to a particle Reynolds number >> 10 (Leonzio, 2020) and the high axial Peclet number (Montebelli et al., 2013);
- constant temperature and pressure profile within the catalyst pellet, according to the adoption of a pseudo-homogeneous reactor configuration (Manenti et al., 2011);
- negligible catalyst deactivation (Manenti et al., 2011);
- catalytic particle effectiveness is equal to one, due to the estimated low value of Thiele modulus (<1) (Leonzio, 2020);
- deviations from ideal gas conditions are neglected (fugacity coefficients are almost equal to one at the reactor operating conditions) (Graaf and Winkelman, 2016).

A system of partial differential equations describing the methanol reactor (molar concentrations, energy and pressure drop equations) is developed in dimensionless form (see Eqs. II.43-II.45):

$$\frac{1}{r_{ad}} \cdot \frac{\partial}{\partial r_{ad}} \left(r_{ad} \cdot \frac{\partial C_{i,ad}}{\partial r_{ad}} \right) - \frac{U_z \cdot R_{tot}^2}{L_{tot} \cdot De} \cdot \frac{\partial \ C_{i,ad}}{\partial \xi} + \frac{r_i}{r_{i,o}} \cdot \frac{r_{i,o} \cdot R_{tot}^2}{Dr \cdot C_{in,CO2}} = 0 \qquad (II.43)$$

$$\frac{1}{r_{ad}} \cdot \frac{\partial}{\partial r_{ad}} \left(r_{ad} \cdot \frac{\partial T_{\ ad}}{\partial r_{ad}} \right) - \left(\sum_{j=1}^{2} \frac{\Delta H_j \cdot Dr \cdot C_{in,CO2}}{Ke \cdot T_{in}} \cdot \frac{R_{tot}^2 \cdot \boldsymbol{r_{i,o}}}{De \cdot C_{in,CO2}} \cdot \frac{\boldsymbol{r_{i,o}}}{\boldsymbol{r_i}} - \frac{U_z \cdot (\sum Cp_i \cdot C_i) \cdot R_{tot}^2}{L_{tot} \cdot Ke} \cdot \frac{\partial \ T_{\ ad}}{\partial \xi} \right) = 0 \qquad (II.44)$$

$$\frac{P_{in}}{L_{tot}} \cdot \frac{dP_{ad}}{d\xi} = -\frac{G}{\rho \cdot g_c \cdot d_p} \cdot \left(\frac{1-\varepsilon}{\varepsilon^3} \right) \cdot \left[\frac{150 \cdot (1-\varepsilon) \cdot \mu}{d_p} + 1.75 \cdot G \right] \qquad (II.45)$$

where r_{ad} is the dimensionless radial coordinate, $r_{ad}=r/R_{tot}$, $C_{i,ad}$ is the dimensionless molar concentration of component i, $C_{i,ad}=Ci/C_{in,CO2}$, Uz is the superficial gas velocity in m/s, R_{tot} is the radius of reactor tube in m, Dr is the radial dispersion coefficient in m^2/s, ξ is the dimensionless axial coordinate, $\xi= z/L_{tot}$, $\boldsymbol{r}_i$ is the reaction rate of i component in mol/m^3s, $\boldsymbol{r_{i,o}}$ is the reaction rate of i component at the system inlet conditions (fresh feed stream composition, reactor inlet temperature and pressure), $C_{in,CO2}$ is the inlet concentration of CO_2 in mol/m^3, T_{ad} is the dimensionless temperature, $T_{ad}=T/T_{in}$, ΔH_j is the heat of reaction for reaction j in J/mol, Ke is the equivalent radial thermal conductivity in J/msK, $C_{p,i}$ is the heat capacity at constant pressure

for component i in J/molK, *Ci* is the molar concentration of component i in mol/m^3, L_{tot} is the length of reactor in m, P_{ad} is the dimensionless pressure, $P_{ad} = P/P_{in}$, P_{in} is the pressure at inlet conditions in Pa, *G* is superficial mass velocity in kg/(s m^2), ρ is gas density in kg/m^3, g_c is a conversion factor in kg/m/s^{2}N, d_p is the nominal diameter of catalyst packing in the bed in m, ε is the bed porosity, μ is viscosity in Pa s.

In the material balance (Eq. II.17), a term with the partial derivative of the superficial velocity, U_z, with the reactor axial coordinate should also appear, in order to provide a full account of the variation of the convective molar flux along the reactor length, expressed as follows (see Eq. II.46):

$$\frac{\partial \ U_z \cdot C_{i,ad}}{\partial \xi} \tag{II.46}$$

However, the axial gradient of superficial velocity is neglected in the numerical integration, because it is expected to be small in comparison to the remaining terms: as a matter of facts, the overall molar flow rate changes no more than 10% along the reactor length, reactor temperature keeps a value quite close to the refrigerant fluid temperature and a slight pressure drop is found, as shown by the results described below.

In the integration procedure, the local value of U_z is expressed as a function of local temperature, pressure and molar flowrate, as follows (see Eq. II.47):

$$U_z = \ U_{in} \cdot \frac{P_{in}}{P} \cdot \frac{T}{T_{in}} \cdot \frac{\sum_i F_i}{F_{tot,in}} \tag{II.47}$$

Similar considerations hold also for the overall molar concentration in the term expressing the variation of the radial dispersive flux (Eq. II.17).

In the above equations, some dimensionless numbers are present, as that resembling the Thiele modulus, ϕ^2_n, when considering the radial dispersion coefficient instead of pellet equivalent diffusivity coefficient (Annesini, 2020) (see Eq. II.48):

$$\phi_n^2 = \frac{\boldsymbol{r_{i,o}} \cdot R_{tot}^2}{Dr \cdot C_{in,CO2}} \tag{II.48}$$

where all quantities are defined above, and β number in the energy balance, as the dimensionless heat of reaction (Fogler, 2004) (see Eq. II.49):

$$\beta = - \frac{\Delta H_j \cdot De \cdot C_{in,CO2}}{Ke \cdot T_{in}} \tag{II.49}$$

where all quantities are also defined above. β is positive for exothermic reactions.

An additional dimensionless number, γ, can be identified in the expression of reaction rates, which is sometimes referred to as the Arrhenius number (Fogler, 2004) (see Eqs. II.50-II.51):

$$k(T) = A \cdot e^{\left(-\frac{E_a}{R \cdot T}\right) \cdot \left(\frac{T_{in}}{T_{in}}\right)} = A \cdot e^{(\gamma) \cdot \left(\frac{T_{in}}{T}\right)} \tag{II.50}$$

$$k(T_{in}) = A \cdot e^{\left(-\frac{E_a}{R \cdot Tin}\right)} = A \cdot e^{(\gamma)} \qquad (II.51)$$

where A is the pre-exponential factor, E_a is the activation energy in J/mol, R is the ideal gas constant in J/molK, T is the temperature in K, T_{in} the temperature in K at the reactor inlet.

Boundary conditions set for the partial differential system of equations are fixed at the reactor inlet according to the following relations (see Eqs. II.52-II.54):

$$C_{i,ad} = \frac{C_{in,i}}{C_{in,CO2}} \qquad (II.52)$$

$$T_{ad} = 1 \qquad (II.53)$$

$$P_{ad} = 1 \qquad (II.54)$$

Boundary conditions at the center of reactor tube (radius equal to 0) are the following (see Eqs. II.55-II.56):

$$\frac{\partial T_{ad}}{\partial r_{ad}} = 0 \qquad (II.55)$$

$$\frac{\partial C_{i,ad}}{\partial r_{ad}} = 0 \qquad (II.56)$$

Boundary conditions at $r = R$ are expressed by the following relations (see Eqs. II.57-II.58):

$$-\frac{Ke \cdot T_{in}}{R_{tot}} \cdot \frac{\partial T_{ad}}{\partial r_{ad}} = U \cdot \left(T_{r,ad}(R,z) \cdot T_{in} - T_{ref}\right) \qquad (II.57)$$

$$\frac{\partial C_{i,ad}}{\partial r_{ad}} = 0 \qquad (II.58)$$

where $\boldsymbol{U}$ is the external heat transfer coefficient in J/(s m^2 K) (between 1000 J/(s m^2 K) and 20000 J/(s m^2 K) (Annesini, 2000)), T_{ref} is the temperature of refrigerant fluid of 523 K, while other terms are defined in previous expressions.

The partial differential system of equations with the above boundary conditions is solved in MATLAB® by using the PDEPE function. Cylindrical coordinates in steady state conditions are considered. To evaluate the radial thermal conductivity of the packed bed, the correlation obtained from Specchia and Sicardi (1980) is used (see Eq. II.59):

$$Ke = K_g \cdot \left(\frac{\varepsilon}{1.5} + \frac{1-\varepsilon}{0.312 \cdot \varepsilon^{2.32} + \frac{K_g}{K_{cat}} \cdot \frac{2}{3}} \right) \qquad (II.59)$$

where ε is the bed void fraction, K_{cat} is the thermal conductivity of catalyst, and K_g is the thermal conductivity of gas according to the following relation (Lovik, 2001), in kW/(m K) (see Eq. II.60):

$$K_g = 0.01234 \cdot 10^{-3} + 1.84375 \cdot 10^{-7} \cdot T \qquad (II.60)$$

where T is the temperature in K. The radial dispersion coefficient is calculated with the following correlation (Smith, 1981) (see Eq. II.61):

$$D_r = \frac{\frac{d_p \cdot \mu}{8}}{(1 + 19.4 \cdot \left(\frac{d_p}{d_t}\right)^2)} \qquad (II.61)$$

where d_p is the catalyst diameter in m, d_t is the tube diameter in m and μ is the viscosity in Pa s. The 2-D model is developed considering 1 tube of the reactor.

II.3 Results and discussion

II.3.1 Results of equilibrium analysis for methanol synthesis

A thermodynamic equilibrium analysis of a methanol reactor in different plant configurations, as i) once-through reactor, ii) reactor with the recycle of unconverted gases after the separation of CH_3OH and H_2O (R=80%) and iii) membrane reactor (α=0.4), is developed in this section with the aim to evaluate CO_2 conversion to CH_3OH, i.e. CH_3OH yield, CO_2 global conversion and CH_3OH selectivity .

In this analysis, the range of temperature is fixed to be 473-553 K, where the industrial catalyst based on $Cu/Al_2O_3/Zn$ would assure satisfactory reaction rates and the thermodynamic equilibrium of reaction 1 is also quite favorable. The commonly suggested range of operating pressure is 15-55 bar.

The results of this equilibrium analysis are reported in Figure II.4, where it is possible to see that temperature has a negative effect, while pressure has a positive effect on CO_2 conversion to CH_3OH, according to the Le Chatelier's principle (it is an exothermic reaction with reduction of mole number). More specifically, Figure II.4a shows CO_2 conversion to CH_3OH and CH_3OH yield varying temperature and pressure, for the once-through reactor. The highest CO_2 conversion is reached at the lowest examined temperature (473 K) and highest examined pressure (55 bar). The results of temperature-dependent analysis clearly show the limitations of direct CO_2 hydrogenation route, since the maximum attainable CO_2 equilibrium conversion is 38% at the conditions considered here.

For the reactor with a recycle of gases (R=80%) after the separation of CH_3OH and H_2O, Figure II.4b shows that, at 55 bar and 473 K, CO_2 conversion to CH_3OH and CH_3OH yields are equal to 69%, with reference to the plant feed stream. Definitely, the system with a recycle stream of H_2-CO_2-CO, after the separation of CH_3OH and H_2O, ensures a higher CH_3OH yield compared to the process arrangement with a mixture of CO_2-H_2 in the reactor feed stream, examined before.

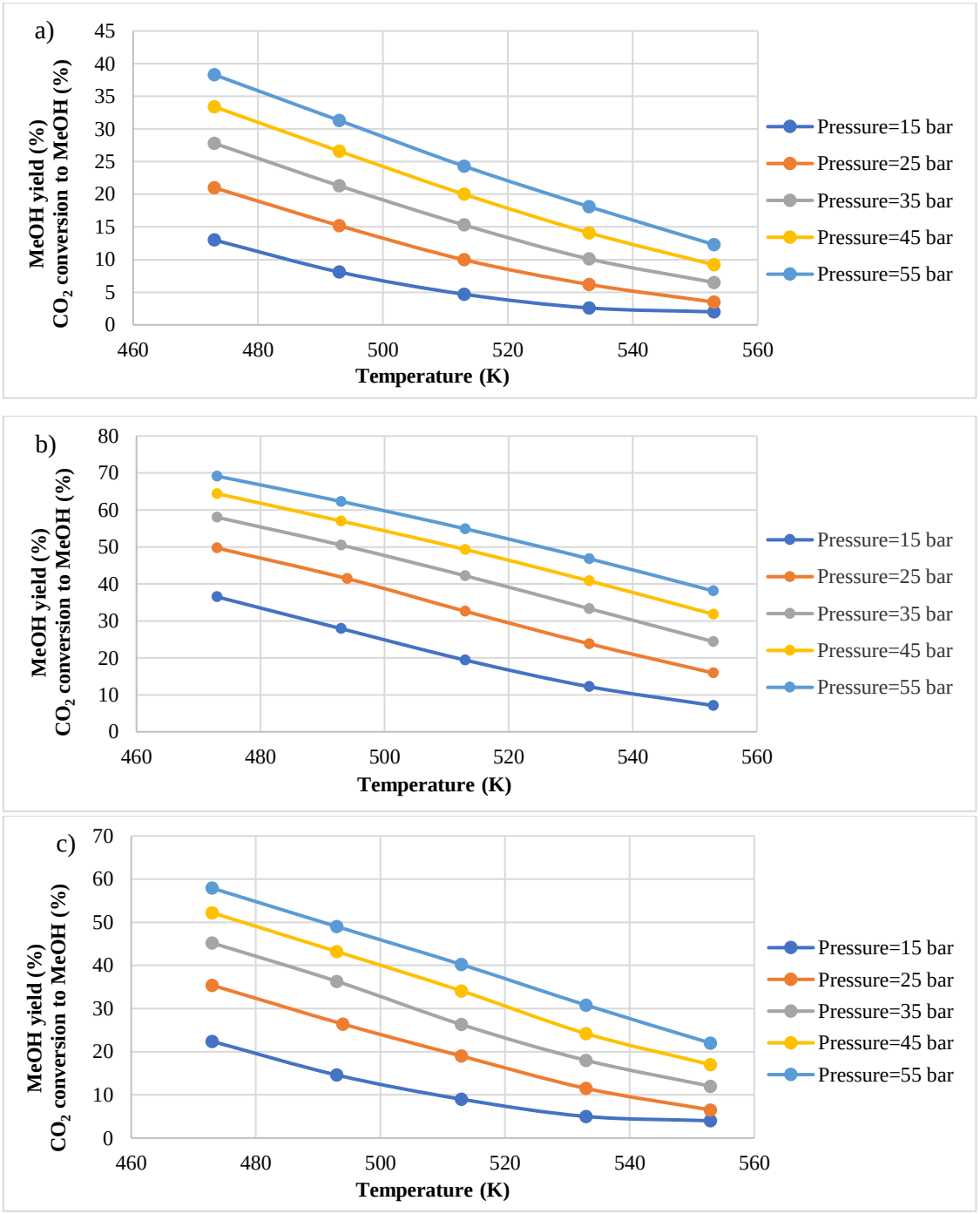

Figure II.4 Equilibrium CO_2 conversion to CH_3OH and CH_3OH yield as a function of temperature and pressure, with stoichiometric CO_2-H_2 ratio (1:3) in the process feeding stream: a) once-through reactor; b) reactor with the recycle of unconverted gases (R=80%) after the separation of CH_3OH and H_2O by condensation; c) membrane reactor permeable to steam (Leonzio et al., 2019)

Figure II.4c shows the equilibrium analysis for a membrane reactor designed to separate H_2O simultaneously to the reaction process. The system ensures a CO_2 conversion higher than that in an once-through reactor, but substantially lower when compared to CO_2 conversion predicted in a reactor with the

recycle of gases after the separation of condensable compounds. In fact, at the same operating conditions, 55 bar and 493 K, the equilibrium CO_2 conversion to CH_3OH is equal to 58%. When compared to the results obtained with the once-through reactor, the higher conversion is due to the removal of water that shifts the reactions towards products. It is worth noticing here that H_2O is also produced by rWGS reaction, so selectivity towards methanol is not helped. The positive effect on conversion process due to H_2O removal is also reported by Zachopoulos and Heracleous (2017).

The results reported in Figure II.4 show that by combining the separation of reaction products, as H_2O and CH_3OH, and by recycling unconverted gases, CO_2 conversion and CH_3OH yield can be improved compared to other cases. A similar behavior is also reported in the studies of Makertiharta et al. (2017), Struis and Stucki (2001).

The presence of CO in the feeding stream is highly advantageous with respect to the methanol synthesis from plain CO_2. According to the Vanden Bussche and Froment (1996) reaction mechanism, increasing CO concentration makes the equilibrium extent of the second reaction (rWGS) to decrease progressively up to the point when it proceeds in the opposite direction, when CO concentration is higher than that at equilibrium, and in these conditions WGS contributes to increase CO_2 availability and therefore methanol yield. Water inhibits methanol synthesis and a further positive effect of CO arises from its ability to "scavenge" excess water via water gas shift. Then, the recycle of CO in the feed allows to obtain a higher CH_3OH yield and carbon conversion at thermodynamic equilibrium.

As a matter of facts, Figure II.5 shows CH_3OH yield and carbon conversion to methanol versus the CO/CO_2 ratio in the feed and the pressure level, at different temperature (the feeding concentration of hydrogen is adjusted in each case according to the stoichiometric conditions). It is evident that a higher amount of CO in the feed allows to obtain a higher CH_3OH yield and carbon conversion at thermodynamic equilibrium. Temperature has a negative effect while pressure has a positive effect also on the cases analyzed here. A value of CH_3OH yield and carbon conversion near to 100% can be obtained only at the lowest temperature (473 K) investigated here, while at the highest temperature (553 K) CH_3OH yield and carbon conversion are equal to 39% at most.

A maximum in CH_3OH production as a function of CO_2/CO ratio occurs at CO_2 concentration equal to 2-5 mol% (Lee et al., 1993; Vanden Bussche and Froment, 1996). As reported also by Skrzypek et al. (1995), if there is no CO in feed, the mole fraction of methanol in the condensable products does not exceed 0.5, in agreement with the stoichiometry of reactions 1 and 2.

The positive effect of H_2 content on the process efficiency is assessed by additional thermodynamic calculations, not shown here. At 493 K and 55 bar, in the case of stoichiometric ratio 1:3, carbon dioxide conversion is equal to 38% (Figure II.3a), while at the same temperature and pressure carbon dioxide equilibrium conversion reaches 54% with a CO_2:H_2 ratio equal to 1:5. The positive effect of H_2 on CO_2 conversion is also reported by Bansode and Urakawa (2014). However, the H_2 conversion decreases with

the increase of just H_2 partial pressure. Khalilpourmeymandi et al. (2017) find that the effect of the relative amount of H_2 on CH_3OH production is higher than that of a relative amount of CO.

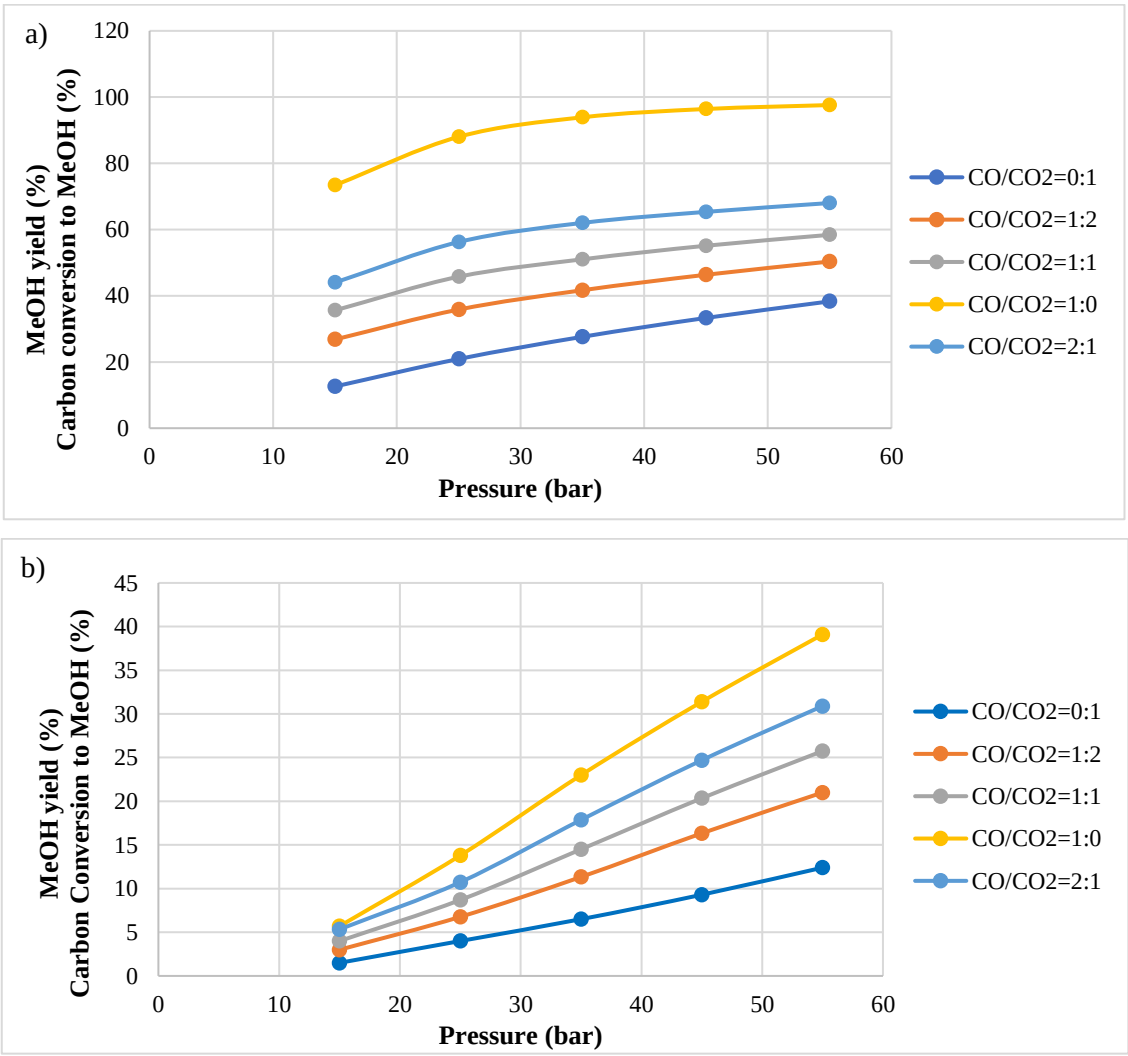

Figure II.4 Equilibrium CH_3OH yield and carbon conversion to methanol for the once-through reactor, as a function of pressure, at different CO/CO_2 ratios, with H_2 content in the feed always adjusted to stoichiometry; a) T=473 K; b) T=553 K (Leonzio et al., 2019)

The global CO_2 conversion as a result of reaction 1 and reaction 2, is also analyzed at the thermodynamic equilibrium, as shown in Figure II.6.

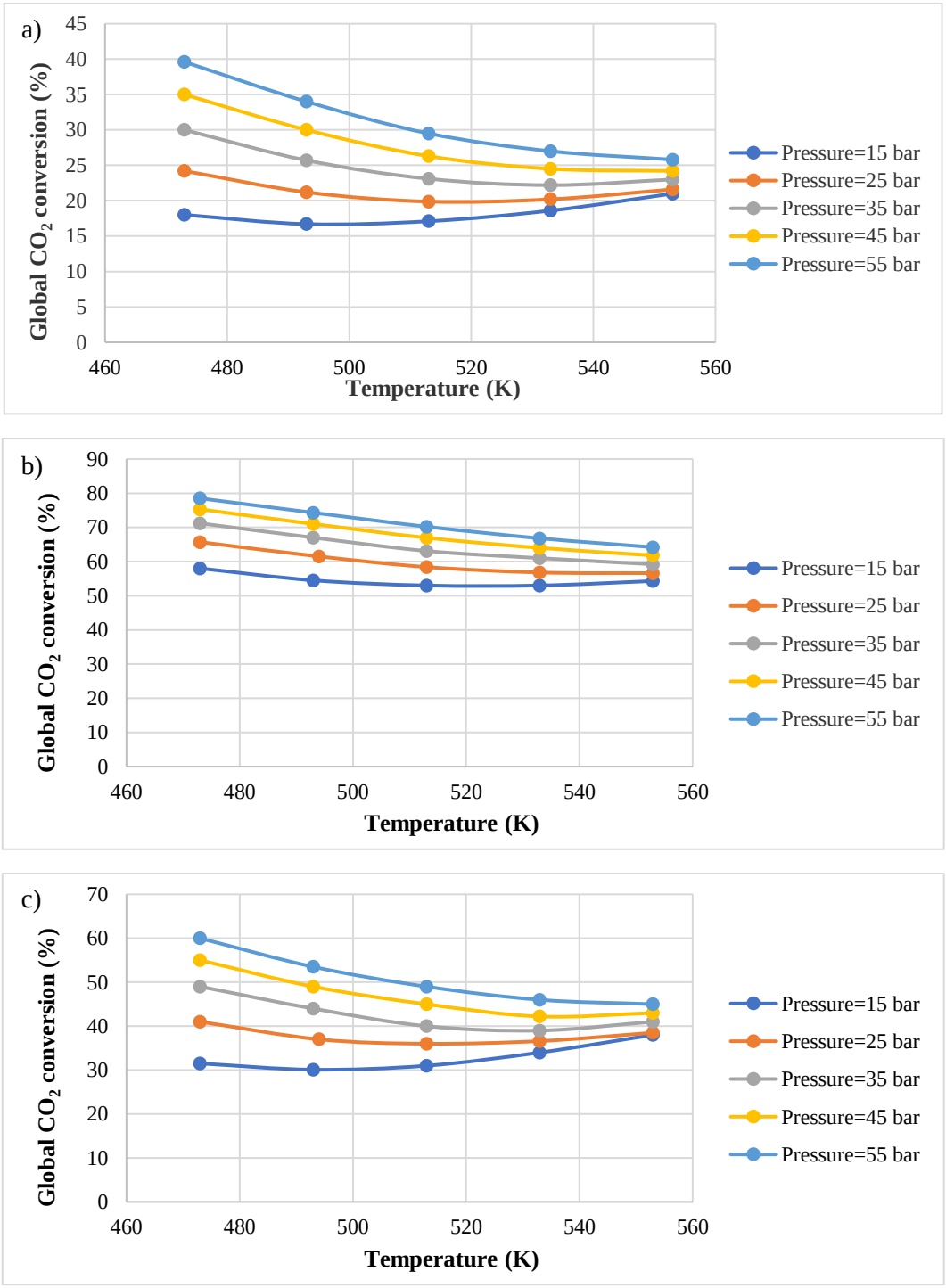

Figure II.6 Overall CO_2 conversion at the equilibrium conditions, as a function of temperature and pressure, with CO_2-H_2 (1:3) in the feeding stream: a) once-through reactor; b) reactor with the recycle of unconverted gases (R=80%) after the separation of CH_3OH and H_2O by condensation; c) membrane reactor permeable to steam (Leonzio et al., 2019)

The global CO_2 conversion shows a minimum in the range of conditions examined in this work. Comparing Figures II.6a and II.4a, as well as for the remaining reactor configurations, shows that, at a lower temperature, reaction 1 mainly occurs, so the system reacts selectively to produce CH_3OH. In fact, at 473

K and 55 bar, CO_2 conversion to CH_3OH in Figure II.4a is equal to 38% while global CO_2 conversion in Figure II.6a is only 40%. However, at a higher temperature, CO_2 reacts more extensively according to the reverse water gas shift (reaction 2) and produces CH_3OH in minor quantity. In fact, at 553 K and 55 bar, CO_2 conversion to CH_3OH in Figure II.3a is 13% while the global CO_2 conversion in figure II.6a is 25%. From Figure II.6, it is also evident that the global CO_2 consumption in the reactor with the recycle of gases reaches the highest values. In fact, at 493 K and 55 bar, the once-through reactor, the reactor with the recycle of unconverted gases and the membrane reactor have respectively a global CO_2 conversion equal to 40%, 79% and 60%.

Figure II.7 shows the selectivity to CH_3OH for the three reactor configurations. The selectivity to CH_3OH (reaction 1) decreases with increasing temperature, due to the favored endothermic reverse water gas shift reaction to CO (reaction 2). Pressure has a positive effect. At a temperature equal to 493 K and a pressure equal to 55 bar, CH_3OH selectivity for once-through reactor, reactor with recycle and membrane reactor is equal respectively to 96%, 88% and 96%. Then the recycle reactor ensures higher CO_2 conversion to CH_3OH, although slightly lower methanol selectivity.

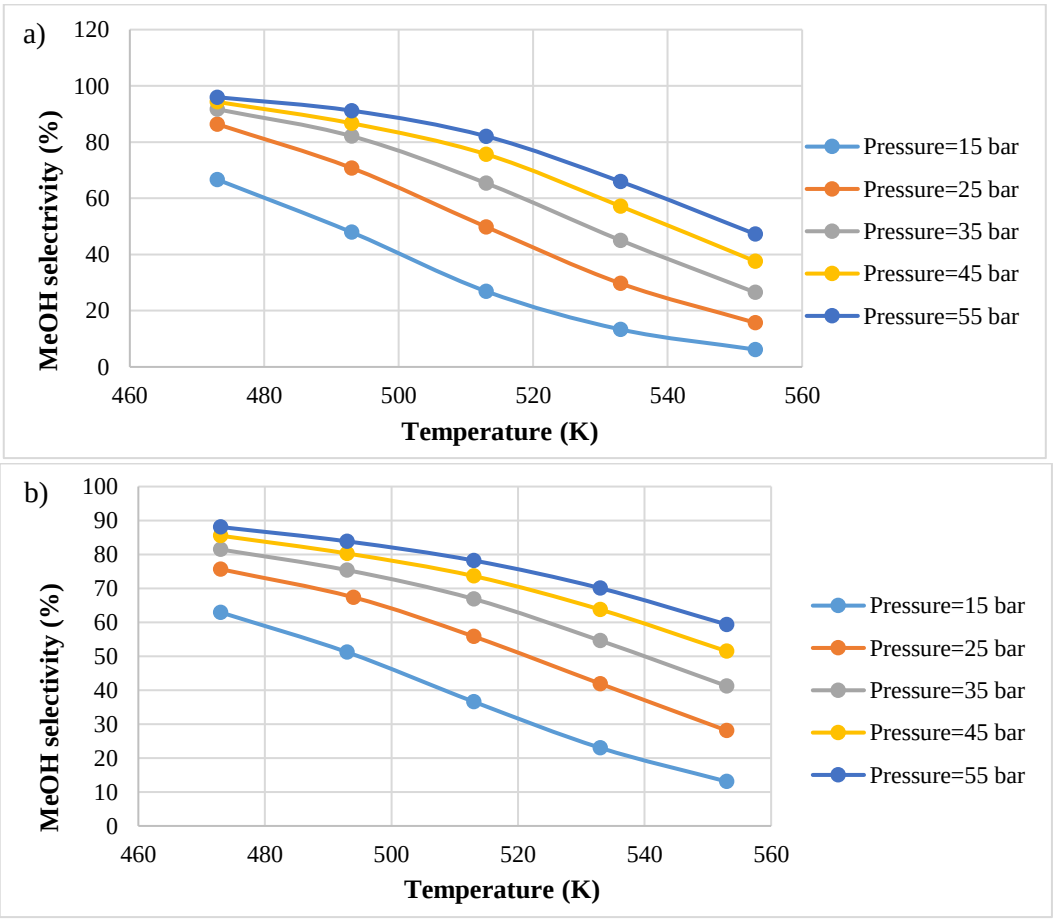

Figure II.7 (Following)

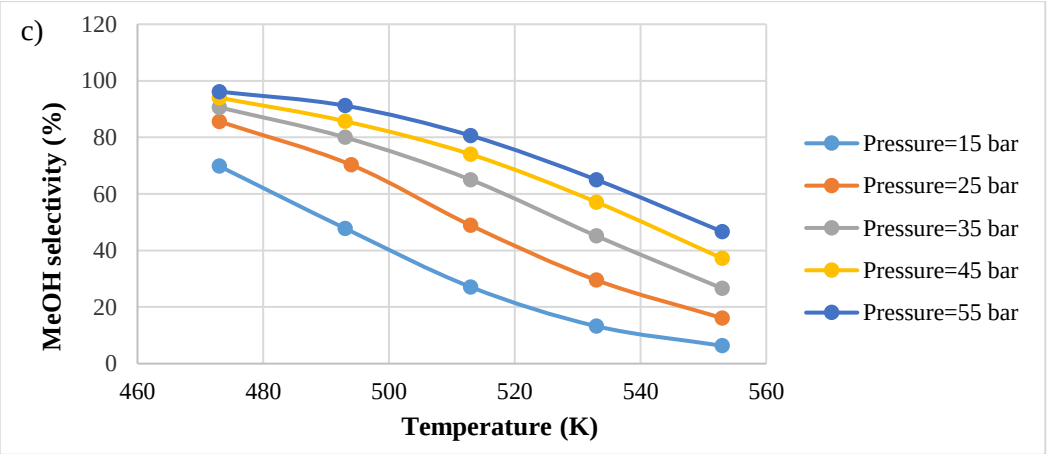

Figure II.7 CH_3OH selectivity from external CO_2-H_2 (1:3) feeding stream at different temperatures and pressures: a) once-through reactor; b) reactor with the recycle of unconverted gases (R=80%) after the separation of CH_3OH and H_2O by condensation; c) membrane reactor permeable to steam (Leonzio et al., 2019)

The thermodynamic analysis is used to analyze the behavior of an adiabatic CH_3OH reactor fed by CO_2 and H_2, in stoichiometric ratio and with the recycle of unconverted gases after the separation of CH_3OH and H_2O by condensation. The inlet temperature and pressure are of 493 K and 55 bar. It is assumed that the reactor exit conditions approach those of equilibrium at 95%.

The extent of reaction 1 as a function of temperature and the corresponding equilibrium curve are obtained, as shown in Figure II.8. Figure II.8a shows the temperature–conversion path of the adiabatic methanol reactor with a recycle ratio of gases of 60% after the condensation of CH_3OH and H_2O. The temperature at the outlet of the real reactor is equal to 544 K, while the methanol yield is equal to 27% with reference to CO_2 in the fresh feed to the plant. Additional results are reported in Table II.2.

Figure II.8b shows the behavior of the adiabatic reactor with a recycle ratio of gases of 80% after the condensation of products (CH_3OH and H_2O). Compared to the previous case, the temperature at the outlet of the adiabatic reactor is slightly different, equal to 547 K, while the extent of reaction 1, or methanol yield, is substantially higher, equal to 37%, as shown in Table II.2. Figure II.8c shows the corresponding results obtained with a recycle ratio of gases of 90% after the separation of CH_3OH and H_2O by condensation. As shown in Table II.6, the outlet temperature is 550 K, while the effective methanol yield is 45%. These results show that an adiabatic methanol reactor with CO_2 and H_2 in the plant external feed allows a higher CH_3OH yield when increasing the recycle ratio, with a corresponding slight increment of the reactor outlet temperature, because of the increased gas flow rate through the reactor and associated heat capacity. It is worth noticing here that, with a process feed stream made of CO_2 and H_2, the heat of reaction is lower compared to that with syngas in the feed: it is about half of the heat of reaction obtained by using syngas in the feed. In fact, starting from CO_2 the heat of reaction is -49 kJ/molCO_2, while starting from syngas, mainly composed by CO, the heat of reaction is -90.7 kJ/molCO.

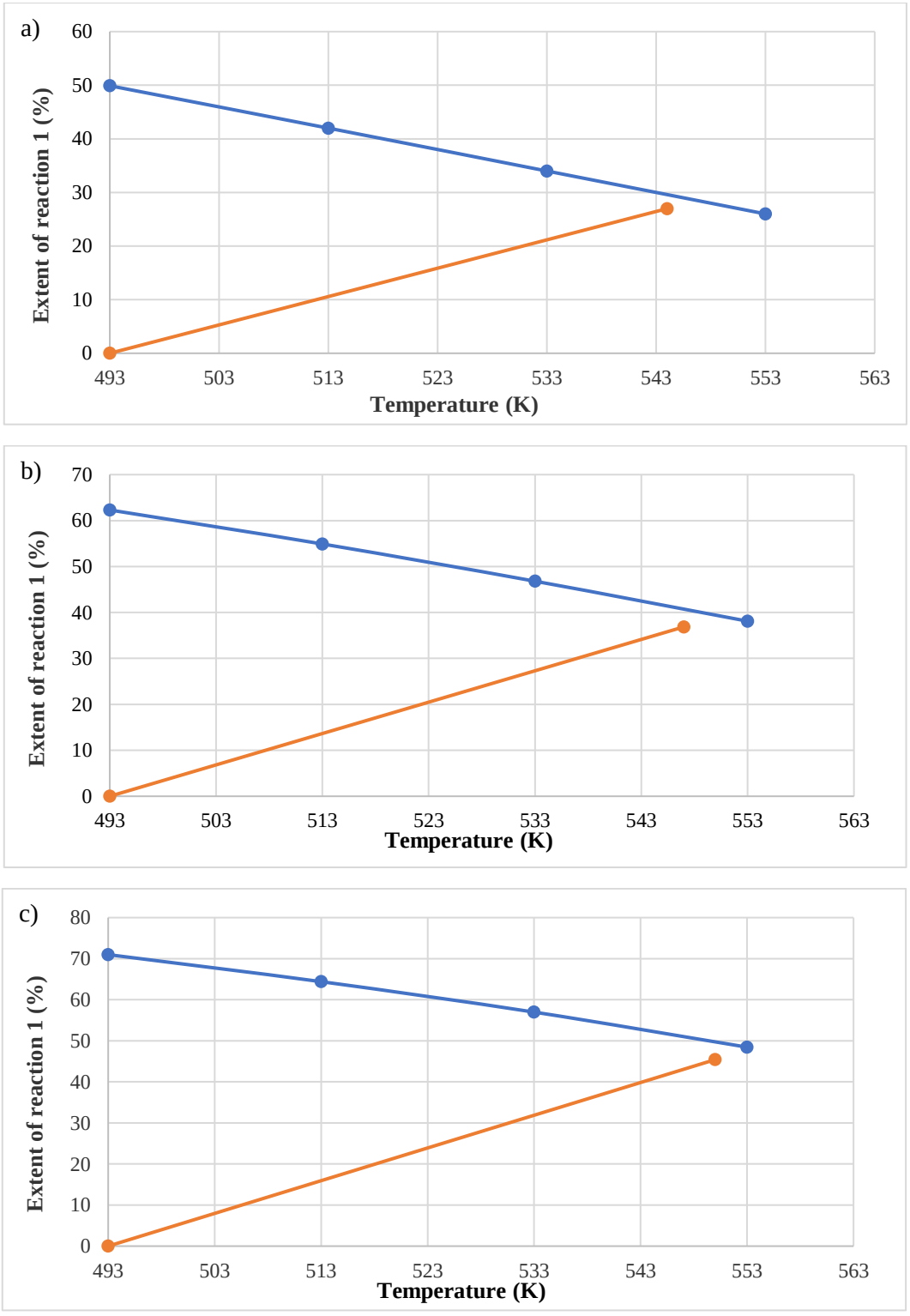

Figure II.8 Extent of reaction 1-vs-temperature trajectory for an adiabatic CH_3OH reactor with the recycle of gases after the separation of CH_3OH and H_2O by condensation (orange line), and corresponding thermodynamic equilibrium limit as a function of temperature (blue line): a) R=60%; b) R=80%; c) R=90% (Leonzio et al., 2019)

Table II.6 Calculated performance indicators for the adiabatic CH_3OH reactor and for the whole process, with different recycle ratio of gases after the separation by condensation of CH_3OH and H_2O (Leonzio et al., 2019)

Recycle ratio	60%	80%	90%
CO_2 flow rate, at the inlet (mol/h) reactor/plant	1.70/1	2.28/1	2.77/1
CO_2 flow rate, at the outlet (mol/h) reactor/plant	1.306/0.617	1.78/0.513	2.19/0.427
CO flow rate, at the inlet (mol/h) reactor/plant	0.11/0	0.264/0	0.42/1
CO flow rate, at the outlet (mol/h) reactor/plant	0.22/0.11	0.37/0.11	0.53/0.1
H_2 flow rate, at the inlet (mol/h) reactor/plant	5.07/3	7.12/3	8.97/3
H_2 flow rate, at the outlet (mol/h) reactor/plant	4.15/2.07	5.89/1.76	7.47/1.49
MeOH production (mol/h)	0.284	0.388	0.478
Temperature, reactor inlet (K)	493	493	493
Temperature, reactor outlet (K) (*)	544	547	550
CO_2 conversion (%) reactor/plant	23.4/47.8	21.9/63.5	20.93/78.1
MeOH yield(%) reactor/plant	16.7/26.9	17/36.8	17.25/45.4
MeOH selectivity (%) reactor/plant	71.2/59.4	77.6/61.1	82.4/61.2

(*) calculated as 95% of CO_2 conversion at the equilibrium

II.3.2 Results of the 1-D mathematical kinetic model for a methanol reactor

The 1-D model is validated considering the work of Yusup et al. (2010). At first, a comparison between a 1-D model with and without the axial dispersion term (0.2 m^2/s) in the molar balance equations is developed. Results show a slight difference between the two models, in agreement with the assumption made in different literature works suggesting to neglect axial dispersion term in the methanol reactor (Manenti et al., 2011, 2013; Meyer et al., 2016;).

This model is useful to investigate the main effects of different variables, as the global heat transfer coefficient at the wall.

In the literature, different values for this coefficient are reported: 1000 J/(s m^2 K) by Bohn (2011), 500 J/(s m^2 K) by Groppi et al. (2012) and 250 J/(s m^2 K) by Luyben (2010). The presence of catalyst pellets increases the heat transfer coefficient at the wall of a packed bed considerably above that in an empty tube, at similar gas flow rate (Smith, 1981). This large increase is due to mixing and turbulence induced by particles and is quite difficult to predict it accurately as a function of process conditions, although some correlations have been proposed. For this reason, a sensitivity analysis is performed varying the value of global heat exchange coefficient over the whole range considered in the literature, and also varying the temperature of the isothermal heat exchange fluid.

Figure II.9 shows temperature axial profiles inside the methanol reactor obtained with different values of the global heat exchange coefficient (300 J/(s m^2 K) in Figure II.8a, 600 J/(s m^2 K) in Figure II.8b and 1000 J/(s m^2 K) in figure II.8c). In each figure, a value equal to 490 K, 510 K and 523 K is assumed for the isothermal heat exchange fluid.

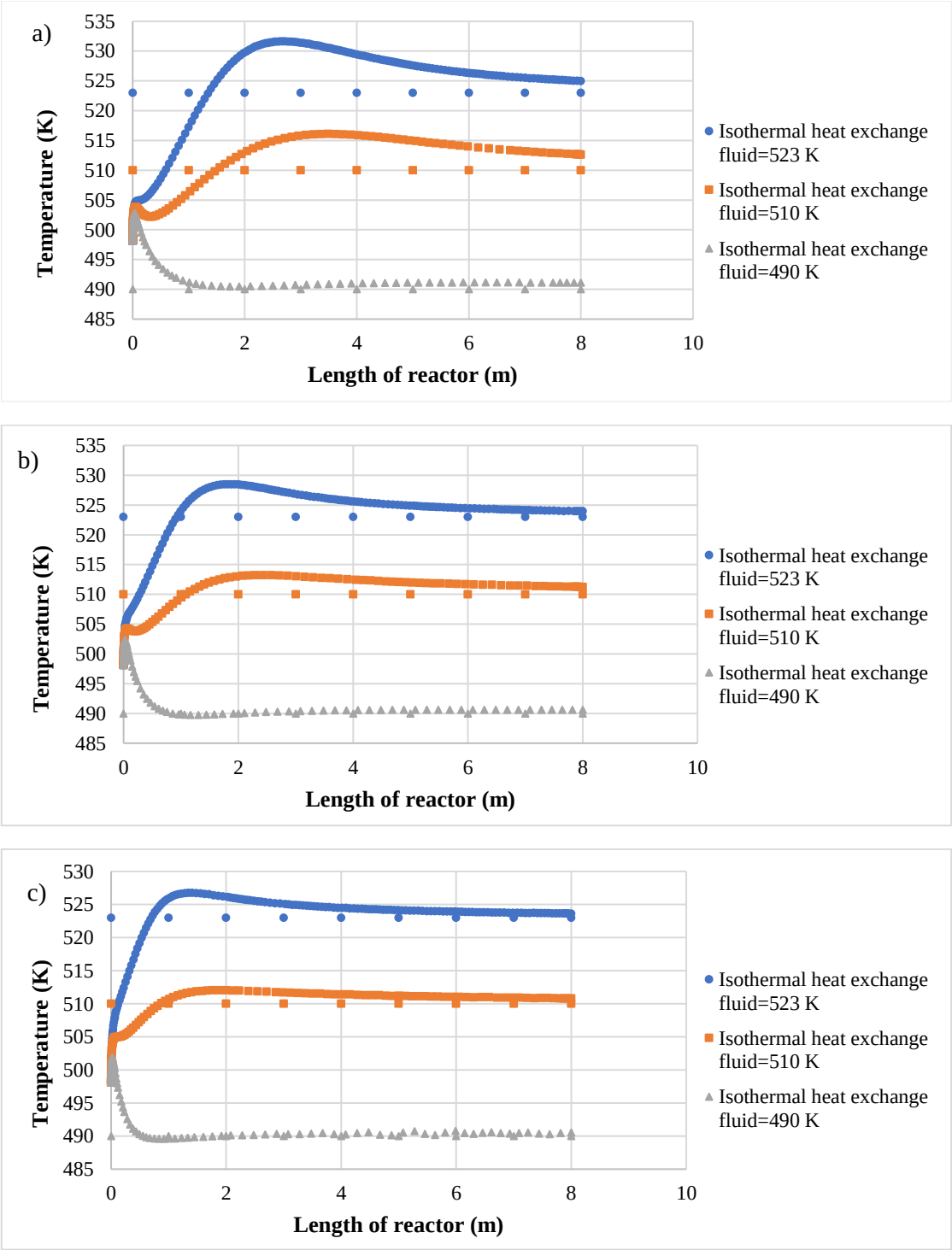

Figure II.9 Calculated temperature profiles inside the CH_3OH reactor for different values of heat exchange fluid temperature and global heat exchange coefficient: a) 300 J/(s m^2 K); b) 600 J/(s m^2 K); c) 1000 J/(s m^2 K) (Leonzio et al., 2019)

Results show that a value equal to 523 K for the heat exchange fluid ensures to have the best results in terms of reaction progress. When the value of the heat exchange coefficient at the wall is smaller, the hot

spot becomes more pronounced, as expected. As a matter of facts, Figure II.9a shows that, with a reduced value of this coefficient and with the intermediate temperature level for the heat exchange fluid (510 K), a second hotspot appears at the entrance of the reactor due to high initial rate of reaction 1 and associated heat release. Moreover, inside the reactor there are two opposite reactions, one exothermic and one endothermic. In all cases examined here, temperature inside the reactor tends asymptotically to the temperature of the isothermal heat exchange fluid.

Fixing the value of global heat exchange coefficient to 1000 J/(s m^2 K), Figure II.10a shows CO_2 conversion along the reactor, as predicted at different values of the isothermal heat exchange fluid, while Figure II.10b shows CH_3OH selectivity at corresponding conditions. More data are reported in Table II.7.

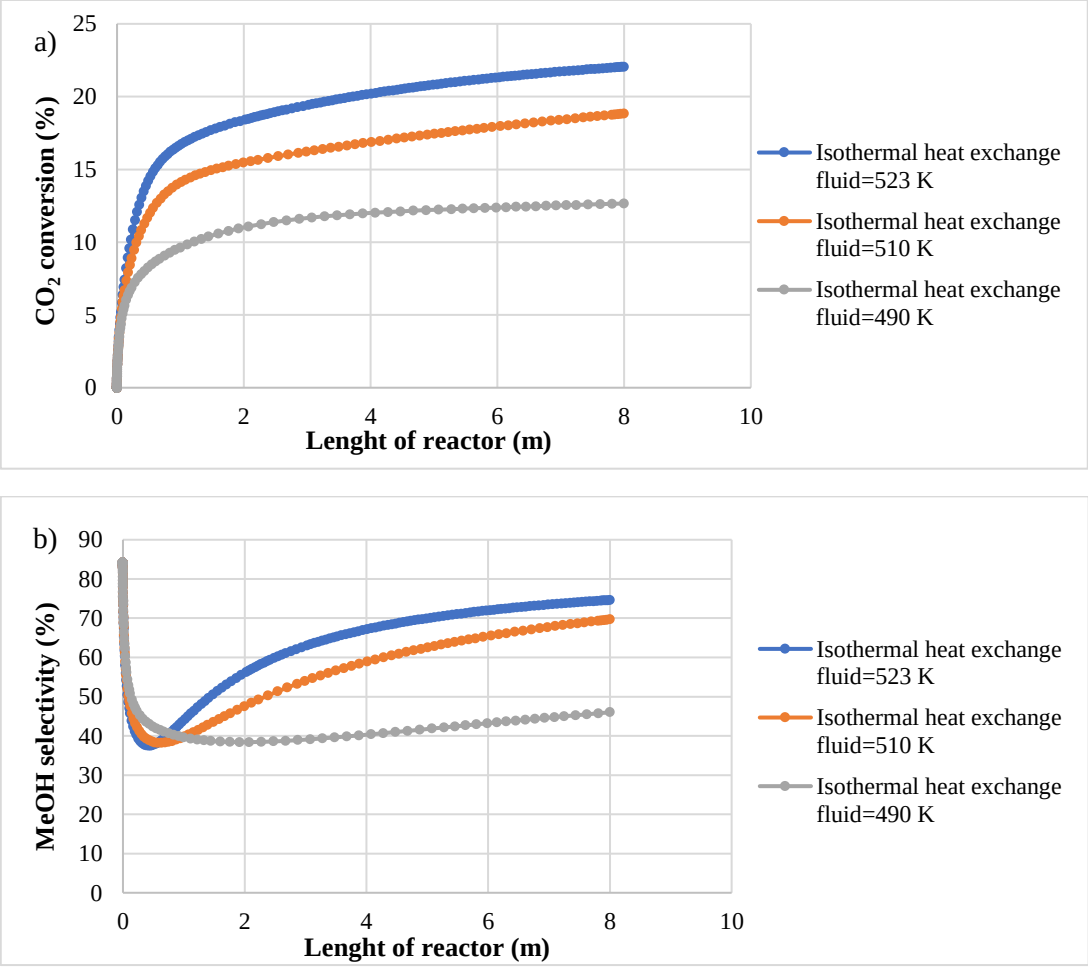

Figure II.10 Additional numerical results obtained with a global heat exchange coefficient equal to 1000 J/(s m^2 K) and at different values of heat exchange fluid temperature: a) Overall CO_2 conversion in the reactor; b) CH_3OH selectivity in the reactor (Leonzio et al., 2019)

Table II.7 Calculated performance indicators for the nearly isothermal CH_3OH reactor and the whole process with a value of global heat exchange coefficient equal to 1000 J/(s m^2 K) and at different temperature of isothermal heat exchange fluid (Leonzio et al., 2019)

Temperature isothermal heat exchange fluid (K)	523.0	510.0	490.0
CO_2 flow rate at the reactor inlet (mol/s)	83.2	92.9	116.7
CO_2 flow rate at the reactor outlet (mol/s)	65.2	75.4	101.8
CO_2 flow rate at plant inlet (mol/s)	25.0	25.0	25.0
CO_2 flow rate at plant outlet (mol/s)	6.5	7.5	10.2
MeOH production (mol/s)	13.4	12.1	6.9
Temperature, reactor inlet (K)	498.0	498.0	498.0
Temperature, reactor outlet (K)	523.6	510.8	490.6
CO_2 conversion, in the whole process (%)	73.9	69.8	59.3
CO_2 conversion, in the reactor (%)	21.6	18.8	12.7
MeOH yield, in the whole process (%)	53.6	48.6	27.4
MeOH yield, in the reactor (%)	16.1	13.1	5.9
MeOH selectivity, in (%)	74.4	69.5	46.3

CO_2 conversion at the outlet of the reactor is equal to 21.6%, 18.8% and 12.7% for an isothermal heat exchange fluid temperature equal to 523 K, 510 K and 490 K, respectively. CH_3OH selectivity is equal to 74.4%, 69.5% and 46.3% for values of isothermal heat exchange fluid temperature equal to 523 K, 510 K and 490 K, respectively. CO_2 conversion and CH_3OH selectivity are both referred to the reactor inlet stream calculated under each process conditions. It is worth mentioning here that, as the outlet reactor temperature increases, CH_3OH selectivity tends to level off, because of the increasing importance of reaction 2.

On the other hand, when considering a lower value of global heat exchange, equal to 300 J/(s m^2 K), Figure II.11a shows CO_2 conversion at different values of isothermal heat exchange fluid temperature, while Figure II.11b shows the corresponding CH_3OH selectivity.

Additional data are reported in Table II.8. At the outlet of the reactor, CO_2 conversion is equal to 22.1%, 19.6%, 12.9%, for values of isothermal heat exchange fluid temperature equal to 523 K, 510 K and 490 K, respectively. Corresponding CH_3OH selectivity at the outlet of reactor is equal to 74.1%, 71.0%, 47.4%, respectively.

These results suggest that, at a fixed temperature of heat exchange fluid, the global heat exchange coefficient has negligible influence on CO_2 conversion and CH_3OH selectivity; this is probably related to the fact that, under each operating condition, the temperature reached in the reactor is quite close to the heat exchange fluid temperature, the influence of which is largely dominant.

It is possible to see that CH_3OH selectivity, just after a high initial value, is decreasing in the first section of the reactor due to the temperature rise. In the second half of the reactor, CH_3OH selectivity increases monotonically according to the temperature trend.

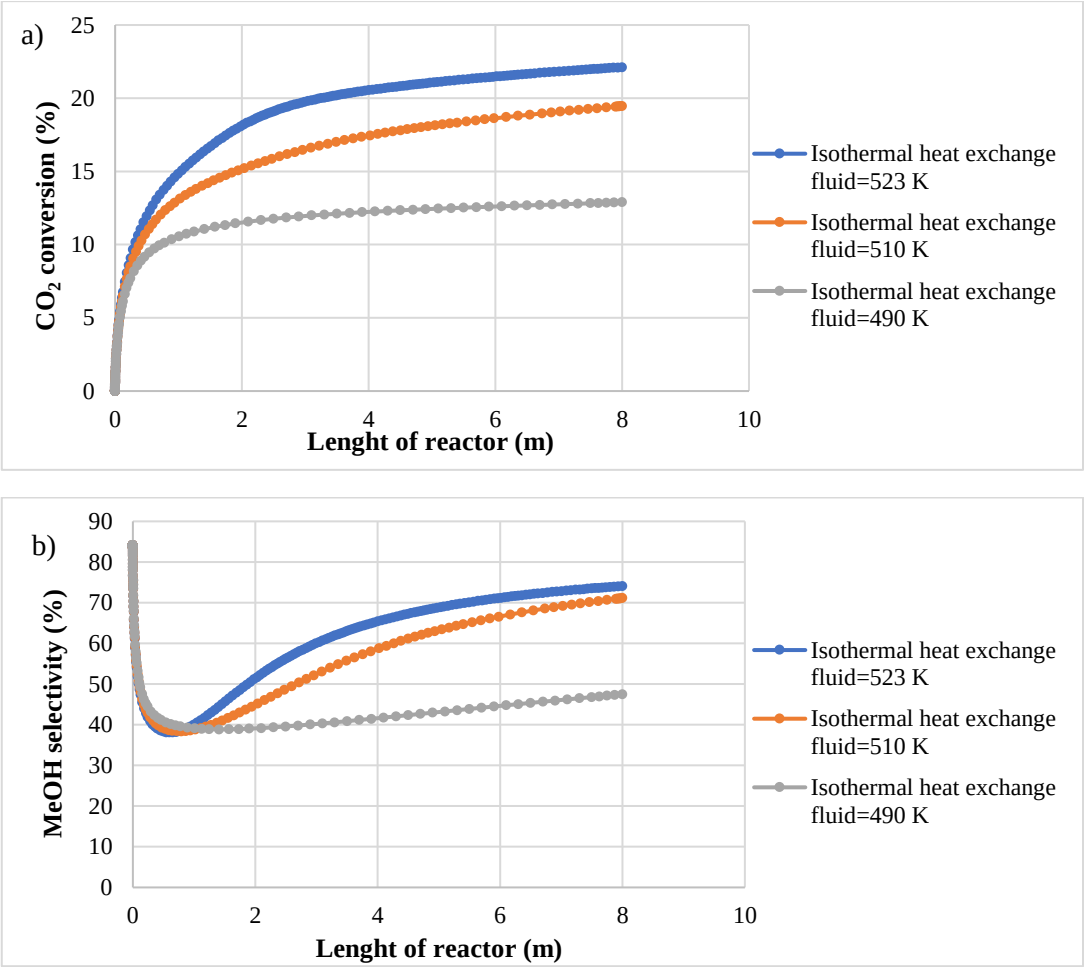

Figure II.11 Additional numerical results obtained with a global heat exchange coefficient equal to 300 J/(s m^2 K) and at different values of heat exchange fluid temperature: a) Overall CO_2 conversion in the reactor; b) CH_3OH selectivity in the reactor (Leonzio et al., 2019)

Table II.8 Calculated performance indicators for the nearly isothermal CH_3OH reactor and the whole process with a value of global heat exchange coefficient equal to 300 J/(s m^2 K) and at different temperature of isothermal heat exchange fluid (Leonzio et al., 2019)

Temperature isothermal heat exchange fluid (K)	523.0	510.0	490.0
CO_2 flow rate at the reactor inlet (mol/s)	83.6	90.7	115.7
CO_2 flow rate at the reactor outlet (mol/s)	65.2	73.0	100.8
CO_2 flow rate at plant inlet (mol/s)	25.0	25.0	25.0
CO_2 flow rate at plant outlet (mol/s)	6.5	7.3	10.1
MeOH production (mol/s)	13.7	12.6	7.1
Temperature, reactor inlet (K)	498.0	498.0	498.0
Temperature, reactor outlet (K)	525.0	512.6	491.1
CO_2 conversion, in the whole process (%)	73.9	70.8	59.7
CO_2 conversion, in the reactor (%)	22.1	19.6	12.9
MeOH yield, in the whole process (%)	54.8	50.4	28.3
MeOH yield, in the reactor (%)	16.4	13.9	6.1
MeOH selectivity, in (%)	74.1	71.0	47.4

Overall, CO_2 conversion and CH_3OH selectivity at the reactor outlet, calculated with different values of heat exchange fluid temperature, show expected trends. For this reason, the mono-dimensional model, despite the well known limitations in the description of local conditions inside the reactor, can be assumed as a valid computational tool in this phase of work regarding the technical feasibility of CO_2 hydrogenation and the choice of operating conditions.

II.3.3 Results of the 2-D mathematical kinetic model for a methanol reactor

Due to few available experimental data, the validation of the developed model is limited to the single work about syngas hydrogenation to methanol reporting the experimental data of a packed bed reactor (Montebelli et al., 2013). These authors describe an industrial packed bed multi-tubular reactor (Lurgy type), once-through, externally cooled by cooling water, fed by syngas at the operating conditions shown in table 3 of their work. The reactor length is assumed to be equal to 12 m; this datum is not reported in the original work by Montebelli et al. (2013). The experimental data and simulation results obtained with the 2-D model, reported in Table II.9 in terms of CO conversion and CH_3OH productivity are close to each other: 75% (experimental) vs 73% (calculated) and 1025 ton/day (experimental) vs 1024 (calculated), respectively. On the other hand, the outlet temperature calculated by the model is somewhat higher than the reported experimental value (547 K vs 515 K): this difference is attributable to the catalyst thermal conductivity, the value of which is not known and is assumed equal to that in Table II.1 in simulations.

Table II.9 Comparison between experimental data (Montebelli et al., 2013) and simulation results obtained with the 2-D model (Leonzio and Foscolo, 2020)

	Experimental (Montebelli et al., 2013)	Calculated
CO conversion (%)	75	73
MeOH productivity (ton/day)	1025	1024
Outlet temperature (K)	515	547

In addition, to further validate the 2-D model, with reference to the structured packing a comparison is made with the corresponding simulations obtained from the 1-D reactor model developed before, by calculating the bulk weighted average molar flow rate profile for each compound, according to the following relation (see Eq. II.62):

$$F_b = \frac{\int_0^{2\pi}\int_0^R U_z(r)F(r,z)rdrd\theta}{\int_0^{2\pi}\int_0^R U_z(r)rdrd\theta} \qquad (II.62)$$

where F is the local molar flow rate in mol/s, U_z the axial velocity in m/s and F_b the weighted average value of axial flow rate on the reactor cross section at height z (Bird, 2002). For this validation, the wall heat transfer coefficient is set to 1500 J/(s m^2 K).

Figure II.12 shows the bulk weighted average molar flow rate profiles obtained with the 2-D model, while Figure II.13 shows the corresponding molar flow rate profiles calculated by the 1-D model: quite small differences are noticeable, attributable to slight radial gradients on the tube cross section, which in this case are limited by the high value of catalyst thermal conductivity.

From these two Figures, it is evident that H_2 and CO_2 molar flow rate decrease, while CH_3OH and H_2O increase along the reactor, respectively. On the other hand, CO is mainly produced in the first section of the reactor, by the reverse water gas shift reaction, while increasing the reactor height it is consumed to produce CH_3OH. Then, a maximum in the profile is present in this case. Figures II.12 and II.13 show that a slightly lower production of CH_3OH is predicted at the outlet of the reactor by the 1-D model, due to the assumption of flat radial profiles.

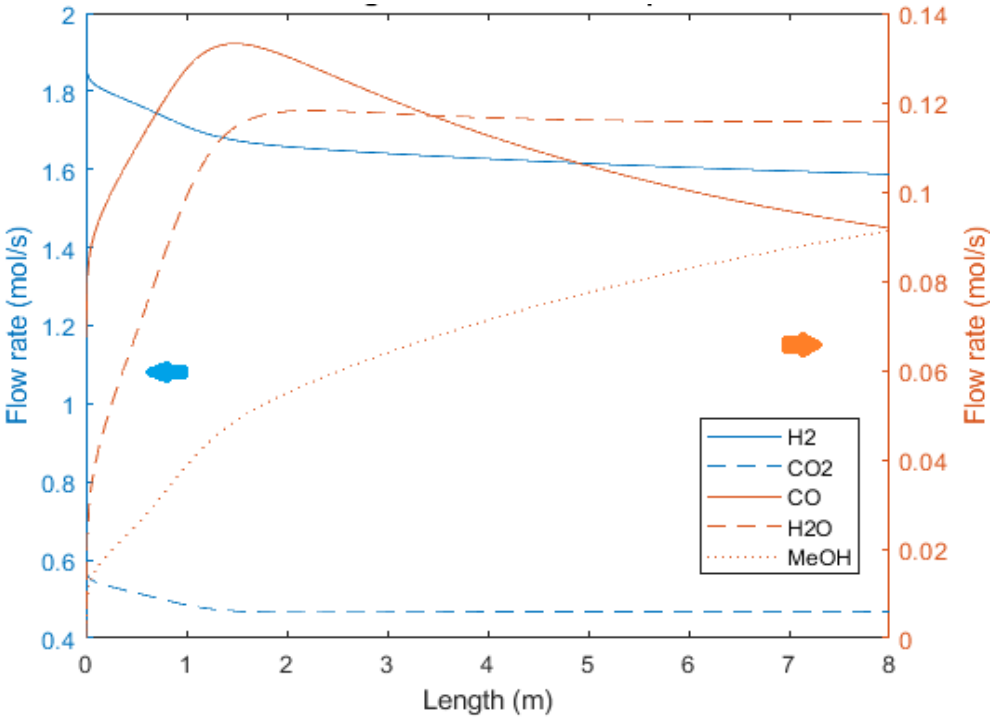

Figure II.12 Bulk weighted average molar flow rates estimated inside a structured CH_3OH reactor as a function of tube length with the 2-D model (Leonzio and Foscolo, 2020)

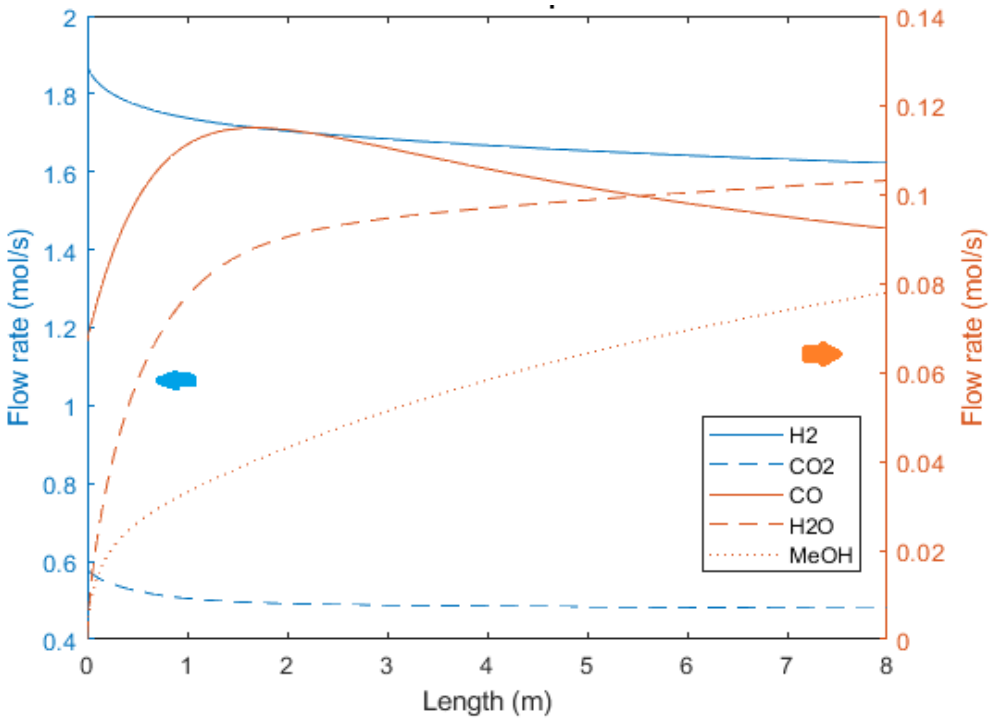

Figure II.13 Gaseous flow rates inside a CH_3OH reactor as a function of tube length, calculated at the same operating conditions as in Figure II.11 with the 1-D model (Leonzio and Foscolo, 2020)

Figure II.14 shows the temperature profile of gas phase inside the CH_3OH reactor, obtained with the 2-D model as a function of dimensionless radius and length. On the other hand, Figure II.15 shows the temperature profile along the CH_3OH reactor calculated with the 1-D model. Considering the outlet temperatures and component flow rates, it results that for a structured packed bed reactor with a quite high thermal conductivity a fairly good agreement is found between 1-D and 2-D models, as also reported in Table II.10. The 2-D model is then validated.

Table II.10 Comparison between the numerical results of 1-D and 2-D model for a structured bed CH_3OH reactor (bulk weighted average values are considered for the 2-D model) (Leonzio and Foscolo, 2020)

	Inlet values		**Outlet values**	
	1-D	**2-D**	**1-D**	**2-D**
Temperature (K)	498	498	525	534
Flow rate (mol/s)				
CO	0.07	0.07	0.09	0.08
H_2	1.88	1.89	1.62	1.59
CO_2	0.58	0.58	0.48	0.47
CH_3OH	0	0	0.08	0.09
H_2O	0	0	0.10	0.11

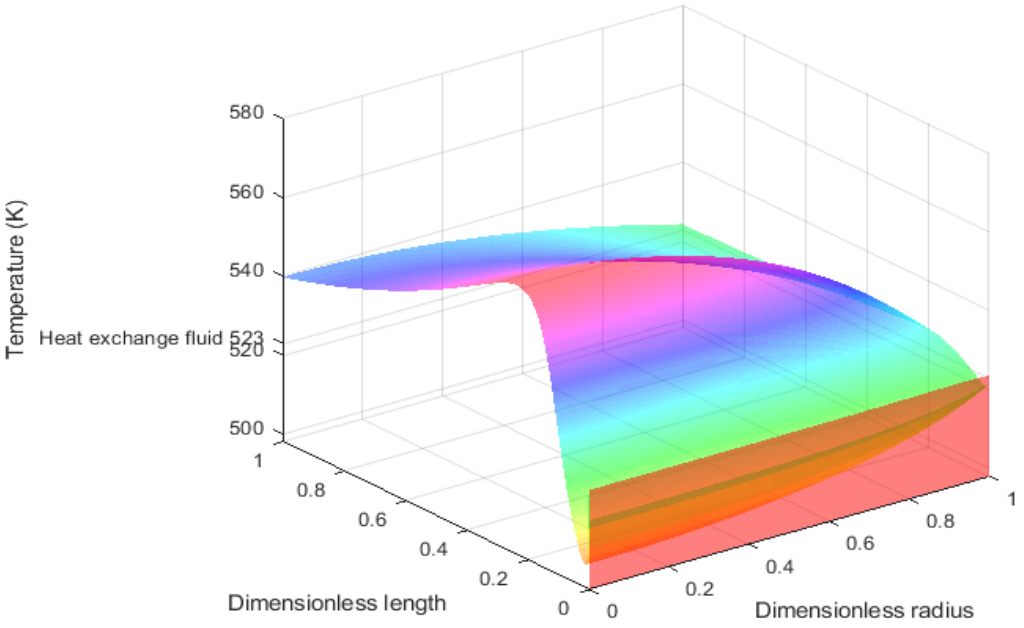

Figure II.14 Tridimensional profile of temperature inside the structured CH_3OH reactor as a function of dimensionless length and tube radius (heat exchange fluid temperature=523 K) (Leonzio and Foscolo, 2020)

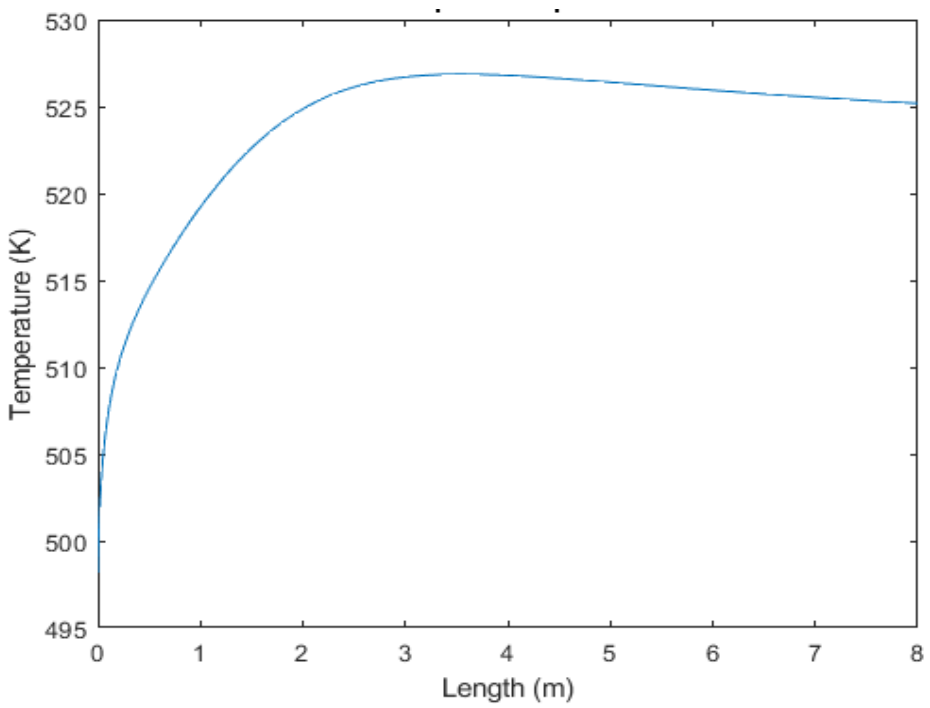

Figure II.15 Temperature profile along the CH_3OH reactor computed with the 1-D model (heat exchange fluid temperature=523 K) (Leonzio and Foscolo, 2020)

Also, from the temperature profiles in Figure II.14, it is evident that, with the structured packing, reactions evolve almost in an uniform way, over the tube cross section, along the second part of the reactor, after the hot spot (a slight radial gradient is present). In fact, a high value for the effective radial thermal conductivity of catalyst bed is obtained in this case: a relatively slight radial gradient of temperature is present. The radial temperature profile in the first section of the reactor, is determined by the fact that the inlet temperature is below the heat exchange fluid temperature, so that the heat flow is directed towards the tube center. The subsequent hot spot, caused by the exothermic CH_3OH reaction, is placed before the middle of the reactor length, in fair agreement with predictions obtained with the 1-D model, although more pronounced.

It is possible to evaluate CO_2 selectivity to CH_3OH (as the ratio between the produced CH_3OH and the consumed CO_2), reactor CH_3OH yield (as the ratio between the produced CH_3OH and CO_2 fed to the reactor) and plant CH_3OH yield (as the ratio between the produced CH_3OH and CO_2 fed to the plant) predicted by the two models, respectively. With the 2-D model, these parameters are found equal to 82%, 16% and 56%, respectively. With the 1-D model instead, the calculated values for these parameters are respectively 75%, 13% and 50%.

A lower value of radial thermal conductivity is considered in the simulation for a packed bed, non-structured reactor. As shown in Figure II.16, in these conditions, the evaluated radial temperature profile is more steep than that found for the structured reactor, and temperature variation along the tube radius is certainly not negligible due to a higher resistance to heat transfer. Moreover, compared to the structured reactor, the hot spot is less pronounced. Higher temperature values are reached at the center of the reactor tube: the highest value is 572 K, at the center of the outlet reactor section. The trend in the first section of the reactor is due to the competition between two different reactions: one exothermic and the other endothermic: after reaching the temperature of the heat exchange fluid, the temperature decreases due to the endothermic reaction and then increases again due to the exothermic reaction. Close to the tube surface, this behavior is mitigated by heat transfer with the heat exchange fluid. In fact, the temperature value tends to be close there to the heat exchange fluid temperature of 523 K. A slight resistance to heat transfer phenomena is present at the wall.

Figure II.17 shows the weighted average molar flow rate profiles for the non-structured reactor. It is evident that a lower molar flow rate of CH_3OH (0.0676 mol/s at the reactor outlet) is predicted respect to the structured reactor, due to the different temperature profile not favoring the reaction kinetics. In fact, CO_2 selectivity to CH_3OH, CH_3OH yield for the reactor and for the plant calculated in this case are respectively 54%, 12% and 42%.

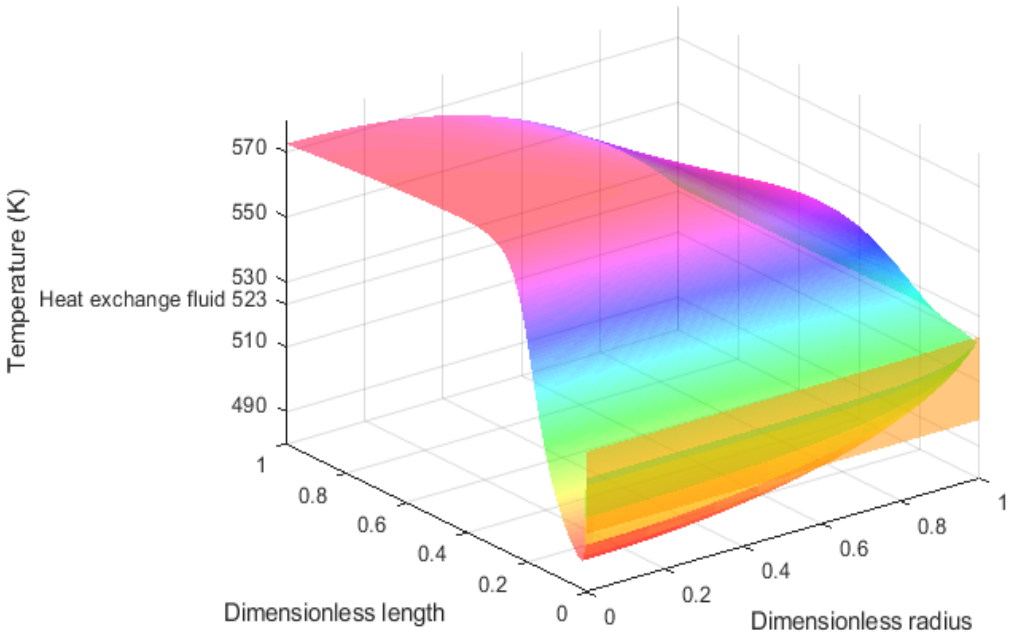

Figure II.16 Tridimensional profile of temperature inside the non-structured packed bed CH_3OH reactor as a function of dimensionless length and tube radius (temperature of the isothermal heat exchange fluid=523 K) (Leonzio and Foscolo, 2020)

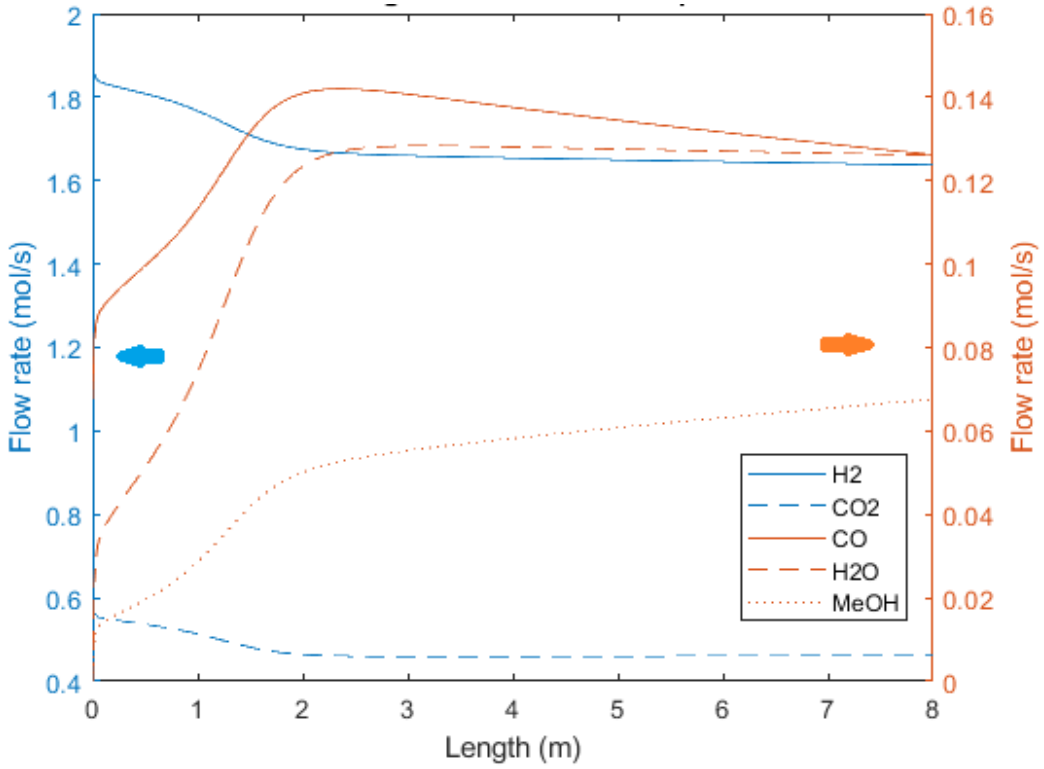

Figure II.17 Bulk weighted average molar flow rates as a function of reactor tube length, for a non-structured catalytic packing (Leonzio and Foscolo, 2020)

With the non-structured packing, the approach to equilibrium at the reactor outlet is predicted more problematic; as a consequence, slight higher recycle flow rates are required. A higher efficiency of a structured reactor compared to a non-structured one is also found in the work of Visconti et al. (2018); their simulations show that the performances of structured catalyst beds based on open cell foams and honeycomb monoliths exceed that of conventional packed beds, especially in compact cooled multi-tubular reactors.

Similar results are also reported in Phan et al. (2010, 2011): by a comparison with a conventional packed bed reactor, the authors claim that the superior activity of a structured reactor is related to its higher radial heat transfer rate, which provides a nearly isothermal catalytic bed for all the studied CO conversion levels (up to 30%). In a similar way, Montebelli et al. (2013) claim that the computed temperature profiles are due the fact that in a structured reactor, heat transfer is mainly due to a conductive mechanism within the continuous metallic matrix of the structured substrate. In the literature, there are few attempts to compare a structured reactor with a packed bed made of catalyst pellets, analyzing and discussing radial phenomena. In fact, the most of published works are about a 1-D methanol reactor model (Manenti et al., 2014; Al-Kalbani et al., 2016) and a 2-D model is introduced only to compare different kinetic models (Meyer et al., 2016) and different catalysts (Hartig and Keil, 1993).

II.3.3.1 Results of sensitivity analysis

Very few data are available in the open literature about the performance of methanol reactors, specifically when CO_2 hydrogenation is considered. An extensive sensitivity analysis is performed to demonstrate furtherly simulation reliability, by investigating the ability to take into account the influence of key operating conditions in a proper quantitative manner.

A sensitivity analysis is carried out for the structured methanol reactor changing the value of the wall heat transfer coefficient. A decrease of the wall heat transfer coefficient to 1000 J/(m^2 s K), as it is predictable, shows a slight increase of temperature, however without significant variation in molar flow rates and outlet compositions. The hot-spot temperature is shifted towards the outlet of the reactor and with a higher value. On the other hand, an increase of the heat transfer coefficient to 3000 J/(m^2 s K), shows a slight decrease of temperature without significant variation of molar flow rates and compositions. The hot-spot temperature is shifted towards the inlet of the reactor.

An additional sensitivity analysis is developed by increasing the inlet temperature of the reactor feed stream to 530 K for the structured reactor, with a wall heat transfer coefficient equal to 1500 J/(m^2 s K). Figure II.18 shows the tridimensional temperature profile inside the CH_3OH reactor, predicted as a function of dimensionless tube radius and length. Heat exchange fluid temperature is set, as in the previous cases, to 523 K. It is clear that, close to the inlet section, the temperature decreases to a minimum value in combination also with the endothermic reverse water gas shift. After that, the temperature increases to achieve the hot spot. No significant variations are present in the position and temperature level of the hot

spot. This trend of temperature influences the molar flow rate of each chemical compound. Figure II.19 shows the weighted average molar flow rate of CH_3OH, H_2O, H_2, CO and CO_2 as a function of length.

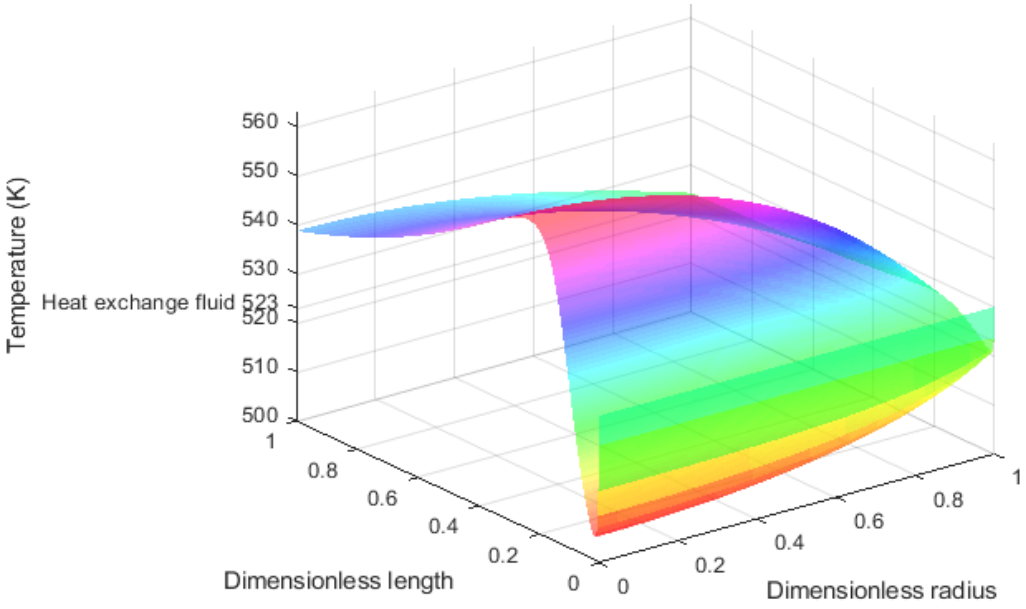

Figure II.18 Tridimensional profile of temperature inside the structured CH_3OH reactor as a function of dimensionless length and tube radius (heat exchange fluid temperature=523 K, inlet reactor temperature=530 K) (Leonzio and Foscolo, 2020)

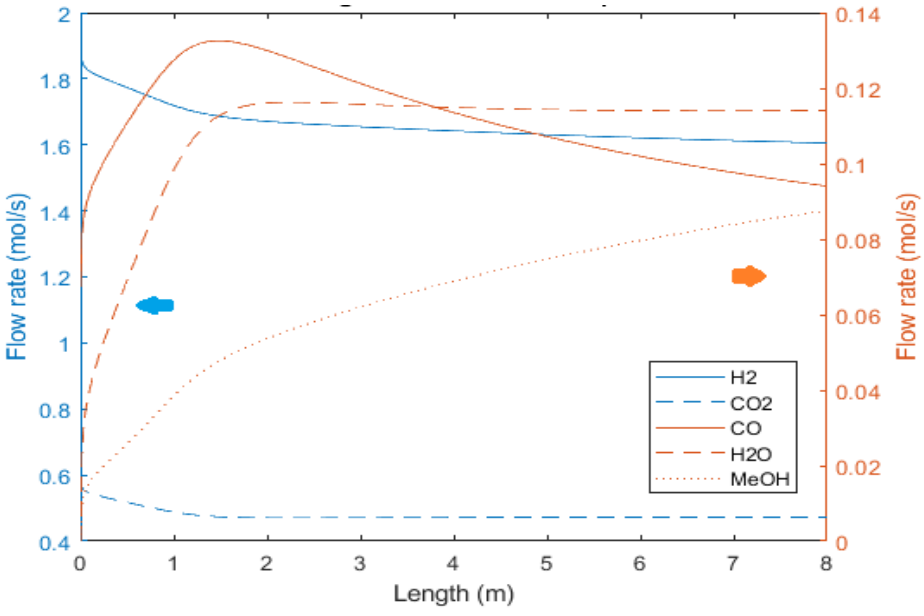

Figure II.19 Bulk weighted average flow rates inside the structured CH_3OH reactor as a functions of tube length (heat exchange fluid temperature=523 K, inlet reactor temperature=530 K) (Leonzio and Foscolo, 2020)

Predicted flow rates of CH_3OH and H_2O at the reactor exit (respectively of 0.09 mol/s and 0.11 mol/s) are lower than those in the base case: this temperature profile reduces the average reaction rates in the reactor. A greater reactor inlet temperature favors the endothermic reverse water gas shift reaction: at the outlet of the reactor, a slightly higher flow rate of CO (0.09 mol/s) is calculated compared to the base case. H_2 flow rate and CO_2 flow rate are respectively of 1.60 mol/s and 0.48 mol/s, slightly higher values compared to the base case.

An additional sensitivity study is performed, by doubling the tube diameter to 0.1016 m, in view of reducing investment costs. As it is well known, the tube diameter is an important choice in the design of a catalytic reactor with the exchange of heat to a fluid flowing on the shell side: the heat exchange surface area per unit tube length is inversely proportional to the tube diameter. Then, as also reported in Montebelli et al. (2013), an increase in tube diameter produces a proportional increase of radial heat transfer resistance. In order to keep constant the contact time with catalyst and the gas velocity, fresh feeding flow rate in each tube and tube number are changed respectively to 9.98 mol/s and 38. Figure II.20 shows the tridimensional temperature profile inside the CH_3OH reactor as a function of dimensionless radius and length. As discussed above, higher temperatures are calculated compared to the base case and a less pronounced hot-spot is found. In particular, the hot spot is located at about 2.4 m and slightly exceeds 556 K. Due to a higher thermal load per unit of heat transfer surface, with the same external heat exchange coefficient, a more pronounced radial temperature gradient is predicted and the computed outlet temperature is higher.

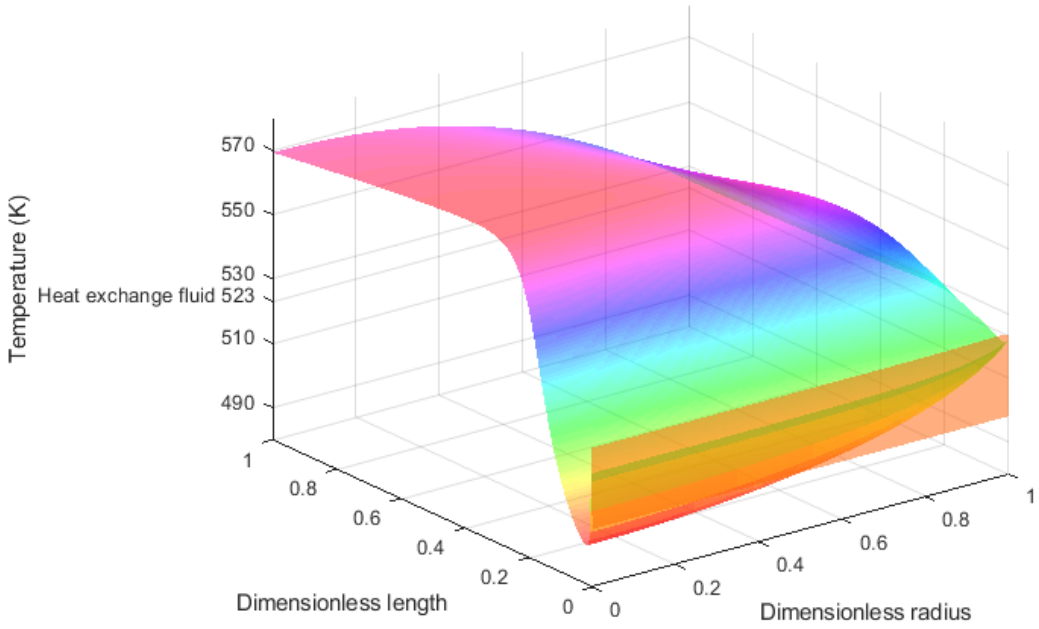

Figure II.20 Tridimensional profile of temperature inside the structured CH_3OH reactor as a function of dimensionless length and tube radius (heat exchange fluid temperature=523 K, tube radius=0.0508 m) (Leonzio and Foscolo, 2020)

Figure II.21 shows the weighted average molar flow rate profile along the tube length, for each component. At the reactor exit, the calculated molar flow rate of CO, H_2, CO_2, CH_3OH and H_2O are respectively 0.48 mol/s, 6.45 mol/s, 1.83 mol/s, 0.28 mol/s, and 0.50 mol/s.

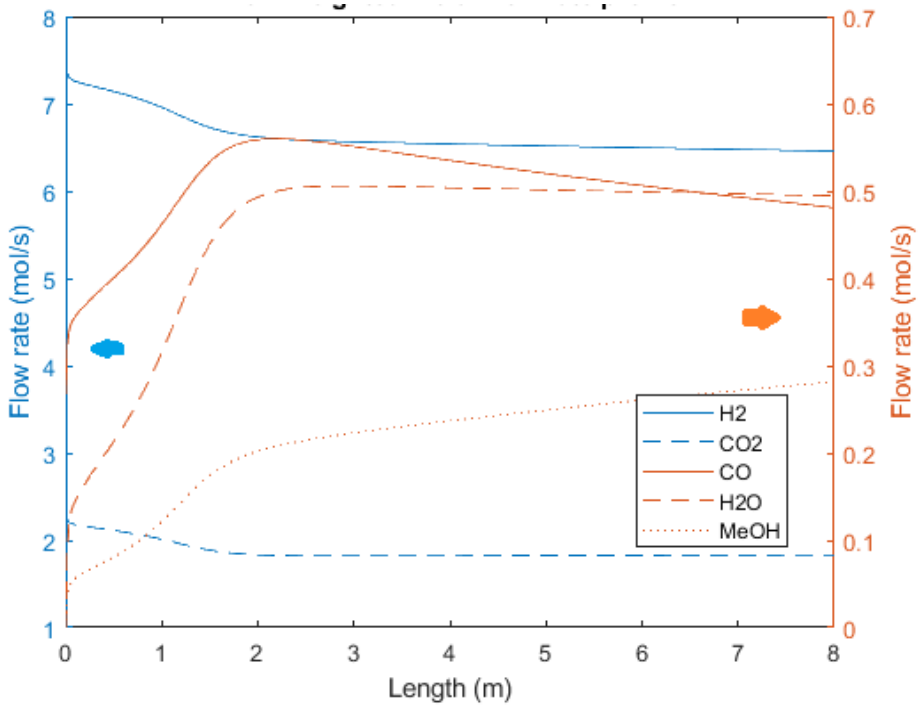

Figure II.21 Bulk weighted average molar flow rates inside the structured CH_3OH reactor as a function of tube length (heat exchange fluid temperature=523 K, tube radius=0.0508 m) (Leonzio and Foscolo, 2020)

For this reactor system, the calculated CO_2 selectivity to CH_3OH, CH_3OH yield within the reactor and within the whole plant are respectively of 57%, 12% and 42%, lower values compared to the base case.

For the base case structured CH_3OH reactor, it is interesting to develop a sensitivity analysis, changing the value of the overall dimensionless number β, defined in the Eq. II.46, by varying the value of radial thermal conductivity.

In particular, it is possible to find a limiting value for which the radial temperature profile corresponding to the hot spot reactor cross section is flat, then the 1-D and 2-D models provide similar results. Radial temperature profiles for the different values of β are shown in Figure II.22. For β of the order of 10^{-4}, or lower than that, a flat radial profile is obtained: the 1-D model is able to describe a structured methanol reactor satisfactorily. It is worth mentioning here that β=0.0087 is in the base case.

A similar sensitivity analysis is considered for a structured CH_3OH reactor with a tube radius of 0.0508 m. In this case, it is found that for values of β lower than 10^{-5} the 1-D and 2-D models provide similar results.

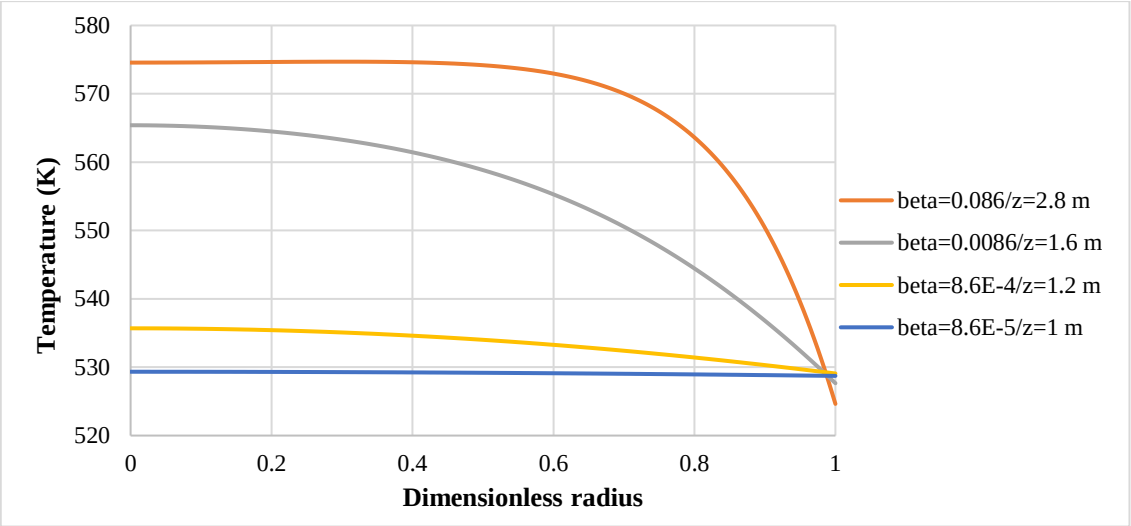

Figure II.22 Radial temperature profile at the hot spot axial coordinate as a function of tube dimensionless radius for different values of the dimensionless number β (Leonzio and Foscolo, 2020)

Sensitivity analyses are developed also for the non-structured reactor for which the 2-D model is able to predict more pronounced radial gradients. At first, the wall heat transfer coefficient is changed to 1000 J/(m^2 s K) and 3000 J/(m^2 s K). No significant variations are present for the component flow rates and compositions. As found in the previous sensitivity analysis, for the case with the wall heat transfer coefficient of 1000 J/(m^2 s K) a slightly increase of temperature is present, while for the case with the wall heat transfer coefficient of 3000 J/(m^2 s K) a slightly decrease of temperature is achieved. These results confirm what reported in Leonzio (2020), where it is shown the increase of heat specific flux at higher values of wall heat transfer coefficient, for a packed bed methanol reactor. Then, with an increase of heat specific flux a decrease of reactor temperature is computed, as expected.

An additional sensitivity analysis is developed by increasing the inlet temperature to 530 K with a value of the wall heat transfer coefficient of 1500 J/(m^2 s K). The temperature profile is shown in Figure II.23. As for the structured reactor, at the inlet reactor, temperature decreases towards a minimum value (higher towards the external radius) and then it increases, achieving, in a nearly asymptotic way, values lower than those predicted for the base case, at the center of the reactor (569 K). In the regions close to the tube wall, temperature drops to that of the refrigerant fluid.

Figure II.24 shows the bulk weighted average molar flow rate profile for each component. Numerical results show that at the outlet of reactor, H_2, CO_2, CO, H_2O, CH_3OH flow rate are respectively of 1.64 mol/s, 0.47 mol/s, 0.12 mol/s, 0.12 mol/s and 0.07 mol/s. Comparing these values with the base case (non-structured reactor) indicates that the temperature profile shown in Figure II.22 reduces the productivity of the reactor. In fact, a lower amount of CH_3OH is produced. To underline the lower efficiency of the system, CO_2 selectivity to CH_3OH, reactor CH_3OH yield and plant CH_3OH yield are calculated and are respectively

equal to 53%, 11% and 40%. CO_2 conversion is reduced of about 1.3% compared to the base case. These results confirm the literature findings by Leonzio (2020), where a lower carbon conversion is found at higher inlet temperatures.

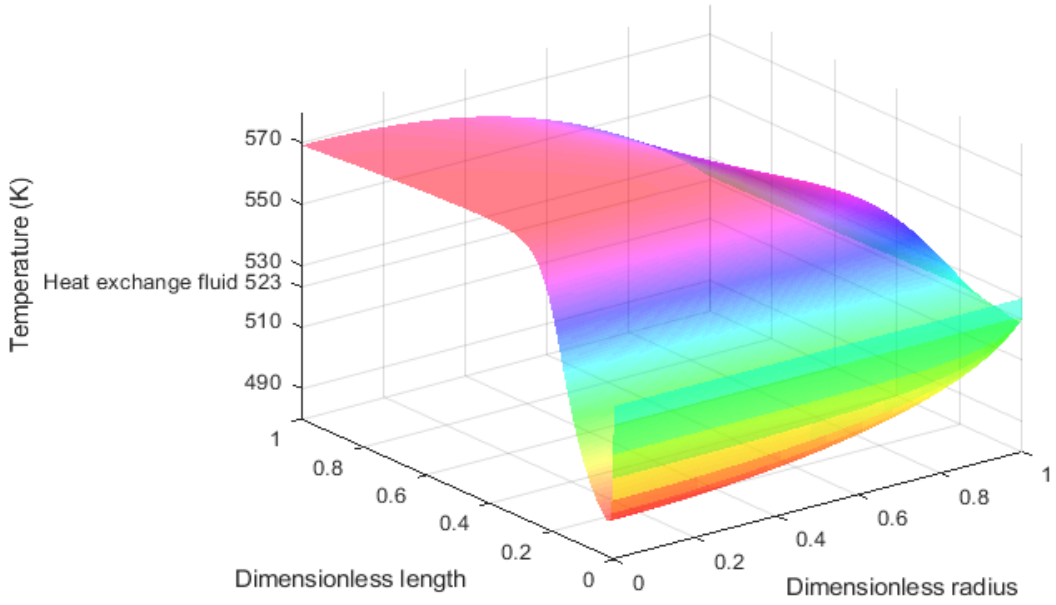

Figure II.23 Tridimensional profile of temperature inside the non-structured CH_3OH reactor as a function of dimensionless length and tube radius (heat exchange fluid temperature=523 K, inlet reactor temperature=530 K) (Leonzio and Foscolo, 2020)

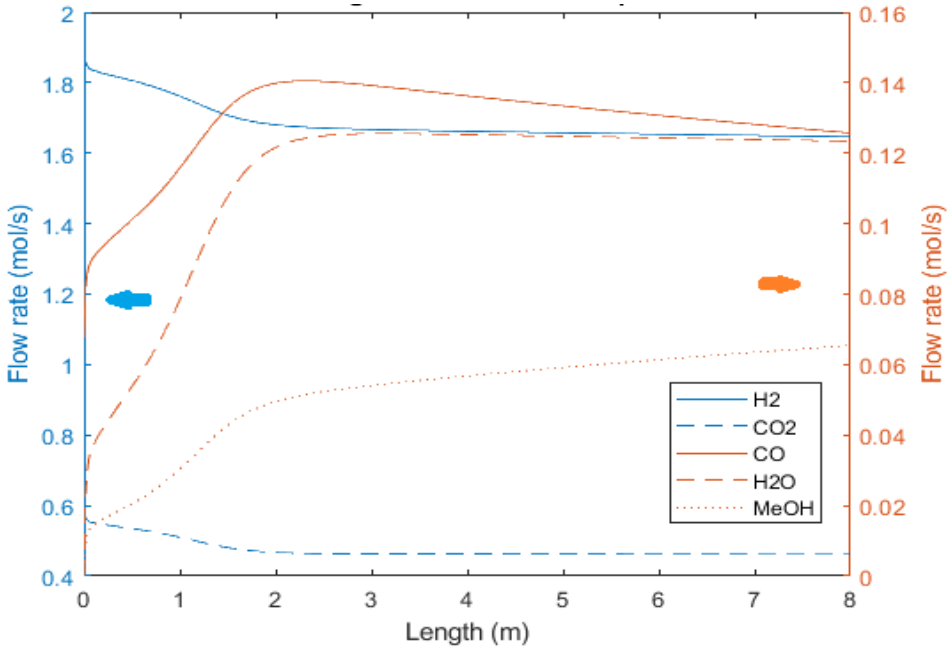

Figure II.24 Bulk weighted average flow rates inside the non-structured CH_3OH reactor as a function of tube length (heat exchange fluid temperature=523 K, inlet reactor temperature=530 K) (Leonzio and Foscolo, 2020)

Finally, an additional study is performed by increasing the tube diameter to 0.1016 m. Figure II.25 shows the calculated temperature profile inside the reactor as a function of radius and length. The maximum temperature is obtained at the outlet of the reactor and is equal to 577 K. Overall, compared to the base case, a wider region of the reactor is predicted to operate at higher temperature, then lower conversion efficiencies are obtained (Manenti et al., 2011).

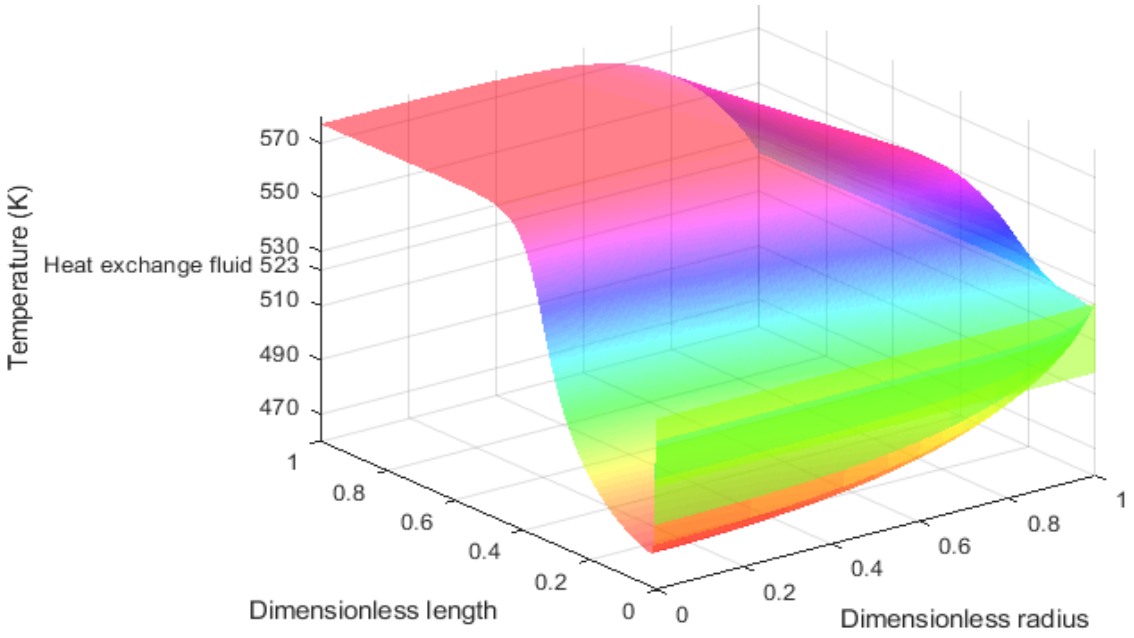

Figure II.25 Tridimensional profile of temperature inside the non-structured CH_3OH reactor as a function of dimensionless length and tube radius (heat exchange fluid temperature=523 K, tube radius=0.0508 m) (Leonzio and Foscolo, 2020)

In fact, CO_2 selectivity to CH_3OH, reactor CH_3OH yield, plant CH_3OH yield are lower and respectively equal to 45%, 10.0% and 36%. At the outlet of the reactor, as shown in Figure II.26, H_2, CO_2, CO, H_2O and CH_3OH calculated flow rates are respectively of 6.59 mol/s, 1.82 mol/s, 0.56 mol/s, 0.52 mol/s and 0.23 mol/s.

As a result, for the non-structured CH_3OH reactor the overall performance is predicted to decrease with increasing tube diameter as in the case of structured reactor, previously considered.

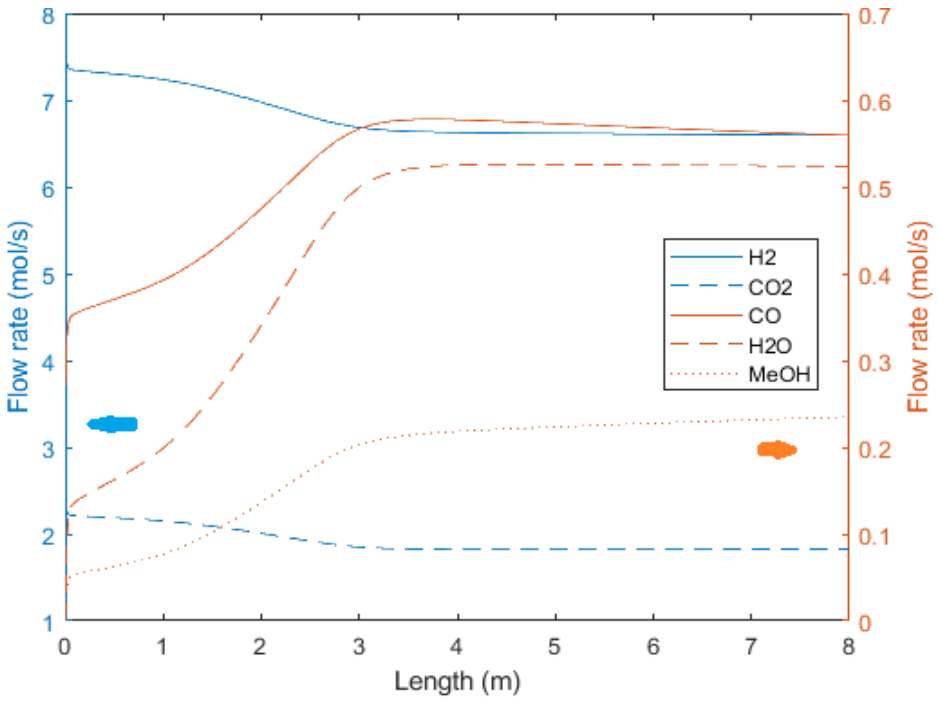

Figure II.26 Bulk weighted average molar flow rates inside the non-structured CH_3OH reactor as a function of tube length (heat exchange fluid temperature=523 K, tube radius=0.0508 m) (Leonzio and Foscolo, 2020)

II.4 Conclusions

A study about CO_2 hydrogenation to CH_3OH is proposed in this chapter. The results show:

- the technical feasibility to produce CH_3OH via CO_2 hydrogenation according to the circular economy (only CO_2 and H_2 in the feed);
- to overcome the thermodynamic limitation of this reaction pathway, an equilibrium analysis shows that, the best reactor configuration consists on the recycle of unconverted gases (CO, CO_2 and H_2) after the separation of H_2O and CH_3OH by condensation: a CO_2 conversion of 69% can be achieved at 55 bar and 473 K;
- the use of CO_2 and H_2 in the feeding stream, instead of a syngas, ensures a lower ΔH for the exothermic reacting system and therefore a reduced reactor temperature increase with reference to that obtainable in the case of a traditional hydrogenation process, which utilizes a syngas feed stream, containing a substantial amount of CO;
- the 1-D mathematical model allows to characterize the overall behavior of a packed bed catalytic reactor operating with recirculation of reactant gases after separation by condensation of products (the best reactor configuration): results show very slight differences between the numerical outputs obtained with and without an axial dispersion term in the mole balance equations;

- this 1-D model also shows that the effect on the reactor performance of the global coefficient of heat exchange with the cooling system is less important than the choice of isothermal heat exchange fluid temperature;
- for the same reactor configuration, fed by CO_2 and H_2, the 2-D model allows to highlight the effect of local fluctuations in temperature and reaction rates for a structured and non-structured reactor packing; these differences are definitely more important for the non-structured reactor, across tube cross sections, because of stronger resistance to radial heat transfer;
- a higher efficiency is predicted for a structured reactor, then a lower recycle flow rate is required in this case (a given methanol yield can be achieved in a structured packing reactor with a comparatively shorter contact time);
- feed temperature and the diameter of the reactor tube have a negative effect on the performance of both reactor topologies, while the wall heat transfer coefficient has a less negative effect on temperature, without a significant variation of molar flow rates;
- in addition to the validation of the 2-D model, by using the few experimental data available in the open literature, the extensive sensitivity analysis carried out allows to check the ability of the 2-D model to answer correctly to changes in key operating conditions: as a result, once model parameters are properly tuned according to experimental data of a reactor campaign, reliable predictions are expected by the model to quantify the effect of different operating conditions and to develop accurate control systems.

Appendix

Methanol–from-carbon-dioxide plants investigated in the literature

Two process schemes for a CH_3OH plant are considered and analyzed in ChemCad®: these are reported in the literature in the work of Perez-Fortes et al. (2016) and Kiss et al. (2016). In both processes, the recycle of unconverted gases (CO, CO_2, H_2) is present, after the separation of CH_3OH and H_2O. Figure S1a shows the scheme of Perez-Fortes et al. (2016), while Figure S1b shows the scheme of Kiss et al. (2016).

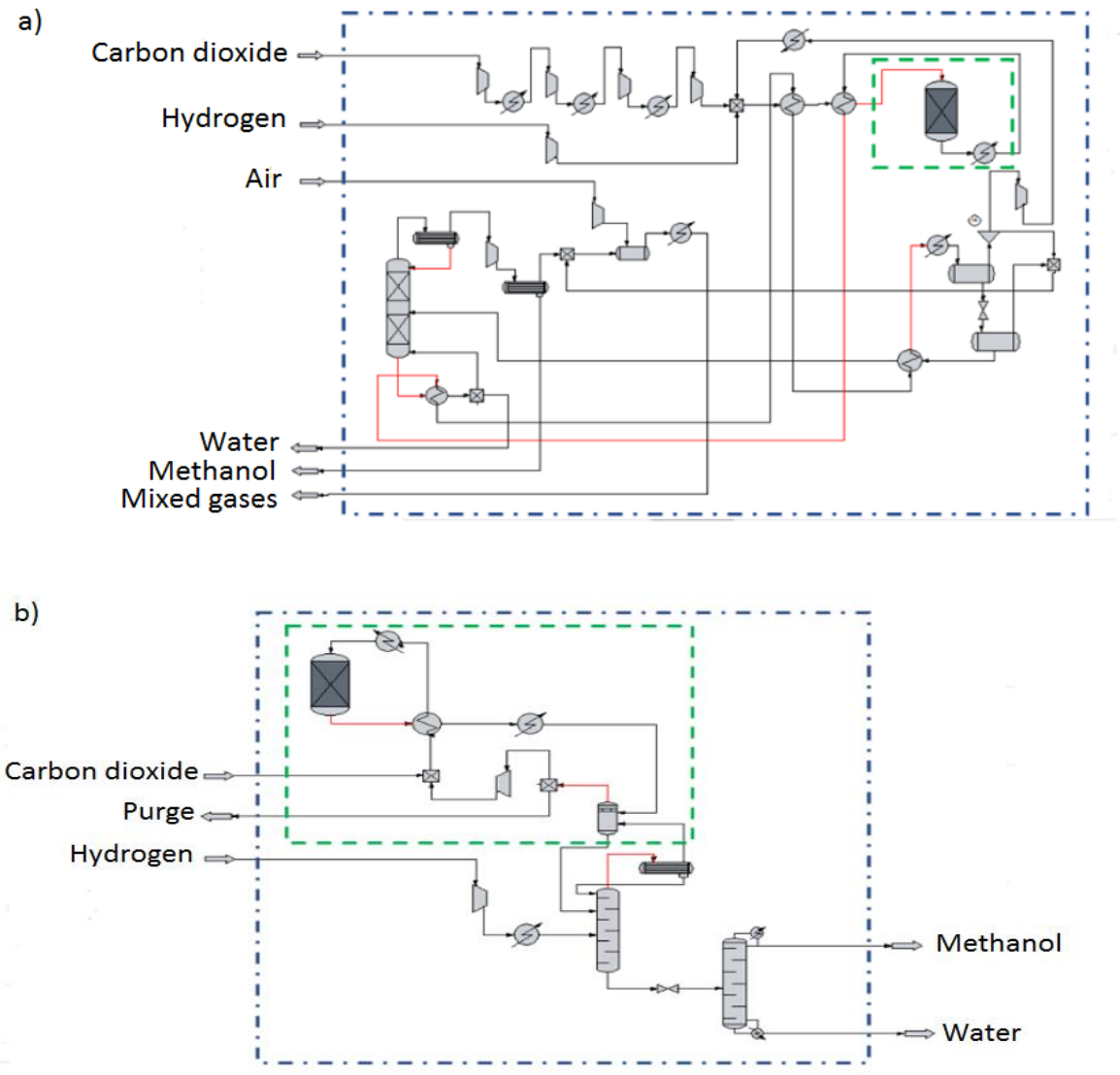

Figure S1 Process scheme for methanol production according to: a) Perez-Fortes et al. (2016), b) Kiss et al. (2016) (green dashed line: boundaries of the reactor section; blue dashed line: boundaries of the plant section).

In the process of Perez-Fortes et al. (2016), the CO_2 feeding stream, captured from a pulverized coal power plant, is compressed through four stages of compression with intermediate cooling from 1 bar to 78 bar, before to be mixed with compressed H_2 at 78 bar. The CH_3OH reactor is modelled as an adiabatic plug flow reactor, using the kinetics of Vanden Bussche and Froment (1996). The reactor operates at 76 bar and 483 K (inlet pressure and temperature) with a volume equal to 42 m^3 and with 44500 kg of $Cu/ZnO/Al_2O_3$ catalyst arranged in pellets forming a packed bed. A heat exchanger removes the heat of reaction producing saturated steam, which expands into two turbines to generate electricity for the CO_2 compressors. The remaining heat is used to heat cycled water that comes from the condenser of a power plant, assuming that the analyzed process is integrated into a power plant. Also, the stream at the exit of the reactor is used to pre-heat the feed stream, to provide heat at the bottom of the distillation column and then to pre-heat the feeding stream to that column. After this thermal integration, CH_3OH and H_2O are separated and the unconverted gases are partially recirculated.

In the process of Kiss et al. (2016), the fresh CO_2 feeding stream is mixed with the recycle gas stream and sent to the feed-effluent heat exchanger. The fresh, wet H_2 feed from chlorine production by salt electrolysis is pressurized to 45 bar before entering the stripper and then is fed to the reactor. The CH_3OH reactor is a multi-tubular reactor with the following characteristics: 12 m of length, 810 tubes of 0.06 m of diameter containing $Cu/ZnO/Al_2O_3$ catalyst. It works in isothermal mode at 523 K and 50 bar. In Kiss et al. (2016), the plant is simulated using the kinetic model of Graaf et al. (1988), while in this Thesis the alternative kinetic mechanism and reaction rates proposed by Vanden Bussche and Froment (1996) are adopted. The stream at the outlet of the reactor is cooled by two heat exchangers and then flashed to separate gases (CO, CO_2, H_2) from the CH_3OH-H_2O mixture. The gas stream, after a tiny purge, is recirculated to the reactor, following compression and mixing with fresh reactants. The CH_3OH-H_2O mixture is sent to the stripper where wet hydrogen is fed in counter-current mode. This dries the hydrogen feed thus removing H_2O and separates light gases (as H_2, CO and CO_2) that are completely recycled. The liquid bottom stream of the stripper is sent to a distillation column for the separation of CH_3OH.

The two plants are modelled in ChemCad® using RKS thermodynamic model for the plant studied by Perez-Fortes et al. (2016) and Non Random Two Liquid (NRTL) thermodynamic model for the plant studied by Kiss et al. (2016), following the choice made in those respective papers.

Table S1 shows that a fairly good agreement between literature and simulation data is present, then the models developed in this work are both validated.

Table S1 Comparison between simulations in ChemCad® and literature data, for the process schemes proposed by Kiss et al. (2016) and Perez Fortes et al. (2016)

	Perez-Fortes et al. (2016)	Kiss et al. (2016)	Simulation of Perez-Fortes et al. (2016)	Simulation of Kiss et al. (2016)
Methanol production (kg/h)	55100	12507	57527	12492
Water production (kg/h)	31700	7346	31664	6065
CO_2 conversion (%), reactor/plant	22.0/93.9	17.2/100.0	22.0/96.5	27/100.0
Gross CO_2 used (kg/kgCH_3OH)	1.37	1.38	1.40	1.37
$[H_2]$-$[CO_2]$/$[CO]$+$[CO_2]$, reactor/plant	2.30/2.0	1.64/2.00	2.31/2.00	3.7/2.00
Heat flow due to reaction (MW)	-23.3	-4.5	-23.7	-5.1

Finally, it is worth recalling here that the reaction mechanism and reaction rates suggested by Vanden Bussche and Froment (1996) are utilized to obtain the results reported in Table S1, differently from the approach by Kiss et al. (2016), who adopt the kinetic model by Graaf et al. (1988). A very close methanol throughput is predicted in the simulations of this Thesis, with the same plant configuration, reactant feed streams and reactor size, as shown on Table S1. According to the Vanden Bussche and Froment kinetic model, the recycle stream is somewhat reduced: this allows for a greater contact time with a consequent higher conversion of CO_2 in the reaction section of the whole plant.

Kinetic model description

In the Vanden Busche and Froment kinetic model, the reaction rate kinetic constants have a temperature dependency characterized by the well known Arrhenius expression (see Eq. S1)

$$k_i = A \cdot e^{\left(\frac{B}{R \cdot T}\right)} \qquad (S1)$$

where R is the constant of universal gas law, in J/mol K, T is temperature in Kelvin, while the values of A and B are reported in Table S2 (Vanden Bussche and Froment, 1996).

Table S2 Values of reaction rate kinetic constants for the kinetic model of Vanden Bussche and Froment (1996) (Leonzio, 2020)

	A	B (J/mol)
k_a ($bar^{-0.5}$)	0.499	17197
k_b (bar^{-1})	$6.62 \cdot 10^{-11}$	124119
k_c	3453.38	0
k_1 (mol/kg s bar^2)	1.07	36696
k_2 (mol/kg s bar)	$1.22 \cdot 10^{10}$	-94765

References

Al-Kalbani, H., Xuan, J., García, S., Wang, H. 2016. Comparative energetic assessment of methanol production from CO2: Chemical versus electrochemical process, Applied Energy 165 1–13.

Ampelli, C., Perathoner, S., Centi, G. 2015 CO_2 utilization: an enabling element to move to a resource- and energy-efficient chemical and fuel production. Phil. Trans. R. Soc. A 373: 20140177.

Annesini, M.C. 2020. Fenomeni di trasporto: fondamenti e applicazioni, Edizioni ingegneria. 2000.

Bansode, A., Urakawa, A., 2014. Towards full one-pass conversion of carbon dioxide to methanol and methanol-derived products. J. Catal. 309 66-70.

Bird, R.B., Stewart, W.E., Lightfoot, E.N., 2002. Transport Phenomena, second edition, John Wiley & Sons.

Bohn, K. 2011. Design configurations of the methanol synthesis loop. Master thesis. Norwegian University of Science and Technology Department of Chemical Engineering;

Fogler, H.S. 2004. Elements of Chemical Reaction Engineering, 4th ed.; New Jersey, USA, Prentice Hall: Upper Saddle River, New Jersey, USA,

Gallucci, F., Basile, A. 2007. A theoretical analysis of methanol synthesis from CO2 and H2 in a ceramic membrane reactor, International Journal of Hydrogen Energy 32 5050–5058.

Graaf, G.H., and Winkelman, J.G.M. 2016. Chemical Equilibria in Methanol Synthesis Including the Water−Gas Shift Reaction: A Critical Reassessment, Ind. Eng. Chem. Res. 55 5854−5864.

Graaf GH, Stamhuis EJ, Beenackers AACM, 1988. Kinetics of low-pressure methanol synthesis. Chem. Eng. Sci. 43 12 3185-3195.

Graaf, G.H., Sijtsema, P.J.J.M., Stamhuis, E.J., and Joosten, G.E.H., 1986. Chemical equilibria in methanol synthesis. Chem. Eng. Sci. 41, 2883

Groppi, G., Tronconi, E., Cortelli, C., Leanza, R. 2012. Conductive monolithic catalysts: development and industrial pilot tests for the oxidation of o-xylene to phthalic an hydride. Ind Eng Chem Res 51 (22) 7590-6.

Hartig, F., Keil, F.J., 1993. Large-scale spherical fixed bed reactors: modeling and optimization, Ind. Eng. Chem. Res. 32 (3), 424-437.

Huš, M., Kopač, D., Štefančič, N.S., Jurković, D.L., Dasireddy, V.D.B.C., Likozar, B. 2017a. Unravelling the mechanisms of CO2 hydrogenation to methanol on Cu-based catalysts using first-principles multiscale modelling and experiments, Catal. Sci. Technol., 7 5900-5913.

Hus, M., Dasireddy, V.D.B.C., Stefancic, N.S., Likozar, B. 2017b. Mechanism, kinetics and thermodynamics of carbon dioxide hydrogenation to methanol on Cu/ZnAl2O4 spinel-type heterogeneous catalysts, Applied Catalysis B: Environmental 207 267–278.

Khalilpourmeymandi, H., Mirvakili, A., Rahimpour, M.R., Shariati, A. 2017. Application of response surface methodology for optimization of purge gas recycling to an industrial reactor for conversion of CO_2 to methanol. Chinese Journal of Chemical Engineering, 25, (5) 676-687.

Kiss, A.A., Pragt, J.J., Vos, H.J., Bargeman, G., de Groot, M.T., 2016. Novel efficient process for methanol synthesis by CO2 hydrogenation. Chemical Engineering Journal 284:260–269.

Kopac, D., Hus, M., Ogrizek, M., Likozar, B. 2017. Kinetic Monte Carlo Simulations of Methanol Synthesis from Carbon Dioxide and Hydrogen on Cu(111) Catalysts: Statistical Uncertainty Study, J. Phys. Chem. C 121 17941−17949.

Lee, J.S., Lee, K.H., Lee, S.Y., Kim, Y.G., 1993. A comparative study of methanol synthesis from COTHz and CO-H, over a Cn-ZnO-A1203 catalyst, J. Catal., 144 414-424.

Leonzio, G. 2020. Mathematical modeling of a methanol reactor by using different kinetic models, Journal of Industrial and Engineering Chemistry, In press.

Lovik, I. 2001. Modelling, Estimation and Optimization of the Methanol Synthesis with Catalyst Deactivation. A thesis submitted in partial fullment of the degree of Doktor Ingenior Norwegian University of Science and Technology Department of Chemical Engineering.

Luyben, LW. 2010. Design and control of a methanol reactor/ column process. Ind Eng Chem Res 49 6150-63

Machado, C.F.R., de Medeiros J.L., and Araújo O.F.Q., 2014. A comparative analysis of methanol production routes: synthesis gas versus CO2 hydrogenation, Proceedings of the 2014 International Conference on Industrial Engineering and Operations Management Bali, Indonesia, January 7 – 9.

Makertiharta IGBN, Dharmawijaya PT, Wenten IG, 2017. Current progress on zeolite membrane reactor for CO2 hydrogenation. AIP Conference Proceedings 1788, 040001.

Manenti, F., Cieri, S., Restelli, M., 2011. Considerations on the steady-state modeling of methanol synthesis fixed-bed reactor. Chemical Engineering Science 66 152–162.

Manenti, F., Leon-Garzon, A.R., Ravaghi-Ardebili, Z., Pirola, C. 2014. Systematic staging design applied to the fixed-bed reactor series for methanol and one-step methanol/dimethyl ether synthesis. Applied Thermal Engineering 70 1228-1237.

Manenti, F., Cieri, S., Restelli, M., Bozzano, G. 2013. Dynamic modeling of the methanol synthesis fixed-bed reactor. Comput Chem Eng 48 325-34

Meyer, J.J., Tan, P., Apfelbacher, A., Daschner, R., Hornung, A. 2016. Modeling of a Methanol Synthesis Reactor for Storage of Renewable Energy and Conversion of CO2 – Comparison of Two Kinetic Models, Chem. Eng. Technol. 39 (2) 233–245.

Montebelli, A., Visconti, C.G., Groppi, G., Tronconi, E., Ferreira, C., Kohler, S. 2013. Enabling small scale methanol synthesis reactors through the adoption of highly structured catalyst. Catal. Today 215 176-185.

Leonzio, G., 2018. State of art and perspectives about the production of methanol, dimethyl ether and syngas by carbon dioxide hydrogenation, Journal of CO_2 utilization, 27, 326-354.

Leonzio, G. 2020. Mathematical modeling of methanol reactor using different kinetic models, Industrial & Engineering Chemistry Research, In press.

Leonzio and Foscolo, 2020. Analysis of a 2-D model of a packed bed reactor for methanol production by means of CO_2 hydrogenation. International Journal of Hydrogen Energy. In press.

Leonzio, G., E. Zondervan, P.U. Foscolo, 2019. Methanol production by CO_2 hydrogenation: Analysis and simulation of reactor performance. International Journal of Hydrogen Energy, 44, 16, 7915-7933

Pérez-Fortes, M., Schöneberger, J.C., Boulamanti, A., Tzimas, E., 2016. Methanol synthesis using captured CO2 as raw material: Techno-economic and environmental assessment. Applied Energy. 161: 718–732.

Phan, X.K., Bakhtiary, H.D., Myrstad, R., Thormann, J., Pfeifer, P., Venvik, H.J., Holmen, A. 2010. Preparation and Performance of a Catalyst-Coated Stacked Foil Microreactor for the Methanol Synthesis, Ind. Eng. Chem. Res. 49 10934–10941

Phan, X.K., Bakhtiary-Davijanya, H., Myrstad, R., Pfeifer, P., Venvika, H.J., Holmen, A. 2011. Preparation and performance of Cu-based monoliths for methanol synthesis, Applied Catalysis A: General 405 1–7.

Skrzypek, J., Lachowska, M., Grzesik, M., Sloczynski, J., Nowak, P., 1995. Thermodynamics and kinetics of low pressure methanol synthesis. The Chemical Engineering Journal 58 101-108.

Slotboom, Y., Bos, M.J., Pieper, J., Vrieswijk, V., Likozar, B., Kersten, S.R.A., Brilman, D.W.F. 2020. Critical assessment of steady-state kinetic models for the synthesis of methanol over an industrial Cu/ZnO/Al2O3 catalyst. Chemical Engineering Journal 389 124181

Smith, J.M. 1981. Chemical Engineering Kinetics, McGraw-Hill College; 3rd edition.

Specchia, V., Sicardi, S., 1980. Modified correlation for the conductive contribution of thermal conductivity in packed bed reactor. Chemical Engineering Communication, 6:1-3, 131-139.

Struis, R.P.W.J., 2001. Stucki S, Verification of the membrane reactor concept for the methanol synthesis. Applied Catalysis A: General 216 117–129.

Vanden Bussche, K.M., Froment, G.F. 1996. A Steady-State Kinetic Model for Methanol Synthesis and the Water Gas Shift Reaction on a Commercial Cu/ZnO/Al2O3 Catalyst, J. Catal. 161 (1) 1-10.

Visconti, C.G., Montebelli, A., Groppi, G., Tronconi, E., Kohler, S. 2018. Highly Conductive Structured Catalysts for the Intensification of Methanol Synthesis in Multitubular Reactors, Methanol Science and Engineering, 519-528.

Yusup, S., Anh, N.P., Zabiri, H. 2010. A Simulation study of an industrial methanol reactor based simplified steady state model, IJRRAS 5 (3) 213-222.

Zachopoulosa A, Heracleous E, 2017. Overcoming the equilibrium barriers of CO2 hydrogenation to methanol via water sorption: A thermodynamic analysis. Journal of CO_2 Utilization 21 360–367.

Nomenclature

Abbreviations

a = specific surface area of heat exchange in [m^2/kg_{cat}]

A = pre-exponential factor

Ci = molar concentration of component I [mol/m^3]

$C_{i,ad}$ = dimensionless molar concentration of component i

$C_{in,CO2}$ = inlet concentration of CO_2 [mol/m^3]

$C_{p,}$ = heat capacity at constant pressure for component i [J/molK]

C_{pm} = average specific heat [J/molK]

$C_{s,i}$ = concentration of component i at the pellet surface [mol/m^3]

C_{wp} = Weisz-Prater parameter

D_e = effective diffusivity [m^2/s]

d_p = equivalent diameter of catalyst particle in the bed [m]

Dr = radial dispersion coefficient [m^2/s]

d_t = tube diameter [m]

E_a = activation energy [J/mol]

F = total molar flow rate [mol/s]

F_b = bulk weight molar flow rate [mol/s]

F_{CH3OH} = molar flow rate of methanol [mol/s]

F_{CO} = molar flow rate of carbon monoxide [mol/s]

F_{CO2} = molar flow rate of carbon dioxide [mol/s]

F_{H2} = molar flow rate of hydrogen [mol/s]

F_{H2O} = molar flow rate of water [mol/s]

F_i = molar flow rate of component i [mol/s]

F_{totin} = total molar flow rate at the inlet of reactor [mol/s]

G = superficial mass velocity [$kg/s\ m^2$]

g_c = conversion factor [$kg/m/s^2N$]

L_{tot} = length of reactor [m]

K_{cat} = thermal conductivity of catalyst [J/msK]

K_e = equivalent radial thermal conductivity [J/msK]

K_{eq1} = equilibrium constant of reaction 1

K_{eq2} =equilibrium constant of reaction 2

K_g = thermal conductivity of gas [kW/mK]

k_1,k_2,k_c,k_a,k_b = reaction costant of methanol synthesis reaction

P_{ad} = dimensionless pressure

p_{CH3OH} = partial pressure of CH_3OH [bar]

p_{CO} = partial pressure of CO [bar]

p_{CO2} = partial pressure of CO_2 [bar]

$P_{e,p}$ = Peclet number of catalyst pellet ($U_z d_p / D_r$)

p_{H2} = partial pressure of H_2 [bar]

p_{H2O} = partial pressure of H_2O [bar]

P = pressure [Pa]

P_r = Prandtl number

R = ideal gas constant [J/molK]

r_{ad} = dimensionless radial coordinate

R_{edpva} = Reynold number according the the diameter of catalyst pellet ($\rho v d_p / \mu$)

$\mathbf{r}_i$ = reaction rate of i component [mol/m^3s]

$\mathbf{r}_{i,o}$ = reaction rate of i component at the system inlet conditions [mol/m^3s]

$r_{obs,i}$ = measured value of the reaction rate for component i [mol/m^3s]

R_p is the pellet radius [m]

R_{tot} = radius of reactor tube [m]

r_1 = reaction rate of reaction 1 [mol/m^3s]

r_2 = reaction rate of reaction 2 [mol/m^3s]

S = tube cross section surface area [m^2]

T = temperature [K]

T_{ad} = dimensionless temperature

T_j = temperature of the heat exchange fluid [K]

U = global coefficient of heat exchange [J/m^2sK]

U_z = superficial gas velocity [m/s]

w = mass of catalyst [kg]

z = reactor length [m]

Greek letters

β = dimensionless heat of reaction

γ = dimensionless number ($\frac{E_a}{R \cdot T}$)

ΔH_j = heat of reaction for reaction j [J/mol]

ΔH_1^{rxn} = heat of reaction for reaction 1 [J/mol]

ΔH_2^{rxn} = heat of reaction for reaction 2 [J/mol]

ε = bed void fraction

μ = viscosity [Pas]

ξ = dimensionless axial coordinate

ρ = gas density [kg/m^3]

ρ_c = density of catalyst particle [kg/m^3]

ϕ_n^2 = Thiele modulus

Chapter III

Design model for CCUS supply chains - Development of a CCUS supply chain for Germany-Part I

The mathematical model for the optimal design of a supply chain for carbon dioxide capture, utilization and storage is described and applied to Germany, the largest emitter in Europe. Carbon dioxide may be stored and/or utilized to produce different compounds: in this application, methanol via methane dry reforming. Using a Mixed Integer Linear Programming model, three different cases are considered, according to the hydrogen production route required to obtain the right syngas composition: hydrogen by external reforming, hydrogen by external water electrolysis, hydrogen by internal steam reforming. Results show that the best option is providing hydrogen by water electrolysis, because a higher amount of carbon dioxide is consumed to produce the same amount of methanol. The proposed best supply chain produces 203 Mton/year of methanol then, Germany would be able to satisfy the world methanol demand in next years. Carbon tax and economic incentives are required to reduce the methanol production cost to 340 €/ton: only in this case the process is economically feasible.

III.1 Introduction

Germany is the country with the highest greenhouse gas (GHG) emissions in Europe, then urgent solutions are need to solve this problem, in order to achieve the environmental target set by the Europe 2020 strategy for 2020. Carbon capture and storage (CCS), carbon capture and utilization (CCU) and carbon capture utilization and storage (CCUS) supply chains can be a valid solution in this context (Egmond and Hekkert, 2012). In the literature, many studies are considered about the analysis of CCS systems, where carbon dioxide (CO_2) is captured and stored in different ways, aiming at climate change mitigation (Bruhn et al., 2016). However, CO_2 utilization is also important according to the circular economy (converting a waste emission into a resource), avoiding that a great amount of CO_2 is only accumulated into oceans or underground and reducing fossil raw materials utilization (Bringezu, 2014). However, CO_2 utilization should not be considered as an alternative technology to CCS, but as a complementary technology to update the overall technology (Joshi, 2014). This consideration brings to the development and study of CCUS frameworks, where CO_2 is stored and used, after its capture and transportation. As already discussed, in the literature CCUS supply chains are mainly about CO_2 enhanced oil recovery (CO_2-EOR) systems, while methanol (CH_3OH) is the most important product that can be obtained from CO_2, with a widespread utilization. A study about a CCUS supply chain, where CO_2 is hydrogenated to CH_3OH production is present in the literature (Ochoa Bique, 2018). Production of methanol by means of CO_2 hydrogenation is actually the subject of Chapter II of this Thesis. However, CH_3OH can be produced from CO_2 through other routes, as methane (CH_4) dry reforming (Wang et al., 2019; Dou et al., 2019). The interest here relies to the fact that CH_4 is progressively becoming more abundant and cheaper thanks to new extraction technologies; in addition, its relatively high content of hydrogen (H_2) makes it the best feedstock for a low carbon

economy and the transition to fully renewable energy sources. This research, then, wants to fill a gap present in the literature, developing a mathematical model of a CCUS supply chain for Germany where CO_2 is stored and used to produce CH_3OH via CH_4 dry reforming. For CH_3OH synthesis, the ratio H_2:CO_2 is 2:1 and not 1:1 as obtained in the syngas then, the additional H_2 needed for the reaction is provided by three different ways (by external reforming, by external water (H_2O) electrolysis, by internal steam reforming) that are compared in economic and environmental point of view, to choose the best one. Ten regions with higher CO_2 emissions are considered in Germany and inside the supply chain, while Altmark is the storage site and Leuna the utilization site. CO_2 is mainly captured from flue gases of power plants, cement and iron and steel industries through different capture technologies. In particular, a deterministic Mixed Integer Linear Programming (MILP) model is developed to design and optimize the framework, through the minimization of the total costs, then according to the economic point of view, as most of works reported in the literature. At this stage, a single optimization is then considered to find the best connection of each element inside the supply chain and the amount of captured, transported, stored and used CO_2 with the amount of produced CH_3OH and the best capture technologies. The aim of this work, is then to suggest an optimal CCUS framework that is able to reduce CO_2 emissions according to the environmental target at the minimum costs, satisfying the national CH_3OH demand.

III.2 Model development

III.2.1 Problem statement

For the developed supply chain, the following assumptions are made:

- capture plants are located at CO_2 sources to avoid the transportation of flue gas and its additional costs (Kalyanarengan Ravi et al., 2017);
- one to one coupling: one source node can be connected to only one capture node in the storage and utilization section and each capture node can receive from only one source node (Kalyanarengan Ravi et al., 2017);
- the mode for transporting CO_2 is always via pipeline, because it is the most mature technology and able to carry a large amount of CO_2 at a low costs. When the CO_2 stream is pure from corrosive contaminants, a pipeline made of carbon steel can be used, while a pipeline made of stainless steal is suggested if NO_x and SO_x or other corrosive compounds are present; moreover, CO_2 is generally transported in supercritical or liquid phase);
- CH_3OH is produced through via CH_4 dry reforming;
- the framework structure remains constant and the mathematical model is in steady state conditions over a horizon of 25 years: the work is focused on the design of the system finding its optimal

topology (then it can be supposed that in this relatively short period few changes will affect raw materials availability and products demand);

- CH_3OH production amount is constant over time due to the stationary conditions and the short considered period, so that it can be sold to a stable price in order to maximize the profit;
- due to the geological characteristics of the selected storage site that can store a very great amount of CO_2, only one storage option is chosen in the model;
- there is one option for CH_4 source, because the selected site can satisfy the required demand and the developed model is simpler;
- the reactor for CH_4 dry reforming producing syngas, the reactor for CH_3OH production from the produced syngas and the additional H_2 source are located in the same utilization site;
- in the case of external production of H_2 by CH_4 steam reforming, additional CO_2 emissions are present (computed from: $CH_4+2H_2O=4H_2+CO_2$) and considered in the developed mathematical model;
- distances between source and utilization/storage sites are calculated from their latitude and longitude (Kalyanarengan Ravi et al., 2017);
- the profitability of the system is estimated by evaluating CH_3OH production cost;

Based on the above assumptions, a mathematical model is developed. The following specifications are given:

- CO_2 sources: locations, yearly CO_2 emissions, CO_2 composition and flow rate of flue gases (Federal Ministry for the Environment, 2014);
- CO_2 capture and compression technologies: used materials and costs (Nguyen and Zondervan, 2018; Zhang et al., 2018);
- CO_2 transportation via pipeline: costs and distances (Serpa et al., 2011; Distance, 2019);
- CH_3OH production plant: location, conversion factor and costs of the considered technology (Lochner, 2011; Hermandez and Martin, 2016; Luu et al., 2015);
- CO_2 storage: location, type, capacity and costs (Hendriks, 1994; Hasan et al., 2014; Roehrl and Toth, 2009);
- CH_4 source: location and costs (Kühn, et al., 2013; Eurostat, 2016);
- CH_4 transportation via pipeline: costs and distances (Lochner, 2011; Distance, 2019);
- H_2 and steam production: location and costs (Turton et al., 2009; Stadler, 2014);
- national CH_3OH demand to be satisfied and target of CO_2 emission reduction to achieve (Ochoa Bique et al., 2018; Federal Ministry for the Environment, 2017);

The following decisions are made:

- which sources to be selected from a given set of sources and which CO_2 quantity to be captured from each selected source;
- which technologies and materials combination should be used for CO_2 capture in each selected source;
- which quantity of CH_4 and H_2 should be used;
- for storage and CH_3OH production sites, which should be the amount of stored and utilized CO_2 and the amount of produced CH_3OH, respectively;

The objective is to minimize the total costs, which includes CO_2 capture and compression costs, CO_2 transportation costs, CO_2 storage costs, production costs (steam/H_2, CH_4 and CH_3OH) and CH_4 transportation costs.

III.2.2 CCUS supply chain model

The supply chain is modelled as a MILP model for which sets, parameters, variables, constraints, equations and the objective function are defined in the following sections. AIMMS (Advanced Interactive Multidimensional Modeling System) is used as programming environment for the implementation of the model.

III.2.2.1 Sets

Each element inside the supply chain is represented by an index. The stationary sources are represented by 'i', capture and compression facilities are represented by 'j', geological storage and utilization sites as 'k'.

III.2.2.2 Parameters

The parameters used in the CCUS supply chain model are the following: CR^{min}, the minimum target for the overall CO_2 reduction (ton/year); CS_i, the total CO_2 emission from each source i (ton/year); F_i, the total flue gas flow rate from each source i (mol/s); XS_i, CO_2 composition in the flue gas from source i (mol%); XL_i, the lowest CO_2 composition processing limit for the capture plant j (mol%); XH_i, the highest CO_2 composition processing limit for the capture plant j (mol%); C_k^{max}, the maximum storage capacity at the storage site k (ton); $MeOH^{dem}$, the national CH_3OH demand that must be satisfied in Germany (ton/year).

III.2.2.3 Variables

For the developed model, binary and continuous variables are used. $X_{i,j,k}$ and $Y_{i,j,k}$ are the considered binary variables, with a value of 1 or 0. In particular, they are used to select the CO_2 storage site and the CO_2 capture technology/material respectively, when they have a value of 1. Continuous variables have a value between 0 and 1: $FR_{i,j,k}$ is used to determine the fraction of CO_2 that is sent to the storage site, $MR_{i,j,k}$ is considered to determine the fraction of CO_2 that it is sent to the utilization site.

III.2.2.4 Constraints

For the developed model, different constraints are taken into account. To ensure that the captured CO_2 is not divided among different storage sites, the following constraint is used (see Eq. III.1):

$$\sum_{(j,k)\in(J,K)} X_{i,j,k} \leq 1 \qquad \forall\, i \in I \qquad (III.1)$$

where $X_{i,j,k}$ is the binary variable defined above. In addition, this constraint allows the one to one coupling assumption between sources and capture systems in the storage section.

To ensure that the maximum storage capacity is not exceeded, the following constraint is used (see Eq. III.2):

$$\sum_{(i,k)\in(I,K)} CS_i \cdot FR_{i,j,k} \leq \frac{C_k^{max}}{TH} \qquad \forall\, k \in K \qquad (III.2)$$

where CS_i is the total CO_2 emission from source 'i', C_k^{max} is the maximum storage capacity of the storage site 'k', TH is the time horizon of the supply chain and $FR_{i,j,k}$ is the continuous variable defined above.

To ensure that the minimum target of CO_2 emissions reduction is achieved, the following constraint is used (see Eq. III.3):

$$\sum_{(i,j,k)\in(I,J,K)} CS_i \cdot FR_{i,j,k} + CS_i \cdot MR_{i,j,k} \geq CR^{min} \qquad (III.3)$$

where CS_i is the total CO_2 emission from source 'i', $FR_{i,j,k}$ and $MR_{i,j,k}$ are the continuous variables defined above and CR^{min} is the minimum target of CO_2 emissions reduction. To consider the additional CO_2 emissions linked to the external H_2 provision through the steam reforming process, in the LHS term of this constraint these emissions are subtracted to CO_2 utilized within the system.

To make sure that when a source is selected no more than 90% of CO_2 is captured from that source, the following restriction is introduced, where $FR_{i,j,k}$ and $MR_{i,j,k}$ are defined above (see Eq. III.4):

$$\sum_{(j)\in(J)} FR_{i,j,k} + MR_{i,j,k} \leq 0.9 \qquad \forall\, (i,k) \in (I,K) \qquad (III.4)$$

Not all the considered technologies can be used to capture CO_2 from a source, with a purity of 90% in CO_2. This depends on the following constraint (see Eq. III.5):

$$\sum_{(k)\in(K)} (XH_j - XS_i) \cdot (XS_i - XL_j) \cdot X_{i,j,k} \geq 0 \qquad \forall\, (i,j) \in (I,J) \quad (III.5)$$

where XS_i is CO_2 composition in flue gas from source "i", XL_j, is the lowest CO_2 composition processing limit for the capture plant "j", XH_j is the highest CO_2 composition processing limit for the capture plant "j"

and $X_{i,j,k}$ is the binary variable defined above. This constraint is valid for the storage section, while the required purity for the utilization section is achieved in the respective site.

To ensure that the national CH_3OH demand is satisfied the following constraint is used (see Eq. III.6):

$$\sum_{(i,j,k)\in(I,J,K)} MR_{i,j,k} \geq MeOH^{dem} \qquad (III.6)$$

where $MeOH^{dem}$ is the CH_3OH demand that must be satisfied and $MR_{i,j,k}$ the methanol production at the given plant.

In the utilization and storage section only one capture technology/material can be chosen for the selected CO_2 source, as defined in the following constraint (see Eq. III.7):

$$\sum_{(j,k)\in(J,K)} Y_{i,j,k} \leq 1 \qquad \forall\, i \in I \qquad (III.7)$$

where $Y_{i,j,k}$ is defined above.

In order to convert the non linear mathematical model in a linear mathematical model through the Glover linearization, the following constraints are used (see Eqs. III.8-9):

$$0 \cdot X_{i,j,k} \leq FR_{i,j,k} \leq 0.9 \cdot X_{i,j,k} \qquad \forall\, (i,j,k) \in (I,J,K) \qquad (III.8)$$

$$0 \cdot Y_{i,j,k} \leq MR_{i,j,k} \leq 0.9 \cdot Y_{i,j,k} \qquad \forall\, (i,j,k) \in (I,J,K) \qquad (III.9)$$

where $FR_{i,j,k}$, $MR_{i,j,k}$, $X_{i,j,k}$ and $Y_{i,j,k}$ are the variables defined above, while 0.9 is used because at least 90% of CO_2 is captured from each source. The nonlinearity arises from the equations related to CO_2 capture and compression costs, where the product between a continuous and a binary variable is present. The continuous variable is that related to the amount of captured CO_2 sent to the utilization or storage section, used to define the amount of treated flue gas, while the binary variable is that related to the choice of CO_2 capture technology. Applying this linearization method it is possible to consider only a continuous variable in the cost equation, with the constraint as defined in Eqs. III.8-III.9.

III.2.2.5 Equations

CO_2 capture and compression costs (€/year) are calculated as follows (see Eq. III.10):

$$CC_{i,j,k} = CDC_{i,j,k} + CIC_{i,j,k} + COC_{i,j,k} \qquad \forall\, (i,j,k) \in (I,J,K) \qquad (III.10)$$

where $CDC_{i,j,k}$ are the flue gas dehydration costs (€/year), $CIC_{i,j,k}$ are the investment costs (€/year) and $COC_{i,j,k}$ are the operating costs (€/year). Generally, flue gas is dehydrated via tri-ethylene glycol absorption with a cost of 9.28 € per ton of CO_2 (including the capital and investment costs) (Kalyanarengan Ravi et al., 2017). For the amine absorption, no dehydration operations are necessary. The investment and operating

costs are a function of flue gas flow rate and CO_2 composition and are calculated as follows (Zhang et al., 2018) (see Eqs. III.11-12):

$$CIC_{i,j,k} = \alpha_{I,j} \cdot Y_{i,j,k} + (\beta_{I,j} \cdot x_{co2,i}{}^{n_{I,j}} + \gamma_{I,j}) \cdot F_{i,j,k}^{m_{I,j}} \quad \forall (i,j,k) \in (I,J,K) \qquad (III.11)$$

$$COC_{i,j,k} = \alpha_{o,j} \cdot Y_{i,j,k} + (\beta_{o,j} \cdot x_{co2,i}{}^{n_{o,j}} + \gamma^{\gamma}{}_{o,j}) \cdot F_{i,j,k}^{m_{o,j}} \quad \forall (i,j,k) \in (I,J,K) \qquad (III.12)$$

where $\alpha_{I,j}, \alpha_{o,j}, \beta_{I,j}, \beta_{o,j}, \gamma_{I,j}, \gamma_{o,j}, n_{I,j}, n_{o,j}, m_{o,j}, m_{I,j}$ are fixed parameters for each process and for each material, as in Table III.1, $x_{CO2,i}$ is CO_2 composition in flue gas, $F_{i,j,k}$ is flue gas flow rate in mol/s and $Y_{i,j,k}$ is the binary variable defined above.

These expressions are obtained considering a CO_2 capture plant followed by a six-stage compression with inter-stage cooling to compress CO_2 up to 150 bar (Hasan et al., 2012a,b).

For the ionic liquid absorption, the following equations are used for the investment and operating costs (€/year) respectively (Nguyen and Zondervan, 2018) (see Eqs. III.13-14):

$$CIC_{i,j,k} = (\alpha_{I,j} \cdot F_{i,j,k} + \beta_{I,j} \cdot Y_{i,j,k}) \cdot x_{co2,i} + \gamma_{I,j} \cdot F_{i,j,k}^{m_{I,j}} \quad \forall (i,j,k) \in (I,J,K) \qquad (III.13)$$

$$COC_{i,j,k} = (\alpha_{o,j} \cdot F_{i,j,k} + \beta_{o} \cdot Y_{i,j,k}) \cdot x_{co2,i} + \gamma_{o,j} \cdot F_{i,j,k}^{m_{o,j}} \quad \forall (i,j,k) \in (I,J,K) \qquad (III.14)$$

where $\alpha_{I,j}, \alpha_{o,j}, \beta_{I,j}, \beta_{o,j}, \gamma_{I,j}, \gamma_{o,j}, m_{o,j}, m_{I,j}$ are fixed parameters as in Table III.1, $x_{CO2,i}$ is CO_2 composition in flue gas, $F_{i,j,k}$ is flue gas flow rate in mol/s and $Y_{i,j,k}$ is the binary parameter defined above.

Table III.2 Data cost for CO_2 capture and compression technologies (Zhang et al., 2018)

Technology	Material	α	β	γ	n	m
		Investment cost ($/year)				
Absorption	MEA	7719	67871	901.000	0.660	0.800
PSA	13X	220462	26720	895.262	0.508	0.804
VSA	13X	91060	23096	7688.408	0.470	0.763
Membrane	FSC-PVAm	177500	16505	18912.000	0.880	0.770
		Investment cost (€/year)				
Absorption	IL	7590.52	2606878.23	33119.84		0.67
		Operating cost ($/year)				
Absorption	MEA	0	24088	0	1.000	1.000
PSA	13X	0	11352	3115.833	1.000	0.974
VSA	13X	0	8167	1580.419	0.590	0.985
Membrane	FSC-PVAm	0	11619	0	0.210	1.000
		Operating cost (€/year)				
Absorption	IL	33172.59	897224.41	187421.22		0.65

A linear model for CO_2 transportation costs via pipeline as proposed by Serpa et al. (2011) is used. The total costs comprise the investment ($TIC_{i,j,k}$) and operating costs ($TOC_{i,j,k}$) according to the following equation (see Eq. III.15):

$$TC_{i,j,k} = CCR \cdot TIC_{i,j,k} + TOC_{i,j,k} \qquad \forall\,(i,j,k) \in (I,J,K) \qquad (III.15)$$

where CCR is the capital cost recovery, calculated at an interest rate, r, of 10% and 25 years, y ($r(1+r)^y/(1+r)^y-1$), and cost terms respectively in M€ and in M€/year are equal to (see Eqs. III.16-III.17):

$$TIC_{i,j,k} = \left(\alpha_t \cdot CS_i \cdot FR_{i,j,k}/MR_{i,j,k} + \beta_t \cdot X_{i,j,k}/Xm_{i,j,k}\right) \cdot F_T \cdot \left(D_{i,k}/d_{i,k} + 16\right) \quad \forall\,(i,j,k) \in (I,J,K) \quad (III.16)$$

$$TOC_{i,j,k} = 4\% \cdot TIC_{i,j,k} \qquad \forall\,(i,j,k) \in (I,J,K) \qquad (III.17)$$

where α_t=0.019 and β_t=0.533 (Serpa et al., 2011), $D_{i,k}$ and $d_{i,k}$ are the distances between source and storage sites and between source and utilization sites, F_T is a terrestrial factor equal to 1.2 (Broek et al., 2010), 16 km are added to distance to consider an additional transportation path (Dahowski et al., 2004), $X_{i,j,k}$ is the variable defined above as $MR_{i,j,k}$ and $FR_{i,j,k}$, $X_{mi,j,k}$ is a parameter equal to 0 if $MR_{i,j,k}$ is 0 else it is 1, CS_i is the amount of CO_2 in Mton/year. The operational costs are taken as 4% of investment costs (Kalyanarengan Ravi et al., 2017).

CO_2 storage costs (€/year) are calculated as the sum of investment costs ($SIC_{i,j,k}$) and operating costs ($SOC_{i,j,k}$) (see Eq. III.18):

$$SC_k = CCR \cdot SIC_k + SOC_k \qquad \forall\,(k) \in (K) \qquad (III.18)$$

with CCR defined above and where the investment costs (€) are calculated according to the following relation (Hendriks, 1994) (see Eq. III.19):

$$SIC_k = (m \cdot d_{well} + b) \cdot N_{well}^{build}{}_k \qquad \forall\,(k) \in (K) \qquad (III.19)$$

where, m and b are parameters respectively equal to 1.53 M€/km and 1.23 M€, d_{well} is the depth of the well CCR is the capital cost recovery (calculated considering an interest rate of 10% and 25 years) and N_{well}^{build} is the number of wells that should be built (Hasan et al., 2014) (see Eq. III.20):

$$N_{well}^{build}{}_k = \frac{\sum_{(i,j)\in(I,J)} CS_i \cdot FR_{i,j,k}}{IC} \qquad \forall\,(k) \in (K) \qquad (III.20)$$

depending on the maximum injection capacity per well IC and stored CO_2. Operating costs (€/year) are calculated as 4% of the investment costs (Kalyanarengan Ravi et al., 2017) (see Eq. III.21):

$$SOC_k = 4\% \cdot SIC_k \qquad \forall\,(k) \in (K) \qquad (III.21)$$

CH_4 production costs from natural gas are close to 0.32 €/m^3 (Eurostat, 2016). When the additional H_2 is provided externally to the system, the amount of CH_4 required by the process is calculated considering that

it is equi-molar to the consumed amount of CO_2, as in the following relation (Luu et al., 2015) (see Eq. III.22):

$$CH_4 + CO_2 + 2H_2 = 2CH_3OH \qquad \Delta H = 65.72\ kJ/mol \qquad (III.22)$$

When the additional H_2 is provided by steam, the amount of CH_4 required by the process is calculated according to the following global relation (see Eq. III.23):

$$3CH_4 + CO_2 + 2H_2O = 4CH_3OH \qquad \Delta H = 296.38\ kJ/mol \qquad (III.23)$$

CH_4 transportation costs via pipeline include the costs for compressors and pipeline, then operative and investment costs. According to Lochner (2011), a linearized expression for these costs (€/km) is the following (see Eq. III-24):

$$CH_4T = 150130 \cdot m_{CH4} \qquad (III.24)$$

where m_{CH4} is the annual capacity in billion cubic meter.

The costs for CH_3OH production via CH_4 dry reforming are 0.32 €/kg (Hernandez and Martin, 2016). The amount of produced CH_3OH can be obtained by the knowledge of CO_2 sent to the utilization section and according to Eqs. III.22 and III.23.

Regarding the additional H_2 required to balance properly the syngas composition, the knowledge of its amount is given by Eq. III.22, when H_2 is provided externally to the system. H_2 production cost via CH_4 steam reforming is 2.94 €/kg, while via H_2O electrolysis is 8.82 €/kg (Stadler, 2014). When H_2 is provided by steam reforming internally to the system, the required amount of steam is given by Eq. III.23. Steam production cost is fixed to 26 €/ton (Turton et al., 2009).

III.2.2.6 Objective function

The objective function of the developed mathematical model is defined by the following relation (see Eq. III.25):

$$\phi = \sum_{(i,j,k)} CC_{i,j,k} + TC_{i,j,k} + SC_k + MeOHP_k + H_2P_{i,j,k}/H_2OP_{i,j,k} + CH_4P_{i,j,k} + CH_4T_{i,j,k} \qquad (III.25)$$

where $CC_{i,j,k}$ are CO_2 capture and compression costs, $TC_{i,j,k}$ are CO_2 transportation costs, SC_k are CO_2 storage costs, $MeOHP_k$ are CH_3OH production costs, $H_2P_{,i,j,k}/H_2OP_{,i,j,k}$ are H_2/steam production costs, $CH_4P_{i,j,k}$ are CH_4 production costs, $CH_4T_{i,j,k}$ are CH_4 transportation costs.

A general scheme for the CCUS supply chain model is shown in Figure III.1.

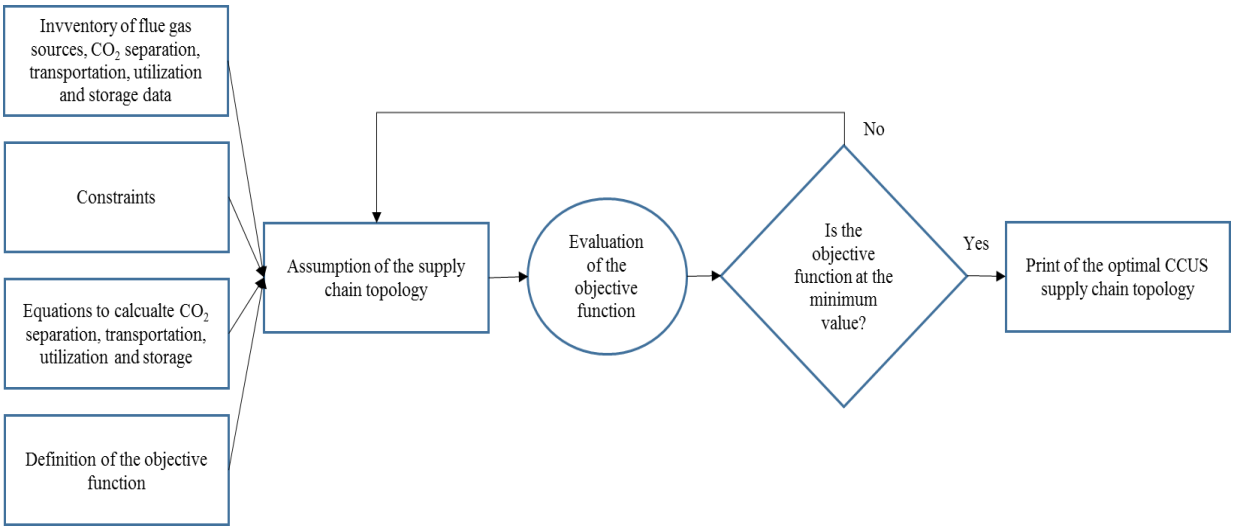

Figure III.3 Structure of the MILP supply chain model (Leonzio and Zondervan, 2020)

III.2.3 Case study

In this section, the data of CO_2 sources, storage and utilization sites in Germany are presented. An accurate analysis about CO_2 emissions in Germany is reported in Figure III.2

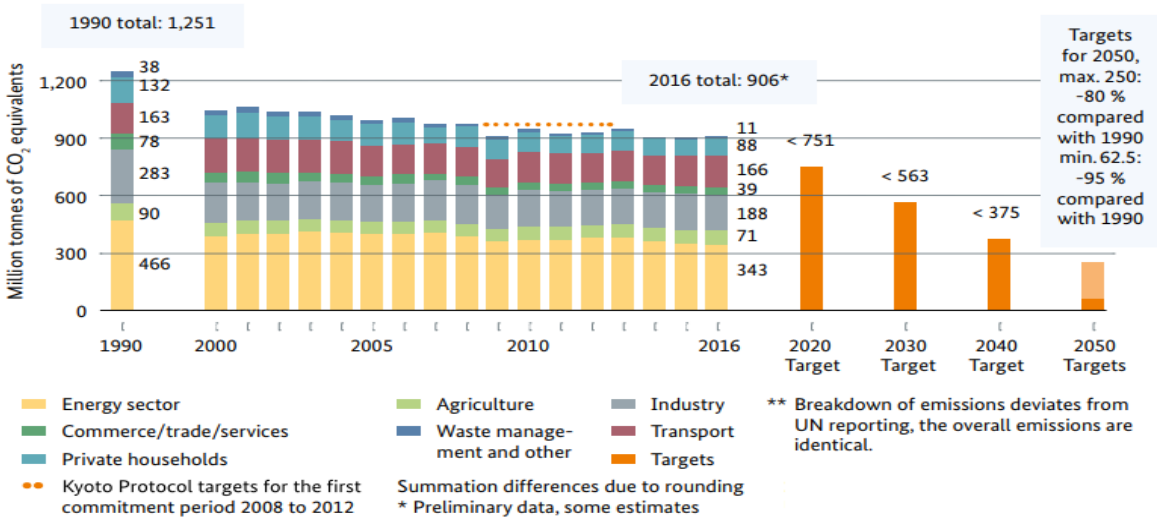

Figure III.2 CO_2 emissions evolution by sector in Germany (Federal Ministry for the Environment, 2017)

CO_2 emissions for the year 2016 are of 906 Mton and according to the environmental protection policy they should be reduced to a value lower than 751 Mton in 2020. Then, a minimum target for CO_2 emissions reduction is set to 160 MtonCO_2/year to design and optimize the CCUS supply chain.

Moreover, the ten regions with higher CO_2 emissions are selected, as reported in Table III.2. Northrhine-Westphalia (307.3 MtCO_2/year), Bavaria (80 MtonCO_2/year), Baden-Württemberg (69.3 MtonCO_2/year),

Lower Saxony (69 MtonCO_2/year), Brandenburg (55 MtonCO_2/year), Saxony (48.7 MtonCO_2/year), Hesse (42.9 MtonCO_2/year), Saxony-Anhalt (27.4 MtonCO_2/year), Berlin (19.8 MtonCO_2/year), Saarland (19.1 MtonCO_2/year) are the chosen German regions with the respective value of CO_2 stationary emissions (Federal Ministry for the Environment, 2014). The nodes are located at the capital cities of each region: Düsseldorf, Munich, Stuttgart, Hannover, Potsdam, Dresden, Wiesbaden, Magdeburg, Berlin, Saarbrucken respectively for Northrhine-Westphalia, Bavaria, Baden-Württemberg, Lower Saxony, Brandenburg, Saxony, Hessen, Saxony-Anhalt, Berlin, Saarland.

It is supposed that power plants, cement industries and steel and iron industries are the main source of CO_2. In particular, power plants generating flue gases are present in Baden-Württemberg, Lower Saxony, Brandenburg, Hessen, Berlin (Energy Charts, 2019; Source watch, 2019). Cement industries are present in Saarland and Saxony (Vdz, 2019), while iron and steel industries are located in Northrhine-Westphalia, Bavaria and Saxony-Anhalt (Twinnin, 2019). CO_2 emission levels are set for each flue gas according to (Zhang et al., 2018).

Table III.3 The main sources of CO_2 emissions in Germany (Leonzio et al.,2019a)

German regions	Node	Flue gas type	CO_2 emissions (Mton/year)	CO_2 in flue gas (mol%)	Flue gas (mol/s)
Northrhine-Westphalia	Dusseldorf	Iron & Steel	307.3	17	$1.30 \cdot 10^6$
Bavaria	Munich	Iron & Steel	80	18	$3.2 \cdot 10^5$
Baden-Württemberg	Stuttgart	Power Plant	69.3	4	$1.25 \cdot 10^6$
Lower Saxony	Hannover	Power Plant	69	14	$3.55 \cdot 10^5$
Brandenburg	Potsdam	Power Plant	55	13	$3.05 \cdot 10^5$
Saxony	Dresda	Cement	48.7	21	$1.67 \cdot 10^5$
Hessen	Wiesbaden	Power Plant	42.9	13	$2.38 \cdot 10^5$
Saxony-Anhalt	Magdeburg	Iron & Steel	27.4	18	$1.10 \cdot 10^5$
Berlin	Berlin	Power Plant	19.8	15	$9.51 \cdot 10^4$
Saarland	Saarbrucken	Cement	19.1	22	$6.26 \cdot 10^4$

Altmark is chosen as centralized storage site. In geological terms, Altmark is located at the North Germany Basin and contains reservoirs suitable for CO_2 storage (Rebscher et al., 2006). It is in the federal state of Sachsen-Anhalt. The reservoir rocks are located at a depth of 3 km, with an overall storage capacity of 508 MtonCO_2 and maximum injection capacity of a well of 912.5 KtonCO_2/year (Ochoa Bique, 2018). Due to the great storage capacity, only one storage site is considered for the model. In addition, a centralized CO_2 storage system may offer economic and technical advantages, easily understandable.

Altmark is also the second largest natural gas field in Europe. For this reason, it is chosen as the main source of CH_4, needed for the dry reforming reaction (Roehrl and Toth, 2009).

Leuna has an existing CH_3OH plant with a capacity of 660 ton/year: for this reason, it is chosen as CH_3OH production site through CH_4 dry reforming (ICIS, 2019). Only one CH_3OH production site is selected in the CCUS supply chain, because it is supposed that the site can satisfy the national demand (then with a high or infinity capacity). In fact, the first aim of this model is to verify that producing a defined amount of CH_3OH and storing a defined amount of CO_2, from a captured amount of CO_2, it is possible to achieve the target set by the environmental policy. Distances between stationary CO_2 source, utilization and storage sites are provided in Table III.3 (Distance, 2019). The distance between Leuna and Altmark is 155 km (Distance, 2019).

Table III.4 Distance between CO_2 source, utilization and storage sites

German Sources		Leuna (km)	Altmark (km)
Northrhine-Westphalia	Düsseldorf	439.6	468.3
Bavaria	Munich	409.7	587.3
Baden-Württemberg	Stuttgart	457.4	576.5
Lower Saxony	Hannover	196	194.9
Brandenburg	Potsdam	165.5	116.2
Saxony	Dresda	151.3	292.8
Hesse	Wiesbaden	397.2	497.1
Saxony-anhalt	Magdeburg	133.6	65.3
Berlin	Berlin	194.5	125.3
Saarland	Saarbrücken	549.9	649.8

In the carbon capture section of the CCUS supply chain, different technologies/materials are used to capture at most 90% of CO_2 from flue gas. For the absorption technology, MEA solution (30%wt), because it is the most used solvent, and the ionic liquid, as 1-butyl-3-methylimidazolium acetate ([bmim][Ac]), due to its energy and capture efficiency, are used (Rochelle et al., 2011; Nguyen and Zondervan, 2018). For the membrane technology, the fixed-site-carrier (FSC) polyvinyl amine (PVAm) material is chosen, because of its high permeability to CO_2 (Hägg and Lindbråthen, 2005). For the pressure swing adsorption (PSA) and vacuum swing adsorption (VSA) technologies, the 13X zeolite is selected as sorption material, because it is the most used and experimentally validated (Xiao et al., 2008).

III.3 Results and discussion

In this section, the results for the proposed CCUS framework for Germany are presented. If the primary goal is to achieve an environmental benefit reducing the overall CO_2 emission up to a certain level, the

design of CCUS is developed minimizing the costs, setting the desired level of CO_2 reduction as a constraint. In the analyzed supply chain, 10 CO_2 sources, 5 technologies for CO_2 capture and compression, 1 CO_2 storage site and 1 CO_2 utilization site are considered.

III.3.1 Results of CCUS supply chain with the addition of hydrogen produced externally to the system by steam reforming (Case A)

The model has 532 (100 Integer) variables and 566 constraints. The CPLEX 12.7.1 is the solver that is selected in AIMMS. Typical CPU times are less than a second and solutions are found with 59 iterations. The computer processor is 2.5 GHz while the memory is 4 GB.

Table III.4 shows the amount of CO_2 that, from the selected sources, is sent to the storage and utilization section.

Table III.5 Topology of the supply chain model for German regions when H_2 is produced externally to the system by steam reforming (Case A) (Leonzio et al., 2019b)

CO_2 source	**Capture technology**	**CO_2 amount (Mton/year)**
	To storage	
Magdeburg	MEA absorption	20.3
	To utilization	
Dusseldorf	MEA absorption	277
Munich	MEA absorption	2.73

Considering also CO_2 emissions due to the H_2 production by steam reforming, the supply chain treats 878 Mton/year of CO_2 emissions altogether: 20.3 Mton/year of CO_2 are sent to the storage site, while 279.73 Mton/year of CO_2 are sent to the utilization site. Magdeburg is the selected CO_2 source capturing CO_2 through the MEA absorption, to send it to the storage site. Dusseldorf and Munich are the selected CO_2 sources capturing CO_2 through the MEA absorption to send it to the utilization section for CH_3OH production. Also, it results that, for flue gas flow rates higher than 10 kmol/s (then high flue gas flow rates), the absorption technology, in particular MEA absorption, is preferred over other capture technologies, due to a lower cost at relative low CO_2 compositions. In fact, important factors in the capture and compression costs are CO_2 composition and flue gas flow rate. Table III.5 shows the optimized costs of the CCUS system in Germany, when H_2 is produced externally to the system by steam reforming. The total supply chain costs are equal to 262 billion€/year. CO_2 capture and compression costs are 3.58 billion€/year, 1.37% of the total costs. CH_4 transportation costs have an influence on the total costs of 1.4%, with a value of 3.69 billion€/year. CH_3OH, H_2 and CH_4 production costs have a higher influence on the total costs, respectively of 50%, 28.5% and 19%.

Table III.6 Optimized cost of CCUS supply chain when H_2 is produced externally to the system by steam reforming (Case A) (Leonzio et al., 2019b)

CO_2 capture and compression costs	3.58	billion€/year
CO_2 transportation costs	5.92	million€/year
CO_2 storage costs	153	million€/year
MeOH production costs	130	billion€/year
CH_4 provision costs	49.7	billion€/year
CH_4 transportation costs	3.3.69	billion€/year
H_2 provision costs	74.6	billion€/year
Supply chain total costs	262	billion€/year

The storage costs are equal to 153 million€/year. These costs consider only the amount of CO_2 and not the well characteristics, even if they are functions of the depth of well and the capacity of injected CO_2. The total CO_2 transportation costs to the storage and utilization sites are equal to 5.92 million€/year. The assumption of having the capture plants in the same location of source plants allows to neglect the transportation costs of flue gas from sources to capture sites in the economic analysis. According to Knoope et al. (2013) the pipeline cost is mostly underestimated.

The amount of required CH_4 and H_2 are respectively of 102 Mton/year and 25.4 Mton/year. On the other hand, 407 Mton/year of CH_3OH are produced in the considered CCUS supply chain scheme.

III.3.2 Results of CCUS supply chain with the addition of hydrogen produced externally to the system by water electrolysis (Case B)

The developed model has 531 (100 Integer) variables and 565 constraints. Also in this case, CPLEX 12.7.1 is the solver that is selected in AIMMS. Typical CPU times are less than a second and solutions are found with 39 iterations. The same computer processor as that of the previous case is used.

The topology of the CCUS supply chain obtained by optimizing the mathematical model is shown in Table III.6, when the additional H_2 is produced externally to the system by H_2O electrolysis, utilizing renewable energy power. The total treated CO_2 emissions are 739 Mton/year: 20.3 Mton/year of CO_2 are sent to the storage while 140 Mton/year of CO_2 are used to produce CH_3OH.

Table III.7 Results of the supply chain model for German regions when H_2 is produced externally to the system by H_2O electrolysis utilizing renewable energy power (Case B) (Leonzio et al., 2019b)

CO_2 source	**Capture technology**	**CO_2 amount (Mton/year)**
	To storage	
Magdeburg	MEA absorption	20.3
	To utilization	
Dusseldorf	MEA absorption	140

As shown in Table III.6, Magdeburg is selected as CO_2 source for the storage section, while Dusseldorf is selected for the utilization section. For both sections, the same capture technology is selected and it is MEA absorption, as according to the considerations provided previously. Table III.7 shows the costs of the supply chain: the total value is 207 billion€/year. CH_3OH, H_2 and CH_4 production costs contribute to the total costs 31.4%, 54% and 12%, respectively. In fact, CH_3OH, H_2 and CH_4 production costs are respectively of 65.1 billion€/year, 112 billion€/year and 24.8 billion€/year. A lower influence is ascribed to other terms. CO_2 capture and compression costs, CO_2 transportation costs, CO_2 storage costs and CH_4 transportation costs are respectively of 3.34 billion€/year, 3.16 million€/year, 153 million€/year and 1.85 billion€/year.

Table III.8 Optimized cost of the CCUS supply chain when H_2 is produced externally to the system by H_2O electrolysis utilizing renewable energy power (Case B) (Leonzio et al., 2019b)

CO_2 capture and compression costs	3.34	billion€/year
CO_2 transportation costs	3.16	million€/year
CO_2 storage costs	153	million€/year
MeOH production costs	65.1	billion€/year
CH_4 provision costs	24.8	billion€/year
CH_4 transportation costs	1.85	billion€/year
H_2 provision costs	112	billion€/year
Supply chain total costs	207	billion€/year

In this CCUS supply chain, the amount of required CH_4 and H_2 are respectively of 50.9 Mton/year and 12.7 Mton/year. Also, 203 Mton/year of CH_3OH are produced.

III.3.3 Results of CCUS supply chain with the addition of hydrogen produced internally to the system by steam reforming (Case C)

As suggested by AIMMS, the developed mathematical model has 531 (100 Integer) variables and 565 constraints. CPLEX 12.7.1 is the selected solver. Typical CPU times are less than a second and solutions are found with 39 iterations. Regarding the computer processor, the same as that of previous cases is used. Table III.8 presents the topology of the CCUS supply chain when the addition of H_2, to correct syngas composition resulting from dry reforming reaction, is provided through a steam reforming process internally to the system, according to the global Eq. III.23. It is possible to see that, results are the same as that of the supply chain considered under the Case B. In fact, the total treated CO_2 emissions are 739 Mton/year: 20.3 Mton/year are sent to the storage, while 140 Mton/year of CO_2 are sent to the utilization. Magdeburg is the selected CO_2 source, with MEA absorption capture technology, for the storage section, while Dusseldorf is the selected CO_2 source, with MEA absorption capture technology as well, for the utilization section.

Table III.9 Results of the supply chain model for German regions when H_2 is produced internally to the system by steam reforming (Case C) (Leonzio et al., 2019b)

CO_2 source	**Capture technology**	**CO_2 amount (Mton/year)**
	To storage	
Magdeburg	MEA absorption	20.3
	To utilization	
Dusseldorf	MEA absorption	140

Table III.9 shows the costs related to the CCUS supply chain considered under the Case C.

Table III.10 Optimized costs of the CCUS supply chain with H_2 produced internally to the system by steam reforming (Case C) (Leonzio et al., 2019b)

CO_2 capture and compression costs	3.34	billion€/year
CO_2 transportation costs	3.16	million€/year
CO_2 storage costs	153	million€/year
MeOH production costs	130	billion€/year
CH_4 provision costs	74.5	billion€/year
CH_4 transportation costs	5.54	billion€/year
H_2O provision costs	2.97	billion€/year
Supply chain total costs	217	billion€/year

The total costs are 217 billion€/year: CH_4 production costs and CH_3OH production costs have a higher influence. In fact, CH_4 production costs (74.5 billion€/year) contribute 34% of the total costs while CH_3OH production costs (130 billion€/year) contribute 60% of the total costs. Other costs have a less influence on the total costs, as illustrated in Table III.9.

The mathematical model calculates also the required CH_4 and steam flow rates. In fact, these are respectively of 153 Mton/year and 114 Mton/year. 407 Mton/year of CH_3OH are produced.

III.3.4 Comparison among the different cases analyzed above

Table III.10 shows the comparison among the different cases analyzed before (Case A, B and C). The comparison between the supply chain with H_2 provided externally by means of CH_4 steam reforming (Case A) and the supply chain with H_2 produced internally to the system, also by steam reforming (Case C), shows that an equal amount of CH_3OH is produced (407 Mton/year). However, a higher amount of CH_4 is consumed in the Case C, because a higher amount of CH_4 enters inside the supply chain to ensure the steam reforming process.

As also explained in the previous section, providing H_2 as in the Case A, additional 140 Mton/year of CO_2 are emitted due to the steam reforming reaction (total treated CO_2 emissions are 878 Mton/year). Then, in order to achieve the minimum target for CO_2 emissions reduction, 300 Mton/year of CO_2 are captured and sent to the utilization or storage site (in particular, 279 Mton/year of CO_2 are used). On the other hand, in the Case B and Case C, the addition of H_2 to syngas does not imply further CO_2 emissions externally to the system: 160 Mton/year of CO_2 are captured, to satisfy the target of CO_2 emissions reduction. As shown in Tables III.6 and III.8, in Case B and Case C, the total treated CO_2 emissions are 739 Mton/year and 140 Mton/year of CO_2 are used for CH_3OH production.

Table III.11 Comparison among Cases A (H_2 externally by reforming), Case B (H_2 externally by electrolysis) and Case C (H_2 internally by reforming) of the CCUS supply chain in Germany (Leonzio et al., 2019b)

H_2 source	Externally by reforming	Externally by electrolysis	Internally by reforming
CCUS supply chain cost (billion€/year)	262	207	217
MeOH production (Mton/year)	407	203	407
CH_4 (Mton/year)	102	50.9	153
H_2 (Mton/year)	25.4	12.7	
H_2O (Mton/year)			114
Total CO_2 emissions (Mton/year)	878	739	739
Additional CO_2 emissions (Mton/year)	140	0	0
Total used CO_2 (Mton/year)	279	140	140
Net reduction of CO_2 emissions(Mton/year)*	160	160	160
MeOH production cost with incentives and carbon tax (€/ton)	340	340	340
Carbon tax (€/ton)	80	80	80
Economic incentives MeOH (€/kWh)	0.044	0.115	0.029
Economic incentives MeOH (€/tonMeOH)	245	615	161
Total required incentives (billion€/year)	124	138	78.3
GW ($kgCO_{2\text{-}eq}$/0.032kgMeOH)	0.01332	0.00732	0.01215

* Without considering additional CO_2 emitted to run the supply chain

It should be mentioned here that, although the amount of CO_2 utilized is the same in both Cases B and C, the global reaction path is different, as illustrated by Eqs. III.22 and III.23. For Case B, the Eq. III.22 shows that the mole ratio between the utilized CO_2 and produced CH_3OH, CO_2:CH_3OH, is equal to 0.5. For Case C instead, according to the Eq. III.23 that ratio is equal to 0.25, i.e. more CH_3OH has to be produced to satisfy the same emission target.

As a result, the Case B (utilization of green H_2) is the most favorable, because allows to consume a higher amount of CO_2 for the same CH_3OH production and renewable H_2, also with a lower environmental impact. The major goal of the supply chain is in fact to reduce CO_2 emissions.

Then, the contribution to the global warming is calculated for Cases A, B and C and it is respectively of 0.01332, 0.00732 and 0.01215 $kgCO_{2\text{-}eq}$/0.032 kgMeOH. It is evident that the lowest environmental impact is provided by the Case B. That Case is also characterized by the lowest total costs (207 billion€/year vs 262 billion€/year for the Case A and 271 billion€/year for the Case C). However, the lowest amount of CH_3OH is obtained in the Case B (203 Mton/year vs 407 Mton/year in the other cases) and the cost of green H_2 is high, so that the highest economic incentives are required for CH_3OH production (615 €/ton vs 245 €/ton for the Case A and 161 €/ton for the Case C) in order to keep its production cost at the level of 340 €/ton, acceptable to the market. The value of carbon tax is assumed to be the same in each case (80 €/ton). Economic incentives to the production of CH_3OH and carbon tax are required to keep the CH_3OH production cost below its selling price of 408 €/ton. Setting the value of carbon tax at 80 €/ton, economic incentives are fixed in order to have a value for CH_3OH production cost of 340 €/ton in all cases. It is found that for Case A, B and C total incentives (due to the CH_3OH production and carbon tax) should be of 124 billion€/ton, 138 billion€/ton and 78.3 billion€/ton, respectively. Another important point, to be considered, is the amount of produced CH_3OH. For Case A and C, 407 Mton/year of CH_3OH are produced, as already shown. For Case B, a lower amount of 203 Mton/year is calculated. Considering that the yearly CH_3OH demand in Germany is 940 kton/year, this suggests that also from this point of view the Case B is preferred. Even compared to the current global CH_3OH demand, the production of the supply chain is very high. However, in the coming decades the need for CH_3OH is expected to grow strongly when new sectors for its utilization are considered, for instance transportation fuel, in order to progressively replace fossil energy sources. Figure III.3 shows the global CH_3OH demand over the last ten years and in the next future (IHS, 2014).

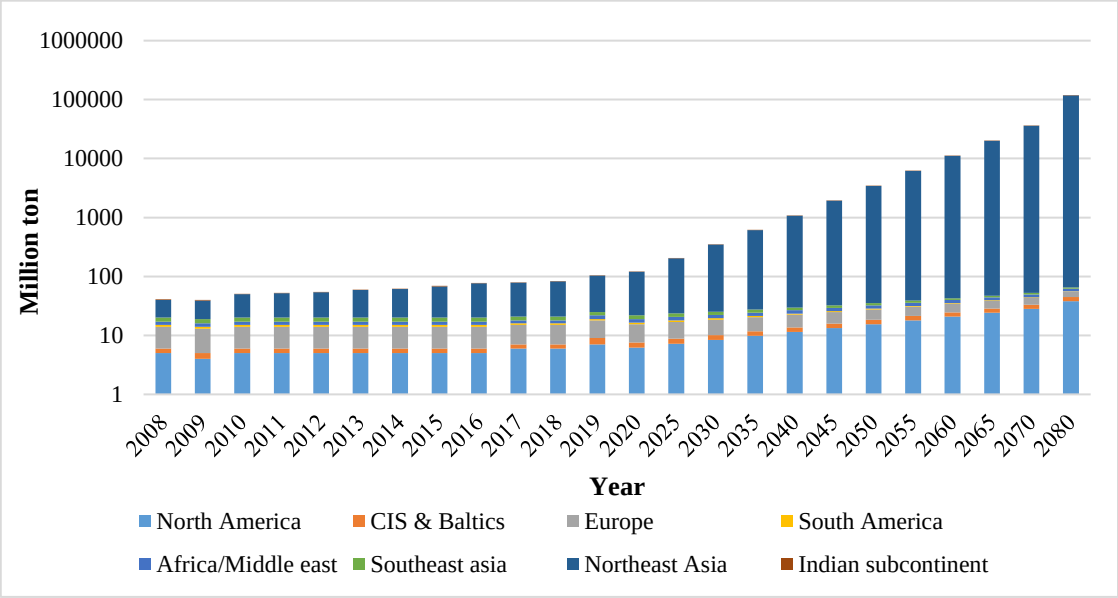

Figure III.3 Actual and forecasted global CH_3OH demand (IHS, 2014)

The current demand for CH_3OH is approximately 100 Mton/year. Southeast Asia is the largest market for CH_3OH. CH_3OH is especially used for the production of formaldehyde (32%) but also in gasoline blending (11%), MTBE (10%) and acetic acid (11%), then it is an essential commodity. The prediction in Figure III.2 suggests that in the next decade 2025-2035 the global need for CH_3OH will approximately increase from 180 to 580 Mton/year. A German CCUS supply chain as that designed in this research may become a global leader in supplying CH_3OH.

A sensitivity analysis is also carried out to evaluate the influence of carbon tax and economic incentives on the CH_3OH production cost for the best case, when H_2 is produced by H_2O electrolysis, exploiting renewable energy power.

An increase of these parameters of 5% is imposed, one by one, and the results are reported in Table III.11. A comparison with the base case, in which the CH_3OH production cost is equal to 340 €/ton is carried out in the residue term. The residue term is defined as the difference between the value obtained in the sensitivity analysis and the CH_3OH production cost in the base case. Results suggest that economic incentives have a higher effect on the CH_3OH production cost. An increase equal to 5% of economic incentives can reduce by about 10% the CH_3OH production cost, making the supply chain more competitive with other technologies. Carbon tax has a lower effect on the analyzed response, determining a decrease of about 1% on the CH_3OH production cost.

Table III.12 Sensitivity analysis for CH_3OH production cost (Case B is considered) (Leonzio et al., 2019b)

Carbon tax	Economic incentives	MeOH production cost (€/ton)	Residue (€/ton)
5%		337	3.28
	5%	309	30.9

Summarizing, to have an attractive dry reforming process for CH_3OH production, Germany needs to produce an amount of CH_3OH greater than 940 kton/year (national demand) and export it.

III.4 Conclusions

In this chapter, an innovative MILP model is developed to suggest the optimal design of a CCUS supply chain in Germany. The model minimizes the total costs, reducing a defined amount of CO_2 emissions in order to achieve the target set by the environmental policy. As the innovative aspect, the captured CO_2 is used to produce CH_3OH via CH_4 dry reforming.

Three different cases are considered, which differ among each other for the H_2 source needed to adjust properly the H_2:CO_2 ratio needed by the methanol reaction. In one case, H_2 is provided externally to the system by steam reforming (additional CO_2 released to the environment is taken into account to preserve the net target for CO_2 emissions reduction). In the second case, H_2 is provide by H_2O electrolysis utilizing renewable energy power. Finally, in the third case, H_2 is provided internally to the system by steam reforming properly combined to dry reforming.

Results show that MEA absorption technology is the preferred capture system for high flow rate of flue gas.

Also, among the considered cases, it also results that providing green H_2 (produced by H_2O electrolysis utilizing renewable power sources) assures a lower environmental impact in terms of global warming (0.0073 $kgCO_2eq$/0.032 kgMeOH), as expected, even if a lower relative amount of CH_3OH is produced. However, in this case, a higher amount of CO_2 is used to produce the same amount of CH_3OH. In any case, by producing CH_3OH through CH_4 dry reforming Germany will have an important role inside the world CH_3OH market for the next future (about 2025-2035), exporting the amount exceeding the national demand. When H_2 is provided by H_2O electrolysis, the CCUS supply chain costs 207 billion€/year and produces 203 Mton/year of CH_3OH. If carbon tax and economic incentives are included, the process can be economically feasible, with a CH_3OH production cost fixed at 340 €/ton.

Reference

Bringezu, S., 2014. Carbon recycling for renewable materials and energy supply: recent trends, long-Term options, and challenges for research and development. J. Ind. Ecol. 18, 327–340.

Broek, M.V.D., Brederode, E., Ramírez, A., Kramers, L., Kuip, M.V.D., Wildenborg, T., Turkenburg, W., Faaij, A., 2010. Environmental modelling & software designing a cost-effective CO2 storage infrastructure using a GIS based linear optimization energy model. Environ. Modell. Softw. 25 (12), 1754–1768,

Bruhn, T., Naims, H., Olfe-Kräutlein, B., 2016. Separating the debate on CO2 utilisation from carbon capture and storage. Environmental Science & Policy 60 38–43.

Dahowski, R., Dooley, J., Davidson, C., Bachu, S., Gupta, N., 2004. A CO2 Storage Supply Curve for North America, Proceedings of the 7. international conference on greenhouse gas control technologies.

Distance, 2019. Available at: http://it.distance.to

Dou, J., Zhang, R., Hao, X., Bao, Z., Wu, T., Wang, B., Yu, F. 2019. Sandwiched SiO2@Ni@ZrO2 as a coke resistant nanocatalyst for dry reforming of methane. Applied Catalysis B: Environmental 254 (2019) 612–623.

Egmond, S., Hekkert, M., 2012. Argument map for carbon capture and storage. Int. J. Greenh. Gas Control 11, 148–159.

Energy Charts, 2019, Available at: https://www.energy-charts.de/osm.htm

Eurostata, 2016. https://www.cbs.nl/en-gb/news/2016/21/gas-price-above-electricity-price-below-eu-average

Federal Ministry for the Environment, Nature conservation, Building and Nuclear safety. The German Government's Climate Action Programme 2020 Cabinet decision of 3 December 2014.

Federal Ministry for the Environment, Nature conservation, Building and Nuclear safety. Climate Action in Figures Facts, Trends and Incentives for German Climate Policy 2017 edition

Hägg, M.B., Lindbråthen, A., 2005. CO2capture from natural gas fired power plants by usingmembrane technology. Ind Eng Chem Res., 44(20):7668–75

Hasan, M.M.F., Boukouvala, F., First, E.L., Floudas, C.A., 2014. Nationwide, regional, and statewide CO2 capture, utilization, and sequestration supply chain network optimization. Ind Eng Chem Res 53, (18), 7489–7506.

Hasan, M.M.F., Baliban, R.C., Elia, J.A., Floudas, C.A. 2012a. Modeling, Simulation, and Optimization of Postcombustion CO2 Capture for Variable Feed Concentration and Flow Rate. 1. Chemical Absorption and Membrane Processes. Ind. Eng. Chem. Res. 51, 15642−15664

Hasan, M.M.F., Baliban, R.C., Elia, J.A., Floudas, C.A. 2012b. Modeling, Simulation, and Optimization of Postcombustion CO2 Capture for Variable Feed Concentration and Flow Rate. 2. Pressure Swing Adsorption and Vacuum Swing Adsorption Processes. Ind. Eng. Chem. Res. 2012b, 51, 15665−15682

Hendriks, C.A., Carbon Dioxide Removal from coal-Fired power plant. In department of science, technology, and society. Utrecht University. 1994: Utrecht, Netherlands.

Hernández, B., Martin, M., Optimal Composition of Biogas for Methanol Production Via Dry Reforming, 2016 AIChE Annual Meeting: Proceedings: Computing and Systems Technology Division: Process Design II, San Francisco

ICIS, 2019.Available at: https://www.icis.com/explore/resources/news/2017/07/28/10128588/germany-s-leuna-methanol-plant-running-well-after-maintenance/

IHS, Global Methanol Report 2014. London, Information Handling Services

Joshi, P.B. 2014. Carbon dioxide utilization: a comprehensive review. Int. J. Chem. Sci.: 12 (4) 1208-1220.

Kalyanarengan Ravi, N., Van Sint Annaland, M., Fransoo, J.C., Grievink, J., Zondervan, E., 2017. Development and implementation of supply chain optimization framework for CO2 capture and storage in the Netherlands. Computer Chemical Engineering 102, 40–51.

Knoope, M.M.J., Ramrez, A., Faaij, A.P.C., 2013. A state of the art review of techno-economic model predicting the costs of CO2 pipeline transport. Int. J. Greenh. Gas Control 16, 241-270.

Leonzio, G., Zondervan, E. 2020. Analysis and optimization of carbon supply chains integrated to a power to gas process in Italy. Journal of Cleaner Production. Under review.

Leonzio, G., Foscolo, P.U., Zondervan, E. 2019a. Sustainable utilization and storage of carbon dioxide: Analysis and design of an innovative supply chain. Computers and Chemical Engineering 131 106569

Leonzio, G., Foscolo, P.U., Zondervan, E. 2019b. An outlook towards 2030: Optimization and design of a CCUS supply chain in Germany. Computers and Chemical Engineering 125 499–513.

Lochner, S., 2011. The Economics of Natural Gas Infrastructure Investments Theory and Model-based Analysis for Europe. Inauguraldissertation zur Erlangung des Doktorgrades der Wirtschafts- und Sozialwissenschaftlichen Fakultät der Universität zu Köln,

Luu, M.T., Milani, D., Bahadori, A., Abbas, A., 2015. A comparative study of CO2 utilization in methanol synthesis with various syngas production technologies. Journal of CO2 Utilization 12, 62–76

Nguyen, T.B.H., Zondervan, E. 2018. Development and comparison of two novel process designs for the selective capture of CO2 from different sources, ACS Sustainable Chemistry & Engineering, 6 (4), 4845-4853.

Ochoa Bique, A., Nguyen, T.B.H., Leonzio, G., Galanopoulos, C., Zondervan, E. 2018. Integration of carbon dioxide and hydrogen supply chains, Computer Aided Chemical Engineering, 43, 1413-1418.

Rebscher, D., May, F., Oldenburg, C.M., 2006. Sequestration of CO2 in the Altmark natural gas field, Germany: Mobility control to extend enhanced gas recovery, Paper LBNL 60157, 2006, Lawrence Berkeley National Laboratory, University of California.

Rochelle, G., Chen, E., Freeman, S., Van Wagener, D., Xu, Q., Voice, A., 2011. Aqueous piperazine asthe new standard for CO2capture technology. Chem Eng J. 171(3):725–33.

Roehrl, A., Toth, F., A critical comparison of geological storage of carbon dioxide and nuclear waste in Germany: status, issues, and policy implications, 8th Conference on Applied Infrastructure Research (INFRADAY), Berlin, Germany, 9-10 October 2009.

Serpa, J., Morbee, J., Tzimas, E., 2011. Technical and Economic Characteristics of a CO2 Transmission Pipeline Infrastructure, JRC62502 1-43.

Source watch, 2019. Available at: https://www.sourcewatch.org/index.php/GKH_Hannover_power_station

Stadler, P. 2014. Cost evaluation of large scale hydrogen production for the aviation industry, Master semester project, Ecole Polytechnique Federal de Lausanne.

Turton, R., Baile, R.C., Whiting, W.B., Shaeiwitz, J.A., Analysis, Synthesis, and Design of Chemical Processes, Prentice Hall PTR, 2009.

Twinning, 2019. Available at: http://www.twinning-israel.info

Vdz, 2019. Available at: https://www.vdz-online.de/en/cement-industry/cement-sector/cementmarkets/

Wang, F., Wang, Y., Zhang, L., Zhu, J., Han, B., Fan, W., Xu, L., Yu, H., Cai, W., Li, Z., Deng, Z., Shi, W. 2019. Performance enhancement of methane dry reforming reaction for syngas production over Ir/Ce0.9La0.1O2-nanorods catalysts. Catalysis today, In proof.

Xiao, D., Xu, S., Brownbill, N.J., Paul, S., Chen, L.H., Pawsey, S., Aussenac, F., Su, B.L., Han, X., Bao, X., Liuad Z., and Blanc, F., 2018. Fast detection and structural identification of carbocations on zeolites by dynamic nuclear polarization enhanced solid-state NMR, Chem. Sci., 2018, 9, 8184–8193.

Zhang, S., Liu, L., Zhang, L., Zhuang, Y., Du. J. 2018. An optimization model for carbon capture utilization and storage supply chain: A case study in Northeas

Nomenclature

Indices

i = carbon dioxide source

j = carbon dioxide capture system

k = carbon dioxide storage site and complementary utilization section

Abbreviations

AIMMS = advanced interactive multidimensional modeling system

CC = carbon dioxide capture and compression costs [€/year]

CCR = capital cost recovery

CCUS = carbon capture utilization and storage

CCU = carbon capture utilization

CDC = flue gas dehydration costs [€/year]

CH_4P = methane production costs [€/year]

CH_4T = methane transportation costs [€/year]

CIC = carbon dioxide capture and compression investment costs [€/year]

COC = carbon dioxide capture and compression operative costs [€/year]

CO_2-EOR = CO_2enhanced oil recovery

GHG = greenhouse gas

F_i = flue gas flow rate from source i [mol/s]

H_2P/H_2OP = hydrogen/steam production cost [€/year]

IC = maximum injection capacity per well [ton/year]

IL = ionic liquid

MEA = monoethanolamine

MeOHP = methanol production cost [€/year]

MILP = mixed integer linear programming

N^{build}_{well} = number of well

PSA = pressure swing adsorption

SC = carbon dioxide storage costs [€/year]

SIC = carbon dioxide storage investment costs [€]

SOC = carbon dioxide storage operative costs [€/year]

TC = carbon dioxide transportation costs [€/year]

TH = time horizon

TIC = carbon dioxide transportation investment costs [M€]

TOC = carbon dioxide transportation operative costs [M€/year]

VSA = vacuum swing adsorption

Parameters

b = parameter in SIC [M€]

C_k^{max} = maximum storage capacity for storage site k [ton]

CR^{min} = minimum target for carbon dioxide reduction [ton/year]

CS_i = carbon dioxide emission from each source i [ton/year]

$D_{i,k}/d_{i,k}$ = distance from sources i to storage/utilization site k [km]

d_{well} = depth of well [km]

F_i/F = flue gas flow rate from each source i [mol/s]

F_t = terrestrial factor

m = parameter in SIC [M€/km], CIC and COC

$MeOH^{dem}$ = national methanol demand [ton/year]

n = parameter in CIC and COC

x_{CO2} = carbon dioxide molar fraction

X_m = parameter equal to 1 if carbon dioxide is transported to methanol production site

XS_i = carbon dioxide composition in the flue gas emission from source i [mol%]

XL_i = lowest carbon dioxide composition processing limit for capture plant j [mol%]

XH_i = highest carbon dioxide composition processing limit for capture plant j [mol%]

Variables

Binary

$X_{i,j,k}$ = 1 if carbon dioxide is captured from source i with technology j and sent to storage site k, otherwise 0

$Y_{i,j,k}$ = 1 if carbon dioxide is capture from source i with technology j and sent to storage/utilization site k, otherwise 0

Continuous

$MR_{i,j,k}$ =fraction of captured carbon dioxide from source i with technology j sent to utilization site k

$FR_{i,j,k}$ = fraction of captured carbon dioxide from source i with technology j sent to storage site k

Greek letters

α = parameter in CIC and COC

α_t = parameter in TIC

β = parameter in CIC and COC

β_t = parameter in TIC

γ = parameter in CIC and COC

Chapter IV

Development of a CCUS supply chain for Germany-Part II

In the previous CCUS supply chain suggested for Germany, an amount of methanol greater than the national demand is produced. To avoid the export of a great amount of methanol, other compounds may be produced inside the system, with the same reduction target of carbon dioxide emissions. In this chapter, an innovative and alternative CCUS supply chain is proposed for Germany. In fact, the production of methanol, concrete by curing, wheat, lignin for polyethylene, calcium carbonate, urea, polyurethane and concrete by red mud is considered from carbon dioxide captured. The proposed framework is modelled as a Mixed Integer Linear Programming model, based on that described at the beginning of Chapter III, and optimized minimizing the total costs. Results show that for the optimal supply chain the total costs are 97.9 billion €/year with a net present value of 675 billion € and a payback period of 2.71 years: the economic profitability may be ensured only by carbon tax. A Monte Carlo simulation is carried out to evaluate the uncertainty regarding the selling price of carbon dioxide based products and their national demand.

IV.1 Introduction

As already discussed, Germany is the country with the highest greenhouse gas (GHG) emissions in Europe. Moreover, it is shown that, carbon capture utilization and storage (CCUS) supply chains can be a valid solution to reduce emissions and to achieve the target set by the environmental policy. With these considerations, in the previous chapter, a CCUS supply chain producing methanol (CH_3OH) via methane (CH_4) dry reforming is proposed. However, an amount of CH_3OH greater than the national demand is produced, in order to achieve the minimum target of carbon dioxide (CO_2) emissions reduction.

In order to reduce the amount of produced CH_3OH, the captured CO_2 can be used to produce many other compounds. In the literature, as discussed in the introduction of this Thesis, different pathways are studied to valorize CO_2 as a waste and to produce then other compounds. In particular, Patricio et al. (2017) provide an estimate of the potential CO_2 utilization in Europe. It is reported that, the potential use of CO_2 in concrete curing is 22.5 Mtpa, in horticulture 22 Mtpa, in lignin 8.4 Mtpa, in propylene polymer 8.3 Mtpa, in mineral carbonation 5.3 Mtpa, in urea fertilizer 3.9 Mtpa, in methanol 2 Mtpa, in polyurethane 0.3 Mtpa, and in bauxite residue carbonation 0.2 Mtpa. These are then the products with a higher potentiality to be obtained by CO_2 in Europe.

Specific data are provided for Germany. In fact, for this country, the potential use of CO_2 in methanol is of 1.33 Mtpa, in mineral carbonation is of 1.34 Mtpa, in concrete curing is of 2.15 Mtpa, in urea is of 0.7 Mtpa, in lignin treatment is of 0.7 Mtpa, in polyurethane of 0.1 Mtpa, in concrete by red mud is of 0.03 Mtpa, in propylene polymer is of 0.1 Mtpa, while in horticulture is of 0.5 Mtpa (Patricio et al., 2017).

According to these considerations, at this research stage, an innovative CCUS supply chain is proposed for Germany to avoid that it will have a dominant role inside the global CH_3OH market. According to the work of Patricio et al. (2017), it is supposed that CO_2 is used to produce methanol by means of the hydrogenation

reaction, urea, concrete by curing, wheat, lignin for polyethylene, calcium carbonate, polyurethane and concrete by red mud. Among the suggested CO_2-based products, polyurethane and not propylene is chosen due to the high level of interest by researchers on its production from CO_2 (Von der Assen et al., 2015), while wheat is considered among other horticulture products due to the great production in Germany (Germany is the second largest producer in Europe, (World-Grain, 2019)).

A similar CCUS system was not considered in the literature before, then the novelty of the work is evident. For the model, the same CO_2 source and storage sites of the previous case are considered, while for each CO_2-based product two utilization sites are taken into account. The deterministic Mixed Integer Linear Programming (MILP) model is developed minimizing the total costs of the system, setting the target of CO_2 emissions reduction as a constraint. The economic objective function is taken into account. As in the previous case, the aim of this research is to design the best carbon supply chain (finding the best connection among each element of the framework, the amount of captured, used and stored CO_2, and the amount of each produced compound) able to reduce CO_2 emissions at the minimum cost, satisfying the national demand of the considered products, before it is realized at industrial scale.

IV.2 Model development

IV.2.1 Problem statement

Main assumptions to develop the mathematical model of this innovative CCUS supply chain are the following:

- one to one coupling: one source node can be connected to only one capture node in the storage and utilization section and each capture node can receive from only one source node (Kalyanarengan Ravi et al., 2017);
- CO_2 capture plants are located at CO_2 source sites to avoid the transportation of flue gas with additional costs;
- CO_2 is transported always via pipeline, as the most economical way to transport a large amount of CO_2 and other options are not considered;
- CO_2 is used for concrete curing, wheat cultivation, lignin treatment for polyethylene production, polyurethane production, calcium carbonate production by mineral carbonation, urea fertilizer production, methanol production via hydrogenation, concrete production by red mud, in different utilization sites located in Germany (Patricio et al., 2017);
- the CCUS supply chain is in steady state conditions considering a period of 25 years, because the aim of this research is to design the framework by finding the optimal topology (it can be supposed that in this relatively short period few changes will affect raw materials availability and products demand);

- the demand of the considered CO_2-based products is constant over time, due to the stationary conditions and the short considered period (then these can be sold at a stable price making the system profitable in an economic sense);
- the selected storage site can receive a great amount of CO_2, then only one storage site is present and chosen (as a matter of facts the Altmark geological storage site by alone provides 54% of the overall CO_2 storage capacity estimated for Germany (Holler and Viebahn, 2011));
- only two different sites are selected for each chemical product obtained from CO_2, then production plants are considered with a great or infinity capacity;
- as suggested in the literature, the distances between CO_2 sources and CO_2 utilization/storage sites are calculated from its respective latitude and longitude (Kalyanarengan Ravi et al., 2017);
- the profitability of the CCUS supply chain is evaluated by considering the net present value (NPV) and the payback period (PBP);

For the mathematical model, the following inputs are provided:

- CO_2 sources: locations, yearly CO_2 emissions, CO_2 composition and flow rate of flue gases (Federal Ministry for the Environment, 2014);
- CO_2 capture and compression technologies: materials and correlations used for the evaluation of costs (Nguyen and Zondervan, 2018; Zhang et al., 2018);
- CO_2 transportation: distances and relative costs (Serpa et al., 2011);
- conversion factors for the production of chemical compounds by using CO_2 (Patricio et al., 2017; Von der Assen et al., 2015; Erda et al., 2015);
- production of chemical compounds by using CO_2: location of plants and costs (Colacem, 2019; Zimmer, 2012; Jönsson and Wallberg, 2009; Plastics-Insight, 2019; Zappa, 2014; Collodi et al., 2017; Hank et al., 2018; Wheatatlas, 2019; Cemnet, 2019; Chemical-technology, 2019; Kali-gmbh, 2019; Thyssenkrupp, 2019; Globalsyngas, 2019; Leonzio et al., 2019a; Dadcoalumina, 2019; Hydro, 2019; Ineos, 2019; Covestro, 2019; Dow, 2019);
- CO_2 storage: location, type, capacity and costs (Hendriks, 1994; Hasan et al., 2014; Roehrl and Toth, 2009);
- national demand of produced chemical compounds and target of CO_2 emissions reduction (Ochoa Bique et al., 2018; Vde, 2019; Bloomberg, 2019; Converting, 2019; Alexy et al., 2000; Plastics, 2019; Wolfgang Tegethoff, 2001; Ourworld, 2019; Tredingeconomics, 2019);

Solving the mathematical model, the following decisions should be taken:

- the amount of CO_2 captured in each source;
- the technology and material used for the capture of CO_2 from the selected CO_2 sources;
- the amount of each compound produced from CO_2;

- the utilization site chosen for the production of chemical compounds;
- the amount of stored/utilized CO_2;
- the best combination between CO_2 sources, CO_2 capture technologies/materials, CO_2 storage/utilization sites.

The objective function minimizes the total costs of the CCUS supply chain, which include CO_2 capture and compression costs, CO_2 transportation costs, CO_2 storage costs and production costs of different CO_2-baed compounds.

IV.2.2 CCUS supply chain model

To develop the model for the CCUS supply chain, it is necessary to define sets, parameters, variables, constraints, equations and objective function.

IV.2.2.1 Sets

In the developed mathematical model, it is necessary to define each component of the CCUS supply chain with an index. CO_2 sources are represented by 'i', CO_2 capture and compression technologies are represented by 'j', CO_2 storage sites and its complementary utilization section as 'k', CH_3OH production sites are indicated by 'm', concrete production sites are represented by 'c', wheat production sites are represented by 'w', lignin treatment sites are represented by 'l', polyurethane production sites are presented by 'p', calcium carbonate production sites are indexed by 'cc', urea fertilizer production sites are represented by 'u', concrete production by red mud sites are represented by 'cr'.

IV.2.2.2 Parameters

Several parameters are used in the suggested model, as the following: CR^{min}, the minimum target for the overall CO_2 reduction (ton/year); CS_i, the total CO_2 emission from each source i (ton/year); F_i, the total flue gas flow rate from each source i (mol/s); XS_i, CO_2 composition in the flue gas from source i (mol%); XL_i, the lowest CO_2 composition processing limit for the capture plant j (mol%); XH_i, the highest CO_2 composition processing limit for the capture plant j (mol%); C_k^{max}, the maximum storage capacity at the storage site k (ton); $MeOH^{dem}$, the national CH_3OH demand that must be satisfied in Germany (ton/year), $Concrete^{dem}$ the national concrete demand that must be satisfied in Germany (ton/year), $Wheat^{dem}$ the national wheat demand that must be satisfied in Germany (ton/year), $Lignin^{dem}$ the national lignin demand that must be satisfied in Germany (ton/year), $Polyurethane^{dem}$ the national polyurethane demand that must be satisfied in Germany (ton/year), $Calcium\ Carbonate^{dem}$ the national calcium carbonate demand that must be satisfied in Germany (ton/year), $Urea^{dem}$ the national urea demand that must be satisfied in Germany (ton/year), Concrete by $red\ mud^{dem}$ the national concrete by red mud demand that must be satisfied in Germany (ton/year).

IV.2.2.3 Variables

In this model, $X_{i,j,k}$ and $Y_{i,j,k}$ are the binary variables (with a value of 1 or 0) used to select CO_2 storage site and CO_2 capture technology/material respectively when these are 1. Continuous variables with a value between 0 and 1 are the following: $FR_{i,j,k}$ to define the fraction of captured CO_2 that is sent to the storage; $Utilization_{i,j,k}$ to define the fraction of captured CO_2 sent to the utilization; $Concrete_{i,j,c}$ to define the fraction of captured CO_2 used for concrete production; $Wheat_{i,j,w}$ to define the fraction of captured CO_2 used for wheat production; $Lignin_{,ij,l}$ to define the fraction of captured CO_2 used for lignin production; $Polyurethane_{i,j,p}$ to define the fraction of captured CO_2 used for polyurethane production; Calcium $carbonate_{i,j,cc}$ to define the fraction of captured CO_2 used for calcium carbonate production; $Urea_{i,j,u}$ to define the fraction of captured CO_2 used for urea production; $Methanol_{i,j,m}$ to define the fraction of captured CO_2 used for CH_3OH production; Concrete by red $mud_{i,j,cr}$ to define the fraction of captured CO_2 used for concrete by red mud production.

IV.2.2.4 Constraints

For the development of the mathematical model, the following constraints are used. To ensure that CO_2 captured from each source does not get distributed to multiple storage sites the following constraint is used (see Eq. IV.1):

$$\sum_{(j,k)\in(J,K)} X_{i,j,k} \leq 1 \qquad \forall\, i \in I \tag{IV.1}$$

where $X_{i,j,k}$ is the binary variable as defined above. In this way, the assumption based on one to one coupling between sources and capture technology is ensured for the storage section.

In order not to exceed the maximum storage capacity, the following constraint is used (see Eq. IV.2):

$$\sum_{(i,j)\in(I,J)} CS_i \cdot FR_{i,j,k} \leq \frac{C_k^{max}}{TH} \qquad \forall\, k \in K \tag{IV.2}$$

where CS_i is the total CO_2 emission from source 'i', C_k^{max} is the maximum storage capacity of the storage site 'k', TH is the time horizon of supply chain and $FR_{i,j,k}$ is the variable defined above.

To ensure that a minimum target of CO_2 emission reduction is achieved, the following constraint is used (see Eq. IV.3):

$$\sum_{(i,j,k)\in(I,J,K)} CS_i \cdot FR_{i,j,k} + CS_i \cdot Utilization_{i,j,k} \geq CR^{min} \tag{IV.3}$$

where CS_i is the total CO_2 emission from source 'i', $FR_{i,j,k}$ and $Utilization_{i,j,k}$ are the continuous variables defined above and CR^{min} is the minimum target of CO_2 emissions reduction.

To ensure that no more than 90% of CO_2 is removed from the selected source the following constraint is used (see Eq. IV.4):

$$\sum_{(j)\in(J)} FR_{i,j,k} + Utilization_{i,j,k} \leq 0.9 \qquad \forall\,(i,k)\ \in (I,K) \qquad (IV.4)$$

where $FR_{i,j,k}$ and $Utilization_{i,j,k}$ are the variables defined.

Not all the considered technologies can be used to capture CO_2 from all sources, as some of them are not capable to remove up to 90% of CO_2 from the feed flue gas and with a product purity of 90% CO_2 at least. This depends on the composition of CO_2 in the feed, as defined by the following constraint (see Eq. IV.5):

$$\sum_{(k)\in(K)} (XH_j - XS_i)\cdot(XS_i - XL_j)\cdot X_{i,j,k} \geq 0 \qquad \forall\,(i,j)\ \in (I,J) \qquad (IV.5)$$

where XS_i is CO_2 composition in flue gas from source "i", XL_j, is the lowest CO_2 composition processing limit for the capture plant "j", XH_j is the highest CO_2 composition processing limit for the capture plant "j" and $X_{i,j,k}$ is the binary variable defined above. According to the above constraint (IV.5), carbon capture technologies should ensure a minimum CO_2 purity level of 90%, in the storage section. Different purity levels, specific for each utilization process, are not considered here, because the distribution of the available CO_2 feedstock among different utilization processes may change. It is supposed then, that the required CO_2 purity is achieved in the utilization site.

To ensure that the national demand of each CO_2-based product is satisfied, the following constraints are used (see Eqs. IV.6-IV.13):

$$\sum_{(i,j,c)\in(I,J,C)} Concrete_{i,j,c} \geq Concrete^{dem} \qquad (IV.6)$$

$$\sum_{(i,j,w)\in(I,J,W)} Wheat_{i,j,w} \geq Wheat^{dem} \qquad (IV.7)$$

$$\sum_{(i,j,l)\in(I,J,L)} Lignin_{i,j,l} \geq Lignin^{dem} \qquad (IV.8)$$

$$\sum_{(i,j,p)\in(I,J,P)} Polyurethane_{i,j,p} \geq Polyurethane^{dem} \qquad (IV.9)$$

$$\sum_{(i,j,cc)\in(I,J,CC)} Calcium\ carbonate_{i,j,cc} \geq Calcium\ Carbonate^{dem} \qquad (IV.10)$$

$$\sum_{(i,j,u)\in(I,J,U)} Urea_{i,j,u} \geq Urea^{dem} \qquad (IV.11)$$

$$\sum_{(i,j,m)\in(I,J,M)} Methanol_{i,j,m} \geq MeOH^{dem} \qquad (IV.12)$$

$$\sum_{(i,j,cr)\in(I,J,CR)} Concrete\ by\ red\ mud_{i,j,cr} \geq Concrete\ by\ red\ mud^{dem} \qquad (IV.13)$$

where the amount of each production should be equal or higher than the respective national demand, in order to ensure that the minimum target of CO_2 emissions reduction is achieved with a limited storage capacity.

To ensure that the amount of captured CO_2 sent to the utilization section is divided among different utilization sites, respecting then material balances, the following constraint is used (see Eq. IV.14):

$$\begin{aligned} Utilization_{i,j,k} = (&Concrete_{i,j,c} + Wheat_{i,j,w} + Lignin_{i,j,l} + Polyurethane_{i,j,p} \\ &+ CalciumCarbonate_{i,j,cc} + Urea_{i,j,u} + Methanol_{i,j,m} \\ &+ Concrete\ by\ red\ mud_{i,j,cr}) \cdot n_{sites} \qquad \forall\ (i,j,k,c,w,l,p,cc,u,m,cr) \\ &\in (I,J,K,C,W,L,P,CC,U,M,CR) \qquad (IV.14) \end{aligned}$$

where $Utilization_{i,j,k}$, $Concrete_{i,j,c}$, $Wheat_{i,j,w}$, $Lignin_{ij,l}$, $Polyurethane_{i,j,p,}$ Calcium $carbonate_{i,j,cc}$, $Urea_{i,j,u}$, $Methanol_{i,j,m}$ and Concrete by red $mud_{i,j,cr}$ are the continuous variables defined above, while n_{sites} is the number of sites for each utilization.

In the utilization and storage section only one capture technology/material can be chosen for the selected CO_2 source, as defined in the following constraint (see Eq. IV.15):

$$\sum_{(j,k)\in(J,K)} Y_{i,j,k} \leq 1 \qquad \forall\ i\ \in I \qquad (IV.15)$$

where $Y_{i,j,k}$ is defined above. In order to convert the nonlinear mathematical model in a linear mathematical model through a Glover linearization (see Chapter III), the following constraints are used (see Eqs. IV.16-IV.17):

$$0\ \cdot X_{i,j,k} \leq FR_{i,j,k} \leq 0.9 \cdot X_{i,j,k} \qquad \forall\ (i,j,k)\ \in (I,J,K) \qquad (IV.16)$$

$$0 \cdot Y_{i,j,k}\ \leq Utilization_{i,j,k} \leq 0.9 \cdot Y_{i,j,k} \qquad \forall\ (i,j,k)\ \in (I,J,K) \qquad (IV.17)$$

where $FR_{i,j,k}$, $Utilization_{i,j,k}$, $X_{i,j,k}$ and $Y_{i,j,k}$ are the variables defined above, while 0.9 is used because at least 90% of CO_2 is captured from each source.

IV.2.2.5 Equations

CO_2 capture and compression costs (€/year) are obtained by the following relation (See Eq. IV.18).

$$CC_{i,j,k} = CDC_{i,j,k} + CIC_{i,j,k} + COC_{i,j,k} \qquad \forall\,(i,j,k) \in (I,J,K) \qquad (IV.18)$$

where $CDC_{i,j,k}$ are the flue gas dehydration costs in €/year, $CIC_{i,j,k}$ are the investment costs in €/year and $COC_{i,j,k}$ are the operating costs in €/year. Generally, the saturated flue gas is dehydrated via tri-ethylene glycol absorption at a cost of 9.28 € per ton of CO_2 (including capital and investment costs) (Kalyanarengan Ravi et al., 2017). For amine absorption, no dehydration operation is necessary. The investment and operating costs as functions of CO_2 composition and flue gas flow rate are calculated as follows (Zhang et al., 2018) (see Eqs. IV.19-IV.20):

$$CIC_{i,j,k} = \alpha_{I,j} \cdot Y_{i,j,k} + (\beta_{I,j} \cdot {x_{co2,i}}^{n_{I,j}} + \gamma_{I,j}) \cdot F_{i,j,k}^{m_{I,j}} \qquad \forall\,(i,j,k) \in (I,J,K) \qquad (IV.19)$$

$$COC_{i,j,k} = \alpha_{o,j} \cdot Y_{i,j,k} + (\beta_{o,j} \cdot {x_{co2,i}}^{n_{o,j}} + \gamma_{o,j}) \cdot F_{i,j,k}^{m_{o,j}} \qquad \forall\,(i,j,k) \in (I,J,K) \qquad (IV.20)$$

where $\alpha_{I,j}$, $\alpha_{o,j}$, $\beta_{I,j}$, $\beta_{o,j}$, $\gamma_{I,j}$, $\gamma_{o,j}$, $n_{I,j}$, $n_{o,j}$, $m_{o,j}$, $m_{I,j}$ are fixed parameters for each process and for each material, as in Table S1 of Appendix, $X_{CO2,i}$ is CO_2 content in flue gas, $F_{i,j,k}$ is flue gas flow rate in mol/s and $Y_{i,j,k}$ is the binary variable defined before.

For ionic liquid absorption, the following equations are used (see Eqs. IV.21-IV.22) for the investment and operating costs (€/year), respectively, also as a function of CO_2 composition and flue gas flow rate (Nguyen and Zondervan, 2018):

$$CIC_{i,j,k} = (\alpha_{I,j} \cdot F_{i,j,k} + \beta_{I,j} \cdot Y_{i,j,k}) \cdot x_{co2,i} + \gamma_{I,j} \cdot F_{i,j,k}^{m_{I,j}} \qquad \forall\,(i,j,k) \in (I,J,K) \qquad (IV.21)$$

$$COC_{i,j,k} = (\alpha_{o,j} \cdot F_{i,j,k} + \beta_{o} \cdot Y_{i,j,k}) \cdot x_{co2,i,} + \gamma_{o,j} \cdot F_{i,j,k}^{m_{o,j}} \qquad \forall\,(i,j,k) \in (I,J,K) \qquad (IV.22)$$

where $\alpha_{I,j}$, $\alpha_{o,j}$, $\beta_{I,j}$, $\beta_{o,j}$, $\gamma_{I,j}$, $\gamma_{o,j}$, $m_{o,j}$, $m_{I,j}$ are fixed parameters, as in Table S1 of Appendix, $X_{CO2,i,}$ is CO_2 composition in flue gas, $F_{i,j,k}$ is flue gas flow rate in mol/s, $Y_{i,j,k}$ is the binary variable defined before.

The evaluation of CO_2 transportation costs via pipeline (M€/year) is proposed by Serpa et al. (2011) as the sum of investment ($TIC_{i,j,k,c,w,l,p,cc,u,m,cr}$) and operating costs ($TOC_{i,j,k,c,w,l,p,cc,u,m,cr}$), according to the following equation (see Eq. IV.23):

$$TC_{i,j,k,c,w,l,p,cc,u,m,cr} = CCR \cdot TIC_{i,j,k,c,w,l,p,cc,u,m,cr} + TOC_{i,j,k,c,w,l,p,cc,u,m,cr} \qquad \forall\,(i,j,k,c,w,l,p,cc,u,m,cr) \in (I,J,K,C,W,L,P,CC,U,M,CR) \qquad (IV.23)$$

With CCR the capital cost recovery, calculated at an interest rate of 10% and 25 years. The investment (M€) and operating costs (M€/year) are expressed by the following relations (see Eqs. IV.24-IV.25):

$$TIC_{i,j,k,c,w,l,p,cc,u,m,cr} = (\alpha_t \cdot CS_i \cdot FR_{i,j,k}/Concrete_{i,j,c}/Wheat_{i,j,w}/Lignin_{i,j,l}/Polyurethane_{i,j,p}/Calcium\ carbonate_{i,j,cc}/Urea_{i,j,u}/Methanol_{i,j,m}/Concrete\ by\ red\ mud_{i,j,cr} + \beta_t \cdot X_{i,j,k}/X_{i,j,c}/X_{i,j,w}/X_{i,j,l}/X_{i,j,p}/X_{i,j,cc}/X_{i,j,u}/X_{i,j,m}/X_{i,j,cr}) \cdot F_T \cdot (D_{i,k}/D_{i,c}/D_{i,w}/D_{i,p}/D_{i,cc}/D_{i,u}/D_{i,m}/D_{i,cr}/D_{i,l} + 16) \quad \forall (i,j,k,c,w,l,p,cc,u,m,cr) \in (I,J,K,C,W,L,P,CC,U,M,CR) \qquad (IV.24)$$

$$TOC_{i,j,k,c,w,l,p,cc,u,m,cr} = 4\% \cdot TIC_{i,j,k,c,w,l,p,cc,u,m,cr} \quad \forall (i,j,k,c,w,l,p,cc,u,m,cr) \in (I,J,K,C,W,L,P,CC,U,M,CR) \qquad (IV.25)$$

where α_t is 0.019 and β_t is 0.533 (Serpa et al., 2011), $D_{i,k}$/ $D_{i,c}$/ $D_{i,w}$/ $D_{i,l}$/$D_{i,p}$/ $D_{i,cc}$/ $D_{i,u}$/ $D_{i,m}$/ $D_{i,cr}$ are the distances respectively between CO_2 sources and storage, concrete production, wheat production, lignin production, polyurethane production, calcium carbonate production, urea production, methanol production, concrete by red mud production sites, F_T is a terrestrial factor equal to 1.2 (Broek et al., 2010), 16 km are added to the distance to consider additional paths related to the process (Dahowski et al., 2004), $FR_{i,j,k}$ $Utilization_{i,j,k}$, $Concrete_{i,j,c}$, $Wheat_{i,j,w}$, $Lignin_{,ij,l}$, $Polyurethane_{i,j,p,}$ Calcium $carbonate_{i,j,cc}$, $Urea_{i,j,u}$, $Methanol_{i,j,m}$ and Concrete by $red\ mud_{i,j,cr}$ are the continuous variables defined above , CS_i is the amount of CO_2 in Mton/year. The operating costs are taken as 4% of the investment costs, as shown in Eq. IV.25 (Kalyanarengan Ravi et al., 2017).

CO_2 storage costs (€/year) are calculated considering the investment costs per year (SIC_k) and the operating costs (SOC_k) also per year, according to the following relation (See Eq. IV.26):

$$SC_k = CCR \cdot SIC_k + SOC_k \qquad \forall (k) \in (K) \qquad (IV.26)$$

with CCR defined above. The investment costs (€) are calculated with the following relation (Hendriks, 1994) (see Eq. IV.27):

$$SIC_k = (m \cdot d_{well} + b) \cdot N_{well}^{build}{}_k \qquad \forall (k) \in (K) \qquad (IV.27)$$

where m and b are parameters respectively equal to 1.53 M€/km and 1.23 M€ (Hendriks, 1994), d_{well} is the depth of the well, and N_{well}^{build} is the number of wells which is needed to be built per year (Hasan et al., 2014) (see Eq. IV.28):

$$N_{well}^{build}{}_k = \frac{\sum_{(i,j)\in(I,J)} CS_i \cdot FR_{i,j,k}}{IC} \qquad \forall (k) \in (K) \qquad (IV.28)$$

depending on the maximum injection capacity per well, IC and stored CO_2. The operating costs (€/year) are 4% of investment costs (Kalyanarengan Ravi et al., 2017) (see Eq. IV.21):

$$SOC_k = 4\% \cdot SIC_k \qquad \forall (k) \in (K) \qquad (IV.29)$$

For the production costs and selling prices of each CO_2-based product and the conversion factors of these compounds from CO_2, it is possible to consider Table IV.1.

Table IV.1 Production cost, selling price and conversion factor for different CO_2-based products (Leonzio et al., 2019b)

CO_2 utilization	**Production cost**	**Selling price**	**Conversion factor**
Concrete curing	21.8 €/ton (Colacem, 2019)	77 €/ton (Colacem, 2019)	0.03 tonCO_2 per ton of produced block (Patricio et al., 207)
Wheat	159 €/ton (Zimmer, 2012)	175 €/ton (Zimmer, 2012)	451-565 mgCO_2 per kg of wheat (Erda et al., 2005)
Lignin	15.4 €/ton (Jonsson and Wallberg, 2009)	500 €/ton (Sikdar et al., 1990)	0.22 tonCO_2 per ton of produced lignin (Patricio et al., 207)
Polyurethane	6377 €/ton (Plastics-Insight, 2019; Dow, 2019)	7966 €/ton (Plastics-Insight, 2019; Dow, 2019)	0.3 kgCO_2 per kg of polyurethane (von der Assen et al., 2015)
Calcium carbonate	65,2 €/ton (Zappa, 2014)	120 €/ton (Zappa, 2014)	0.25 tonCO_2 per ton of steel slag (*) (Patricio et al., 207)
Urea	257 €/ton (Collodi et al., 2017)	287 €/ton (Fao, 2019)	0,74 tonCO_2 per ton of urea (Patricio et al., 207)
Methanol	608 €/ton (Hank et al., 2018)	408 €/ton (Emshng-tech, 2019)	1.7 tonCO_2 per ton of produced methanol (Patricio et al., 207)
Concrete by red mud	20.95 €/ton (Colacem, 2019)	77 €/ton (Colacem, 2019)	0.053 tonCO_2 per ton of red mud (Patricio et al., 207)

(*)it has been also assumed that 0.30 ton of $CaCO_3$ salable on the market are obtained per ton of steel slag.

IV.2.2.6 Objective function

Equation IV.30 shows the objective function for the analyzed CCUS supply chain model (see Eq. IV.30):

$$\emptyset = \sum_{(i,j,k,c,w,l,p,cc,u,m,cr)} CC_{i,j,k} + TC_{i,j,k,c,w,l,p,cc,u,m,cr} + SC_k + CP_c + WP_w + LP_l + PP_p + CCP_{cc} + UP_u + MP_m + CRP_{cr} \quad (IV.30)$$

where $CC_{i,j,k}$ are CO_2 capture and compression costs, $TC_{i,j,k,c,w,l,p,cc,u,m,cr}$ are CO_2 transportation costs, SC_k are CO_2 storage costs, MP_m are CH_3OH production costs, CP_c are concrete curing production costs, WP_w are wheat production costs, LP_l are lignin production costs, PP_p are polyurethane production costs, CCP_{cc} are calcium carbonate production costs, UP_u are urea production costs, CRP_{cr} are concrete by red mud production costs.

IV.2.3 Case study

The analysis of CO_2 emissions, CO_2 sources selected for the CCUS supply chain in Germany and the target for emissions reduction that should be achieved are already discussed in the respective sections of the previous chapter. These considerations are true also for the selected CO_2 storage site, as Altmark.

For each chemical compound, two utilization sites are selected: Ennigerloh and Hannover for concrete curing, because conventional concrete industries are already present there (Cemnet, 2019), Munich and Hannover for wheat cultivation (Wheatatlas, 2019), Cologne and Münchsmünster for lignin utilization, because conventional polyethylene plants are already present there (Ineos, 2019; Chemical-technology, 2019), Schwarzheide and Leverkusen for polyurethane production, because industries producing polyurethane in a conventional way are present there (Chemical-technology, 2019; Covestro, 2019), Salzgitter and Bremen for calcium carbonate production because traditional industries for calcium carbonate are present there (En.stahl, 2019), Kassel and Hagen for urea production because conventional plants for urea production are present there (Kali-gmbh, 2019; Thyssenkrupp, 2019), Leuna and Wesseling for methanol production because conventional methanol plants are present there (Globalsyngas, 2019; ICIS, 2019), Rackwitz and Hamburg for concrete production by red mud because alumina plants are already present there (Dadcoalumina, 2019; Hydro, 2019). The selected CO_2 sources are reported in figure IV.1a, while CO_2 utilization and storage sites chosen for the CCUS supply chain are shown in Figure IV.1b.

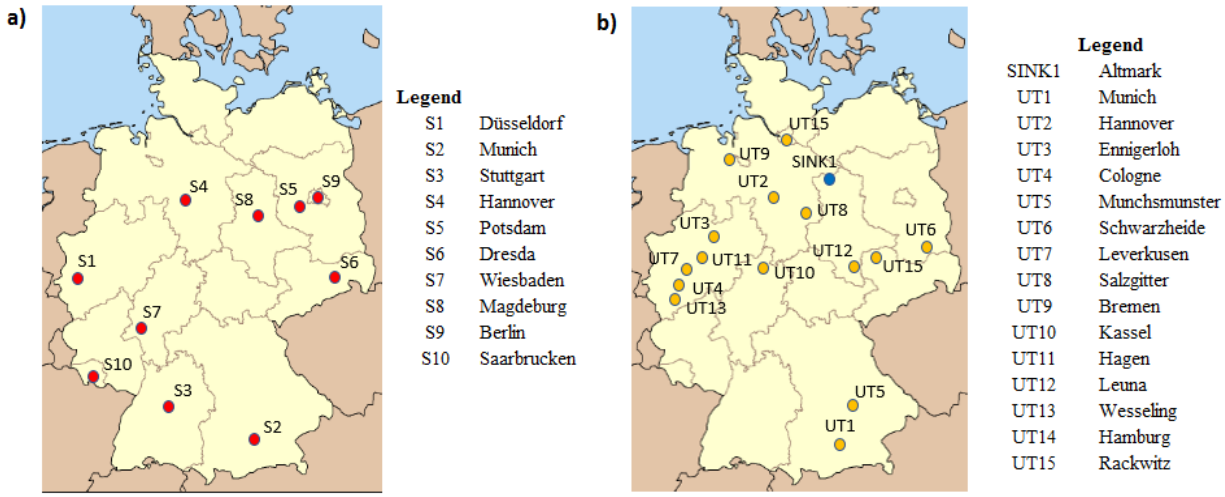

Figure IV.1 a) Selected CO_2 sources; b) Selected CO_2 utilization and storage sites in Germany for the developed CCUS supply chain (Leonzio et al., 2019b)

Distances between stationary CO_2 source, utilization and storage sites are provided in the Appendix (Tables S2-S10).

In the carbon capture section of the CCUS supply chain, different technologies/materials are used to capture at most 90% of CO_2 from flue gas. For absorption technology, MEA solution (30%wt), because it is the most used solvent, PZ (40% wt), due to its energy efficient and stable thermal performance, and ionic liquid (1-butyl-3-methylimidazolium acetate), due to its energy and capture efficiency are used (Rochelle et al., 2011; Nguyen and Zondervan, 2018). For membrane technology, POE1 and POE2 materials are selected

due to their CO_2/N_2 selectivity, while FSC-PVAm material is chosen, because of its high permeability to CO_2 (Hägg and Lindbråthen, 2005). For pressure swing adsorption (PSA) and vacuum swing adsorption (VSA) technologies, different zeolites are selected as sorption materials: 13X, AHT, MVY, and WEI. The first zeolite is the most used, also validated experimentally (Xiao et al., 2008), while the others are selected due to their costs (Hasan et al. 2015).

Table IV.2 shows the national German demand for the selected chemical compounds that the developed CCUS supply chain should satisfy.

Table IV.2 National German demand for different CO_2-based chemical compounds (Leonzio et al., 2019b)

CO_2-based product	**National German demand**
Concrete	5.32 Mton/year (Vdz, 2019)
Wheat	21.5 Mton/year (Bloomberg, 2019)
Lignin	0.41 Mton/year (Converting, 2019; Alexy et al., 2000)
Polyurethane	12.2 Mton/year (Plastics, 2019)
Calcium carbonate	65.4 Mton/year (Wolfgang Tegethoff, 2001)
Urea fertilizer	1.48 Mton/year (Ourworld, 2019; Tredingeconomics, 2019)
Methanol	940 kton/year (Ochoa Bique et al., 2018)
Concrete by red mud	21.8 Mton/year (Vdz, 2019)

IV.3 Results and discussion

At first, a sensitivity analysis is carried out varying the national demand of the produced CO_2-based compounds; secondly, a study considering uncertainties in the demand and the selling price of these products is developed through the Monte Carlo simulation. The model, formulated as MILP model, has 144430 constraints, 110789 variables (280 integer). CPLEX 12.7.1 is the selected solver and the solving times are about 6 seconds, with 726 iterations. The used computer contains an Intel Core i-3 processor at 2.5 GHz with 4 GB of RAM.

IV.3.1 Results of sensitivity analysis

From a literature search, the national demand of CO_2-based chemical compounds is found, as shown in Table IV.2. However, in a realistic vision, the overall demand should not be satisfied by the sustainable production suggested here, and the production through a conventional process should be considered. Then, a sensitivity analysis is developed changing the national demand fixed in the model, as a percent (10%, 20%, 30%, 40%, 50%, 60%, 70%, 80%, 90%, 100%) of the total national demand for each chemical compound.

The total costs of supply chain, net present value and payback period for all considered cases are listed in Table IV.3: increasing the amount of these products according to a percentage of total national demand, the

total costs of CCUS supply chain and net present value increase from 29 billion€/year to 103 billion€/year and from 113 billion€ to 747 billion€, respectively, while the payback period decreases from 5.82 years to 2.65 years. In the economic analysis, a carbon tax of 80 €/tonCO_2, an interest rate of 4% and taxes at 45% are considered.

Table IV.3 Results of CCUS supply chain optimizations as a function of different values of CO_2-based compounds national demand (Leonzio et al., 2019b)

Percent of total national demand (%)	Total costs (Billion€/year)	NPV (Billion€)	PBP (Years)
10	29	113	5.82
20	37.2	200	4.25
30	48.7	265	3.74
40	57	333	3.41
50	65.1	343	3.41
60	73.3	470	3.01
70	82.3	542	2.89
80	90	607	2.80
90	97.9	675	2.72
100	103	747	2.65

Assuming that the best economic case is suggested by the highest value of net present value, in this research the best realistic case is when 90% of total demand for each CO_2-based compound is produced within the CCUS supply chain. The topology of this best CCUS supply chain is shown in Figure IV.2 (the topologies of other CCUS chains are shown in the Appendix, see Figures from 1 to 9).

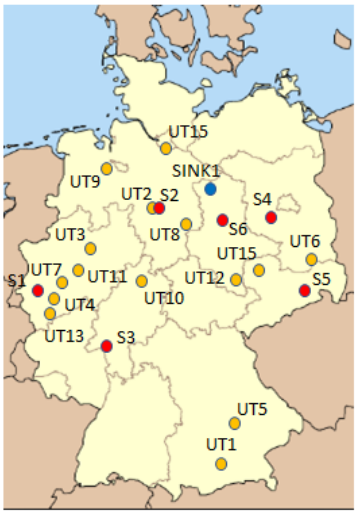

CO_2 Utilization/Storage	Production	CO_2 Source
SINK1 Altmark		S6 Magdeburg
UT1 Munich	Wheat	S1 Dusseldorf
UT2 Hannover	Concrete curing and Wheat	S1 Dusseldorf
UT3 Ennigerloh	Concrete curing	S1 Dusseldorf
UT4 Cologne	Lignin	S1 Dusseldorf
UT5 Munchsmunster	Lignin	S1 Dusseldorf
UT6 Schwarzheide	Polyurethane	S1 Dusseldorf
UT7 Leverkusen	Polyurethane	S1 Dusseldorf
UT8 Salzgitter	Calcium carbonate	S3-S2-S4-S5 Wiesbaden-Hannover-Potsdam-Dresda
UT9 Bremen	Calcium carbonate	S3-S2-S4-S6 Wiesbaden-Hannover-Potsdam-Dresda
UT10 Kassel	Urea	S1 Dusseldorf
UT11 Hagen	Urea	S1 Dusseldorf
UT12 Leuna	Methanol	S2 Hannover
UT13 Wesseling	Methanol	S2 Hannover
UT14 Hamburg	Concrete by red mud	S1 Dusseldorf
UT15 Rackwitz	Concrete by red mud	S1 Dusseldorf

Figure IV.2 Results of CCUS supply chain design optimization considering 90% of national demand of produced CO_2-based chemical compounds (Leonzio et al., 2019b)

For the selected best case, shown in Figure IV.2, the trend of cash flows is reported in Figure IV.3, considering a life time of the CCUS chain equal to 25 years, with 2 years for the construction. Satisfying 90% of total national demand, the CCUS supply chain has a total cost of 97.9 billion€/year with a net present value of 675 billion€ and a payback period of 2.71 years. As suggested by the payback period, being lower than 3 years, the framework is a good and attractive solution due to the use of carbon tax.

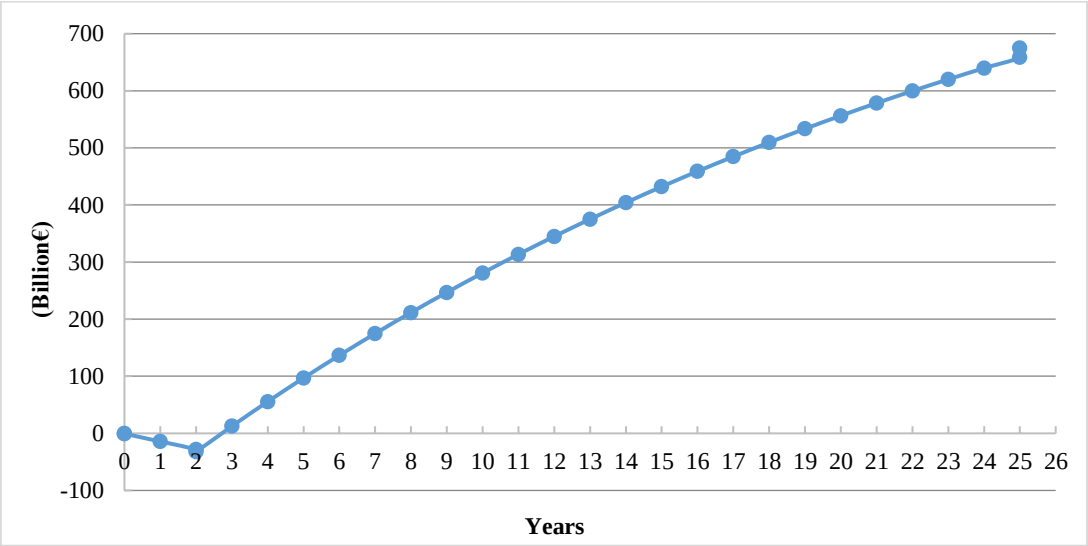

Figure IV.3 Cash flows diagram for the CCUS supply chain where 90% of national demand of CO_2-based products is satisfied (Leonzio et al., 2019b)

For this case, CO_2 capture and compression costs are 14.9 billion€/year, CO_2 transportation costs are 0.46 billion€/year, CO_2 storage costs are 0.153 billion€/year, while the total production costs of different compounds are 82.4 billion€/year. Table IV.4 shows the amount of CO_2 from each selected CO_2 source that is sent to the utilization and storage site thought the selected capture technology/material.

Magdeburg is the source selected for the storage option and in this source site, CO_2 is captured through MEA absorption. Dresden, Wiesbaden, Berlin, Munich, Potsdam, Magdeburg, Saarbrucken are the sources selected for the utilization option, where CO_2 is captured through PZ absorption. The target about CO_2 emissions reduction is fulfilled, then 160 MtonCO_2/year are reduced by the system (this number considers CO_2 sent to both utilization and storage section). Among four different capture technologies with different materials, only one capture technology with two different materials is selected in the design of this carbon supply chain. It is interesting to see how the absorption technology is selected for the storage and utilization section with two different materials: MEA for the storage option and PZ for the utilization option. Among these, PZ is preferred over MEA, because it is present in more choices with high and low flow rate of captured CO_2. In fact, as reported by Kalyanarengan Ravi et al. (2017), PZ has a lower cost than MEA,

then, it is preferred inside the supply chain. It is possible to suppose that PZ is chosen for all utilization options, because the respective selected sources have a similar CO_2 composition, between 13 mol% and 22 mol%.

However, for the same CO_2 source as Magdeburg, two different materials for the absorption are used. This suggests that the choice of capture technology/material depends not only on CO_2 composition and on flue gas flow rate, but also on its final use, as the storage or utilization option. In fact, the design of the CCUS supply chain, as a multi-scale process, is developed not in a hierarchical way (step by step starting from micro-scale decisions, as the choice of materials, to arrive at kilometer scale as the supply chain optimization) but in a simultaneous way (by considering simultaneous selection of materials and processes for CO_2 capture, CO_2 sources, utilization and sequestration sites), then considering the overall system in tandem (Papadopoulos and Seferlis, 2017). This is an important result for the design of a supply chain including both CO_2 utilization and storage site: the selection of a capture technology/material depends on CO_2 composition, flue gas flow rate and CO_2 final use.

Even if the singular capture option of MEA absorption can have a higher cost than other technologies/materials as PZ absorption (Hasan et al., 2015), inside the CCUS supply chain after the overall optimization, MEA absorption can have a lower cost and then it is the preferred option by considering the destination of CO_2.

Table IV.4 Topology of CCUS supply chain optimization where 90% of national demand of CO_2-based products is satisfied (Leonzio et al., 2019b)

CO_2 source	**Capture technology/material**	**CO_2 amount (Mton/year)**
	To storage	
Magdeburg	MEA Absorption	20.32
	To utilization	
Dresda	PZ Absorption	43.83
Wiesbaden	PZ Absorption	38.61
Berlin	PZ Absorption	0.99
Munich	PZ Absorption	1.44
Potsdam	PZ Absorption	33.28
Magdeburg	PZ Absorption	4.34
Saarbruken	PZ Absorption	17.19

As shown in Figure IV.2, CO_2 from Saarbrucken source site is used to produce wheat, concrete, lignin, polyurethane, calcium carbonate. CO_2 from Potsdam source site is used to produce calcium carbonate and concrete by red mud. CO_2 from Berlin source site is used for the production of urea fertilizer while CO_2 from Munich source site produces methanol. CO_2 from Dresda, Wiesbaden, Magdeburg and Saarbrucken

source sites is sent to the calcium carbonate production. The amount of CO_2-based chemical compounds that is produced is shown in Table IV.5: the national demand is satisfied and a higher amount of calcium carbonate is produced.

Then, Germany is able to export an amount of calcium carbonate, however the produced quantity is lower than the global demand of 4500 Mton/year and the European demand 1080 Mton/year (Wolfgang Tegethoff, 2001; CCA, 2016). In the base case, the specific cost (€/tonCO_2 captured) for all products utilization is higher than the corresponding cost of storage: as a results the storage capacity is completely exhausted over 25 years (the time horizon of the supply chain), all products but one reach the national demand (the minimum production level imposed by constraints) and the product with the cheapest production cost (calcium carbonate) is obtained at a rate about double than the national demand, although lower than the European demand.

Table IV.5 Amount of CO_2-based chemical compounds produced inside the CCUS supply chain (Leonzio et al., 2019b)

CO_2-based chemical compound	**Production (Mton/year)**
Methanol	0.85
Concrete curing	4.79
Wheat	19.35
Lignin	0.38
Polyurethane	11.00
Calcium Carbonate	120
Urea	1.34
Concrete by red mud	19.15

IV.3.2 Results considering the uncertainties

The selling price and the national demand of CO_2-based chemical compounds show generally variations. Ozkir and Basligil (2013) underline the complicate nature of a carbon supply chain, characterized by a high level of uncertainties. For this reason for the best supply chain defined above, an analysis is developed, by changing these two parameters (selling price and national demand of CO_2-based chemical compounds) in the range between -50% and +50% of the base case values, mentioned before (Table IV.1).

Table IV.6 shows the results obtained by changing the selling price of CO_2-based chemical compounds.

Table IV.6 Results of CCUS supply chain by changing the selling price of CO_2-based chemical compounds compared to the base case (Leonzio et al., 2019b)

Variation of selling price (%)	NPV (Trillion€)	PBP (years)
(-50)	0.266	3.79
(-40)	0.348	3.38
(-30)	0.430	3.12
(-20)	0.511	2.94
(-10)	0.593	2.82
base case	0.675	2.72
(+10)	0.756	2.64
(+20)	0.838	2.58
(+30)	0.920	2.53
(+40)	1	2.49
(+50)	1.08	2.45

How it should be, by increasing the selling price for each compound, the NPV increases while the PBP decreases. On the other hand, by decreasing the selling price, the NPV decreases while the PBP increases. With the value of mean (0.675 trillion€ and 2.86 years), standard deviation (0.271 trillion€ and 0.42 years), maximum (1.08 trillion€ and 3.79 years) and minimum (0.266 trillion€ and 2.45 years) obtained by sensitivity analysis, a Monte Carlo simulation is carried out by means of RiskAMP software by using a normal distribution. Figure IV.4a and IV.4b show respectively the frequency and the cumulative probability for NPV, while Figure IV.5a and IV.5b show the frequency and the cumulative probability for PBP, respectively. Considering the uncertainty of selling price for CO_2-based compounds, the most probable values for NPV and PBP are in the range between 1.1 and 1.2 trillion€ and 3.85 years, respectively.

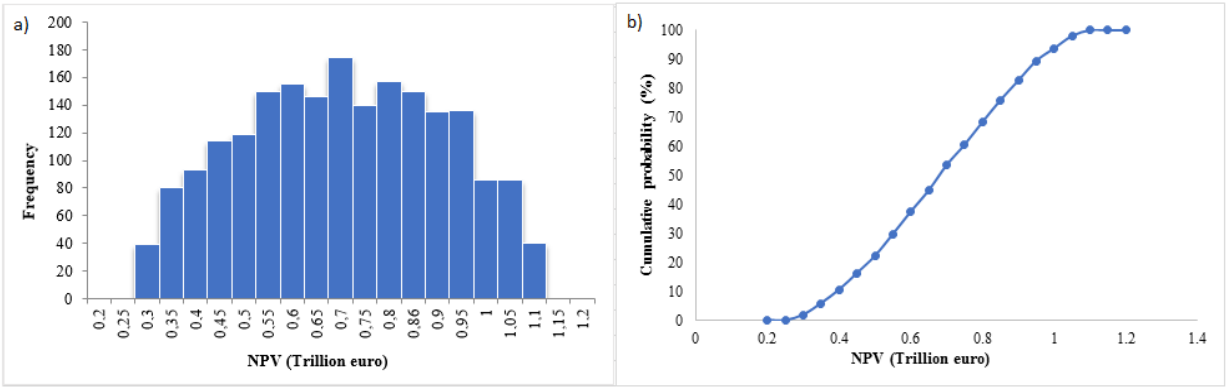

Figure IV.4 Results of NPV according to the Monte Carlo simulation with uncertainty in the selling price of CO_2-based chemical compounds: a) frequency; b) cumulative probability (Leonzio et al., 2019b)

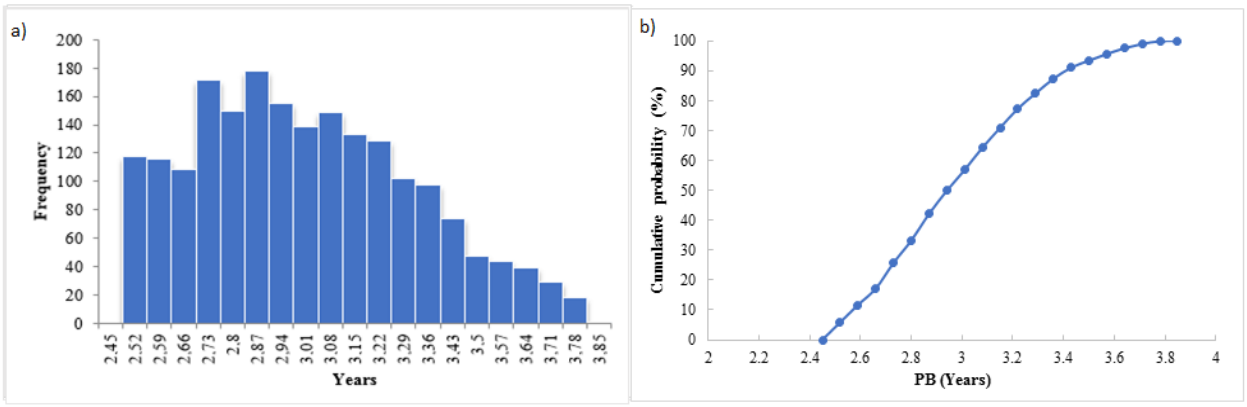

Figure IV.5 Results of PBP according to the Monte Carlo simulation with uncertainty in the selling price of CO_2-based chemical compounds: a) frequency; b) cumulative probability (Leonzio et al., 2019b)

The sensitivity analysis is focused on the utilization section of the supply chain: as a matter of fact, the overall amount of captured CO_2 cannot be reduced because of the environmental constraint and a similar consideration is true for the stored fraction (already at its maximum level in the base case). So, when a change is imposed in the global quantity of CO_2 transformed into products, the quantity of each product is affected to reach the objective at minimum costs. Table IV.7 shows the results obtained by changing the national demand of CO_2-based chemical compounds between -50% and +50% of base case values, defined before (Table IV.2). By increasing the national demand for each compound, the NPV increases while the PBP decreases. On the other hand, by decreasing the national demand, the NPV decreases while the PB time increases.

Table IV.7 Results of CCUS supply chain by changing the national demand of CO_2-based chemical compounds compared to the base case (Leonzio et al., 2019b)

Percent of national demand (%)	**Total cost (Billion€/year)**	**NPV (Billion€)**	**PBP (years)**
(-50)	61	368	3.29
(-40)	68.2	429	3.11
(-30)	76	491	2.97
(-20)	83.4	547	2.87
(-10)	90.8	613	2.79
base case	97.9	675	2.72
(+10)	106	736	2.66
(+20)	110	805	2.61
(+30)	120	860	2.57
(+40)	125	926	2.53
(+50)	126	982	2.50

Also in this case, a Monte Carlo simulation is developed to evaluate the uncertainty regarding the national demand of chemical compounds. The value of mean (0.676 trillion€ and 2.78 years), standard deviation (0.205 trillion€ and 0.25 years), maximum (982 billion€ and 3.28 years) and minimum (613 billion€ and 2.5 years) are considered for normal distribution. Figure IV.6a and IV.6b show the frequency and cumulative probability for NPV, while Figure IV.7a and IV.7b present the frequency and cumulative probability for PBP. It is found that considering the variation about the national demand of CO_2-based chemical compounds, the most probable values for NPV and PBP are, respectively, in the range of 1.04 and 1.12 trillion€ and 3.32 years.

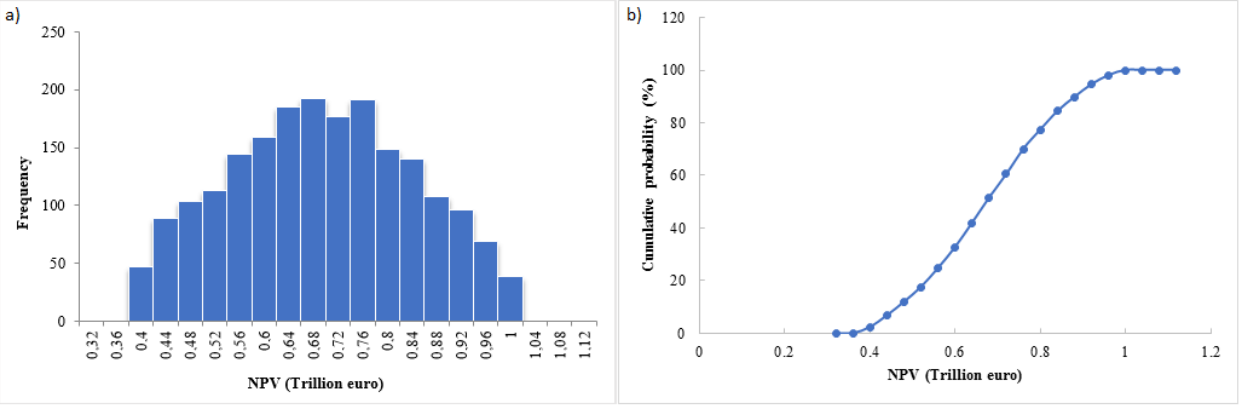

Figure IV.6 Results of NPV according to the Monte Carlo simulation with uncertainty in the national demand of CO_2-based chemical compounds: a) frequency; b) cumulative probability (Leonzio et al., 2019b)

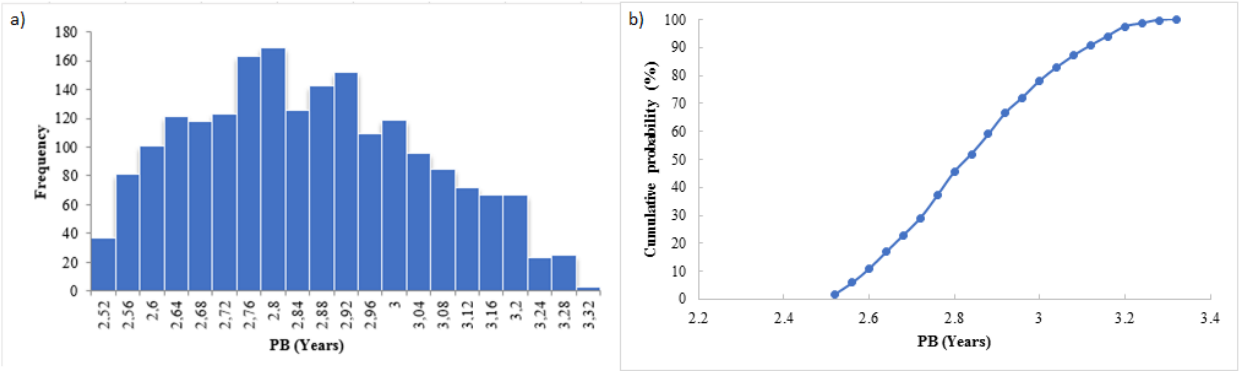

Figure IV.7 Results of PBP according to the Monte Carlo simulation with uncertainty in the national demand of CO_2-based chemical compounds: a) frequency; b) cumulative probability (Leonzio et al., 2019b)

It is possible to deduce from the values of PBP that in the two considered scenarios the CCUS supply chain is economically feasible considering the use of carbon tax.

IV.4 Conclusions

An innovative CCUS supply chain is proposed for Germany, which should solve the environmental problem related to CO_2 emissions. To avoid the production of a large amount of CH_3OH, as found in the previous study, in this framework, different compounds are considered to be produced from CO_2. In particular, the products with a higher potentiality according to the literature are taken into account: methanol, concrete by curing, wheat, lignin for polyethylene, calcium carbonate, urea, polyurethane and concrete by red mud. A similar CCUS scheme has not been considered in the literature so far.

The proposed mathematical model is a MILP type and it is able to design the supply chain minimizing the total costs setting the amount of CO_2 that should be reduced as a constraint. In the optimal design, the total costs of the CCUS supply chain are 97.9 billion€/year with a NPV of 675 billion€ and a PBP of 2.71 years. Results show that for high flue gas flow rate, absorption is the preferred capture technology, while PZ is the preferred material (capture costs are in the order of 100 €/ton CO_2 captured). Moreover, the selection of CO_2 capture technology/material is also depending on the final use of CO_2 due to the simultaneous optimization of supply chain. A sensitivity analysis according to the Monte Carlo simulation is performed to evaluate the uncertainty about the selling price and national demand of CO_2-based chemical compounds. Variations between -50% and +50% compared to the base case are evaluated. Considering the uncertainty of selling price, the most probable values for NPV and PBP are in the range between 1.1 and 1.2 trillion€ and 3.85 years, respectively. Considering the uncertainty of national demand, the most probable values for NPV and PBP are respectively in the range of 1.04 and 1.12 trillion€ and 3.32 years. Profitable solutions are in any cases ensured due to the carbon tax only.

Appendix

Table S1 Cost data for capture and compression technologies (Zhang et al., 2018; Nguyen and Zondervan, 2018)

Process	Material	α	β	γ	n	m
		investment cost ($/year)				
Absorption	MEA	7719	67871	901.000	0.660	0.800
Absorption	PZ	0	59956	226.932	0.566	0.800
PSA	13X	220462	26720	895.262	0.508	0.804
PSA	AHT	214535	17833	4607.297	0.744	0.813
PSA	MVY	162447	22468	6408.791	1.000	0.797
PSA	WEI	142320	19332	6076.357	0.610	0.779
VSA	13X	91060	23096	7688.408	0.470	0.763
VSA	AHT	113969	24939	2659.383	0.468	0.786
VSA	MVY	119259	21652	8101.014	1.000	0.795
VSA	WEI	180953	15644	7751.257	0.874	0.802
Membrane	FSC PVAm	177500	16505	18912.000	0.880	0.770
Membrane	POE-1	568	19151	29669.274	0.778	0.735
Membrane	POE-2	53960	19967	28462.417	0.656	0.744
		investment cost (€/year)				
Absorption	IL	7590.52	2606878.23	33119.84		0.67
		operating cost ($/year)				
Absorption	MEA	0	24088	0	1.000	1.000
Absorption	PZ	0	26825	0	0.945	0.966
PSA	13X	0	11352	3115.833	1.000	0.974
PSA	AHT	0	7040	983.893	0.626	1.000
PSA	MVY	0	7265	1328.677	0.756	1.000
PSA	WEI	0	6398	1257.721	0.554	0.991
VSA	13X	0	8167	1580.419	0.590	0.985
VSA	AHT	0	8545	1725.654	0.842	0.996
VSA	MVY	0	9117	1839.193	1.000	1.000
VSA	WEI	0	7378	1493.500	0.753	1.000
Membrane	FSC PVAm	0	11619	0	0.210	1.000
Membrane	POE-1	0	12798	0	0.134	0.980
Membrane	POE-2	0	13556	0	0.135	0.984
		operating cost (€/year)				
Absorption	IL	33172.59	897224.41	187421.22		0.65

Table S2 Distance between German carbon sources and wheat utilization sites (Distance, 2019)

CO_2 Source		CO_2 Utilization	Distance (km)
Northrhine-Westphalia	Düsseldorf	Munich	486.91
Bavaria	Munich	Munich	0
Baden-Württemberg	Stuttgart	Munich	190.53
Lower Saxony	Hannover	Munich	488.69
Brandenburg	Potsdam	Munich	485.67
Saxony	Dresda	Munich	359.59
Hesse	Wiesbaden	Munich	324.7
Saxony-anhalt	Magdeburg	Munich	443.86
Berlin	Berlin	Munich	504.92
Saarland	Saarbrücken	Munich	356.65

CO_2 Source		CO_2 Utilization	Distance (km)
Northrhine-Westphalia	Düsseldorf	Hannover	239.96
Bavaria	Munich	Hannover	488.69
Baden-Württemberg	Stuttgart	Hannover	401.45
Lower Saxony	Hannover	Hannover	0
Brandenburg	Potsdam	Hannover	226.24
Saxony	Dresda	Hannover	312.58
Hesse	Wiesbaden	Hannover	274.66
Saxony-anhalt	Magdeburg	Hannover	131.9
Berlin	Berlin	Hannover	249.91
Saarland	Saarbrücken	Hannover	398.02

Table S3 Distance between German carbon sources and concrete curing utilization sites (Distance, 2019)

CO_2 Source		CO_2 Utilization	Distance (km)
Northrhine-Westphalia	Düsseldorf	Hannover	239.96
Bavaria	Munich	Hannover	488.69
Baden-Württemberg	Stuttgart	Hannover	401.45
Lower Saxony	Hannover	Hannover	0
Brandenburg	Potsdam	Hannover	226.24
Saxony	Dresda	Hannover	312.58
Hesse	Wiesbaden	Hannover	274.66
Saxony-anhalt	Magdeburg	Hannover	131.9
Berlin	Berlin	Hannover	249.91
Saarland	Saarbrücken	Hannover	398.02

CO_2 Source		CO_2 Utilization	Distance (km)
Northrhine-Westphalia	Düsseldorf	Ennigerloh	109.93
Bavaria	Munich	Ennigerloh	483.28
Baden-Württemberg	Suttgart	Ennigerloh	349.82
Lower Saxony	Hannover	Ennigerloh	130.94
Brandenburg	Potsdam	Ennigerloh	349.81
Saxony	Dresda	Ennigerloh	405.45
Hesse	Wiesbaden	Ennigerloh	195.66
Saxony-anhalt	Magdeburg	Ennigerloh	248.97
Berlin	Berlin	Ennigerloh	375.12
Saarland	Saarbrücken	Ennigerloh	298.33

Table S4 Distance between German carbon sources and lignin utilization sites (Distance, 2019)

CO_2 Source		CO_2 Utilization	Distance (km)
Northrhine-Westphalia	Düsseldorf	Koeln	48.62
Bavaria	Munich	Koeln	473.42
Baden-Württemberg	Stuttgart	Koeln	321.21
Lower Saxony	Hannover	Koeln	191.65
Brandenburg	Potsdam	Koeln	403.69
Saxony	Dresda	Koeln	443.66
Hesse	Wiesbaden	Koeln	161.46
Saxony-anhalt	Magdeburg	Koeln	301.58
Berlin	Berlin	Koeln	429.73
Saarland	Saarbrücken	Koeln	245.87

CO_2 Source		CO_2 Utilization	Distance (km)
Northrhine-Westphalia	Düsseldorf	Münchsmünster	445.13
Bavaria	Munich	Münchsmünster	70.07
Baden-Württemberg	Stuttgart	Münchsmünster	183.74
Lower Saxony	Hannover	Münchsmünster	424.28
Brandenburg	Potsdam	Münchsmünster	415.96
Saxony	Dresda	Münchsmünster	293.85
Hesse	Wiesbaden	Münchsmünster	288.72
Saxony-anhalt	Magdeburg	Münchsmünster	374.28
Berlin	Berlin	Münchsmünster	435.57
Saarland	Saarbrücken	Münchsmünster	345.2

Table S5 Distance between German carbon sources and polyurethane utilization sites (Distance, 2019)

CO_2 Source		CO_2 Utilization	Distance (km)
Northrhine-Westphalia	Düsseldorf	Schwarzheide	492.39
Bavaria	Munich	Schwarzheide	405.84
Baden-Württemberg	Stuttgart	Schwarzheide	448.43
Lower Saxony	Hannover	Schwarzheide	299.7
Brandenburg	Potsdam	Schwarzheide	115.99
Saxony	Dresda	Schwarzheide	48.06
Hesse	Wiesbaden	Schwarzheide	423.55
Saxony-anhalt	Magdeburg	Schwarzheide	169.39
Berlin	Berlin	Schwarzheide	120.33
Saarland	Saarbrücken	Schwarzheide	545.9

CO_2 Source		CO_2 Utilization	Distance (km)
Northrhine-Westphalia	Düsseldorf	Leverkusen	26.06
Bavaria	Munich	Leverkusen	461.49
Baden-Württemberg	Stuttgart	Leverkusen	295.8
Lower Saxony	Hannover	Leverkusen	240.72
Brandenburg	Potsdam	Leverkusen	445.38
Saxony	Dresda	Leverkusen	471.92
Hesse	Wiesbaden	Leverkusen	138.22
Saxony-anhalt	Magdeburg	Leverkusen	343.07
Berlin	Berlin	Leverkusen	471.93
Saarland	Saarbrücken	Leverkusen	200.2

Table S6 Distance between German carbon sources and calcium carbonate utilization sites (Distance, 2019)

CO_2 Source		CO_2 Utilization	Distance (km)
Northrhine-Westphalia	Düsseldorf	Salzgitter	271.44
Bavaria	Munich	Salzgitter	454.67
Baden-Württemberg	Stuttart	Salzgitter	385.83
Lower Saxony	Hannover	Salzgitter	52.16
Brandenburg	Potsdam	Salzgitter	182.34
Saxony	Dresda	Salzgitter	260.42
Hesse	Wiesbaden	Salzgitter	275.86
Saxony-anhalt	Magdeburg	Salzgitter	82.92
Berlin	Berlin	Salzgitter	207.62
Saarland	Saarbrücken	Salzgitter	404.11

CO_2 Source		CO_2 Utilization	Distance (km)
Northrhine-Westphalia	Düsseldorf	Bremen	248.08
Bavaria	Munich	Bremen	582.82
Baden-Württemberg	Stuttgart	Bremen	478.63
Lower Saxony	Hannover	Bremen	100.15
Brandenburg	Potsdam	Bremen	296.41
Saxony	Dresda	Bremen	405.3
Hesse	Wiesbaden	Bremen	335.09
Saxony-anhalt	Magdeburg	Bremen	217.77
Berlin	Berlin	Bremen	315.56
Saarland	Saarbrücken	Bremen	445.39

Table S7 Distance between German carbon sources and urea utilization sites (Distance, 2019)

CO_2 Source		CO_2 Utilization	Distance (km)
Northrhine-Westphalia	Düsseldorf	Kassel	189.8
Bavaria	Munich	Kassel	383.78
Baden-Württemberg	Stuttgart	Kassel	283.25
Lower Saxony	Hannover	Kassel	118.31
Brandenburg	Potsdam	Kassel	272.89
Saxony	Dresda	Kassel	296.94
Hesse	Wiesbaden	Kassel	163.11
Saxony-anhalt	Magdeburg	Kassel	172.22
Berlin	Berlin	Kassel	299.97
Saarland	Saarbrücken	Kassel	291.63

CO_2 Source		CO_2 Utilization	Distance (km)
Northrhine-Westphalia	Düsseldorf	Hagen	50.68
Bavaria	Munich	Hagen	463.82
Baden-Württemberg	Stuttgart	Hagen	311.73
Lower Saxony	Hannover	Hagen	191.75
Brandenburg	Potsdam	Hagen	400.95
Saxony	Dresda	Hagen	437.81
Hesse	Wiesbaden	Hagen	152.05
Saxony-anhalt	Magdeburg	Hagen	298.7
Berlin	Berlin	Hagen	427.16
Saarland	Saarbrücken	Hagen	238.72

Table S8 Distance between German carbon sources and methanol utilization sites (Distance, 2019)

CO_2 Source		CO_2 Utilization	Distance (km)
Northrhine-Westphalia	Düsseldorf	Leuna	364.93
Bavaria	Munich	Leuna	355.8
Baden-Württemberg	Stuttgart	Leuna	348.16
Lower Saxony	Hannover	Leuna	195.55
Brandenburg	Potsdam	Leuna	139.55
Saxony	Dresda	Leuna	123.6
Hesse	Wiesbaden	Leuna	299.26
Saxony-anhalt	Magdeburg	Leuna	93.42
Berlin	Berlin	Leuna	164.11
Saarland	Saarbrücken	Leuna	425.17

CO_2 Source		CO_2 Utilization	Distance (km)
Northrhine-Westphalia	Düsseldorf	Wesseling	46.88
Bavaria	Munich	Wesseling	446.45
Baden-Württemberg	Stuttgart	Wesseling	276.85
Lower Saxony	Hannover	Wesseling	256.22
Brandenburg	Potsdam	Wesseling	454.96
Saxony	Dresda	Wesseling	473.96
Hesse	Wiesbaden	Wesseling	121.84
Saxony-anhalt	Magdeburg	Wesseling	352.89
Berlin	Berlin	Wesseling	481.75
Saarland	Saarbrücken	Wesseling	177.08

Table S9 Distance between German carbon sources and concrete by red mud utilization sites (Distance, 2019)

CO_2 Source		CO_2 Utilization	Distance (km)
Northrhine-Westphalia	Düsseldorf	Hamburg	338.62
Bavaria	Munich	Hamburg	612.55
Baden-Württemberg	Stuttgart	Hamburg	534.12
Lower Saxony	Hannover	Hamburg	132.71
Brandenburg	Potsdam	Hamburg	242.59
Saxony	Dresda	Hamburg	377.26
Hesse	Wiesbaden	Hamburg	404.2
Saxony-anhalt	Magdeburg	Hamburg	192.97
Berlin	Berlin	Hamburg	255.73
Saarland	Saarbrücken	Hamburg	523.16

CO_2 Source		CO_2 Utilization	Distance (km)
Northrhine-Westphalia	Düsseldorf	Rackwitz	390.28
Bavaria	Munich	Rackwitz	371.16
Baden-Württemberg	Stuttgart	Rackwitz	373.32
Lower Saxony	Hannover	Rackwitz	209.61
Brandenburg	Potsdam	Rackwitz	117.15
Saxony	Dresda	Rackwitz	103.5
Hesse	Wiesbaden	Rackwitz	327.33
Saxony-anhalt	Magdeburg	Rackwitz	93.05
Berlin	Berlin	Rackwitz	140.22
Saarland	Saarbrücken	Rackwitz	453.12

Table S10 Distance between German carbon sources and storage site (Distance, 2019)

CO_2 Source		CO_2 Storage	Distance (km)
Northrhine-Westphalia	Düsseldorf	Altmark	371.31
Bavaria	Munich	Altmark	527.64
Baden-Württemberg	Stuttgart	Altmark	484.29
Lower Saxony	Hannover	Altmark	131.63
Brandenburg	Potsdam	Altmark	118.96
Saxony	Dresda	Altmark	255.17
Hesse	Wiesbaden	Altmark	383.76
Saxony-anhalt	Magdeburg	Altmark	84.28
Berlin	Berlin	Altmark	135.32
Saarland	Saarbrücken	Altmark	512.5

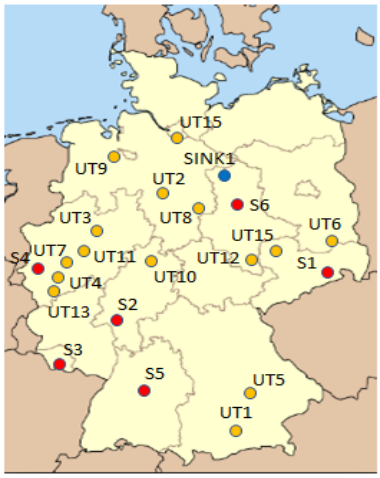

CO_2 Utilization/Storage	Production	CO_2 Source
SINK1 Altmark		S6 Magdeburg
UT1 Munich	Wheat	S4 Dusseldorf
UT2 Hannover	Concrete curing and Wheat	S3-S4 Saarbrucken-Dusseldorf
UT3 Ennigerloh	Concrete curing	S3 Saarbrucken
UT4 Cologne	Lignin	S4 Dusseldorf
UT5 Munchsmunster	Lignin	S4 Dusseldorf
UT6 Schwarzheide	Polyurethane	S4 Dusseldorf
UT7 Leverkusen	Polyurethane	S4 Dusseldorf
UT8 Salzgitter	Calcium carbonate	S1-S2-S5 Dresda-Wiesbaden-Stuttgart
UT9 Bremen	Calcium carbonate	S5 Stuttgart
UT10 Kassel	Urea	S5 Stuttgart
UT11 Hagen	Urea	S5 Stuttgart
UT12 Leuna	Methanol	S5 Stuttgart
UT13 Wesseling	Methanol	S5 Stuttgart
UT14 Hamburg	Concrete by red mud	S4 Dusseldorf
UT15 Rackwitz	Concrete by red mud	S4 Dusseldorf

Figure S4 Results of CCUS supply chain design considering 10% of national demand of produced chemical compounds

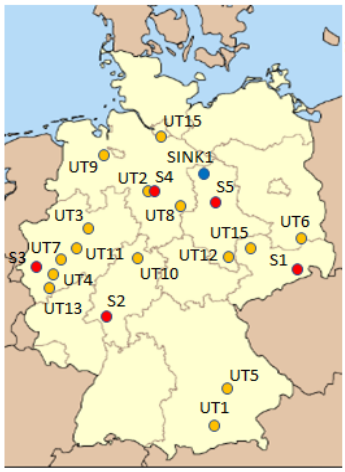

CO_2 Utilization/Storage	Production	CO_2 Source
SINK1 Altmark		S5 Magdeburg
UT1 Munich	Wheat	S4 Hannover
UT2 Hannover	Concrete curing and Wheat	S4 Hannover
UT3 Ennigerloh	Concrete curing	S4 Hannover
UT4 Cologne	Lignin	S3 Dusseldorf
UT5 Munchsmunster	Lignin	S3 Dusseldorf
UT6 Schwarzheide	Polyurethane	S4 Hannover
UT7 Leverkusen	Polyurethane	S4 Hannover
UT8 Salzgitter	Calcium carbonate	S1-S2-S4-S5 Dresda-Wiesbaden-Hannover-Magdeburg
UT9 Bremen	Calcium carbonate	S1-S2-S4-S6 Dresda-Wiesbaden-Hannover-Magdeburg
UT10 Kassel	Urea	S4 Hannover
UT11 Hagen	Urea	S4 Hannover
UT12 Leuna	Methanol	S3 Dusseldorf
UT13 Wesseling	Methanol	S3 Dusseldorf
UT14 Hamburg	Concrete by red mud	S3 Dusseldorf
UT15 Rackwitz	Concrete by red mud	S3 Dusseldorf

Figure S5 Results of CCUS supply chain design considering 20% of national demand of produced chemical compounds

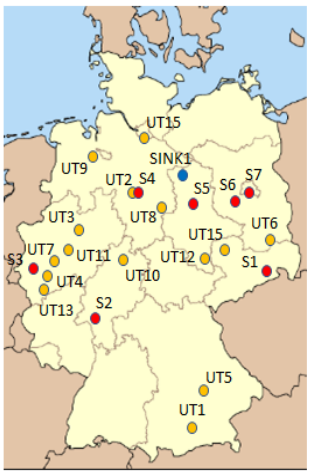

CO_2 Utilization/Storage	Production	CO_2 Source
SINK1 Altmark		S5 Magdeburg
UT1 Munich	Wheat	S4 Hannover
UT2 Hannover	Concrete curing and Wheat	S4 Hannover
UT3 Ennigerloh	Concrete curing	S4 Hannover
UT4 Cologne	Lignin	S3 Dusseldorf
UT5 Munchsmunster	Lignin	S3 Dusseldorf
UT6 Schwarzheide	Polyurethane	S7 Berlin
UT7 Leverkusen	Polyurethane	S7 Berlin
UT8 Salzgitter	Calcium carbonate	S1-S2-S4-S5-S6 Dresda-Wiesbaden-Hannover-Magdeburg-Potsdam
UT9 Bremen	Calcium carbonate	S1-S2-S4-S5-S7 Dresda-Wiesbaden-Hannover-Magdeburg-Potsdam
UT10 Kassel	Urea	S3 Dusseldorf
UT11 Hagen	Urea	S3 Dusseldorf
UT12 Leuna	Methanol	S4 Hannover
UT13 Wesseling	Methanol	S4 Hannover
UT14 Hamburg	Concrete by red mud	S3 Dusseldorf
UT15 Rackwitz	Concrete by red mud	S3 Dusseldorf

Figure S6 Results of CCUS supply chain design considering 30% of national demand of produced chemical compounds

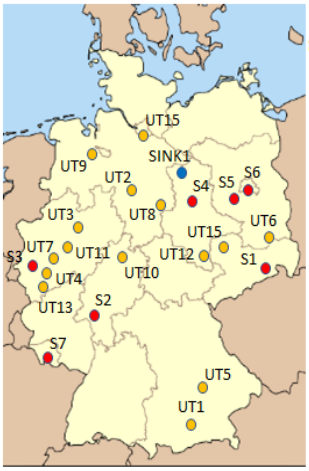

CO_2 Utilization/Storage	Production	CO_2 Source
SINK1 Altmark		S4 Magdeburg
UT1 Munich	Wheat	S3 Dusseldorf
UT2 Hannover	Concrete curing and Wheat	S6-S3 Berlin-Dusseldorf
UT3 Ennigerloh	Concrete curing	S6 Berlin
UT4 Cologne	Lignin	S3 Dusseldorf
UT5 Munchsmunster	Lignin	S3 Dusseldorf
UT6 Schwarzheide	Polyurethane	S3 Dusseldorf
UT7 Leverkusen	Polyurethane	S3 Dusseldorf
UT8 Salzgitter	Calcium carbonate	S1-S2-S4-S5-S7 Dresda-Wiesbaden-Magdeburg-Potsdam-Saarbrucken
UT9 Bremen	Calcium carbonate	S1-S2-S4-S5-S8 Dresda-Wiesbaden-Magdeburg-Potsdam-Saarbrucken
UT10 Kassel	Urea	S3 Dusseldorf
UT11 Hagen	Urea	S3 Dusseldorf
UT12 Leuna	Methanol	S3 Dusseldorf
UT13 Wesseling	Methanol	S3 Dusseldorf
UT14 Hamburg	Concrete by red mud	S4 Dusseldorf
UT15 Rackwitz	Concrete by red mud	S5 Dusseldorf

Figure S7 Results of CCUS supply chain design considering 40% of national demand of produced chemical compound

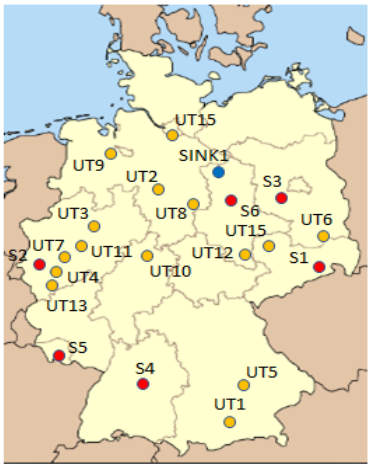

CO_2 Utilization/Storage	Production	CO_2 Source
SINK1 Altmark		S6 Magdeburg
UT1 Munich	Wheat	S5 Saarbrucken
UT2 Hannover	Concrete curing and Wheat	S4-S5 Stuttgart-Saarbrucken
UT3 Ennigerloh	Concrete curing	S5 Stuttgart
UT4 Cologne	Lignin	S5 Saarbrucken
UT5 Munchsmunster	Lignin	S5 Saarbrucken
UT6 Schwarzheide	Polyurethane	S2 Dusseldorf
UT7 Leverkusen	Polyurethane	S2 Dusseldorf
UT8 Salzgitter	Calcium carbonate	S3-S2 Potsdam-Dusseldorf
UT9 Bremen	Calcium carbonate	S3-S3 Potsdam-Dusseldorf
UT10 Kassel	Urea	S3 Potsdam
UT11 Hagen	Urea	S4 Potsdam
UT12 Leuna	Methanol	S1 Dresda
UT13 Wesseling	Methanol	S1 Dresda
UT14 Hamburg	Concrete by red mud	S2 Dusseldorf
UT15 Rackwitz	Concrete by red mud	S2 Dusseldorf

Figure S8 Results of CCUS supply chain design considering 50% of national demand of produced chemical compounds

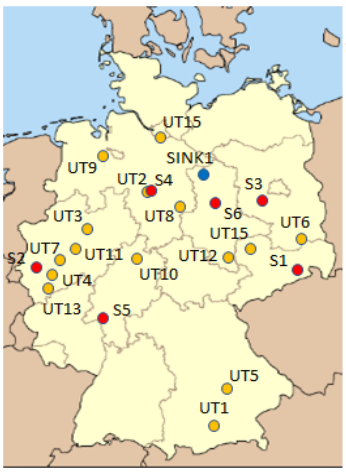

CO_2 Utilization/Storage	Production	CO_2 Source
SINK1 Altmark		S6 Magdeburg
UT1 Munich	Wheat	S2 Dusseldorf
UT2 Hannover	Concrete curing and Wheat	S2 Dusseldorf
UT3 Ennigerloh	Concrete curing	S2 Dusseldorf
UT4 Cologne	Lignin	S2 Dusseldorf
UT5 Munchsmunster	Lignin	S2 Dusseldorf
UT6 Schwarzheide	Polyurethane	S2 Dusseldorf
UT7 Leverkusen	Polyurethane	S2 Dusseldorf
UT8 Salzgitter	Calcium carbonate	S3-S4-S1-S5 Potsdam-Hannover-Dresda-Wiesbaden
UT9 Bremen	Calcium carbonate	S3-S4-S1-S6 Potsdam-Hannover-Dresda-Wiesbaden
UT10 Kassel	Urea	S2 Dusseldorf
UT11 Hagen	Urea	S2 Dusseldorf
UT12 Leuna	Methanol	S4 Hannover
UT13 Wesseling	Methanol	S4 Hannover
UT14 Hamburg	Concrete by red mud	S2 Dusseldorf
UT15 Rackwitz	Concrete by red mud	S2 Dusseldorf

Figure S9 Results of CCUS supply chain design considering 60% of national demand of produced chemical compounds

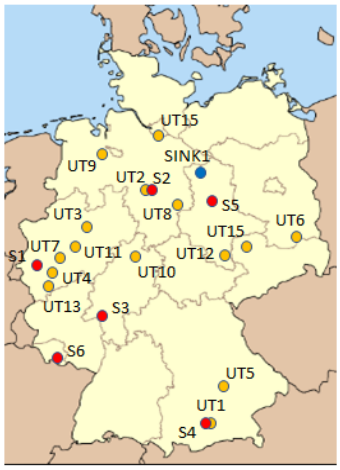

CO_2 Utilization/Storage	Production	CO_2 Source
SINK1 Altmark		S5 Magdeburg
UT1 Munich	Wheat	S4 Munich
UT2 Hannover	Concrete curing and Wheat	S4-S1 Munich-Dusselford
UT3 Ennigerloh	Concrete curing	S1 Dusseldorf
UT4 Cologne	Lignin	S6 Saarbrucken
UT5 Munchsmunster	Lignin	S6 Saarbrucken
UT6 Schwarzheide	Polyurethane	S4 Munich
UT7 Leverkusen	Polyurethane	S4 Munich
UT8 Salzgitter	Calcium carbonate	S3-S2-S4-S5 Wiesbaden-Hannover-Munich-Magdeburg
UT9 Bremen	Calcium carbonate	S3-S2-S4-S6 Wiesbaden-Hannover-Munich-Magdeburg
UT10 Kassel	Urea	S4 Munich
UT11 Hagen	Urea	S4 Munich
UT12 Leuna	Methanol	S4 Munich
UT13 Wesseling	Methanol	S4 Munich
UT14 Hamburg	Concrete by red mud	S1 Dusseldorf
UT15 Rackwitz	Concrete by red mud	S1 Dusseldorf

Figure S10 Results of CCUS supply chain design considering 70% of national demand of produced chemical compounds

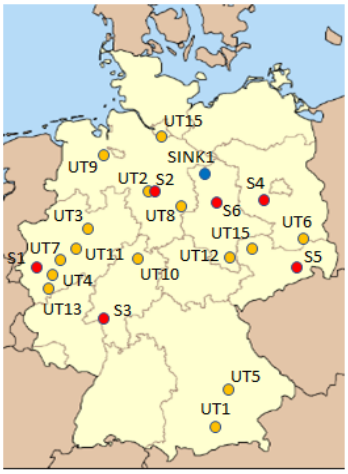

CO_2 Utilization/Storage	Production	CO_2 Source
SINK1 Altmark		S6 Magdeburg
UT1 Munich	Wheat	S1 Dusseldorf
UT2 Hannover	Concrete curing and Wheat	S1 Dusseldorf
UT3 Ennigerloh	Concrete curing	S1 Dusseldorf
UT4 Cologne	Lignin	S1 Dusseldorf
UT5 Munchsmunster	Lignin	S1 Dusseldorf
UT6 Schwarzheide	Polyurethane	S1 Dusseldorf
UT7 Leverkusen	Polyurethane	S1 Dusseldorf
UT8 Salzgitter	Calcium carbonate	S3-S2-S4-S5 Wiesbaden-Hannover-Potsdam-Dresda
UT9 Bremen	Calcium carbonate	S3-S2-S4-S6 Wiesbaden-Hannover-Potsdam-Dresda
UT10 Kassel	Urea	S1 Dusseldorf
UT11 Hagen	Urea	S1 Dusseldorf
UT12 Leuna	Methanol	S2 Hannover
UT13 Wesseling	Methanol	S2 Hannover
UT14 Hamburg	Concrete by red mud	S1 Dusseldorf
UT15 Rackwitz	Concrete by red mud	S1 Dusseldorf

Figure S11 Results of CCUS supply chain design considering 80% of national demand of produced chemical compounds

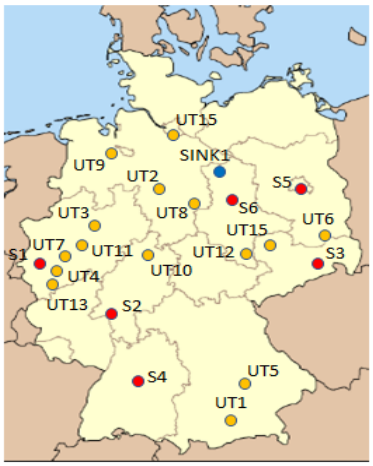

CO_2 Utilization/Storage	Production	CO_2 Source
SINK1 Altmark		S6 Magdeburg
UT1 Munich	Wheat	S1 Dusseldorf
UT2 Hannover	Concrete curing and Wheat	S1-S5 Dusseldorf-Berlin
UT3 Ennigerloh	Concrete curing	S5 Berlin
UT4 Cologne	Lignin	S1 Dusseldorf
UT5 Munchsmunster	Lignin	S1 Dusseldorf
UT6 Schwarzheide	Polyurethane	S1 Dusseldorf
UT7 Leverkusen	Polyurethane	S1 Dusseldorf
UT8 Salzgitter	Calcium carbonate	S2-S3-S4 Wiesbaden-Dresda-Stuttgart
UT9 Bremen	Calcium carbonate	S2-S3-S5 Wiesbaden-Dresda-Stuttgart
UT10 Kassel	Urea	S1 Dusseldorf
UT11 Hagen	Urea	S1 Dusseldorf
UT12 Leuna	Methanol	S4 Stuttgart
UT13 Wesseling	Methanol	S4 Stuttgart
UT14 Hamburg	Concrete by red mud	S1 Dusseldorf
UT15 Rackwitz	Concrete by red mud	S1 Dusseldorf

Figure S12 Results of CCUS supply chain design considering 100% of national demand of produced chemical compounds

References

Alexy, P., Kosıkova, B., Podstranska, G., 2000. The effect of blending lignin with polyethylene and polypropylene on physical properties, Polymer 41, 4901–4908.

Bloomberg, 2019. Available at: hhtp://www.bloomberg.com

Broek, M.V.D., Brederode, E., Ramírez, A., Kramers, L., Kuip, M.V.D., Wildenborg, T., Turkenburg, W., Faaij, A., 2010. Environmental modelling & software designing a cost-effective CO2 storage infrastructure using a GIS based linear optimization energy model. Environ. Modell. Softw. 25 (12), 1754–1768

Cemnet, 2019. Available at: https://www.cemnet.com/global-cement-report/country/germany

CCA, 2016. Available at: https://www.ima-europe.eu/sites/ima-europe.eu/files/publications/Renewability%20short%20statement_FINAL.PDF

Chemical-technology, 2019. Available at: https://www.chemicals-technology.com/projects/lyondellbasellhdpepl/; https://www.chemicals-technology.com/projects/schwarzheide/

Colacem, 2019. Available at: https://www.colacem.com/ww/en

Collodi, G., Azzaro, G., Ferrari N., 2017. Techno-Economic evaluation of HYCO plant integrated to Ammonia/Urea or methanol production with ccs. IEAGHG technical report 2017-03.

Converting, 2019. Available at: http://www.convertingquarterly.com/industry-news1/european-pe-film-demand-remains-strong-in-2016-exceeds-74-million-tonnes-up-1-over-2015

Covestro, 2019. Available at: hhtp://www.covestro.de

Dadcoalumina, 2019. Available at: http://www.dadcoalumina.com/about/

Dahowski, R., Dooley, J., Davidson, C., Bachu, S., Gupta, N., 2004. A CO2 Storage Supply Curve for North America, Proceedings of the 7. international conference on greenhouse gas control technologies.

Dow, 2019. Available at: hhtp://www.dow.com

En.stahl, 2019. Available at: en.stahl-online.de

Emshng-tech, 2019. Available at: www.emshng-tech.com

Erda, L., Wei, X., Hui, J., Yinlong, X.,Yue, L., Liping, B., Liyong, X., 2005. Climate change impacts on crop yield and quality with CO2 fertilization in China. Philos Trans R Soc Lond B Biol Sci., 360(1463) 2149–2154.

Fao, 2019. Available at: www.fao.org

Federal Ministry for the Environment, Nature conservation, Building and Nuclear safety. The German Government's Climate Action Programme 2020 Cabinet decision of 3 December 2014.

Globalsyngas, 2019. Available at: https://www.globalsyngas.org/resources/world-gasification-database/wesseling-methanol-plant-vi

Hägg, M.B., Lindbråthen, A., 2005. CO2capture from natural gas fired power plants by usingmembrane technology. Ind Eng Chem Res., 44(20):7668–75

Hank, C., Gelpke, S., Schnabl, A., White, R.J., Full, J., Wiebe, N., Smolinka, T., Schaadt, A., Henning, H.M., Hebling, C., 2018. Economics & carbon dioxide avoidance cost of methanol production based on

renewable hydrogen and recycled carbon dioxide – power-to-methanol, Sustainable Energy & Fuels, 6, 1113-1364

Hasan, M.M.F., First, E.L., Boukouvala, F., Floudas, C.A., 2015. A multi-scale framework for CO2 capture, utilization, and sequestration: CCUS and CCU, Computers and Chemical Engineering 81, 2–21.

Hasan, M.M.F., Boukouvala, F., First, E.L., Floudas, C.A., 2014. Nationwide, regional, and statewide CO2 capture, utilization, and sequestration supply chain network optimization. Ind Eng Chem Res 53, (18), 7489–7506.

Hendriks, C.A., Carbon Dioxide Removal from coal-Fired power plant. In department of science, technology, and society. Utrecht University. 1994: Utrecht, Netherlands.

Holler, S., Viebahn, P., 2011. Assessment of CO2 storage capacity in geological formations ofGermany and Northern Europe, Energy Procedia 4, 4897–4904.

Hydro, 2019. Available at: https://www.hydro.com/en/about-hydro/hydro-worldwide/germany/rackwitz/hydro-aluminium-gieberei-rackwitz-gmbh/

ICIS, 2019.Available at: https://www.icis.com/explore/resources/news/2017/07/28/10128588/germany-s-leuna-methanol-plant-running-well-after-maintenance/

Ineos, 2019. Available at: https://www.hydro.com/en/about-hydro/hydro-worldwide/germany/rackwitz/hydro-aluminium-gieberei-rackwitz-gmbh/

Jönsson, A.S., Wallberg, O., 2009. Cost estimates of kraft lignin recovery by ultrafiltration, Desalination, 237, Issues 1–3, 254-267.

Kali-gmbh, 2019. Available at: http://www.kali-gmbh.com/uken/company/locations/

Kalyanarengan Ravi, N., Van Sint Annaland, M., Fransoo, J.C., Grievink, J., Zondervan, E., 2017. Development and implementation of supply chain optimization framework for CO2 capture and storage in the Netherlands. Computer Chemical Engineering 102, 40–51.

Leonzio, G., Foscolo, P.U., Zondervan, E., 2019a. An outlook towards 2030: optimization and design of a CCUS supply chain in Germany, Computer and Chemical Engineering Journal, 125 499-513.

Leonzio, G., Foscolo, P.U., Zondervan, E., 2019b. Sustainable utilization and storage of carbon dioxide: Analysis and design of an innovative supply chain. Computers and Chemical Engineering 131 106569

Nguyen, T.B.H., Zondervan, E. 2018. Development and comparison of two novel process designs for the selective capture of CO2 from different sources, ACS Sustainable Chemistry & Engineering, 6 (4), 4845-4853.

Ochoa Bique, A., Nguyen, T.B.H., Leonzio, G., Galanopoulos, C., Zondervan, E. 2018. Integration of carbon dioxide and hydrogen supply chains, Computer Aided Chemical Engineering, 43, 1413-1418.

Ourworld, 2019. Available at: https://ourworldindata.org/fertilizer-and-pesticides

Ozkır, V., Baslıgil, H., 2013. Multi-objective optimization of closed-loop supply chains in uncertain environment. J. Clean. Prod. 41:114-125.

Papadopoulos, A.I., Seferlis, P., 2017. Process Systems and Materials for CO2 Capture: Modelling, Design, Control and Integration, John Wiley & Sons Ltd,

Patricio, J., Angelis-Dimakis, A., Castillo-Castillo, A., Kalmykova, Y., Rosado, L. 2017a. Region prioritization for the development of carbon capture and utilization technologies. Journal of CO2 Utilization 17, 50–59.

Plastics-Insight, 2019. Available at: https.//www.plasticsinsight.com

Plastics, 2019. Available at: https://www.plasticseurope.org/application/files/5715/1717/4180/Plastics_the_facts_2017_FINAL_for_website_one_page.pdf

Rochelle, G., Chen, E., Freeman, S., Van Wagener, D., Xu, Q., Voice, A., 2011. Aqueous piperazine asthe new standard for CO2capture technology. Chem Eng J. 171(3):725–33.

Roehrl, A., Toth, F., A critical comparison of geological storage of carbon dioxide and nuclear waste in Germany: status, issues, and policy implications, 8th Conference on Applied Infrastructure Research (INFRADAY), Berlin, Germany, 9-10 October 2009.

Serpa, J., Morbee, J., Tzimas, E., 2011. Technical and Economic Characteristics of a CO2 Transmission Pipeline Infrastructure, JRC62502 1-43.

Sikdar, S.K., Bier, M., Todd, P., 1990. Frontier in bioprocessing, CRC Press. Boca Raton, Florida.

Thyssenkrupp, 2019. Available at: https://www.thyssenkrupp-industrial-solutions.com/en/locations/europe-cis/uhde-high-pressure-technologies-germany/

Tredingeconomics, 2019. Availablet at: https://tradingeconomics.com/germany/permanent-cropland-percent-of-land-area-wb-data.html;

Vde, 2019.Available at: https://www.vdz-online.de/en/cement-industry/cement-sector/cementmarkets/

Von der Assen, N., Sternberg, A., Katelhon, A., Bardow, A., 2015, Environmental potential of carbon dioxide utilization in the polyurethane supply chain, Faraday Discuss., 183, 291-307.

Wheatatlas, 2019. Available at: http://wheatatlas.org/country/environment/DEU/0?AspxAutoDetectCookieSupport=1

Wolfgang Tegethoff, F., Calcium Carbonate: From the Cretaceous Period into the 21st Century, 2001. Springer Basel AG.

World-Grain, 2019. Available at: https://www.world-grain.com/articles/12540-germanys-wheat-production-bounces-back

Xiao, D., Xu, S., Brownbill, N.J., Paul, S., Chen, L.H., Pawsey, S., Aussenac, F., Su, B.L., Han, X., Bao, X., Liuad Z., and Blanc, F., 2018. Fast detection and structural identification of carbocations on zeolites by dynamic nuclear polarization enhanced solid-state NMR, Chem. Sci., 2018, 9, 8184–8193.

Zappa, W., Pilot-scale Experimental Work on the Production of Precipitated Calcium Carbonate (PCC) from Steel Slag for CO2 Fixation, Thesis submitted in partial fulfilment of the requirements for the degree of Master of Science in Technology Department of Energy Technology School of Engineering, Aalto University Espoo, 11th August 2014.

Zhang, S., Liu, L., Zhang, L., Zhuang, Y., Du. J. 2018. An optimization model for carbon capture utilization and storage supply chain: A case study in Northeastern China, Applied Energy 231 194–206

Zimmer, Y., Production Cost in the EU and in Third Countries: past Trends, Structures and Levels Global Partners: Workshop on the Outlook for EU Agriculture by COPA, COGECA, European Crop Protection & Fertilizers Europe Brussels, June 27th 2012;

Nomenclature

Indices

i = carbon dioxide source

j = carbon dioxide capture system

k = carbon dioxide storage sites and complementary utilization section

m = methanol production site

c = concrete production site

w = wheat production site

l = lignin production site

p = polyurethane production site

cc = calcium carbonate production site

u = urea production sit

cr = concrete by red mud production sit

Abbreviations

AIMMS = advanced interactive multidimensional modeling system

CC = carbon dioxide capture and compression capture costs [€/year]

CCUS = carbon capture utilization and storage [€/year]

CCP = calcium carbonate production costs

CCR = capital cost recovery

CDC = flue gas dehydration costs [€/year]

CIC = carbon dioxide capture and compression investment costs [€/year]

COC = carbon dioxide capture and compression operative costs [€/year]

CP = concrete curing production costs [€/year]

CRP = concrete by red mud production costs [€/year]

F_i/F = flue gas flow rate from source i [mol/s]

GHG = greenhouse gas

IC = maximum injection capacity per well [ton/year]

LP = lignin production costs [€/year]

MEA = monoethanolamine

MILP = mixed integer linear programming

N^{build}_{well} = number of well

NPV = net present value [€]

PBP = payback period [year]

PP = polyurethane production costs [€/year]

PSA = pressure swing adsorption

PZ = piperazine

SC = carbon dioxide storage costs [€/year]

SIC = carbon dioxide storage investment costs [€]

SOC = carbon dioxide storage operative costs [€/year]

TC = carbon dioxide transportation costs [€/year]

TH = time horizon

TIC = carbon dioxide transportation investment costs [M€]

TOC = carbon dioxide transportation operative costs [M€/year]

UP = urea production costs [€/year]

WP = wheat production costs [€/year]

Parameters

b = parameter in SIC [M€]

Calcium $Carbonate^{dem}$ = national calcium carbonate demand [ton/year]

$Concrete^{dem}$ = national concrete demand [ton/year]

Concrete by $red\ mud^{dem}$ = national concrete by red mud demand [ton/year]

C_k^{max} = maximum storage capacity at the storage site k [ton]

CR^{min} = minimum target for carbon dioxide reduction [ton/year]

CS_i = total carbon dioxide emission from each source i [ton/year]

$D_{i,k}/D_{i,c}/D_{i,w}/D_{i,p}/D_{i,cc}/D_{i,u}/D_{i,m}/D_{i,cr}/D_{i,l}$ = distance from source i to storage k/concrete c/wheat w/polyurethane p/calcium carbonate cc/urea u/methanol m/concrete by red mud/lignin l production site [km]

d_{well} = depth of well [km]

F_i/F = flue gas flow rate from each source i [mol/s]

F_t = terrestrial factor

$Lignin^{dem}$ = national lignin demand [ton/year]

m = parameter in SIC [M€/km], CIC and COC

$MeOH^{dem}$ = national methanol demand [ton/year]

n = parameter in CIC and COC

$Polyurethane^{dem}$ = national polyurethane demand [ton/year]

X = parameter equal to 1 if carbon dioxide is transported to a specific utilization site

x_{CO2} = carbon dioxide molar fraction

XS_i = carbon dioxide composition in the flue gas emission from source i [mol%]

XL_i = lowest carbon dioxide composition processing limit for capture plant j [mol%]

XH_i = highest carbon dioxide composition processing limit for capture plant j [mol%]

$Urea^{dem}$ = national urea demand [ton/year]

$Wheat^{dem}$ = national wheat demand [ton/year]

Variables

Binary

$X_{i,j,k}$ = 1 if carbon dioxide is captured from source i with technology j and sent to storage site k, otherwise 0

$Y_{i,j,k}$ = 1 if carbon dioxide is capture from source i with technology j and sent to storage/utilization site k, otherwise 0

Continuous

$Calcium\ carbonate_{i,j,cc}$ = fraction of captured carbon dioxide from source i with technology j sent to calcium carbonate production site cc

$Concrete\ by\ red\ mud_{i,j,cr}$ = fraction of captured carbon dioxide from source i with technology j sent to concrete production site by red mud cr

$Concrete_{i,j,c}$ = fraction of captured carbon dioxide from source i with technology j sent to concrete production site c

$FR_{i,j,k}$ = fraction of captured carbon dioxide from source i with technology j sent to storage site k

$Lignin_{I,j,l}$ = fraction of captured carbon dioxide from source i with technology j sent to lignin production site l

$Methanol_{i,j,m}$ = fraction of captured carbon dioxide from source i with technology j sent to methanol production site m

$Polyurethane_{i,j,p}$ = fraction of captured carbon dioxide from source i with technology j sent to polyurethane production site p

$Urea_{i,j,u}$ = fraction of captured carbon dioxide from source i with technology j sent to urea production site u

$Utilization_{i,j,k}$ = fraction of captured carbon dioxide from source i with technology j sent to overall utilization site k

$Wheat_{i,j,w}$ = fraction of captured carbon dioxide from source i with technology j sent to wheat production site w

Greek letters

α = parameter in CIC and COC

α_t = parameter in TIC

β = parameter in CIC and COC

β_t = parameter in TIC

γ = parameter in CIC and COC

Chapter V

Development of a CCUS supply chain for Italy

The mathematical model for the design of a carbon capture utilization and storage supply chain is applied for Italy in this chapter. The Mixed Integer Linear Programming model is considered, to minimize the total costs and reduce significantly carbon dioxide emissions, as required by national objectives to mitigate climate change. Carbon dioxide can be stored or utilized to produce through a power to gas system methane that is fed to the gas grid. In particular, different carbon capture utilization and storage supply chains with different storage sites (saline aquifers) are taken into account. Results show that the framework with the off-shore Adriatic sea as storage site is the most appropriate system, due to a low supply chain cost and the lowest level of economic incentives, as compared to other cases. The total costs of this supply chain are $7.34 \cdot 10^4$ *million €/year (953 €/ton*CO_2 *captured) and 16.1 Mton/year of methane are produced. The suggested supply chain does not result economically favorable without substantial financial incentives (80 €/ton*CO_2 *for carbon tax and 260 €/MWh for methane production). Comparing the developed supply chains that include simultaneous utilization and storage of carbon dioxide with a carbon capture and utilization supply chain shows that the latter is economically less favorable.*

V.1 Introduction

The strategic actions for Italy to reduce greenhouse gas emissions (GHG) are as follows: further dissemination of renewable energies, promoting of energy-efficiency projects that maximize sustainability benefits with the de-carbonization of energy system, doubling public investments allocated for research and development of clean-energy technologies, from € 222 million in 2013 to € 444 million in 2021. Also, it is necessary to reduce the final energy consumption by a total of 10 $Mton_{eq}$, to reach a 28% share of renewables in total energy consumption and a 55% share of renewables in electricity consumption, by 2030 (Italy's national energy strategy, 2017).

In this context, power to gas systems have an important role, because these processes can contribute to achieve the above objectives, exploiting renewable energies, reducing carbon dioxide (CO_2) emissions and also satisfying the national methane (CH_4) demand (Parra et al., 2017). In a power to gas system, renewable electric energy can be transformed into storable CH_4 via electrolysis and subsequent CO_2 hydrogenation through methanation, via the Sabatier reaction (Leonzio, 2017; Ma et al., 2018). Power to gas system is a promising way to manage and store fluctuating electricity produced by renewable energy sources, then a highly effective integration of renewables is obtained, reducing CO_2 emissions. It is clear that, these systems will have an important role inside the green and circular economy (Styring et al., 2011).

Studies related to the applicability of a power to gas process in Italy are published in the literature. In Guandalini et al. (2017), the potential application of a power to gas system using renewable energies is considered for the near future of Italy. In Colbertaldo et al. (2018) the role of a power to gas system in an integrated multi-energy system (especially transport sector) is studied.

The integration of a power to gas system in a carbon capture utilization (CCUS) supply chain has not been considered in the literature before. These considerations bring to the development of a CCUS supply chain integrated to a power to gas system in Italy. Moreover, the production of CH_4 is specifically selected for the Italian regions because the potential production of methanol (CH_3OH), investigated already in the literature, is very low there (Patricio et al., 2017). On the other hand, Italy would have the opportunity to satisfy the national CH_4 demand, producing methane by hydrogenation of CO_2. In addition, an existing capillary network for CH_4 distribution is present in Italy.

For the supply chain, ten Italian regions, those with grater CO_2 emissions, are selected as CO_2 sources, Verbania is selected as the utilization site with a power to gas plant, while different saline aquifers (Malossa San Bartolomeo, Pesaro sea, off-shore Adriatic sea, Cornelia, off-shore Marche, off-shore Calabria ionic sea, Sulcis area) are selected as potential storage sites. Seven CCUS supply chain configurations, each with a different storage site, are considered to be described through a deterministic Mixed Integer Linear Programming (MILP) model. Another point of strength for this work is the comparative evaluation of the different carbon supply chains, each of them with different storage sites, and the comparison with a carbon capture utilization (CCU) system to understand the importance of the storage site in the management of CO_2.

V.2 Model development

V.2.1 Problem statement

For the developed carbon supply chain, the following assumptions are made:

- capture plants and CO_2 sources are located at the same place, to avoid the transportation of flue gas from CO_2 source to capture treatment sites;
- one to one coupling: one source node can be connected to only one capture node in the storage and utilization section and each capture node can receive from only one source node (Kalyanarengan Ravi et al., 2017);
- CO_2 is transported from source to storage and utilization sites always via pipeline, chosen as the most efficient system;
- CH_4 is produced by the catalytic Sabatier reaction with complete CO_2 hydrogenation, in a power to gas system, where hydrogen (H_2) is produced by water electrolysis through proton exchange membrane (PEM) electrolyzer using renewable power energy, as solar energy (a portion of electricity from network is any case present (Matzen and Demirel, 2016)) (Parra et al., 2017; Leonzio, 2017; Di Felice and Micheli, 2015; ENI, 2019);

- for the power to gas system, the material balance, based on the stoichiometric conditions of Sabatier reaction, is taken into account to evaluate the amount of CH_4 that is produced from the captured CO_2 sent to the utilization section;
- the structure, and consequently the mathematical model, is in steady state conditions over a horizon time of 25 year: the aim of the research is, in fact, to design the supply chain at its optimum conditions;
- CH_4 production is constant over time due to the stationary conditions and it is sent to the gas grid;
- CH_4 produced in the CO_2 utilization section can be sold at a stable price, set by market;
- distances between source and utilization/storage sites are calculated from their latitude and longitude (Kalyanarengan Ravi et al., 2017);
- the profitability of the framework is estimated by evaluating CH_4 production cost, including also the electrolyzer process;
- only one storage and utilization site are considered for each supply chain due to the high storage capacity and high assumed production capacity;

With these assumptions, a mathematical model is developed for the supply chain, when the following information is provided:

- CO_2 sources: locations, yearly CO_2 emissions, CO_2 composition and flow rate of flue gases (Green report, 2017; Green, 2014);
- CO_2 capture and compression technologies: used materials and costs (Nguyen and Zondervan, 2018; Zhang et al., 2018);
- CO_2 transportation: costs and distances (Serpa et al., 2011; Distance, 2019);
- power to gas plant: location and CH_4 production cost (Reichert, 2012; Renewable Energy, 2012);
- CO_2 storage sites: location, type, capacity and costs (Hendriks, 1994; Hasan et al., 2014; Donda et al., 2011; Plaisant et al., 2017; Moia et al., 2012);

The model so developed allows to decide which CO_2 sources to use from a given set of sources and the yearly CO_2 flow rate to be captured from each selected source; which technology and material combinations should be used for the CO_2 capture process from each selected source; the amount of captured CO_2 sent to the storage and utilization and the amount of produced CH_4.
The objective function minimizes the total costs, including CO_2 capture and compression costs, CO_2 transportation costs, CO_2 storage costs, CH_4 production costs via power to gas.

V.2.2 CCUS supply chain model

To develop a mathematical model as a MILP model for each CCUS and CCU supply chain, sets, parameters, variables, constraints, equations and the objective function should be defined, as in the

following sections. AIMMS (Advanced Interactive Multidimensional Modeling System) software is used to model the supply chains analyzed in this study.

V.2.2.1 Sets

Sets are considered to define each element inside the supply chain. CO_2 sources are indicated by "i", CO_2 capture technologies are indicated by "j", while CO_2 geological storage and utilization sites are indicated by "k".

V.2.2.2 Parameters

Several parameters are used in the suggested model, as the following: CR^{min}, the minimum target for the overall CO_2 reduction (ton/year); CS_i, the total CO_2 emission from each source i (ton/year); F_i, the total flue gas flow rate from each source i (mol/s); XS_i, CO_2 composition in the flue gas from source i (mol%); XL_i, the lowest CO_2 composition processing limit for the capture plant j (mol%); XH_i, the highest CO_2 composition processing limit for the capture plant j (mol%); C_k^{max}, the maximum storage capacity at the storage site k (ton);

V.2.2.3 Variables

To select a specific CO_2 source, a CO_2 capture plant and a CO_2 storage site a binary variable $X_{i,j,k}$ is introduced (1, if CO_2 from source 'i' is captured using a technology/material combination in capture plant 'j' and is stored in storage site 'k'; 0, otherwise). To choose the CO_2 capture technology/material a binary variable $Y_{i,j,k}$ is used (1 if CO_2 is captured from source 'i', with capture technology/material 'j' and it is sent to the storage/utilization site 'k'; 0 otherwise). To determine the CO_2 fraction that is captured from each source, 0-1 continuous variables are used: $FR_{i,j,k}$ (the fraction of CO_2 captured from source 'i' using capture plant 'j' and stored to the storage site 'k'), $MR_{i,j,k}$ (the fraction of CO_2 captured from source 'i' using capture plant 'j' and processed in the methane production site 'k').

V.2.2.4 Constraints

The following constraint for $X_{i,j,k}$, the variable defined above, ensures that the captured CO_2 is not divided in many storage sites (see Eq. V.1)

$$\sum_{(j,k)\in(J,K)} X_{i,j,k} \leq 1 \qquad \forall\, i \in I \tag{V.1}$$

This constraint also guarantees the one to one coupling assumption between sources and capture systems in the storage section.

Each storage site has a maximum storage capacity that should be not exceeded through the following constraint (see Eq. V.2):

$$\sum_{(j,i)\in(J,I)} CS_i \cdot FR_{i,j,k} \leq \frac{C_k^{max}}{TH} \qquad \forall \quad k \in K \qquad (V.2)$$

where CS_i is the total CO_2 emission from source 'i', C_k^{max} is the maximum storage capacity of the storage site 'k', TH is the time horizon of supply chain in year and $FR_{i,j,k}$ is the continuous variable defined above. To achieve the minimum target related to CO_2 emissions reduction, the following constraint is used (see Eq. V.3):

$$\sum_{(i,j,k)\in(I,J,K)} CS_i \cdot FR_{i,j,k} + CS_i \cdot MR_{i,j,k} \geq CR^{min} \qquad (V.3)$$

where CS_i is the total CO_2 emission from source 'i', $FR_{i,j,k}$ and $MR_{i,j,k}$ are the continuous variables defined above and CR^{min} is the minimum target for CO_2 emission reduction.

For each selected source, no more than 90% of CO_2 is captured, then the following constraint is set (see Eq. V.4)

$$\sum_{j \in J} FR_{i,j,k} + MR_{i,j,k} \leq 0.9 \qquad \forall\, (i,k) \in (I,K) \qquad (V.4)$$

where $FR_{i,j,k}$ and $MR_{i,j,k}$ are the continuous variables defined above.

Not all the considered technologies can be used to capture CO_2 from all sources with a product purity of 90% for CO_2 (Kalayanarengan Ravi et al., 2017). This depends on the composition of CO_2 in the feed, and the following constraint is considered (see Eq. V.5):

$$\sum_{(k)\in(K)} (XH_j - XS_i) \cdot (XS_i - XL_j) \cdot X_{i,j,k} \geq 0 \qquad \forall\, (i,j) \in (I,J) \qquad (V.5)$$

where XS_i is CO_2 composition in flue gas emission from source "i", XL_j is the lowest CO_2 composition processing limit for the capture technology "j", XH_j is the highest CO_2 composition processing limit for the capture technology "j" (mol%). This specific for CO_2 purity is assumed for the storage site, while for the utilization site the required purity is achieved in the methanol production site.

Only one capture technology/material should be selected for each CO_2 source in the utilization and storage section, then the following constraint is set (see Eq. V.6):

$$\sum_{(j,k)\in(J,K)} Y_{i,j,k} \leq 1 \qquad \forall\ i \in I \qquad (V.6)$$

In order to convert the non linear mathematical model into a linear one, the glover linearization is applied, considering the following constrains (see Eqs. V.7-V.8):

$$0 \cdot Y_{i,j,k} \leq MR_{i,j,k} \leq 0.9 \cdot Y_{i,j,k} \qquad \forall\, (i,j,k) \in (I,J,K) \qquad (V.7)$$

$$0 \cdot X_{i,j,k} \leq FR_{i,j,k} \leq 0.9 \cdot X_{i,j,k} \qquad \forall (i,j,k) \in (I,J,K) \qquad (V.8)$$

where $FR_{i,j,k}$, $X_{i,j,k}$, $MR_{i,j,k}$ and $Y_{i,j,k}$ are already defined, while 0.9 is used because at most 90% of CO_2 is captured from each CO_2 source.

The national annual CH_4 demand of 70.9 billion m^3/year (46.5 Mton/year) (Alverà, 2017), is not a constraint of practical relevance, because the overall amount of captured CO_2 is not enough to produce CH_4 at this rate.

V.2.2.5 Equations

The total CO_2 capture and compression costs (€/year) are obtained by the following relation (see Eq. V.9):

$$CC_{i,j,k} = CDC_{i,j,k} + CIC_{i,j,k} + COC_{i,j,k} \qquad \forall (i,j,k) \in (I,J,K) \qquad (V.9)$$

where $CDC_{i,j,k}$ are the flue gas dehydration costs, $CIC_{i,j,k}$ are the investment costs and $COC_{i,j,k}$ are the operating costs. Generally, the saturated flue gas is dehydrated via tri-ethylene glycol absorption with a cost of 9.28 € per ton of CO_2 (including capital and investment costs) (Kalayanarengan Ravi et al., 2017). For amine absorption, no dehydration is necessary. The investment and operating costs (€/year) are a function of flue gas flow rate and CO_2 composition and are provided by the following correlations (Zhang et al., 2018) (see Eqs. V.10-V.11):

$$CIC_{i,j,k,} = \alpha_{I,j} \cdot Y_{i,j,k} + (\beta_{I,j} \cdot {x_{co2,i}}^{n_{I,j}} + \gamma_{I,j}) \cdot {F_{i,j,k}}^{m_{I,j}} \qquad \forall (i,j,k) \in (I,J,K) \qquad (V.10)$$

$$COC_{i,j,k} = \alpha_{o,j} \cdot Y_{i,j,k} + (\beta_{o,j} \cdot {x_{co2,i}}^{n_{o,j}} + \gamma_{o,j}) \cdot {F_{i,j,k}}^{m_{I,j}} \qquad \forall (i,j,k) \in (I,J,K) \qquad (V.11)$$

where $\alpha_{I,j}$, $\alpha_{o,j}$, $\beta_{I,j}$, $\beta_{o,j}$, $\gamma_{I,j}$, $\gamma_{o,j}$, $n_{I,j}$, $n_{o,j}$, $m_{o,j}$, $m_{I,j}$ are fixed parameters depending on the used process and material (see table S1 of chapter IV), $x_{CO2,i}$ is CO_2 composition in flue gas from source "i", $F_{i,j,k}$ is flue gas flow rate in mol/s, $Y_{i,j,k}$ is the binary variable defined above. For absorption with ionic liquids, different correlations for the investment and operating costs (€/year) are used, respectively, as follows (Nguyen and Zondervan, 2018) (see Eq. V.12-V.13):

$$CIC_{i,j,k} = (\alpha_{I,j} \cdot F_{i,j,k} + \beta_{I,j} \cdot Y_{i,j,k}) \cdot {x_{co2,i}} + \gamma_{I,j} \cdot {F_{i,j,k}}^{m_{I,j}} \qquad \forall (i,j,k) \in (I,J,K) \qquad (V.12)$$

$$COC_{i,j,k} = (\alpha_{o,j} \cdot F_{i,j,k} + \beta_{o,j} \cdot Y_{i,j,k}) \cdot {x_{co2,i}} + \gamma_{o,j} \cdot {F_{i,j,k}}^{m_{O,j}} \qquad \forall (i,j,k) \in (I,J,K) \qquad (V.13)$$

where $\alpha_{I,j}$, $\alpha_{o,j}$, $\beta_{I,j}$, $\beta_{o,j}$, $\gamma_{I,j}$, $\gamma_{o,j}$, $m_{o,j}$, $m_{I,j}$ are fixed parameters (see table S1 of chapter IV), $x_{CO2,i}$ is CO_2 composition in flue gas from source "i", $F_{i,j,k}$ is flue gas flow rate in mol/s and $Y_{i,j,k}$ is the binary variable defined above.

A linear model for CO_2 transportation costs is used, as proposed by Serpa et al. (2011). The total costs (M€/year) comprise the investment costs ($TIC_{i,j,k}$) and the operating costs ($TOC_{i,j,k}$) according to the following equation (see Eq. V.14):

$$TC_{i,j,k} = CCR{\cdot}TIC_{i,j,k} + TOC_{i,j,k} \qquad \forall\,(i,j,k)\ \in (I,J,K) \qquad (V.14)$$

with CCR the capital cost recovery factor, calculated at an interest rate of 10% and 25 years, while other terms (respectively in M€ and M€/year) are (see Eqs. V.15-V.16):

$$TIC_{i,j,k} = \left(\alpha_t \cdot CS_i \cdot FR_{i,j,k} + \beta_t \cdot X_{i,j,k}/P_{i,j,k}\right) \cdot F_T \cdot \left(D_{i,k}/P_{i,k} + 16\right)\ \forall\,(i,j,k)\ \in (I,J,K) \quad (V.15)$$

$$TOC_{i,j,k} = 4\% \cdot TIC_{i,j,k} \qquad \forall\,(i,j,k)\ \in (I,J,K) \qquad (V.16)$$

where α_t is 0.019 and β_t is 0.533 (Serpa et al., 2011), $D_{i,k}$ and $P_{i,k}$ are the distance between source and storage sites and between source and utilization sites respectively, F_T is a terrestrial factor, corresponding to 1.2 (Broek et al., 2010), 16 km are added to the distance to consider additional paths related to process (Dahowski et al., 2004), $X_{i,j,k}$ is the binary variable defined before, $P_{i,j,k}$ is a parameter with a value of 1 if CO_2 is transported to the utilization section, CS_i is the amount of CO_2 in Mton/year. The operational costs are taken as 4% of investment costs (Kalayanarengan Ravi et al., 2017).

The total CO_2 storage costs (€/year) comprise the investment costs (SIC_k) (€) and the operating costs (SOC_k) (€/year), as in the following relation (see Eq. V.17):

$$SC_k = CCR{\cdot}SIC_k + SOC_k \qquad \forall\,k\ \in K \qquad (V.17)$$

with CCR defined above, where the investment costs are calculated as (Hendriks, 1994) (see Eq. V.18):

$$SIC_k = (m \cdot d_{well} + b) \cdot N_{well}^{build}{}_k \qquad \forall\,k\ \in K \qquad (V.18)$$

where m and b are parameters corresponding to 1.53 M€/km and 1.23 M€ respectively (Ochoa Bique, 2018), d_{well} is the depth of the well, and N_{well}^{build} is the number of wells which need to be built (Hasan et al., 2014) (see Eq. V.19):

$$N_{well}^{build}{}_k = \frac{\sum_{(i,j)\in(I,J)} CS_i \cdot FR_{i,j,k}}{IC} \qquad \forall\,k\ \in K \qquad (V.19)$$

as a function of stored CO_2 and of maximum injection capacity per well. The operating costs (€/year) are 4% of investment costs (Kalayanarengan Ravi et al., 2017) (see Eq. V.20):

$$SOC_k = 4\% \cdot SIC_k \qquad \forall\,k\ \in K \qquad (V.20)$$

CH_4 production costs in a power to gas process considering the overall system (methane reactors, ancillary equipment and electrolyzer system for hydrogen production) is set to 300 €/MWh (Reichert, 2012; Leonzio, 2017; Hassan et al., 2019; Ma et al., 2018). These high costs are due to the high cost of electricity, that in Italy is about 130 €/MWh (Clean Energy Wire, 2018). In fact, Reichert (2012) shows in his work a sensitivity analysis of CH_4 production costs and for an electricity cost of the same order of the Italian value, the considered CH_4 production costs are suggested. Ma et al. (2018) report that CH_4 generation costs via

power to gas are between 13.5 €/kWh and 17 €/kWh in 2014, based on the electric price of 5 €/kWh. When the cost of electricity in Italy is taken into account, the value of 364 €/MWh is obtained for the CH_4 production costs. This last value is comparable with that reported by Reichert (2012).

Reichert (2012) shows also that the production costs of 1 MWh of H_2 via electrolysis are 209 €. Considering that to produce 1 MWh of CH_4, 1.19 MWh of H_2 are required, the corresponding costs for H_2 are 250 €. Then, 83% of CH_4 production costs has to be related to H_2 costs. Of course, lower H_2 production costs can be achieved if the electrolyzer is operating only during off-pick hours and days, assuming a plant storage section for hydrogen that ensures continuous operation of the methanation reactor.

V.2.2.6 Objective function

The objective function of carbon supply chain considering the minimization of the total costs is given as (see Eq. V.21):

$$\emptyset = \sum_{(i,j,k)} CC_{i,j,k} + TC_{i,j,k} + CH_4P_k + SC_k \qquad (V.21)$$

where $CC_{i,j,k}$ are CO_2 capture and compression costs, $TC_{i,j,k}$ are CO_2 transportation costs, SC_k are CO_2 storage costs, CH_4P_k are CH_4 production costs. In the optimized system, the total costs are minimized with the constraint to safeguard the reduction of CO_2 emissions required by the climate change issue.

V.2.3 Case study

The trend of CO_2 emissions in Italy is shown in Figure V.1, where CO_2 emissions include power industry, additional industrial combustion, non-combustion, buildings and transport emissions.

Figure V.1 Trend of carbon dioxide emissions in Italy by sector (Green report, 2017)

Even if CO_2 emissions in 2016 were lower compared to 1990, in absolute terms (352 Mton CO_2 in 2016 against 423 Mton CO_2 in 1990), per capita (6 ton/year in 2016 against 7.4 in 1990), and in relation to the results of economic activities (0.171 ton CO_2/kUSD in 2016 against to 0.243 ton CO_2/kUSD in 1990), a CO_2 reduction trend could not be found since 2014 (Green report, 2017). In fact, since 2014 CO_2 emissions have increased, and in 2015 CO_2 emissions increased by 1.3% compared to 2014.

Actually, the national target for CO_2 emissions in 2030 is 275 MtonCO_2/year (Gracceva et al., 2017).

Ten Italian regions, those with higher CO_2 emissions, are selected as sources for the supply chain, as shown in Table V.1.

Table V.1 Data about CO_2 source sites for the selected Italian regions inside the supply chain (Green, 2014; Zhang, 2018)

	CO_2 source	CO_2 emissions (Mton/year)	CO_2 in flue gas (mol%)	Flue gas (mol/s)
1	Puglia	68.6	17	$2.91 \cdot 10^5$
2	Lombardy	46.8	18	$1.87 \cdot 10^5$
3	Sicily	41.5	4	$7.48 \cdot 10^5$
4	Lazio	28.2	14	$1.45 \cdot 10^5$
5	Sardinia	26.4	13	$1.46 \cdot 10^5$
6	Veneto	22.5	21	$7.72 \cdot 10^6$
7	Emilia Romagna	21.8	13	$1.21 \cdot 10^5$
8	Piedmont	19.7	18	$7.89 \cdot 10^4$
9	Liguria	17.6	15	$8.45 \cdot 10^4$
10	Tuscany	16.8	11	$1.11 \cdot 10^5$

The nodes for the framework are located at the capital cities of each region (selected as CO_2 source): Bari, Milan, Palermo, Rome, Cagliari, Venice, Bologna, Turin, Genoa, Florence, respectively for Puglia, Lombardy, Sicily, Lazio, Sardinia, Veneto, Emilia Romagna, Piedmont, Liguria, Tuscany.

Seven CO_2 storage sites are selected for the CCUS supply chains: Malossa San Bartolomeo, Pesaro sea, off-shore Adriatic sea, Cornelia, off-shore Marche, off-shore Calabria ionic sea, Sulcis area are the storage sites, as shown in Figure V.2 (Moia et al., 2012). These areas contain geological reservoirs mineralized by sea water and are called saline aquifers. These are characterized by conditions of temperature and pressure favorable to store CO_2 above the critical point. CO_2 storage in saline aquifers is considered as a suitable technology, probably because it provides the largest potential storage volume (Bachu, 2000; Burnol et al., 2015). Generally, the estimation of storage capacity in saline aquifers is very complex due to different physical and chemical trapping mechanisms, that simultaneously occur at different rates and timescales (Bradshaw et al., 2007). Table V.2 characterizes each CO_2 storage site, defining the storage capacity, depth of well and maximum injection capacity.

Figure V.2 CO_2 storage and CO_2 utilization sites of CCUS and CCU supply chains

Table V.2 Characterization of CO_2 storage sites in the CCUS supply chains of Italy (Moia et al., 2012; Donda et al., 2011; Plaisant et al., 2017)

Storage site	Maximum storage capacity ($MtonCO_2$)	Depth of well (m)	Maximum injection capacity (Mton/year)
Malossa San Bartolomeo	380	1590	0.3
Pesaro sea	240	1400	0.5
Off-shore Adriatic sea	820	1400	1
Cornelia	200	1400	0.5
Off-shore Marche	400	1270	1
Off-shore Calabria ionic	100	1280	1
Area Sulcis	15	1250	0.2

Verbania is chosen as CO_2 utilization site, replacing an existing biogas plant, producing 27540 m^3/day of biogas form livestock effluents (cattle and swine) (Renewable Energy, 2012). Then, the utilization section is chosen in a site where CH_4 could be already produced with a traditional system (the upgrading of biogas). Regarding the renewable energy for the electrolyzer system, solar energy is expected to be the most available renewable energy source in the coming future for Italy and many photovoltaic systems are already installed in this region (Colbertaldo et al., 2018; ENI, 2019).

Only one utilization site is taken into account in this research, because it is supposed with unlimited production capacity. Indeed, a multiplicity of power to gas systems would be needed to satisfy the national demand, requiring a more complex supply chain. In this analysis, the considered production center symbolizes all possible power to gas systems in Italy and provides a first estimate of CO_2 between the utilization and storage sections. Moreover, only one utilization site is considered because few biogas plants, seen as potential locations of a power tog as system, are present in Italy.

In fact, Lombardy, Emilia Romagna, Veneto and Piedmont are the most important regions hosting biogas plants in Italy. The oldest plant is in Rome at the Malagrotta landfill and is in operation since the mid-90s. It is capable of treating about 200 m^3/h of biogas (collected from the urban waste landfill). The upgraded bio-methane is not injected into the grid and is used as biofuel in vehicles. Other plants are demonstration plants and no one is connected to the gas grid (Maggioni and Pieroni, 2016). Finally, an important industrial plant producing bio-methane from organic wastes is located in Montello (Montello, 2018).

In Figure V.2, the utilization site chosen for the supply chains is shown on the map of Italy. Overall, the study is of course a simplification of the reality and the grid size of supply chain optimization is rather large (geographic region). The outcomes of such large grids also lead to "centralized" strategies.

Distances between stationary CO_2 source, utilization and storage sites are provided in Table V.3 (Distance, 2019).

Table V.3 Distance (km) between CO_2 source and storage and utilization sites (Distance, 2019)

	Verbania	Malossa San Bartolomeo	Pesaro sea	Off-shore Adriatic sea	Cornelia	Off-shore Marche	Off-shore Calabria Ionic	Area Sulcis
Puglia	986.4	894.5	536.8	293.3	493.5	466.3	481.5	1009.2
Lombardy	102.3	37.6	369.9	577.9	587.3	584.6	1057.3	883.1
Sicily	1569.2	1477.3	1192.5	1248	1136.2	1109	474.3	465.6
Lazio	674.5	582.6	300.9	212.2	206.9	303.2	511.4	593.4
Sardinia	978.8	893.6	912.2	810	815	810.1	942.3	
Veneto	362.2	231.4	297.4	203	326.9	512	1017.4	911.3
Emilia Romagna	316.6	224.7	235.4	367.3	193.1	231.2	874	760.4
Piedmont	153	176.1	479.8	720.4	509.9	702.8	1174.3	929.4
Liguria	220.8	183.3	444.8	670.1	471	660.6	481.8	760.1
Tuscany	416.7	324.8	255.9	402.1	299	403.7	756	676.4

Regarding capture technology, the absorption using monoethanolamine solution (MEA) at 30wt% or ionic liquid (IL) as 1-butyl-3-methylimidazolium acetate ([bmim][Ac]), pressure swing (PSA) and vacuum swing (VSA) adsorption using the zeolite 13X, membrane using the fixed-site-carrier (FSC) polyvinyl amine (PVAm) are available in the design of supply chains, because these are the most used and more efficient (Wang et al., 2011; Nguyen and Zondervan, 2018).

V.3 Results and discussion

The CCUS supply chains taken into account have 7 different CO_2 storage sites, with a high storage capacity, keeping the same CO_2 source and utilization sites. Then, 7 different CCUS supply chains are considered, in addition to 1 CCU system.

To solve the model, CPLEX 12.7.1 is the solver that is selected. The computer processor is 2.5 GHz while the memory is 4 GB.

The MILP model of CCUS supply chains is made of 711 variables (50 integer variables) and 684 constraints. The solution is found in some seconds and with a maximum of 100 iterations. For the CCU supply chain, the MILP model is composed by 460 variables (50 integer variables) and 482 constraints. The problem is solved in 1.69 s with 142 iterations.

Results of CCUS and CCU supply chains are shown in Table V.4, indicating for each considered carbon supply chain, the selected CO_2 sources, the capture technology/material chosen for each source and the amount of CO_2 that is stored or used (also shown in Figure V.3). It is possible to see that changing CO_2 storage changes the selected carbon capture technology/material inside the supply chain. In fact, the different storage sites have different characteristics influencing, in addition to the different distances, the terms inside the objective function and then the results.

Table V.4 Topology of CCUS and CCU supply chains (*For the number see Table V.1)

Storage site	**Destination of captured CO_2 - Regions of Capture**		**Capture technology in each Region**	**Yearly rate of CO_2 captured in each Region (Mton/year)**
Malossa san Bartolomeo (a)	Utilization	1, 7, 8	1=Membrane 7=MEA absorption 8=MEA absorption	1=24.4 7=19.6 8=17.7
	Storage	2	2=MEA absorption	2=15.3
Pesaro sea (b)	To utilization	1,7,8	1=Membrane 7=MEA absorption 8=MEA absorption	1=30 7=19.6 8=17.7
	To storage	2	2=IL Absorption	2=9.6
Off-shore Adriatic sea (c)	To utilization	1,7,8	1=MEA absorption 7=MEA absorption 8=MEA absorption	1=6.82 7=19.6 8=17.7
	To storage	2	2=MEA absorption	2=32.8
Cornelia (d)	To utilization	1,7,8	1=MEA absorption 7=MEA absorption 8=MEA absorption	1=39.6 7=11.6 8=17.7
	To storage	7	7=MEA absorption	7=8
Off-shore Marche (e)	To utilization	1,7,8	1=Membrane 7=Membrane 8=PSA	1=39.6 7=3.64 8=17.7
	To storage	7	7=IL absorption	7=16

Table V.4 (Continued)

Storage site	Destination of captured CO_2 - Regions of Capture		Capture technology in each Region	Yearly rate of CO_2 captured in each Region (Mton/year)
Off-shore Calabria Ionic (f)	To utilization	1,7,8	1=MEA absorption 7=MEA absorption 8=MEA absorption	1=35.6 7=19.6 8=17.7
	To storage	9	9=IL absorption	9=4
Area Sulcis (g)	To utilization	1,7,8	1=Membrane 7=Membrane 8=Membrane	1=39 7=19.6 8=17.7
	To storage	5	5=PSA	5=0.6
(h)	To utilization	2,7,8	2=MEA absorption 7=Membrane 8=IL absorption	2=39.6 7=16.9 8=17.7
	To storage	-	-	-

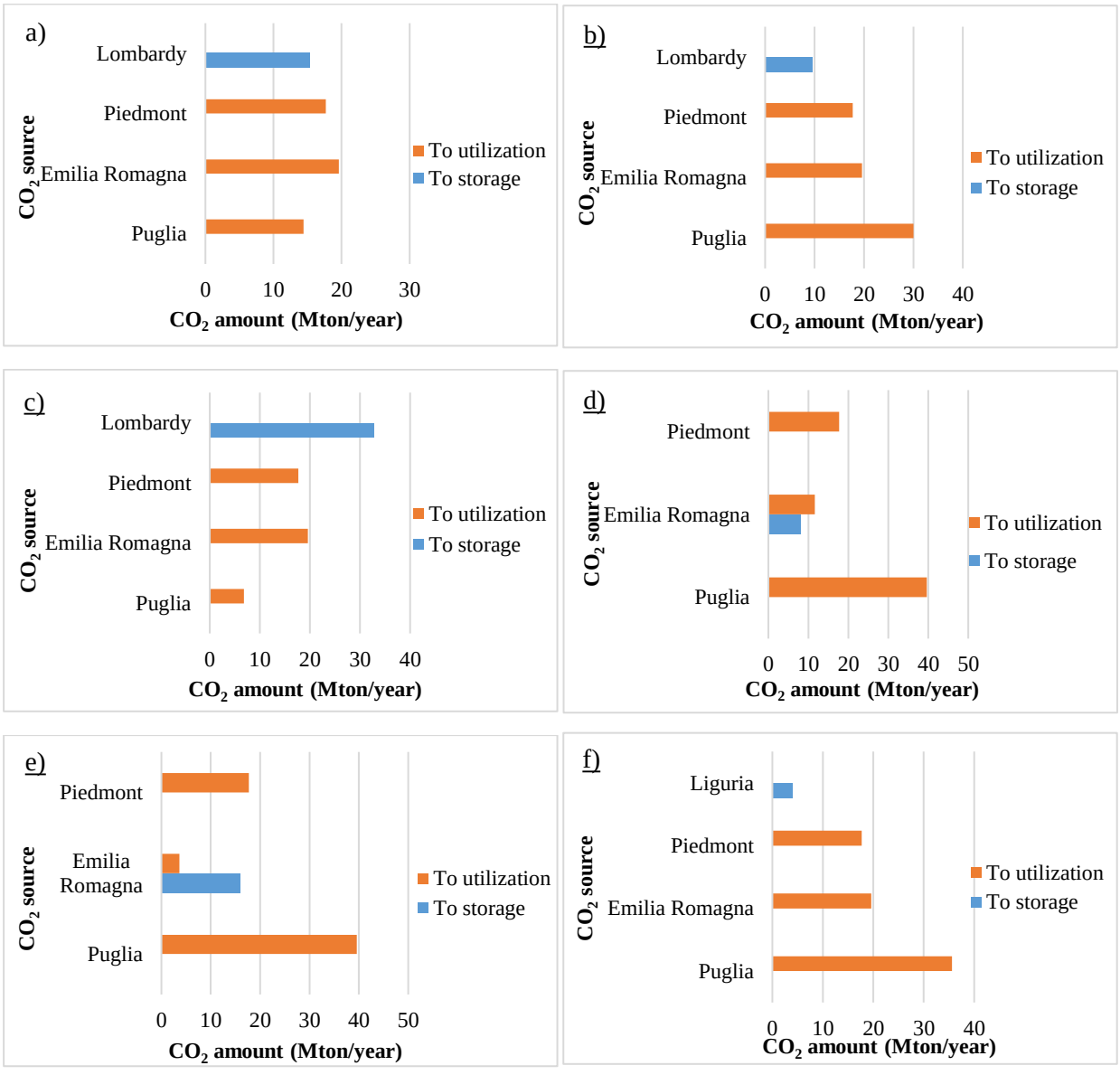

Figure V.3 (Following)

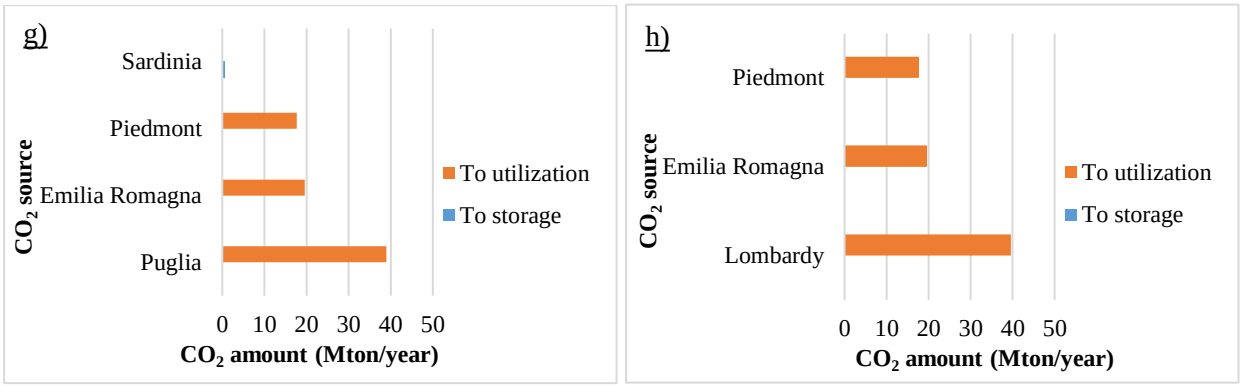

Figure V.3 Amount of CO_2 captured from each source and sent to utilization and/or storage: a) CCUS supply chain with Malossa San Bartolomeo as storage site; b) CCUS supply chain with Pesaro sea as storage site; c) CCUS supply chain with off-shore Adriatic sea as storage site; d) CCUS supply chain with Cornelia as storage site; e) CCUS supply chain with offshore Marche as storage site; f) CCUS supply chain with offshore Calabria Ionic storage site; g) CCUS with Area Sulcis as storage site; h) CCU supply chain.

The topology of these supply chains is also summarized in Figure V.4.

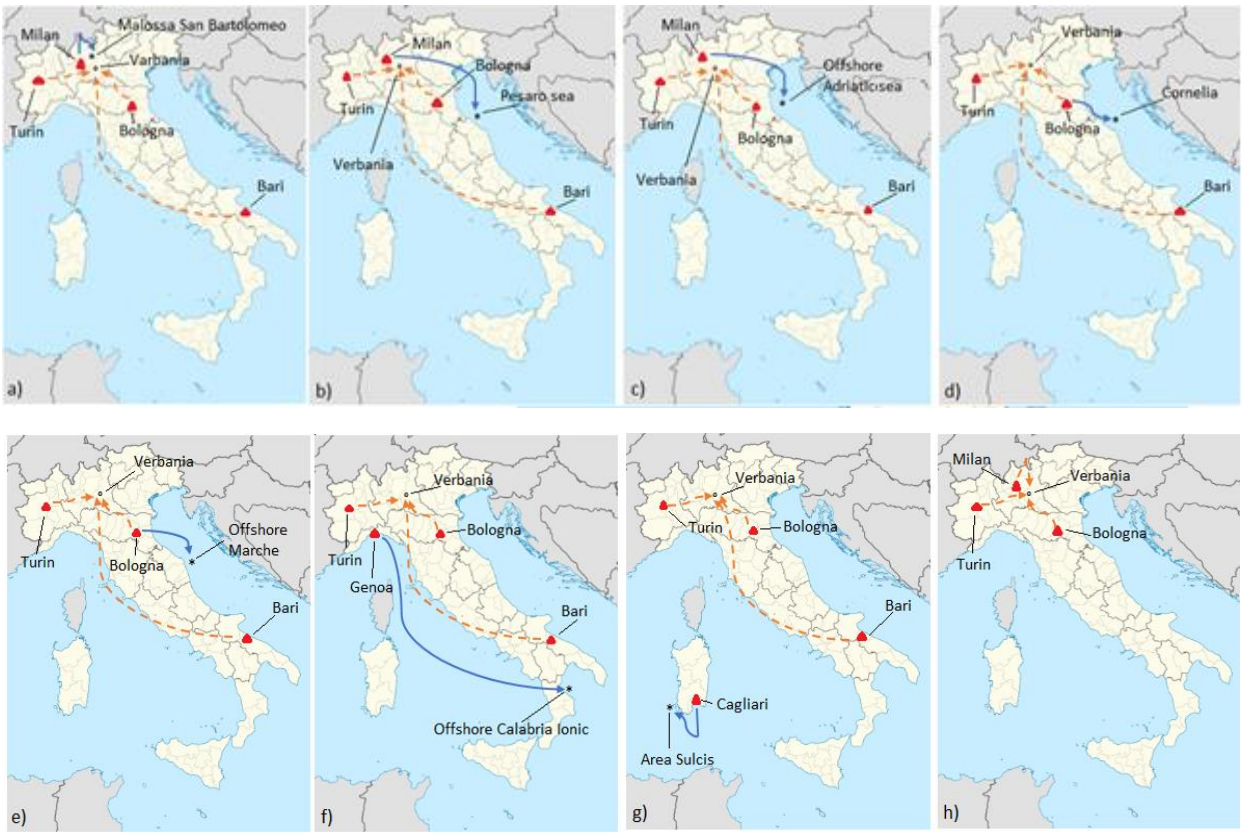

Figure V.4 Results of carbon supply chain network: a) CCUS supply chain with Malossa San Bartolomeo as storage site; b) CCUS supply chain with Pesaro sea as storage site; c) CCUS supply chain with Offshore Adreatico sea as storage site; d) CCUS supply chain with Cornelia as storage site; e) CCUS supply chain with Offshore Marche as storage site; f) CCUS supply chain with Offshore Calabria Ionic storage site; g) CCUS with Area Sulcis as storage site; h) CCU supply chain. (Legend: ▲ CO_2 source; * storage site; ° utilization site, – – – CO_2 transportation from source to utilization, —— CO_2 transportation from source to storage).

Overall, from the results it is evident that MEA absorption is the most convenient technology for CO_2 capture from flue gas, due to lower costs. Membrane capture system is also preferred in some cases, followed, in three cases, by ionic liquid absorption. Membrane and ionic liquid absorption are generally better utilized due to relative low costs (Hasan et al., 2012; Nguyen and Zondervan, 2018). VSA is never selected and used in the supply chains, as also reported in Kalyanarengan Ravi et al. (2017) and Zhang et al. (2018). In only one case PSA is chosen as capture technology.

In particular, when Malossa San Bartolomeo is used as storage site, CO_2 from Lombardy region is sent to the storage using MEA absorption, while Puglia, Emilia Romagna and Piedmont are CO_2 sources related to the utilization section, using for the first source a membrane system and MEA absorption for the others. Here membrane system is chosen due to the highest CO_2 flow rate than that in other sources treated with MEA absorption.

In the CCUS supply chain with Pesaro as storage site, MEA absorption is also used in connection to the utilization section, in particular for Emilia Romagna and Piedmont CO_2 sources. An additional CO_2 source in the utilization section is Puglia, treated by a membrane system. For the storage section, this CCUS supply chain considers Lombardy as CO_2 source using IL absorption. Also in this case, a membrane system is selected for the highest CO_2 flow rate while IL absorption for the lowest CO_2 flow rate.

In the alternative CCUS supply chain with off-shore Adriatic sea as storage site, MEA absorption is used for all selected CO_2 sources. Here, Puglia, Emilia Romagna and Piedmont are CO_2 sources for the utilization section, while Lombardy is CO_2 source for the storage section.

This same condition is present in the CCUS supply chain with Cornelia as storage site. However, Puglia, Emilia Romagna, Piedmont are CO_2 sources for the utilization section, while Emilia Romagna is CO_2 source for the storage section.

In these two cases, MEA absorption is selected because it can allow to reach the lowest total costs of the supply chain.

Also, in the CCUS supply chain with off-shore Calabria Ionic as storage site, MEA absorption is the preferred capture technology. In fact, all CO_2 sources related to the utilization (Puglia, Emilia Romagna, Piedmont) use MEA absorption as capture technology. In the storage section, Liguria uses IL absorption to capture CO_2, due to the lowest flue gas flow rate.

The second preferred capture technology, membrane system, is used for the CCUS supply chains with off-shore Marche and Area Sulcis as storage sites. In the second case, membrane system is used for all CO_2 sources related to the utilization section (Puglia, Emilia Romagna, Piedmont), while PSA, with the lowest flue gas flow rate and relative low CO_2 composition, is used for the storage section. In the first case, membrane is also used for two CO_2 sources in the utilization section (Puglia and Emilia Romagna), while PSA and IL absorption are selected for the other CO_2 sources.

On the other hand, in the CCU supply chain, the chosen CO_2 sources are Lombardy, Emilia Romagna and Piedmont that use, respectively, MEA absorption, membrane (due to the lowest costs) and IL absorption (due to the lowest flue gas flow rate) as capture systems.

In all considered cases, the minimum target for reduction of CO_2 emissions is achieved.

In addition to the topology, an economic analysis is shown in Table V.5 and in Figure V.5. Here costs, methane yields, revenues, set carbon tax and economic incentives, net methane production costs are presented for each considered supply chain.

Table V.5 Economic results of the analyzed carbon supply chains (* for storage site see Table V.4; ° the total costs are not considering carbon tax and economic incentives, then a higher value than revenue is obtained.

Storage site (*)	**Cost categories (milion€/year)**		**Methane Yield (Mton/year)**	**Revenue (million€/year)**	**Carbon tax (€/ton)**	**Economic incentives (€/MWh)**	**net Methane production costs (€/MWh)**
a	CO_2 capture and compression	358.6	22.5	87600	80	260	23.4
	CO_2 storage	193					
	CO_2 transportation	1.52					
	Methane production	101127					
	Total costs °	101700					
b	CO_2 capture and compression	508.3	24.5	95600	80	260	24.6
	CO_2 storage	67.3					
	CO_2 transportation	1.52					
	Methane production	110300					
	Total costs°	110900					
c	CO_2 capture and compression	999.4	16.1	62700	80	260	19.1
	CO_2 storage	115					
	CO_2 transportation	1.52					
	Methane production	72300					
	Total costs°	73400					
d	CO_2 capture and compression	202.7	25.1	97900	80	260	24.4
	CO_2 storage	56.11					
	CO_2 transportation	1.52					
	Methane production	112900					
	Total costs°	113200					
e	CO_2 capture and compression	858	22.2	86500	80	260	24.1
	CO_2 storage	52.8					
	CO_2 transportation	1.52					
	Methane production	99800					
	Total costs°	100700					

Table V.5 (Continued)

Storage site (*)	Cost categories (milion€/year)		Methane Yield (Mton/year)	Revenue (million€/year)	Carbon tax (€/ton)	Economic incentives (€/MWh)	net Methane production costs (€/MWh)
f	CO_2 capture and compression	1960	26.5	108000	80	270	19.4
	CO_2 storage	13.26					
	CO_2 transportation	1.52					
	Methane production	119500					
	Total costs°	121500					
g	CO_2 capture and compression	33.34	27.8	10400	80	270	15.2
	CO_2 storage	9.8					
	CO_2 transportation	1.52					
	Methane production	125000					
	Total costs°	125100					
h	CO_2 capture and compression	2750	28	113000	80	270	21.8
	CO_2 storage	-					
	CO_2 transportation	1.52					
	Methane production	126000					
	Total costs°	128800					

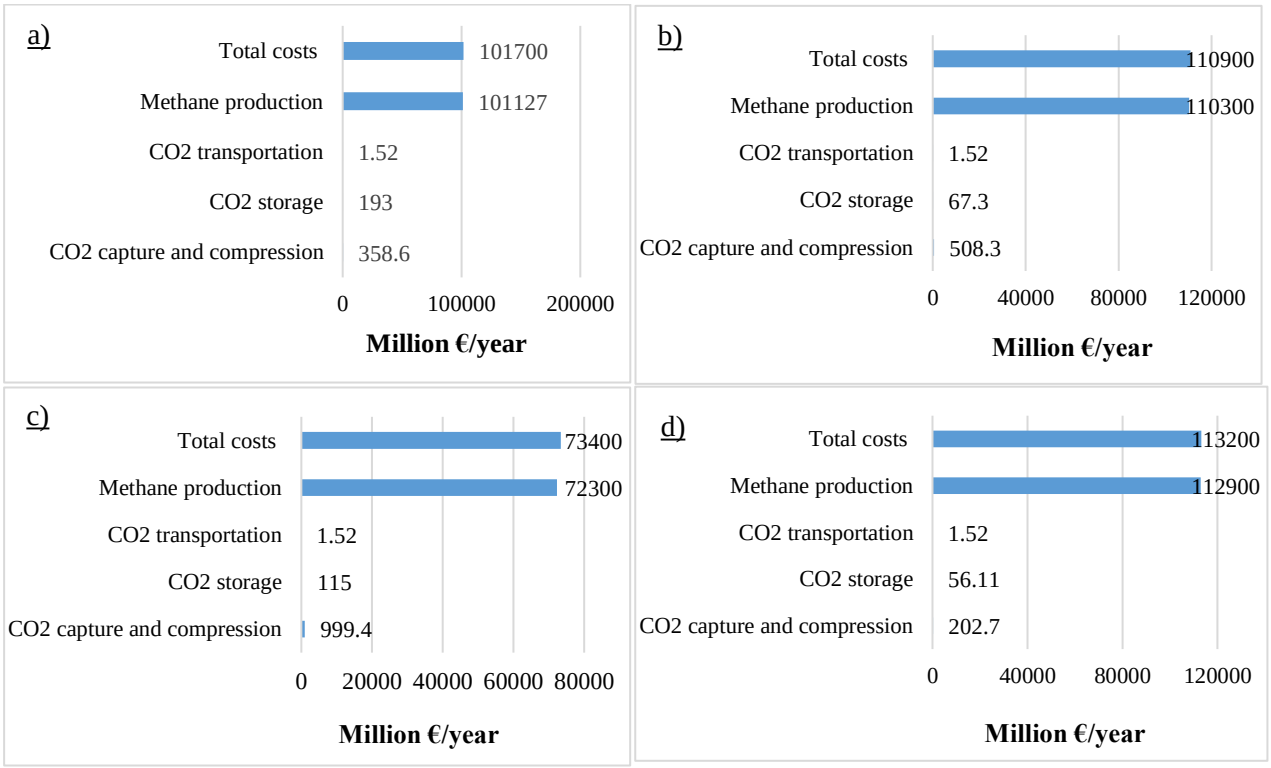

Figura V.6 (Following)

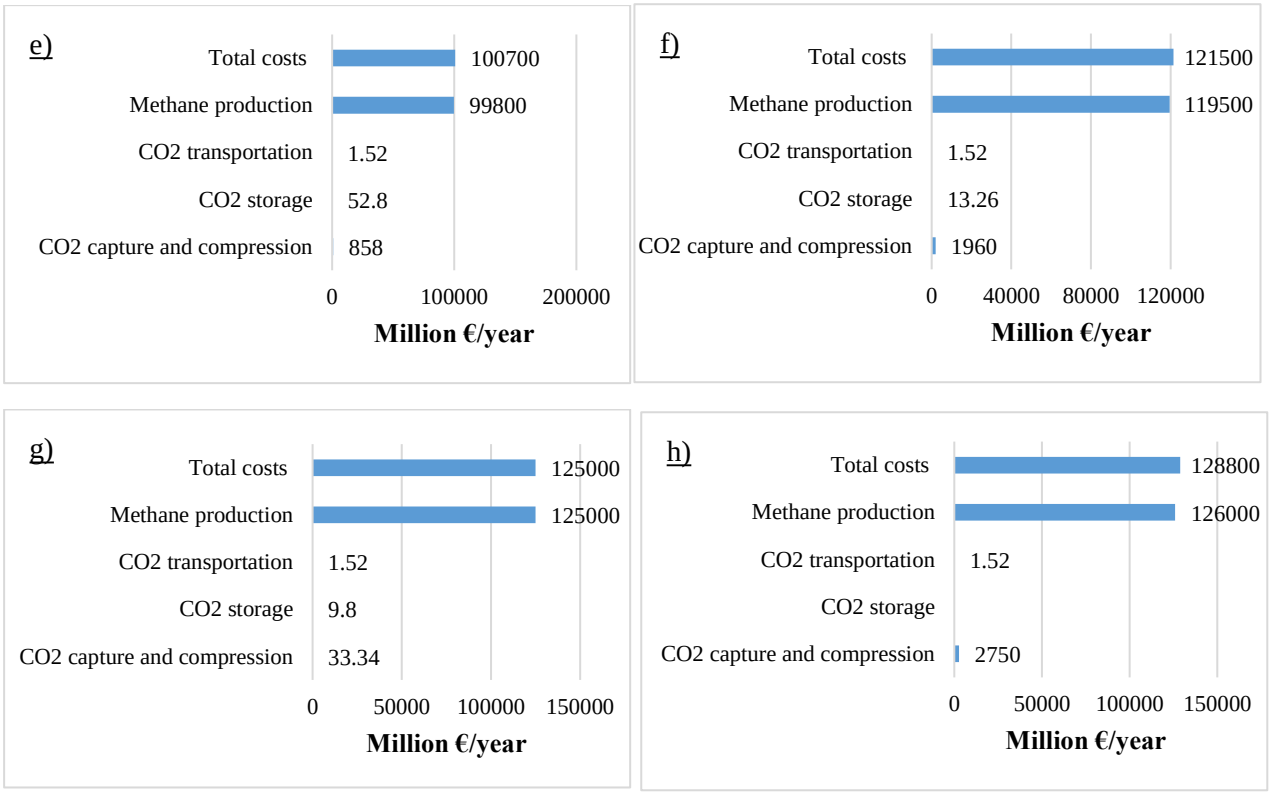

Figure V.6 Cost analysis of: a) CCUS supply chain with Malossa San Bartolomeo as storage site; b) CCUS supply chain with Pesaro sea as storage site; c) CCUS supply chain with off-shore Adriatic sea as storage site; d) CCUS supply chain with Cornelia as storage site; e) CCUS supply chain with off-shore Marche as storage site; f) CCUS supply chain with off-shore Calabria Ionic as storage site; g) CCUS with Area Sulcis as storage site; h) CCU supply chain

With Malossa San Bartolomeo used as storage site inside the CCUS supply chain, the optimized total costs are as follows: the total costs are $1.017 \cdot 10^5$ million€/year (301.64 €/MWh or 1321 €/tonCO_2 captured) with CO_2 capture and compression costs of $3.586 \cdot 10^2$ million€/year, CH_4 production costs of $1.011 \cdot 10^5$ million€/year, CO_2 transportation costs of 1.520 million €/year and 193 million €/year are CO_2 storage costs. When Pesaro sea is used as storage site in the CCUS supply chain, the optimized total costs are $1.109 \cdot 10^5$ million€/year (301.90 €/MWh or 1440 €/tonCO_2 captured). In particular, CO_2 compression and capture costs are 508.30 million€/year, CO_2 transportation costs are equal to 1.520 million€/year, CO_2 storage costs are 67.30 million€/year while CH_4 production costs through a power to gas process are $1.103 \cdot 10^5$ million€/year.

For the off-shore Adriatic sea as storage site, the optimized total costs of CCUS supply chain are $7.340 \cdot 10^4$ million€/year (304.62 €/MWh or 953 €/tonCO_2 captured). CO_2 compression and capture costs are $9.994 \cdot 10^2$ million€/year, CO_2 transportation costs are 1.52 million€/year, CO_2 storage costs are 115 million€/year while CH_4 production costs are $7.23 \cdot 10^4$ million€/year.

For the CCUS supply chain with Cornelia as storage site, the total costs are $1.132 \cdot 10^5$ million€/year (300.77 €/MWh or 1470 €/tonCO_2 captured), CO_2 storage costs and CH_4 production costs are respectively 56.11 million€/year and $1.129 \cdot 10^5$ million€/year. CO_2 compression and capture costs are 202.70 million€/year while CO_2 transportation costs are 1.52 million€/year.

When off-shore Marche is used as storage site, the total costs are $1.007 \cdot 10^5$ million€/year (302.65 €/MWh or 1308 €/tonCO_2 captured), while CO_2 storage costs and CH_4 production costs are respectively 52.80 million€/year and $9.98 \cdot 10^4$ million€/year. CO_2 transportation costs are 1.52 million€/year while CO_2 capture and compression costs are 858 million€/year.

For the CCUS supply chain with off-shore Calabria Ionic as storage site, the total costs are $1.215 \cdot 10^5$ million€/year (304.89 €/MWh or 1577 €/tonCO_2 captured). CO_2 compression and capture costs are $1.96 \cdot 10^3$ million€/year, CO_2 transportation costs are 1.52 million€/year, CO_2 storage costs are 13.26 million€/year while CH_4 production costs are $1.195 \cdot 10^5$ million€/year.

The total costs of CCUS supply chain with Area Sulcis as storage site are of $1.251 \cdot 10^5$ million€/year (299.96 €/MWh or 1627 €/tonCO_2 captured), including CO_2 capture and compression costs (33.34 million€/year), CH_4 production costs ($1.250 \cdot 10^5$ million€/year), CO_2 storage costs (9.80 million€/year) and CO_2 transportation costs (1.52 million€/year).

The analysis of costs for the CCU supply chain follows: total costs are $1.288 \cdot 10^5$ million€/year (306.43 €/MWh or 1671 €/tonCO_2 captured), CO_2 compression and capture costs are $2.750 \cdot 10^3$ million€/year, CO_2 transportation costs are 1.52 million€/year, CH_4 production costs are $1.260 \cdot 10^5$ million€/year, while 28 Mton/year of CH_4 are produced. The supply chain has the highest costs.

It is possible to see, that the total costs of a carbon supply chain with a power to gas system in the utilization section is in the range of 953 €/tonCO_2 captured and 1671 €/tonCO_2 captured. These high values are due to high CH_4 production costs that are in the range of $7.23 \cdot 10^4$ million€/year and $1.26 \cdot 10^5$ million€/year.

In fact, as also shown in Figure V.6, from the above analysis is evident that the main item in global costs is CH_4 production costs with the power to gas process that includes also H_2 production by means of electrolyzers. Here, the most significant contribution is the electrolysis process (Graf et al., 2014; Müller-Syring et al., 2013; Hassan et al., 2019). To support these results, Gotz et al. (2016) write that a power to gas process might play an important role in the future energy system, however, technical and economic barriers have to be overcome before it can become commercially successful. This determines a significant effect on the totals cost of supply chain.

The relatively high cost of CO_2 capture is also reported by Steeneveldt et al. (2006) and Kalayanarengan Ravi et al. (2017).

The amount of CH_4 that is produced for all considered supply chains is around 20 Mton/year. In particular, the highest amount of CH_4 is produced in the CCU supply chain (28 Mton/year) followed by the CCUS supply chain with Area Sulcis as storage site (27.8 Mton/year), while the lowest amount of CH_4 is produced in the CCUS supply chain with off-shore Adriatic sea as storage site (16.1 Mton/year). The different amount

of produced CH_4 depends on storage capacity: if a lower storage capacity is present, a higher amount of CH_4 is produced with the aim to achieve the same target of CO_2 emissions reduction.

For all analyzed cases, considering that CH_4 can be sold at a price of 25 €/MWh (Eurostat, 2018) revenues are calculated, as reported in Table V.5. Revenues are between $1.13 \cdot 10^5$ million€/year and $1.04 \cdot 10^4$ million€/year.

However, in order to have a positive profit, economic incentives and carbon tax should be considered. Then, for the considered supply chains, the costs for ton of captured CO_2 should decrease with these considerations.

Economic incentives, in fact, should be obtained according to the Directive 2013/12/5 by feeding methane into the gas network and according to the Directive 6/12/2012 for the production of H_2 in an electrolyzers using renewable power. A carbon tax equal to 80 €/tonCO_2 should be considered, even if not yet established in Italy (In Italy, actually, carbon tax is not present, however the average value of carbon tax present in Europe is considered for this study (Effective Carbon Price, 2018)). With this level of carbon tax, for each analyzed case, the value of economic incentives is found in order to have a positive profit. The calculation is done in the following way. A new value for the total costs of a supply chain is obtained subtracting to the optimized total costs carbon tax and economic incentives, while the profit margin is obtained as new total costs less revenues. At a fixed value of carbon tax, then economic incentives are progressively changed in calculations until a positive profit is obtained.

Generally, economic incentives should be in the range of 260 €/MWh and 270 €/MWh of CH_4 produced.

In these conditions, it is possible to conclude that the required incentives represent a high fraction of the total costs, (for example these are 86% of total costs for the CCUS supply chain with Malossa San Bartolomeo storage site), then the power to gas system still remains not convenient as a chemical storage of energy (Di Costanzo, 2017). A substantial development of technologies involved in the power to gas system and the increase of exploitation of renewable energy resources are needed to make this system interesting for the issue of energy storage.

Considering economic incentives and carbon tax, net CH_4 production costs are calculated and estimated to be in the range 15.2 €/MWh and 24.6 €/MWh.

Net CH_4 production cost is influenced by the total costs of supply chain (and by the structure of the supply chain defined by a particular storage site) and by the amount of produced CH_4. The storage site then influences the optimized structure of the system and then its total costs. Keeping constant the global amount of captured CO_2, at lower total costs, a lower net CH_4 production cost is ensured, while a higher amount of CH_4 ensures a lower net CH_4 production cost. The combined effect of these two parameters determines the effective CH_4 production cost.

The comparison of different cases shown in Table V.5 shows that the CCUS supply chain with off-shore Adriatic sea as storage site ensures to have a low total cost of supply chain, with the lowest value of economic incentives, compared to the other cases. In fact, in this case the estimated net CH_4 production

cost is 19.1 €/MWh while economic incentives are 260 €/MWh. Considering economic incentives and carbon tax, the net total costs of supply chain is, instead, of 59.69 €/tonCO_2 captured, a value comparable with those reported in literature (Zhang et al., 2018).

For the best CCUS supply chain, considering the data reported by Matzen and Demirel (2016), $7.09 \cdot 10^5$ GJ/year of renewable energies, through photovoltaic systems, are required by the electrolyzer producing 7.41 Mton/year of H_2. About 54 electrolyzers with a capacity of 10 MW should be considered for this carbon supply chain (Dolman and Madden, 2015).

In the CCUS supply chain with Area Sulcis as storage site, even if a lower net CH_4 production cost is obtained (15.2 €/MWh), however, higher economic incentives (270 €/MWh) are required.

Regarding the CCU supply chain, this is clearly not a good economic choice: even if economic incentives of 260 €/MWh are considered, this system is not profitable.

Actually, CH_4 production in Italy is 6 billion m^3/year (3.9 Mton/year) (Global Energy Statistical Yearbook, 2018), while CH_4 demand is 46.5 Mton/year. To satisfy this demand, Italy should import the remaining CH_4 (about 43 Mton/year). Using the CCUS supply chain with off-shore Adriatic sea as storage site, producing 16.1 Mton/year of CH_4 (about 35% of national demand), it is possible to reduce the import of CH_4 to 26.9 Mton/year.

The obtained results suggest that CO_2 storage is very important to have the most economically profitable supply chain with the established reduction of emissions. CCS technology alone has the potential to reduce greenhouse gas emission by 20% by 2050 (Todd, 2011). Actually, a plain CCU has not sense. CO_2 is captured for environmental problems, and to assure a significant reduction of emissions it is necessary to store it, because the annual amount of CO_2 emitted in the atmosphere is simply much larger than the demand of CO_2-based products. In CCU systems, the CO_2 demand is limited by the amount of chemicals that have to be produced, i.e. CO_2 sources at smaller scales should be used (IEA and UNIDO, 2011). CO_2 utilization should not be considered as an alternative technology to carbon capture and storage, but as a complementary technology realizing the overall technology of CCUS inside the circular economy (Bringezu et al., 2014).

According to the COP21 Paris agreement, CCU systems should be considered further to reduce emissions and to achieve the fixed targets, in addition to storage systems. As reported by Ericson et al. (2015) and Mikkelsen et al. (2010), CCU system is a technology used to improve the development of CCS systems through CCUS systems.

CO_2 utilization itself does not allow the direct reduction of emissions, but only reduces the used fossil raw resources (Naims, 2016). It is worth to underline that CO_2 incorporated in each product will ultimately be emitted again into the atmosphere, then, according to the lifetime of each product, CO_2 might just be stored for days or weeks to years or even decades (Styring et al., 2011; von der Assen et al., 2013). For these reasons, a CCU supply chain does not allow the primary strategic ambition to contribute significantly to mitigating climate change but rather needs to be considered as a component in a larger mitigation strategy (Bruhn et al., 2016). Cuéllar-Franca and Azapagic (2015), Sternberg and Bardow (2015), von der Assen

and Bardow (2014) demonstrate that CCU systems have not necessarily a positive effect on the environment but are more related to political strategies of resources utilization, reducing the used amount of fossil raw materials or process energies. Then it is important also the storage that is recognized as an emission reduction instrument.

Several actions have to be developed to promote the CCUS supply chain: capture technologies need to be improved until they become commercially competitive, best options for CO_2 transportation networks need to be ascertained, storage sites have to be identified, industrial processes that use CO_2 as feedstock need to be deployed, and the general public should know and recognize the "CCUS chain" as an alternative to CO_2 emissions mitigation (Perez Fortes et al., 2014).

V.4 Conclusions

In this chapter, a power to gas system, producing methane, is integrated in different CCUS supply chains (with different storage sites as saline aquifers) and in a CCU supply chain for Italy, that is an European Country with noticeable GHG emissions. In literature, no power to gas systems are integrated in a carbon supply chain, then the novelty of this investigation is clear.

The systems are designed through MILP models, minimizing the total costs and reducing the amount of CO_2 emissions according to the environmental policy.

Results show that in each CCUS supply chain, financial incentives (related to carbon tax and CH_4 production from renewable energy) are required for the economic feasibility. A comparison of the considered frameworks shows that with the supply chain using the off-shore Adriatic sea storage site, the supply chain cost is low, with the lowest required economic incentives, then it is the best economic solution. For this system, total costs are $7.34 \cdot 10^4$ million€/year without economic incentives, and 16.1 Mton/year of CH_4 are produced, so that the net CH_4 production cost is 19 €/MWh when a proper level of incentives is considered (80 €/ton of avoided carbon dioxide emission and 260 €/MWh of methane produced). In this way, Italy can reduce the import of methane substantially, as mentioned above.

The obtained results show that, a CCU supply chain system is not a good solution, due to the high net CH_4 production cost and the highest level of economic incentives, although a higher CH_4 production is ensured. Then, it is important to have a storage site inside the supply chain. In fact, carbon capture and storage aims at climate change mitigation, according to the environmental policy, while carbon capture and utilization aims to reduce fossil resources consumption by reusing the emitted carbon dioxide and shifting industrial processes toward renewables. The option of CO_2 utilization alone is not sufficient to achieve national and international climate change mitigation; the support of carbon storage is required.

References

Alverà, M., 2017. Snam Rete Gas Ten-year network development plan of the natural gas transmission network 2017-2026, Document prepared by Snam Rete Gas S.p.A. In compliance with the D.L. 93 of 11 June 2011 and subse quent amendments and additions.

Bachu, S., 2000. Sequestration of CO2 in geological media: Criteria and approach for site selection in response to climate change. Energy Convers Manage 41, 953–70.

Bradshaw, J., Bachu, S., Bonijoly, D., Burruss, R., Holloway, S., Christensen, N.P., et al. 2007. CO2 storage capacity estimation: Issues and development of standards. Int J Greenh Gas Control 1, 62–8.

Bringezu, S., 2014. Carbon recycling for renewable materials and energy supply: recent trends, long-Term options, and challenges for research and development. J. Ind. Ecol. 18, 327–340.

Broek, M.V.D., Brederode, E., Ramírez, A., Kramers, L., Kuip, M.V.D., Wildenborg, T., Turkenburg, W., Faaij A., 2010. Environmental modelling & software designing a cost-effective CO2 storage infrastructure using a GIS based linear optimization energy model. Environ. Modell. Softw. 25 (12). 1754–1768.

Bruhn, T., Naims, H., Olfe-Kräutlein, B., 2016. Separating the debate on CO2 utilisation from carbon capture and storage, Environmental Science & Policy 60, 38–43.

Burnol, A., Thinon, I., Ruffine, L., Herri, J.M., 2015. Influence of impurities (nitrogen and methane) on the CO 2 storage capacity as sediment-hosted gas hydrates–Application in the area of the Celtic Sea and the Bay of Biscay. Int J Greenh Gas Control 35, 96–109

Clean energy wire, 2018. Available at: https://www.cleanenergywire.org/news/german-households-and-industry-pay-highest-power-prices-europe

Colbertaldo, P., Guandalini, G., Campanari, S., 2018. Modelling the integrated power and transport energy system: The role of power-to-gas and hydrogen in long-term scenarios for Italy, Energy 154, 592-601.

Cuéllar-Franca, R.M., Azapagic, A., 2015. Carbon capture, storage and utilization technologies: a critical analysis and comparison of their life cycle environmental impacts. J. CO2 Util. 9, 82–102.

Dolman, M., Madden, B., Dunbar water electrolyser feasibility study, May 2015, Available at: https://sustainingdunbar.org/files/2015/12/Dunbar-WE-feasibility-study-P3-report_final_12.05.15.pdf

Dahowski, R., Dooley, J., Davidson, C., Bachu, S., Gupta, N., 2004. A CO2 Storage Supply Curve for North America. Proceedings of the 7. international conference on greenhouse gas control technologies.

Di Costanzo, F., 2017. Analisi energetica ed economica di un sistema "Power to gas" con produzione biologica di metano. [Laurea magistrale], Università di Bologna, Corso di Studio in Ingegneria energetica [LM-DM270].

Di Felice, L., Micheli, F., 2015. From Biomass to SNG, Process Intensification for Sustainable Energy Conversion, First Edition. Edited by Fausto Gallucci and Martin van Sint Annaland. John Wiley & Sons, Ltd.

Distance, 2019. Available at: http://it.distance.to

Donda, F., Volpia, V., Persoglia, S., Parushev, D., 2011. CO2 storage potential of deep saline aquifers: The case of Italy. International Journal of Greenhouse Gas Control 5, 327–335.

Effective Carbon price, 2018. Available at: http://www.oecd.org/env/tools-evaluation/carbon-prices.htm

ENI, 2019. Available at: http://www.eniscuola.net/en/argomento/solar/solar-knowledge/some-more-numbers-in-italy/

Ericson, A., Bozzuto, C., Krutka, H., Tomski, P., Angielski, S., Phillips, J., 2015. Fossil Forward: Revitalizing CCS—Bringing Scale and Speed to CCS Deployment. National Coal Council. Ericson, A., Bozzuto, C., Krutka, H., Tomski, P., Angielski, S., Phillips, J., 2015. Fossil Forward: Revitalizing CCS—Bringing Scale and Speed to CCS Deployment. National Coal Council.

Eurostat, 2018. Available at: https://ec.europa.eu/eurostat/statistics-explained/index.php?title=File:Gas_prices_for_non-household_consumers,_second_half_2017_(EUR_per_kWh).png#filehistory

Global Energy Statistical Yearbook, 2018. Available at: https://yearbook.enerdata.net/natural-gas/world-natural-gas-production-statistics.html

Gotz, M., Lefebvre, J., Morsa, F., McDaniel Koch, E., Graf, F., Bajohr, S., Reimert, R., Kol, T., 2016. Review Renewable Power-to-Gas: A technological and economic review, Renewable energy, 85, 1371-1390.

Gracceva, F., De Luca, E., Fidanza, A., Del Nero, P., Giuffrida, L.G., Felici, B., Pona, C., Zini, A., (2017) Analisi trimestrale del sistema energetico italiano. Report 1/2017. ISSN 2531-4750 (2017).

Graf, F., Götz, M., Henel, M., Schaaf, T., Tichler R., Abschlussbericht "Techno-ökonomische Studie von Power-to-Gas-Konzepten", Bonn 2014 Available at: http://www.dvgw-innovation.de/fileadmin/dvgw/angebote/forschung/innovation/pdf/g3_01_12_tp_b_d.pdf

Green Report, 2017. Available at: http://www.greenreport.it/

Green, 2014, Available at: https://www.google.de/search?q=percentuale+emissioni+co2+regioni+italiane&source=lnms&tbm=isch&sa=X&ved=0ahUKEwi22_WKvtHeAhVJFywKHaQTACUQ_AUIDigB&biw=1366&bih=608#imgrc=_Q4uMiUoDub58M.

Guandalini, G., Robinius, M., Grube, T., Campanari, S., Stolten, D., 2017. Long-term power-to-gas potential from wind and solar power: A country analysis for Italy, International Journal of Hydrogen Energy, 42, 13389-13406.

Hasan, M.M.F., Boukouvala, F., First, E.L., Floudas, C.A., 2014. Nationwide. regional. and statewide CO2 capture. utilization. and sequestration supply chain network optimization. Ind Eng Chem Res 53. (18). 7489–7506.

Hasan, M.M.F.. Baliban, R.C.. Elia, J.A.. Floudas, C.A.. 2012. Modeling. simulation. and optimization of postcombustion CO2capture for variable feed concentration and flowrate. 1. Chemical absorption and membrane processes. Ind Eng Chem Res. 51 (48) 15642–64.

Hassan, A., Patel, M.K., Parra, D., 2019. An assessment of the impacts of renewable and conventional electricity supply on the cost and value of power-to-gas, International Journal of Hydrogen Energy, 44, 9577-9593.

Hendriks, C.A., Carbon Dioxide Removal from coal-Fired power plant. In department of science. technology. and society. Utrecht University. 1994: Utrecht. Netherlands.

IEA and UNIDO, 2011. Technology Roadmap—Carbon Capture and Storage in Industrial Applications. International Energy Agency (IEA) and the United Nations Industrial Development Organization (UNIDO).

Italy's National Energy Strategy 2017, https://www.mise.gov.it/images/stories/documenti/BROCHURE_ENG_SEN.PDF

Kalyanarengan Ravi, N., Van Sint Annaland, M., Fransoo, J.C., Grievink, J., Zondervan, E., 2017. Development and implementation of supply chain optimization framework for CO2 capture and storage in the Netherlands. Comp. Chem. Eng. 102. 40–51.

Leonzio G., 2017. Design and feasibility analysis of Power-to-gas plant in Germany. Journal of Cleaner Production. 162, 609-623.

Ma, J., Li, Q., Kühn, M., Nakaten, N., 2018. Power-to-gas based subsurface energy storage: A review, Renewable and Sustainable Energy Reviews 97, 478–496.

Maggioni, L., Pieroni, C., 2016. Deliverable D5.2: Report on the biomethane injection into national gas grid. http://www.isaac-project.it/wp-content/uploads/2017/07/D5.2-Report-on-the-biomethane-injection-into national-gas-grid.pdf,

Matzen, M., Demirel, Y., 2016. Methanol and dimethyl ether from renewable hydrogen and carbon dioxide: alternatve fuels production and life cycle assessment, Journal of Cleaner Production, 139, 1068-1077.

Mikkelsen, M., Jorgensen, M., Krebs, F.C., 2010. Theteraton challenge. A review of fixation and transformation of carbon dioxide. Energy Environ. Sci. 3, 43–81.

Moia, F., Fais, S., Pisanu, F., Sardu, G., Casero, P., Guandalini, R., Agate, G., Beretta, S., Cappelletti, F., Colucci, F., 2012. La fattibilità dello stoccaggio geologico della CO2 negli acquiferi salini profondi nell'onshore e offshore italiano, 1º Congresso dell'Ordine dei Geologi di Basilicata,"Ricerca, Sviluppo ed Utilizzo delle Fonti Fossili: Il Ruolo del Geologo", Potenza, 30 Novembre - 2 Dicembre 2012.

Montello, 2019. Available at: http://www.montello-spa.it/recycling-organic-waste/?lang=en

Müller-Syring, G., Henel, M., Köppel, W., Mlaker, H., Sterner, M., Höcher T., Entwicklung von modularen Konzepten zur Erzeugung, Speicherung und Einspeisung von Wasserstoff und Methan ins Erdgasnetz Abschlussbericht DVGW-Projekt G1-07-10 DBI Gas- und Umwelttechnik GmbH, Bonn (2013) Available at: http://www.dvgw-innovation.de/fileadmin/dvgw/angebote/forschung/innovation/pdf/g1_07_10.pdf

Naims, H., 2016. Economics of carbon dioxide capture and utilization—a supply and demand perspective, Environ Sci Pollut Res 23, 22226–22241

Nguyen, T.B.H., Zondervan, E. 2018. Ionic Liquid as a Selective Capture Method of CO2 from Different Sources: Comparison with MEA, ACS Sustainable Chemistry & Engineering, 6 (4), 4845-4853.

Ochoa Bique, A., Nguyen, T.B.H., Leonzio, G., Galanopoulos, C., Zondervan, E. 2018. Integration of carbon dioxide and hydrogen supply chains, Computer Aided Chemical Engineering, 43, 1413-1418.

Parra, D., Zhang, X., Bauer, C., Patel, M.K., 2017. An integrated techno-economic and life cycle environmental assessment of power-to-gas systems, Applied Energy 193, 440–454.

Patricio, J., Angelis-Dimakisb, A., Castillo-Castillo, A., Kalmykova, Y., Rosado, L., 2017. Region prioritization for the development of carbon capture and utilization technologies, Journal of CO2 Utilization 17, 50–59.

Pérez-Fortes M., Bocin-Dumitriu A., Tzimas E., 2014. CO2 Utilization Pathways: Techno-Economic Assessment and Market Opportunities, Energy Procedia 63, 7968 – 7975.

Plaisant, A., Maiu, A., Maggio, E., Pettinau, A., 2017. Pilot-scale CO2 sequestration test site in the Sulcis basin (SW Sardinia): Preliminary site characterization and research program. Energy Procedia 114, 4508 – 4517.

Reichert, F., 2012. Wind-to-Gas-to-Money? Economics and Perspectives of the Power-to-Gas Technology. Aalborg University Department of Development and Planning MSc (Eng) Sustainable Energy Planning and Management. master thesis.

Renewable Energy, National Report on current status of biogas production – Italy WP5 – deliverables 5.1, http://act-clean.eu/downloads/D5.1_ITALY_National_Report.pdf (2012).

Serpa, J., Morbee, J., Tzimas, E., 2011. Technical and Economic Characteristics of a CO2 Transmission Pipeline Infrastructure, JRC62502 1-43.

Sternberg, A., Bardow, A., 2015. Power-to-what? Environmental assessment of energy storage systems. Energy Environ. Sci. 8, 389–400.

Steeneveldt, R., Berger, B., Torp, T.A., 2006. CO2 Capture and storage, Closing the Knowing–Doing Gap, Chemical Engineering Research and Design, 84, (A9), 739– 763.

Styring, P., Jansen, D., de Coninck, H., Reith, H., Armstrong, K., 2011. Carbon Capture and Utilization in the Green Economy. Centre for Low Carbon Futures, York. TheLocal, 2014. Vattenfall Abandons Research on CO2 Storage. The Local. UoS, 2016. Carbon Capture, Utilisation and Storage & Conventional Power. University of Sheffield.

Todd, A.C., 2011. CCS – A multidisciplinary global activity for a global challenge. Chemical Engineering Research and Design, 89, 1443-1445.

von der Assen, N., Jung, J., Bardow, A., 2013. Life-cycle assessment of carbon dioxide capture and utilization: avoiding the pitfalls. Energy Environ. Sci. 6, 2721–2734.

von der Assen, N., Bardow, A., 2014. Life cycle assessment of polyols for polyurethane production using CO2 as feedstock: insights from an industrial case study. Green Chem. 16, 3272–3280.

Wang, M., Lawal, A., Stephenson, P., Sidders, J., Ramshaw, C., 2011. Post-combustion CO2 capture with chemical absorption: A state-of-the-art review, Chemical Engineering Research and Design, 89, 1609-1624.

Zhang, S., Liu, L., Zhang, L., Zhuang, Y., Du. J. 2018. An optimization model for carbon capture utilization and storage supply chain: A case study in Northeastern China, Applied Energy 231 194–206

Nomenclature

Indeces

i = carbon dioxide source

j = carbon dioxide capture system

k = carbon dioxide geological storage sites and methane production site

Abbreviations

AIMMS = advanced interactive multidimensional modeling system

CCR = capital cost recovery

CCUS = carbon capture utilization and storage

CCU = carbon capture and utilization

CC = carbon dioxide capture and compression costs [€/year]

CDC = flue gas dehydration costs [€/year]

CH_4P = methane production costs [€/year]

CIC = carbon dioxide capture and compression investment costs [€/year]

COC = carbon dioxide capture and compression operating costs [€/year]

GHG = greenhouse emissions

IC = maximum injection capacity per well [ton/year]

IL = ionic liquid

MEA = monoethanolamine

MILP = mixed integer linear programming

N^{build}_{well} = number of well

PEM = proton exchange membrane

PSA = pressure swing adsorption

SC = carbon dioxide storage cost [€/year]

SIC = carbon dioxide investment storage costs [€]

SOC = carbon dioxide operating storage costs [€/year]

VSA = vacuum swing adsorption

TC = carbon dioxide transportation costs [€/year]

TH = time horizon

TIC = carbon dioxide investment transportation costs [M€]

TOC = carbon dioxide operating transportation costs [M€/year]

Parameters

b = parameter in SIC [M€]

C_k^{max} = maximum storage capacity for storage site k [ton]

CR^{min} = minimum target for carbon dioxide reduction [ton/year]

CS_i = carbon dioxide emissions from each source i [ton/year]

$D_{i,k}$ = distance between carbon source and storage site [km]

$P_{i,k}$ = distance between carbon source and utilization site [km]

P = parameter equal to 1 if carbon dioxide is transported to utilization site

d_{well} = depth of well [km]

F_i/F = flue gas flow rate from each source i [mol/s]

F_t = terrestrial factor

m = parameter in SIC [M€/km], in CIC and COC

n = parameter in CIC and COC

x_{CO2} = carbon dioxide molar fraction

XS_i = carbon dioxide composition in the flue gas emission from source i [mol%]

XL_i = lowest composition processing limit for capture plant j [mol%]

XH_i = highest composition processing limit for capture plant j [mol%]

Variables

Binary

$X_{i,j,k}$ = 1 if carbon dioxide from source 'i', is captured using capture plant 'j' and stored in storage site 'k', 0 otherwise

$Y_{i,j,k}$ = 1 if carbon dioxide is captured from source 'i' with the technology 'j' and sent to storage/utilization site 'k', 0 otherwise

Continuous

$FR_{i,j,k}$ = fraction of the carbon dioxide captured from source 'i' using the capture plant 'j' and sent to storage site 'k'

$MR_{i,j,k}$ = fraction of the carbon dioxide captured from source 'i' using the capture plant 'j' and sent to utilization site 'k'

Greek letters

α = parameter in CIC and COC

α_t = parameter in TIC

β = parameter in CIC and COC

β_t = parameter in TIC

γ = parameter in CIC and COC

Chapter VI

Development of a CCUS supply chain for the UK

The UK is the second largest emitter Country of carbon dioxide in Europe, then urgent actions are required to mitigate any adverse effect on GHG accumulation in the atmosphere. For this reason, the Mixed Integer Linear Programming model is applied in this chapter to develop a carbon capture utilization and storage supply chain for the UK. Three different frameworks, with different storage sites (saline aquifers) as Bunter Sandstone, Scottish off-shore and Ormskirk Sandstone are taken into account. Several attractive potential utilization options are considered: calcium carbonate, concrete, tomatoes, polyurethane, methanol and methane production. Total costs are minimized to design and optimize these carbon supply chains, while reducing significantly carbon dioxide emissions. Results show that the system with Bunter Sandstone as storage site is the most economically profitable solution, due to the highest value of net present value (0.554 trillion€) and lowest value of payback period (2.85 years). Only carbon tax is needed to have a profitable solution from an economic point of view. Total costs are 1.04 billion€/year.

VI.1 Introduction

Carbon capture utilization and storage (CCUS) supply chains would have an important role for the UK economy, improving the de-carbonization of industries, generating low carbon power and allowing the production of hydrogen (H_2) with a low carbon footprint (Department for business, energy and industrial strategy, 2019). CCUS systems can also promote the development of bio-energies. Then, it is clear, that these frameworks are vital to the low carbon transformation of the UK and its ambition to establish the world's first net-zero carbon industrial cluster by 2040, and at least one low-carbon cluster by 2030. The UK Committee on Climate Change (CCC), underlined that CCUS supply chains are important to meet the future targets of emissions reduction (OGC, 2018). Also, this technology could help strengthen the long-term competitiveness of the UK's industrial regions, in Scotland, South Wales, Humberside, Merseyside and Teesside. On the other hand, CCUS systems generate economic value with also job creation and retention (OGC, 2018).

Another important consideration is that the geology of the UK can support the realization of carbon supply chains, as reported by the Global Carbon Capture and Storage Institute (GCCSI), analyzing each nation's suitability and preparedness for CCUS development (GCCSI, 2016). In fact, the UK has valuable resources and significant carbon dioxide (CO_2) storage capability.

Today, innovative companies across the UK are developing cutting edge CCUS technologies, there are world leading academic institutions focused on driving cost reductions and existing industries have the skills and capability required to deploy CCUS at large scale.

The government has taken first actions to reduce costs of these systems and to consider their deployment but no concrete actions or realizations are made.

In the literature, a model for a CCUS supply chain integrating carbon and H_2 supply chains in the UK and producing methanol (CH_3OH) by CO_2 hydrogenation is developed by Quarton and Samsatli (2020). More CO_2-based products are not considered to be produced inside a CCUS for the UK. The work presented in this chapter wants to overcome this gap. In fact, CO_2 utilization routes with a high value of technology readiness level (TRL) are taken into account, such as calcium carbonate, concrete, tomatoes and polyurethane production (Alberici et al., 2017). Also, CH_3OH and methane (CH_4) production are considered, because these routes are often taken into account in the literature and differ from the previous ones for an hydrogenation reaction being involved. Also, a considerable amount of CO_2 is expected to be consumed for these products in the projections for the year 2030 in the UK (Alberici et al., 2017). Then, a deterministic Mixed Integer Linear Programming (MILP) model of a CCUS supply chain for the UK is developed, considering regions with higher emissions. In particular, three different frameworks are suggested: these have a different storage site, a saline aquifer, such as Bunter Sandstone in the southern North Sea, Scottish off-shore in the central North Sea and Ormskirk Sandstone in the Irish East Sea. The aim of this work is then to design and optimize these CCUS supply chains minimizing total costs while reducing a significant amount of CO_2, according to the environmental target. The best case is then chosen for the UK.

VI.2 Model development

VI.2.1 Problem statement

In order to develop the mathematical model the following assumptions are made:

- one to one coupling: one source node can be connected to only one capture node in the storage and utilization section and each capture node can receive from only one source node (Kalyanarengan Ravi et al., 2017);
- to avoid the transportation of flue gas with additional costs, CO_2 sources and capture plants are located at the same site (Kalyanarengan Ravi et al., 2017);
- within the supply chain CO_2 is transported via pipeline because, it is the most mature infrastructure able to transport high flow rates of CO_2 at low costs;
- CO_2 is assumed to produce polyurethane, concrete, calcium carbonate and tomatoes as well as CH_3OH and CH_4 (Alberici et al., 2017);
- the supply chain is considered to be operating at steady state conditions for a period of 25 years: the work is focused on the design of the system finding its optimal topology;
- the demand for CO_2-based products is considered constant over time and these can be sold at a stable selling price (Hasan et al., 2015; Zhang et al., 2018): the supply chain is evaluated at an average time disregarding major fluctuations for the design of production plants;

- only one storage site is present inside the CCUS supply chain able to store an amount of CO_2 equal to emissions that need to be reduced to achieve the minimum target imposed by the environmental policy;
- for the utilization section, no more than two production sites are considered for each CO_2-based product, then production plants are considered with a great or infinity capacity;
- distances between nodes inside the supply chain are evaluated according to their latitude and longitude (Kalyanarengan Ravi et al., 2017);
- the economic feasibility is found through the calculation of the net present value (NPV) and payback period (PBP);

In addition to these assumptions, some inputs are provided to define the mathematical model:

- CO_2 sources: type, location and yearly CO_2 and flue gas emissions (Department of Business, Energy and Industrial Strategy, 2018; NAEI, 2019);
- CO_2 capture and compression process: materials and technologies with respective total costs (Nguyen and Zondervan, 2018; Zhang et al., 2018);
- CO_2 transportation: distances and respective costs (Serpa et al., 2011; NHC, 2019);
- for each CO_2-based product a conversion factor is taken into account (Patricio et al., 2017; Ancona et al., 2019; Von der Assen et al., 2015; Department for Environment Food and Rural Affairs, 2019);
- CO_2 utilization: location and production costs (Hank et al., 2018; Reichert, 2012; Van der Velden, 2019; Colacem 2019; Zappa, 2014; Sheldon, 2017; Natural gas, 2019; Prea, 2019; Basf, 2019; Apsgroup, 2019; MPA, 2019; Hanson, 2019; BCCF, 2019);
- CO_2 storage: location and respective costs (Bentham, 2006; Kolstera et al., 2018; Babaei et al., 2016; Kirk, 2005; Gammer et al., 2011; Hendriks, 1994);
- National demand for each product and CO_2 reduction targets (Reportlinker, 2019; EIA, 2019; ONS, 2019; Britishgrowers, 2019; MPA, 2019; Bide et al., 2019);

The mathematical model is able to provide the optimal connection between CO_2 sources, CO_2 utilization and storage sites. CO_2 sources are selected with the respective capture technologies/materials and connected with the utilization and storage section. The optimal amount of captured and transported CO_2 is determined in addition to the amount of each CO_2-based product.

The objective is to minimize total costs, which include CO_2 capture and compression costs, CO_2 transportation costs, CO_2 storage costs and production costs of the different CO_2-based products.

VI.2.2 CCUS supply chain model

In this section, sets, parameters, variables, constraints and equations are defined for the model of the CCUS supply chain. The model is a MILP type and it is solved by using AIMMS (Advanced Interactive Multidimensional Modeling System) software.

VI.2.2.1 Sets

Each element inside the CCUS supply chain is identified by an index. CO_2 sources are represented by 'i', CO_2 capture and compression technologies are represented by 'j', CO_2 storage sites and its complementary utilization section as 'k', CH_3OH plants are indicated by 'm', power to gas plants are indicated by 'g', polyurethane plants are indicated by 'p', tomatoes production sites are indicated by 't', concrete plants are indicated by 'c', calcium carbonate plants are represented by 'd'.

VI.2.2.2 Parameters

The parameters used in the CCUS supply chain model are the following: CR^{min}, the minimum target for the overall CO_2 reduction (ton/year); CS_i, the total CO_2 emission from each source i (ton/year); F_i, the total flue gas flow rate from each source i (mol/s); XS_i, CO_2 composition in the flue gas from source i (mol%); XL_i, the lowest CO_2 composition processing limit for the capture plant j (mol%); XH_i, the highest CO_2 composition processing limit for the capture plant j (mol%); C_k^{max}, the maximum storage capacity at the storage site k (ton);

VI.2.2.3 Variables

Continuous and binary variables are used to define the model for the CCUS supply chain. To select the storage site and the capture technology/material the following binary variables are introduced respectively: $X_{i,j,k}$ and $Y_{i,j,k}$.. Continuous variables are introduced to define the fraction of captured CO_2 that is sent to the storage ($FR_{i,j,k}$), to the utilization ($Utilization_{i,j,k}$), to CH_3OH production ($Methanol_{i,j,m}$), to CH_4 production ($Methane_{i,j,g}$), to polyurethane production ($Polyurethane_{i,j,p}$), to tomatoes growing ($Tomato_{i,j,t}$), to concrete curing ($Concrete_{i,j,c}$) and to calcium carbonate production ($CalciumCarbonate_{i,j,d}$). A value between 0 and 1 is assumed for these continuous variables.

VI.2.2.4 Constraints

The following constraints are introduced in the mathematical model. CO_2 cannot be sent to multiple storage sites, then the following constraint is used (see Eq. VI.1):

$$\sum_{(j,k)\in(J,K)} X_{i,j,k} \leq 1 \qquad \forall\, i \in I \tag{VI.1}$$

with $X_{i,j,k}$ the binary variable already defined. In addition, this inequality ensures the one to one coupling between CO_2 sources and capture technologies in the storage section.

CO_2 storage site is characterized by a defined storage capacity that cannot be exceeded, then the following constraint is used (see Eq. VI.2):

$$\sum_{(i,j)\in(I,J)} CS_i \cdot FR_{i,j,k} \leq \frac{C_k^{max}}{TH} \qquad \forall\, k \in K \qquad (VI.2)$$

where CS_i is the total CO_2 emissions from source 'i', C_k^{max} is the maximum storage capacity of the storage site 'k', TH is the time horizon of supply chain in year and $FR_{i,j,k}$ is the variable defined above.

The defined CCUS supply chain should achieve the minimum target for CO_2 emissions reduction, then this constraint is defined as (see Eq. VI.3):

$$\sum_{(i,j,k)\in(I,J,K)} CS_i \cdot FR_{i,j,k} + CS_i \cdot Utilization_{i,j,k} \geq CR^{min} \qquad (VI.3)$$

with CS_i the total CO_2 emissions from source 'i', $FR_{i,j,k}$ and $Utilization_{i,j,k}$ the variables defined above and CR^{min} the minimum target of CO_2 emissions reduction. The whole amount of CO_2 that is captured and sent to the utilization and storage section should be higher than the minimum target for emissions reduction.

For a selected CO_2 source, not all CO_2 can be processed by a selected capture technology: at most only 90% of CO_2 can be captured, as defined by the following constraint (see Eq. VI.4):

$$\sum_{(j)\in(J)} FR_{i,j,k} + Utilization_{i,j,k} \leq 0.9 \qquad \forall\, (i,k) \in (I,K) \qquad (VI.4)$$

with $FR_{i,j,k}$ and $Utilization_{i,j,k}$ the continuous variables defined above.

Not all the considered technologies can be used to capture CO_2 with a product purity of 90% for CO_2. This depends on the composition of CO_2 in the feed, as defined by the following constraint (see Eq. VI.5):

$$\sum_{(k)\in(K)} (XH_j - XS_i) \cdot (XS_i - XL_j) \cdot X_{i,j,k} \geq 0 \qquad \forall\, (i,j) \in (I,J) \qquad (VI.5)$$

where XS_i is CO_2 composition in flue gas emissions from source i, XL_j, is the lowest limit of processing composition for the capture plant j, XH_j is the highest limit of processing composition for the capture plant j, $X_{i,j,k}$ is the variable defined above. This constraint is required for the storage section, while in the utilization section a purity higher or lower than 90% can be required and achieved in the respective site.

The amount of CO_2 that is sent to the utilization section is divided among the different utilization options, according to the following material balance constraint (see Eq. VI.6):

$$Utilization_{i,j,k} = (Concrete_{i,j,c} + Tomato_{i,j,t} + Polyurethane_{i,j,p} + CalciumCarbonate_{i,j,d} + Methanol_{i,j,m} + Methane_{i,j,g} +) \cdot n_{sites} \qquad \forall\, (i,j,k,c,t,p,d,m,g) \in (I,J,K,C,T,P,D,M,G) \qquad (VI.6)$$

with $Utilization_{i,j,k}$, $Methanol_{i,j,m}$, $Methane_{i,j,g}$, $Polyurethane_{i,j,p}$, $Tomato_{i,j,t}$, $Concrete_{i,j,c}$ and $CalciumCarbonate_{i,j,d}$, the variables defined above and n_{sites} is the number of each utilization sites.

In the utilization and storage section, only one capture technology/material can be chosen for the selected CO_2 source, as defined in the following constraint (see Eq. VI.7):

$$\sum_{(j,k)\in(J,K)} Y_{i,j,k} \leq 1 \qquad \forall \quad i \in I \qquad (VI.7)$$

with $Y_{i,j,k}$ the binary variable defined before.

In order to convert the mathematical model to a linear one, a Glover linearization (see Chapter III) is applied by using these constraints (see Eqs. VI.8-VI.9):

$$0 \cdot X_{i,j,k} \leq FR_{i,j,k} \leq 0.9 \cdot X_{i,j,k} \qquad \forall\,(i,j,k) \in (I,J,K) \qquad (VI.8)$$

$$0 \cdot Y_{i,j,k} \leq Utilization_{i,j,k} \leq 0.9 \cdot Y_{i,j,k} \qquad \forall\,(i,j,k) \in (I,J,K) \qquad (VI.9)$$

where $FR_{i,j,k}$, $X_{i,j,k}$, $Utilization_{i,j,k}$ and $Y_{i,j,k}$ are already defined, while 0.9 is used because at least 90% of CO_2 is captured from each CO_2 source.

VI.2.2.5 Equations

In the mathematical model of carbon supply chain, equations for CO_2 capture and compression costs, CO_2 transportation costs and CO_2 storage costs are given. CO_2 capture and compression costs (€/year) are determined according to the following relation (see Eq. VI.10):

$$CC_{i,j,k} = CDC_{i,j,k} + CIC_{i,j,k} + COC_{i,j,k} \qquad \forall\,(i,j,k) \in (I,J,K) \qquad (VI.10)$$

where $CDC_{i,j,k}$ are the flue gas dehydration costs (€/year) equal to 9.28 €/tonCO_2 (Kalyanarengan Ravi et al., 2017), $CIC_{i,j,k}$ are the investment costs (€/year) and $COC_{i,j,k}$ are the operating costs (€/year). The investment and the operating costs expressions are as follows (Zhang et al., 2018) (see Eqs. VI.11-VI.12):

$$CIC_{i,j,k} = \alpha_{I,j} \cdot Y_{i,j,k} + (\beta_{I,j} \cdot {x_{co2,i}}^{n_{I,j}} + \gamma_{I,j}) \cdot F_{i,j,k}^{m_{I,j}} \qquad \forall\,(i,j,k) \in (I,J,K) \qquad (VI.11)$$

$$COC_{i,j,k} = \alpha_{o,j} \cdot Y_{i,j,k} + (\beta_{o,j} \cdot {x_{co2,i}}^{n_{o,j}} + \gamma_{o,j}) \cdot F_{i,j,k}^{m_{o,j}} \qquad \forall\,(i,j,k) \in (I,J,K) \qquad (VI.12)$$

where $\alpha_{I,j}$, $\alpha_{o,j}$, $\beta_{I,j}$, $\beta_{o,j}$, $\gamma_{I,j}$, $\gamma_{o,j}$, $n_{I,j}$, $n_{o,j}$, $m_{o,j}$, $m_{I,j}$ are fixed parameters for each process and for each material (see table S1 of Chapter IV), $x_{CO2,i}$ is CO_2 content in flue gas for the selected CO_2 source, $F_{i,j,k}$ is flue gas flow rate in mol/s and $Y_{i,j,k}$ is the binary parameter defined before. However, for ionic liquid absorption, modified equations can be used (see Eqs. VI.13-VI.14) (Nguyen and Zondervan, 2018):

$$CIC_{i,j,k} = (\alpha_{I,j} \cdot F_{i,j,k} + \beta_{I,j} \cdot Y_{i,j,k}) \cdot x_{co2,i} + \gamma_{I,j} \cdot F_{i,j,k}^{m_{I,j}} \qquad \forall\,(i,j,k) \in (I,J,K) \qquad (VI.13)$$

$$COC_{i,j,k} = (\alpha_{o,j} \cdot F_{i,j,k} + \beta_{o,j} \cdot Y_{i,j,k}) \cdot x_{co2,i,} \quad + \gamma_{o,j} \cdot F_{i,j,k}^{m_{o,j}} \quad \forall (i,j,k) \in (I,J,K) \qquad (VI.14)$$

with $\alpha_{I,j}$, $\alpha_{o,j}$, $\beta_{I,j}$, $\beta_{o,j}$, $\gamma_{I,j}$, $\gamma_{o,j}$, $m_{o,j}$, $m_{I,j}$ fixed parameters (see table S1 of Chapter IV), $x_{CO2,i,}$ CO_2 composition in flue gas, $F_{i,j,k}$ flue gas flow rate in mol/s, $Y_{i,j,k}$ the binary variable defined above.

CO_2 is transported within the CCUS supply chain via pipeline and the relation to calculate these costs is reported by Serpa et al. (2011), where the total costs ($TC_{i,j,k,c,t,p,d,m,g}$ in M€/year) are the sum of the investment ($TIC_{i,j,k,c,t,p,d,m,g}$ in M€) and the operating costs ($TOC_{i,j,k,c,t,p,d,m,g}$ in M€/year) (see Eq. VI.15):

$$TC_{i,j,k,c,t,p,d,m,g} = CCR \cdot TIC_{i,j,k,c,t,p,d,m,g} + TOC_{i,j,k,c,t,p,d,m,g} \qquad \forall (i,j,k,c,t,p,d,m,g) \in (I,J,K,C,T,P,D,M,G) \qquad (VI.15)$$

where CCR is the capital cost recovery, calculated at an interest rate of 10% and 25 years. The investment and operating costs (M€/year) are determined from these relations (see Eq. VI.16):

$$\begin{aligned} TIC_{i,j,k,c,t,p,d,m,g} &= \big(\alpha_t \\ &\cdot CS_i \cdot FR_{i,j,k}/Concrete_{i,j,c}/Tomato_{i,j,t}/Polyurethane_{i,j,p}/Calcium\ carbonate_{i,j,d} \\ &/Methanol_{i,j,m}/Methane_{i,j,g} + \beta_t \cdot X_{i,j,k}/X_{i,j,c}/X_{i,j,t}/X_{i,j,p}/X_{i,j,d}/X_{i,j,m}/X_{i,j,g}\big) \cdot F_T \\ &\cdot \big(D_{i,k}/D_{i,c}/D_{i,t}/D_{i,p}/D_{i,d}/D_{i,m}/D_{i,g} + 16\big) \quad \forall (i,j,k,c,t,p,d,m,g) \\ &\in (I,J,K,C,T,P,D,M,G) \end{aligned} \qquad (VI.16)$$

$$TOC_{i,j,k,c,t,p,d,m,g} = 4\% \cdot TIC_{i,j,k,c,t,p,d,m,g} \qquad \forall (i,j,k,c,t,p,d,m,g) \in (I,J,K,C,T,P,D,M,G) \qquad (VI.17)$$

where α_t is 0.019 and β_t is 0.533 (Serpa et al., 2011), $D_{i,k}/D_{i,c}/D_{i,t}/ D_{i,p}/D_{i,d}/D_{i,m}/ D_{i,g}$ are the distance respectively between CO_2 sources and storage site, concrete production site, tomatoes production site, polyurethane production site, calcium carbonate production site, CH_3OH production site, CH_4 production site, F_T is a terrestrial factor of 1.2 (Broek et al., 2010), 16 km are added to the distance to consider additional paths related to process (Dahowski et al., 2004), $FR_{i,j,k}$, $Methanol_{i,j,m}$, $Methane_{i,j,g}$, $Polyurethane_{i,j,p}$, $Tomato_{i,j,t}$, $Concrete_{i,j,c}$ and $CalciumCarbonate_{i,j,d}$, are the continuous variables already defined, $X_{i,j,k}$, $X_{i,j,c}$, $X_{i,j,t}$, $X_{i,j,d}$, $X_{i,j,m}$, $X_{i,j,g}$ are 1 if the respective continuous variable is not 0, CS_i is the amount of CO_2 in Mton/year. The operating costs are 4% of investment costs (Kalyanarengan Ravi et al., 2017).

CO_2 storage costs (SC_k in €/year) are the sum of investment (SIC_k in €) and operating costs (SOC_k in €/year) (Kalyanarengan Ravi et al., 2017) (see Eq. VI.18):

$$SC_k = CCR \cdot SIC_k + SOC_k \qquad \forall (k) \in (K) \qquad (VI.18)$$

whit CCR defined above. The investment costs are determined from the following relation (Hendriks, 1994) (see Eq. VI.19):

$$SIC_k = (m \cdot d_{well} + b) \cdot N_{well}^{build}{}_k \qquad \forall\,(k) \in (K) \qquad (VI.19)$$

where m and b are parameters respectively of 1.53 M€/km and 1.23 M€ (Hendriks, 1994), d_{well} is the depth of the well, and N_{well}^{build} is the number of wells which need to be built evaluated according to this relation (Hasan et al., 2014) (see Eq. VI.20):

$$N_{well}^{build}{}_k = \frac{\sum_{(i,j)\in(I,J)} CS_i \cdot FR_{i,j,k}}{IC} \qquad \forall\,(k) \in (K) \qquad (VI.20)$$

as a function of the maximum injection capacity per well, IC, and the amount of stored CO_2. The operating costs are 4% of investment costs (see Eq. VI.21) (Kalyanarengan Ravi et al., 2017).

$$SOC_k = 4\% \cdot SIC_k \qquad \forall\,(k) \in (K) \qquad (VI.21)$$

Production costs and selling prices of CO_2-based products are shown in Table VI.1.

Table VI.1 Selling price and production cost of CO_2-based products for the CCUS supply chain of the UK (Leonzio et al., 2020)

CO_2-based product	Production cost	Selling price
Methanol	608 €/ton (Hank et al., 2018)	705 €/ton (National Statistics, 2019)
Methane	300 €/MWh (Reichert, 2012)	0.028 €/kWh (Eurostat, 2019)
Polyurethane	1349 €/ton	2590 €/ton (National Statistics, 2019)
Tomato growing	0.85 €/kg (Van den Velden, 2019)	1.45 €/kg (Department for Environment Food and Rural Affairs, 2019)
Concrete	21.8 €/ton (Colacem, 2019)	32.6 €/ton (RMS, 2019)
Calcium carbonate	65.2 €/ton (Zappa, 2014)	120 €/ton (Zappa, 2014)

The conversion factors for the compounds produced are: 1.7 tonCO_2/tonCH_3OH (Patricio et al., 2017), 1 moleCO_2/moleCH_4 (Ancona et al., 2019), 0.3 kgCO_2/kg polyurethane (von der Assen et al., 2015), 2.6 ton tomato/tonCO_2 (Patricio et al., 2017; Department for Environment Food and Rural Affairs, 2019), 0.03 tonCO_2/ton concrete (Patricio et al., 2017), 0.25 tonCO_2/ton steel slag (Patricio et al., 2017).

VI.2.2.6 Objective function

The objective function of the mathematical model for the CCUS supply chain is defined as (see Eq. VI.22):

$$\emptyset = \sum_{(i,j,k,c,t,p,d,m,g)} CC_{i,j,k} + TC_{i,j,k,c,t,p,d,m,g} + SC_k + CP_c + CP_t + CP_p + CP_d + CP_m + CP_g \qquad (VI.22)$$

where $CC_{i,j,k}$ are CO_2 capture and compression costs, $TC_{i,j,k,c,t,p,d,m,g}$ are CO_2 transportation costs, SC_k are CO_2 storage costs, CP_c are concrete production costs, CP_t are tomatoes production costs, CP_p are

polyurethane production costs, CP_d are calcium carbonate production costs, CP_m are methanol production costs, CP_g are methane production costs. This objective function is minimized to design the system.

VI.2.3 Case study

The European Member Countries have agreed to reduce European emissions by at least 40% below 1990 levels, by 2030. To achieve this aim, the UK should reduce CO_2 emissions by 53% compared to 1990 levels (Committee on Climate Change, 2019). In the UK, total CO_2 emissions in 1990 were of 596.3 Mton, then in 2030 they should be below 320 Mton (Department of Business, Energy and Industrial Strategy, 2019). Actually, CO_2 emissions are of 357.5 Mton then, to achieve the target for 2030, an additional reduction of 10.5% is required (Department of Business, Energy and Industrial Strategy, 2018).

For the CCUS supply chain, only CO_2 emissions from industrial and commercial sectors are considered. Four regions, represented by their main city, with greater emissions are selected. The regions of interest are: Wales (14.2 Mton/year), Scotland (13.3 Mton/year), the North West (15.5 Mton/year), Yorkshire and the Humber (18 Mton/year). The nodes are located respectively at Cardiff, Edinburgh, Manchester, Leeds. Total CO_2 emissions in the CCUS supply chain for these regions are equal to 61 Mton/year. These should be reduced by 10.5%, as discussed above. The minimum target of emissions reduction to be obtained by the model is 6.4 Mton/year. CO_2 is mainly emitted by power plants (NAEI, 2019), whose flue gases have a CO_2 composition in the range of 4-15 mol% (Zhang et al., 2018), as reported in Table VI.2, which also shows flue gas flow rates.

Table VI.2 Characterization of CO_2 sources selected for the CCUS supply chain in the UK (Leonzio et al., 2020)

Region	Node	Flue gas type	CO_2 composition (mol%)	CO_2 (Mton/year)	Flue gas (mol/s)
Wales	Cardiff	Power plant	10	14.2	102313
Scotland	Edinburgh	Power plant	12	13.3	79857
North West	Manchester	Power plant	14	15.5	79771
Yorkshire and the Humber	Leeds	Power plant	13	18	99763

In the UK, CO_2 can be stored in oil and gas fields or in saline aquifers (Department of Energy and Climate Change, 2010). The first option is the most important storage type for the UK, with low risks, and with potentially enough storage capacity. The total storage capacity can be considered in the range of 7.4-9.9 $GtCO_2$ (Department of Energy and Climate Change, 2010).

Saline aquifer storages have potentially a large-scale distribution around the UK. The total storage capacity in the UK is in the range of 7.1-14.3 $GtCO_2$ (the potential theoretical capacity exceeds those of oil and gas

fields) and these are present in the Irish Sea, southern North Sea, and northern/central North Sea (Department of Energy and Climate Change, 2010). Because of their much larger capacity, saline aquifers are selected in this study for the CCUS supply chain. Three different storage sites near to the selected CO_2 sources are identified, one for each CCUS supply chain: Bunter Sandstone in the southern North Sea, Scottish off-shore in the Central North Sea and Ormskirk Sandstone in the Irish East Sea. The main characteristics of these storage sites are reported in Table VI.3.

Table VI.3 Data about CO_2 storage sites considered for CCUS supply chains of the UK (Leonzio et al., 2020)

Storage location	Southern North Sea		
Storage area	Bunter Sandstone		Bentham (2006)
Storage site	1\44		Bentham (2006)
Storage capacity	10	$MtonCO_2$	Bentham (2006)
Storage depth	1600	m	Bentham (2006)
Injection capacity per well	2	$MtonCO_2$/year	Kolstera et al. (2018)
Storage location	Central North sea		
Storage area	Scottish off-shore		
Storage site	Forties		Babaei et al. (2016)
Storage capacity	121	$MtonCO_2$	Babaei et al. (2016)
Storage depth	2217	m	Babaei et al. (2016)
Injection capacity per well	3	$MtonCO_2$/year	Babaei et al. (2016)
Storage location	Irish east sea		
Storage area	Ormskirk Sandstone		Kirk (2005)
Storage site	4		Kirk (2005)
Storage capacity	11.5	$MtonCO_2$	Kirk (2005)
Storage depth	500	m	Kirk (2005)
Injection capacity per well	2	$MtonCO_2$/year	Kirk (2005)

CO_2 sources and CO_2 storage sites are reported in Figure VI.1.

Figure VI.13 CO_2 source ( ) and CO_2 storage site (*) suggested for CCUS supply chains of the UK (Leonzio et al., 2020)

In the utilization section, CO_2 is used to produce calcium carbonate, concrete, tomatoes, polyurethane, CH_3OH and CH_4. In addition to CH_3OH and CH_4 obtained from CO_2 hydrogenation, for the other compounds, the corresponding consumed CO_2 is expected to be considerable according to projections for the year 2030.

For the year 2030, the value of UK demand for calcium carbonate, concrete, tomatoes, polyurethane are respectively of 5-43 KtonCO_2/year, 0-100 KtonCO_2/year, 108-2018 KtonCO_2/year, 0-100 KtonCO_2/year (Alberici et al., 2017). All of these processes have also a high value of TRL (Alberici et al., 2017). Tomatoes are chosen for horticultural production because, they have the highest production (Department for

Environment Food and Rural Affairs, 2019) ahead of cucumbers, peppers and aubergines amongst those suggested as agricultural products that can be obtained from CO_2 in the UK (Alberici et al., 2017).

For each CO_2-based product, different production sites are suggested. For CH_3OH production Billingham is selected (Sheldon, 2017), for CH_4 production Isle of Grain and Avonmouth are selected (Natural Gas, 2019), for polyurethane production Manchester (Prea, 2019) and Alfreton (Basf, 2019) are suggested, for tomatoes growing Teesside and the Isle of Wight (Apsgroup, 2019) are considered, for concrete production York (MPA, 2019) and Wallasey (Hanson, 2019) are suggested, while for calcium carbonate production Lifford, Birmingham and Fort William are suggested (BCCF, 2019). At maximum two utilization sites are considered for each CO_2-based product, because the aim is to find a first distribution of CO_2 between the utilization and storage section in order to reduce emissions. These production sites have then a high production capacity. Utilization sites are shown in Figure VI.2.

Figure VI.14 CO_2 utilization sites suggested for CCUS supply chains of the UK (methanol production site, methane production site, polyurethane production site, tomatoes production site, concrete production site, calcium carbonate production site) (Leonzio et al., 2020)

The UK national demand of each of these CO_2-based products is the following: for CH_3OH $1.64 \cdot 10^{-4}$ Mton/year (Reportlinker, 2019), for methane 51.4 Mton/year (EIA, 2019), for polyurethane 0.15 Mton/year (ONS, 2019), for tomatoes $7.5 \cdot 10^{-2}$ Mton/year (Britishgrowers, 2019), for concrete 4.14 Mton/year (MPA, 2019), for calcium carbonate $6.53 \cdot 10^{-1}$ Mton/year (Bide et al., 2019).

Distances between stationary CO_2 source, utilization and storage sites are provided in the Appendix (Tables S1-S5).

For CO_2 capture, the same capture technologies/materials as reported in Chapter IV are considered: absorption technology, with materials such as monoethanolamine (MEA) (30%wt), piperazine (PZ) (40% wt) and ionic liquids (IL) (1-butyl-3-methylimidazolium acetate) ([bmim][Ac]), membrane technology with POE1, POE2 and FSC-PVAm, pressure swing adsorption (PSA) and vacuum swing adsorption (VSA) technologies with 13X, AHT, MVY and WEI.

VI.3 Results and discussion

In this section, results for CCUS supply chains developed for the UK are presented. The models formulated as MILP models and developed in AIMMS are solved thorough CPLEX 12.7.1. The model has 6423 (112 integer) variables and 7614 constraints. The computer processor is 2.5 GHz with 4 GB memory.

VI.3.1 Results of the CCUS supply chain with Bunter Sandstone as storage site

Table VI.4 shows the optimal topology of the CCUS supply chain with Bunter Sandstone as storage site, showing the amount of CO_2 that is sent to the utilization or storage from the selected source. The optimal solution is found in 0.58 seconds and in 54 iterations.

Table VI.4 Topology of the CCUS supply chain in the UK with Bunter Sandstone storage site (Leonzio et al., 2020)

CO_2 source	**CO_2 capture technology/material**	**CO_2 amount (Mton/year)**
	To storage	
Leeds	MEA absorption	0.4
	To utilization	
Leeds	PZ absorption	6

The system manages 61 Mton/year of CO_2 (in the four regions taken in the account in this study) and captures 6.4 Mton/year of CO_2. 6 Mton/year of CO_2 are sent to the utilization section, while 0.4 Mton/year of CO_2 are sent to the storage. The minimum target for CO_2 emissions reduction is achieved. For both cases,

Leeds is the selected CO_2 source. For the storage section, MEA absorption is the suggested capture technology, while for the utilization section PZ absorption is selected. As found in Chapter IV, the absorption technology is the preferred choice due to lower costs than for other technologies. The lower costs of absorption are also reported in Hasan et al. (2012), comparing absorption, membrane, PSA and VSA technologies at different flue gas flow rate and CO_2 composition. Also, it is possible to verify that the selection of capture material depends on the final use of CO_2, in addition to its treated amount, as found in Chapter IV of this thesis. For a fixed CO_2 composition, as in this case study, PZ material is preferred at higher flow rates due to lower costs, as shown by Kalyanarengan Ravi et al. (2017). For lower flow rates, the costs of MEA and PZ are comparable and MEA absorption capture technology is suggested.

As expected the selected CO_2 source is connected to a storage site in the Yorkshire and the Humber region (with Leeds as main city), because it is nearby. This reduces CO_2 transportation costs. In the utilization section, CO_2 is used to produce calcium carbonate, with the amount of 5.4 Mton/year, higher than the national demand (0.653 Mton/year (Bide et al., 2019)), then a substantial fraction of produced calcium carbonate should be exported to other Countries. Calcium carbonate is produced at Lifford, Birmingham and at Fort William. The graphical topology of this optimized supply chain is shown in Figure VI.3.

Figure VI. 3 Topology of the optimized CCUS supply chain with Bunter Sandstone as storage site (CO_2 source site, * CO_2 storage site, calcium carbonate production site, → to CO_2 storage site, → to CO_2 utilization site) (Leonzio et al., 2020)

CO_2 capture and compression costs are 0.687 billion€/year, CO_2 transportation costs are 2.16 million€/year, CO_2 storage costs are 0.765 million€/year, while calcium carbonate production costs are 0.352 billion€/year. At optimal conditions, the total costs of this CCUS supply chain are 1.04 billion€/year. CO_2 capture and compression costs have the highest influence on the total costs, as also found in other supply chains reported in the literature (Hasan et al., 2014; Kalyanarengan Ravi et al., 2017; Zhang et al., 2018). Calcium carbonate production costs also have a high influence on the total costs.

An economic analysis is carried out to evaluate the NPV and PBP. For this supply chain, it is found that at the optimal conditions, the NPV is 0.554 trillion€, while the PBP is 2.85 years. The system is economically profitable only when considering carbon tax (80 €/tonCO_2) and without considering other additional economic incentives.

The cost of polyurethane production is covered by confidentiality obligations, then a sensitivity analysis is developed in order to verify that the suggested value is not significant for the obtained results. In this sensitivity analysis different production costs, lower than the selling price (between 1349 €/ton and 2158 €/ton), are considered. The results of CCUS supply chain optimization are independent by the polyurethane production cost (a total cost of the supply chain of 1.04 billion€/year is obtained in all different exanimated cases).

VI.3.2 Results of the CCUS supply chain with Scottish off-shore as storage site

The optimal topology of the CCUS supply chain with Scottish off-shore as storage site is reported in Table VI.5. 54 iterations are used to solve the model in 0.81 seconds.

Table VI.5 Topology of the CCUS supply chain for the UK with Scottish off-shore as storage site (Leonzio et al., 2020)

CO_2 source	**CO_2 capture technology/material**	**CO_2 amount (Mton/year)**
	To storage	
Edinburgh	VSA-WEI	4.84
	To utilization	
Leeds	PZ Absorption	1.56

The system involves 61 Mton/year of CO_2 (in the four regions taken in the account in this study) and captures 6.4 Mton/year from those emissions, according to the established environmental target. In this case, 4.84 Mton/year of captured CO_2 are sent to the storage section, while 1.56 Mton/year of captured CO_2 are sent to the utilization. For the storage section, Edinburgh is the source selected in this case with VSA technology using WEI material as selected capture process. In the utilization section, Leeds CO_2 source is

chosen by the model, with PZ absorption as capture technology. Flue gas from Edinburgh has a CO_2 composition of 12 mol%, slightly lower than CO_2 composition of flue gas from Leeds (13 mol%). However, the flue gas flow rate from Edinburgh is higher than that from Leeds. These results regarding the choice of capture technology are in agreement with those reported in the literature by Hasan et al. (2012): at a comparable CO_2 composition (just above 10 mol%), for relatively low flue gas flow rates the absorption technology is the suggested choice, while for relatively high flue gas flow rates the VSA process is suggested due to lower costs. Regarding the capture material, PZ is selected due to lower costs at lower CO_2 compositions for a fixed amount of flue gas flow rate (Kalyanarengan Ravi et al., 2017). The WEI zeolite material is chosen because the flue gas flow rate of Leeds is not so high (Zhang et al., 2018).

As in the previous case study, the selected CO_2 source from which CO_2 is sent to the storage is the nearest site in order to reduce CO_2 transportation costs. In the utilization section, CO_2 is used to produce calcium carbonate (1.4 Mton/year) at Lifford, Birmingham and at Fort William. A somewhat higher amount than the national demand is produced, then it would need to be exported to other Countries. The topology of this CCUS supply chain is shown in Figure VI.4.

Figure VI. 4 Topology of the optimized CCUS supply chain with Scottish off-shore as storage site (CO_2 source site, * CO_2 storage site, calcium carbonate production site, to CO_2 storage site, to CO_2 utilization site) (Leonzio et al., 2020)

The total costs of the supply chain are of 0.425 billion€/year. CO_2 capture and compression costs, CO_2 transportation costs, CO_2 storage costs and production costs of calcium carbonate are respectively of 0.323 billion€/year, 3.57 million€/year, 7.76 million€/year and 91.5 million€/year. CO_2 capture and compression costs have the highest influence on the total costs as in the previous case study and as reported elsewhere in the literature (Hasan et al., 2014; Kalyanarengan Ravi et al., 2017; Zhang et al., 2018). Capture and compression costs are followed by calcium carbonate production costs, CO_2 storage costs and CO_2 transportation costs. A more detailed economic analysis is carried out for the optimized system, in order to evaluate its profitability. The NPV and PBP are calculated and are respectively of 0.12 trillion€ and 5.27 years. In this analysis, only a carbon tax of 80 €/tonCO_2 is considered. A profitable system is obtained with a PBP period of about 5 years.

VI.3.3 Results of the CCUS supply chain with Ormskirk Sandstone storage site

The optimal structure of the CCUS supply chain with the storage site in the East Irish Sea is reported in Table VI.6. The optimal solution is found with 54 iterations in 0.8 seconds.

Table VI.6 Topology of the CCUS supply chain for the UK with Ormskirk Sandstone as storage site (Leonzio et al., 2020)

CO_2 source	**CO_2 capture technology/material**	**CO_2 amount (Mton/year)**
	To storage	
Manchester	MEA Absorption	0.46
	To utilization	
Leeds	PZ Absorption	5.94

The system involves 61 Mton/year of CO_2, globally (in the four regions taken in the account in this study) and chooses to capture 6.4 Mton/year of these emissions from selected sources. A small amount of CO_2 is sent to the storage: only 0.46 Mton/year are sent to the Ormskirk Sandstone storage site. 5.94 Mton/year of CO_2 are sent to the utilization section to produce calcium carbonate. As far as the storage section is concerned, Manchester, with a CO_2 composition of 14 mol%, is the selected source: once more it is the nearest source to the storage site and for this reason it is selected. For the utilization section, Leeds (i.e. the Yorkshire and the Humber region with a CO_2 composition of 13 mol%) is the chosen CO_2 source. For both of them absorption technology is the selected process. However, two different capture materials are selected: for the storage section, MEA is selected while for the utilization section, PZ solution is suggested. As in the first case study (the CCUS supply chain with Bunter Sandstone as storage site), absorption technology is selected due to lower costs compared to other capture technologies (Hasan et al., 2012).

However, for higher flow rates the PZ solution is the best material because it can ensure lower costs compared to MEA (Kalyanarengan Ravi et al., 2017). The optimized topology of this developed CCUS supply chain is shown in Figure VI.5.

Figure VI.5 Topology of the optimized CCUS supply chain with Ormskirk Sandstone as storage site (CO_2 source site, * CO_2 storage site, calcium carbonate production site, to CO_2 storage site, to CO_2 utilization site) (Leonzio et al., 2020)

5.35 Mton/year of calcium carbonate are produced in the utilization section (at Lifford, Birmingham and at Fort William). Some of the produced calcium carbonate needs to be exported. Inside the optimized supply chain, CO_2 capture and compression costs are 0.682 billion€/year, CO_2 transportation costs are 2.18 million€/year, CO_2 storage costs are 0.477 million€/year, while calcium carbonate production costs are 0.349 billion€/year. The total costs of the optimized CCUS supply chain are equal to 1.03 billion€/year. As already discussed, capture and compression costs mostly influence the total costs, followed by calcium carbonate production costs, CO_2 transportation costs and CO_2 storage costs. To evaluate the economic feasibility of the supply chain, the value of NPV and PBP are found. As in previous cases, only a carbon tax is considered with a value of 80 €/tonCO_2. Results show that the NPV is equal to 0.549 trillion€, while

the PBP is 2.86 years. Profitability is ensured by the optimized CCUS supply chain with Ormskirk Sandstone as storage site.

VI.3.4 Comparison among the CCUS supply chains developed above

A comparison among the different CCUS supply chains developed here is shown in Table VI.7.

Table VI.7 Comparison among the CCUS supply chains for the UK (Leonzio et al., 2020)

Storage site	Bunter Sandstone	Scottish off-shore	Ormskirk Sandstone
Treated CO_2 (Mton/year)	61	61	61
Captured CO_2 (Mton/year)	6.4	6.4	6.4
Minimum target for CO_2 reduction (Mton/year)	6.4	6.4	6.4
Total costs of CCUS supply chain (billion€/year)	1.04	0.425	1.03
Produced CO_2-based product	calcium carbonate	calcium carbonate	calcium carbonate
Amount of CO_2-based product (Mton/year)	5.4	1.4	5.35
Net present value (trillion€)	0.554	0.12	0.549
Payback period (years)	2.85	5.27	2.86
Production cost of CO_2-based product (€/ton)(*)	193	304	193

(*) in this evaluation economic incentives and carbon tax are not considered

The systems consider the same amount of CO_2 emissions of 61 Mton/year and capture the same amount of CO_2 (6.4 Mton/year) from the selected sources according to the minimum target for emissions reduction. Only calcium carbonate is produced in these supply chains due to lower production costs to achieve the target for CO_2 reduction. 5.4 Mton/year, 1.4 Mton/year and 5.35 Mton/year of calcium carbonate are produced in the CCUS supply chain with Bunter Sandstone, Scottish off-shore and Ormskirk Sandstone as storage site respectively. This amount of calcium carbonate is higher than the national demand so a fraction of it should be exported and sold on the international market. The CCUS supply chain with the lowest costs is that with Scottish off-shore as storage site. However, it is found that the CCUS supply chain with the highest value of NPV and the lowest PB time is that using Bunter Sandstone as storage site. For this structure, the NPV is 0.554 trillion€ while the PB time is 2.85 years. Calcium carbonate production cost is 193 €/ton (without considering economic incentives or a carbon tax). The CCUS supply chain with Bunter Sandstone storage site is the best suggested solution according to the model.

VI.3.5 Further enhancement of CCUS supply chains developed for UK

In the supply chain models developed in previous sections, the production of a single good (calcium carbonate) in substantial excess of the UK national demand is predicted to be obtained by the optimized supply chains, because of its low cost in relation to other utilization options and of the limited capacity of each CO_2 storage site. Market generally would not like such conditions, so a new case study is considered

here for the UK. In fact, for the above frameworks it is assumed that for all CO_2-based products the respective production should not exceed the double of the corresponding national demand. These constraints are then introduced into the mathematical model.

For the CCUS supply chain with Bunter Sandstone as storage site, the new optimal structure, calculated in 1.36 seconds, is reported in Table VI.8.

Table VI.8 Topology of the CCUS supply chain for the UK with Bunter Sandstone as storage site when constraints about the national demand of CO_2-based products are taken into account

CO_2 source	**CO_2 capture technology/material**	**CO_2 amount (Mton/year)**
	To storage	
Leeds	IL Absorption	0.4
	To utilization	
Leeds	PZ Absorption	5.999
Manchester	PZ Absorption	0.001

As in the previous cases, the system treats 61 Mton/year of CO_2 emissions and captures 6.4 Mton/year of CO_2, that are sent to the storage Bunter Sandstone (0.4 Mton/year) and to the utilization section (6 Mton/year). In particular, Leeds is connected with the capture site using IL absorption, while Manchester and again Leeds are connected to the utilization section through PZ absorption. As shown in Chapter III, the absorption is the preferred technology. Overall, the choice of the capture material depends on the final use of CO_2, but PZ due to its low costs is the preferred choice.

The new framework produces CH_3OH (328 ton/year), CH_4 (1.56 Mton/year), concrete (8.28 Mton/year), calcium carbonate (1.31 Mton/year), in an amount equal or lower than the double of respective national demand that must to be satisfied. The national demand is satisfied for all products except for CH_4. It is evident that a situation more friendly for the market is ensured, and the minimum target for CO_2 emissions reduction according to the environmental policy is satisfied also under this scenario.

Figure VI.6 shows the optimized topology of the CCUS supply chain with Bunter Sandstone as storage site.

Figure VI.6 Topology of the optimized CCUS supply chain with Bunter Sandstone as storage site when constraints about the national demand of CO_2-based products are taken into account (CO_2 source site, * CO_2 storage site, calcium carbonate production site, methanol production site, methane production site, concrete production site, to CO_2 storage site, to CO_2 utilization site)

Despite a greater flexibility in the offer of CO_2-based products on the market, compared to the optimized base case, this CCUS supply chain has a higher cost, 8 billion€/year. In particular, CO_2 capture and compression costs are 0.687 billion€/year, CO_2 transportation costs are 2.16 million€/year, CO_2 storage costs are 0.765 million€/year, CH_3OH production costs are 0.2 million€/year, CH_4 production costs are 7.04 billion€/year, concrete production costs are 0.181 billion€/year and calcium carbonate production costs are 85.2 million€/year. It is evident that CH_4 production cost has the highest influence on the total costs of the CCUS supply chain, followed by carbon capture and compression costs and concrete production costs. However, production of a certain amount of methane is necessary in order to reach the objective to reduce carbon dioxide emissions as requested by environmental constraints, under conditions imposed on the supply chain.

It results that economic incentives and carbon tax are required to have a positive NPV. For CH_4, CH_3OH, concrete and calcium carbonate the considered economic incentives are in the order of 270 €/MWh, 0.13 €/kWh, 0.5 €/ton and 0.5 €/ton. Carbon tax is set at 80 €/ton. Under these assumptions, the value of NPV

is 42.3 billion€, while the value of PBP is 4.56 years. For the CCUS supply chain with Scottish offshore as storage site, the optimal topology, calculated in 0.55 seconds, is reported in Table VI.9.

Table VI.9 Topology of the CCUS supply chain for the UK with Scottish offshore as storage site when constraints about the national demand of CO_2-based products are taken into account

CO_2 source	**CO_2 capture technology/material**	**CO_2 amount (Mton/year)**
	To storage	
Edinburgh	MEA Absorption	4.84
	To utilization	
Edinburgh	PZ Absorption	0.001
Leeds	PZ Absorption	1.55

Overall, 61 Mton/year of CO_2 emissions are treated and 6.4 Mton/year of CO_2 are captured: 4.84 Mton/year of CO_2 are sent to the storage section through MEA absorption, while 1.56 Mton/year of CO_2 are sent to the utilization section considering Edinburgh and Leeds are sources. In this last case, PZ absorption is used. Absorption technology is the preferred choice. In the utilization section, concrete (3.61 Mton/year), CH_3OH (328 ton/year) and calcium carbonate (1.31 Mton/year) are produced. CH_3OH and calcium carbonate are equal to the double of national demand, while concrete is lower than the respective national demand (4.14 Mton/year). Figure VI.7 shows the topology of the considered supply chain.

Figure VI.7 Topology of the optimized CCUS supply chain with Scottish offshore as storage site when constraints about the national demand of CO_2-based products are taken into account (CO_2 source site, * CO_2 storage site, calcium carbonate production site, methanol production site, concrete production site, → to CO_2 storage site, → to CO_2 utilization site)

The total costs of this framework is 0.48 billion€/year (higher than the base case).
In particular, CO_2 capture and compression costs are 0.305 billion€/year, CO_2 transportation costs are 3.58 million€/year, CO_2 storage costs are 7.76 million€/year, CH_3OH production costs are 0.2 million€/year, concrete production costs are 78.7 million€/year and calcium carbonate production costs are 85.2 million€/year. Carbon capture and compression costs have the highest influence on the total costs. The system has a positive NPV considering only carbon tax at 80 €/ton. In fact, the value of NPV is 4.55 billion€, while the PBP is 3.47 years.
The same analysis is carried out for the CCUS supply chain with Ormskirk Sandstone as storage site. After the optimization achieved in 0.58 seconds, the obtained topology is shown in Table VI.10.

Table VI.10 Topology of the CCUS supply chain for the UK with Ormskirk Sandstone as storage site when constraints about the national demand of CO_2-based products are taken into account

CO_2 source	**CO_2 capture technology/material**	**CO_2 amount (Mton/year)**
	To storage	
Manchester	MEA Absorption	0.46
	To utilization	
Manchester	PZ Absorption	5.94

This framework captures 6.4 Mton/year of CO_2 from the selected source at Manchester with two different capture technologies (MEA absorption for the storage site and PZ absorption for the utilization section). In the utilization section, CO_2 is used to produce CH_3OH (328 ton/year), CH_4 (1.54 Mton/year), concrete (8.28 Mton/year) and calcium carbonate (1.31 Mton/year). Only CH_4 production does not achieve the national demand (51.4 Mton/year). Figure VI.8 describes the obtained topology.
The total costs of the framework is 7.87 billion€/year (higher than the base case). In particular, CO_2 capture and compression costs are 0.664 billion€/year, CO_2 transportation costs are 2.19 million€/year, CO_2 storage costs are 0.477 million€/year, CH_3OH production costs are 0.2 million€/year, CH_4 production costs are 6.9 billion€/year, concrete production costs are 0.181 billion€/year and calcium carbonate production costs are 85.2 million€/year. CH_4 production costs and carbon capture and compression costs have the higher influence on total costs.
At the same level of economic incentives considered for the CCUS supply chain with Bunter Sandstone as storage site, the NPV is positive and equal to 42.1 billion€ while the PBP is 4.54 years.

Figure VI.8 Topology of the optimized CCUS supply chain with Ormskirk Sandstone as storage site when constraints about the national demand of CO_2-based products are taken into account (CO_2 source site, * CO_2 storage site, calcium carbonate production site, methanol production site, methane production site, concrete production site, to CO_2 storage site, to CO_2 utilization site)

Overall, the obtained results suggest that it is possible to diversify the production in the UK avoiding a great amount of only one product. In this case, for the CCUS supply chain with Scottish offshore as storage site, economic incentives are not required and only carbon tax is needed to have a positive NPV. On the other hand, the other frameworks ensure also CH_4 production, however economic incentives are necessary. Among the two systems with a comparable PBP, the supply chain with Bunter Sandstone as storage site allows to have a higher value of NPV.

VI.4 Conclusions

In this chapter, three different CCUS supply chains for the UK are designed considering different storage sites (Bunter Sandstone, Scottish off-shore and Ormskirk Sandstone). These systems are modelled as MILP models and optimized through the minimization of total costs. Products for which the production process has a high value for TRL are considered: calcium carbonate, tomatoes, concrete and polyurethane. In projections for the year 2030, these products also meet a high national demand in terms of consumed CO_2. CH_3OH and CH_4, obtained from CO_2 hydrogenation reaction with renewable hydrogen, are also considered, as in many literature studies.

Results show that the CCUS supply chain with Bunter Sandstone as storage site is the most economically profitable system, due to the highest value of NPV (0.554 trillion€/year) and the lowest value of PB time (2.85 years), considering only carbon tax, at a value of 80 €/tonCO_2. The supply chain costs 1.04 billion€/year and reduces 6.4 Mton/year of CO_2 emissions. The captured CO_2 is used to produce 5.4 Mton/year of calcium carbonate, an amount greater than the national demand then, a proportion should be exported. All the considered CCUS supply chains are economically feasible considering only carbon tax.

To avoid the production of a great amount of calcium carbonate, the mathematical model is updated considering constraints about the production of CO_2-based products (this should not exceed the double of the corresponding national demand). In this case, more compounds are produced at a rate acceptable to the market, and only the system with Scottish offshore as storage site requires carbon tax to have a positive NPV. For the other case studies, economic incentives are also needed.

It has been shown how using a mathematical model to find the optimal configuration of alternative carbon dioxide storage and utilization chains, studies can be undertaken to find strategies for achieving the stringent CO_2 reduction targets that the UK seeks to achieve.

Appendix

Table S1 Distances between CO_2 sources and storage sites (NHC, 2019)

Cardiff	Bunter Sandstone	475	km
Cardiff	Forties	819	km
Cardiff	Ormskirk Sandstone	286	km
Edinburgh	Bunter Sandstone	341	km
Edinburgh	Forties	414	km
Edinburgh	Ormskirk Sandstone	179	km
Manchester	Bunter Sandstone	287	km
Manchester	Forties	587	km
Manchester	Ormskirk Sandstone	144	km
Leeds	Bunter Sandstone	227	km
Leeds	Forties	570	km
Leeds	Ormskirk Sandstone	207	km

Table S2 Distances between CO_2 source and utilization sites (NHC, 2019)

Cardiff	Billingham	384.24	km
Cardiff	London	211.52	km
Cardiff	Isle of Grain	269.06	km
Cardiff	Avonmouth	47.41	km
Cardiff	Manchester	263.97	km
Cardiff	Alfreton	217.5	km
Cardiff	Isle of Wight	157.6	km
Cardiff	York	309.84	km
Cardiff	Wallasey	216.29	km
Cardiff	Lifford	141.65	km
Cardiff	Fort William	606.71	km

Table S3 Distances between CO_2 source and utilization sites (NHC, 2019)

Edinburgh	Billingham	188.38	km
Edinburgh	London	518.15	km
Edinburgh	Isle of Grain	546.35	km
Edinburgh	Avonmouth	489.88	km
Edinburgh	Manchester	233.11	km
Edinburgh	Alfreton	322.69	km
Edinburgh	Isle of Wight	585.38	km
Edinburgh	York	244.04	km
Edinburgh	Wallasey	266.98	km
Edinburgh	Lifford	380.24	km
Edinburgh	Fort William	166.44	km

Table S4 Distances between CO_2 source and utilization sites (NHC, 2019)

Manchester	Billingham	107.43	km
Manchester	London	290.91	km
Manchester	Isle of Grain	325.25	km
Manchester	Avonmouth	262.12	km
Manchester	Manchester	0	km
Manchester	Alfreton	95.56	km
Manchester	Isle of Wight	352.41	km
Manchester	York	78.97	km
Manchester	Wallasey	67.23	km
Manchester	Lifford	147.32	km
Manchester	Fort William	382.76	km

Table S5 Distances between CO_2 source and utilization sites (NHC, 2019)

Leeds	Billingham	76.18	km
Leeds	London	284.02	km
Leeds	Isle of Grain	313.85	km
Leeds	Avonmouth	279.62	km
Leeds	Manchester	41.88	km
Leeds	Alfreton	89.96	km
Leeds	Isle of Wight	359.37	km
Leeds	York	37.15	km
Leeds	Wallasey	107.6	km
Leeds	Lifford	158.27	km
Leeds	Fort William	392.42	km

References

Alberici, S., Noothout, P., Mir, G.U.R., Stork, M., Wiersma (Ecofys), F., with technical input from Mac Dowell, N., Shah, N., Fennell P., Assessing the potential of CO2 utilization in the UK, Final report, Ecofys 2017 by order of: UK Department for Business, Energy & Industrial Strategy (BEIS).

Ancona, M.A., Antonucci, V., Branchini, L., Catena, F., De Pascale, A., Di Blasi, A., Ferraro, M., Italiano, C., Melino, F., Vita, A., 2019. Thermal integration of a high-temperature co-electrolyzer and experimental methanator for Power-to-Gas energy storage system, Energy Conversion and Management 186, 140–155.

Apsgroup, 2019. Available at: https://apsgroup.uk.com/discover

Babaei, M., Govindan, R., Korre, A., Shi, J.Q., Durucana, S., Quinn, M., McCormac, M., 2014. CO2 storage potential at Forties oilfield and the surrounding Paleocene sandstone aquifer accounting for leakage risk through abandoned wells, Energy Procedia 63, 5164 – 5171

Basf, 2019. Available at: www.basf.com

Bentham, M., An assessment of carbon sequestration potential in the UK – Southern North Sea case study, Tyndall Centre for Climate Change Research, 2006.

Bide, T., Brown, T.J., Idoine, N., Mankelow, J.M., 2019. United Kingdom Minerals Yearbook 2018, British Geological Survey Open Report, OR/19/018, 63 pp.

BCCF, 2019. Available at: http://www.calcium-carbonate.org.uk/uklocations.asp

Britishgrowers, 2019. Available at: http://www.britishgrowers.org/british-growing/

Broek, M.V.D., Brederode, E., Ramírez, A., Kramers, L., Kuip, M.V.D., Wildenborg, T., Turkenburg, W., Faaij, A., 2010. Environmental modelling & software designing a cost-effective CO2 storage infrastructure using a GIS based linear optimization energy model. Environ. Modell. Softw. 25 (12), 1754–1768

Committee on Climate Change, 2019. Available at: https://www.theccc.org.uk/wp-content/uploads/2015/11/Fifth-Carbon-Budget_Ch2_Overview-of-climate science-and-international-circumstances.pdf

Colacem, 2019. Available at: www.colacem.com

Dahowski, R., Dooley, J., Davidson, C., Bachu, S., Gupta, N., 2004. A CO2 Storage Supply Curve for North America, Proceedings of the 7. international conference on greenhouse gas control technologies

Department for business, energy and industrial strategy, 2019. Available at: https://assets.publishing.service.gov.uk/government/uploads/system/uploads/attachment_data/file/819648/ccus-business-models-consultation.pdf

Department of Business, Energy and Industrial Strategy, 2018. Local authority carbon dioxide emissions estimates 2016, Statistical Release: National Statistics.

Department of Energy & Climate Change, 2010, CO2 Storage in the UK - Industry Potential

Department for Environment Food & Rural Affairs, 2019. Available at: http://www.defra.gov.uk/statistics/foodfarm/landuselivestock/bhs/

EIA, 2019. Available at: https://www.eia.gov/beta/international/analysis.php?iso=GBR

Eurostat, 2019. Available at: https://ec.europa.eu/eurostat/statistics-explained/index.php/Natural_gas_price_statistics

Gammer, D., A. Green, ETI, S. Holloway, BGS, Smith, G., Senergy, The Energy Technologies Institute's UK CO2 Storage Appraisal Project (UKSAP), SPE Offshore Europe Oil and Gas Conference and Exhibition held in Aberdeen, UK, 6–8 September 2011

GCCSI, 2016. Carbon Capture and Storage Readiness Index.

Hank, C., Gelpke, S., Schnabl, A., White, R.J., Full, J., Wiebe, N., Smolinka, T., Schaadt, A., Henning, H.M., and Hebling, C., 2018. Economics & carbon dioxide avoidance cost of methanol production based on renewable hydrogen and recycled carbon dioxide – power-to-methanol, Sustainable Energy Fuels, 2, 1244-1261.

Hasan, M.M.F., Boukouvala, F., First, E.L., Floudas, C.A., 2014. Nationwide, Regional, and Statewide CO2 Capture, Utilization, and Sequestration Supply Chain Network Optimization, Ind. Eng. Chem. Res. 53, 7489−7506.

Hasan, M.M.F., Baliban, R.C., Elia, J.A., Floudas, C.A., 2012b. Modeling, simulation, and optimization of postcombustion CO2 capture for variable feed concentration and flow rate.2. Pressure swing adsorption and vacuum swing adsorption processes. Ind EngChem Res., 51, (48), 15665–82.

Hasan, M.M.F., First, E.L., Boukouvala, F., Floudas, C.A., 2015. A multi-scale framework for CO2capture, utilization, andsequestration: CCUS and CCU, Computers and Chemical Engineering 81, 2–21.

Hanson, 2019. Available at: https://www.hanson.co.uk/en/hanson-location-finder

Hendriks, C.A., 1994. Carbon Dioxide Removal from coal-Fired power plant. In department of science, technology, and society. Utrecht University. Utrecht, Netherlands.

Kalyanarengan Ravi, N., Van Sint Annaland, M., Fransoo, J.C., Grievink, J., Zondervan, E., 2017. Development and implementation of supply chain optimization framework for CO2 capture and storage in the Netherlands. Computer Chemical Engineering 102, 40–51.

Kirk. K.L., 2005. Potential for storage of carbon dioxide in the rocks beneath the East Irish Sea. British Geological Survey Internal Report, CR/05/127N. 24pp.

Kolstera, C., Agadad, S., Mac Dowell, N., Krevord, S., 2018. The impact of time-varying CO2 injection rate on large scale storage in the UK Bunter Sandstone, International Journal of Greenhouse Gas Control 68, 77–85.

Leonzio, G., Bogle, D., Foscolo, P.U., Zondervan, E. 2020. Optimization of CCUS supply chains in the UK: A strategic role for emissions reduction. Chemical Engineering Research and Design, 155 211-228.

MPA, 2019. Available at: https://mineralproducts.org/documents/Facts-at-a-Glance-2018.pdf

NAEI, 2019. Available at: http://naei.beis.gov.uk/reports/reports?section_id=4

Natural gas, 2019. Available at: https://assets.publishing.service.gov.uk/government/uploads/system/uploads/attachment_data/file/820685/Chapter_4.pdf

National Statistics, 2019. Available at: https://www.ons.gov.uk/businessindustryandtrade/manufacturingandproductionindustry/datasets/ukmanufacturerssalesbyproductprodcom

Nguyen, T.B.H., Zondervan, E. 2018. Ionic Liquid as a Selective Capture Method of CO2 from Different Sources: Comparison with MEA, ACS Sustainable Chemistry & Engineering, 6 (4), 4845-4853.

NHC, 2019. Available at: www.nhc.noaa.gov

OGC, 2018. Available at: http://oilandgasclimateinitiative.com/wp-content/uploads/2018/11/Potential-Value-of-CCUS-to-the-UK-Economy.pdf

ONS, 2019. Available at: https://www.ons.gov.uk/businessindustryandtrade/manufacturingandproductionindustry/datasets/ukmanufacturerssalesbyproductprodcom

Patricio, J., Angelis-Dimakisb, A., Castillo-Castillo, A., Kalmykova, Y., Rosado, L., 2017. Region prioritization for the development of carbon capture and utilization technologies, Journal of CO2 Utilization 17, 50–59.

Prea, 2019. Available at: http://www.prea.co.uk/

Quarton, C.J., Samsatli, S., 2020. The value of hydrogen and carbon capture, storage and utilisation in decarbonising energy: Insights from integrated value chain optimization, Applied Energy 257, 113936.

Reichert F., 2012 Wind-to-Gas-to-Money? Economics and Perspectives of the Power-to-Gas Technology. Aalborg University Department of Development and Planning MSc (Eng) Sustainable Energy Planning and Management. master thesis.

RMS, 2019. Available at: rmsconcrete.co.uk/prices/

Serpa, J., Morbee, J., Tzimas, E., 2011. Technical and Economic Characteristics of a CO2 Transmission Pipeline Infrastructure, doi:10.2790/30861.

Sheldon, D., 2017. Methanol Production – A Technical History A review of the last 100 years of the industrial history of methanol production and a look into the future of the industry, Johnson Matthey Technology Review, 61, 3, 172-182, 2017.

Van den Velden, 2019. Available at: https://www.holanda.es/media/106863/5)%20n.%20van%20der%20velden-producci%C3%B3n%20%E2%80%9Clocal-for-local%E2%80%9D%20de%20tomates%20en%20invernadero%20posibilidades%20y%20comentarios.pdf

von der Assen, N., Sternberg, A., Katelhon A., and Bardow, A., 2015. Environmental potential of carbon dioxide utilization in the polyurethane supply chain, Faraday Discuss., 183, 291-307.

Zappa, W., 2014. Pilot-scale Experimental Work on the Production of Precipitated Calcium Carbonate (PCC) from Steel Slag for CO2 Fixation, PhD thesis.

Zhang, A., Liu, L., Zhang, L., Zhuang, Y., Du, J. 2018. An optimization model for carbon capture utilization and storage supply chain: A case study in Northeastern China, Applied Energy 231, 194–206.

Nomenclature

Indices

i = carbon dioxide source

j = carbon dioxide capture system

k = carbon dioxide storage site and complementary utilization section

m = methanol production site

g = methane production site

p = polyurethane production site

t = tomato production site

c = concrete production site

d = calcium carbonate production site

Abbreviations

AIMMS = advanced interactive multidimensional modeling system

CC = carbon dioxide capture and compression costs [€/year]

CDC = flue gas dehydration costs [€/year]

CIC = carbon dioxide capture and compression investment costs [€/year]

COC = carbon dioxide capture and compression operating costs [€/year]

CCUS = carbon capture utilization and storage

CP = concrete production costs [€/year]

CP = tomato production costs [€/year]

CP = polyurethane production costs [€/year]

CP = calcium carbonate production costs [€/year]

CP = methanol production costs [€/year]

CP = methane production costs [€/year]

IC = maximum injection capacity per well [ton/year]

IL = ionic liquid

MEA = monoethanolamine

MILP = mixed integer linear programming

NPV = net present value

PBP = payback period

PSA = pressure swing adsorption

PZ = piperazine

SC = carbon dioxide storage cost [€/year]

SIC = carbon dioxide investment storage costs [€]

SOC = carbon dioxide operating storage costs [€/year]

TC = carbon dioxide transportation costs [€/year]

TH = time horizon

TIC = investment carbon dioxide transportation costs [M€]

TOC = operating carbon dioxide transportation costs [M€/year]

TRL = technology readiness level

VSA = vacuum swing adsorption

Variables

Continuous variables

$FR_{i,j,k}$ = fraction of captured carbon dioxide from source i with technology j sent to storage site k

$Utilization_{i,j,k}$ = fraction of captured carbon dioxide from source i with technology j sent to overall utilization site k

$Methanol_{i,j,m}$ = fraction of captured carbon dioxide from source i with technology j sent to methanol production site m

$Methane_{i,j,g}$ = fraction of captured carbon dioxide from source i with technology j sent to methane production site g

$Polyurethane_{i,j,p}$ = fraction of captured carbon dioxide from source i with technology j sent to polyurethane production site p

$Tomato_{i,j,t}$ = fraction of captured carbon dioxide from source i with technology j sent to tomato growing t

$Concrete_{i,j,c}$ = fraction of captured carbon dioxide from source i with technology j sent to concrete curing c

$CalciumCarbonate_{i,j,d}$ = fraction of capture carbon dioxide from source i with technology j sent to calcium carbonate production site d

Binary variables

$X_{i,j,k}$ = 1 if carbon dioxide is captured from source i with technology j and sent to storage site k, otherwise 0

$Y_{i,j,k}$ = 1 if carbon dioxide is capture from source i with technology j and sent to storage/utilization site k, otherwise 0

Parameters

b = parameter in SIC

C_k^{max} = maximum storage capacity for storage site k [ton]

CR^{min} = minimum target for overall carbon dioxide reduction [ton/year]

CS_i = carbon dioxide emissions from source i [ton/year]

$D_{i,k}/D_{i,c}/D_{i,t}/D_{i,p}/D_{i,d}/D_{i,m}/D_{i,g}$ = distance from source i to storage k/concrete c/tomato t/polyurethane p/calcium carbonate d/methanol m/methane g production site [km]

d_{well} = depth of well [km]

F_i/F = flue gas flow rate from source i [mol/s]

F_t = terrestrial factor

m = parameter in SIC

m = parameter in CIC and COC

n = parameter in CIC and COC

X = parameter equal to 1 if carbon dioxide is transported to a specific utilization site

x_{CO2} = carbon dioxide molar fraction

XL_i = lowest composition processing limit for capture technology j [mol%]

XH_i = highest composition processing limit for capture technology j [mol%]

XS_i = carbon dioxide composition in the flue gas emission from source i [mol%]

Greek letters

α = parameter in CIC and COC

α_t = parameter in TIC

β = parameter in CIC and COC

β_t = parameter in TIC

γ = parameter in CIC and COC

Chapter VII

Definition of a new objective function for CCUS supply chains

A more complete and realistic objective function than that in the previous studies is considered and minimized in order to determine the optimal design of carbon capture utilization and storage systems. The objective function includes carbon tax remission, economic incentives and revenues that are subtracted from total costs. Then mixed integer linear programming models with this new objective function are developed for a carbon capture utilization and storage supply chain in Germany, Italy and the UK, considering for each of them the same utilization and storage options as in the previous studies. For each framework, the most significant values of cost parameters on the market referred to the last years are considered in a scenario analysis. Results show that carbon tax influences only the total value of the objective function while, economic incentives and revenues have a significant effect also on the topology of the supply chain.

VII.1 Introduction

For the carbon capture utilization and storage (CCUS) supply chains of Germany, Italy and the UK previously examined, the objective function of the mathematical model is represented by total costs that are minimized. It is found that economic incentives obtained for a sustainable production, and carbon tax remission, the importance of which is already underlined in the literature, are required to have a profitable solution from an economic point of view (for the framework in Italy and in Germany producing only methanol (CH_3OH) carbon tax remission and economic incentives are required, for the framework in the UK and in Germany producing more products only carbon tax remission is needed). Moreover, for these systems, CO_2-based products can be sold generating revenues.

Then, for a more complete and realistic description of these systems, carbon tax, revenues and economic incentives are considered in the objective function and subtracted to total costs (CO_2 capture and compression costs, CO_2 storage costs, CO_2 transportation costs and production costs of CO_2-based products). This new objective function is minimized in order to design carbon supply chains and find their best topology. A more complex objective function is therefore suggested than those reported in the literature, considering generally total costs only.

It is necessary to keep in mind and put more attention on the uncertainties of these models deriving by decades-long time horizons, such as climate conditions, geophysical properties of storage reservoirs, economic parameters and environmental policies. The complicated and dynamic nature of a supply chain determines a high level of uncertainty on decisions concerning it, as also reported by Ozkir and Basligil (2013).

Then, the aim of the research work described in this chapter is to develop a deterministic mixed integer linear programming (MILP) model for CCUS supply chains considered for Italy, Germany and the UK as in the previous studies with this new objective function, in order to have a more realistic design.

In addition, as an innovative point, in line with what is reported and suggested in the literature about the uncertainty, different levels of economic incentives, carbon tax and revenues are considered, aiming to evaluate their effect on the supply chain design. As another objective of this work, the influence of the market on the design of these frameworks is analyzed.

VII.2 Model development

For the CCUS supply chain of Germany, Italy and the UK the mathematical model is developed as in previous, respective Chapters. Only the objective function is changed. The MILP models are solved using AIMMS software (Advanced Interactive Multidimensional Modeling).

VII.2.1 Objective function

Revenues, economic incentives and carbon tax are included in the expression of the objective function: the maximum profit is sought for the system. For CCUS supply chains in Italy and in Germany producing only methanol (CH_3OH) via methane (CH_4) dry reforming, the objective function ϕ is the following (see Eq. VII.1):

$$\phi = total\ costs - revenues - economic\ incentives - carbon\ tax\ remission \qquad (VII.1)$$

For the CCUS supply chain producing different products in Germany and in the UK, the objective function ϕ is (see Eq. VII.2):

$$\phi = total\ costs - revenues - carbon\ tax\ remission \qquad (VII.2)$$

When no economic incentives are required for the profitability of a CCUS system, as it is the case of these supply chains (see Chapters IV and VI), then a simplification of the objective function is considered.
In both equations, total costs are given by CO_2 capture and compression costs, CO_2 transportation costs, CO_2 storage costs and production costs of different CO_2-based products. Economic incentives are obtainable because of the sustainable production route of products, while carbon tax is avoided to the extent of the captured CO_2. Revenues are obtained from selling the obtained CO_2-based products. These objective functions are minimized in order to design the best supply chain.

VII.2.2 Case study

For the CCUS supply chain of Italy, Germany and the UK, the case study has been discussed in the previous, respective Chapters. It is interesting here to analyze the variation of the market. Then, for CCUS supply chains of Italy, the carbon tax is considered over three different levels: 20 €/tonCO_2, 80 €/tonCO_2 and 140 €/tonCO_2 (OECD, 2013), while economic incentives assume these values: 240 €/MWh, 270 €/MWh and 300 €/MWh (Leonzio and Zondervan, 2020).

For the CCUS supply chain of Germany producing only CH_3OH, the variation of carbon tax is at three different levels: 20 €/tonCO_2, 80 €/tonCO_2 and 140 €/tonCO_2 (OECD, 2013), while economic incentives assume a value of 0.092 euro/kWh, 0.111 euro/kWh and 0.129 euro/kWh (Leonzio et al., 2019a). Methanol selling price is supposed to be between 90 €/ton and 540 €/ton (Mikulski, 2018).

For the CCUS supply chain in Germany producing methanol, urea, concrete, wheat, polyurethane, calcium carbonate and lignin, the carbon tax is changed as in the previous case study, while economic incentives are not considered in this case, due to the economic convenience of selling CO_2-based products. However, selling prices are changed. The lowest value of selling price for methanol, concrete, wheat, lignin, polyurethane, calcium carbonate and urea is fixed at 90 €/ton, 34 €/ton, 125 €/ton, 480 €/ton, 6384 €/ton, 108 €/ton, 253 €/ton, respectively; while the highest selling price for methanol, concrete, wheat, lignin, polyurethane, calcium carbonate and urea is fixed at 540 €/ton, 138 €/ton, 260 €/ton, 750 €/ton, 7250 €/ton, 132 €/ton and 369 €/ton, respectively (Mikulski, 2018; European Commission, 2019; Gosselink, 2011; PlasticsInsight, 2019; PCI, 2019; Fao, 2019; WSDOT, 2019).

For the CCUS supply chain of the UK, the carbon tax is considered to be equal to 20 €/tonCO_2, 80 €/tonCO_2 and 140 €/tonCO_2 (OECD, 2013), respectively. Economic incentives are not required, then only selling prices are changed. For methanol, methane, polyurethane, tomatoes, concrete and calcium carbonate the lowest selling price assumed inside the market is respectively 690 €/ton, 0.0178 €/kWh, 2260 €/ton, 1.12 €/kg, 15.18 €/ton, 108 €/ton. On the other hand, the highest selling price of these is respectively 3510 €/ton, 0.028 €/kWh, 2590 €/ton, 2.68 €/kg, 153 €/ton and 132 €/ton (Office for National Statistics, 2019; Department for Business, Energy and Industrial Strategy, 2019; Department for Environment, Food and Rural Affairs, 2019; WSDOT, 2019; PCI, 2019).

VII.3 Results and discussion

In this section, the results are presented of sensitivity analyses for CCUS supply chains in Italy integrated by a power to gas system, for the CCUS supply chain in Germany producing CH_3OH via CH_4 dry reforming and different CO_2-based compounds, and for the CCUS of the UK producing mainly calcium carbonate. The influence of the market on the CCUS supply chains design is evaluated and analyzed. CPLEX 12.7.1 is the solver that is selected, while the computer processor is 2.5 GHz and the memory is 4 GB.

VII.3.1 Results for CCUS supply chains in Italy

A first sensitivity analysis is developed for CCUS supply chains in Italy, changing carbon tax and economic incentives according to a low level (20 €/ton and 240 €/MWh, respectively for carbon tax and economic incentives), medium level (80 €/ton and 270 €/MWh, respectively for carbon tax and economic incentives) and high level (140 €/ton and 300 €/MWh, respectively for carbon tax and economic incentives) (OECD, 2013; Leonzio and Zondervan, 2020). The selling price of methane is set at 25 €/MWh (Eurostat, 2019).

Results are reported in Tables S1-S3 of the Appendix. Results show that, changing carbon tax and economic incentives, the total value of the objective function and the amount of produced CH_4 are changed, and also the topology of the system changes. Overall, for all supply chains, the amount of CH_4 produced per year is between 16.1 Mton/year and 101 Mton/year, while the total value of the objective function ranges between 15.5 billion€/year and -70 billion€/year. Positive values of the objective function suggest that the system is not economically profitable. At the low values of carbon tax and economic incentives, a negative profit is present. For the CCUS supply chain with Malossa San Bartolomeo as storage site, the total value of the objective function, the amount of CH_4 and the avoided (overall captured) CO_2 are shown in 3D plots in figure VII.1a, VII.1b, and VII.1c respectively.

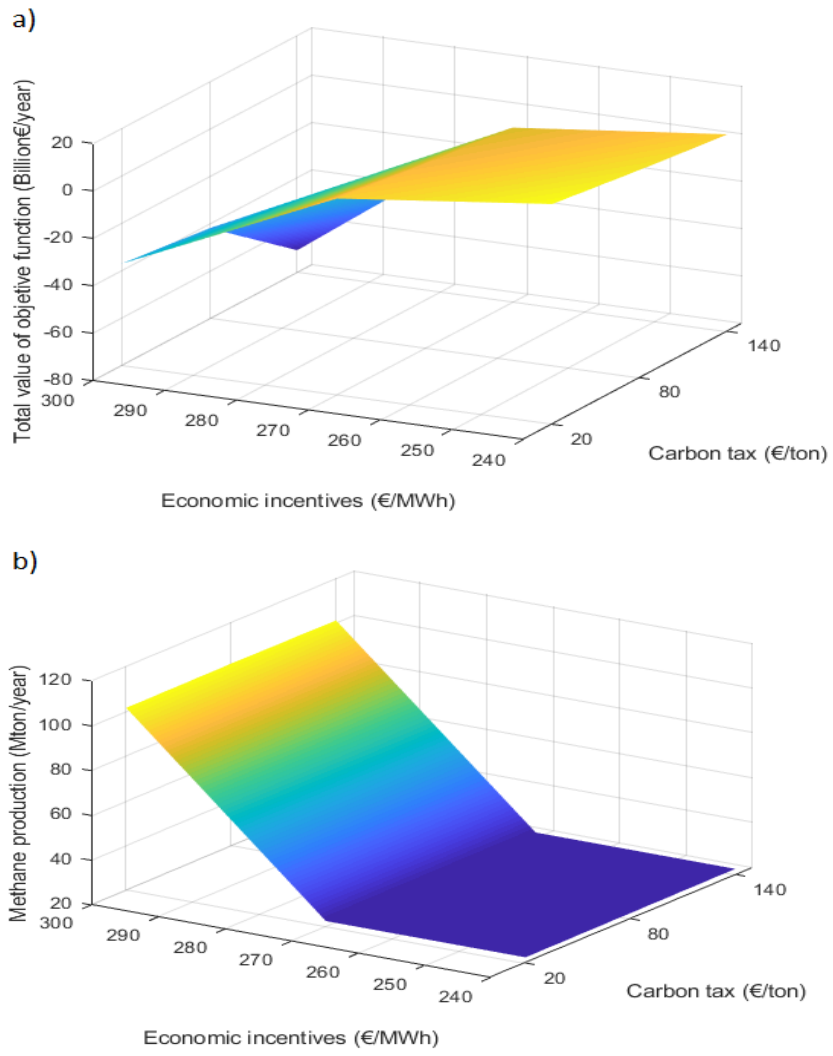

Figure VII.1 (Following)

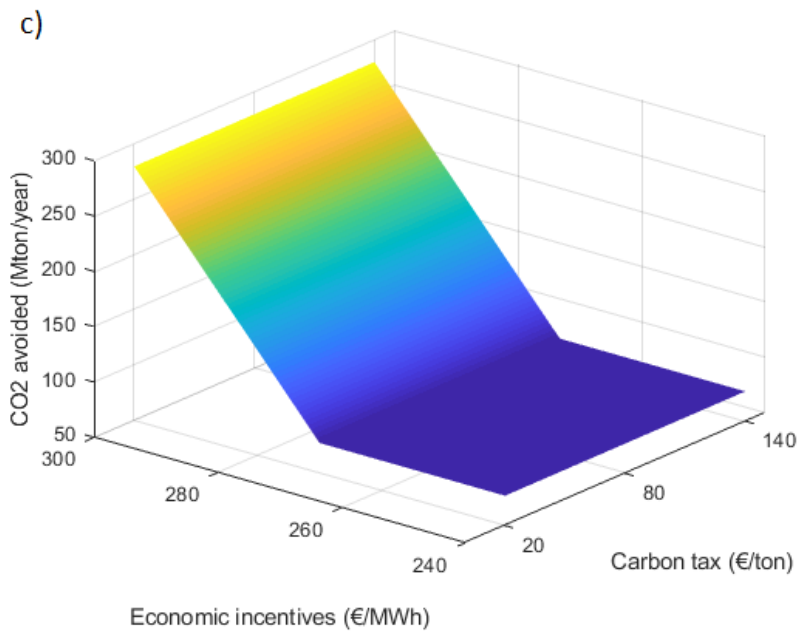

Figure VII.1 a) Total value of the objective function; b) Methane production; c) Avoided CO_2 as a function of carbon tax and economic incentives for the CCUS supply chain of Italy with Malossa San Bartolomeo as storage site (Leonzio et al., 2020)

It is possible to see that the overall captured CO_2 assumes values between 77 Mton/year and 279 Mton/year, the amount of produced CH_4 assumes values between 22.5 Mton/year and 101 Mton/year while the total value of the objective function is between 2.65 billion€/year and -70.7 billion€/year. Moreover, CH_4 production and avoided CO_2 have the same trend, and a positive value of the objective function (corresponding to economic loss) is found for a lower amount of CH_4 and captured CO_2. On the other hand, negative values of the objective function are present for higher captured CO_2 and CH_4 production. In this last case, higher values of incomes due to revenues (for selling more CH_4) and carbon tax remission are ensured. In addition, it is found that a higher CH_4 production and corresponding lower CO_2 emissions are ensured when economic incentives are higher; these results point to the value of "multi-objective optimization" considering both economic and environmental aspects in future studies.

As discussed in the next section, the carbon tax alone has no influence on the amount of produced CH_4 and captured CO_2 (then on the topology of the system), but only on the total value of the objective function.

To show that the topology is modified in this sensitivity analysis, Table S1, S2 and S3 of the Appendix report also the topology of different CCUS supply chains in Italy with different storage sites, all investigated at the low, medium and high level of carbon tax and economic incentives, respectively.

It is evident that, at a high level of these parameters, all CO_2 that can be captured in all sources is sent to the utilization for CH_4 production, maximizing the profit of the system. In fact, at the low and medium value of the considered parameters CO_2 reduction is of 77 Mton/year (the minimum target to achieve CO_2 reduction required by the environmental policy), while at a high value of considered parameters, 279

Mton/year of CO_2 are reduced and used in the power to gas system to produce 101 Mton/year of CH_4. In the first case, a reduced number of sources are selected while in the second case, all sources are selected. The effect of the investigated parameters is positive on the amount of captured CO_2 and selected carbon sources. Considering the structure of the objective function, when carbon tax and economic incentives are increased in order to decrease the value of the objective function, revenues should also increase. If revenues increase, the amount of produced CH_4 increases and so does also the amount of captured CO_2 from the selected sources.

Overall, monoethanolamine (MEA) absorption is the preferred choice and pressure swing adsorption (PSA) is chosen in one case only. Also in Chapter V, MEA absorption is the best choice due to low costs. The low cost for the PSA capture technology is reported also by Kalyanarengan Ravi et al. (2017). Membrane and IL absorption are used and preferred for higher carbon dioxide content streams (Hasan et al., 2012).

The sensitivity analysis carried out above is changing both carbon tax and economic incentives together. It is interesting to perform an additional analysis changing only carbon tax according to its low, medium and high level, in order to check its specific effect on the results. Selling price of methane and economic incentives are respectively of 25 €/MWh and 270 €/MWh. It is found that carbon tax has no effect on the topology and methane production: it influences only the total value of the objective function. Table S4 of the Appendix shows in more details that the topology of the CCUS supply chain with Malossa San Bartolomeo as storage site does not change for all values of carbon tax remission.

Figure VII.2 and VII.3 show respectively the trend of the total value of the objective function and CH_4 produced, while Figure VII.4 shows the amount of captured CO_2 for the different values of carbon tax.

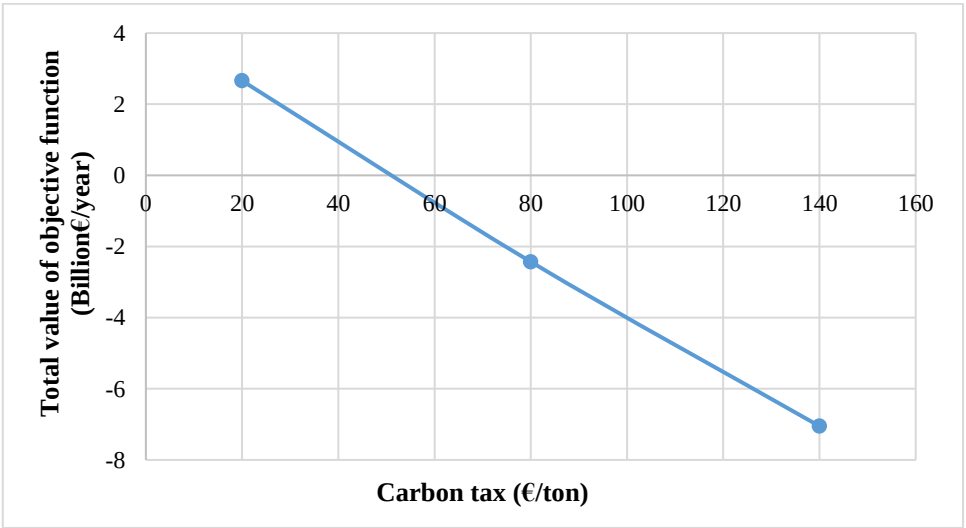

Figure VII.2 Trend of the total value of the objective function versus carbon tax for the CCUS supply chain with Malossa San Bartolomeo as storage site (Leonzio et al., 2020)

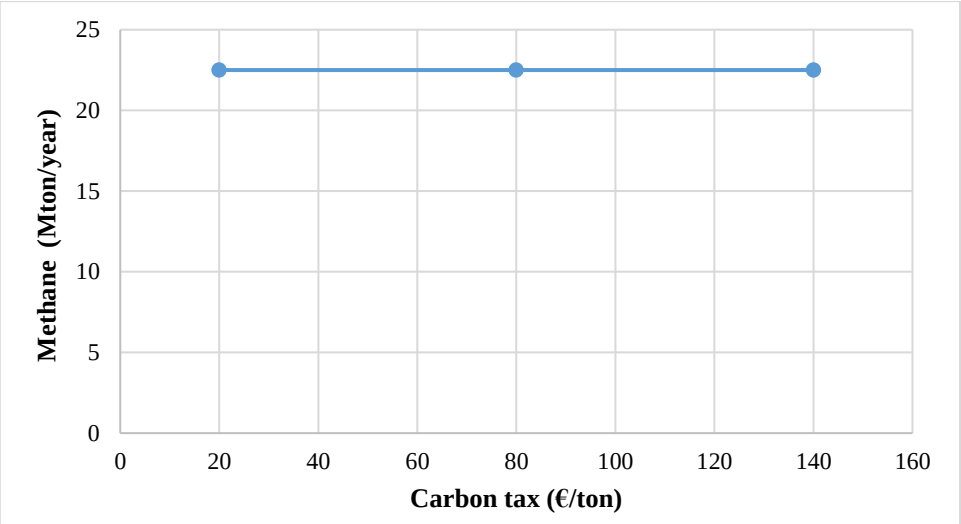

Figure VII.3 Trend of methane production versus carbon tax for the CCUS supply chain with Malossa San Bartolomeo as storage site (Leonzio et al., 2020)

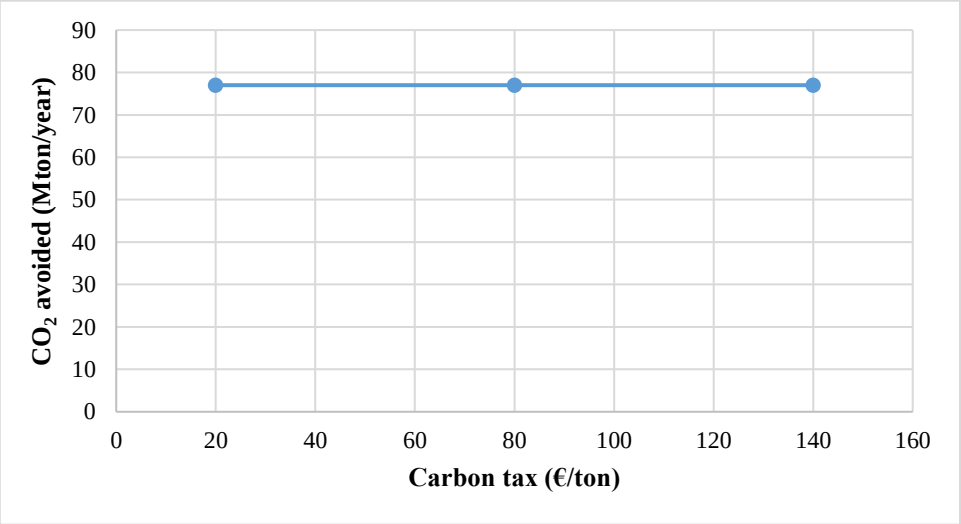

Figure VII.4 Trend of avoided carbon dioxide versus carbon tax for the CCUS supply chain with Malossa San Bartolomeo as storage site (Leonzio et al., 2020)

The total value of the objective function ranges between 2.66 billion€/year and -7.05 billion€/year: only at high values of carbon tax the system is economically profitable. 22.5 Mton/year of CH_4 are produced while 77 Mton/year of CO_2 are avoided. These results confirm that the topology of the CCUS supply chain is mainly changed due to the variation of economic incentives, while carbon tax influences only the value of the objective function. Then, if it is desirable to have a fixed topology of CCUS supply chain, the profitability of the system can be obtained changing the value of carbon tax (high values are preferred, of course).

The results obtained for this supply chain with Malossa San Bartolomeo as storage site are valid also for the other CCUS supply chains in Italy. A comparison between the results of these sensitivity analyses and the supply chain of Malossa San Bartolomeo, optimized in Chapter V without considering regulatory and market incentives in the objective function, is reported in Table VII.1.

Table VII.13 Comparison between the CCUS supply chain with Malossa San Bartolomeo developed in Chapter V and the results obtained in this work with the new objective function (Leonzio et al., 2020)

		Total value of objective function (billion€/year)	CO_2 to storage (Mton/year)	CO_2 to utilization (Mton/year)	Captured CO_2 (Mton/year)
Chapter V		101.7	15.2	61.8	77
This work:					
Variation of economic incentives and carbon tax	low level	12.8	15.2	61.8	77
	medium level	-2.43	15.2	61.8	77
	high level	-70.7	-	279	279
Variation of carbon tax	low level	2.66	15.2	61.8	77
	medium level	-2.43	15.2	61.8	77
	high level	-7.05	15.2	61.8	77

From the comparison presented in Table VII.1, it is evident that in most cases examined here the same CO_2 distribution of the base case is found. Only at the high level of carbon tax and economic incentives CO_2 is captured from all sources, at the maximum rate, to produce CH_4 (279 Mton/year of CO_2 are avoided). Regarding values assumed by the objective function, a direct comparison between the base case and this sensitivity study is not possible, because it is expressed in a different way. As far as this study is concerned, increasing the value of carbon tax and economic incentives provides a more negative value of the objective function, suggesting a more profitable economic condition.

VII.3.2 Results for the CCUS supply chain producing methanol in Germany

For the CCUS supply chain in Germany, producing CH_3OH via CH_4 dry reforming, a sensitivity analysis is carried out changing together carbon tax and economic incentives according to the low (20 €/ton and 0.092 €/kWh, respectively for carbon tax and economic incentives), medium (40 €/ton and 0.111 €/kWh, respectively for carbon tax and economic incentives) and high (140 €/ton and 0.129 €/kWh, respectively for carbon tax and economic incentives) levels (OECD, 2013; Leonzio et al., 2019a). CH_3OH selling price is set at 408 €/ton (Emshng-tech, 2019). Results show that the topology of the system is changed, as in the previous study of CCUS supply chains in Italy.

In particular, Table S5 of the Appendix shows the total value of the objective function and CH_3OH production obtained in this analysis for Germany. The value of the objective function is between 16.3 billion€/year and -197 billion€/year, respectively for the low and high value of the investigated parameters. CH_3OH production is between 203 Mton/year and 968 Mton/year, respectively for low value and high value of carbon tax and economic incentives.

In a more comprehensive way, Figure VII.5 shows the 3D plots for the value of the objective function (Figure VII.5a), CH_3OH production (Figure VII.5b) and avoided CO_2 (Figure VII.5c) as a function of carbon tax and economic incentives. The range of the objective function and CH_3OH production are already mentioned above, while the avoided CO_2 emissions are between 160 Mton/year and 665 Mton/year. The captured CO_2 and CH_3OH production have the same trend as for the supply chain of Italy: they are increasing for higher values of economic incentives, while are not affected by carbon tax. An opposite trend is found for the value of the objective function that is also influenced by the value of carbon tax. With higher economic incentives, a higher amount of CH_3OH production is favored, and then a higher amount of CO_2 is captured producing a higher income from the avoided carbon tax. These factors reduce the value of the objective function.

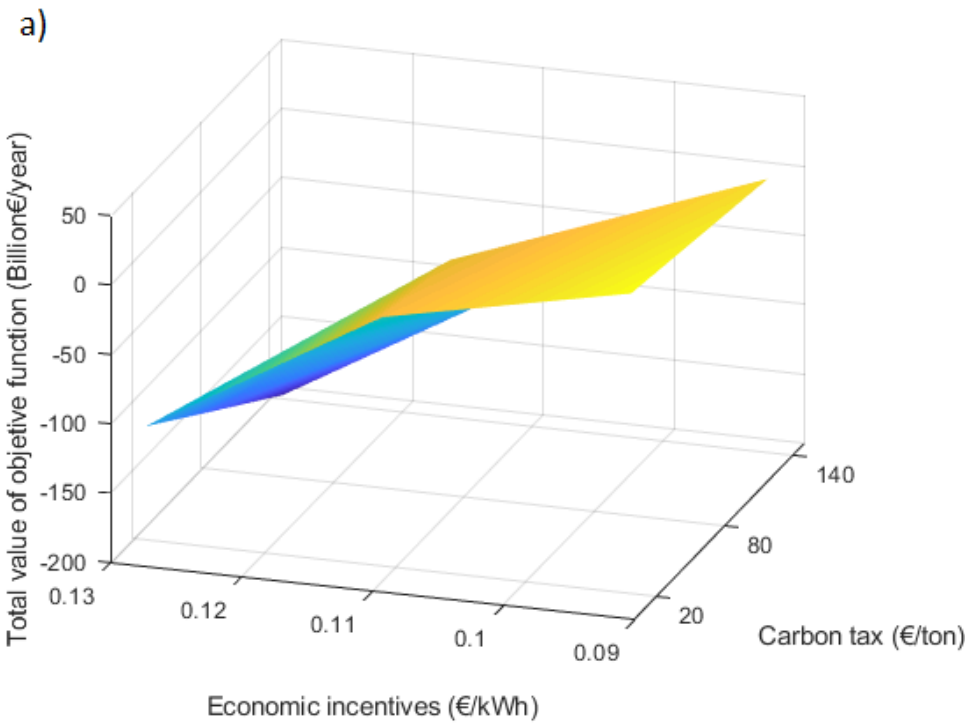

Figure VII.5 (Following)

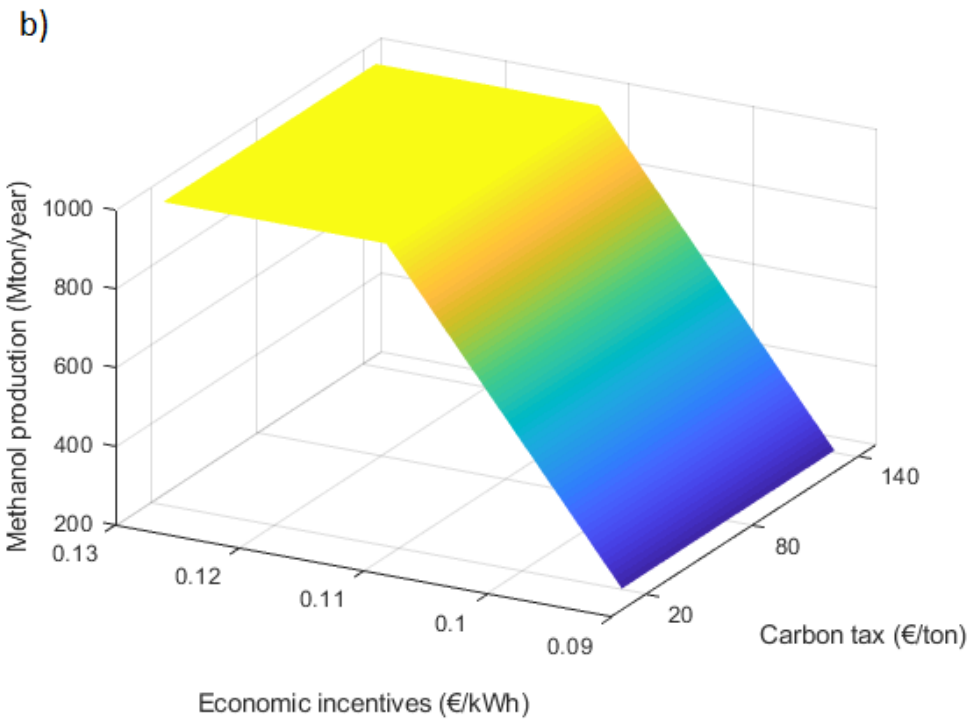

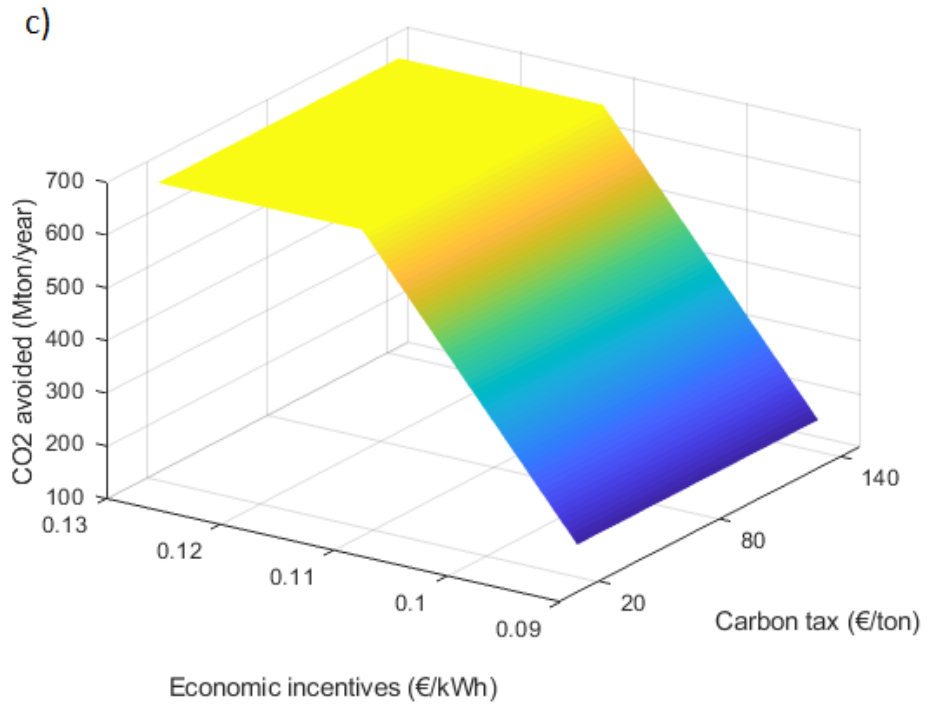

Figure VII.5 a) Total value of the objective function; b) CH_3OH production; c) Avoided CO_2 as a function of carbon tax and economic incentives for the CCUS supply chain of Germany producing CH_3OH (Leonzio et al., 2020)

Table S6 of the Appendix shows the topology of the supply chain at the low level of the investigated parameters, while Table S7 of the Appendix shows the topology at the medium and high level of the parameters investigated here. At the low level of carbon tax and economic incentives, 163 Mton/year of CO_2 are captured and sent to the storage or to the utilization section. The minimum target of CO_2 reduction is achieved. At the medium and high level of the investigated parameters, all CO_2 sources are selected and the maximum amount of CO_2 is captured and sent to the utilization section. 665 Mton/year of CO_2 are captured to produce 968 Mton/year of CH_3OH. The previous considerations about the CCUS in Italy are still valid: carbon tax and economic incentives have a positive effect on the selected sources through revenues. Increasing carbon tax and economic incentives, in order to minimize the objective function, causes revenues to increase producing more CH_3OH with a higher level of CO_2 captured from more sources. In the optimized supply chain, MEA absorption is the best choice due to a low cost compared to other technologies. As in the previous study, an additional sensitivity analysis is performed in order to evaluate only the effect of carbon tax on the results. CH_3OH selling price and economic incentives are of 408 €/ton and 0.111 €/kWh, respectively (Vita et al., 2018; Leonzio et al., 2019a). Figure VII.6 and VII.7 show respectively the value of the objective function and the amount of CH_3OH produced for different values of carbon tax: the amount of CH_3OH is constant at 203 Mton/year, as shown in Figure VII.7. As in Figure VII.6, the total value of the objective function is between 15.8 billion€/year for a carbon tax of 20 €/ton and -2.89 billion€/year for a value of carbon tax of 140 €/ton. Figure VII.8 shows the trend of captured CO_2 as a function of carbon tax: it is constant (160 Mton/year) as CH_3OH production.

Due to the constant production of CH_3OH, the topology of the supply chain, as for the case study regarding Italy, is not influenced by carbon tax: this is shown in Table S8 of the Appendix section.

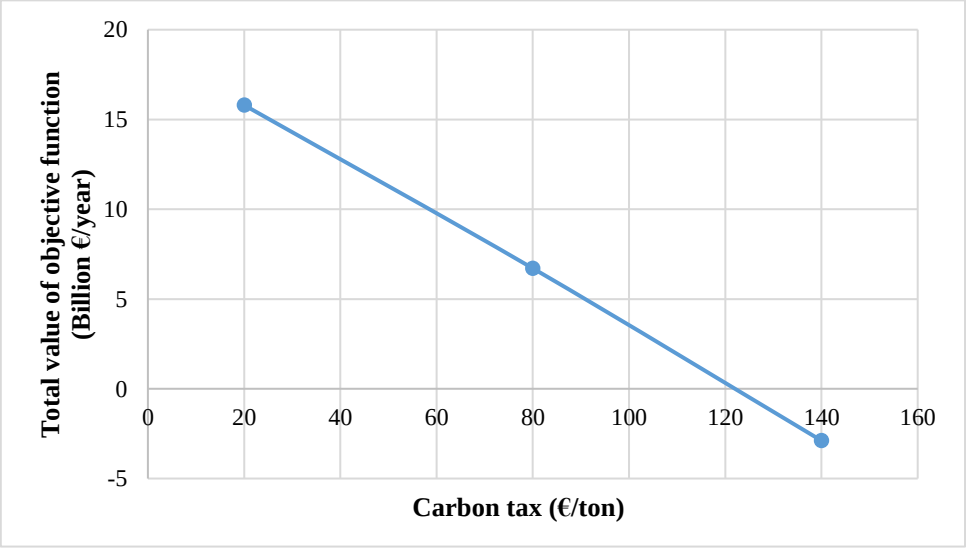

Figure VII.6 Trend of the total value of the objective function versus carbon tax for the CCUS supply chain producing only CH_3OH in Germany (Leonzio et al., 2020)

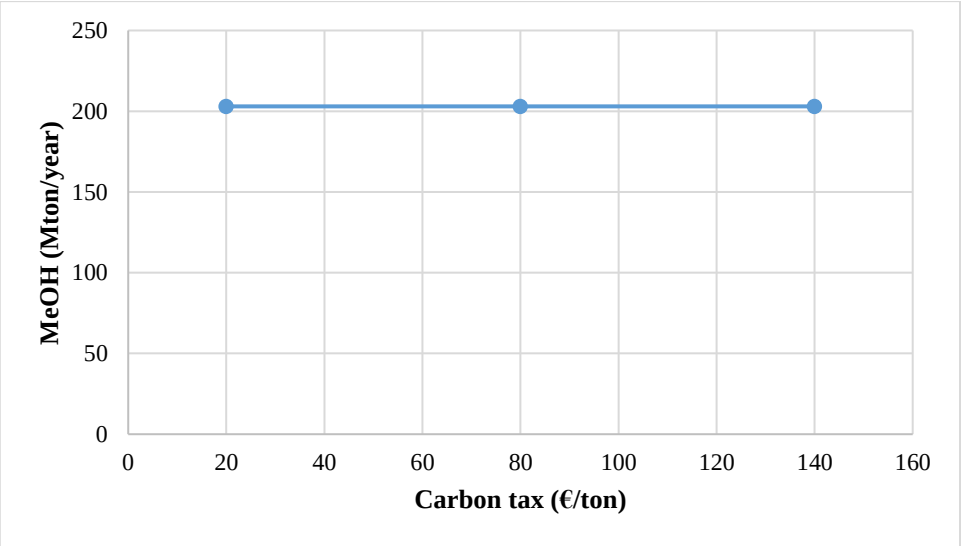

Figure VII.7 Trend of CH_3OH production versus carbon tax for the CCUS supply chain producing only CH_3OH in Germany (Leonzio et al., 2020)

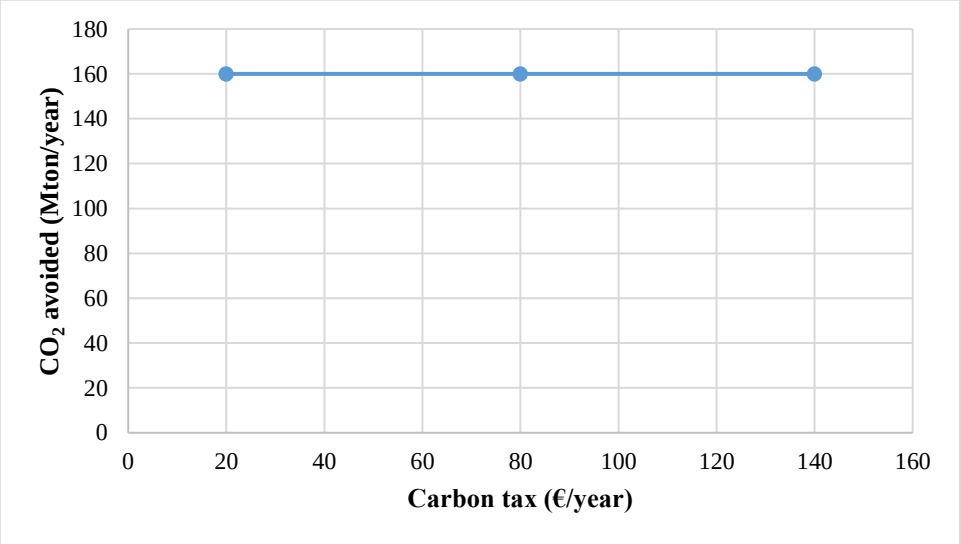

Figure VII.8 Trend of captured CO_2 versus carbon tax for the CCUS supply chain producing only CH_3OH in Germany (Leonzio et al., 2020)

In this optimized scheme, 160 Mton/year of CO_2 are captured (20.3 Mton/year of CO_2 are sent to the storage section, while 140 Mton/year are sent to the utilization section) from Magdeburg and Dusseldorf sources through MEA absorption. Also, it is possible to see that changing carbon tax causes the minimum target of CO_2 reduction to be achieved. If the market has an oscillatory trend, then a sensitivity analysis changing the selling price of CH_3OH should be considered. The lowest (90 €/ton) and highest price (540 €/ton) of CH_3OH in last years are taken into account for this study, while carbon tax is set to 80 €/ton and economic

incentives to 0.111 €/kWh (Mikulski, 2018). Results show that the topology of the system and CH_3OH production are changed in addition to the total value of the objective function, as shown in Figure VII.9.

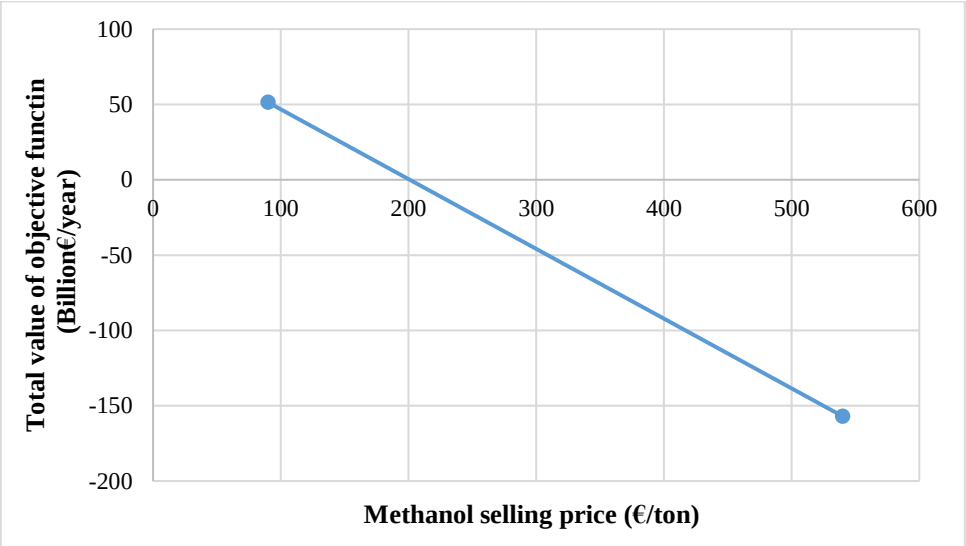

Figure VII.9 Trend of the total value of the objective function versus CH_3OH selling price for the CCUS supply chain producing only CH_3OH in Germany (Leonzio et al., 2020)

The value of the objective function is between 51.4 billion€/year and -157 billion€/year, respectively for a value of CH_3OH selling price of 90 €/ton and 540 €/ton. In the first case, a negative profit is obtained. CH_3OH production is shown in Figure VII.10: production increases from 203 Mton/year to 968 Mton/year.

Figure VI.10 Trend of CH_3OH production versus CH_3OH selling price for the CCUS supply chain producing only CH_3OH in Germany (Leonzio et al., 2020)

Table S9 and S10 of the Appendix show the topology of the system, respectively at the lowest and highest value of CH_3OH selling price.

At the lowest value of CH_3OH selling price, 160 Mton/year of CO_2 emissions are avoided using PSA and MEA absorption. At the highest value of CH_3OH selling price, the maximum amount of CO_2 is captured from all sources, reducing overall emissions by 665 Mton/year. Then, as carbon tax and economic incentives, revenues also have a positive effect on the selected CO_2 sources. If carbon tax and economic incentives are fixed, increasing revenues, with the aim to minimize the objective function, makes the amount of produced compounds grow as well as CO_2 captured from an increasing number of sources.

As in the previous case study, a comparison between the supply chain developed in Chapter III, considered as the base case, and the results of these sensitivity analyses is shown in Table VII.2.

Table VII.2 Comparison between the CCUS supply chain producing CH_3OH in Germany developed in Chapter III (base case) and the results of sensitivity analyses with the new objective function (Leonzio et al., 2020)

		Total value of objective function (billion€/year)	CO_2 to storage (Mton/year)	CO_2 to utilization (Mton/year)	Captured CO_2 (Mton/year)
Chapter III		207	20.3	140	160
This work:					
Variation of economic incentives and carbon tax	low level	16.3	20.3	140	160
	medium level	-30		665	665
	high level	-197		665	665
Variation of carbon tax	low level	15.8	20.3	140	160
	medium level	6.71	20.3	140	160
	high level	-2.98	20.3	140	160
Variation selling price	low level	51.4	20.3	140	160
	high level	-157	-	665	665

From the above comparison, it is evident that at the low level the distribution of CO_2 between the storage and the utilization is the same as that of the base case (Chapter III). Increasing the value of carbon tax and economic incentives together, and the selling price, CO_2 is captured from all sources and sent to the utilization section. No changes are predicted when only carbon tax is varied. Regarding the value of the objective function, also in this case its expression in the base case is different compared to that used in the sensitivity analysis, then a direct comparison is impossible. However, in the sensitivity analysis, negative values are obtained by increasing the values of parameters, ensuring then a positive profit.

VII.3.3 Results for the CCUS supply chain producing different products in German

A sensitivity analysis is developed for the CCUS supply chain producing different products in Germany. In this case, no economic incentives are considered while carbon tax is changed assuming these values: 20 €/ton, 80 €/ton and 140 €/ton, as in the previous analyses (OECD, 2013) The selling price of methanol, concrete, wheat, lignin, polyurethane, calcium carbonate, urea is respectively of 408 €/ton, 77 €/ton, 175 €/ton, 500 €/ton, 7966 €/ton, 120 €/ton and 287 €/ton (Leonzio et al., 2019b). As the results obtained in previous case studies, only the total value of the objective function is influenced by carbon tax, as shown in Figure VII.11, where a value of -18.94 trillion€/year is predicted for a carbon tax of 20 €/ton while a value of -19.02 trillion€/year is obtained for a carbon tax of 140 €/ton. A small variation of the total value is observed in this case: carbon tax has a lower effect on the objective function compared to the previous studies, because in this sensitivity analysis CO_2 is always captured from all sources, at the maximum available quantity, and utilized to produce different goods.

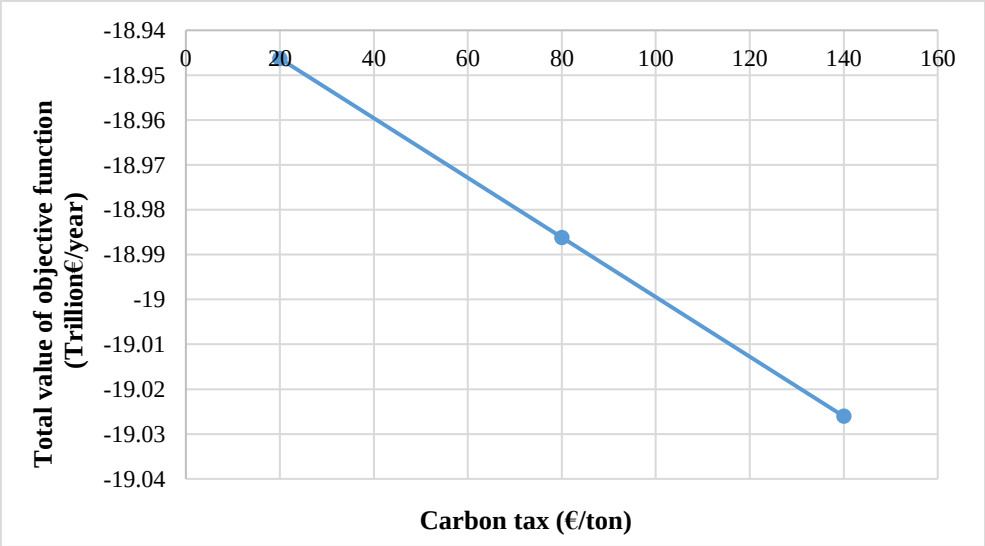

Figure VII.11 Trend of the total value of the objective function versus carbon tax for the CCUS supply chain producing different products in Germany (Leonzio et al., 2020)

As a consequence of this, the amount of produced CO_2-based compounds, shown in Figure VII.12, and the revenues, are constant in this case. From Figure VII.12, it is possible to observe that calcium carbonate, concrete by red mud, polyurethane, concrete curing are the compounds whose production is greater.

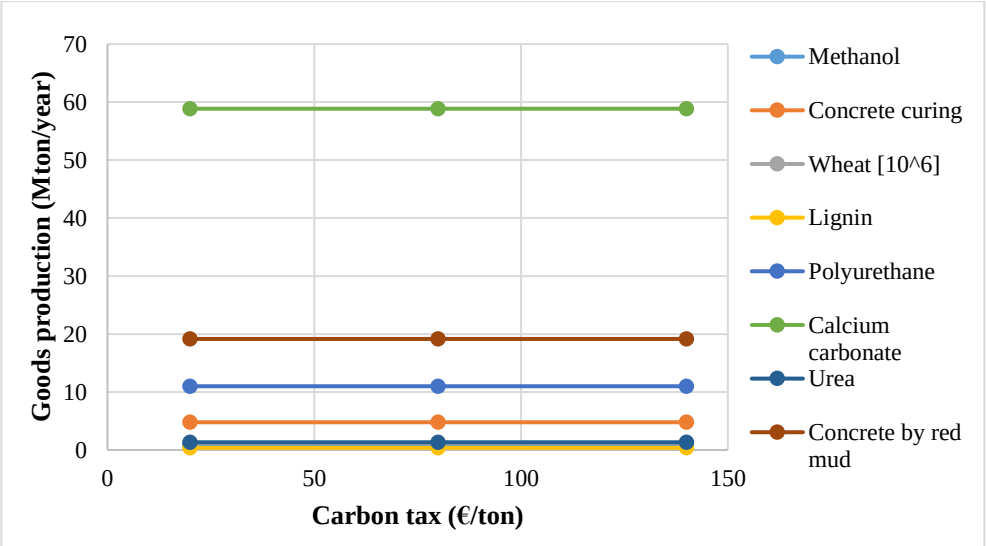

Figure VII.12 Trend of the production of different goods versus carbon tax for the CCUS supply chain producing different compounds in Germany (Leonzio et al., 2020)

The topology is shown in Table S11 of the Appendix . Regarding the topology, as mentioned above all CO_2 sources are selected and for each of them, the maximum amount of CO_2 is captured: a reduction of emissions equal to 665 Mton/year is registered, as shown in Figure VII.13.

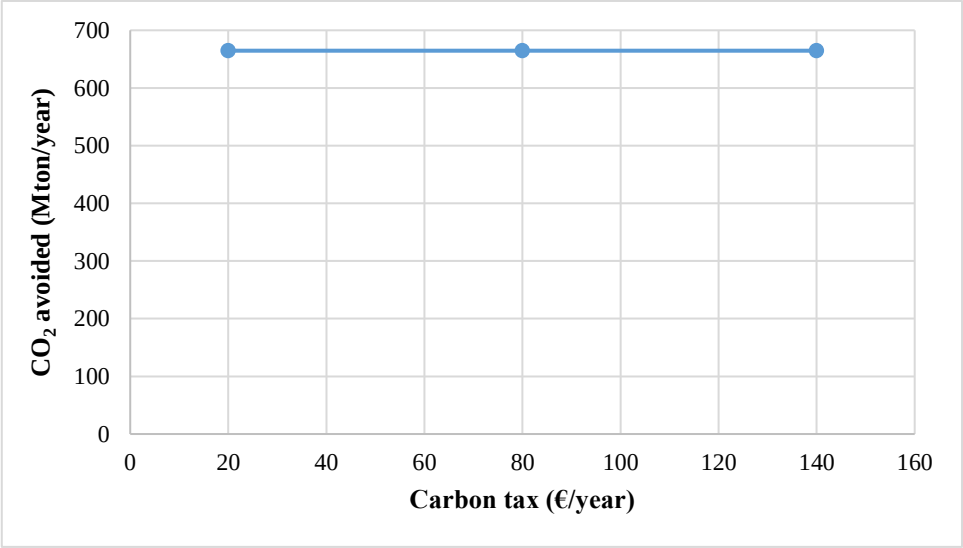

Figure VII.13 Trend of avoided CO_2 versus carbon tax for the CCUS supply chain producing different products in Germany (Leonzio et al., 2020)

Absorption using PZ is the selected capture technology due to low costs compared to MEA absorption (Kalyanarengan Ravi, 2017). These results suggest that the carbon tax is not relevant if modification on

topology or amount of CO_2-based products should be obtained. An additional sensitivity analysis is carried out changing the revenues, considering the lowest and highest value of selling price on the market, in recent years. At the lowest level, methanol, concrete, wheat, lignin, polyurethane, calcium carbonate and urea have a selling price of 90 €/ton, 34 €/ton, 125 €/ton, 480 €/ton, 6384 €/ton, 108 €/ton, 253 €/ton, 34 €/ton, respectively; at the highest level, methanol, concrete, wheat, lignin, polyurethane, calcium carbonate and urea have a price of 540 €/ton, 138 €/ton, 260 €/ton, 750 €/ton, 7250 €/ton, 132 €/ton and 369 €/ton, respectively (Mikulski, 2018; European Commission, 2019; Gosselink, 2011; PlasticsInsight, 2019; PCI, 2019; Fao, 2019; WSDOT, 2019). In this analysis, the carbon tax is set to 80 €/ton. As the previous analysis, from this study the results suggest that CO_2 is captured from all sources and sent to the utilization section, as shown in Table S12 of the Appendix. Absorption PZ is the selected capture technology due to economic advantages (Kalyanarengan Ravi, 2017).

The total value of the objective function and the amount of CO_2-based products are predicted to change in this case, as shown respectively in Figure VII.14 and VII.15. In these Figures, the level -1 is referred to the case with the lowest selling price, while the level 1 is referred to the case with the highest selling price. The total value of the objective function ranges between -1.24 trillion€/year and -119.8 trillion€/year, respectively for the lowest and highest values of selling price. Figure VII.15 shows that, although the global utilization of CO_2 is not changed, there is a variation in two products (lignin and wheat): if the production of lignin decreases there is an increase in wheat production. It is possible to conclude that topology is changed by revenues even if the structure of the system is the same. As in the previous case study, the topology is influenced by revenues.

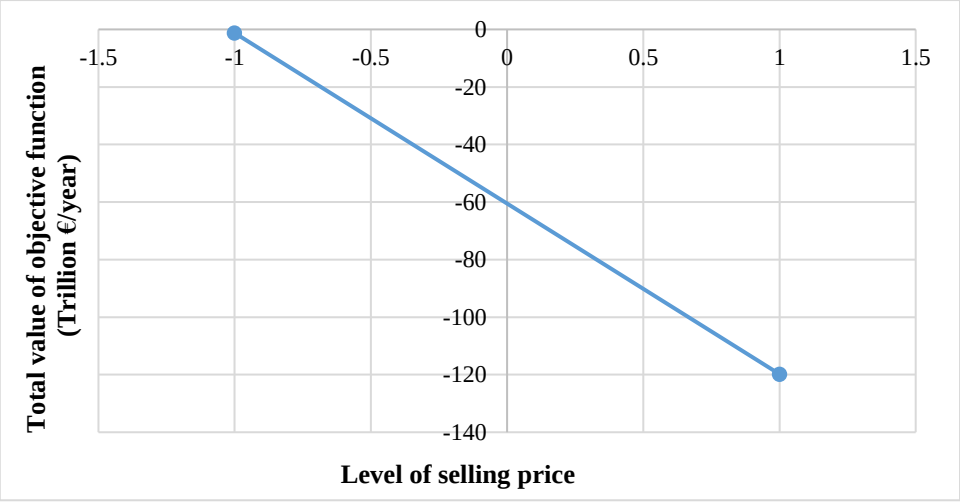

Figure VII.14 Trend of the total value of the objective function versus the level of selling price for CCUS supply chain producing different products in Germany (level=-1 lowest value of selling price, level=1 highest value of selling price) (Leonzio et al., 2020)

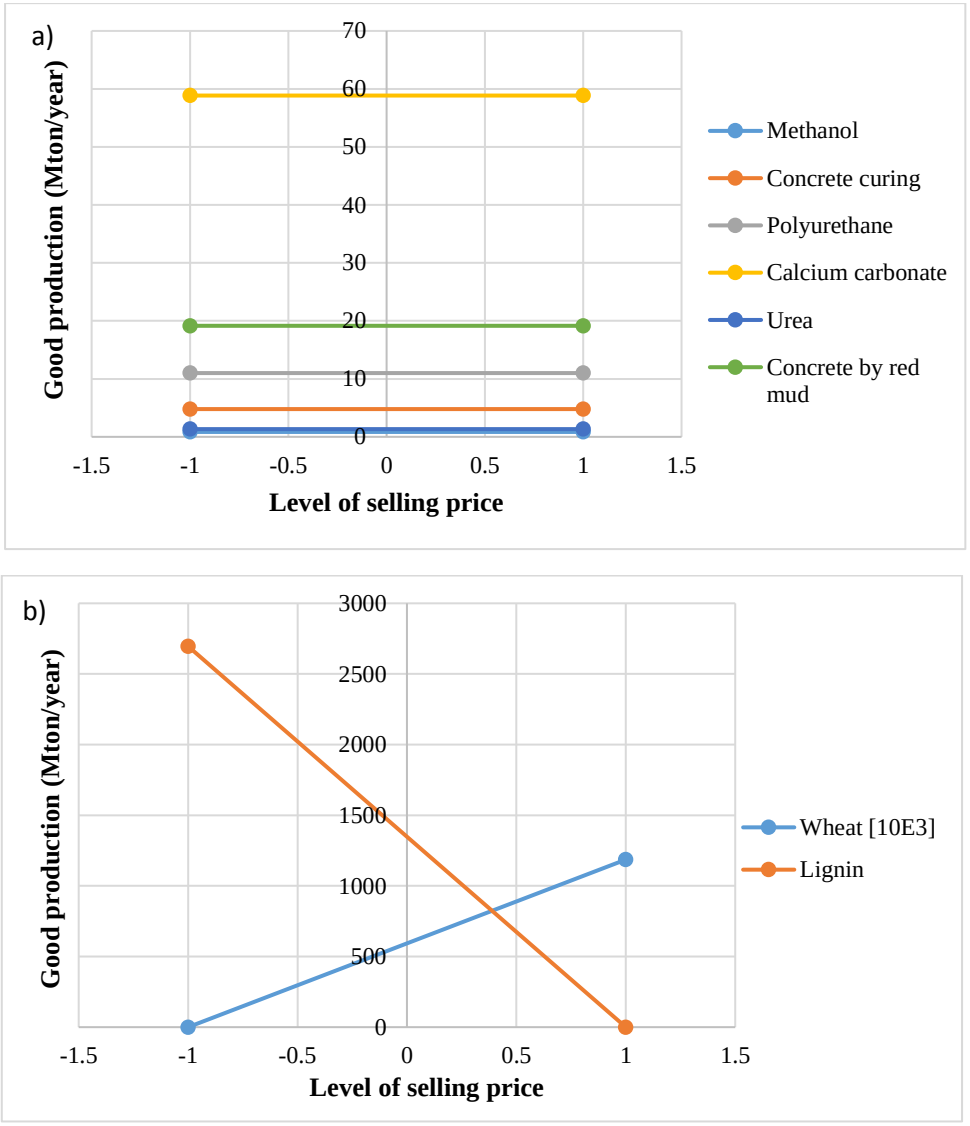

Figure VII.15 Trend of the production of different compounds for the CCUS supply chain in Germany: a) constant trend for all but two products, b) variation in lignin and wheat production (level=-1 lowest value of selling price, level=1 highest value of selling price) (Leonzio et al., 2020)

A comparison between the supply chain developed in Chapter IV and those analyzed in these sensitivity analyses is reported in Table VII.3. It is evident that considering carbon tax and revenues in the objective function produces a substantial variation of the topology compared to the base case in all conditions. In the base case, 20.3 Mton/year of CO_2 are sent to the storage, while 140 Mton/year of CO_2 are sent to the utilization. Overall, 160 Mton/year of CO_2 are captured. In the sensitivity analysis with the new defined objective function, CO_2 is captured from all sources, then 665 Mton/year of CO_2 are captured and sent to the utilization. In all cases of the sensitivity analysis, a positive profit is ensured. In particular, increasing the values of the investigated parameters produces a more profitable supply chain.

Table VII.3 Comparison between the CCUS supply chain producing more products in Germany developed in Chapter IV (base case) and the sensitivity analyses with the new defined objective function (Leonzio et al., 2020)

		Total value of objective function (billion €/year)	CO_2 to storage (Mton/year)	CO_2 to utilization (Mton/year)	Captured CO_2 (Mton/year)
Chapter IV		97.9	20.3	140	160
This work:					
Variation of carbon tax	low level	-18946		665	665
	medium level	-18986		665	665
	high level	-19026		665	665
Variation selling price	low level	-1241		665	665
	high level	-119798		665	665

VII.3.4 Results for the CCUS supply chain producing different products in the UK

Finally, a sensitivity analysis is developed for the CCUS supply chain producing different products in the UK. Economic incentives are not considered while carbon tax is changed assuming these values: 20 €/ton, 80 €/ton and 140 €/ton, as in the previous analyses (OECD, 2013). The selling price of CH_3OH, CH_4, polyurethane, tomatoes, concrete and calcium carbonate is respectively of 705 €/ton, 0.028 €/kWh, 2590 €/ton, 1.45 €/kg, 32.6 €/ton and 120 €/ton (National Statistics, 2019; Eurostat, 2019; Department for Environment Food and Rural Affairs, 2019; RMS, 2019, Zappa, 2014). Results show that changing carbon tax only the total value of the objective function is changed and this parameter has no effect on the topology and polyurethane production. Table S13 of the Appendix section reports the topology of the CCUS supply chain with Bunter Sandstone as storage site for different levels of carbon tax, while Figure VII.16 shows the constant trend of polyurethane production.

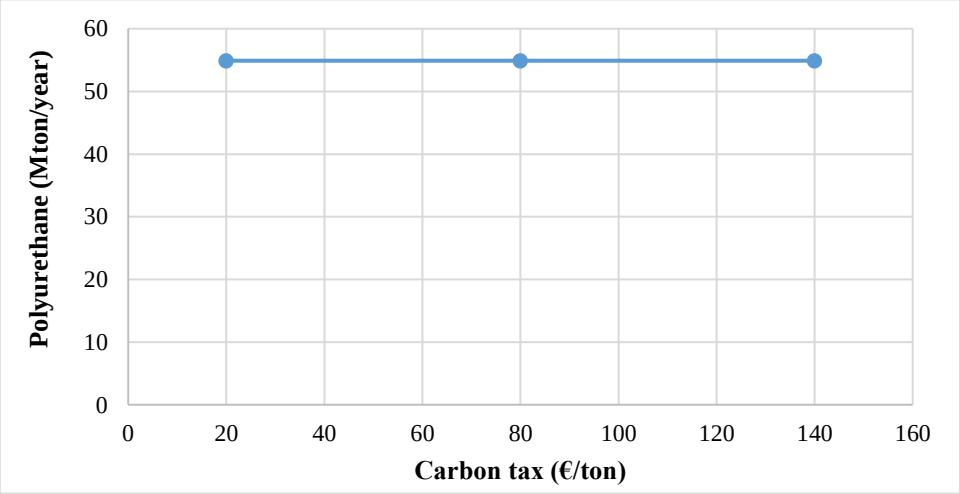

Figure VII.16 Trend of polyurethane production versus carbon tax for the CCUS supply chain in the UK with Bunter Sandstone as storage site

On the other hand, Figure VII.17 shows the trend of the total value of the objective function for the considered CCUS supply chain at different level of carbon tax, while Figure VII.18 show the trend of captured CO_2. The total value of the objective function is in the range of -241.66 billion€/year and -247.15 billion€/year, respectively for a carbon tax of 20 €/ton and 140 €/ton. 54.9 Mton/year of CO_2 are avoided through the application of this framework.

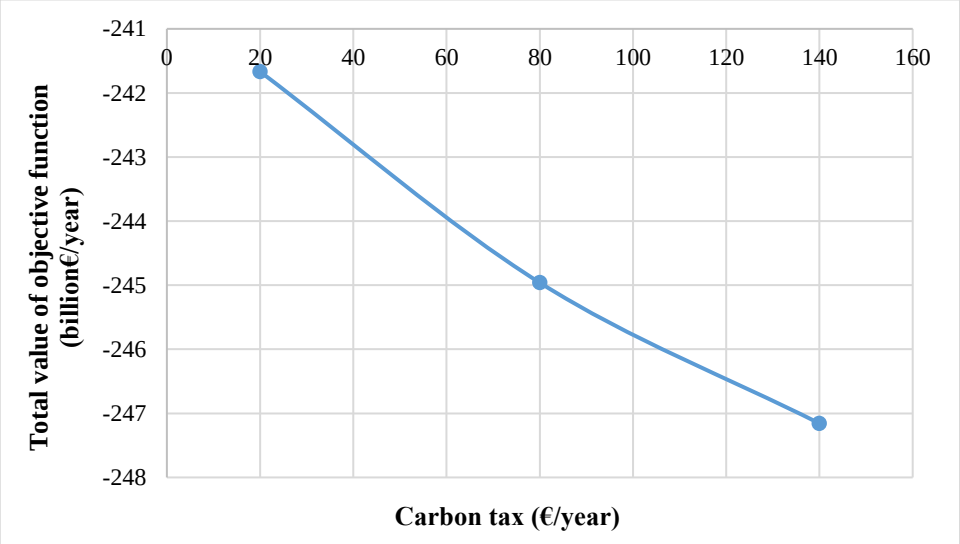

Figure VII.17 Trend of the total value of the objective function versus carbon tax for the CCUS supply chain in the UK with Bunter Sandstone as storage site.

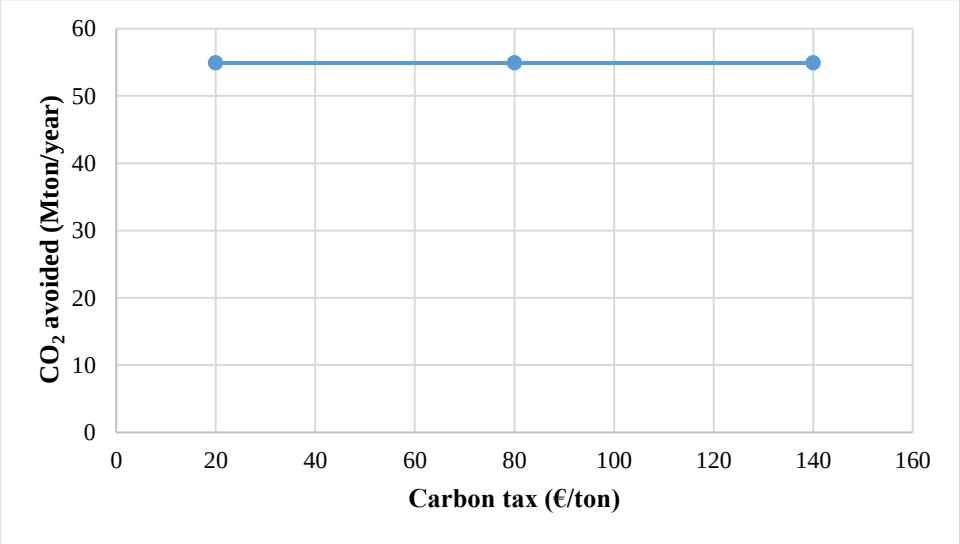

Figure VII.18 Trend of avoided CO_2 versus carbon tax for the CCUS supply chain in the UK with Bunter Sandstone as storage site

An additional sensitivity analysis, is performed changing the revenues, considering the lowest and highest value of selling price for the different CO_2-based products. The lowest value of selling price for CH_3OH, CH_4, polyurethane, tomatoes, concrete and calcium carbonate is respectively of 690 €/ton, 0.0178 €/kWh, 2260 €/ton, 1.12 €/kg, 15.18 €/ton and 108 €/ton. The highest level of selling price for CH_3OH, CH_4, polyurethane, tomatoes, concrete and calcium carbonate is respectively of 3510 €/ton, 0.028 €/kWh, 2590 €/ton, 2.68 €/kg, 153 €/ton and 132 €/ton (National Statistics, 2019; Eurostat, 2019; Department for Environment Food and Rural Affairs, 2019; RMS, 2019, Zappa, 2014). Carbon tax is set to 80 €/ton. Results of this analysis shows that the total value of the objective function is changed, as reported in Figure VII.19, where -1 is referred to the case with the lowest values of selling price, while 1 is referred to the case with the highest values of selling price. The total value of the objective function is between -165 billion€/year and -259 billion€/year.

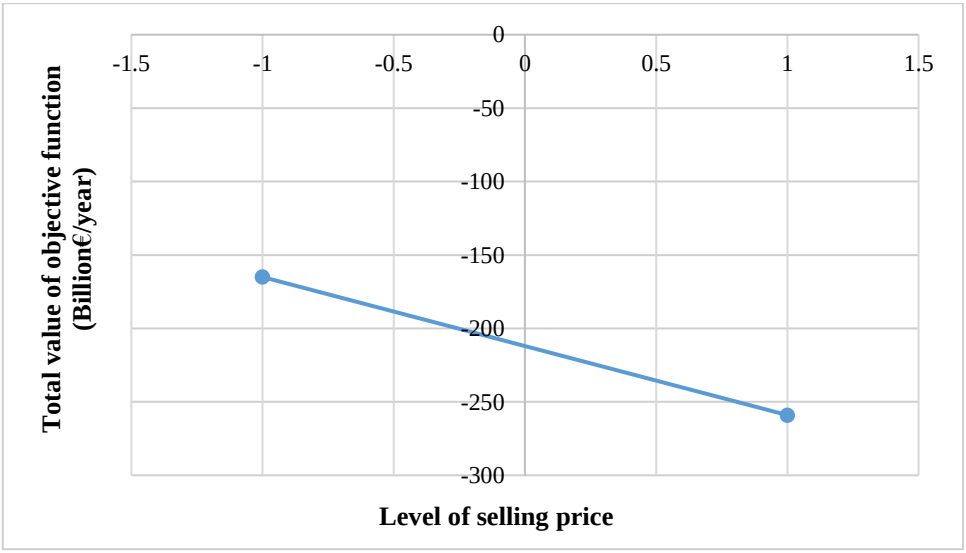

Figure VII.19 Trend of the total value of the objective function versus the level of selling price for CCUS supply chain in the UK with Bunter Sandstone as storage site (level=-1 lowest value of selling price, level=1 highest value of selling price)

In addition, the topology is changed because, even if the global structure of the system is constant as in Table S14 of the Appendix section, different products are produced at the lowest and highest level of selling price. In particular, at the lowest value of selling price 183 Mton/year of polyurethane is produced, while at the highest value of selling price 143 Mton/year of tomatoes are ensured. The same result of the previous case studies is then obtained here regarding the influence of revenues on the design of a supply chain. To have a comparison with the CCUS supply chain developed in Chapter VI, Table VII.4 is considered.

Table VII.4 Comparison between the CCUS supply chain in the UK with Bunter Sandstone as storage site developed in Chapter VI (base case) and the sensitivity analyses with the new defined objective function

		Total value of objective function (billion€/year)	CO_2 to storage (Mton/year)	CO_2 to utilization (Mton/year)	CO_2 captured (Mton/year)
Chapter VI		1.04	0.4	6	6.4
This work:					
Variation of carbon tax	low level	-241.67		54.9	54.9
	medium level	-244.96		54.9	54.9
	high level	-247.16		54.9	54.9
Variation selling price	low level	-164.8		54.9	54.9
	high level	-259.31		54.9	54.9

Also in this case, carbon tax and revenues considered in the objective function affect the topology of the supply chain in a significant way. In fact, in the base case the captured CO_2 is distributed between the utilization and the storage section, while considering these two parameters all CO_2 that can be captured from all source is captured and sent to the utilization section, maximizing the profit. 54.9 Mton/year of CO_2 are captured. In all cases of the sensitivity analysis, a positive profit is ensured. In particular, increasing the values of the investigated parameters produces a more profitable supply chain.

VII.4 Conclusions

In this Chapter, a sensitivity analysis is developed for CCUS supply chains in Italy, Germany (producing either methanol or a variety of products) and the UK, using a novel objective function to update MILP models developed in previous Chapters. This allows a more realistic design and optimization of the supply chain. Carbon tax remission, economic incentives and revenues are changed by considering three different levels of their values, according to the market.

Overall, in a first analysis, carbon tax and economic incentives are changed together; then, only carbon tax is changed to evaluate its specific effect and lastly, revenues are changed considering the lowest and highest value of selling price for the compounds to be produced. With reference to the different supply chains considered here, results show that:

a) carbon tax influences only the total value of the objective function, while the topology of the supply chain and the amounts of different products are not affected. If the aim is to change only the profit of the system without changing the topology, it is suggested to change only the value of carbon tax.

b) economic incentives influence the topology of CCUS supply chains. In particular, economic incentives have a positive effect on the number of CO_2 sources included in the optimized supply chain: increasing the value of this parameter enlarges the number of selected sources and increases the amount of CO_2 that is

effectively captured, above the minimum target for emissions reduction fixed by the environmental requirements.

c) revenues influence the structure and also the topology of CCUS supply chains. As expected, the effect of increasing revenues is predicted to be positive on the number of selected CO_2 sources and on the amount of CO_2 that is actually captured, progressively closer to the maximum admissible amount from the selected sources.

Appendix

1. Results of sensitivity analysis for CCUS supply chains in Italy at the low level of carbon tax and economic incentives

Table S3 Results of CCUS supply chains in Italy at the low level of carbon tax and economic incentives (Leonzio et al., 2020)

Storage site	Source	Capture technology	CO_2 amount (Mton/year)	Objective function (Billion€/year)	Methane production (Mton/year)
Malossa San Bartolomeo	To storage			12.8	22.5
	Lombardy	PSA adsorption	15.2		
	To utilization				
	Puglia	MEA absorption	61.8		
	Sicily	MEA absorption	0.024		
Pesaro	To storage			13.3	24.5
	Lombardy	MEA absorption	9.6		
	To utilization				
	Puglia	MEA absorption	61.8		
	Sicily	MEA absorption	5.62		
Offshore Adriatic sea	To storage			9.39	16.1
	Lombardy	MEA absorption	32.8		
	To utilization				
	Puglia	MEA absorption	44.2		
Cornelia	To storage			14.7	25.1
	Emilia Romagna	MEA absorption	8		
	To utilization				
	Puglia	MEA absorption	61.8		
	Lombardy	MEA absorption	7.22		
Offshore Marche	To storage			11.9	22.2
	Emilia Romagna	MEA absorption	16		
	To utilization				
	Puglia	MEA absorption	61		
Offshore Calabria ionic	To storage			14.4	26.5
	Liguria	IL absorption	4		
	To utilization				
	Puglia	MEA absorption	61.8		
	Lombardy	MEA absorption	11.2		
Area Sulcis	To storage			14.8	27.8
	Sardina	MEA absorption	0.6		
	To utilization				
	Puglia	MEA absorption	61.8		
	Lombardy	MEA absorption	14.6		

Table S4 (Continued)

Storage site	Source	Capture technology	CO_2 amount (Mton/year)	Objective function (Billion€/year)	Methane production (Mton/year)
(-)	To utilization			15.5	28
	Lombardy	MEA absorption	39.6		
	Piedmonte	MEA absorption	17.7		
	Emilia Romagna	Membrane	19.6		

2. Results of sensitivity analysis for the CCUS supply chains in Italy at the medium level of carbon tax and economic incentives

Table S5 Results of CCUS supply chains of Italy at the medium level of carbon tax and economic incentives (Leonzio et al., 2020)

Storage site	Source	Capture technology	CO_2 amount (Mton/year)	Objective function (Billion€/year)	Methane production (Mton/year)
Malossa San Bartolomeo	To storage			-2.43	22.5
	Lombardy	MEA absorption	15.2		
	To utilization				
	Sicily	MEA absorption	37.4		
	Sardinia	MEA absorption	4.17		
	Veneto	MEA absorption	20.3		
Pesaro	To storage			-2.4	24.5
	Lombardy	MEA absorption	9.6		
	To utilization				
	Sicily	MEA absorption	37.4		
	Sardinia	MEA absorption	9.77		
	Veneto	MEA absorption	20.3		
Offshore Adriatic sea	To storage			-2.41	16.1
	Lombardy	MEA absorption	32.8		
	To utilization				
	Sicily	MEA absorption	37.4		
	Veneto	MEA absorption	6.82		
Cornelia	To storage			-2.51	15.1
	Emilia Romagna	MEA absorption	8		
	To utilization				
	Lombardy	MEA absorption	31.6		
	Sicily	MEA absorption	37.4		
Offshore Marche	To storage			-2.74	22.2
	Emilia Romagna	MEA absorption	16		
	To utilization				
	Lombardy	MEA absorption	23.6		
	Sicily	MEA absorption	37.4		

Table S3 (Continued)

Storage site	Source	Capture technology	CO_2 amount (Mton/year)	Objective function (Billion€/year)	Methane production (Mton/year)
Offshore Calabria ionic	To storage			-2.27	26.5
	Liguria	MEA absorption	4		
	To utilization				
	Puglia	MEA absorption	61.8		
	Lombardy	MEA absorption	11.2		
Area Sulcis	To storage			-2.37	27.8
	Sardinia	MEA absorption	0.6		
	To utilization				
	Puglia	MEA absorption	61.8		
	Lombardy	MEA absorption	14.6		
(-)	To utilization			-1.76	28
	Lombardy	MEA absorption	39.6		
	Piedmont	MEA absorption	17.7		
	Emilia Romagna	Membrane	19.6		

3. Results of sensitivity analysis for the CCUS supply chains in Italy at the high level of carbon tax and economic incentives.

Table S6 Results of CCUS supply chains of Italy at the high level of carbon tax and economic incentives (Leonzio et al., 2020)

Storage site	Source	Capture technology	CO_2 amount (Mton/year)	Objective function (Billion€/year)	Methane production (Mton/year)
Malossa San Bartolomeo	To storage			-70.7	101
Pesaro				-67.1	101
Offshore Adriatic sea	To utilization			-46.4	101
Cornelia	Puglia	MEA absorption	61.8	-47	101
	Lombardy	MEA absorption	42.1		
Offshore Marche	Sicily	MEA absorption	37.4	-47	101
	Lazio	MEA absorption	25.3		
Offshore Calabria Ionic	Sardinia	MEA absorption	23.8	-47.1	101
	Veneto	MEA absorption	20.3		
Area Sulcis	Emilia Romagna	MEA absorption	19.6	-47.1	101
	Piedmont	MEA absorption	17.7		
(-)	Liguria	MEA absorption	15.8	-46.5	101
	Tuscany	MEA absorption	15.2		

4. Results of sensitivity analysis for the CCUS supply chain in Italy with Malossa San Bartolomeo as storage site at different values of carbon tax.

Table S4 Topology of the CCUS supply chain in Italy with Malossa San Bartolomeo as storage site at different values of carbon tax (Leonzio et al., 2020)

CO_2 Source	**Capture technology**	**CO_2 amount (Mton/year)**
To storage		
Lombardy	MEA absorption	15.2
To utilization		
Sicily	MEA absorption	37.4
Sardinia	MEA absorption	4.17
Veneto	MEA absorption	20.3

5. Results of sensitivity analysis for the CCUS supply chain producing only methanol in Germany at different levels of carbon tax and economic incentives.

Table S5 Total value of objective function and methanol production for the CCUS supply chain in Germany changing carbon tax and economic incentives (only methanol is produced) (Leonzio et al., 2020)

Parameters	**Total value of objective function (billion€/year)**	**Methanol production (Mton/year)**
Low value	16.3	203
Medium value	-30	968
High value	-197	968

Table S6 Topology of the CCUS supply chain producing methanol in Germany at the low level of investigated parameters (carbon tax and economic incentives) (Leonzio et al., 2020)

CO_2 source	**Capture technology**	**CO_2 amount (Mton/year)**
To storage		
Magdeburg	MEA absorption	20.3
To utilization		
Dusseldorf	MEA absorption	140

Table S7 Topology of the CCUS supply chain producing methanol in Germany at the medium and high level of investigated parameters (carbon tax and economic incentives) (Leonzio et al., 2020)

CO_2 source	**Capture technology**	**CO_2 amount (Mton/year)**
To storage		
-	-	-
To utilization		
Dusseldorf	MEA absorption	277
Munich	MEA absorption	72
Stuttgart	MEA absorption	62.4
Hannover	MEA absorption	62.1
Potsdam	MEA absorption	49.5
Dresda	MEA absorption	43.8
Wiesbaden	MEA absorption	38.6
Magdeburg	MEA absorption	24.7
Berlin	MEA absorption	17.8
Saarbruken	MEA absorption	17.2

6. Results of sensitivity analysis for the CCUS supply chain producing only methanol in Germany at different values of carbon tax.

Table S8 Topology of the CCUS supply chain producing methanol in Germany at different values of carbon tax (Leonzio et al., 2020)

CO_2 source	**Capture technology**	**CO_2 amount (Mton/year)**
To storage		
Magdeburg	MEA absorption	20.3
To utilization		
Dusseldorf	MEA absorption	140

7. Results of sensitivity analysis for the CCUS supply chain producing only methanol in Germany at different values of methanol selling price.

Table S9 Topology of the CCUS supply chain producing methanol in Germany at the lowest value of methanol selling price (Leonzio et al., 2020)

CO_2 source	**Capture technology**	**CO_2 amount (Mton/year)**
To storage		
Magdeburg	PSA adsorption	20.3
To utilization		
Dusseldorf	MEA absorption	140

Table S10 Topology of the CCUS supply chain producing methanol in Germany at the highest value of methanol selling price (Leonzio et al., 2020)

CO_2 source	**Capture technology**	**CO_2 amount (Mton/year)**
To storage		
To utilization		
Dusseldorf	MEA absorption	277
Munich	MEA absorption	72
Stuttgart	MEA absorption	62.4
Hannover	MEA absorption	62.1
Potsdam	MEA absorption	49.5
Dresda	MEA absorption	43.8
Wiesbaden	MEA absorption	38.6
Magdeburg	MEA absorption	24.7
Berlin	MEA absorption	17.8
Saarbruken	MEA absorption	17.2

8. Results of sensitivity analysis for the CCUS supply chain producing different products in Germany at different values of carbon tax.

Table S11 Topology of the CCUS supply chain producing different products in Germany at different values of carbon tax (Leonzio et al., 2020)

CO_2 source	**Capture technology**	**CO_2 amount (Mton/year)**
To storage		
-	-	-
To utilization		
Dusseldorf	PZ absorption	277
Munich	PZ absorption	72
Stuttgart	PZ absorption	62.4
Hannover	PZ absorption	62.1
Potsdam	PZ absorption	49.5
Dresda	PZ absorption	43.8
Wiesbaden	PZ absorption	38.6
Magdeburg	PZ absorption	24.7
Berlin	PZ absorption	17.8
Saarbruken	PZ absorption	17.2

9. Results of sensitivity analysis for the CCUS supply chain producing different products in Germany at different values of selling prices.

Table S12 Topology of the CCUS supply chain producing different products in Germany at different values of selling price (Leonzio et al., 2020)

CO_2 source	**Capture technology**	**CO_2 amount (Mton/year)**
To storage		
-	-	-
To utilization		
Dusseldorf	PZ absorption	277
Munich	PZ absorption	72
Stuttgart	PZ absorption	62.4
Hannover	PZ absorption	62.1
Potsdam	PZ absorption	49.5
Dresda	PZ absorption	43.8
Wiesbaden	PZ absorption	38.6
Magdeburg	PZ absorption	24.7
Berlin	PZ absorption	17.8
Saarbruken	PZ absorption	17.2

10. Results of sensitivity analysis for the CCUS supply chain in the UK with Bunter Sandstone as storage site at different values of carbon tax.

Table S13 Topology of the CCUS supply chain in the UK with Bunter Sandstone as storage site at different values of carbon tax

CO_2 source	**Capture technology**	**CO_2 amount (Mton/year)**
To storage		
To utilization		
Leeds	PZ absorption	16.2
Cardiff	PZ absorption	12.78
Edinburgh	PZ absorption	11.97
Manchester	PZ absorption	13.95

11. Results of sensitivity analysis for the CCUS supply chain in the UK with Bunter Sandstone as storage site at different values of selling prices.

Table S14 Topology of the CCUS supply chain in the UK with Bunter Sandstone as storage site at different values of selling price for CO_2-based compounds

CO_2 source	**Capture technology**	**CO_2 amount (Mton/year)**
	To storage	
	To utilization	
Leeds	PZ absorption	16.2
Cardiff	PZ absorption	12.78
Edinburgh	PZ absorption	11.97
Manchester	PZ absorption	13.95

References

Department for Environment, Food and Rural Affairs, 2019. Available at: https://www.gov.uk/government/statistics/agricultural-price-indices

Department for Business, Energy and Industrial Strategy, 2019. Available at: https://www.gov.uk/government/statistical-data-sets/prices-of-fuels-purchased-by-manufacturing-industry

Emshng-tech, 2019. Available at: www.emshng-tech.com

European Commission, 2019. Available at: https://ec.europa.eu/agriculture/markets-and-prices/price-monitoring/monthly-prices_en

Eurostat, 2019. Available at: https://ec.europa.eu/eurostat/statistics-explained/index.php?title=File:Gas_prices_for_non-household_consumers,_second_half_2017_(EUR_per_kWh).png#filehistory, accessed May 10, 2019.

Eurostat, 2019. Available at: https://ec.europa.eu/eurostat/statistics-explained/index.php/Natural_gas_price_statistics

Fao, 2019. Available at: www.fao.org

Gosselink, R.J.A. Lignin as a Renewable Aromatic Resource for the Chemical Industry, PhD Thesis, Wageningen University, Wageningen, NL. 2011.

Hasan, M.M.F., Baliban, R.C., Elia, J.A., Floudas, C.A. 2012. Modeling, simulation, and optimization of postcombustion CO2capture for variable feed concentration and flowrate. 1. Chemical absorption and membrane processes. Ind Eng Chem Res, 51, (48), 15642–64.

Kalyanarengan Ravi, N., Van Sint Annaland, M., Fransoo, J.C., Grievink, J., Zondervan, E. 2017. Development and implementation of supply chain optimization framework for CO2 capture and storage in the Netherlands. Computer Chemical Engineering, 102, 40–51.

Leonzio G., Zondervan, E. 2020. Analysis and optimization of carbon supply chain integrated by power to gas process in Italy, Journal of Cleaner Production, under review.

Leonzio, G., Foscolo, P.U., Zondervan, E., Bogle, D. 2020. Scenario Analysis of Carbon Capture, Utilization (Particularly Producing Methane and Methanol), and Storage (CCUS) Systems. Ind. Eng. Chem. Res. In press.

Leonzio, G., Foscolo, P.U., Zondervan, E. 2019a. An outlook towards 2030: Optimization and design of a CCUS supply chain in Germany, Computers and Chemical Engineering, 125, 499–513.

Leonzio, G., Foscolo, P.U., Zondervan, E. 2019b. Sustainable utilization and storage of carbon dioxide: analysis and design of an innovative supply chain, Computers and Chemical Engineering, 131, 106569.

Mikulski, M., MCK, TUDelft, Public final report-Methanol as an alternative fuel for vessels, Technical report 2018. 10.13140/RG.2.2.29463.11686

National Statistics, 2019. Available at: https://www.ons.gov.uk/businessindustryandtrade/manufacturingandproductionindustry/datasets/ukmanufacturerssalesbyproductprodcom

OECD, 2013. Available at: https://www.oecd.org/env/tools-evaluation/Effective-Carbon-Prices-in-France.pdf

Office for National Statistics, 2019. Available at: https://www.ons.gov.uk/businessindustryandtrade/manufacturingandproductionindustry/datasets/ukmanufacturerssalesbyproductprodcom

Ozkır, V., Baslıgil, H. 2013. Multi-objective optimization of closed-loop supply chains in uncertain environment. J. Clean. Prod. 41, 114-125.

PCI, 2019. Available at: https://www.pcimag.com/articles/105429-huber-announces-price-increase-for-industrial-ground-calcium-carbonate

PlasticsInsight, 2019. Available at: https://www.plasticsinsight.com/resin-intelligence/resin-prices/polyurethane/

RMS, 2019. Available at: rmsconcrete.co.uk/prices/

Vita, A., Italiano, C., Previtali, D., Fabiano, C., Palella, A., Freni, F., Bozzano, G., Pino, L., Manenti, F. 2018. Methanol synthesis from biogas: A thermodynamic analysis, Renewable Energy, 118, 673-684

WSDOT, 2019. Available at: https://www.wsdot.wa.gov/NR/rdonlyres/2788838C-B426-4E21-ADE5-B5CDA80E643D/0/ConcretePavement.pdf

Zappa, W., 2014. Pilot-scale Experimental Work on the Production of Precipitated Calcium Carbonate (PCC) from Steel Slag for CO2 Fixation, PhD thesis.

Nomenclature

Abbreviation

AIMMS = advanced interactive multidimensional modeling system

CCUS = carbon capture utilization and storage

IL = ionic liquid

MEA = monoethanolamine

MILP = mixed integer linear programming

PSA = pressure swing adsorption

PZ = piperazine

Chapter VIII

Life cycle assessment analysis of CCUS supply chains

Carbon capture utilization and storage supply chains aim to reduce carbon dioxide emissions, however energy is required for their operations, producing an additional environmental impact. For these systems, a life cycle assessment allows to verify the effective reduction of emissions. In this Chapter, the methodology of life cycle assessment is applied to the best carbon capture utilization and storage supply chains developed for Italy, Germany and the UK. Results show that these Countries will be able to achieve the carbon dioxide reduction target fixed by the environmental policy. A sensitivity analysis is carried out increasing the amount of carbon dioxide sent to the utilization section and reducing that sent to the storage section, keeping constant the overall amount of captured carbon dioxide. Overall, for the framework of Germany and the UK, a higher environmental impact is produced at a higher utilization rate of carbon dioxide, contrarily to the study about the Italian case, where a power to gas system is present. Power to gas is the most attractive and mature process that contributes to reduce the environmental impact, although its cost is still high and technical and economic improvements are needed to make cheaper the "green" hydrogen production for carbon dioxide hydrogenation.

VIII.1 Introduction

Carbon supply chains, with the aim to reduce carbon dioxide (CO_2) emissions, require a significant amount of energy for their operations (especially for CO_2 capture and conversion processes) and this causes an additional environmental penalty that contrasts their aim. It was estimated that the increase in fuel consumption per kWh, for plants that capture 90% of CO_2 by using the best current technologies ranges from 24 to 40% for new supercritical pulverized coal plants, from 11 to 22% for natural gas combined cycle plants, and from 14 to 25% for coal-fired integrated gasification combined cycle systems, compared to similar plants without capture and storage systems (IPCC, 2005).

Therefore, it is necessary to know if a specific carbon supply chain is favorable from an environmental point of view. To this purpose, a life cycle assessment (LCA) analysis should be developed. It is a green metric that considers all inputs and outputs in a process, analyzed in their entire life (Von der Assen et al., 2014a). Moreover, it was stated that "*the LCA is a technique compiling an inventory of relevant inputs and outputs of a product system; evaluating the potential environmental impacts associated with those inputs and outputs; and interpreting the results of the inventory and impact phases in relation to the objectives of the study*" (ISO 14040, 2009; ISO 14044, 2006).

The literature survey indicates that environmental analyses were considered for carbon capture utilization and storage (CCUS) supply chains where CO_2 is mainly used for the enhanced oil recovery and to produce polyols, dimethyl ether and algae (Fernandez-Dacosta et al., 2018; Yue and You, 2015). No other CO_2-based products were taken into consideration for a LCA analysis of a carbon supply chain. Also, the previous studies were not considering the application of a LCA analysis on a CCUS supply chain at large

scale (e.g. taking into account a supply chain developed for an entire Nation with the respective consumption and production data).

This study will contribute to fill these gaps. Then a LCA analysis is developed for the best CCUS supply chain developed for Germany, Italy and the UK, as described in the previous Chapters, and producing different CO_2-based products.

As in other literature works, the aim of this research is to verify that the developed systems can effectively reduce CO_2 emissions according to the environmental target. Moreover, a sensitivity analysis is developed for these supply chains to evaluate the influence of storage and utilization sections on the environmental results: a variable part of the captured CO_2 is sent to the utilization section to produce different compounds, instead of being stored. This analysis can help the choice between CO_2 utilization or storage in order to create a more environmentally friendly system.

VIII.2 Materials and methods

The LCA analysis is a quantitative methodology used to evaluate the environmental impact according to the ISO 14044 and ISO 14040 (ISO 14040, 2009; ISO 14044, 2006). Four important phases characterize this analysis: goal and scope, life cycle inventory (LCI) phase, life cycle impact assessment (LCIA) phase and interpretation phase (Von der Assen et al., 2014a; ISO 14040, 2009; ISO 14044, 2006). To develop the LCA analysis, GaBi software is used (Education license, version 6) (Thinkstep, 2019).

VIII.2.1 Goal and scope

The goal of this study is to evaluate the environmental performances of the developed CCUS supply chains (at large scale) producing different CO_2-based products in Germany and in the UK and methane in Italy. It is necessary to demonstrate that the suggested CCUS supply chains achieve the target set by the European environmental policy, especially in terms of CO_2 emissions. For this reason, a yearly-based LCA analysis is considered. A sensitivity analysis is carried out to verify the influence of the utilization and storage sections on the environmental impact and, for a more complete analysis, different impact categories are considered (acidification potential (AP), eutrophication potential (EP), ozone depletion potential (ODP), abiotic depletion potential (ADP) fossil and elements, fresh water aquatic ecotoxity potential (FAETP), human toxicity potential (HTP), marine aquatic ecotoxicity potential (MAETP), photochemical ozone creation potential (POCP), terrestrial ecotoxicity potential (TETP)). In this case, then, conditions ensuring higher sustainability are identified.

VIII.2.1.1 Functional unit

The considered CCUS supply chains have multi-functionalities (Von der Assen et al., 2014a). In order to define the functional unit, a system expansion methodology is applied, allowing the joint evaluation of all

functions, since the functional unit is expanded to contain all functions (Fernandez-Dacosta et al., 2018). Then the functional unit is defined as a harmonized basket provided by the combination of all products. For the CCUS supply chain in Germany (Chapter IV) the functional unit is the following: 76.7 Mton of cement+$1.22 \cdot 10^{11}$ kWh of electricity+13.6 Mton of iron and steel+4.79 Mton of concrete curing+19.4 Mton of wheat+0.378 Mton of treated lignin+11 Mton of polyurethane+120 Mton of calcium carbonate+1.34 Mton of urea+0.846 Mton of methanol (CH_3OH)+19.2 Mton of concrete by red mud+20.3 Mton of stored CO_2. For the CCUS supply chain in Italy (Chapter V) the functional unit is, instead, the following: 66.92 Mton of steel+$22.48 \cdot 10^9$ kWh of electricity+16.1 Mton of methane (CH_4)+32.8 Mton of stored CO_2. For the CCUS supply chain of the UK (Chapter VI) the functional unit is the following: $7.36 \cdot 10^{10}$ MJ of electrical energy+5.4 Mton of calcium carbonate+0.4 Mton of stored CO_2. In all cases, the amount of products and stored CO_2 are considered, keeping in mind the results provided by the optimization of these systems in AIMMS (Advanced Interactive Multidimensional Modeling System).

Then a definition of functional unit in absolute terms is considered (referred to the whole amount of each product, as calculated in the design of the supply chain by the computational model), according to the goal of this research, that is the LCA analysis of the supply chains optimized in AIMMS, to verify the effective reduction of CO_2 emissions compared to the environmental target.

VIII.2.1.2 System boundaries

Cradle-to-gate analyses are performed for supply chains, where CO_2 is also considered as a feedstock (economic flow) and not only as an emission (Von der Assen et al., 2014a) (the use and disposal of CO_2-based products is not considered in these analyses).

System boundaries, describing which processes of the CCUS supply chain in Germany are included in the assessment, are shown in Figure VIII.1. Inside the system boundaries, in the upstreams processes, three different inlets are present: power plants, cements plants and steel and iron plants. In the section downstream of storage and utilization processes, where the captured CO_2 is used or stored, nine outlet streams are present, namely different products of CO_2 utilization routes (CH_3OH, urea, concrete curing, concrete by red mud, wheat, polyurethane, calcium carbonate, lignin) and the stored CO_2. CO_2 capture and compression and CO_2 transportation are considered to be inside up- and downstream boundaries.

Figure VIII.2 shows the system boundaries for the CCUS supply chain in Italy. Inside the system boundaries, in the upstream processes, flue gas sources are present (a power plant and iron and steel plants). In the section downstream of the utilization process and storage section, methane and stored CO_2 are considered. Also in this case, CO_2 capture and compression and transportation are included between the upstream and downstream boundaries.

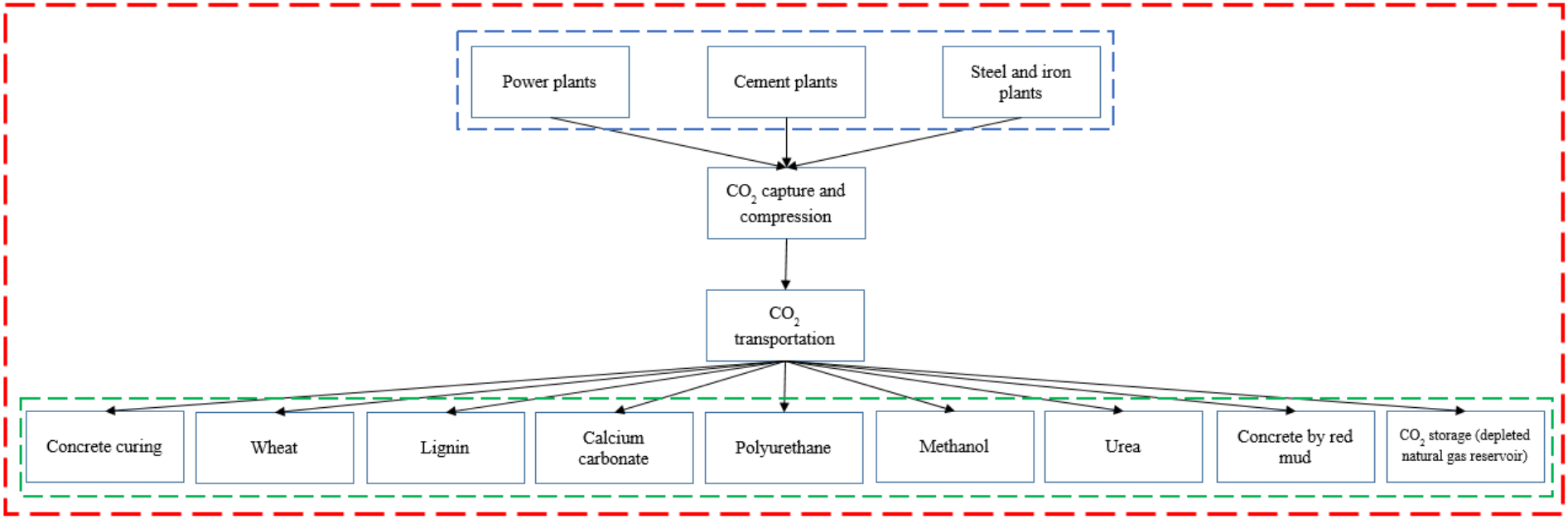

Figure VIII.1 System boundaries for the CCUS supply chain in Germany - red line: system boundaries; green line: downstream processes (production of CO_2-based compounds and CO_2 storage); blue line: upstream processes (Leonzio et al., 2020)

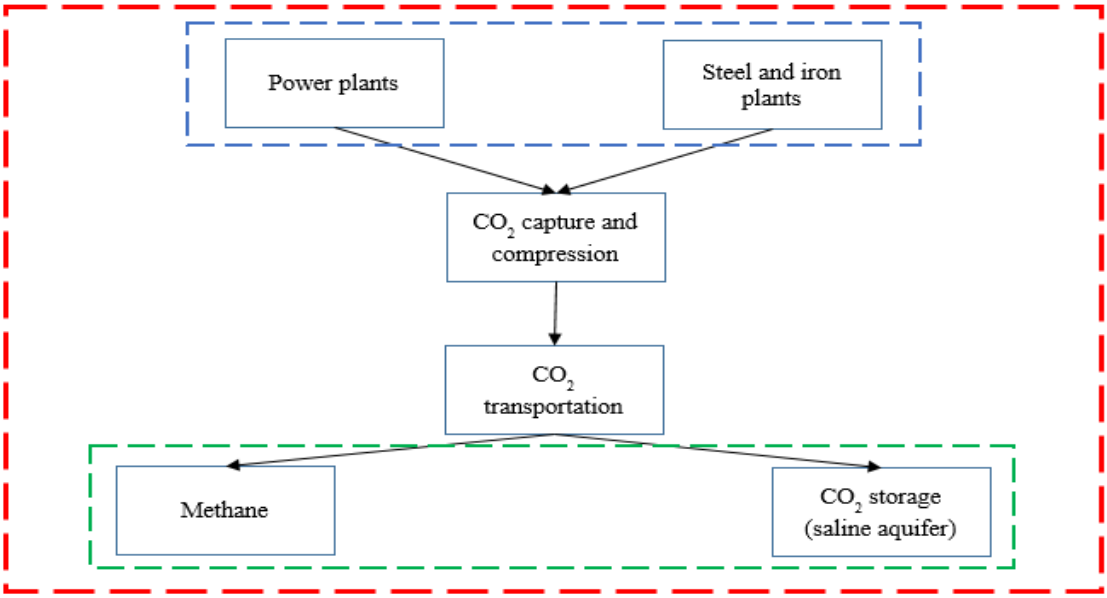

Figure VIII.2 System boundaries for the CCUS supply chain in Italy - red line: system boundaries; green line: downstream processes (production of methane and CO_2 storage); blue line: upstream processes (Leonzio et al., 2020)

Figure VIII.3 shows the system boundaries considered for a cradle-to-gate LCA analysis of CCUS supply chain in the UK. In the upstream processes, CO_2 sources are present (power plants). In the downstream processes, calcium carbonate production and CO_2 storage are considered. Between them, CO_2 capture and compression and CO_2 transportation are analyzed.

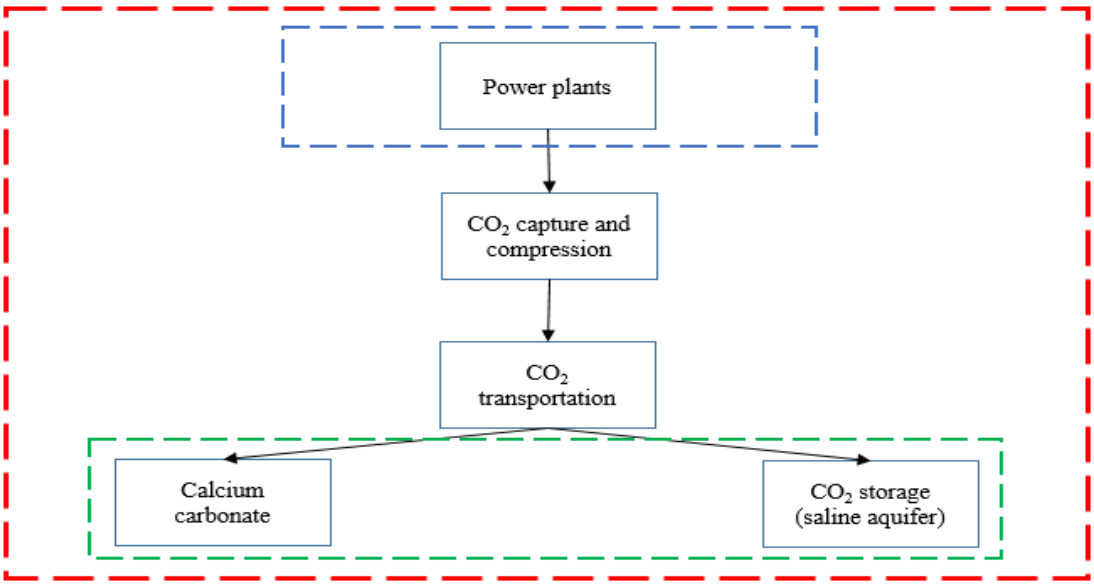

Figure VIII.3 System boundaries for the CCUS supply chain in Italy - red line: system boundaries; green line: downstream processes (production of methane and CO_2 storage); blue line: upstream processes (Leonzio et al., 2020)

For all supply chains, the utilization options are chosen as the most economically appealing CO_2-based products for the respective Countries, according to the literature.

For the three supply chains, in the upstream processes related to CO_2 sources, system boundaries include also the construction of plants, the extraction or production of raw materials and their transportation calculated using the database of GaBi software (Thinkstep, 2019). The infrastructure and transport of raw materials with their production are also considered for CO_2 transportation, according to literature sources (Koornneef et al., 2008). Infrastructures are considered only for CO_2 capture with MEA absorption, due to the scarce availability of data (Giordano et al., 2018). For the utilization processes, infrastructure data are not available, however, the production of raw materials is considered inside the system boundary. Since natural reservoirs are assumed (a saline aquifer, located in the offshore Adriatic sea, for the CCUS supply chain of Italy and in the Bunter Sandstone for the CCUS supply chain of the UK and a depleted natural gas reservoir, located in Altmark, for the CCUS supply chain of Germany), no infrastructures are necessary, excluding the energy required for the process of storage (Wildbolz, 2007).

VIII.2.2 Life cycle inventory phase

In the LCI phase, all input and output data for all processes of CCUS supply chains are provided. In particular, the results for large-scale supply chains obtained by the optimization and design with AIMMS software are considered. Based on these process data, an inventory list is calculated. In particular, all elementary flows entering the process (technosphere) from nature (environment) in the form of resources, and leaving the process in the form of resources, deposited goods, emissions to air, fresh water, sea water, agricultural and industrial soil are taken into account.

An inventory analysis of processes absent in the database of GaBi software (Thinkstep, 2019), is here considered integrating and comparing to each other, data already reported in the literature. These processes are especially important for CO_2 utilization, storage and transportation. For the CCUS supply chain of Germany, an inventory analysis is performed for production from CO_2 of CH_3OH, calcium carbonate, polyurethane, urea, wheat, concrete curing, concrete by red mud and lignin treatment.

Tables VIII.1 and VIII.2 show respectively the inventory analysis for CH_3OH production by CO_2 hydrogenation and for hydrogen (H_2) production by water (H_2O) electrolysis, considering the work of Biernacki et al. (2018), Michailos et al. (2018), Kajaste et al. (2018), Matzen and Demirel (2016). It is also considered the recycle of unconverted gases to CH_3OH reactor, after the separation of H_2O and CH_3OH, with an efficiency of 80%. In summary, 1.7 ton of CH_3OH are produced per ton of inlet CO_2 (Patricio et al., 2017).

Table VIII.1 Inventory analysis for CH_3OH synthesis via CO_2 hydrogenation in the CCUS supply chain of Germany (Biernacki et al., 2018; Michailos et al., 2018; Kajaste et al., 2018; Matzen and Demirel, 2016; Patricio et al., 2017)

Input of the process		
H_2	0.23	ton
CO_2	1.70	ton
Aluminum oxide	0.01	ton
Copper oxide	0.08	ton
Zinc oxide	0.04	ton
Water	5.45	ton
Energy	0.13	MWh
Output of the process		
Wastewater	0.68	m^3
CO_2	0.34	ton
Methanol	1	ton

Table VIII.2 Inventory analysis for the electrolyzer in CH_3OH production process in the CCUS supply chain of Germany (Biernacki et al., 2018; Michailos et al., 2018; Kajaste et al., 2018; Matzen and Demirel, 2016; Patricio et al., 2017)

Input of the process		
Water	2.22	ton
Traditional energy	141.96	kWh
Renewable energy	6.11	kWh
Output of the process		
Oxygen	1.97	ton
H_2	0.23	ton
Waste water	0.12	m^3
VOC	5.23	g
CO	47.67	g
NOx	41.31	g
PM_{10}	15.16	g
$PM_{2.5}$	7.50	g
SOx	276.67	g
CH_4	47.06	g
CO_2	28.22	kg
SF6	0.92	mg
C_2F_6	0.10	g
Black carbon	0.25	g
POC	0.48	g

Table VIII.3 shows the inventory analysis for calcium carbonate production from CO_2, considering the literature works of Mattila et al. (2014) and Zappa (2014) and that the ratio between the ton of used CO_2 and the ton of steel slag is 0.25.

Table VIII.3 Inventory analysis for calcium carbonate production process from CO_2 in the CCUS supply chain of Germany (Mattila et al., 2014; Zappa, 2014)

Input of the process		
Steel slag	3.3	ton
CO_2	0.83	ton
NH_4Cl solvent	0.03	ton
Electricity	107.40	kWh
Water	2.10	ton
Steam	37500	MJ
Output of the process		
Calcium carbonate	1.00	ton
Waste water	2.01	ton

An inventory analysis for lignin treatment with CO_2 is presented in Table VIII.4, according to the work of Bernier and Lavigne (2013) and considering that 0.22 ton of CO_2 per ton of lignin are provided (Patricio et al., 2017).

Table VIII.4 Inventory analysis for lignin treatment process with CO_2 in the CCUS supply chain of Germany (Bernier and Lavigne; 2013; Patricio et al., 2017)

Input of the process		
Natural gas	0.46	ton
CO_2	0.22	ton
H_2SO_4	0.17	ton
NaOH	0.08	ton
$CaCO_3$	0.17	ton
Water	3.56	ton
Electricity	7.33	kWh
Output of the process		
SO_2	6.75×10^{-9}	ton
NO_x	3.38×10^{-7}	ton
CO	3.82×10^{-7}	ton
Lignin	1	ton

Polyurethane is produced by polyols and isocyanate. The former reactant is obtained by CO_2, while the latter one is obtained by carbon monoxide (CO) produced via CH_4 steam reforming. All inputs and outputs for these processes are shown in Table VIII.5, according to the work of Von der Assen et al. (2015). For

polyurethane production from CO_2, the ratio between used CO_2 and polyurethane is 0.3 (Patricio et al., 2017).

Table VIII.5 Inventory analysis for polyurethane production from CO_2 in the CCUS supply chain of Germany (Von der Assen et al., 2015; Patricio et al., 2017)

Polyurethane production (flexible foam)		
Input of the process		
Polyols	0.713	kg
Electricity	1.5	MJ
TDI	0.285	kg
Output of the process		
Flexible foam	1	kg
GW	0.051	$kgCO_{2\text{-eq}}$
Isocyanate production		
Input of the process		
Toluene	0.15	kg
Electricity	3.77	MJ
CO	0.09	kg
Nitirc acid	0.21	kg
Output of the process		
TDI	0.285	kg
Steam reforming		
Input of the process		
CH_4	0.066	kg
Electricity	0.353	MJ
Heat	0.747	MJ
Output of the process		
H_2	0.020	kg
CO	0.092	kg
Polyols production		
Input of the process		
Starter	0.019	kg
Propylene oxide	0.395	kg
CO_2	0.299	kg
Output of process		
Polyols	0.713	kg

An inventory analysis for urea production from CO_2 is shown in Table VIII.6, according to the work of Antonetti et al. (2017). Here 0.74 ton of CO_2 are used to produce 1 ton of urea (Patricio et al., 2017).

Table VII.6 Inventory analysis for urea production from CO_2 in the CCUS supply chain of Germany (Antonetti et al., 2017; Patricio et al., 2017)

Input of the process			
NH_3		0.57	ton
CO_2		0.74	ton
Energy		0.05	MWh
Output of the process			
NH_3 emissions		0.004	ton
Wastewater		0.48	ton
	NH_3	0.03	ton
	CO_2	0.02	ton
	Urea	0.005	ton
	water	0.43	ton
Urea		1	ton

An environmental burden and inventory analysis for wheat growing enhanced by CO_2 is shown in Table VIII.7, considering the work of Biswas et al. (2010, 2008) and that 500 mg of CO_2 are required to produce 1 kg of wheat (Leonzio et al., 2019).

Table VIII.7 Inventory analysis for wheat production in the CCUS supply chain of Germany (Biswas et al., 2010; 2008; Leonzio et al., 2019)

Input of the process		
CO_2	0.5	kg
Output of the process		
Wheat	1	ton
GW	275	$kgCO_{2\text{-}eq}$

Inventory analyses for concrete produced by red mud and concrete curing are shown respectively in Table VIII.8 and VIII.9, comparing data reported by Nikbin et al. (2018) and by Gursel and Horvath (2012). The GWP and cumulative energy demand (CED) are respectively of 330.74 $kgCO_{2\text{-}eq}$ and 2848.5 MJ for concrete production by red mud (1 ton) (Nikbin et al., 2018). The GWP and CED are, instead, respectively of 292 $kgCO_{2\text{-}eq}$ and 1374.68 MJ for concrete curing (1 ton) (Nikbin et al., 2018; Carboncure, 2019). In concrete curing, 0.03 ton of CO_2 are required for 1 ton of concrete (Patricio et al., 2017), while in concrete by red mud production the ratio between the ton of CO_2 and the ton of red mud is 0.17.

Table VIII.8 Inventory analysis for concrete production by red mud and CO_2 in the CCUS supply chain of Germany (Nikbin et al., 2018; Gursel and Horvath, 2012; Patricio et al., 2017)

Input of the process		
Cement	0.222	ton
Red mud	0.074	ton
Coarse Agg	0.129	ton
Fine Agg.	0.106	ton
Leca	0.197	ton
Limestone	0.118	ton
Water	0.150	ton
Superplasticizer	0.004	ton
CO_2	0.013	ton
Output of the process		
Concrete	1	ton
CO	0.04619	ton
Lead	0.000012	ton
NO_X	0.00075	ton
PM_{10}	0.00002	ton
SO_2	0.00076	ton
VOC	0.00057	ton

Table VIII.9 Inventory analysis for concrete curing in the CCUS supply chain of Germany (Nikbin et al., 2018; Gursel and Horvath, 2012; Patricio et al., 2017)

Input of the process		
Cement	0.285	ton
Water	0.145	ton
Fine aggregates	0.118	ton
Coarse aggregates	0.145	ton
Leca	0.190	ton
Limestone	0.114	ton
Super-plasticize	0.003	ton
CO_2	0.030	ton
Output of the process		
CO	0.056	ton
Lead	0.00001	ton
NOx	0.001	ton
PM_{10}	0.00003	ton
SO_2	0.001	ton
VOC	0.001	ton
Concrete	1.000	ton

In the CCUS supply chain of Italy, CH_4 is produced from CO_2 with a power to gas process. Table VIII.10 shows the inventory analysis for the methanation process, (Sabatier reaction) supposing a complete CO_2 conversion to CH_4 (Reiter et al., 2015; Sternberg and Bardow, 2016).

Table VIII.10 Inventory analysis for the methanation process (Sabatier reaction) in the CCUS supply chain of Italy (Reiter et al., 2015; Sternberg and Bardow, 2016)

Input of the process		
CO_2	2.75	kg
H_2	0.46	kg
Electricity	0.33	kWh
Output of the process		
CH_4	1	kg
Waste heat	8.26	MJ
H_2O	2.29	kg

In the CCUS supply chain of the UK, calcium carbonate is produced then, for this production process the same considerations of the CCUS supply chain of Germany are taken into account.

In all considered CCUS supply chains, CO_2 is also stored: it is supposed that electrical energy is used to inject CO_2 and the required energy is $2.86 \cdot 10^{-2}$ kWh/kgCO_2 (Wildbolz, 2007). Emission by leakages occurs in a very long term, then these are not considered in the LCA analysis. Regarding CO_2 transportation, infrastructures and energy data are considered according to the work of Koornneef et al. (2008) and Wildbolz (2007), respectively. It is supposed that the energy for CO_2 recompression is necessary for a distance over 400 km and it is of 0.011 kWh/(ton km) (Wildbolz, 2007). No leakage emissions are considered due to their negligible value (Bouman et al., 2015).

For the inventory analysis of CO_2 capture with piperazine absorption, the required energy is considered. Von der Aben et al. (2015) suggest a value of 0.80 GJ/tonCO_2, while 0.86 GJ/tonCO_2 are necessary for the absorption of CO_2 with MEA. Infrastructures and emission data for this last technology are proposed by Giordano et al. (2018).

The LCI results, provided by GaBi software, about the CCUS supply chain in Germany are summarized in Table VIII.11. It is worth noticing that, in the output, the greatest contribution to elementary flows is made by the emissions to fresh water (63.4%) followed by the emissions to air (35.8%). Other terms are negligible. Elementary flows can be expressed also in kg$CO_{2\text{-eq}}$. In the input, 5.24×10^{11} kg$CO_{2\text{-eq}}$ of resources are present. In the output, 7.08×10^{11} kg$CO_{2\text{-eq}}$ of emissions to air are calculated. As a weak point in this analysis, it is found that the steam production in the calcium carbonate process and CO_2 source in Munich provide the highest contribution to the emissions to air.

Table VIII.11 LCI results: elementary flows for the CCUS supply chain in Germany

Input		
Resources	5.95×10^{13}	kg
Output		
Resources	1.98×10^{9}	kg
Deposited goods	3.20×10^{11}	kg
Emissions to air	2.20×10^{13}	kg
Emissions to fresh water	3.90×10^{13}	kg
Emissions to sea water	1.72×10^{11}	kg
Emissions to agricultural soil	5.98×10^{5}	kg
Emissions to industrial soil	4.98×10^{5}	kg

To allocate the environmental impact to a co-product, the price allocation method is adopted for CO_2 sources, where the main product is co-produced with CO_2.

The considered prices for CO_2, electricity, cement and steel are respectively 80 €/ton, 0.15 €/kWh, 80 €/ton and 589 €/ton (Focus Economics, 2019; Boyer and Ponssard, 2013; Europe, 2019; OECD, 2013).

The LCI results, then the elementary flows, are also obtained by GaBi software for the CCUS supply chain in Italy, as shown in Table VIII.12.

Table VIII.12 LCI results: elementary flows for the CCUS supply chain in Italy

Input		
Resources	2.49×10^{12}	kg
Output		
Resources	1.78×10^{10}	kg
Deposited goods	8.03×10^{10}	kg
Emissions to air	5.65×10^{11}	kg
Emissions to fresh water	2.04×10^{12}	kg
Emissions to sea water	1.54×10^{9}	kg
Emissions to agricultural soil	4.95×10^{3}	kg
Emissions to industrial soil	3.92×10^{4}	kg

In the output, the greatest impact is due to the emissions to fresh water and the emissions to air that contribute respectively for 75.4% and 20.9% to the total output flow. The deposited goods contribute with 2.97% to the total flow while other contributions are negligible. Inputs and outputs are expressed also as $kgCO_{2\text{-}eq}$: resources in input are $2.83\times10^{8}\,kgCO_{2\text{-}eq}$ while emissions to air in the output are $9.67\times10^{10}\,kgCO_{2\text{-}eq}$. The highest contribution is due to CO_2 sources in Lombardy and Puglia (iron and steel plant). Also in this case, a price allocation is considered for CO_2 sources. The considered price for CO_2, electricity and

steel are respectively of 80 €/ton, 0.15 €/kWh and 589 €/ton (Portdata, 2019; Focus Economics, 2019; OECD, 2013).

The LCI results for the CCUS supply chain of the UK are reported in Table VIII.13.

Table VIII.13 LCI results: elementary flows for the CCUS supply chain in the UK

Input		
Resources	$2.35 \cdot 10^{12}$	kg
Output		
Resources	$8.75 \cdot 10^{4}$	kg
Deposited goods	$2.75 \cdot 10^{10}$	kg
Emissions to air	$4.44 \cdot 10^{11}$	kg
Emissions to fresh water	$1.71 \cdot 10^{12}$	kg
Emissions to sea water	$2.36 \cdot 10^{11}$	kg
Emissions to agricultural soil	239	kg
Emissions to industrial soil	$4.4 \cdot 10^{3}$	kg

In the output, a higher impact is due to emissions to fresh water and emissions to air that contribute respectively with 70.7% and 18.4% to the total output flow. The deposited goods contributes with 1.14% to total flow while other contributions can be neglected. Input and output can be expressed also like $kgCO_{2eq}$: resources in input are $2.26 \cdot 10^{10}$ $kgCO_{2eq}$ while emissions to air in output are $3.21 \cdot 10^{10}$ $kgCO_{2eq}$. A price allocation is considered for CO_2 source in Leeds. The considered price for CO_2 and electricity are respectively of 80 €/ton and 0.2 €/kWh (Portdata, 2019; OECD, 2013).

VIII.3 Results

The results of LCA analysis are here presented for all CCUS supply chains. The magnitude of environmental burden is evaluated through two different steps: classification and characterization. In these steps, the LCI results are combined and organized into impact categories and then into impact indicators at the midpoint level using the CML 2001 methodology, implemented in GaBi software (Von der Assen et al., 2014a; Guinee et al., 2002; PE International, 2010; Thinkstep, 2019) (LCIA phase). In the last phase of this environmental analysis, the interpretation of the results in terms of significant issues and sensitivity analysis is developed (interpretation phase).

VIII.3.1 Life cycle impact assessment phase for the CCUS supply chain of Germany

At first, the GWP is the environmental impact category that is considered, because the first aim of this analysis is to verify the target suggested by the environmental policy regarding CO_2 emissions. Results for

other impact categories, like AP, EP, ODP, ADP fossil and elements, FAETP, HTP, MAETP, POCP, TETP are shown in the Appendix (see Table S1).

Results show that the value of GWP is of 1.94×10^{11} $kgCO_{2\text{-}eq}$: the suggested CCUS supply chain can achieve what established in the environmental policy by the Government environmental regulations. In fact, the Federal Ministry for the Environment (2017) stated that in Germany, CO_2 emissions should be lower than 751 Mton in 2020 and in the suggested scheme, considering also emissions from the not selected sources, total CO_2 emissions are of 640 Mton. The greatest CO_2 emissions inside the CCUS supply chain, come from CO_2 source in Munich (steel and iron plant) with 7.85×10^{10} $kgCO_{2\text{-}eq}$, followed by steam production in the precipitated calcium carbonate process, with 1.95×10^{10} $kgCO_{2\text{-}eq}$, by CO_2 source in Potsdam (power plant) with 1.65×10^{10} $kgCO_{2\text{-}eq}$, by the process for the production of propylene oxide in polyurethane production, with 1.53×10^{10} $kgCO_{2\text{-}eq}$, and by the process to produce concrete by red mud, with 6.42×10^{9} $kgCO_{2\text{-}eq}$.

VIII.3.2 Life cycle impact assessment phase for the CCUS supply chain of Italy

Also for the CCUS supply chain in Italy, the goal of this analysis is to verify that the supply chain reduces CO_2 emissions to a value lower than that established by the environmental policy for 2030, equal to 275 Mton (Gracceva et al., 2017). For this reason, only the GWP impact category is considered. Results show that for the analyzed CCUS supply chain, the value of GWP is 9.62×10^{10} $kgCO_{2\text{-}eq}$. Considering other CO_2 sources not selected for the supply chain, the total CO_2 emissions are of 249 Mton. A value lower than the target is then obtained, showing that the suggested solution can reduce effectively CO_2 emissions in Italy. Inside the supply chain, the processes with a greater contribution to CO_2 emissions are the iron and steel plant in Puglia (6.32×10^{10} $kgCO_{2\text{-}eq}$) and the iron and steel plant in Lombardy (1.09×10^{10} $kgCO_{2\text{-}eq}$). For a complete analysis other impact categories like AP, EP, ODP, ADP fossil and elements, FAETP, MAETP, POCP, TEP are reported in the Appendix (see Table S2).

VIII.3.3 Life cycle impact assessment phase for the CCUS supply chain of the UK

The goal of the UK is to reduce CO_2 emissions to a value lower than that established by the environmental policy, equal to 54.6 Mton for 2030 (Department of Business, Energy and Industrial Strategy, 2018). Results show that for the developed CCUS supply chain, the value of GWP is of 9.37×10^{9} $kgCO_{2\text{-}eq}$. Considering other CO_2 sources not selected for the supply chain, total CO_2 emissions are of 52.37 Mton. A value lower than the target is obtained then, the suggested CCUS solution can reduce effectively CO_2 emissions in the UK. Inside the supply chain, the process that has a higher contribution to CO_2 emissions is the power plant, with 7.79×10^{9} $kgCO_{2eq}$.

For a complete analysis, other impact categories are reported in Appendix (see Table S3).

VIII.4. Discussion

VIII.4.1 Interpretation phase for the CCUS supply chain of Germany

From the above section, it is noticeable that significant issues (processes that contribute most to the overall result) are: the precipitated calcium carbonate process, due to a high environmental impact of steam production, CO_2 sources (in particular Munich, Potsdam), propylene oxide formation in the polyurethane production section and concrete production by red mud.

A sensitivity analysis is carried out to evaluate the influence of storage and utilization section inside the suggested topology of the supply chain. In particular, for CO_2 captured from Magdeburg, the amount that is sent to the storage section is tentatively utilized in different percentages, for the separate production of different species (concrete by red mud or curing, wheat, lignin upgrading, urea, methanol, polyurethane and calcium carbonate).

With three different case studies, only 25%, 50% and 75% of the whole CO_2 originally stored in the base case, is maintained in the storage section in this sensitivity analysis, while the remaining captured CO_2 is sent to the utilization, in order to increase the production of one product.

Results are shown in Table VIII.14: for a complete picture of the environmental impact, all impact categories are considered. While the GWP is expected to be increased by increasing the utilization rate of CO_2, other impacts could be increased, constant or decreased.

Table VIII.14 Results of sensitivity analysis when increasing carbon dioxide utilization rate in each utilization section; arrows indicate the variation of each impact category with reference to the base case (↑/↓ low variation (<5%), ↔ constant value, ↑/↓ medium variation (<50%), ⇑/⇓ high variation (>50%)) (Leonzio et al., 2020)

	GWP	AP	EP	ODP	ADP elements	ADP fossil	FAETP	HTP	MAETP	POCP	TETP
Methanol	↑	↔	↔	↔	↑	↓	↑	↓	↔	↔	↓
Concrete curing	↑	↑	↑	↔	↔	↓	↓	↑	↔	⇑	↑
Urea	↑	↑	↑	↑	↑	↑	↓	↑	↔	↑	↔
Wheat	⇑	↔	↔	↔	↔	↓	↓	↓	↔	↔	↓
Lignin treatment	↑	↑	↔	↑	↑	↑	↔	↑	↑	↑	↔
Polyurethane	↑	↑	↑	↑	⇑	↑	↑	↑	↑	↑	↑
Calcium carbonate	↑	↑	↔	↔	↑	↓	↔	↑	↑	↑	↑
Concrete by red mud	↑	↑	↑	↔	↔	↓	↔	↑	↔	↑	↑

Assuming that the fraction of CO_2 sent to the utilization section is used to produce CH_3OH, and that the captured CO_2 is stored at a rate of only 25%, 50%, 75% of the base case, the calculated CH_3OH production

is 9.8 Mton, 6.8 Mton and 3.8 Mton, respectively. Keeping constant the amount of captured CO_2, and reducing the amount of CO_2 sent to storage (i.e. producing more CH_3OH), the AP, EP, ODP, MAETP, POCP remain constant. On the other hand, the GWP, ADP elements and FAETP fossil increase compared to the base case. However, the GWP increases only slightly compared to base case. The opposite trend is observed for the ADP fossil, HTP and TETP. Overall, the variation of these impact categories is not significant compared to the base case.

In the following analysis, CO_2 that is not stored is used for concrete curing: when the stored amount of CO_2 is only 25%, 50%, 75% of the base case, CO_2-cured concrete is 513 Mton, 343 Mton and 174 Mton, respectively. Results show that for the ODP, ADP elements and MAETP no variations are present. The GWP, AP, EP, HTP, POCP, TETP are increased then, a higher environmental impact is present, especially for the POCP. The highest value that is achieved for the GWP is 3.46×10^{11} $kgCO_{2\text{-eq}}$, when the stored CO_2 is only 25% of the base case. Reductions are present for the FAETP and ADP fossil. Overall, producing a higher amount of CO_2-cured concrete increases the environmental impact.

In the following analysis, CO_2 that is not stored is used to produce urea. When the stored CO_2 is only 25%, 50%, 75% of the base case, the urea production is of 21.9 Mton, 15.5 Mton and 8.2 Mton, respectively. Results show that the TETP and MAETP have a constant trend, while the GWP, AP, EP, ADP fossil, HTP and POCP increase. The highest value for GWP is 2.28×10^{11} $kgCO_{2\text{-eq}}$. On the other hand, only the FAETP is reduced increasing CO_2 sent to the utilization section. Overall, like in the previous case, the increase of urea production is not favorable to the reduction of the environmental impact.

CO_2 that is not stored is sent to the utilization section to produce wheat. The total CO_2-assisted production of wheat, when the stored CO_2 is only 25%, 50% and 75% of that sent to the storage section in the base case, is respectively $3.05\cdot10^{10}$ ton, $2.03\cdot10^{10}$ ton and $1.02\cdot10^{10}$ ton. With an increasing amount of CO_2 utilized for wheat production, only the GWP increases and a higher value compared to the base case is obtained (8.55×10^{12} $kgCO_{2\text{-eq}}$ compared to 1.94×10^{11} $kgCO_{2\text{-eq}}$ of the base case). This suggests a higher environmental impact, even if a reduction of ADP fossil, FAETP, HTP and TETP is predicted. Other impact categories like POCP, MAETP, ADP elements, ODP, EP and AP present a constant trend.

CO_2 not stored is sent to the utilization for lignin treatment: when only 25%, 50% and 75% of CO_2 sent to the storage section in the base case is stored, the respective amount of lignin that is upgraded is 69.7 Mton, 46.6 Mton and 23.5 Mton. Overall, increasing the lignin that is treated determines a higher environmental impact. In fact, the GWP, AP, ODP, ADP elements, ADP fossil, HTP, MAETP and POCP increase. However, as in the methanol case, no significant variations are obtained. For example, the highest value of GWP is 2.06×10^{11} $kgCO_{2\text{-eq}}$. On the other hand, the TETP and FAETP show no variations.

When increasing the amount of CO_2 sent to the utilization for polyurethane production, it is evident that the environmental impact increases. The highest variation compared to the base case is present for the ADP elements, while for other impact categories no significant variations compared to the base case are obtained.

The highest GWP is 2.88×10^{11} $kgCO_{2\text{-eq}}$. When only 25%, 50% and 75% of CO_2 sent to the storage section in the base case is stored, the amount of polyurethane that is produced is respectively 62 Mton, 45 Mton and 28 Mton.

In the following sensitivity analysis, the amount of CO_2 that is not stored is sent to the utilization for the production of calcium carbonate. When only 25%, 50%, 75% of CO_2 sent to the storage section in the base case is stored, the amount of calcium carbonate that is produced is respectively 135 Mton, 131 Mton and 126 Mton. A constant trend is present for the EP, ODP and FAETP. Increasing the utilization option, a reduction is obtained only for the ADP fossil, while an increment is obtained for other impact categories. The highest value for GWP is 1.96×10^{11} $kgCO_{2\text{-eq}}$. However, no significant variations compared to base case are present.

In the last sensitivity analysis, CO_2 not stored is sent to the utilization for the production of concrete by red mud. When only 25%, 50% and 75% of CO_2 sent to the storage in the base case is actually stored, the amount of concrete produced is respectively 1.16 billion ton, 783 Mton and 401 Mton. A constant trend is present for the ODP, ADP elements, FAETP and MAETP. Generally, increasing the amount of CO_2 sent to the utilization section, the GWP, AP, EP, HTP, POCP and TETP increase, while only the ADP fossil decreases. The highest value of GWP is 5.79×10^{11} $kgCO_{2\text{-eq}}$, calculated when only 25% of CO_2 is stored in the storage section compared to the base case. However, no substantial variations are predicted compared to the base case for these impact categories.

The sensitivity analysis suggests that the storage site is important inside the CCUS supply chain in order to reduce the environmental impact, in terms of GWP. In fact, in all cases, the GWP is increased by increasing the amount of CO_2 sent to the utilization section, for the same amount of captured CO_2. Only few impact categories are reduced in these sensitivity analyses and only for some CO_2-based products.

Comparing the different case studies, a lower overall environmental impact is obtained when additional CH_3OH is produced. On the other hand, the highest GWP value is obtained with wheat production.

A higher environmental impact in terms of GWP at a higher utilization rate of CO_2 is due to a higher specific environmental impact of utilization processes compared to that of the storage system. This result is in agreement with the work of Cuellar-Franca and Azapagic (2015) where a comparison between a CCS and a CCU was presented: on average, the GWP of a CCS is significantly lower than that of CCU option. For example, for the biodiesel production in a CCU, the GWP is four times higher than that of a CCS, while the carbon mineralization and the EOR have a GWP that is 2.9 and 1.8 times higher than that of a CCS, respectively. Then, even if the utilization solution can help to reduce costs because of the generated profit (a better economic potential is ensured), it can not help to reduce the environmental impact in terms of GWP.

As a result, the storage section is important and should be designed at the optimal operating conditions. Also, the storage is important because the demand of chemicals does not have the capacity to sink enough

CO_2 emissions in order to achieve carbon reduction targets (Cuellar-Franca and Azapagic, 2015). The same consideration about the importance of a carbon storage was reported by Aldaco et al. (2019) comparing a CCU with a CCS system. A lower GWP, obtained for a carbon supply chain with the storage option, is also reported by Fernandez-Dacosta et al. (2018): CCUS systems present higher CO_2 emission reductions than CCU systems. A higher potential of climate change mitigation is ensured when the storage option is taken into account.

For the other impact categories, a comparison with the literature cannot be performed because a complete LCA analysis for CCUS supply chains, with the emerging technologies in the utilization section and considering all impact categories, has not been developed yet. In fact, Cuellar-Franca and Azapagic (2015) in their work suggested, for future works, to consider a wider range of LCA impacts, rather than focusing only on the GWP, as well as to consider various utilization options of CO_2, as done for the supply chains developed in this Thesis.

Although LCA studies and respective results for new CO_2 utilization processes will undoubtedly evolve, the LCA analysis at this stage will help to provide suggestions for future researches aiming at higher energy and environmental advantages (National Academies of Sciences, Engineering, and Medicine, 2019).

With these considerations, a LCA study is carried out considering a higher efficiency for CH_3OH synthesis, in terms of global CO_2 conversion, that should reduce CO_2 emissions at the outlet of the chemical reactor. The sensitivity analysis previously developed is repeated at these operating conditions, with the aim to verify if, with a higher efficiency of the process, a higher CO_2 utilization rate can reduce the environmental impact. Results are shown in Table VIII.15.

Table VIII.15 Results of sensitivity analysis when increasing carbon dioxide utilization rate to methanol and varying carbon dioxide conversion; arrows indicate the variation of each impact category with reference to the base case (⇔ constant value; ⇑/⇓ low variation (< 5%) upwards/downwards) (Leonzio et al., 2020)

CO_2 conversion	GWP	AP	EP	ODP steady state	ADP elements	ADP fossil	FAETP	HTP	MAETP	POCP	TETP
100%	⇔	⇔	⇔	⇔	⇑	⇓	⇑	⇓	⇔	⇔	⇓
90%	⇔	⇔	⇔	⇔	⇑	⇓	⇑	⇓	⇔	⇔	⇔

It is evident that increasing the utilization rate of CO_2 and improving the efficiency of CH_3OH synthesis, with the same amount of captured CO_2, the GWP is constant, as other impact categories.

In any case, when the global CO_2 conversion of CH_3OH synthesis is fixed at 90%, ADP elements and FAETP increase, while ADP fossil and HTP decrease. When global CO_2 conversion is 100%, also TETP decrease, suggesting a lower environmental impact.

It is shown that improving the efficiency of a CH_3OH process allows to send a higher amount of CO_2 to the utilization section without increasing the value of GWP, compared to the base case. However, it is difficult

to realize a CH_3OH process based on CO_2 hydrogenation with these high efficiencies, and many investigations would be needed to this aim, with environmental and energetic advantages.

VIII.4.2 Interpretation phase for the CCUS supply chain of Italy

The previous results for the CCUS supply chain of Italy suggest that significant issues are related to CO_2 sources, especially Puglia and Lombardy, where iron and steel plant are present.

As for the previous supply chain, a sensitivity analysis is developed keeping constant the amount of captured CO_2, while increasing the amount of emissions sent to the utilization for CH_4 production and reducing those sent to the storage. 25%, 50%, 75% of CO_2 sent to the storage section in the base case is stored in this analysis and the rest is sent to the utilization for CH_4 production. The amount of CH_4 that is produced in the respective case study is of 25 Mton, 22 Mton and 19 Mton. In the base case, 16.1 Mton of methane are produced. Results are shown in Table VIII.16: the GWP is reduced, then, for this supply chain in Italy, the utilization is preferred over the storage because a lower GWP can be obtained.

Regarding other impact categories, a better environmental impact is also obtained, because all of them are reduced, except the EP that is constant. The storage is not favorable to reduce the environmental impact. These results suggest that the power to gas technology is a process cleaner and more environmentally friendly than the storage option and other utilization systems (evaluated for the CCUS supply chain in Germany). In fact, no CO_2 emissions are present at the outlet of chemical reactor. CO_2 conversion and CH_4 selectivity reach values close to 100%, especially under stoichiometric conditions (Stangeland et al., 2015).

Table VIII.17 Results of the sensitivity analysis regarding different impact categories when higher fractions of CO_2 flow rate are utilized for methane production; arrows indicate variations with respect to the base case (⇔ constant value, ↓/↑ low variation (<5%), ⇓/⇑ medium variation (<50%)) (Leonzio et al., 2020)

GWP	AP	EP	ODP steady state	ADP elements	ADP fossil	FAETP	MAETP	POCP	TETP
↓	↓	⇔	↓	↓	↓	↓	⇓	↓	⇓

VIII.4.3 Interpretation phase for the CCUS supply chain of the UK

The previous results for the CCUS supply chain of the UK suggest that the power plant (CO_2 source) and the thermal energy production from biomass in calcium carbonate process are significant issues.

A sensitivity analysis is developed increasing the amount of CO_2 sent to the utilization for calcium carbonate production and reducing the amount of CO_2 sent to the storage, keeping constant the amount of captured CO_2. Only 25%, 50%, 75% of CO_2 sent to the storage section in the base case is stored in this analysis and the rest is sent to the utilization for calcium carbonate production. The amount of calcium carbonate that is produced for the respective case is of 5.7 Mton, 5.6 Mton and 5.5 Mton. In the base case,

5.4 Mton of calcium carbonate are produced. Results, as in Table VIII.18, show that the GWP, is increased if CO_2 is not sent to the storage but to the utilization. Then, for this analyzed supply chain, the utilization is not preferred over the storage, because a higher GWP is obtained. This result agrees with the results obtained for the CCUS supply chain of Germany. The same considerations are valid for other impact categories.

Table VIII.18 Results of the sensitivity analysis regarding different impact categories when higher fractions of CO_2 flow rate are utilized for calcium carbonate production; arrows indicate variations with respect to the base case (↓/↑ low variation (<5%))

GWP	AP	EP	ODP steady state	ADP elements	ADP fossil	FAETP	HTP	MAETP	POCP	TETP
↑	↑	↑	↑	↑	↑	↑	↑	↑	↑	↑

VIII.5 Conclusions

In this Chapter, a LCA analysis is carried out for large scale CCUS supply chains developed previously for Germany, Italy and the UK. Compared to the existing literature, processes and products not considered before are taken into account for this environmental analysis.

The LCA results show that for the CCUS supply chain of Germany, Italy and the UK the value of GWP is respectively of: 1.94×10^{11} $kgCO_{2\text{-}eq}$, 9.62×10^{10} $kgCO_{2\text{-}eq}$ and 9.37×10^{9} $kgCO_{2\text{-}eq}$. These results suggest that these Countries can reduce CO_2 emissions according to the environmental target using carbon supply chains.

For all supply chains, a sensitivity analysis is performed increasing the utilization rate of CO_2: keeping constant the captured CO_2, 25%, 50% and 75% of CO_2 sent to the storage in the base case is effectively stored in this analysis, while the remaining part is sent to the utilization section. For the CCUS supply chain of Germany (for which CH_3OH, urea, wheat, concrete, calcium carbonate, polyurethane, lignin are the considered utilization processes) and the UK (where calcium carbonate is produced) a higher environmental impact is present increasing the utilization rate of CO_2. In this case, the storage section is important in order to achieve a lower environmental impact. On the other hand, for the CCUS supply chain of Italy, where CH_4 is produced via a power to gas system, a lower environmental impact is present at higher utilization rate of CO_2. Then, the power to gas is a process cleaner and more environmentally friendly than the storage option and other utilization systems. The power to gas system therefore resulted to be the most realistic and mature process that avoids the increase of the environmental impact with its utilization. It is worth noticing here that hydrogen is assumed to be obtained by means of an electrolysis process utilizing green power sources.

Appendix

Table S1 Results of LCIA analysis for the CCUS supply chain of Germany

AP	1.57×10^{9}	$kgSO_{2eq}$
EP	3.04×10^{10}	$kgPhosphate_{eq}$
ODP steady state	3.76×10^{3}	$kgR11_{eq}$
ADP elements	4.25×10^{5}	$kgSb_{eq}$
ADP fossil	3.44×10^{12}	MJ
FAETP	7.43×10^{10}	$kgDCB_{eq}$
HTP	5.27×10^{10}	$kgDCB_{eq}$
MAETP	4.54×10^{14}	$kgDCB_{eq}$
POCP	1.84×10^{8}	$kgethene_{eq}$
TETP	1.49×10^{9}	$kgDCB_{eq}$

Table S2 Results of LCIA analysis for the CCUS supply chain of Italy

AP	4.67×10^{8}	$kgSO_{2eq}$
EP	1.15×10^{11}	$kgPhosphate_{eq}$
ODP steady state	368	$kgR11_{eq}$
ADP elements	2.27×10^{4}	$kgSb_{eq}$
ADP fossil	1.96×10^{12}	MJ
FAETP	9.27×10^{10}	$kgDCB_{eq}$
MAETP	1.02×10^{13}	$kgDCB_{eq}$
POCP	7.88×10^{7}	$kgethene_{eq}$
TETP	4.42×10^{7}	$kgDCB_{eq}$

Table S3 Results of LCIA analysis for the CCUS supply chain of the UK

AP	9.02×10^{7}	$kgSO_{2eq}$
EP	7.34×10^{6}	$kgPhosphate_{eq}$
ODP steady state	0.0132	$kgR11_{eq}$
ADP elements	1.25×10^{3}	$kgSb_{eq}$
ADP fossil	1.47×10^{11}	MJ
FAETP	1.88×10^{7}	$kgDCB_{eq}$
HTP	1.62×10^{9}	$kgDCB_{eq}$
MAETP	1.1×10^{13}	$kgDCB_{eq}$
POCP	7.21×10^{6}	$kgethene_{eq}$
TETP	1.39×10^{8}	$kgDCB_{eq}$

References

Aldaco, R., Butnar, I., Margallo, M., Laso, J., Rumayor, M., Dominguez-Ramos, A., Irabien, A., Dodds, P.E., 2019. Bringing value to the chemical industry from capture, storage and use of CO2: A dynamic LCA of formic acid production, Science of the Total Environment 663, 738–753

Antonetti, E., Iaquaniello, G., Salladini, A., Spadaccini, L., Perathoner, S., and Centi, G., 2017. Waste-to-Chemicals for a Circular Economy: The Case of Urea Production (Waste-to-Urea), ChemSusChem 10, 912 – 920.

Bernier, E., Lavigne, C., 2013. Life cycle assessment of kraft lignin for polymer applications, Int J Life Cycle Assess, 18, 520–528.

Biernacki, P., Rother, T., Paul, W., Werner, P., Steinigeweg, S., 2018. Environmental impact of the excess electricity conversion into methanol, Journal of Cleaner Production 191, 87-98.

Biswas, W.K., Graham, J., Kelly, K., John, M.B. 2010. Global warming contributions from wheat, sheep meat and wool production in Victoria, Australia e a life cycle assessment, Journal of Cleaner Production 18, 1386-1392.

Biswas, W.K., Barton L., Carter, D. 2008. Global warming potential of wheat production inWestern Australia: a life cycle assessment, Water and Environment Journal 22, 206–216.

Bouman, E.A., Ramirez, A., Hertwich, E.G. 2015. Multiregional environmental comparison of fossil fuel power generation—Assessment of the contribution of fugitive emissions from conventional and unconventional fossil resources, International Journal of Greenhouse Gas Control, 33, 1-9.

Boyer, M., Ponssard. J.P., Economic analysis of the European cement industry. 2013. <hal-00915646>

Carboncure, 2019. Available at: www.carboncure.com

Cuellar-Franca, R.M., Azapagic, A., 2015. Carbon capture, storage and utilisation technologies: a critical analysis and comparison of their life cycle environmental impacts. J. CO2 Util. 9, 82–102.

Department of Business, Energy and Industrial Strategy, 2018 UK Greenhouse gas emissions, provisional figures, Statistical Release: National Statistics, 28 March 2019.

Europe, 2019. https://ec.europa.eu/eurostat/statistics-explained/index.php/Electricity_price_statistics

Fernández-Dacosta, C., Stojcheva, V., Ramirez, A., 2018. Closing carbon cycles: Evaluating the performance of multi-product CO2 utilisation and storage configurations in a refinery, Journal of CO2 Utilization, 23, 128-142.

Focus Economics, 2019. https://www.focus-economics.com/commodities/base-metals/steel-europe

Giordano, L., Roizard, D., Favre, E., 2018. Life cycle assessment of post-combustion CO2 capture: A comparison between membrane separation and chemical absorption processes, International Journal of Greenhouse Gas Control 68, 146–163.

Gracceva F., De Luca E., Fidanza A., Del Nero P., Giuffrida L.G., Felici B., Pona C., Zini A., 2017 Analisi trimestrale del sistema energetico italiano. Report 1/2017. ISSN 2531-4750 (2017).

Guinee, J.B., Gorree, M., Heijungs, R., Huppes, G., Kleijn, R., Sleeswijk, A.W., Haes, H.Au.D., Bruijn, J.A.D., Duin, R.V., Hujbregts, M.A.J., 2002. Handbook on Life Cycle Assessment: Operational Guide to the ISO Standards. Kluwer Academic Publisher, Dordrecht.

Gursel, A.P., Horvath, A., 2012. Green Concrete LCA Tool. Univ. California, Berkeley, CA.

IPCC, 2005, IPCC special report on Carbon dioxide Capture and Storage. Prepared by Working Group III of the Intergovernmental Panel on Climate Change [Metz, B., O. Davidson, H.C. de Coninck, M. Loos and L.A. Meyer (eds.)], Cambridge University Press, Cambridge, United Kingdom and New York, NY, USa, 442 pp.

ISO 14040:2009, Environmental management – Life cycle assessment – Principles and framework, European Committee for Standardisation, Brussels.

ISO 14044:2006, Environmental management – Life cycle assessment – Requirements and guidelines, European Committee for Standardisation, Brussels.

Kajaste, R., Hurme M., and Oinas, P. 2018. Methanol-Managing greenhouse gas emissions in the production chain by optimizing the resource base, AIMS Energy, 6(6)1074–1102.

Koornneef J., van Keulen T., Faaij A., Turkenburg W. 2008. Life cycle assessment of a pulverized coal power plant with post-combustion capture, transport and storage of CO2. International Journal of Greenhouse Gas Control 2, 448-467.

Leonzio, G., Foscolo, P.U., Zondervan, E., 2019, Sustainable utilization and storage of carbon dioxide: analysis and design of an innovative supply chain, Computers and Chemical Engineering, 135, 5, 106569.

Leonzio, G., Bogle, D., Foscolo, P.U. 2020. Life cycle assessment of a carbon capture utilization and storage supply chain in Italy and Germany: comparison between carbon dioxide storage and utilization systems. To be submitted.

Mattila, H.P., Hudd, H., Zevenhoven, R., 2014. Cradle-to-gate life cycle assessment of precipitated calcium carbonate production from steel converter slag, Journal of Cleaner Production 84, 611-618.

Matzen, M., Demirel, Y., 2016a. Methanol and dimethyl ether from renewable hydrogen and carbon dioxide: Alternative fuels production and life-cycle assessment, Journal of Cleaner Production 139, 1068-1077.

Michailos, S., Sanderson, P., Zaragoza, A.V., McCord, S., Armstrong, K., Styring, P., 2018. Methanol Worked Examples for the TEA and LCA Guidelines for CO2 Utilization,

National Academies of Sciences, Engineering, and Medicine. 2019. Gaseous Carbon Waste Streams Utilization: Status and Research Needs. Washington, DC: The National Academies Press. doi: https://doi.org/10.17226/2523.

Nikbin, I.M., Aliaghazadeh, M., Charkhta, S., Fathollahpour, A. 2018. Environmental impacts and mechanical properties of lightweight concrete containing bauxite residue (red mud), Journal of Cleaner Production 172, 2683-2694.

OECD, 2013. Effective Carbon Prices, http://www.oecd.org/env/tools-evaluation/carbon-prices.htm

Patricio, J., Angelis-Dimakis, A., Castillo-Castillo, A., Kalmykova, Y., Rosado, L., 2017. Region prioritization for the development of carbon capture and utilization technologies, Journal of CO2 Utilization 17, 50–59.

PE International, 2010. PE international database. Extensions: Ib inorganic intermediates, XIV Constr. Mater. Last updated: 2010.

Portdata 2019. Available at: https://www.pordata.pt/en/Europe/Electricity+prices+for+households+and+industrial+users+(Euro+ECU)-1477-211472

Reiter, G., Lindorfer, J. 2015. Global warming potential of hydrogen and methane production from renewable electricity via power-to-gas technology, Int J Life Cycle Assess, 20, 477–489

Stangeland, K., Kalai, D., Li, H., Yu, Z., 2017. CO_2 methanation: the effect of catalysts and reaction conditions, Energy Procedia 105, 2022 – 2027.

Sternberg A., and Bardow, A. 2016. Life Cycle Assessment of Power-to-Gas: Syngas vs Methane, ACS Sustainable Chem. Eng. 4, 4156−4165.

Thinkstep, 2019, Available at: https://www.thinkstep.com/.

Von der Assen, N., Voll, P., Peters M., and Bardow, A., 2014a. Life cycle assessment of CO2 capture and utilization: a tutorial review, Chem. Soc. Rev., 43, 7982—7994.

von der Assen, N., Sternberg, A., Katelhon, A., Bardow, 2015. Environmental potential of carbon dioxide utilization in the polyurethane supply chain, Faraday Discuss., 183, 291–307.

von der Aben, V.N. From Life-Cycle Assessment towards Life-Cycle Design of Carbon Dioxide Capture and Utilization, 2015, Diese Dissertation ist auf den Internetseiten der Universitatsbibliothekonline verfugbar.

Wildbolz, C. 2007. Life Cycle Assessment of Selected Technologies for CO2 Transport and Sequestration, Diploma Thesis, No. 2007MS05

Yue D., You F., 2015, Integration of geological sequestration and microalgae biofixation supply chains for better greenhouse gas emission abatement, Chemical Engineering Transactions, 45, 487-492.

Zappa, W., Pilot-scale Experimental Work on the Production of Precipitated Calcium Carbonate (PCC) from Steel Slag for CO2 Fixation, Thesis submitted in partial fulfilment of the requirements for the degree of Master of Science in Technology Department of Energy Technology School of Engineering, Aalto University Espoo, 11th August 2014.

Nomenclature

Abbreviations

ADP = abiotic depletion potential

AIMMS = advanced interactive multidimensional modeling system

AP = acidification potential

CED = cumulative energy demand

CCU = carbon capture and utilization

CCUS = carbon capture utilization and storage

CCS = carbon capture and storage

EP =eutrophication potential

FAETP = fresh water aquatic ecotoxity potential

GWP = global warming potential

HTP = human toxicity potential

LCA = life cycle assessment

LCI = life cycle inventory

LCIA = life cycle impact assessment

MAETP = marine aquatic ecotoxicity potential

MEA = monoethanolamine

ODP = ozone depletion potential

POCP = photochemical ozone creation potential

TETP = terrestrial ecotoxicity potential

Chapter IX

Multi-objective optimization of CCUS supply chains

In this Chapter, the best carbon capture utilization and storage supply chains, previously developed for Germany, Italy and the UK, are reformulated as bi-objective problems. The amount of captured carbon dioxide is maximized while total costs are minimized at the same time. Results show that, for the resolution of this multiple objective optimization problem, the augmented ε-constraint method is more efficient than the traditional ε-constraint method, and the respective Pareto fronts with trade-off conditions are obtained. A scenario on this plot for the three carbon supply chains is suggested for the decision makers, considering only the economic objective function (the scenario with the minimum value of net total cost is selected) or both objective functions (the scenario with the shortest distance from the Utopia point is chosen). It is found that, the scenario suggested for the CCUS supply chain of Germany is closer to Utopia conditions than those suggested for the other two supply chains: a better trade-off between the two objective functions is then achieved, even if the system has the highest costs.

IX.1 Introduction

Generally, carbon capture utilization and storage (CCUS) supply chains are designed and optimized considering an economic objective function, expressing total costs or the net present value or the total profit, that should be minimized or maximized according to the specific case. No environmental objective functions, considering for example the reduction of emissions that should be maximized, are taken into account. Moreover, most of these objective functions are considered one at a time.

As discussed in the introduction of this Thesis, no studies about carbon capture utilization and storage supply chains have simultaneously considered economic and environmental aspects, through a multi-objective optimization (MOO) problem. Only the work of Yue and You (2015) considered economic and environmental performances of a CCUS supply chain, cultivating algae for biofuels production, however the system is solved using the Life Cycle Optimization framework.

Actually, MOO problems have gained a wide popularity in sustainability studies and several objective functions are simultaneously optimized rather than being considered as additional constraints inside the developed mathematical model (Grossman and Guillen-Gosalbez, 2010; Limleamthong and Guillen-Gosalbez, 2017). In the literature, multi-objective optimization problems are generally solved for oil and gas sector (Ghaithan et al., 2017; Attia et al., 2019; Azadeh et al., 2017), bioenergy (Razm et al., 2019), biofuels (Camber and Sowlati, 2016) agriculture (Roghanian and Cheraghalipour, 2019) and sustainable (Balaman et al., 2018; Resat and Unsal, 2019; Mele et al., 2011; You et al., 2012; Pinto-Varela et al., 2011) supply chains.

Studies about the application of MOO to CCUS supply chains are then lacking, despite the interest of this kind of optimization in other research fields.

For this reason, in order to fill this gap, the best supply chains developed for Germany (producing more CO_2-based products), for Italy (with Adriatic sea as storage site) and for the UK (with Bunter Sandstone as storage site) are re-formulated as deterministic MOO problems. For these CCUS supply chains, total costs are minimized while the amount of captured carbon dioxide (CO_2) is maximized, according to a bi-objective optimization problem: an economic as well as an environmental objective function are taken into consideration simultaneously. For the resolution of these problems, the ε-constraint and the augmented ε-constraint methods are compared, with the aim to find the Pareto front, suggesting all possible solutions as trade-off between the two objective functions. Some methods are suggested to select one scenario for decision makers, among those found through the Pareto front. The aim of this work is then to design and optimize the previous CCUS frameworks considering economic and environmental aspects simultaneously.

IX.2 Model development

For the CCUS supply chain of Germany, Italy and the UK the mathematical model is developed as in previous, respective Chapters. However, the constraint about achieving the minimum target of CO_2 emissions reduction is not considered and two objective functions are taken into account, as defined below. For each system, the Mixed Integer Linear Programming (MILP) model is solved using AIMMS (Advanced Interactive Multidimensional Modeling) software, according to the ε-constraint method and the augmented ε-constraint.

IX.2.1 Objective functions

In the considered bi-objective problems, two objective functions are considered (see Eqs. IX.1-IX.2):

$$\phi_1 = Total\ costs \qquad (IX.1)$$

$$\phi_2 = Captured\ carbon\ dioxide \qquad (IX.2)$$

Then, an economic and an environmental objective function are considered. The total costs of a CCUS supply chain consider CO_2 capture and compression costs, CO_2 transportation costs, CO_2 storage costs and the production costs of different CO_2-based products. This objective function should be minimized, while the overall CO_2 captured inside the CCUS supply chain should be maximized. A trade-off between these two objective functions is obtained.

IX.2.2 The ε-constraint method

The ε-constraint method, also known as the constraint transformation method, is a posteriori method introduced by Haimes et al. (1971) for convex and non convex problems. For detailed information about the ε-constraint method and its advantages over other techniques to solve multi-objective problems please refer to Reza Norouzi et al. (2014), Rezvani et al. (2015), Mavrotas (2009) and Miettinen (1999). Moreover,

the application of this methodology for the multi optimization of supply chains can be found in Mota et al. (2015), Santibañez-Aguilar et al. (2011), You et al. (2012) and Cucek et al. (2012).

In the-ε constraint method, the initial multi-objective optimization problem is transformed into a single optimization problem with a sequence of other objective functions set as constraints (Brisset and Gillon, 2015). Then, assuming the following multi optimization problem (Mavrotas, 2009):

$$\max(f_1(x), f_2(x), \dots f_p(x))$$

S.t. (subject to)

$$x \in S \qquad (IX.3)$$

where x is the vector of decision variables, $f_1(x), \dots, f_p(x)$ are the p objective functions and S is the feasible region, it can be transformed by the ε-constraint method in the following problem (Mavrotas, 2009):

$$\max \; f_1(x)$$

S.t.

$$f_2(x) \geq \varepsilon \qquad \varepsilon \in \{\varepsilon_{l,2}, \dots . \varepsilon_{h,2}\} \qquad (IX.4)$$

$$f_3(x) \geq \varepsilon \qquad \varepsilon \in \{\varepsilon_{l,3}, \dots . \varepsilon_{h,3}\}$$

$$\dots\dots$$

$$f_p(x) \geq \varepsilon \qquad \varepsilon \in \{\varepsilon_{l,p}, \dots . \varepsilon_{h,p}\}$$

$$x \in S$$

where $\varepsilon_{l,i}$ and $\varepsilon_{h,i}$ are generally obtained from the single optimization problems and f_1 is the objective function with the highest priority (Ghaithan et al., 2017). For each mathematical model related to CCUS supply chains, at first the single objective functions (total costs and captured CO_2) are optimized in order to find the range of the ε parameter. After that, total costs are minimized putting the amount of captured CO_2 as a constraint for several points inside the ε range, divided in identical intervals. In fact, cost minimization has always more importance than the other objectives for real-life cases due to harsh competitive conditions (Resat and Unsal, 2019). This allows to find the plot of Pareto front, mainly composed by non dominated or non inferior solutions, defined as "*a feasible solution to a multi-objective programming problem to which exists no other feasible solution that will yield an improvement in one objective without causing a degradation in at least one other objective*" (Cohon, 2008). In other words, there is no solution that optimizes all objectives simultaneously in the decision space (Avci and Selim, 2017). In this work, the Pareto front is built considering ten sections of equal dimension, because they are able to provide a good representation. The Utopia and Nadir points are found respectively as the best and worse conditions for both objective functions.

IX.2.3 The augmented ε-constraint mehod

The augmented ε-constraint method is a posteriori hybrid method, obtained combining the ε-constraint method and the lexicographic method (Mavrotas, 2009; Khorram et al., 2010; van Elzakker et al., 2017). It is developed in order to overcome the following limitations of the ε-constraint method: the calculation of ε range, the efficiency of the obtained solutions (some dominated solutions can be provided), the presence of insignificant extreme sections in the Pareto front and a lower efficiency due to high resolution time required for a large number of objective functions (Mavrotas, 2009; Ochoa Robles, 2018). Also, Liu and Papageorgiou (2013) reported that the main disadvantage of the ε-constraint method is that the generated solutions depend on the selected ε range. While Ogumerem et al. (2018) reported that this method can not ensure the feasibility and efficiency of solutions, that should be verified once the complete set of solutions has been obtained.

According to the augmented ε-constraint method, the lexicographic method is used to build the payoff table (table with results obtained from the individual optimization of objective functions), in order to define the ε range within which, to perform the multi optimization according to the ε-constraint method, generating all efficient solutions (Razm et al., 2019; Attia et al., 2019). According to the lexicographic method, the first objective function, with a higher priority, is optimized obtaining its optimal value. Then, the second objective function is also optimized fixing the first objective function at its optimal value, found in the previous step. After that, the third objective function is optimized constraining the first and the second objective functions at their optimal value. This procedure is repeated until all objective functions are considered and the obtained values are used to build the payoff table. Then, the ε-constraint method is applied: one objective function is minimized or maximized while the others are constrained inside the respective range found with the lexicographic method and divided in sections of equal dimension. In this way, efficient solutions are considered on the Pareto front without extreme insignificant solutions and the processing time is accelerated avoiding redundant iterations (Cambero and Sowlati, 2016).

For the considered CCUS supply chains, according to the above method, one extreme point of the Pareto front is found minimizing total costs, without considering the captured CO_2 objective function. After that, the captured CO_2 is maximized with total costs constrained to the previous value. The other extreme point is found maximizing the captured CO_2 without considering total costs objective function. After that, total costs are minimized with the captured CO_2 constrained to the previous value. These two extreme points, calculated with the lexicographic method, provide the ε range, where to apply the ε-constraint method: total costs are minimized setting the captured CO_2 as a constraint. Total costs are minimized for the same reason defined in the ε-constraint method (Resat and Unsal, 2019). The calculation is done for some points inside the considered ε range. According to these considerations, the Pareto front is built with ten sections of equal dimensions, suggesting a trade-off relation between the two objective functions. These points are sufficient to visualize all regions of the Pareto front, between the two extreme points. This Pareto front allows the decision maker to compromise between economic and environmental objectives (Attia et al., 2019). Also

in this case, the Utopia and Nadir points correspond to the optimal and worse conditions, respectively, for both objective functions.

IX.3 Results and discussion

In this section, the Pareto fronts obtained for the different CCUS supply chains (in Italy, Germany and the UK) are presented and discussed. To this aim, the ε-constraint and augmented ε-constraint methods are used.

IX.3.1 Results for the CCUS supply chain of Germany

The optimal solutions are found in 5.55 s with 1151 iterations, using CPLEX 12.7.1 solver. Figure IX.1 shows the Pareto front for the CCUS supply chain of Germany, obtained with the ε-constraint method: it is divided in 11 points, delimiting 10 intervals of equal dimension. Overall, this curve can be divided mainly in three different sections. On the whole, the extreme sections on the right and left side of the curve are of minor interest, as explained below.

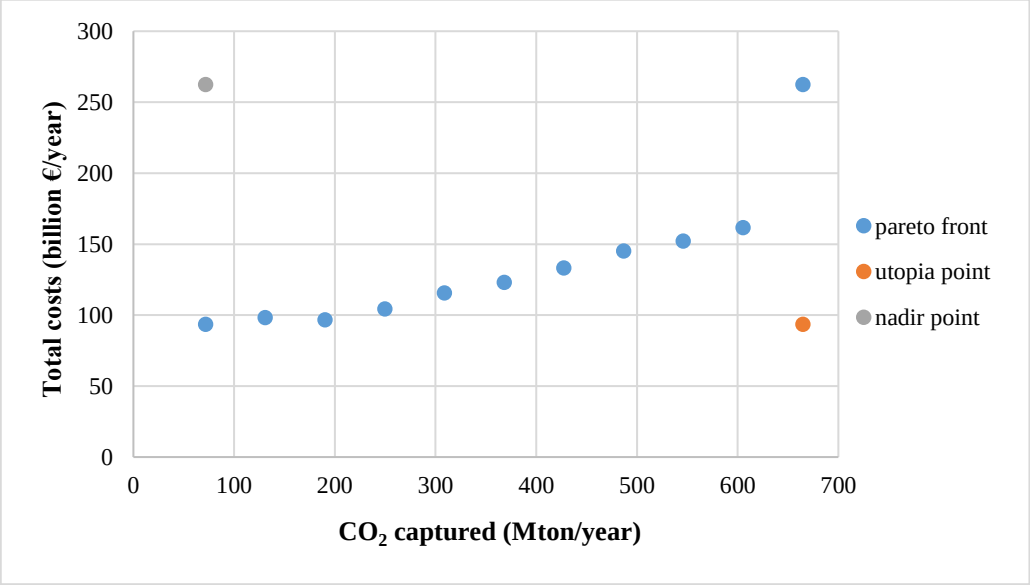

Figure IX.15 Pareto front obtained with the ε-constraint method for the CCUS supply chain of Germany producing different CO_2-based products (Leonzio et al., 2020)

The extreme point on the right side is important if a decision maker is interested on the captured CO_2. Here, there is a high variation on total costs without a big effect on the captured CO_2. For the right extreme point, there is in fact a high variation on total costs with a small variation on the captured CO_2: a high slope is present. In particular, there is a variation on total costs equal to 38.4% with a variation on the captured CO_2 of 8.9%. The extreme point on the left side, on the other hand, can be interesting if a decision maker is

interested on total costs, mainly. There is, in fact, a high variation on the captured CO_2 without a significant effect on total costs. A low slope is present: an increase on total costs of 4.85% with an average variation on the captured CO_2 equal to 45.1%. A moderate slope is present for the intermediate points: a significant improvement up to 68.9% in the captured CO_2 is evident with an increase in total costs of 40.2%. For these intermediate points, it is possible to improve one objective function, but producing a worse condition for the other one. The Nadir point is found at 71.6 Mton/year of captured CO_2 and at 263 billion€/year of total costs. The Utopia point corresponds to 665 Mton/year of captured CO_2 and at 93.5 billion€/year of total costs.

It is interesting to understand the behavior of the extreme point on the left side. With a deeper analysis, it is found that the system on the extreme point on the left side is changing the capture technology. In particular, at the maximum amount of captured CO_2, the WEI vacuum swing adsorption (VSA) is used for the utilization and storage section, replacing the piperazine (PZ) absorption in the utilization section and the pressure swing adsorption (PSA) in the storage section, used in other points.

The two extreme points on the left and right side of the Pareto front can be omitted by using the augmented ε-constraint. With this method, the optimal solutions are found in about 5.34 s with 2149 iterations. Compared to the previous method of resolution, the augmented ε-constraint methodology ensures to carry out higher iterations in a lower time, then it is more efficient, considering the time resolution parameter (Azadeh et al., 2017). Figure IX.2 shows the obtained Pareto front, built with 11 points dividing the curve in 10 pieces of equal dimensions. It is evident that for all points it is possible to improve one objective function but producing a worse condition for the other one.

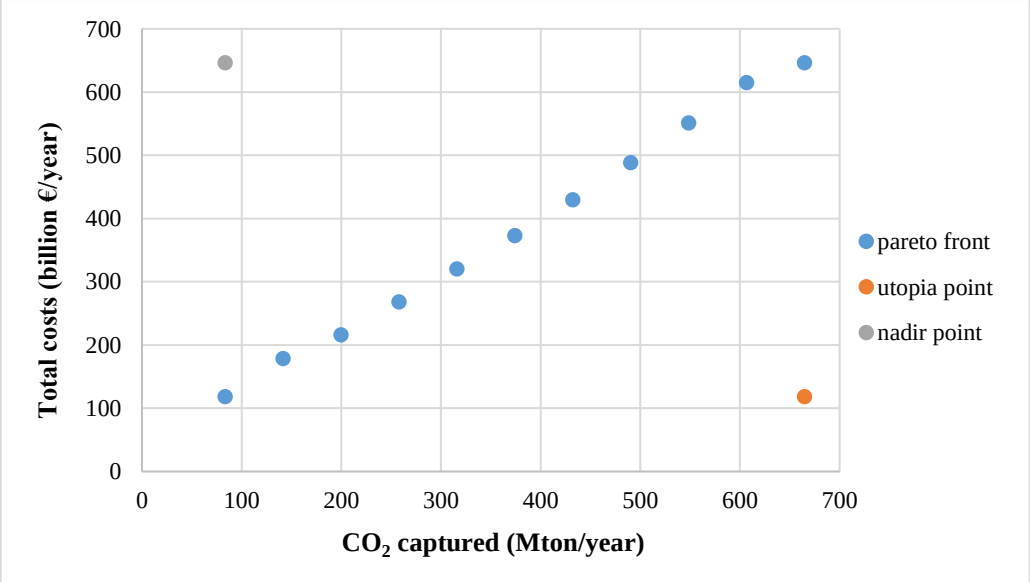

Figure IX.2 Pareto front obtained with the augmented ε-constraint method for the CCUS supply chain of Germany producing different CO_2-based products (Leonzio et al., 2020)

For this Pareto front, an increase of captured CO_2 equal to 87.4% determines an increase of total costs equal to 81.6%. The PZ absorption is used as capture technology in all cases defined on the Pareto front. Nadir and Utopia points are found: the Nadir point is at 83.5 Mton/year of captured CO_2 and at 646 billion€/year of total costs, while the Utopia point is at 665 Mton/year of captured CO_2 and at 119 billion€/year of total costs.

All points on the Pareto front are valid solutions, however, it is possible to choose one of these that has the shortest distance from the Utopia point, defined as the ideal condition (Ochoa Bique et al., 2019; Roghanian and Cheraghalipour, 2019). The calculation is done considering the normalized values of captured CO_2 and total costs and applying the Pythagorean theorem. The selected point is at 374 Mton/year of captured CO_2 and at 373 billion€/year of total costs: Table IX.1 shows the topology of the CCUS supply chain in the selected situation.

Table IX.7 Topology of the CCUS supply chain of Germany producing different CO_2-based products for the point on the Pareto front with the shortest distance from the Utopia point (Leonzio et al., 2020)

CO_2 source	**Capture technology**	**CO_2 amount (Mton/year)**
To storage		
To utilization		
Dusseldorf	PZ absorption	277
Munich	PZ absorption	0.01
Hannover	PZ absorption	62.1
Potsdam	PZ absorption	0.25
Dresda	PZ absorption	3.3
Wiesbaden	PZ absorption	7.18
Magdeburg	PZ absorption	24.7

All captured CO_2 is sent to the utilization section to produce 0.846 Mton/year of methanol (CH_3OH), 4.79 Mton/year of concrete curing, 19.35 Mton/year of wheat, 26.01 Mton/year of lignin, 11 Mton/year of polyurethane, 78.08 Mton/year of calcium carbonate, 373.55 Mton/year of urea and 19.15 Mton/year of concrete by red mud. The PZ absorption is the selected capture technology for all CO_2 sources.

For the problem with the single objective optimization, i.e. minimizing total costs as in Chapter IV of this Thesis, it is found that total costs are 97.9 billion€/year while the captured CO_2 are 160 Mton/year. Then the selected point on the Pareto front, with the shortest distance from the Utopia point, ensures a higher amount of captured CO_2 (a difference of 57.22%), although a higher value of total costs is estimated (a difference of 73.74%) compared to the condition obtained by the single optimization problem.

The previous point on the Pareto front is selected considering both objective functions. However, if a decision maker is more interested on money expenditure, it is possible to express the captured CO_2 in terms of costs, through the carbon tax, and subtract it to the total costs of supply chain, in order to obtain the net total cost. The value of carbon tax is set to 80 €/ton in this analysis. The point of Pareto front with the minimum net total cost, then can be selected. Figure IX.3 shows that this point is the first one on the left side: the amount of captured CO_2 is 83.5 Mton/year while total costs are 118.64 billion€/year (the net total cost is 112 billion€/year).

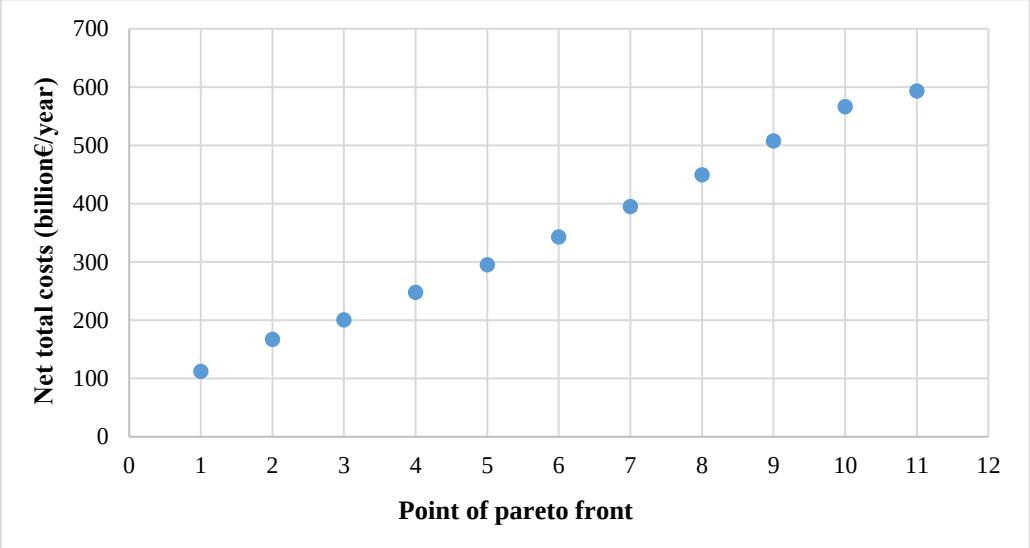

Figure IX.3 Net total cost for the points of Pareto front for the CCUS supply chain of Germany producing different CO_2-based products (Leonzio et al., 2020)

The topology of the CCUS supply chain for this suggested scenario is shown in Table IX.2: all captured CO_2 is sent to the utilization section by using the PZ absorption as capture technology.

Table IX.2 Topology of the CCUS supply chain of Germany producing different CO_2-based products for the point on the Pareto front with the minimum net total cost (Leonzio et al., 2020)

CO_2 source	**Capture technology**	**CO_2 amount (Mton/year)**
To storage		
To utilization		
Dusseldorf	PZ absorption	2.43
Munich	PZ absorption	0.01
Hannover	PZ absorption	62.10
Wiesbaden	PZ absorption	0.08
Magdeburg	PZ absorption	18.87

In the CCUS supply chain 0.846 Mton/year of CH_3OH, 4.79 Mton/year of concrete curing, 19.35 Mton/year of wheat, 0.378 Mton/year of lignin, 11 Mton/year of polyurethane, 69.55 Mton/year of calcium carbonate, 1.33 Mton/year of urea and 19.15 Mton/year of concrete by red mud are produced from the captured CO_2. However, compared to the problem with the single optimization, as in Chapter IV, this selected scenario ensures a lower amount of captured CO_2 and higher overall (gross) total costs.

IX.3.2 Results for the CCUS supply chain of Italy

The optimal solutions are found in about 0.53 s with 193 iterations, using CPLEX 12.7.1 solver. Figure IX.4 shows the Pareto front obtained with the ε-constraint method for the CCUS supply chain of Italy, with Adriatic offshore as storage site. The plot is built with 11 points dividing the all curve in 10 pieces of equal dimensions.

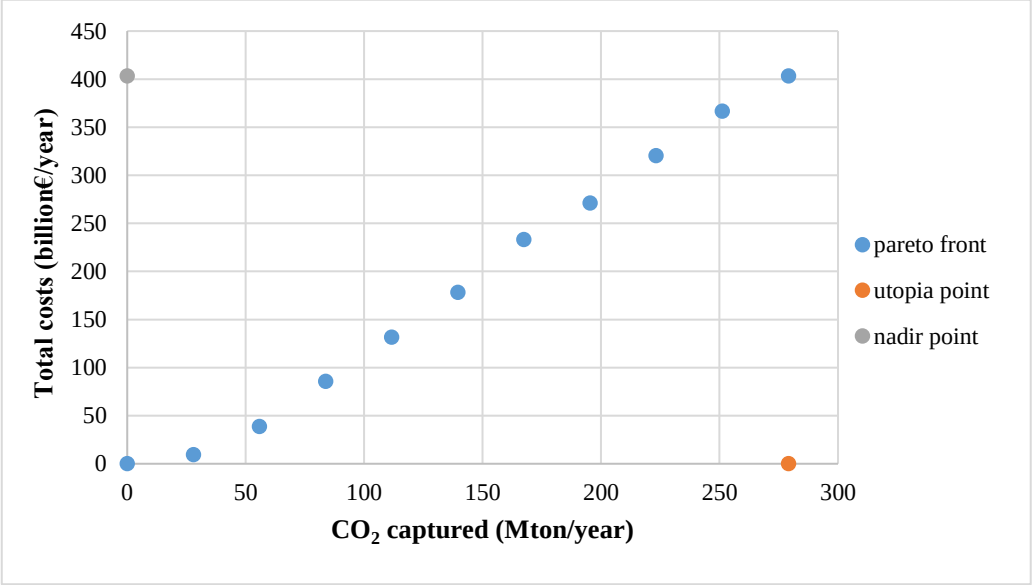

Figure IX.4 Pareto front obtained with the ε-constraint method for the CCUS supply chain of Italy with Adriatic offshore as storage site (Leonzio et al., 2020)

In the model, a constraint about the national demand of methane (CH_4) that should be satisfied is not present then, the minimum cost is obtained when no CO_2 is captured. For this reason, the Pareto front starts from the origin of axes. Overall, an intermediate slope is found: there is an increment of 89% in captured CO_2 with an increment of 97.5% in total costs. Also, the variation of the Pareto front on the left side reflects the variation on capture technology. In fact, on the origin of axes, no capture technologies are needed. On the other hand, in the second point where there is the change, VSA, membrane, PSA and monoethanolamine (MEA) absorption are used for the different carbon sources in the utilization section, while MEA absorption is used in the storage section. The Utopia and Nadir points are found. The coordinates of the first one are

at 279 Mton/year of captured CO_2 and at 0 billion€/year of total costs, while the coordinates of the second one are at 0 Mton/year of captured CO_2 and at 403 billion€/year of total costs.

Also for this CCUS supply chain, the Pareto front is built with the augmented ε-constraint method in order to neglect the extreme sections that are not interesting. In this case, the solving time is about 0.03 s with 198 iterations (in a lower time more iterations are done compared to the ε-constraint method suggesting its more efficiency (Azadeh et al., 2017)). The Pareto front so obtained is shown in Figure IX.5: there is a variation of captured CO_2 of 87.73% with a variation of total costs of 99.4%. Then, an average slope is present, and an improvement of one objective function determines a worse condition for the other one.

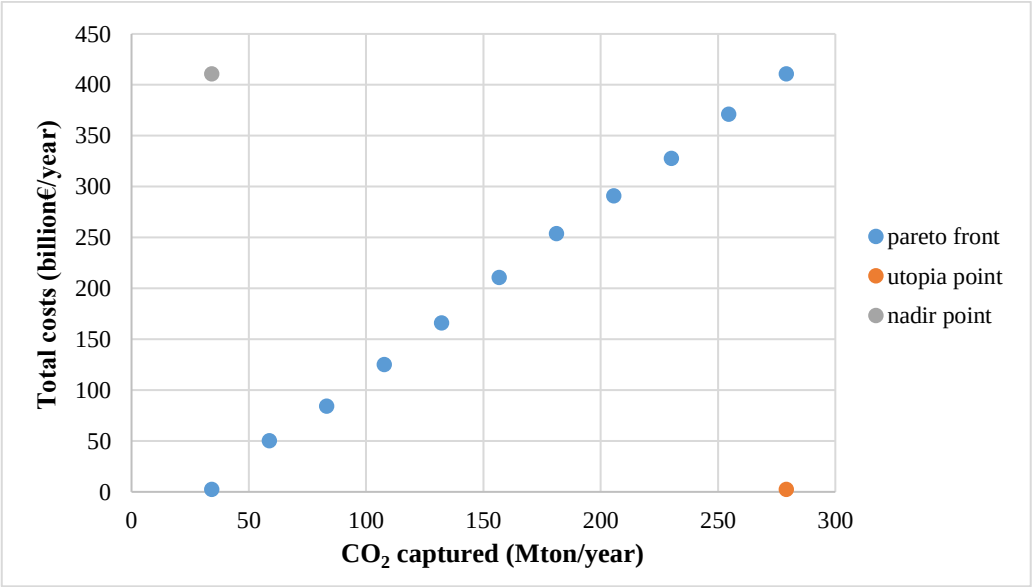

Figure IX.5 Pareto front obtained with the augmented ε-constraint method for the CCUS supply chain of Italy with Adriatic offshore as storage site (Leonzio et al., 2020)

It is possible to notice a variation on the used capture technology between the first point on the left side and the following ones. However, this is not significant for the trend of Pareto front, composed by non dominated solutions. In particular, in the first point of the left side, MEA absorption is used in the utilization section, while PSA is used for the storage section. In other solutions, VSA, MEA absorption, PSA and membrane are the selected capture technologies in the utilization section, while MEA absorption is used in the storage section. The Utopia and Nadir points are considered. The Nadir point is found at 34.2 Mton/year of captured CO_2 and 411 billion€/year of total costs. The Utopia point is found at 279 Mton/year of captured CO_2 and 2.43 billion€/year of total costs.

Among different non dominated points, it is possible to choose one with the shortest distance from the Utopia point, calculated as in the previous case study (Ochoa Bique et al., 2019). This methodology aims

to consider both objective functions. It is found that starting from the left side of the plot, the fifth point has the shortest distance: the captured CO_2 is 132 Mton/year while total costs are 166 billion€/year. The topology of this scenario is shown in Table IX.3.

Table IX.3 Topology of the CCUS supply chain of Italy with Adriatic offshore as storage site for the point on the Pareto front with the shortest distance from the Utopia point (Leonzio et al., 2020)

CO_2 source	**Capture technology**	**CO_2 amount (Mton/year)**
	To storage	
Lombardy	MEA absorption	32.8
	To utilization	
Puglia	MEA absorption	61.8
Sicily	Membrane	17.9
Emilia Romagna	MEA absorption	19.6

The system produces 36.1 Mton/year of CH_4. In the single optimization problem minimizing total costs, it is found that total costs are 73.4 billion€/year while 77 Mton/year of CO_2 emissions are reduced, as reported in Chapter V. Then, in the single optimization problem, lower costs are obtained (a 55.77% of difference is present) but also a lower amount of CO_2 is captured (a difference of 41.73% is obtained) compared to the solution of the bi-optimization problem.

Also in this case, it is possible to choose a scenario on the Pareto front evaluating the net total cost (the difference between total costs and that due to the carbon tax), when considering only one objective function, in this case costs, as shown in Figure IX.6. The decision maker should be interested on a scenario with the minimum net total cost. The first point on the left side is not a realistic one, because at the fixed carbon tax of 80 €/ton, the net total cost is negative. The realistic point with the minimum net total cost is the second one on the left side (45.5 billion€/year): for this scenario the amount of captured CO_2 is of 58.7 Mton/year, while the supply chain costs 50.16 billion€/year. A higher amount of CO_2 at lower costs is captured compared to the single optimization problem of Chapter V. In particular, the difference between the two problems are of 31.7% and 23.8% respectively for the captured CO_2 and total costs. 9.29 Mton/year of CH_4 are produced in the scenario with the minimum net total cost.

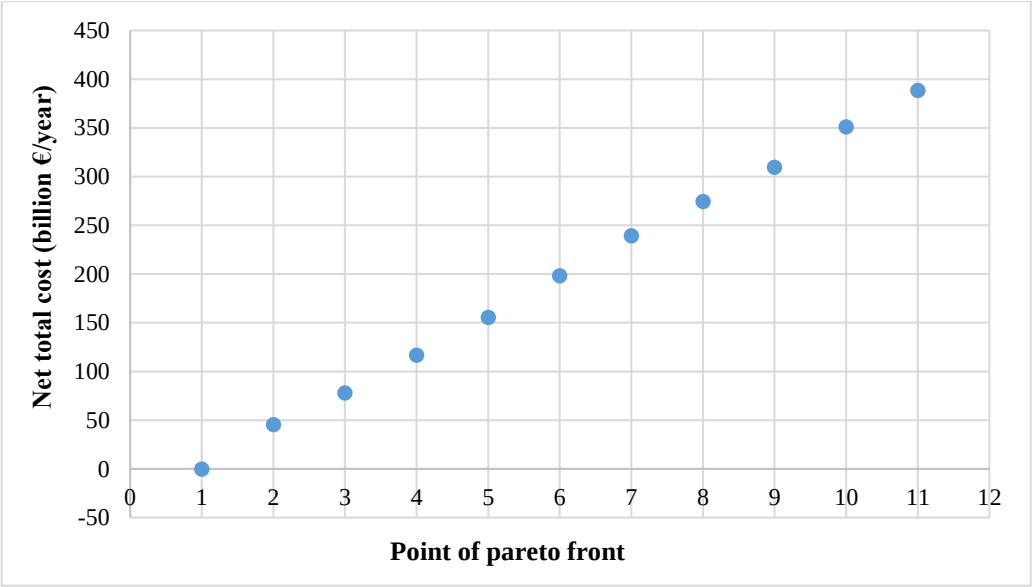

Figure IX.6 Net total cost for the points of Pareto front of the CCUS supply chain of Italy with Adriatic offshore as storage site (Leonzio et al., 2020)

The topology of the CCUS supply chain in this scenario is reported in Table IX.4.

Table IX.4 Topology of the CCUS supply chain of Italy with Adriatic offshore as storage site for the point on the Pareto front with the minimum net total cost (Leonzio et al., 2020)

CO_2 source	**Capture technology**	**CO_2 amount (Mton/year)**
	To storage	
Lombardy	MEA absorption	32.8
	To utilization	
Puglia	MEA absorption	6.26
Emilia Romagna	MEA absorption	19.6

IX.3.3 Results for the CCUS supply chain of the UK

The model is solved in about 0.62 s with 101 iterations, through CPLEX 12.7.1 solver. Figure IX.7 shows the Pareto front for the CCUS supply chain of the UK obtained with the ε-constraint method. The plot is divided in 10 pieces of equal dimensions and starts from the origin of axes because constraints regarding the national demand of CO_2-based products that should be satisfied are not considered.

It is possible to divide the Pareto front in three sections. On the right side, a high slope is present: there is a variation on total costs of 93.8% with a small variation on captured CO_2 equal to 10%. A variation of total

costs is present without significant variations on captured CO_2. On the left side of the Pareto front, overall, a low slope is present and a variation on the captured CO_2 is found without significant variations in total costs. An intermediate slope characterizes the central section of the Pareto front. Here, for a variation on captured CO_2 of 66.7% there is a variation on total costs of 72.8%. Then, as for the supply chains considered previously, in this section a slight improvement of captured CO_2 objective function produces a worse condition for total costs.

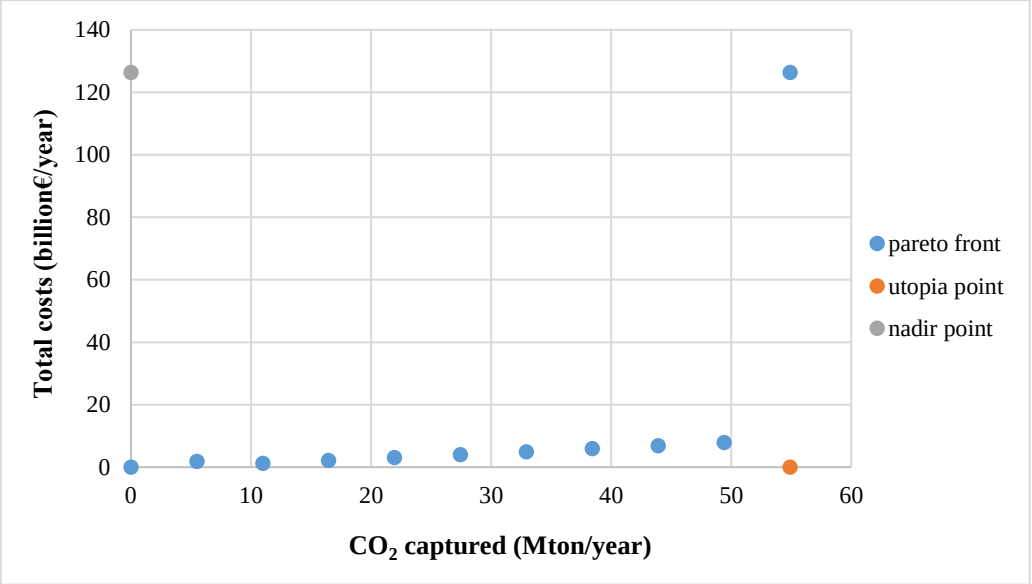

Figure IX.7 Pareto front obtained with the ε-constraint method for the CCUS supply chain of the UK with Bunter Sandstone as storage site (Leonzio et al., 2020)

The nature of the extreme point on the right side is due to a variation on capture technology. In fact, for this scenario, the model suggests to use the WEI VSA for the utilization section for CH_4 production and not to send CO_2 to the storage section. In the preceding points, the PZ absorption is used in the utilization section, while the MEA absorption is used in the storage section.

The Nadir point is found at 0 ton/year of captured CO_2 and at 126 billion€/year of total costs. The Utopia point is found at 54.9 Mton/year of captured CO_2 and at 0 costs.

The augmented ε-constraint method is applied also for this bi-objective optimization problem, in order to avoid the extreme insignificant sections on the Pareto front. The model is solved in about 0.14 s with 101 iterations. Compared to the previous used method, the same iterations are carried out by the augmented ε-constraint method in a lower time, showing its better efficiency (Azadeh et al., 2017). Figure IX.8 shows the obtained plot of Pareto front, divided in 10 pieces of equal dimensions. An average slope is present: the captured CO_2 variation is 78.1% while that of total costs is 92.8%. The two important points, Nadir and

Utopia, are found. The Nadir point is found at 12 Mton/year of captured CO_2 and at 9.6 billion€/year of total costs. The Utopia point is found at 54.9 Mton/year of captured CO_2 and at 0.687 billion€/year of total costs. Generally, the PZ absorption technology is used in the utilization section for all considered cases to capture CO_2.

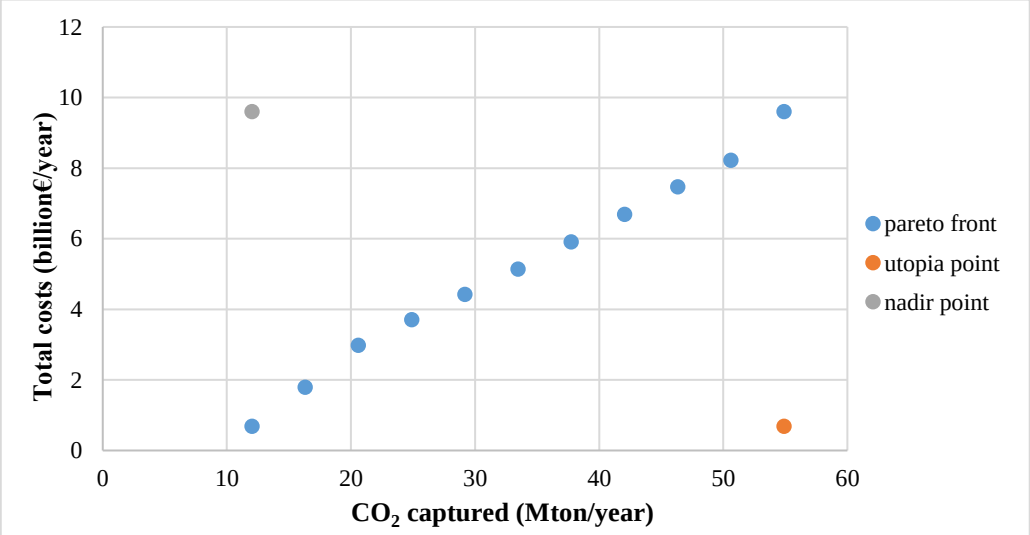

Figure IX.8 Pareto front obtained with the augmented ε-constraint method for the CCUS supply chain of the UK with Bunter Sandstone as storage site (Leonzio et al., 2020)

All points on the Pareto front are valid solutions, however, to choose one among them, the previous methods are used. At first, the distances from the Utopia point are evaluated considering the normalized values of total costs and captured CO_2 and using the Pythagorean theorem: the point with the minimum distance is the sixth from the left side. For this scenario, the amount of captured CO_2 is 33.5 Mton/year while total costs are 5.14 billion€/year. Table IX.5 shows the topology of the supply chain in this condition. The supply chain produces 29.8 Mton/year of calcium carbonate.

Table IX.5 Topology of the CCUS supply chain of the UK with Bunter Sandstone as storage site for the point on the Pareto front with the shortest distance from the Utopia point (Leonzio et al., 2020)

CO_2 source	**CO_2 capture technology**	**CO_2 amount (Mton/year)**
	To storage	
Leeds	MEA absorption	0.4
	To utilization	
Leeds	PZ absorption	15.8
Cardiff	PZ absorption	3.3
Manchester	PZ absorption	13.95

In the single optimization problem minimizing only total costs, as in Chapter VI, it is found that total costs are of 1.04 billion€/year while 6.4 Mton/year of CO_2 are captured. Then, in the bi-optimization problem, a higher amount of CO_2 is captured (a difference of 80.9% is present) at higher costs (the difference is of 79.8%).

The selection of one point on the Pareto front can be done by a decision maker putting more attention on costs. Then, as for the previous CCUS supply chains, the net total cost is evaluated for each scenario defined by the Pareto front, as shown in Figure IX.9. Also in this case, the first point on the left side is not realistic because a negative net total cost is present. Then the second point from the left side can be selected due to the lowest net total cost (0.5 billion€/year), calculated as the difference between total costs and the income obtained with carbon tax, set at 80 €/ton.

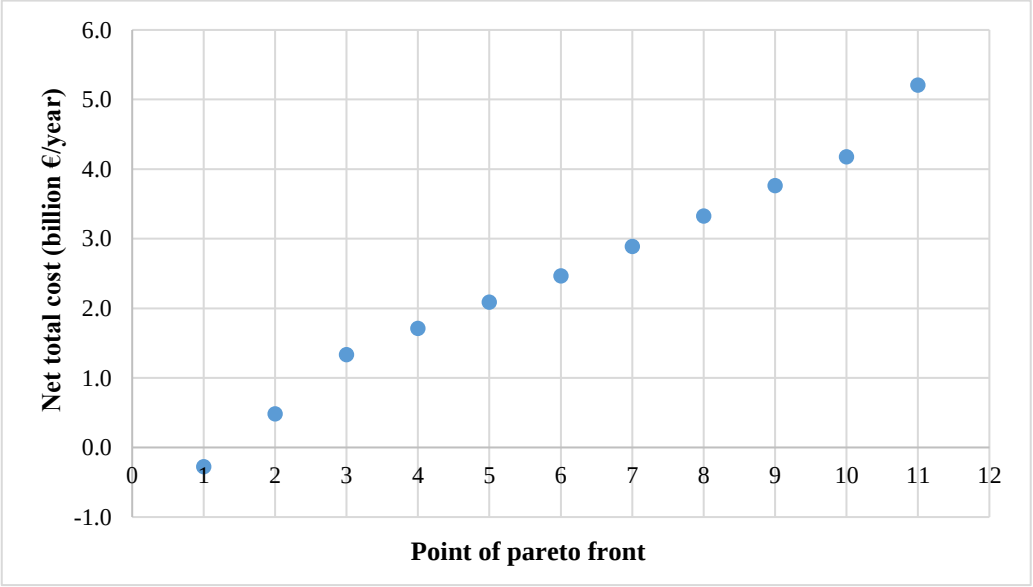

Figure IX.9 Net total cost for the points of Pareto front of the CCUS supply chain of the UK with Bunter Sandstone as storage site (Leonzio et al., 2020)

For this scenario, the topology of CCUS supply chain is reported in Table IX.6. 14.3 Mton/year of calcium carbonate are produced from the captured CO_2. 16.3 Mton/year of CO_2 are captured while the carbon supply chain costs 1.79 billion€/year. Compared to the single optimization problem, a higher amount of CO_2 is captured (a difference of 60.8%) in the bi-optimization problem, however with higher costs (a difference of 41.9%).

Table IX.6 Topology of the CCUS supply chain of the UK with Bunter Sandstone as storage site for the point on the Pareto front with the minimum net total cost (Leonzio et al., 2020)

CO_2 source	**CO_2 capture technology**	**CO_2 amount (Mton/year)**
	To storage	
Leeds	MEA absorption	0.4
	To utilization	
Leeds	PZ absorption	15.8
Manchester	PZ absorption	0.11

IV.3.4 Comparison of the different CCUS supply chains

It is interesting to compare the different CCUS supply chains in terms of Pareto front. Figure IX.11 shows a comparison between the different normalized Pareto fronts, obtained with the augmented ε-constraint method for the CCUS supply chain of Italy, Germany and the UK. Overall, the CCUS supply chain of Germany producing different products as methanol, concrete, wheat, lignin, polyurethane, calcium carbonate and urea has the highest values of total costs and captured CO_2. The lowest costs are obtained in the CCUS supply chain of the UK, while average values of total costs are for the CCUS supply chain of Italy. The same considerations are valid for the other objective function, related to the captured CO_2.

In all cases, for the three Pareto fronts the linear trend suggests that there is an increase of total costs and a simultaneous increase of captured CO_2. This variation is lower for the CCUS supply chain of Germany, where the slope is estimated to be the slowest. On the other hand, the CCUS supply chain of Italy has a highest slope and then a higher variation of costs.

However, for the CCUS supply chain of Germany the Pareto optimal front defines a region of feasible objective space that is extended lower than that related to the other two CCUS supply chains. This can be explained by the additional constraints related to the national demand of different products that should be satisfied and that are present only in the model of CCUS supply chain for Germany.

Although a lower extended objective space, the CCUS supply chain of Germany is the closest to the Utopia conditions. In fact, the minimum distance between the chosen point on the Pareto front and the respective ideal point (Utopia) is of 0.588, 0.607 and 0.660, respectively for the system of Germany, the UK and Italy. A better trade-off between the two objective functions is then achieved in the model describing the CCUS supply chain of Germany, even if the system has the highest costs.

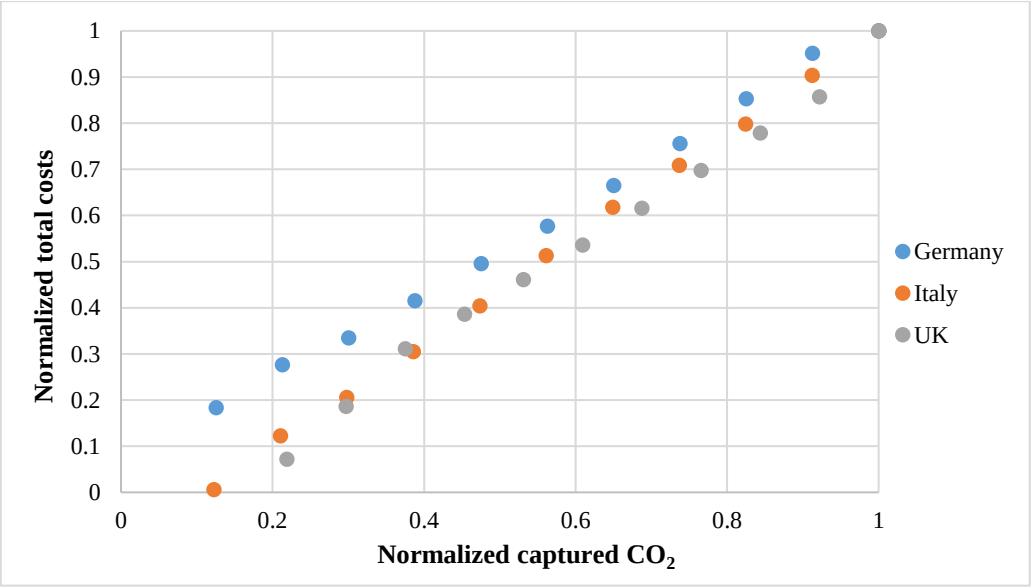

Figure IX.11 Normalized Pareto fronts obtained with the augmented ε-constraint method for the CCUS supply chain of Italy, Germany and the UK, respectively (Leonzio et al., 2020)

IX.4 Conclusions

In this Chapter, a deterministic bi-objective optimization model is suggested for the CCUS supply chains of Germany, Italy and the UK, treated before as a single optimization problem, minimizing total costs. Now these problems are reformulated as MILP models with the aim to minimize total costs and maximize the amount of captured CO_2 simultaneously. Results show the best efficiency for the augmented ε-constraint method due to a lower resolution time, compared to the traditional ε-constraint method. A trade-off among the two conflicting objective functions in the same framework is found through the Pareto front and two guides for a decision maker choosing a single scenario are shown. The first one suggests a scenario with the lowest net total cost, then setting more importance to the economic objective function. The second one suggests a scenario with the shortest distance from the Utopia point, providing importance to both objective functions. Regarding this last method, it is found that the CCUS supply chain of Germany is closer to the ideal conditions, compared to other carbon systems, even if higher costs are computed in this case.

References

Attia, A.M., Ghaithan, A.M., Duffuaa, S.O., 2019. A multi-objective optimization model for tactical planning of upstream oil & gas supply chains, Computers and Chemical Engineering 128 216–227.

Avci, M.G., Selim, H., 2017. A Multi-objective, simulation-based optimization framework for supply chains with premium freights, Expert Systems With Applications 67, 95–106.

Azadeh, A., Shafiee, F., Yazdanparast, R., Heydari, J., Fathabad, A.M., 2017. Evolutionary multi-objective optimization of environmental indicators of integrated crude oil supply chain under uncertainty, Journal of Cleaner Production 152 295-311.

Balaman, S.Y., Matopoulos, A., Wright, D.G., Scott, J. 2018. Integrated optimization of sustainable supply chains and transportation networks for multi technology bio-based production: A decision support system based on fuzzy ε-constraint method, Journal of Cleaner Production 172, 2594-2617

Brisset, S., Gillon, F., Approaches for multi-objective optimization in the eco-design of electric systems, Eco-friendly Innovations in Electricity Transmission and Distribution Networks, 2015.

Cambero, C. Sowlati, T., 2016. Incorporating social benefits in multi-objective optimization of forestbased bioenergy and biofuel supply chains, Applied Energy 178 721–735.

Cohon. J.L., Multiobjective Programming and Planning. Academic Press, 2008.

Cucek L., Varbanov P.S., Klemeš J.J., Kravanja Z. 2012. Total footprints-based multicriteria optimisation of regional biomass energy supply chains. Energy 44 (1) 135–45.

Ghaithan, A.M., Attia, A., Duffuaa, S.O., 2017. Multi-objective optimization model for a downstream oil and gas supply chain, Applied Mathematical Modelling 52 689–708

Grossmann, I.E., Guillen-Gosalbez, G., 2010. Scope for the application of mathematical programming techniques in the synthesis and planning of sustainable processes. Comput. Chem. Eng. 34 1365-1376.

Haimes, Y., Lasdon, L., Wismer, D., 1971. On a Bicriterion Formulation of the Problems of Integrated System Identification and System Optimization. IEEE Trans. Syst. Man Cybern. 1 296–297.

Khorram, E., Zarepisheh, M., Ghaznavi-ghosoni, B.A., 2010. Sensitivity analysis on the priority of the objective functions in lexicographic multiple objective linear programs. Eur. J. Oper. Res. 207 1162‑1168.

Leonzio, G., P.U. Foscolo, E. Zondervan, 2020. Multi-objective optimization of CCUS supply chains for the European countries with higher carbon dioxide emissions. To be Submitted.

Limleamthong, P., Guillen-Gosalbez, G., 2017. Rigorous analysis of Pareto fronts in sustainability studies based on bilevel optimization: Application to the redesign of the UK electricity mix, Journal of Cleaner Production 164 1602-1613.

Liu, S., Papageorgiou, L.G., 2013. Multiobjective optimisation of production, distribution and capacity planning of global supply chains in the process industry. Omega, Management science and environmental issues 41 9 369–382.

Mavrotas, 2009. G. Effective implementation of the e-constraint method in Multi-Objective Mathematical Programming problems, Applied Mathematics and Computation 213 455–465

Mele, F.D., Kostin, A.M., Guill En-Gos Albez, G., Jim Enez, L., 2011. Multiobjective model for more sustainable Fuel supply chains. A case study of the sugar cane industry in Argentina. Ind. Eng. Chem. Res. 50 4939-4958.

Miettinen, K., 1999. Nonlinear Multiobjective Optimization. USA: Kluwer, Boston, MA.

Mota, B., Gomes, M.I., Carvalho, A., Barbosa-Povoa, A.P. 2015. Towards supply chain sustainability: economic, environmental and social design and planning. J Clean Prod 105 14–27.

Ochoa Bique, A., Maia, L.K.K., La Mantia, F., Manca, D., Zondervan, E., 2019. Balancing costs, safety and CO2 emissions in the design of hydrogen supply chains, Computers and Chemical Engineering 129 106493

Ochoa Robles, M.J., 2018. Multi-objective optimization strategies for design and deployment of hydrogen supply chains, PhD thesis, Institut National Polytechnique de Toulouse (Toulouse INP).

Ogumerem, G.S., Kim, C., Kesisoglou, I., Diangelakis, N.A., Pistikopoulos, E.N., 2018. A multi-objective optimization for the design and operation of a hydrogen network for transportation fuel, Chemical Engineering Research and Design 131 279–292

Pinto-Varela, T., Barbosa-Povoa, A.P.F.D., Novais, A.Q., 2011. Bi-objective optimization approach to the design and planning of supply chains: economic versus environmental performances. Comput. Chem. Eng. 35 1454-1468.

Razm, S., Nickel, S., Sahebi, H., 2019. A multi-objective mathematical model to redesign of global sustainable bioenergy supply network, Computers and Chemical Engineering 128 1–20

Resat, H.G., Unsal, B., 2019. A novel multi-objective optimization approach for sustainable supply chain: A case study in packaging industry, Sustainable Production and Consumption 20 29–39

Reza Norouzi, M., Ahmadi, A., Esmaeel Nezhad, A., Ghaedi, A., 2014. Mixed integer programming of multi-objective security constrained hydro/thermal unit commitment. Renew. Sustain. Energy Rev. 29 (0) 911-923.

Rezvani, A., Gandomkar, M., Izadbakhsh, M., Ahmadi, A., 2015. Environmental/economic scheduling of a micro-grid with renewable energy resources. J. Clean. Prod. 87 (0) 216-226.

Roghanian, E., Cheraghalipour, A., 2019. Addressing a set of meta-heuristics to solve a multi-objective model for closed-loop citrus supply chain considering CO2 emissions, Journal of Cleaner Production 239 118081.

Santibañez-Aguilar, J.E., González-Campos, J.B., Ponce-Ortega, J., Serna-González, M., El-Halwagi, M., 2011. Optimal planning of a biomass conversion system considering economic and environmental aspects. Ind Eng Chem Res 50 (14) 8558–70

van Elzakker, M.A.H., Maia, L.K.K., Grossmann, I.E., Zondervan, E., 2017. Optimizing environmental and economic impacts in supply chains in the FMCG industry, Sustainable production and consumption, 11 68–79.

You, F., Tao, L., Graziano, D.J., Snyder, S.W., 2012. Optimal design of sustainable cellulosic biofuel supply chains: multiobjective optimization coupled with life cycle assessment and input-output analysis. AIChE J. 58 1157-1180.

Yue D., You F., Integration of geological sequestration and microalgae biofixation supply chains for better greenhouse gas emission abatement, 2015. Chemical Engineering Transactions, 45 487-492.

Nomenclature

Abbreviations

AIMMS = advanced interactive multidimensional modeling system

CCUS = carbon capture utilization and storage

MEA = monoethanolamine

MOO = multiple objective optimization

PSA = pressure swing adsorption

PZ = piperazine

VSA = vacuum swing adsorption

Chapter X

Stochastic optimization of CCUS supply chains

In this Chapter, a two stage stochastic mixed integer linear programming model is developed for the best carbon capture utilization and storage supply chain in Italy, Germany and the UK, defined in previous Chapters. Few works are present in the literature about this topic, then this research wants to overcome this limitation, considering carbon supply chains producing different products. The objective of these proposed models is to minimize the expected total costs, under the uncertainties of the production cost of carbon dioxide based compounds, achieving at the same time the minimum target for carbon dioxide emissions reduction. The optimal design of these supply chains is then suggested. The expected total costs for the carbon capture utilization and storage supply chain of Italy, Germany and the UK are respectively 77.3 billion€/year, 98.0 billion€/year, 1.05 billion€/year. A comparison with the respective deterministic model is considered through the evaluation of the expected value of perfect information and the value of stochastic solution. Results show that the uncertain production cost in the stochastic model does not have a significant effect on the results, then there are few advantages on solving the stochastic model instead of the deterministic one, when considering the fluctuation of this parameter.

X.1 Introduction

Carbon capture utilization and storage (CCUS) supply chains developed in previous Chapters are presented as deterministic models, without considering the uncertainties of parameters. However, different factors influence the planning of carbon supply chains. Regarding the storage site, uncertainties are related to the permeability, capacity and porosity of reservoirs (Lee et al., 2017; Keating et al., 2011). In addition to these, uncertainties are present inside a supply chain due to the fluctuation of carbon dioxide (CO_2) sources, variability of construction and operation costs and unpredictable events (Han et al., 2012; Zhang et al., 2014; Malaeb et al., 2019). Also, external factors, such as carbon policy, technology, engineering performance and market forces can influence the design of these systems (Middleton and Yaw, 2018). There are different ways to consider the uncertainties of a supply chain: chance constrained programming (Liu and Iwamura, 1998), robust optimization (Mulvey et al., 1995), fuzzy mathematical programming (Zimmermann, 2010) and the most popular, the two stage stochastic model (Govindan et al., 2017).

In the Introduction of this Thesis, it is mentioned that stochastic models are mainly applied to carbon capture and storage (CCS) supply chains. Few works are considering a stochastic model for CCUS supply chains and specifically the fluctuation of production costs of carbon-dioxide-based species: there is a clear lack of these models applied to CCUS supply chains.

The aim of this Chapter is to overcome this limitation, considering CCUS supply chains producing a variety of CO_2-based products: a two stage stochastic model is used to design the best CCUS supply chains that were developed before for Germany, Italy and the UK, respectively in Chapter IV, V and VI. In particular, the CCUS supply chain of Germany produces methanol (CH_3OH), urea, wheat, concrete by curing and red mud, calcium carbonate, polyurethane and lignin. The CCUS supply chain of Italy produces methane (CH_4)

and has the storage site in the offshore Adriatic sea, while the considered CCUS supply chain for the UK produces calcium carbonate and has the Bunter Sandstone as storage site. The expected total costs are minimized in order to optimize the systems, finding the best topology.

In the analyses of this Chapter, the production costs of different CO_2-based products are characterized by uncertainty and then are considered as stochastic parameters with a discrete normal probability distribution. The results are compared with the respective deterministic one in order to evaluate the influence of uncertainties on the design of carbon systems: the expected value of perfect information (EVPI) and the value of stochastic solution (VSS) are evaluated.

X.2 Model development

A two stage stochastic programming model for the design of CCUS supply chains is presented in this section. Advanced Interactive Multidimensional Modeling (AIMMS) software is used to solve this stochastic Mixed Integer Linear Programming (MILP) model.

X.2.1 Problem statement

For each CCUS supply chain, the same assumptions made in the respective previous Chapters (IV, V and VI) are taken into account for this new model. Moreover, it is assumed for all frameworks that stochastic parameters, the production costs of different CO_2-based products, have a normal discrete distribution of probability, with mean value defined by the previous deterministic treatment (stationary conditions) and standard deviation of ±20% with respect to the stationary condition. In addition, different discrete scenarios are defined by means of the stochastic parameters (specific production costs of each compound and its respective probability).

Under the uncertainty, given the information already presented previously, the best connection between each element of the supply chain and the amount of treated CO_2 and produced compounds are found, through the minimization of the objective function, expressing the expected total costs.

XI.2.2 CCUS supply chain model

X.2.2.1 Sets

The same indexes used in the previous models (Chapter IV for the CCUS of Germany, Chapter V for the CCUS of Italy and Chapter VI for the CCUS of the UK) are considered here for each supply chain. The index “s” is added, to identify a particular scenario of the stochastic problem, with a respective probability, as shown below.

X.2.2.2 Parameter

The same parameters defined in each respective previous Chapter (IV, V and VI) are considered here for the stochastic model.

X.2.2.3 Variables

According to the stochastic formulation, decision variables are classified into first stage (here-and-now) variables and second stage (wait-and-see) variables (Zhou et al., 2019). First stage variables are design variables then, these are insensitive to uncertainty. The design variables should be determined before uncertainty is taken into account. In the considered models, these first stage variables are the binary variables $X_{i,j,k,s}$ to choose the storage site for all scenarios and $Y_{i,j,k,s}$ to choose the capture technology in all scenarios: i.e. variables X and Y do not change as scenarios mutate, at this stage. Second stage variables are operation variables, defined after having known uncertainty. These can compensate and correct the decisions taken at the first stage, in order to have the best compromise. In the developed stochastic models, second stage variables define the amount of captured CO_2 that is sent to the utilization and storage section. Then, these are the continuous variables. A common second stage variable for all carbon supply chains is $FR_{i,j,k,s}$ that defines the amount of captured CO_2 sent to the storage section for each scenario. For the CCUS supply chain of Italy, $MR_{i,j,k,s}$ is used to define the amount of CO_2 sent to the power to gas system for each scenario. For the CCUS supply chain of Germany, $Utilization_{i,j,k,s}$ defines the amount of captured CO_2 sent to the utilization section for each scenario; in particular, $Concrete_{i,j,c,s}$ defines the amount of CO_2 captured for concrete production in each scenario; $Wheat_{i,j,w,s}$ defines the amount of CO_2 captured for wheat production in each scenario; $Lignin_{,I,j,l,s}$ defines the amount of CO_2 captured for lignin production in each scenario; $Polyurethane_{i,j,p,s}$ defines the amount of CO_2 captured for polyurethane production in each scenario; $Calcium\ carbonate_{i,j,cc,s}$ defines the amount of CO_2 captured for calcium carbonate production in each scenario; $Urea_{i,j,u,s}$ defines the amount of CO_2 captured for urea production in each scenario; $Methanol_{i,j,m,s}$ defines the amount of CO_2 captured for CH_3OH production in each scenario; $Concrete\ by\ red\ mud_{i,j,cr,s}$ defines the amount of CO_2 captured for concrete by red mud production in each scenario. For the CCUS supply chain of the UK, as continuous second stage variables are defined: $Utilization_{i,j,k,s}$ for the amount of captured CO_2 sent to the utilization section in each scenario, $Methanol_{i,j,m,s}$ for the amount CO_2 sent to methanol production in each scenario, $Methane_{i,j,g,s}$ for the amount of CO_2 sent to CH_4 production in each scenario, $Polyurethane_{i,j,p,}$ for the amount of CO_2 sent to polyurethane production in each scenario, $Tomato_{i,j,t,s}$ for the amount of CO_2 sent to tomato production in each scenario, $Concrete_{i,j,c,s}$ for the amount of CO_2 sent to concrete production in each scenario and to $CalciumCarbonate_{i,j,d,s}$ for the amount of CO_2 sent to calcium carbonate production in each scenario.

X.2.2.4 Constraint

For the considered supply chains, similar constraints are taken into account. The captured CO_2 can not be divided among multiple storage sites and also the one to one coupling principle should be considered for the storage site, then the following constraint is taken into consideration (see Eq. X.1):

$$\sum_{(j,k)\in(J,K)} X_{i,j,k,s} \leq 1 \qquad \forall\,(i,s)\ \in (I,S) \qquad (X.1)$$

where $X_{i,j,k,s}$ is the binary variable defined above. The storage site has a maximum capacity to store emissions, as expressed in the following relation (see Eq. X.2):

$$\sum_{(i,j)\in(I,J)} CS_i \cdot FR_{i,j,k,s} \leq \frac{C_k^{max}}{TH} \qquad \forall\,(k,s)\ \in (K,S) \qquad (X.2)$$

in which CS_i is the total CO_2 emission from each source 'i', C_k^{max} is the maximum storage capacity of the storage site 'k', TH is the time horizon of the supply chain in years, and $FR_{i,j,k,s}$ is defined above.

The supply chain should achieve at least the minimum target for CO_2 emissions reduction, as shown in the following constraint (see Eq. X.3):

$$Total\ captured\ CO_{2_s} \geq CR^{min} \qquad \forall\, s\ \in S \qquad (X.3)$$

where CR^{min} is the minimum target of CO_2 emissions reduction while the total captured CO_2 in each scenario is defined considering CO_2 emissions and its fraction sent to the utilization and storage sections (in particular the total captured CO_2 is expressed as $\sum_{i,j,k} CS_i \cdot FR_{i,j,k,s} + CS_i \cdot Utilization_{i,j,k,s}$ for the CCUS supply chain of Germany and the UK and as $\sum_{i,j,k} CS_i \cdot FR_{i,j,k,s} + CS_i \cdot MR_{i,j,k,s}$ for the CCUS supply chain of Italy).

From a selected source, no more than 90% of CO_2 is captured, as defined in the following constraint (see Eq. X.4):

$$Fraction\ of\ captured\ CO_2\ in\ a\ source_s \leq 0.9 \qquad \forall\, s\ \in S \qquad (X.4)$$

where the fraction of captured carbon dioxide from a specific source i, is expressed as $\sum_{i,j,k} FR_{i,j,k,s} + Utilization_{i,j,k,s}$ for the supply chain of Germany and the UK, and $\sum_{i,j,k} FR_{i,j,k,s} + MR_{j,k,s}$ for the CCUS supply chain of Italy.

In order to capture CO_2 with a purity equal to or higher than 90%, its content in the flue gas streams should be constrained between a minimum (XL_j) and maximum (XH_j) level (see Eq. X.5):

$$\sum_{(k)\in(K)} (XH_j - XS_i) \cdot (XS_i - XL_j) \cdot X_{i,j,k,s} \geq 0 \qquad \forall\,(i,j,s)\ \in (I,J,S) \qquad (X.5)$$

where XS_i is CO_2 composition in flue gas from source i, XL_j, is the lowest limit for CO_2 composition processed by the capture plant j, XH_j is the highest limit for CO_2 composition processed by the capture plant

j and $X_{i,j,k,s}$ is defined above. This relation is valid for the storage site, while different or higher purity is required in the utilization site and this needs to be achieved in each respective site.

Only one capture technology/material should be selected for each CO_2 source, as defined by the following constraint (see Eq. X.6):

$$\sum_{(j,k)\in(J,K)} Y_{i,j,k,s} \leq 1 \quad \forall\ (i,s)\ \in (I,S) \qquad (X.6)$$

where $Y_{i,j,k,s}$ is defined above. For the CCUS supply chain of Germany, it is supposed that the produced amount of different products should be equal or higher than the national demand, as defined in this relation (see Eq. X.7):

$$Produced\ amount\ of\ a\ product_s \geq National\ demand \qquad \forall\ s\ \in S \qquad (X.7)$$

This constraint is not considered for the CCUS supply chain of Italy and the UK.

Overall, as done in the previous deterministic treatment, the developed mathematical model is made linear by using the glover linearization (see Chapter III), expressed by the following constraints (see Eqs. X.8-X.10):

$$0 \cdot Y_{i,j,k,s}\ \leq Utilization_{i,j,k,s} \leq 0.9 \cdot Y_{i,j,k,s} \qquad \forall\ (i,j,k,s)\ \in (I,J,K,S) \qquad (X.8)$$

$$0 \cdot Y_{i,j,k,s}\ \leq MR_{i,j,k,s} \leq 0.9 \cdot Y_{i,j,k,s} \qquad \forall\ (i,j,k,s)\ \in (I,J,K,S) \qquad (X.9)$$

$$0 \cdot X_{i,j,k,s}\ \leq FR_{i,j,k,s} \leq 0.9 \cdot X_{i,j,k,s} \qquad \forall\ (i,j,k,s)\ \in (I,J,K,S) \qquad (X.10)$$

with the continuous ($Utilization_{i,j,k,s}$ and $MR_{i,j,k,s}$) and binary ($X_{i,j,k,s}$ and $Y_{i,j,k,s}$) variables defined above, while 0.9 is considered because at least 90% of CO_2 should be captured from a selected source.

For the CCUS supply chains of the UK and Germany, CO_2 sent to the utilization section is distributed to the different production sites according to the following material balances (see Eqs. X.11-X.12):

$$\begin{aligned} &Utilization_{i,j,k,s} \\ &\quad = Concrete_{i,j,c,s} \cdot n_{sites,c,s} + Wheat_{i,j,w,s} \cdot n_{sites,w,s} + Lignin_{i,j,l,s} \cdot n_{sites,l,s} \\ &\quad + Polyurethane_{i,j,p,s} \cdot n_{sites,p,s} + CalciumCarbonate_{i,j,cc,s} \cdot n_{sites,cc,s} + Urea_{i,j,u,s} \\ &\quad \cdot n_{sites,u,s} + Methanol_{i,j,m,s} \cdot n_{sites,m,s} + ConcreteByRedMud_{i,j,cr,s} \\ &\quad \cdot n_{sites,cr,s} \qquad \forall\ (i,j,k,c,w,l,p,cc,u,m,cr,s) \\ &\quad \in (I,J,K,C,W,L,P,CC,U,M,CR,S) \qquad (X.11) \end{aligned}$$

where $Utilization_{i,j,k,s}$, $Concrete_{i,j,c,s}$, $Wheat_{i,j,w,s}$, $Lignin_{ij,l,s}$, $Polyurethane_{i,j,p,s}$, Calcium $carbonate_{i,j,cc,s}$, $Urea_{i,j,u,s}$, $Methanol_{i,j,m,s}$ and Concrete by red $mud_{i,j,cr,s}$ are the continuous variables defined above, $n_{sites,c,s}$, $n_{sites,w,s}$, $n_{sites,l,s}$, $n_{sites,p,s}$, $n_{sites,cc,s}$, $n_{sites,u,s}$, $n_{sites,m,s}$, $n_{sites,cr,s}$ are the number of sites for each respective product.

$$Utilization_{i,j,k,s} = Concrete_{i,j,c,s} \cdot n_{sites,c,s} + Tomato_{i,j,t,s} \cdot n_{sites,t,s} + Polyurethane_{i,j,p,s} \cdot n_{sites,p,s} + CalciumCarbonate_{i,j,d,s} \cdot n_{sites,d,s} + Methanol_{i,j,m,s} \cdot n_{sites,m,s} + Methane_{i,j,g,s} \cdot n_{sites,g,s} \quad \forall (i,j,k,c,t,p,d,m,g,s) \in (I,J,K,C,T,P,D,M,G,S) \qquad (X.12)$$

with $Utilization_{i,j,k,s}$, $Methanol_{i,j,m,s}$, $Methane_{i,j,g,s}$, $Polyurethane_{i,j,p,s}$, $Tomato_{i,j,t,s}$, $Concrete_{i,j,c,s}$ and $CalciumCarbonate_{i,j,d,s}$ are the second stage variables defined above and $n_{sites,c,s}$, $n_{sites,t,s}$, $n_{sites,p,s}$, $n_{sites,d,s}$, $n_{sites,m,s}$, $n_{sites,g,s}$ are the number of sites for each respective product.

In addition to the above constraints, non-anticipativity (state of art) constraints are assumed for the first stage variables: their value is the same for all scenarios (Escudero et al., 2010; Messina and Mitra, 1997). With these constraints, it is assumed that the decision should depend only on information available at the time of the decision and not on future observations (Mitra et al., 2016; Bakker et al., 2019).

X.2.2.5 Equations

Equations are defined for CO_2 capture and compression costs, CO_2 transportation costs and CO_2 storage costs, evaluated for each scenario. The same equations defined in Chapter IV, V and VI are used.

X.2.2.6 Objective function

Considering a deterministic equivalent problem for the two stage stochastic model, the objective function is defined by the following relation (Mitra et al., 2016; Yang et al., 2017; Bakker et al., 2019) (see Eq. X.13):

$$\phi = \sum_{s} probability_s \cdot Total\ costs_s \qquad (X.13)$$

with the value of probability for each scenario and the value of total costs of framework in each scenario. Total costs of each scenario are multiplied by the probability of occurrence of that scenario (Yeh et al., 2015). The probability is obtained considering that random production costs have a discrete normal probability distribution with a finite number of realizations, sampled randomly using the Monte Carlo method (Messina and Mitra, 1997; Zhang et al., 2019; Trochu et al., 2019). To this aim, RiskAMP in Excel is used. Total costs are provided as the sum of CO_2 capture and compression costs, CO_2 transportation costs, CO_2 storage costs and production costs of different CO_2-based products. This objective function is minimized in order to provide an expected annual value of total costs and to design the supply chains under uncertainties. The optimal level of various decision variables that minimizes the expected total costs is suggested for the stochastic mixed integer linear programming model.

X.2.3 Case study

The case study of Italy has been already discussed in Chapter V. As mentioned before, CH_4 production cost is the stochastic parameter. In the stationary condition CH_4 production cost is of 300 €/MWh, while a standard deviation of ±20% of this expected value is considered under uncertainty. With this assumption, the discrete normal distribution of the stochastic parameter, related to CH_4 production cost, is obtained through the Monte Carlo sampling technique (Zhang et al., 2019), as shown in Figure X.1: 21 scenarios with the respective probability are considered.

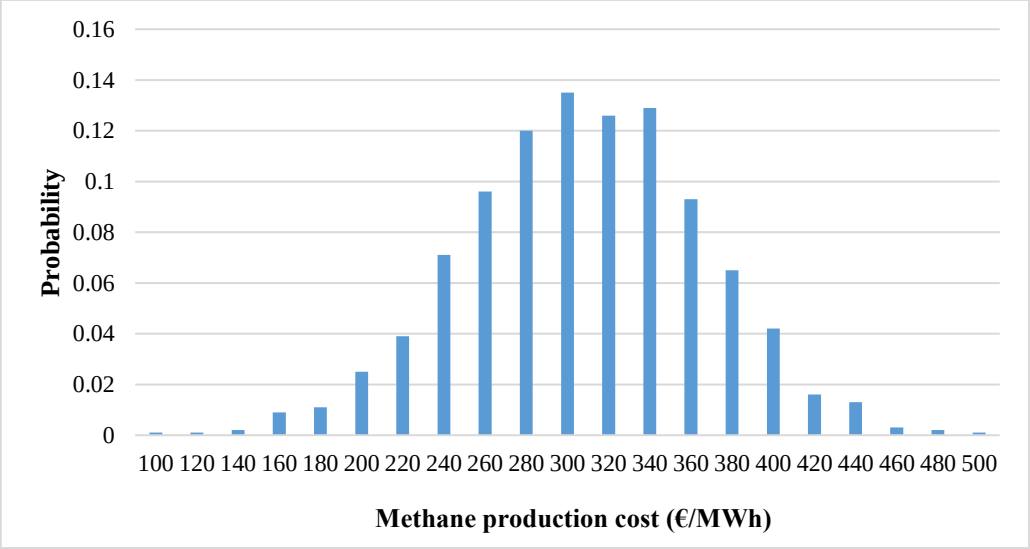

Figure X.16 Discrete normal distribution for the stochastic parameter as CH_4 production cost for the CCUS supply chain of Italy with the Adriatic offshore as storage site (Leonzio et al., 2020)

The case study for the CCUS supply chain of the UK has been discussed in Chapter VI. Also in this case, the production costs of different products are the stochastic parameters. The production costs of CH_3OH, CH_4, polyurethane, tomato, concrete and calcium carbonate are respectively of 608 €/ton, 300 €/MWh, 1349 €/ton, 0.85 €/kg, 21.8 €/ton, 65.2 €/ton. However, an uncertainty with standard deviation of ±20% with respect to the expected values is considered for each production cost, obtaining the discrete normal distribution, as shown in Figure X.2.

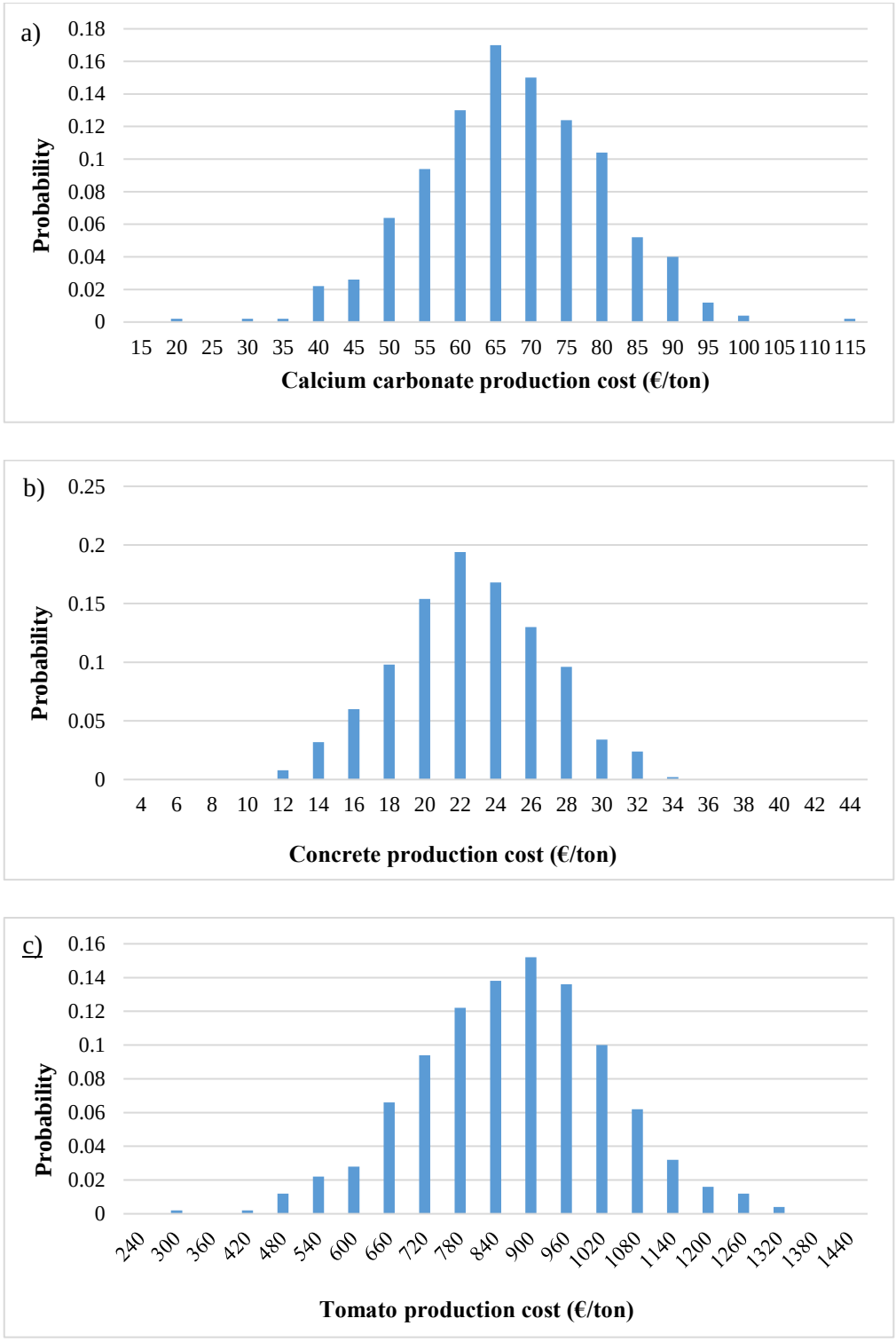

Figure X.17 (Following)

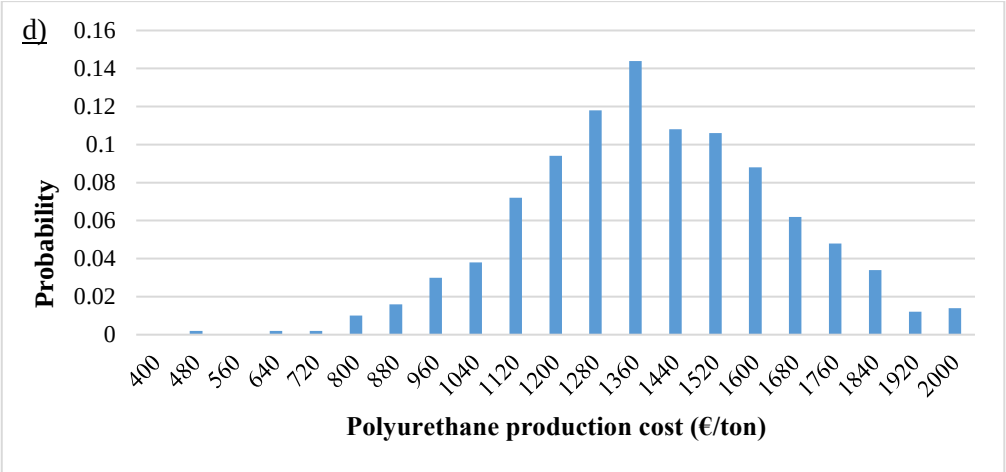

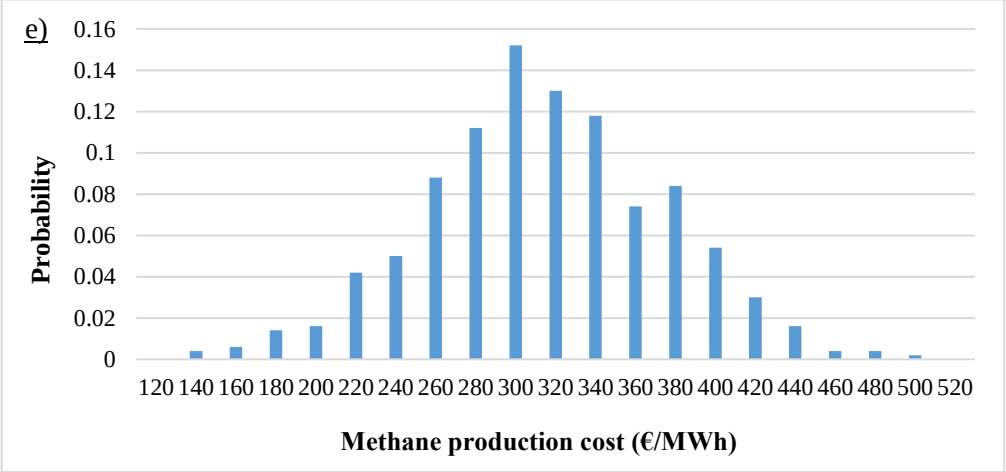

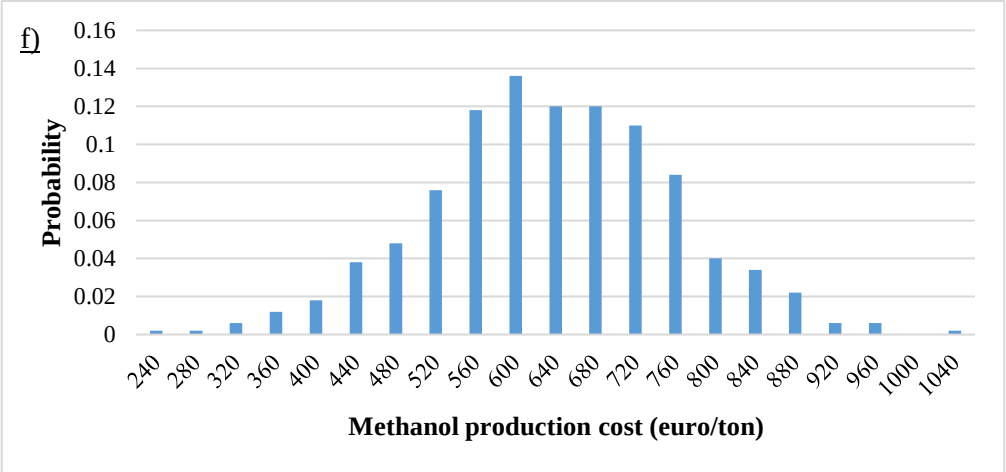

Figure X.2 Discrete normal distribution for the stochastic parameter: a) calcium carbonate production cost; b) concrete production cost; c) tomato production cost; d) polyurethane production costs; e) CH_4 production costs; f) CH_3OH production costs for the CCUS supply chain of the UK with the Bunter Sandstone as storage site

The Monte Carlo sampling technique is used to obtain the discrete normal distribution of production cost for each compound. Also in this case, 21 scenarios are considered. To evaluate the overall probability for each scenario, the product of each probability for each compound is considered, according to the probability composed of independent, compatible events.

The case study for the CCUS supply chain of Germany has been discussed in Chapter IV. The production cost of different CO_2-based products is the stochastic parameter. The production cost of concrete, wheat, lignin, polyurethane, calcium carbonate, urea, methanol, concrete by red mud are respectively the following: 21.8 €/ton, 159 €/ton, 15.4 €/ton, 6377 €/ton, 65.2 €/ton, 257 €/ton, 608 €/ton, 20.95 €/ton. These values are considered in a stationary condition. However, an uncertainty between ±20% of the expected value (applied in the deterministic model) is considered for each production cost, obtaining for each scenario a value of probability, as reported in Figure X.3. Here, only 7 scenarios are considered to avoid a numerical model too big to converge without serious problems. As in the previous case, Monte Carlo technique is used to this aim and the overall probability for each scenario is evaluated as the product of the probability of each product, as done for the CCUS of the UK.

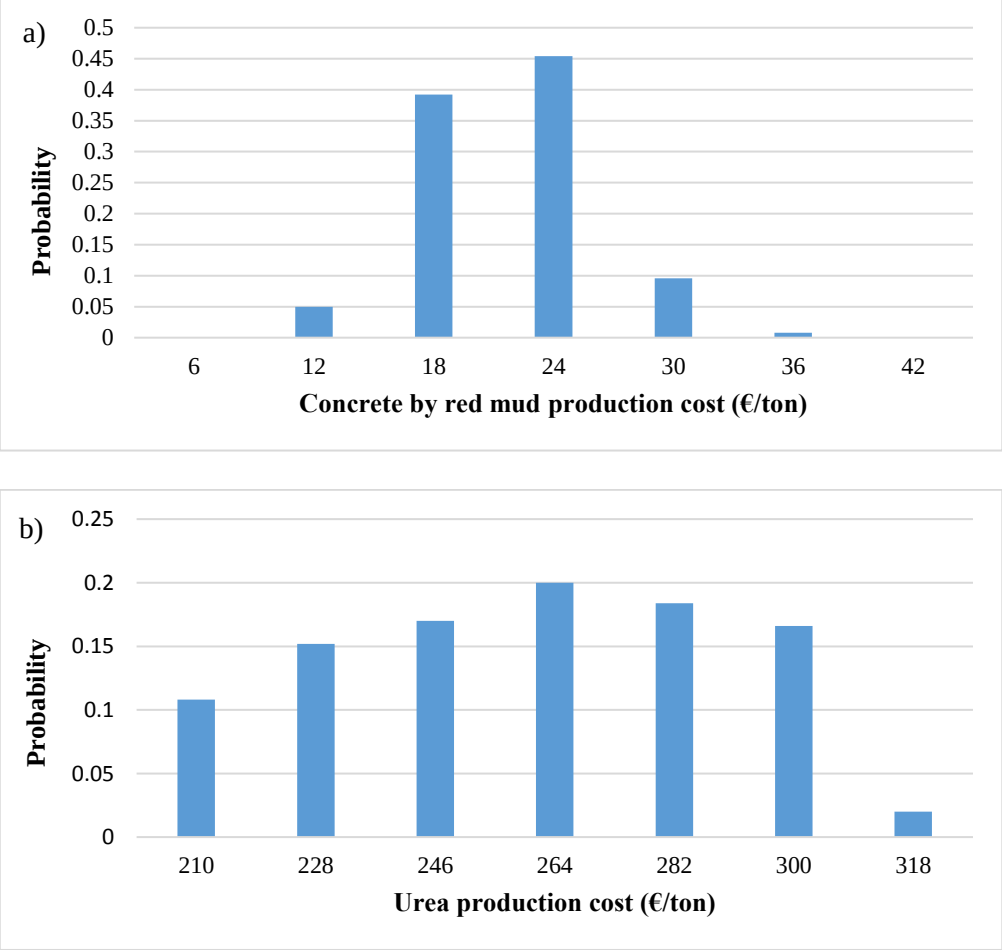

Figure X.18 (Following)

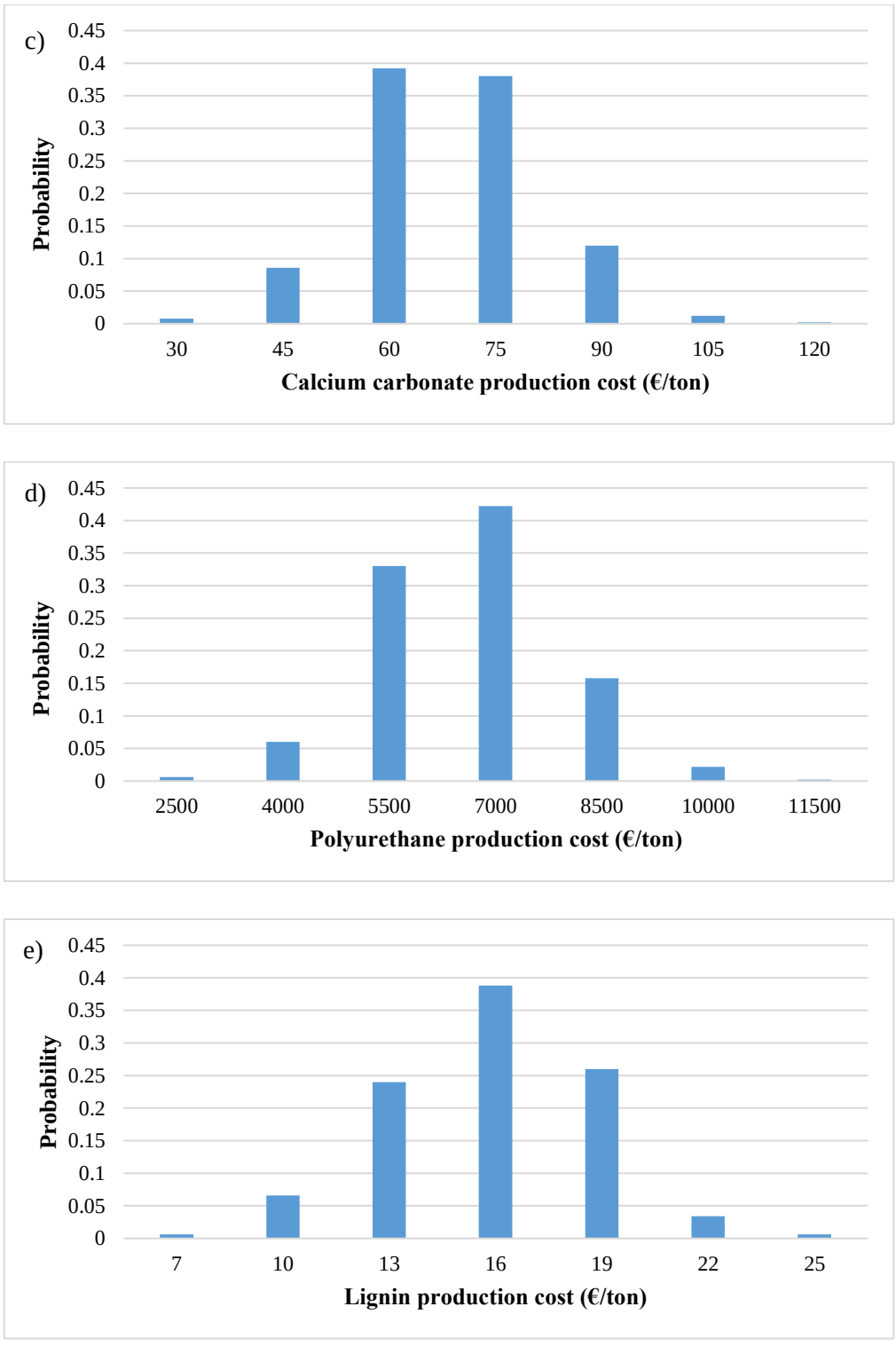

Figure X.19 (Following)

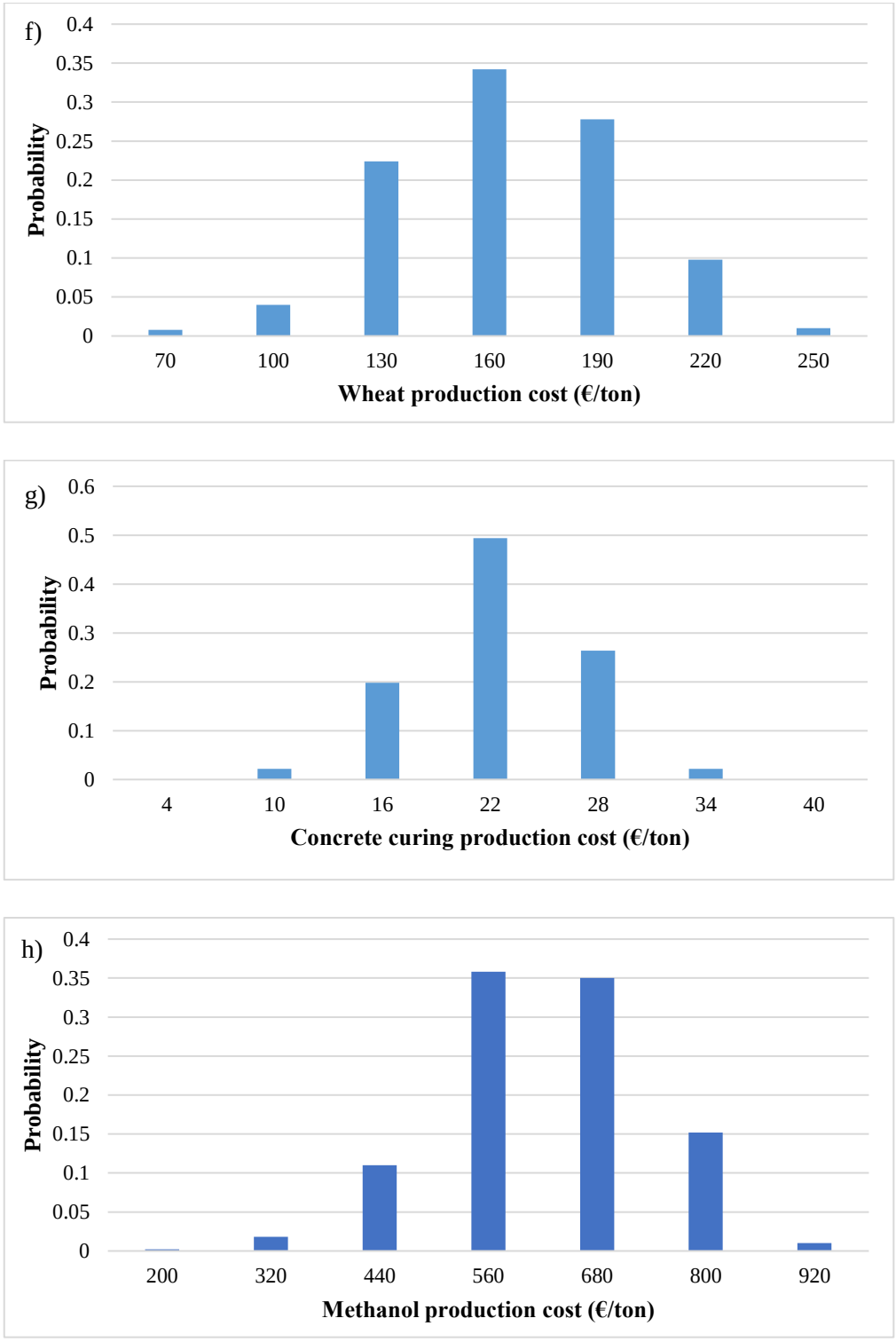

Figure X.3 Discrete normal distribution for the stochastic parameter: a) concrete by red mud production cost; b) urea production cost; c) calcium carbonate production cost; d) polyurethane production costs; e) lignin production costs; f) wheat production costs g) concrete curing production costs; h) CH_3OH production costs for the CCUS supply chain of the Germany

X.2.4 Monte Carlo method

Monte Carlo method is a computer simulation technique used to have an estimation of the entire probability distribution of an outcome, in this case of a random parameter. Common probability distributions include: normal, lognormal, uniform, triangular, pert, discrete. The most common used distribution is the normal one, according to the following relation (see Eq. X.14):

$$f(x) = \frac{1}{\sigma\sqrt{2\pi}} e^{-\frac{(x-\mu)^2}{2\sigma^2}} \qquad (X.14)$$

with σ standard deviation and μ mean. Different steps are followed to build the probability distribution curve of a stochastic parameter. At first, it is necessary to choose the probability distribution law and the value of its characteristic parameters are defined (in our case standard deviation and mean for the normal distribution). After that, a random number between 0 and 1 is associated and the value of investigated stochastic parameter is found (the value of x as according to Eq. X.14). These steps are repeated until 1000 times. The obtained values are used to evaluate the frequency of sampling (the number of times the x is obtained), then the probability distribution curve.

X.3 Results and discussion

X.3.1 Results for the CCUS supply chain of Italy

The model is solved in 0.38 seconds, through 980 iterations, using CPLEX 12.7.1 as solver. The computer processor is 2.5 GHz while the memory is 4 GB. When CH_4 production cost is subjected to fluctuations (as shown in Figure X.1), then it is random, the expected value of the objective function and then the expected value of total costs for the CCUS supply chain with offshore Adriatic sea as storage site is 77.3 billion€/year.

First and second stage variables are calculated. Regarding the first stage variable related to the choice of storage site, it is found that CO_2 should be captured from Lombardy region and sent to the storage site. Regarding the first stage variable related to the choice of capture technology, it is preferable to capture CO_2 with PSA adsorption, as also suggested in Kalyanarengan Ravi et al. (2017). However, after knowing the uncertainty, recourse actions are taken and the variables defining the amount of captured CO_2 sent to the utilization and storage section are defined for each scenario.

It is suggested, for each scenario under the uncertainty, to capture in total 77 Mton/year of CO_2: 44.2 Mton/year are sent to the utilization section, while 32.8 Mton/year are sent to the storage section. Overall, 16.1 Mton/year of CH_4 are produced. Even if the amount of captured CO_2 is the same for different scenarios, different carbon sources and capture technologies are suggested (MEA and IL absorption, membrane, PSA, VSA). In this case, MEA absorption is the most used capture technology due to a lower cost. This solution illustrates that it is impossible, under the uncertainty, to find a solution that is ideal for all circumstance.

However, for all cases, CO_2 is distributed between the utilization and storage section in order to achieve the minimum target for reduction of emissions to the atmosphere. Then, capturing an amount higher than the last one or choosing only the utilization option would never take place with a perfect forecast.
It is interesting to analyze the cost distribution and then the value of total costs for each considered scenario, as in Figure X.4, where the respective probabilities are considered.

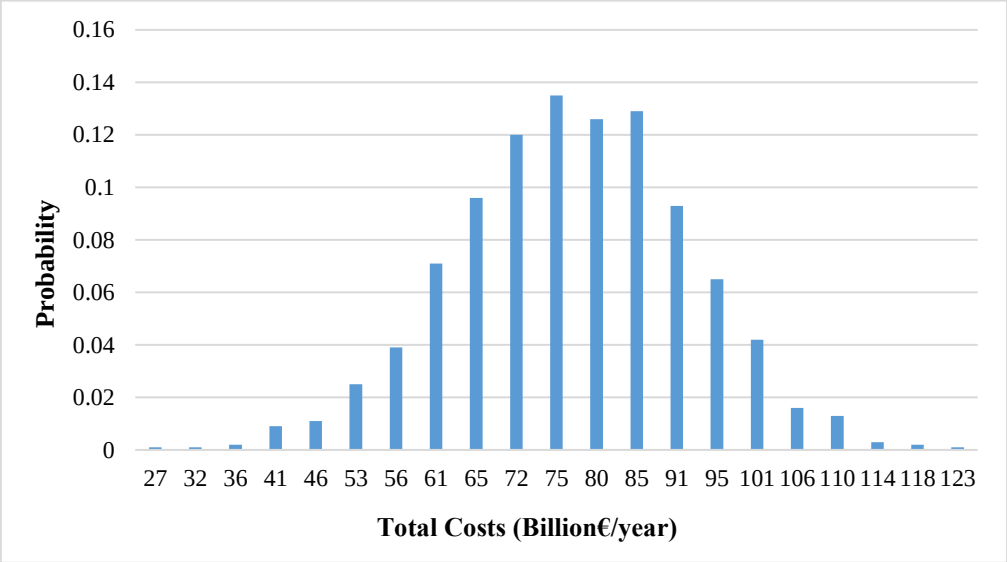

Figure X.4 Costs distribution for the CCUS supply chain of Italy with offshore Adriatic sea as storage site obtained with the stochastic problem (Leonzio et al., 2020)

The topology of the supply chain for the scenario with the highest probability is shown in Table X.1 (the scenario is the number 11 with a probability of 0.135). In this case, the total costs of supply chain are 75 billion€/year while 16.1 Mton/year of CH_4 are produced.

Table X.8 Topology of the CCUS supply chain in Italy with offshore Adriatic sea as storage site for the scenario with the highest probability (Leonzio et al., 2020)

CO_2 source	**CO_2 capture technology**	**CO_2 amount (Mton/year)**
To storage		
Lombardy	MEA absorption	33
To utilization		
Emilia Romagna	MEA absorption	20
Piedmont	MEA absorption	18
Veneto	Membrane	7

For this scenario, CO_2 is captured from Lombardy through MEA absorption and sent to the storage section. Also, CO_2 is captured from Emilia Romagna and Piedmont through MEA absorption, from Veneto from membrane and sent to the utilization section in Verbania for CH_4 production. In this case, membrane technology is used due to a higher carbon dioxide content.

Some parameters are calculated in order to evaluate the stochastic optimization results and compare these to their deterministic counterpart. These parameters are the Expected Value of Perfect Information and the Value of Stochastic Solution.

The EVPI measures the value of knowing future with certainty and in particular, the amount that a decision maker would be willing to pay to have a perfect information about future before that uncertainties will be bared (Birge and Louveaux, 2011). This parameter is calculated as the difference between the wait-and-see (WS) solution and the stochastic here-and-now (HN) solution. The first, the wait-and-see solution, is calculated by weighting each deterministic scenario with its corresponding probability.

For the CCUS supply chain of Italy with offshore Adriatic sea as storage site, it results that the wait-and-see solution is 78.6 billion€/year. This means, if it were possible to know perfectly the future, the total system costs would only be 78.6 billion€/year. However, future can not be predicted, then by solving the stochastic program it is found for the supply chain an expected value of costs equal to 77.3 billion€/year. The EVPI of 1.3 billion€/year suggests how much is worth knowing future with certainty. In particular, the EVPI/WS ratio of 1.64% shows not a big influence of uncertainty on the obtained solution, then it is not worthwhile to have better forecast about the different scenarios (Felfel et al., 2015). A value of EVPI < 1.66% of the stochastic solution underlines that an extra effort is not required to have information about future.

The VSS suggests the possible gain for solving the stochastic model over a deterministic one and in particular, the cost to ignore uncertainty for a decision maker. This suggests the importance of solving a stochastic problem. The VSS is calculated as the difference between the stochastic here-and-now solution and the EEV defined as the expectation of the expected value (EV) solution (Birge and Louveaux, 2011). Two steps are required: at first the EV solution is calculated and then the EEV solution is found. In particular, firstly, the EV solution is obtained by solving a single deterministic problem that uses the expected value of random variables. Secondly, the solutions for the first stage variables obtained in the first step are set in the stochastic problem that provides in this way the EEV solution (Stefansdottir and Grunow, 2018).

For the considered CCUS supply chain of Italy, a value for VSS of 1.6 billion€/year is found (the respective value of EEV is 75.7 billion€/year): solving the stochastic problem rather than the corresponding deterministic problem, 1.6 billion€/year can be saved. It is interesting to evaluate the VSS/EEV ratio that is 2.06%, that is the gain of the two stages stochastic model over the deterministic one (Felfel et al., 2105). Due to the low value of this ratio, it is not recommended to solve a complex problem as the stochastic one. In fact, as found in the above results the uncertainty has no a big influence on the obtained results.

X.3.2 Results for the CCUS supply chain of the UK

The MILP model developed for the CCUS supply chain of the UK is solved in 15.94 seconds with 1402 iterations. The used solver is CPLEX 12.7.1 while, the computer processor is 2.5 GHz and the memory is 4 GB. For this carbon supply chain, random data are present about the production cost of CO_2-based compounds (CH_3OH, CH_4, polyurethane, tomato, concrete and calcium carbonate). In this case, an expected value for the objective function and then for the total costs of the system is found and it is equal to 1.05 billion€/year. In the optimized problem, the first stage variables are the same for all scenarios. Regarding the binary variable related to the definition of the storage section, it is found that CO_2 can be captured from the Yorkshire and the Humber region and sent to the Bunter Sandstone storage site. Regarding the variable characterizing the choice of capture technology, the PZ absorption is the preferable choice, due to a lower cost compared to the MEA absorption (Kalyanarengan Ravi et al. 2017). Second stage variables are, instead, different for each scenario and are related to the recourse actions that should be taken after knowing the uncertainty. Second stage variables define the amount of captured CO_2 that is sent to the utilization and storage section. Under the uncertainty, it is suggested to capture an amount of CO_2 that allows to achieve the minimum target of emissions reduction (6.4 Mton/year). In particular, 6 Mton/year of CO_2 are sent to the utilization section, while 0.4 Mton/year of CO_2 are sent to the storage section. This picture is the same for each scenario. However, different amount of calcium carbonate and polyurethane can be produced in each scenario, as shown in Figure X.5. Other CO_2-based compounds are not produced. Also, in each scenario, different carbon sources are selected to capture CO_2, although PZ absorption is the capture technology mainly used in the utilization section while VSAWEI is the capture technology used in the storage section. The PZ absorption is chosen as explained above, while VSAWEI is selected due to the relatively small flow rate and higher carbon dioxide composition (Zhang et al., 2018; Hasan et al., 2013).

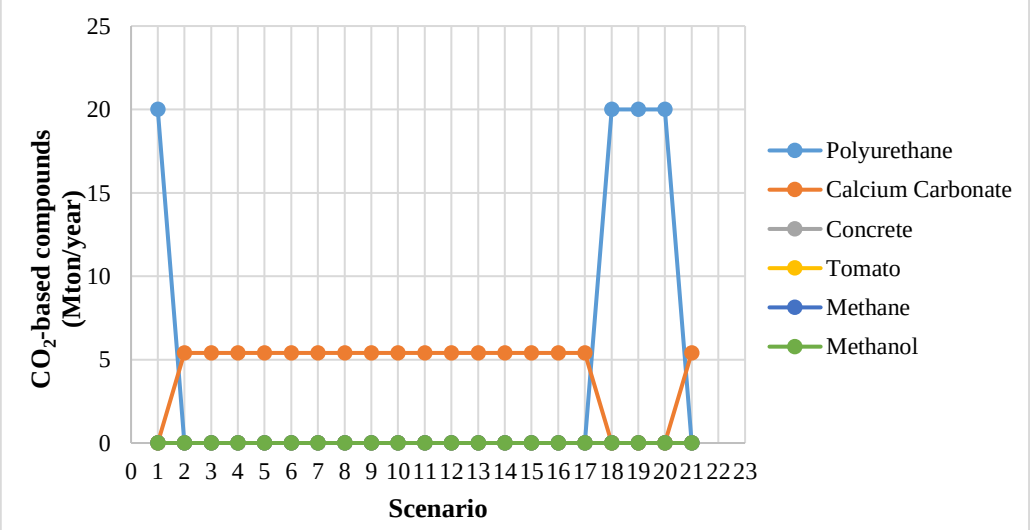

Figure X.5 Amount of CO_2-based compounds produced in different scenarios in the two stages stochastic problem for the CCUS supply chain of the UK with Bunter Sandstone as storage site (Leonzio et al., 2020)

Also in this case study, with random variables is impossible to find an ideal solution for all scenarios under all circumstances, even if for all scenarios CO_2 is distributed between the utilization and storage section with the same ratio, achieving the minimum target for emissions reduction. Then, with a perfect forecast, it is preferable to have both utilization and storage sections, then the importance of one storage site, as found in Chapter V.

Figure X.6 shows the costs distribution for the CCUS supply chain of the UK: for each scenario the value of total costs and the respective probabilities are reported (the scenarios with a probability equal to zero are not taken into account in this plot). Scenario 11 has the highest probability of 0.32 while the respective costs are equal to 1.04 billion€/year. For this case, the topology of the supply chain is reported in Table X.2.

For this scenario, CO_2 is captured from Leeds and sent to the utilization (6 Mton/year) and to the storage (0.4 Mton/year) section. PZ absorption is used in the utilization section, while VSA WEI is used in the storage section. The selection of these capture technologies is explained above.

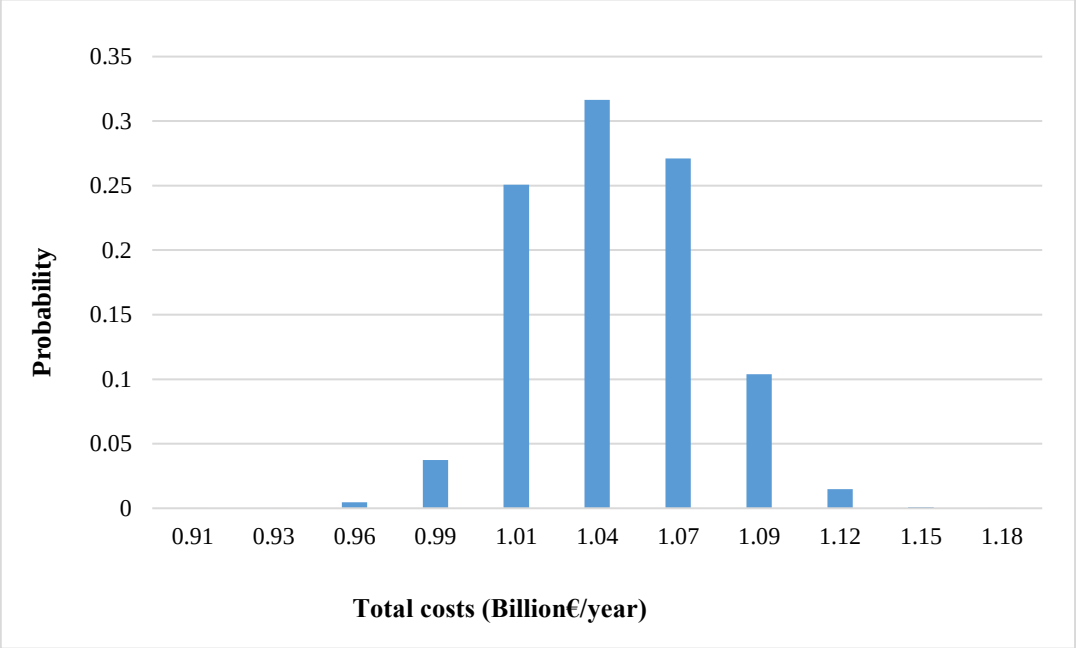

Figure X.6 Costs distribution for the CCUS supply chain of the UK with Bunter Sandstone as storage site obtained with the stochastic problem (Leonzio et al., 2020)

Table X.9 Topology of the CCUS supply chain in the UK with Bunter Sandstone as storage site for the scenario with the highest probability (Leonzio et al., 2020)

CO_2 source	**CO_2 capture technology**	**CO_2 amount (Mton/year)**
	To storage	
Leeds	VSA WEI	0.4
	To utilization	
Leeds	PZ absorption	6

The performance of the stochastic approach is evaluated calculating the expected value of perfect information and the value of stochastic solution, with the meaning explained in the previous case study. When considering three significant digits to express the expected total costs and related economic indices, the model does not detect any difference between the wait-and-see and the here-and-now solution, for the EVPI calculation; when assuming numerical errors much smaller than this level of outputs precision, a difference of 0.18 million€/year is detected, over an expected total cost of 1.05 billion€/year, negligible in relative terms, although still important in absolute terms. Then, in this second case, 0.18 million€/year, the EVPI value, is the amount that a decision maker could pay for having a perfect information in advance on how uncertainties will be revealed. This small value suggests that the uncertainty on the solution is not significant.

Regarding the VSS, the value of the expectation of the expected value is equal to the stochastic here-and-now solution (1.05 billion€/year). Then, the value of VSS is 0: it is not necessary to solve the more complex stochastic problem, as also found in the results of EVPI. The uncertainty is not significant, then it is not important to solve the two stage stochastic problem. It is not advantageous to use the proposed stochastic modelling approach to design the supply chain, when production costs of CO_2-based products are stochastic parameters.

X.3.3 Results for the CCUS supply chain of Germany

Also for the CCUS supply chain of Germany, the two stages stochastic model is solved in 114.33 seconds through 10112 iterations. CPLEX 12.7.1 is the used solver while, the computer processor is 2.5 GHz and the memory is 4 GB.

In the model, the production cost of CH_3OH, concrete, wheat, lignin, polyurethane, calcium carbonate, urea are random and are not defined by a fixed value. In this conditions, the expected value of the objective function expressing the total costs of the supply chain is 98.0 billion€/year.

First and second stage variables are also evaluated. First stage variables are the same of the previous study case, suggesting then the selection of storage site and capture technology. These are equal for all scenarios. It results that for the selection of the storage site CO_2 is captured from Magdeburg and sent to Altmark storage site. Regarding the capture technology the PZ absorption is preferred for the selected carbon

sources, due to lower costs (Kalyanarengan Ravi et al. 2017). Second stage variables, suggesting the amount of captured CO_2 sent to the utilization and storage site, are related to the recourse actions that a decision maker makes after knowing uncertainty. Figure X.7 shows the amount of overall captured CO_2, sent to the utilization and storage site for each scenario.

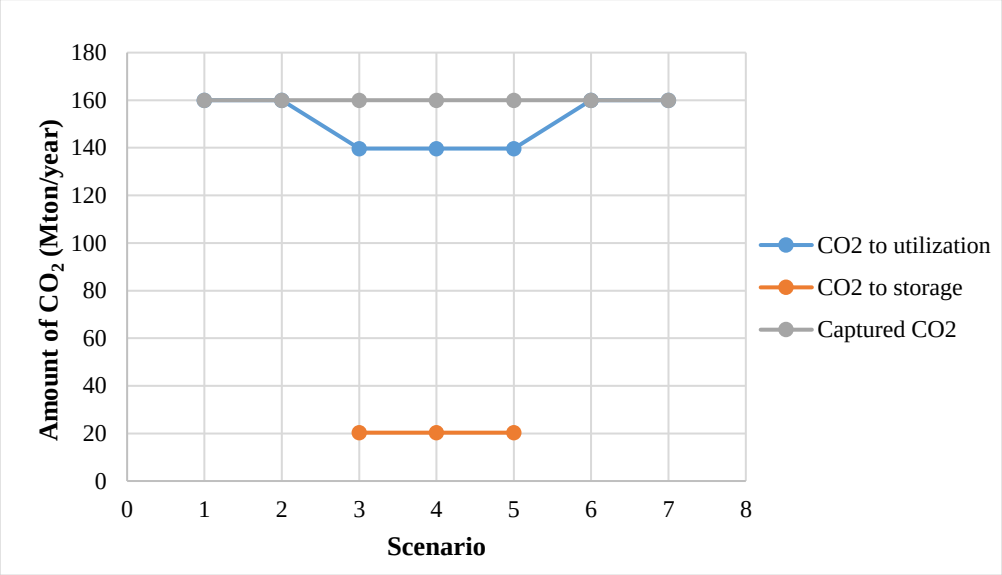

Figure X.7 Amount of CO_2 sent to the utilization and storage section and the total amount of captured CO_2 defined in the second stage variables of the stochastic problem for each scenario in the CCUS supply chain of Germany producing different CO_2-based products (Leonzio et al., 2020)

Results show that for scenarios 1, 2, 6 and 7 all captured CO_2 (160 Mton/year) is sent to the utilization section for the production of different compounds. For other scenarios, the captured CO_2 is sent to the utilization (140 Mton/year) and storage section (20 Mton/year). In both cases, the amount of CO_2 captured allows achieving the minimum target for emissions reduction. Only in few scenarios all captured CO_2 is sent entirely to the utilization section: with a perfect forecast, it is preferable to have a storage and an utilization section inside the supply chain, as in the previous case studies.

The amount of different CO_2-based products in each scenario is reported in Figure X.8.

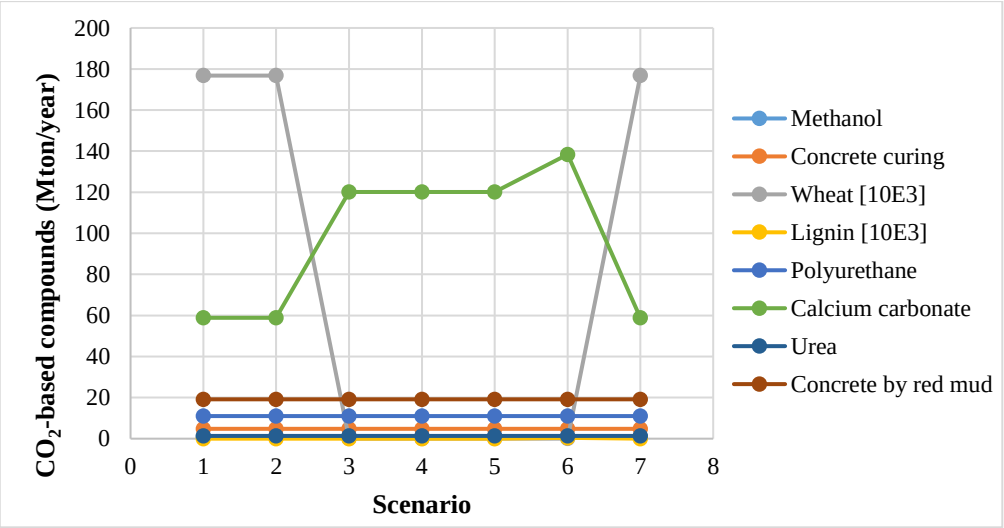

Figure X.8 Amount of CO_2-based compounds produced in different scenarios in the two stages stochastic problem for the CCUS supply chain of Germany (Leonzio et al., 2020)

CH_3OH, Concrete curing, polyurethane, urea, concrete by red mud are characterized by a constant production in each scenario, respectively 0.85 Mton/year, 4.8 Mton/year, 11 Mton/year, 1.3 Mton/year and 19 Mton/year. Wheat, lignin and calcium carbonate have a variation in their production in some scenarios. Figure X.9 shows the cost distribution for the CCUS supply chain of Germany with the respective probability (the scenario with a probability equal to 0 is not taken into account in this plot). The scenario number 4 has the highest probability of 0.97 while total costs of the system are 98.1 billion€/year. For this condition, the topology of the supply chain is shown in Table X.3: in the utilization and storage section CO_2 is captured with the PZ absorption, for reasons explained above.

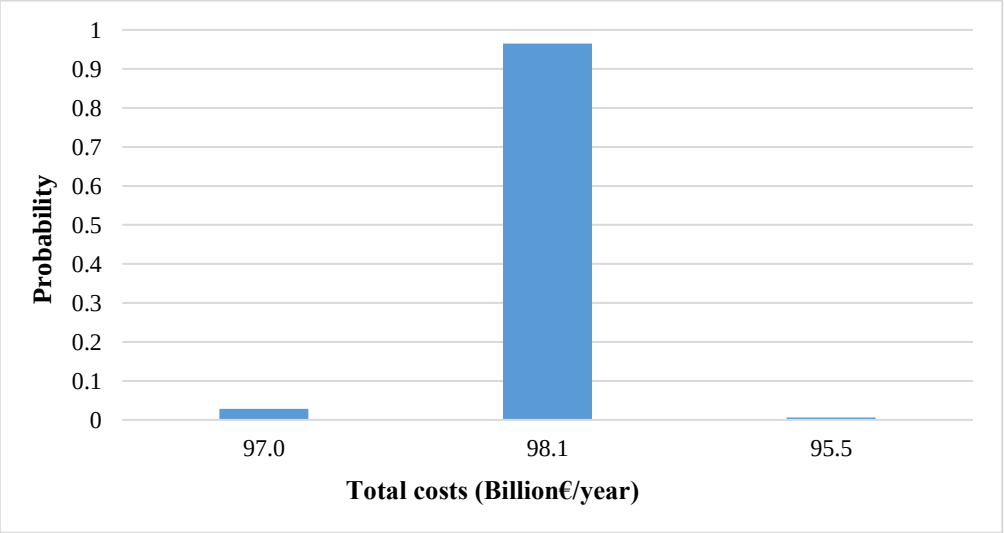

Figure X.9 Costs distribution for the CCUS supply chain of Germany producing different CO_2-based products obtained with the stochastic problem (Leonzio et al., 2020)

Table X.10 Topology of the CCUS supply chain of Germany producing different CO_2-based products for the scenario with the highest probability (Leonzio et al., 2020)

CO_2 source	**CO_2 technology**	**CO_2 amount (Mton/year)**
To storage		
Madgeburg	PZ absorption	20
To utilization		
Munich	PZ absorption	1
Hannover	PZ absorption	52
Dresda	PZ absorption	44
Wiesbaden	PZ absorption	39
Madgeburg	PZ absorption	4

In particular, 20 Mton/year of CO_2 are captured from Magdeburg and sent to the storage site Altmark, while an overall 140 Mton/year of CO_2 are captured from Munich, Hannover, Dresda, Wiesbaden and Magdeburg and sent to the production of the considered products.

Also for this carbon supply chain, parameters as EVPI and VSS are evaluated in order to analyze the importance of uncertainty. It is found that the EVPI for the stochastic model is 8.31 billion€/year (this amount will be paid by a decision maker to know future with certainty), while the wait-and-see solution is 106 billion€/year (it is the cost of the system if it were possible to know perfectly the future). In particular, the EVPI solution is only 8.48% of the stochastic objective function value, then there is not a big influence of uncertainty on the solution and the effort to have information about future is not recommended. In fact, the EVPI/WS ratio is only 7.81%.

Regarding the VSS parameter, it is found a value of 0.1 billion€/year, as the possible gain solving the stochastic model over the deterministic one (the value of the EEV is of 97.9 billion€/year). Negligible values are related to the VSS/EEV ratio and the percentage of VSS over the stochastic objective function: few advantages are obtainable solving the stochastic problem over the deterministic one. In fact, as found with the EVPI, the uncertainty is not so significant on the obtained solution.

X.4 Conclusions

In this Chapter, a two stage stochastic model with recourse actions is developed for the best carbon framework developed for Italy, Germany and the UK as in the previous Chapters, with the aim to find an optimal network and then assist a decision making body. The production costs of different CO_2-based products are the stochastic parameters for which a probability with normal distribution is obtained with the

Monte Carlo technique. The expected total costs of these systems is minimized: these stochastic MILP models are described by deterministic equivalent problems using non-anticipativity (state of art) constraints.

It is found that the expected total costs for the CCUS supply chain of Italy, Germany and the UK is respectively 77.3 billion€/year, 98.0 billion€/year, 1.05 billion€/year.

The comparison with the respective deterministic model is made evaluating the EVPI and the VSS. For the CCUS supply chain of Italy the EVPI and VSS are respectively 1.29 billion€/year and 1.56 billion€/year.

For the CCUS supply chain of the UK the value of EVPI and VSS are respectively 0.18 million€/year (assuming numerical errors much smaller than the considered level of outputs precision, equal to 0.1%) and 0 €/year.

While it is found that the value of EVPI and VSS are respectively 8.31 billion€/year and 0.1 billion€/year for the CCUS supply chain of Germany.

Overall, results show that the uncertainties in production costs don't have a big influence on the modeling of these carbon systems, then few advantages are present solving the stochastic problem over the deterministic one, when considering the fluctuation of the stochastic parameter investigated here. This conclusion is then limited to consider the production cost of CO_2-based compounds as the stochastic parameter. Of course, considering different stochastic parameters may lead to more significant differences between the deterministic and the stochastic approach (a broader analysis extended to other parameters that may vary would be necessary here). On the other hand, the choice of production cost as stochastic parameter was suggested by its novelty, compared to the literature.

References

Bakker, H., Dunke, F., Nickel, S. 2019. A structuring review on multi-stage optimization under uncertainty: Aligning concepts from theory and practice, Omega, in Press.

Birge, J.R., Louveaux, F., 2011. Introduction to Stochastic Programming, second ed. Springer, New York.

Escudero, L.F., Garín, M.A., Pérez, G. and Unzueta, A. 2012. Lagrangean decomposition for large-scale two-stage stochastic mixed 0-1 problems, TOP 20: 347

Felfel, H., Ayadi O., Masmoudi, F. 2015. A stochastic programming approach for a multi-site supply chain planning in textile and apparel industry under demand uncertainty, International Journal of Supply and Operations Management, 2, 3, 925-946

Govindan, K., Fattahi, M., Keyvanshokooh, E. 2017. Supply chain network design under uncertainty: a comprehensive review and future research directions. Eur J Oper Res 263 108–41.

Han, J.H., Lee, I.B. 2012. Multiperiod stochastic optimization model for carbon capture and storage infrastructure under uncertainty in CO2 emissions, product prices, and operating costs. Ind Eng Chem Res 51 11445–57.

Hasan, M.M.F., Boukouvala, F., Floudas, C.A., 2013. Optimization of CO2 Capture, Utilization and Sequestration (CCUS) supply chain networks. AIChE Annual Meeting in San Fransisco November 08

Kalyanarengan Ravi, N., Van Sint Annaland, M., Fransoo, J.C., Grievink, J., Zondervan, E., 2017. Development and implementation of supply chain optimization framework for CO2 capture and storage in the Netherlands. Computer Chemical Engineering 102, 40–51.

Keating, G.N., Middleton, R.S., Viswanathan, H.S., Stauffer, P.H., Pawar, R.J. 2011. How storage uncertainty will drive CCS infrastructure. Energy Proc 4 2393–400.

Lee, S.Y., Lee, J.U., Lee, I.B., Han, J. 2017. Design under uncertainty of carbon capture and storage infrastructure considering cost, environmental impact, and preference on risk, Applied Energy 189 725–738

Leonzio, G., Foscolo, P.U., Zondervan, E. 2020. Design and analysis of CCUS supply chains for European countries under the uncertainty. To be submitted.

Liu, B., Iwamura, K. 1998. Chance constrained programming with fuzzy parameters. Fuzzy Sets Syst 94 227–37.

Malaeb, R., Tarhini, H., Alnouri, S.Y. 2019. Capturing the effects of oil price uncertainty in carbon integration network design. Ind Eng Chem Res 58 3131–45.

Messina, E., Mitra, G. 1997. Modelling and analysis of multistage stochastic programming problems: A software environment, European Journal of Operational Research 101 343-359

Middleton, R.S., Yaw, S. 2018. The cost of getting CCS wrong: uncertainty, infrastructure design, and stranded CO2. Int J Greenh Gas Control 70 1–11.

Mitra, S., Garcia-Herreros, P., Grossmann, I.E. 2016. A cross-decomposition scheme with integrated primal–dual multi-cuts for two-stage stochastic programming investment planning problems, Math. Program., Ser. B 157:95–119

Mulvey, J.M., 1995. Vanderbei RJ, Zenios SA. Robust optimization of large-scale systems. Oper Res 43 264–81.

Stefansdottir, B., Grunow, M. 2018. Selecting new product designs and processing technologies under uncertainty: Two-stage stochastic model and application to a food supply chain, International Journal of Production Economics 201 89–101

Trochu, J., Chaabane, A., Ouhimmou, M. 2019. A two-stage stochastic optimization model for reverse logistics network design under dynamic suppliers' locations, Waste Management 95 569–583

Yang, Y., Zhang, S., Xiao, Y., 2017. Optimal design of distributed energy resource systems based on two-stage stochastic programming. Appl. Therm. Eng. 110,1358-1370.

Yeh, K., Whittaker, C., Realffa, M.J., Lee, J.H. 2015. Two stage stochastic bilevel programming model of a pre-establishedtimberlands supply chain with biorefinery investment interests, Computers and Chemical Engineering 73 141–153

Zhang, X., Duncan, I.J., Huang, G., Li, G. 2014. Identification of management strategies for CO2 capture and sequestration under uncertainty through inexact modeling. Appl Energy 113 310–7.

Zhou, H., Zhang, H., Qiu, R., Lv, M., Xiang, C., Long, Y., Liang, Y. 2019. A two-stage stochastic programming model for the optimal planning of a coal-to-liquids supply chain under demand uncertainty, Journal of Cleaner Production 228 10-28

Zhang, S., Zhuang, Y., Liu, L., Zhang, L., Du, J. 2019. Risk management optimization framework for the optimal deployment of carbon capture and storage system under uncertainty, Renewable and Sustainable Energy Reviews 113 109280

Zhang, S., Liu, L., Zhang, L., Zhuang, Y., Du, J., 2018. An optimization model for car- bon capture utilization and storage supply chain: a case study in northeastern china. Appl Energy 231, 194–206.

Zimmermann, H.J. 2010. Fuzzy set theory. Wiley Interdiscip Rev Comput Stat 2 317–32.

Nomenclature

Abbreviations

AIMMS = advanced interactive multidimensional modeling system

CCUS = carbon capture utilization and storage

EVPI = expected value of perfect information

IL = ionic liquid

MEA = monoethanolamine

MILP = mixed integer linear programming

NPV = net present value

PBP = payback period

PSA = pressure swing adsorption

PZ = piperazine

TH = time horizon

VSA = vacuum swing adsorption

VSS = value of stochastic solution

Parameters

C_k^{max} = maximum storage capacity for storage site k [ton]

CS_i = carbon dioxide emissions from source i [ton/year]

CR^{min} = minimum target for overall carbon dioxide reduction [ton/year]

XL_i = lowest composition processing limit for capture technology j [mol%]

XH_i = highest composition processing limit for capture technology j [mol%]

XS_i = carbon dioxide composition in the flue gas emission from source i [mol%]

Variables

Binary

$X_{i,j,k,s}$ = 1 if carbon dioxide is captured from source i with technology j and sent to storage site k, in the scenario s, otherwise 0

$Y_{i,j,k,s}$ = 1 if carbon dioxide is capture from source i with technology j and sent to storage/utilization site k, in the scenario s, otherwise 0

Continuous

$MR_{i,j,k,s}$ =fraction of captured carbon dioxide from source i with technology j sent to utilization site k, under the scenario s

$FR_{i,j,k}$ = fraction of captured carbon dioxide from source i with technology j sent to storage site k, under the scenario s

$Calcium\ carbonate_{i,j,cc,s}$ = fraction of captured carbon dioxide from source i with technology j sent to calcium carbonate production site cc, under the scenario s

$Concrete\ by\ red\ mud_{i,j,cr,s}$ = fraction of captured carbon dioxide from source i with technology j sent to concrete production site by red mud cr, under the scenario s

$Concrete_{i,j,c,s}$ = fraction of captured carbon dioxide from source i with technology j sent to concrete production site c, under the scenario s

$Lignin_{I,j,l,s}$ = fraction of captured carbon dioxide from source i with technology j sent to lignin production site l, under the scenario s

$Methanol_{i,j,m,s}$ = fraction of captured carbon dioxide from source i with technology j sent to methanol production site m, under the scenario s

$Polyurethane_{i,j,p,s}$ = fraction of captured carbon dioxide from source i with technology j sent to polyurethane production site p, under the scenario s

$Urea_{i,j,u,s}$ = fraction of captured carbon dioxide from source i with technology j sent to urea production site u, under the scenario s

$Utilization_{i,j,k,s}$ = fraction of captured carbon dioxide from source i with technology j sent to overall utilization site k, under the scenario s

$Wheat_{i,j,w,s}$ = fraction of captured carbon dioxide from source i with technology j sent to wheat production site w, under the scenario s

$Methane_{i,j,g,s}$ = fraction of captured carbon dioxide from source i with technology j sent to methane production site g, under the scenario s

$Polyurethane_{i,j,p,s}$ = fraction of captured carbon dioxide from source i with technology j sent to polyurethane production site p, under the scenario s

$Tomato_{i,j,t,s}$ = fraction of captured carbon dioxide from source i with technology j sent to tomato growing t, under the scenario s

$Concrete_{i,j,c,s}$ = fraction of captured carbon dioxide from source i with technology j sent to concrete curing c, under the scenario s

$CalciumCarbonate_{i,j,d,s}$ = fraction of capture carbon dioxide from source i with technology j sent to calcium carbonate production site, under the scenario s

Chapter XI

Improvement of CCUS supply chain model

In carbon capture utilization and storage supply chains previously developed it is supposed that for the utilization section the level of carbon dioxide purity should be achieved in the respective production site. This assumes the utilization of two different pipelines, one for the storage and one for the utilization section. In this Chapter, the previous mathematical model is modified in order to have an unique pipeline network for the entire supply chain; the level of carbon dioxide purity is at least 90% at the outlet of capture system and carbon dioxide is considered almost pure, after compression stages followed by refrigeration/separation stages up to 150 bar to feed carbon dioxide to the pipeline. This specification is valid for both sections of supply chain. Then, about pure carbon dioxide is available for distribution to utilization and storage sites. This new model is applied for the carbon capture utilization and storage supply chain of Germany producing different products. The system is designed and optimized through the minimization of total costs. Results show that the new supply chain costs 0.104 trillion€/year;therefore the minimum target for emissions reduction is achieved at a higher cost compared to the previous corresponding scheme of Chapter IV. As a result, the high level of carbon dioxide purity imposed on the capture section as a whole implies only slightly higher costs.

XI.1 Introduction

In previous Chapters, the carbon capture utilization and storage (CCUS) supply chains are designed considering two different pipelines: one for the utilization and one for the storage section. This means that the level of carbon dioxide (CO_2) purity is different for these two sections. For the storage section, supposing that the capture technology is followed by stages of compressors with inter-stage cooling, an almost pure CO_2 stream at 150 bar is obtained. For the utilization section, where also a medium-low CO_2 purity is in some cases required (Pieri et al., 2018), it is supposed that the needed level of purity is achieved in the respective utilization site. However, for CO_2 transportation is better to have an unique network at a given level of CO_2 purity. It is important to mention that impurities will affect the phase change of the whole CO_2 flow, pipeline transport process, pipeline transport capacity, pipeline crack propagation and pipeline corrosion and protection, etc. (Yang et al., 2017).

Table XI.11 Input for impurity limits in CO_2 transport.

Impurity	Limit in CO_2	Impurity	Limit in CO_2
CO_2	>95 vol%	CO	4750 ppm
H_2O	no free water	H_2S	235 ppm
Ar		SO_2	75 ppm
CH_4	together <5 vol%	HCN	70 ppm
H_2		COS	235 ppm
NO_2	75 ppm	NH_3	550 ppm

The European Commission (2011) provides some recommendations on impurity limits, as in Table XI.1 that however suggests different limits for each specific case.

With these considerations, in this Chapter the previous mathematical model of CCUS supply chain is improved in order to consider only one pipeline structure, that is able to ensure a high CO_2 purity for both utilization and storage section. In fact, almost pure CO_2 at 150 bar in supercritical conditions is considered. A new deterministic integer linear programming (MILP) model is then developed. The CCUS supply chain of Germany, producing different CO_2-based products is taken into account for this analysis. The framework is designed and optimized minimizing total costs while reducing emissions according to the environmental target.

XI.2 Model development

XI.2.1 Problem statement

The same assumptions considered in Chapter IV are taken into account for this new model. Moreover, in addition to these, it is supposed, as mentioned in the introduction, that an unique pipeline with the same high CO_2 purity level is considered. The same remaining information as in Chapter IV is provided, then the model is able to find the best connection among each element inside the framework, the amount of treated CO_2 and the produced CO_2-based compounds.

XI.2.2 CCUS supply chain model

To develop the model for the CCUS supply chain, it is necessary to define sets, parameters, variables, constraints, equations and objective function. AIMMS (Advanced Interactive Multidimensional Modeling System) software is used to model the supply chain analyzed in this study.

XI.2.2.1 Sets

The same sets described in Chapter IV are considered in this new model.

XI.2.2.2 Parameters

The same parameters discussed in Chapter IV are considered in this new model.

XI.2.2.3 Variables

In this model only one binary variable is considered: $Y_{i,j,k}$ used to choose the capture technology/material when it assumes a value equal to 1. The same continuous variables of Chapter IV are taken into account to define the fraction of CO_2 that is sent to the storage and utilization section (with the fraction sent to each specific site).

XI.2.2.4 Constraints

For the development of this mathematical model, different constraints are used. The storage site has a limited capacity then, the following constraint is considered (see Eq. XI.1):

$$\sum_{(i,j)\in(I,J)} CS_i \cdot FR_{i,j,k} \leq \frac{C_k^{max}}{TH} \qquad \forall\, k \in K \qquad (XI.1)$$

where CS_i is the total CO_2 emission from source 'i', C_k^{max} is the maximum storage capacity of the storage site 'k', TH is the time horizon of supply chain and $FR_{i,j,k}$ is the defined variable.

The minimum target for emissions reduction should be achieved, as defined in the following constraint (see eq. XI.2):

$$\sum_{(i,j,k)\in(I,J,K)} CS_i \cdot FR_{i,j,k} + CS_i \cdot Utilization_{i,j,k} \geq CR^{min} \qquad (XI.2)$$

where CS_i is the total CO_2 emission from source 'i', $FR_{i,j,k}$ and $Utilization_{i,j,k}$ are the defined continuous and CR^{min} is the minimum target of CO_2 emissions reduction.

To ensure that no more than 90% of CO_2 is removed from the selected source the following constraint is used (see Eq. XI.3):

$$\sum_{(j)\in(J)} FR_{i,j,k} + Utilization_{i,j,k} \leq 0.9 \qquad \forall\, (i,k) \in (I,K) \qquad (XI.3)$$

where $FR_{i,j,k}$ and $Utilization_{i,j,k}$ are the defined variables.

A level of CO_2 purity at least of 90% should be ensured at the outlet of capture plants, both in the utilization and storage section. The achievement of this requirement depends on the composition of CO_2 in the feed, as defined by the following constraint (see Eq. XI.4):

$$\sum_{(k)\in(K)} (XH_j - XS_i) \cdot (XS_i - XL_j) \cdot Y_{i,j,k} \geq 0 \qquad \forall\, (i,j) \in (I,J) \qquad (XI.4)$$

where XS_i is CO_2 composition in flue gas from source "i", XL_j, is the lowest CO_2 composition processing limit for the capture plant "j", XH_j is the highest CO_2 composition processing limit for the capture plant "j" and $Y_{i,j,k}$ is the binary variable defined above. It is evident that the main difference between this model and that described in Chapter IV is this constraint. By using the binary variable $Y_{i,j,k}$ it is ensured that the capture technology is always able to achieve a CO_2 purity of at least 90% and a series of compressors with inter-stage cooling are able to feed almost pure CO_2 at 150 bar to the distribution pipeline network in the utilization and storage section. In the previous model, using the binary variables $X_{i,j,k}$ this condition was ensured only for the storage section.

To ensure that the national demand of each CO_2-based product is satisfied, the following constraints are used (see Eqs. XI.5-XI.12):

$$\sum_{(i,j,c)\in(I,J,C)} Concrete_{i,j,c} \geq 0{,}9 \cdot Concrete^{dem} \quad (XI.5)$$

$$\sum_{(i,j,w)\in(I,J,W)} Wheat_{i,j,w} \geq 0{,}9 \cdot Wheat^{dem} \quad (XI.6)$$

$$\sum_{(i,j,l)\in(I,J,L)} Lignin_{i,j,l} \geq 0{,}9 \cdot Lignin^{dem} \quad (XI.7)$$

$$\sum_{(i,j,p)\in(I,J,P)} Polyurethane_{i,j,p} \geq 0{,}9 \cdot Polyurethane^{dem} \quad (XI.8)$$

$$\sum_{(i,j,cc)\in(I,J,CC)} Calcium\ carbonate_{i,j,cc} \geq 0{,}9 \cdot Calcium\ Carbonate^{dem} \quad (XI.9)$$

$$\sum_{(i,j,u)\in(I,J,U)} Urea_{i,j,u} \geq 0{,}9 \cdot Urea^{dem} \quad (XI.10)$$

$$\sum_{(i,j,m)\in(I,J,M)} Methanol_{i,j,m} \geq 0{,}9 \cdot MeOH^{dem} \quad (XI.11)$$

$$\sum_{(i,j,cr)\in(I,J,CR)} Concrete\ by\ red\ mud_{i,j,cr} \geq 0{,}9 \cdot Concrete\ by\ red\ mud^{dem} \quad (XI.12)$$

suggesting that the amount of each production should be equal or higher than 90% of the respective national demand, as established in Chapter IV.

According to the material balance, expressed by the following constraint, the captured CO_2 sent to the utilization section is distributed among different sites (see Eq. XI.13):

$$Utilization_{i,j,k} = (Concrete_{i,j,c} + Wheat_{i,j,w} + Lignin_{i,j,l} + Polyurethane_{i,j,p} + CalciumCarbonate_{i,j,cc} + Urea_{i,j,u} + Methanol_{i,j,m} + Concrete\ by\ red\ mud_{i,j,cr}) \cdot n_{sites} \quad \forall\ (i,j,k,c,w,l,p,cc,u,m,cr) \in (I,J,K,C,W,L,P,CC,U,M,CR) \quad (XI.13)$$

where $Utilization_{i,j,k}$, $Concrete_{i,j,c}$, $Wheat_{i,j,w}$, $Lignin_{ij,l}$, $Polyurethane_{i,j,p}$, $Calcium\ carbonate_{i,j,cc}$, $Urea_{i,j,u}$, $Methanol_{i,j,m}$ and $Concrete\ by\ red\ mud_{i,j,cr}$ are the defined continuous variables, while n_{sites} is the number of sites for each utilization.

For the overall supply chain, only one capture technology/material can be chosen for the selected CO_2 source, as defined in the following constraint (see Eq. XI.14):

$$\sum_{(j,k)\in(J,K)} Y_{i,j,k} \leq 1 \qquad \forall\, i \in I \qquad (XI.14)$$

where $Y_{i,j,k}$ is defined above. This constraint also ensure the on one to one coupling between sources and capture technologies.

The Glover linearization is used in order to convert the non-linear mathematical model in a linear one then, the following constraints are considered (see Eqs. XI.15-XI.16):

$$0 \cdot Y_{i,j,k} \leq FR_{i,j,k} \leq 0.9 \cdot Y_{i,j,k} \qquad \forall\, (i,j,k) \in (I,J,K) \qquad (XI.15)$$

$$0 \cdot Y_{i,j,k} \leq Utilization_{i,j,k} \leq 0.9 \cdot Y_{i,j,k} \qquad \forall\, (i,j,k) \in (I,J,K) \qquad (XI.16)$$

with $FR_{i,j,k}$, $Utilization_{i,j,k}$ and $Y_{i,j,k}$ are the defined variables, while 0.9 is used because at least 90% of CO_2 is captured from each source. The variable $X_{i,j,k}$ (introduced in the model of Chapter IV) is not considered in this new model, because it is not needed, then the variable $FR_{i,j,k}$ is constrained between the variable $Y_{i,j,k}$, as defined by the glover linearization.

XI.2.2.5 Equations

The same equations of Chapter IV, for CO_2 capture and compression costs, CO_2 transportation costs, CO_2 storage costs and production costs of CO_2-based products are taken into account in this new model.

XI.2.2.6 Objective function

As in Chapter IV, the objective function is expressing the total cost of CCUS supply chain, including CO_2 capture and compression costs, CO_2 transportation costs, CO_2 storage costs and the production costs of CO_2-based products. This objective function is minimized in order to design the framework.

XI.2.3 Case study

The description of CO_2 sources, CO_2 storage and utilization sites has been done in the respective section of Chapter IV. The same capture technologies/materials are used to reduce CO_2 emissions according to the minimum environmental target for CO_2 reduction of 160 Mton/year. The national demand of different compounds has been defined in Chapter IV.

XI.3 Results and discussion

The model, formulated as a MILP model, has 144559 constraints, 110648 variables (140 integer). CPLEX 12.7.1 is the selected solver and the solving times are about 7.15 seconds, with 312 iterations. The used computer contains an Intel Core i-3 processor at 2.5 GHz with 4 GB of RAM.

The topology obtained by the minimization of total costs is reported in Table XI.2.

Table XI.2 Topology of the new CCUS supply chain optimization where 90% of national demand of CO_2-based products is satisfied

CO_2 source	**Capture technology**	**CO_2 amount (Mton/year)**
	To storage	
Potsdam	PZ Absorption	20.32
	To utilization	
Dusseldorf	PZ Absorption	23.65
Munich	PZ Absorption	0.01
Hannover	PZ Absorption	62.10
Potsdam	PZ Absorption	29.18
Wiesbaden	PZ Absorption	0.08
Magdeburg	PZ Absorption	24.66

From Table XI.2 it results that CO_2 is captured from Potsdam and it is sent to the storage section through piperazine (PZ) absorption. On the other hand, CO_2 is captured from Dusseldorf, Munich, Hannover, Potsdam, Wiesbaden and Magdeburg and it is sent to the utilization section using PZ absorption. As found in Chapter IV, absorption is the preferred capture technology, while PZ is the most convenient material as reported in the work of Kalyanarengan Ravi et al. (2017). Overall, 160 Mton/year of emissions are captured, respecting the minimum target for emissions reduction. In the utilization section, the following compounds are produced: methanol (CH_3OH) (0.846 Mton/year), concrete by curing (4.79 Mton/year), wheat (19.4 Mton/year), lignin (0.378 Mton/year), polyurethane (11 Mton/year), calcium carbonate (120 Mton/year), urea (1.34 Mton/year) and concrete by red mud (19.2 Mton/year). All products, except calcium carbonate, are produced for an amount equal to 90% of national demand. Then the additional amout of calcium carbonate that is produced can be exported, as already discussed in Chapter IV. In fact the same amount of CO_2-based compounds is produced in both models.

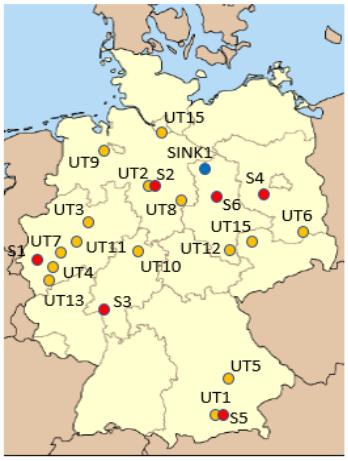

CO_2 Utilization/Storage		CO_2-based product		CO_2 Source
SINK1	Altmark		S4	Potsdam
UT1	Munich	Wheat	S5	Munich
UT2	Hannover	Concrete curing and Wheat	S1-S5	Dusseldorf-Munich
UT3	Ennigerloh	Concrete curing	S1	Dusseldorf
UT4	Cologne	Lignin	S3	Wiesbaden
UT5	Munchsmunster	Lignin	S3	Wiesbaden
UT6	Schwarzheide	Polyurethane	S1	Dusseldorf
UT7	Leverkusen	Polyurethane	S1	Dusseldorf
UT8	Salzgitter	Calcium carbonate	S1-S2-S4-S6	Dusseldorf-Hannover-Potsdam-Magdeburg
UT9	Bremen	Calcium carbonate	S1-S2-S4-S6	Dusseldorf-Hannover-Potsdam-Magdeburg
UT10	Kassel	Urea	S1	Dusseldorf
UT11	Hagen	Urea	S1	Dusseldorf
UT12	Leuna	Methanol	S1	Dusseldorf
UT13	Wesseling	Methanol	S1	Dusseldorf
UT14	Hamburg	Concrete by red mud	S6	Magdeburg
UT15	Rackwitz	Concrete by red mud	S6	Magdeburg

Figure XI.20 Results of the new CCUS supply chain design optimization considering 90% of national demand of produced CO_2-based chemical compounds

Figure XI.1 shows connections between CO_2 sources and specific utilization sites.

The CCUS supply chain costs 0.104 trillion€/year, a cost that is 5% higher than that obtained in the base model of Chapter IV (97.9 billion€/year). Then, ensuring an unique pipeline for the utilization and storage section with almost pure CO_2 does not determine a significant increase of costs compared to the previous model. CO_2 capture and compression costs are 17.1 billion€/year, CO_2 transportation costs are 4.25 billion€/year, CO_2 storage costs are 22 million€/year, CH_3OH production costs are 0.514 billion€/year, concrete curing costs are 0.104 billion€/year, wheat production costs are 3.08 billion€/year, lignin production costs are 5.82 million€/year, polyurethane production costs are 70 billion€/year, calcium carbonate production costs are 7.83 billion€/year, urea production costs are 0.343 billion€/year and concrete by red mud production costs are 0.401 billion€/year.

The economic analysis shows that the net present value (NPV) of the framework is positive considering only carbon tax then, the system is economically feasible. In particular, a value of 0.616 trillion€ is obtained. Also, a value of payback period (PBP) of 5.7 years is ensured.

XI.4 Conclusions

In this Chapter, an improvement of mathematical models for CCUS supply chains previously discussed is suggested. It is assumed an unique pipeline for CO_2 transportation, the same for the utilization and storage section. This pipeline is characterized by almost pure CO_2 compressed at 150 bar. Then, the mathematical model previously developed is changed to this aim. The new MILP model can design carbon supply chains minimizing total costs. The CCUS supply chain for Germany producing more products is considered in this analysis. Results show that in these conditions, a relatively higher total cost is obtained, compared to the case described in Chapter IV. A significant variation is not present. In fact, total costs for this new model are 0.104 trillion€/year compared to 97.9 billion€/year for the previous system. For this new scheme, only the carbon tax is required to have a profitable solution: the NPV is 0.616 trillion€, while the PBP is 5.7 years.

References

European Commission, 2011. Towards a transport infrastructure for large-scale CCS in Europe.

Kalyanarengan Ravi, N., Van Sint Annaland, M., Fransoo, J.C., Grievink, J., Zondervan, E., 2017. Development and implementation of supply chain optimization framework for CO2 capture and storage in the Netherlands. Computer Chemical Engineering 102, 40–51.

Pieri, T., Nikitas, A., Castillo-Castillo A., Angelis-Dimakis, A. 2018. Holistic Assessment of Carbon Capture and Utilization Value Chains. Environments. 5, 108.

Yang, Y., Tao, H., Yang, J., Shang, Q., Cao, S. 2017. Research on CO2 Quality Pipeline Transportation Based on Yanchang Oilfield CC

Nomenclature

Abbreviations

AIMMS = advanced interactive multidimensional modeling system

CCUS = carbon capture utilization and storage

IL = ionic liquid

MEA = monoethanolamine

MILP = mixed integer linear programming

NPV = net present value

PBP = payback period

PSA = pressure swing adsorption

PZ = piperazine

TH = time horizon

VSA = vacuum swing adsorption

Parameters

$Calcium\ Carbonate^{dem}$ = national calcium carbonate demand [ton/year]

$Concrete^{dem}$ = national concrete demand [ton/year]

$Concrete\ by\ red\ mud^{dem}$ = national concrete by red mud demand [ton/year]

C_k^{max} = maximum storage capacity for storage site k [ton]

CR^{min} = minimum target for carbon dioxide reduction [ton/year]

CS_i = carbon dioxide emissions from each source i [ton/year]

$Lignin^{dem}$ = national lignin demand [ton/year]

$MeOH^{dem}$ = national methanol demand [ton/year]

$Polyurethane^{dem}$ = national polyurethane demand [ton/year]

XS_i = carbon dioxide composition in the flue gas emission from source i [mol%]

XL_i = lowest carbon dioxide composition processing limit for capture plant j [mol%]

XH_i = highest carbon dioxide composition processing limit for capture plant j [mol%]

$Urea^{dem}$ = national urea demand [ton/year]

$Wheat^{dem}$ = national wheat demand [ton/year]

Variables

Binary

$Y_{i,j,k}$ = 1 if carbon dioxide is capture from source i with technology j and sent to storage/utilization site k, otherwise 0

Continuous

Calcium carbonate$_{i,j,cc}$ = fraction of captured carbon dioxide from source i with technology j sent to calcium carbonate production site cc

Concrete by red mud$_{i,j,cr}$ = fraction of captured carbon dioxide from source i with technology j sent to concrete production site by red mud cr

Concrete$_{i,j,c}$ = fraction of captured carbon dioxide from source i with technology j sent to concrete production site c

$FR_{i,j,k}$ = fraction of captured carbon dioxide from source i with technology j sent to storage site k

Lignin$_{I,j,l}$ = fraction of captured carbon dioxide from source i with technology j sent to lignin production site l

Methanol$_{i,j,m}$ = fraction of captured carbon dioxide from source i with technology j sent to methanol production site m

Polyurethane$_{i,j,p}$ = fraction of captured carbon dioxide from source i with technology j sent to polyurethane production site p

Urea$_{i,j,u}$ = fraction of captured carbon dioxide from source i with technology j sent to urea production site u

Utilization$_{i,j,k}$ = fraction of captured carbon dioxide from source i with technology j sent to overall utilization site k

Wheat$_{i,j,w}$ = fraction of captured carbon dioxide from source i with technology j sent to wheat production site w

Chapter XII

XII. General conclusions and outlooks

In this Thesis, strategies are described and evaluated by means of numerical models to combine capture and sequestration of carbon dioxide, so to reduce the impact on climate change, with its economic utilization, in order to develop the so called carbon capture, utilization and storage (CCUS) supply chains. To highlight the opportunity to convert CO_2 into useful products, a potential utilization route of carbon dioxide is investigated in greater details, i.e. its conversion to methanol by means of the hydrogenation reaction, amenable to important industrial applications.

An innovative mathematical model, built according to the mixed integer linear programming (MILP) approach, for a CCUS supply chain is proposed. The model is developed using Advanced Interactive Multidimensional Modeling (AIMMS) software and applied to the European Countries with higher emissions (Germany, Italy and the UK). In particular, the model is able to consider different options in the utilization section and it is applied in a deterministic (single and multi objective optimization problem) and in a stochastic form.

Moreover, 1-D and 2-D mathematical models are developed in MATLAB® for a methanol (CH_3OH) packed bed catalytic reactor, operating in steady state inside a process with pure carbon dioxide (CO_2) and H_2 feedstock and with recycle of unconverted gases after the separation of CH_3OH and water (H_2O) by condensation. The model is proposed following the analysis of different options for the layout of the chemical conversion process (once through, recirculation and membrane assisted reactor), demonstrating the superior efficiency of this reactor configuration.

The following is a summary of main findings.

In Chapter II, through an equilibrium analysis of CH_3OH reactors fed by pure CO_2 and H_2, it is found that the reactor with the separation of CH_3OH and H_2O by condensation and with the recycle of unconverted gases ensures high efficiencies: for example a CO_2 conversion of 69% can be achieved at 55 bar and 473 K. Applying the 1-D mathematical kinetic model to this reactor configuration, it is found that the axial dispersion term can be neglected. On the other hand, simulating the same reactor with the 2-D model, it is found that this model is needed for a structured and a non structured reactor, to describe temperature and conversion radial variations, as well as the influence of packing thermal conductivity. Higher efficiencies are predicted for the structured reactor, characterized by greater thermal conductivity: a given CH_3OH yield is achieved with a shorter contact time. A sensitivity analysis is carried out for both models. For the 1-D model, varying the global heat exchange coefficient and the temperature of the isothermal heat exchange fluid shows the dominant effect of the temperature level of the heat exchange fluid on the final temperature reached in the reactor, as well as on the outlet carbon dioxide conversion and methanol selectivity.

For the 2-D model, a sensitivity analysis shows that feed temperature and the diameter of reactor tube have a negative effect on the performances, while the wall heat transfer coefficient has a slight negative effect on temperature without a significant variation on molar flow rates and then on the performances. Moreover, when CO_2 and H_2 are used in the process feeding stream, a lower ΔH characterizes the exothermic reacting system and therefore a reduced reactor temperature increase takes place along the reactor compared to the system using syngas in the feed.

In Chapter III, the innovative mathematical model for a CCUS supply chain is presented. Moreover, the proposed model is applied to Germany, where CH_3OH is produced via methane (CH_4) dry reforming. Total costs are minimized and results show that providing hydrogen (H_2) by water electrolysis ensures a lower environmental impact in terms of global warming and a higher amount of CO_2 is used to produce the same amount of CH_3OH. However, an amount of CH_3OH greater than the national demand is produced, then Germany will have an important role inside the world CH_3OH market for the next future (about 2025-2035). In any case, the CCUS supply chain costs 207 billion€/year and produces 203 Mton/year of CH_3OH. Considering carbon tax and economic incentives the system is economically feasible.

In Chapter IV, in order to overcome the problem of the CCUS supply chain developed in the previous Chapter, related to a probably too high CH_3OH production, the proposed MILP model is extended to consider more utilization options (CH_3OH, concrete by curing, wheat, lignin for polyethylene, calcium carbonate, urea, polyurethane and concrete by red mud). Minimizing total costs, it is found that the optimized total costs of the CCUS supply chain are 97.9 billion€/year with a NPV of 675 billion€ and a PBP of 2.71 years. Only carbon tax is required to have a profitable solution. Considering the uncertainty of selling price, it is found that the most probable values for NPV and PBP are in the range between 1.1 and 1.2 trillion€ and 3.85 years, respectively. Considering the uncertainty of national demand of CO_2-based compounds, the most probable values for NPV and PBP are respectively in the range of 1.04 and 1.12 trillion€ and 3.32 years.

In Chapter V, the deterministic MILP model for a CCUS supply chain is applied to Italy: CO_2 after capture is stored and used to produce CH_4 through a power to gas system. Minimizing total costs, it is found that economic incentives and carbon tax are required to have a profitable system from an economic point of view. Also, the supply chain with offshore Adriatic sea as storage site is predicted as best case, because in this case a comparatively low total cost and the lowest level of economic incentives are calculated. For this framework, total costs are $7.34 \cdot 10^4$ million€/year without economic incentives, and 16.1 Mton/year of CH_4 are produced, so that the net CH_4 production cost is 19 €/MWh when a proper level of incentives is considered (80 €/ton of carbon tax and 260 €/MWh of produced CH_4). In this way, Italy can reduce the import of methane substantially. A comparison with a carbon capture and utilization (CCU) supply chain shows that this last framework is not a good solution, due to a higher net CH_4 production cost and the highest level of economic incentives: it is important to have a storage site inside the supply chain.

In Chapter VI, the deterministic MILP model for a CCUS supply chain is applied to the UK. Total costs are minimized: results show that the CCUS supply chain with Bunter Sandstone as storage site is the most economically viable system, due to the highest value of NPV (0.554 trillion€) and the lowest value of PBP (2.85 years), considering only carbon tax, at a value of 80 €/tonCO_2. The supply chain costs 1.04 billion€/year. The captured CO_2 is used to produce 5.4 Mton/year of calcium carbonate, an amount greater than the national demand, then a portion of it should be exported. To avoid the production of a great amount of calcium carbonate, the mathematical model is updated considering a constraint about the production of CO_2-based products (this should be equal to or lower than the double of national demand). In this case, more compounds are produced with an acceptable amount compared to the market and only the system with Scottish offshore as storage site requires carbon tax to have a positive NPV. For the remaining case studies, economic incentives are also needed.
As a further step in the design of CCUS networks, the objective function of the deterministic MILP model is improved by taking into account carbon tax remission, revenues and economic incentives in the objective function, as in Chapter VII. With a scenario analysis, these new parameters are changed according to three different levels, as suggested by the market. It results that:

a) carbon tax influences only the total value of the objective function, and not the topology of the supply chain and the amount of different products. As a consequence, carbon tax level should be changed, if the aim is to modify only the profit of the system, without changing the topology.
b) economic incentives influence the topology of CCUS supply chain, with a positive effect on the number of CO_2 sources selected in the network and on the amount of CO_2 captured from each source.
c) revenues influence the structure of CCUS supply chains, with the same positive effect on the CO_2 sources selected and on the amount of CO_2 captured.

An additional important aspect is to verify that supply chains can effectively reduce CO_2 emissions, due to their additional energy requirements, by means of a life cycle assessment (LCA) analysis, as done in Chapter VIII. The LCA results show that, for the best CCUS supply chain of Germany, Italy and the UK, the value of global warming potential (GWP) is respectively equal to 1.94×10^{11} $kgCO_{2\text{-}eq}$, 9.62×10^{10} $kgCO_{2\text{-}eq}$ and 9.37×10^{9} $kgCO_{2\text{-}eq}$. Then CCUS supply chains are able to effectively reduce emissions, according to the environmental target. For all supply chains, a sensitivity analysis is also performed increasing the utilization rate of CO_2: keeping constant the amount of CO_2 captured, 25%, 50% and 75% of CO_2 sent to the storage in the base case is effectively stored in this analysis, while a corresponding, additional part is sent to the utilization section. For the CCUS supply chain of Germany, producing different CO_2-based products, and the UK, producing calcium carbonate, a higher environmental impact is determined when increasing the utilization rate of CO_2. In these cases, the storage section is therefore important in order to achieve a lower environmental impact. On the other hand, for the CCUS supply chain of Italy, where CH_4 is produced via a power to gas system, a lower environmental impact is present at a

higher utilization rate of CO_2. Then, the power to gas system is a process cleaner and more environmentally friendly than the storage option and other utilization systems, under conditions when hydrogen is obtained via water electrolysis utilizing renewable energy sources.

The single objective optimization problem, characterized by the minimization of total costs, is improved and a deterministic multi objective problem is investigated and solved in Chapter IX. Total costs are minimized while the amount of captured CO_2 is simultaneously maximized, for the best CCUS supply chain of Germany, Italy and the UK. Results show better efficiency of the augmented ε-constraint method due to a lower resolution time, compared to the traditional ε-constraint method. The Pareto front is found for each framework, suggesting convenient trade-off between the two objective functions, and two guidelines are suggested for a decision maker in order to select the best scenario. This is based on the shortest distance from the Utopia point, giving importance to both objective functions. The alternative choice considers the minimum net total cost, making predominant the economic objective function. It results that the CCUS supply chain of Germany is closer to ideal conditions, compared to the other carbon supply systems examined here, even if higher costs are computed in that case.

The two stage stochastic model is presented in Chapter X and utilized for the best supply chain of Germany, Italy and the UK, considering the production costs of CO_2-based compounds as stochastic parameters.

The expected total costs of these systems are minimized: for the CCUS supply chain of Italy, Germany and the UK they are equal to 77.3 billion€/year, 98.0 billion€/year, 1.05 billion€/year, respectively. Comparing these results with those of the respective deterministic models, by means of the expected value of perfect information (EVPI) and the value of stochastic solution (VSS), it is found that the considered stochastic parameters do not have a big influence on the modelling of carbon supply chains, then very few advantages are offered by solving the stochastic problem instead of the deterministic one, when the stochastic parameter is the production cost of CO_2-based compounds.

In Chapter XI, a new deterministic version of the innovative model for carbon supply chains is suggested, considering an unique pipeline network for CO_2 distribution, in the utilization and storage section. The new MILP model that minimizes total costs is applied to the supply chain producing more compounds in Germany. Results show that the high level of CO_2 purity imposed to all captured streams implies only a slightly higher total cost compared to the system reported in Chapter IV (0.104 trillion€/year). For this new scheme, only carbon tax is required to reach profitability from an economic point of view: the NPV is 0.616 trillion€, while the PBP is 5.7 years.

Regarding future work, it would be interesting to consider more complex CCUS supply chains taking into account, at the same time, a multiplicity of carbon sources, storage sites and utilization sites, trying to design a more realistic picture for each Country. This would imply to eliminate the assumption of only one storage site, or the restriction to only two utilization sites, with a substantial production capacity, so to keep the ratio between utilization and storage above a given threshold limit dictated by the need to establish a circular carbon economy.

In addition, following the development of a supply chain model like that described in this Thesis, applied to different Countries and under different constraints, it would be interesting to extend the model to a CCUS supply chain involving the whole Europe that should achieve a reduction of CO_2 emissions according the COP21 agreement.

To enlarge and better characterize the basket of carbon-dioxide-based compounds, of their dynamic market demand and most convenient production processes (economically and environmentally speaking – green chemistry), realization of a comprehensive data bank would strongly help an even more reliable application of such models, as a result of combined efforts in economic and engineering research.